

LOAN DOCUMENT

DTIC ACCESSION NUMBER		PHOTOGRAPH THIS SHEET	INVENTORY ①																				
	LEVEL																						
	WL-TR-97-4039 DOCUMENT IDENTIFICATION Apr 97																						
		DISTRIBUTION STATEMENT A Approved for public release; Distribution Unlimited																					
		DISTRIBUTION STATEMENT																					
<table border="1"><tr><td colspan="2">ACCESSION FOR</td></tr><tr><td>NTIS</td><td>ORIGIN</td></tr><tr><td>DTIC</td><td>TRAC</td></tr><tr><td>UNANNOUNCED</td><td></td></tr><tr><td>JUSTIFICATION</td><td></td></tr><tr><td colspan="2">BY</td></tr><tr><td colspan="2">DISTRIBUTION/</td></tr><tr><td colspan="2">AVAILABILITY CODES</td></tr><tr><td>DISTRIBUTION</td><td>AVAILABILITY AND/OR SPECIAL</td></tr><tr><td>A-1</td><td></td></tr></table>		ACCESSION FOR		NTIS	ORIGIN	DTIC	TRAC	UNANNOUNCED		JUSTIFICATION		BY		DISTRIBUTION/		AVAILABILITY CODES		DISTRIBUTION	AVAILABILITY AND/OR SPECIAL	A-1		DATE ACCESSIONED	
ACCESSION FOR																							
NTIS	ORIGIN																						
DTIC	TRAC																						
UNANNOUNCED																							
JUSTIFICATION																							
BY																							
DISTRIBUTION/																							
AVAILABILITY CODES																							
DISTRIBUTION	AVAILABILITY AND/OR SPECIAL																						
A-1																							
DISTRIBUTION STAMP		DATE RETURNED																					
19970703 057		REGISTERED OR CERTIFIED NUMBER																					
DATE RECEIVED IN DTIC																							
PHOTOGRAPH THIS SHEET AND RETURN TO DTIC-FDAC																							

H
A
N
D
L
E

W
I
T
H

C
A
R
E

WL-TR-97-4039

**PROCEEDINGS OF THE ANNUAL
MECHANICS OF COMPOSITES
REVIEW (2ND)**



Sponsored by:

**Air force Materials Laboratory
Nonmetallic Materials Division**

and

**Air Force Office of Scientific Research
Directorate of Aerospace Sciences**

APRIL 1997

FINAL REPORT FOR PERIOD 26-28 OCTOBER 1976

Approved for public release; distribution unlimited

**MATERIALS DIRECTORATE
WRIGHT LABORATORY
AIR FORCE MATERIEL COMMAND
WRIGHT-PATTERSON AFB OH 45433-7734**

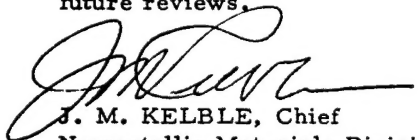
REPORT DOCUMENTATION PAGE			Form Approved OMB No. 0704-0188	
Public reporting burden for this collection of information is estimated to average 1 hour per response, including the time for reviewing instructions, searching existing data sources, gathering and maintaining the data needed, and completing and reviewing the collection of information. Send comments regarding this burden estimate or any other aspect of this collection of information, including suggestions for reducing this burden, to Washington Headquarters Services, Directorate for Information Operations and Reports, 1215 Jefferson Davis Highway, Suite 1204, Arlington, VA 22202-4302, and to the Office of Management and Budget, Paperwork Reduction Project (0704-0188), Washington, DC 20503.				
1. AGENCY USE ONLY (Leave blank)	2. REPORT DATE April 1997	3. REPORT TYPE AND DATES COVERED Final Report 26-28 October 1976		
4. TITLE AND SUBTITLE PROCEEDINGS OF THE ANNUAL MECHANICS OF COMPOSITES REVIEW (2ND)		5. FUNDING NUMBERS		
6. AUTHOR(S)				
7. PERFORMING ORGANIZATION NAME(S) AND ADDRESS(ES) Air Force Materials Laboratory Nonmetallic Materials Division Wright-Patterson AFB OH 45433		8. PERFORMING ORGANIZATION REPORT NUMBER		
9. SPONSORING/MONITORING AGENCY NAME(S) AND ADDRESS(ES) Materials Directorate Wright Laboratory Air Force Materiel Command Wright-Patterson AFB Ohio 45433-7734 POC: Tammy Oaks, WL/MLBM, 937-255-3068		10. SPONSORING/MONITORING AGENCY REPORT NUMBER WL-TR-97-4039		
11. SUPPLEMENTARY NOTES				
12a. DISTRIBUTION AVAILABILITY STATEMENT APPROVED FOR PUBLIC RELEASE; DISTRIBUTION IS UNLIMITED			12b. DISTRIBUTION CODE	
13. ABSTRACT (Maximum 200 words) This report contains the basic unedited vu-graphs of the presentations at the "Mechanics" of Composites Review" sponsored jointly by the Non-metallic Materials Division of the Air Force Materials Laboratory and the Directorate of Aerospace Sciences of the Air Force Office of Scientific Research. The presentations cover current in-house and contract programs under the sponsorship of these two organizations.				
14. SUBJECT TERMS epoxy-matrix composites; composite materials; resin matrix composites; composite bonded joints; fatigue of graphite/epoxy composites; fracture and fatigue of bi-materials			15. NUMBER OF PAGES 346	
			16. PRICE CODE	
17. SECURITY CLASSIFICATION OF REPORT UNCLASSIFIED	18. SECURITY CLASSIFICATION OF THIS PAGE UNCLASSIFIED	19. SECURITY CLASSIFICATION OF ABSTRACT UNCLASSIFIED	20. LIMITATION OF ABSTRACT SAR	

FOREWORD

This report contains the basic unedited Vu-graphs of the presentations at the "Mechanics of Composites Review" sponsored jointly by the Non-metallic Materials Division of the Air Force Materials Laboratory and the Directorate of Aerospace Sciences of the Air Force Office of Scientific Research. The presentations cover current in-house and contract programs under the sponsorship of these two organizations.

Since this is a review of on-going programs, much of the information in this report has not been published as yet and is subject to changes. But timely dissemination of the rapidly expanding technology of advanced composites is deemed highly desirable. Works in the area of mechanics of composites have long been typified by disciplined approaches. It is hoped that such a high standard of rigor is reflected in the majority, if not all, of the presentations in this report.

Feedback and open critique of the presentations are welcome. Special thanks are due to James M. Whitney of the Nonmetallic Materials Division for his effort in organizing this review. Again, suggestions and recommendations from all participants will be most important in the planning of future reviews.



J. M. KELBLE, Chief
Nonmetallic Materials Division
Air Force Materials Laboratory

AGENDA
MECHANICS OF COMPOSITES REVIEW
OCTOBER 26 - 28, 1976

TUESDAY, OCTOBER 26

		<u>PAGE</u>
8:00 AM	REGISTRATION	
8:30	OPENING REMARKS: Brian Quinn, Director of Aerospace Sciences, Air Force Office of Scientific Research	
8:45	MOISTURE EFFECTS ON EPOXY-MATRIX COMPOSITES: George S. Springer, University of Michigan	1
9:30	COFFEE BREAK	
10:00	ENVIRONMENTAL EXPOSURE EFFECTS ON COMPOSITE MATERIALS: Lawrence J. Broutman, Illinois Institute of Technology	11
10:45	DURABILITY OF FIBER REINFORCED RESIN MATRIX COMPOSITES: James M. Whitney, Air Force Materials Laboratory	25
12:00	LUNCH	
1:00 PM	ENVIRONMENTAL EFFECTS ON THE THERMOMECHANICAL BEHAVIOR OF COMPOSITES: Thomas S. Cooke, Southwest Research Institute	51
1:45	ANALYSIS AND DESIGN OF COMPOSITE BONDED JOINTS UNDER A DYNAMIC TYPE LOAD: Jack R. Vinson, University of Delaware	59
2:30	COFFEE BREAK	
3:00	EFFECT OF COMPRESSION ON FATIGUE OF GRAPHITE/EPOXY COMPOSITES: James T. Ryder, Lockheed Corporation	71
3:45	COMPOSITE STRUCTURE OPTIMAL DESIGN BY ENERGY METHODS: Michael Murphy, Norwich University	95
4:30	EFFECTS OF ENVIRONMENT, AND DAMPING AND COUPLING PROPERTIES OF COMPOSITE LAMINATES ON PANEL FLUTTER: Satish Kulkarni, Materials Science Corporation	103
5:15	ADJOURN	

<u>WEDNESDAY, OCTOBER 27</u>	<u>PAGE</u>
8:00 AM FRACTURE AND FATIGUE OF BI-MATERIALS: James W. Mar, Massachusetts Institute of Technology	117
8:45 BIAxIAL TESTING OF GRAPHITE/EPOXY COMPOSITES CONTAINING STRESS CONCENTRATIONS: Isaac Daniel, IIT Research Institute	123
9:30 COFFEE BREAK	
10:00 RESPONSE OF GRAPHITE COMPOSITES TO LASER RADIATION: Kenneth G. Kibler, General Dynamics	153
10:45 DEFECT-PROPERTY RELATIONSHIPS IN COMPOSITE MATERIALS: Kenneth L. Reifsnider, Virginia Polytechnic Institute and State University	159
11:30 FATIGUE IN ADHESIVELY BONDED LAMINATES: James A. Alic, Wichita State University	177
12:00 LUNCH	
1:00 PM ULTRASONIC PROCEDURES FOR THE DETERMINATION OF BOND STRENGTH: Joseph L. Rose, Drexel University	
1:45 FAILURE MECHANISMS AND CRITERIA IN COMPOSITE MATERIALS: Nicholas J. Pagano, Air Force Materials Laboratory	183
2:30 COFFEE BREAK	
3:00 ULTRASONIC NON-DESTRUCTIVE TESTING OF COMPOSITE MATERIALS: Yih-Hsing Pao, Cornell University	199
3:45 BIAxIAL FATIGUE OF COMPOSITES: Philip H. Francis, Southwest Research Institute	209
4:15 TIME-DEPENDENT FRACTURE OF COMPOSITES: Richard A. Schapery, Texas A&M University	221
5:00 ADJOURN	

THURSDAY, OCTOBER 28

PAGE

8:00 AM	EXPLORATORY DEVELOPMENT OF PROBABILISTIC CHARACTERIZATION AND TESTING TECHNIQUES FOR FATIGUE BEHAVIOR OF COMPOSITE LAMINATES: Robert A. Heller, Jann N. Yang, John J. McGowan, George Washington University	225
	ANALYSIS OF FATIGUE DATA: Jann N. Yang, George Washington University	251
8:45	DYNAMICS OF COMPOSITE MATERIALS: George Herrmann, Stanford University	261
9:30	COFFEE BREAK	
10:00	CONTINUUM THEORY OF FRACTURE: Morton E. Gurtin, Carnegie-Mellon University	269
10:30	LINEAR AND NONLINEAR EFFECTS IN THE VIBRATION OF ELASTIC STRUCTURES: Lawrence W. Rehfield, Georgia Institute of Technology	273
11:15	MECHANICS OF COMPOSITE MATERIALS: Gilbert A. Hegemier, University of California, San Diego	281
12:00	LUNCH	
1:00 PM	RESPONSE OF CANTILEVER PLATE (FAN BLADE) DUE TO IMPACT LOADING: Pei Chi Chou, Drexel University	301
1:45	MECHANICS OF COMPOSITE MATERIALS WITH DIFFERENT MODULI IN TENSION AND COMPRESSION: Robert M. Jones, Southern Methodist University	315
2:30	STUDY OF RESIDUAL STRESSES IN COMPOSITES: Thomas B. McDonough, Aeronautical Research Associates of Princeton, Inc.	
3:00	ADJOURN	

MECHANICS OF COMPOSITES REVIEW

LIST OF ATTENDEES AS OF OCTOBER 14, 1976

Alic, John A.
Dept. of Mechanical Engineering
Wichita State University
Wichita, Kansas 67208

Brinson, Halbert F.
Virginia Polytechnic Institute & State
University
College of Engineering
Engineering Science & Mechanics
Blacksburg, Virginia 24061

Broutman, Lawrence L.
Dept. of Metallurgical Engineering
Illinois Institute of Technology
Chicago, Illinois 60616

Bunshah, Ron F.
Professor of Engineering
School of Engineering & Applied Science
University of California
Los Angeles, California 90024

Chou, Pei Chi
Drexel University
Mechanics & Structures Group
32nd & Chestnut Streets
Philadelphia, Pennsylvania 19104

Chou, S. C.
Army Materials & Mechanics
Research Center
Watertown, Massachusetts

Cooke, Thomas S.
Dept. of Materials Science
Southwest Research Institute
P.O. Drawer 28510
San Antonio, Texas 78284

Daniel, Isaac M.
IIT Research Institute
Mechanics of Materials Division
10 West 35th Street
Chicago, Illinois 60616

Dastin, Samuel
Grumman Aerospace Corporation
South Oyster Bay Road
Bethpage, New York 11714

Eisenmann, James
General Dynamics Convair
Aerospace Division
P.O. Box 748
Fort Worth, Texas 67101

Fogg, Larry
Lockheed Aircraft Corporation
Lockheed California Company
Burbank, California 91520

Francis, Philip H.
Southwest Research Institute
Dept. of Mechanical Sciences
P.O. Drawer 28510
8500 Culebra Road
San Antonio, Texas 78284

Garbo, Samuel
McDonnell Douglas Corporation
B32/Level 2/Dept 234
St. Louis, Missouri

Gurtin, Morton E.
Dept. of Mathematics
Carnegie-Mellon University
Pittsburgh, Pennsylvania 15213

Hegemier, Gilbert A.
Dept. of Applied Mechanics &
Engineering Science
University of California, San Diego
LaJolla, California 92037

Henneke, Edmund G.
Virginia Polytechnic Institute &
State University
College of Engineering
Engineering Science & Mechanics
Blacksburg, Virginia 24061

Herrmann, George
Dept. of Applied Mechanics
Stanford University
Stanford, California 94035

Hofer, Kenneth E., Jr.
IIT Research Institute
10 West 35th Street
Chicago, Illinois 60616

Hoffman,
Rockwell International Corporation
Los Angeles Aircraft Division
5701 West Imperial Highway
Los Angeles, California 90009

Jeans, Lawrence
Northrop Corporation
3901 West Broadway
Hawthorne, California 90250

Jones, Robert M.
Solid Mechanics Center
Southern Methodist University
Dallas, Texas 75222

Kibler, Kenneth G.
General Dynamics Convair
Aerospace Division
Fort Worth, Texas 76101

Konishi, Donald
Rockwell International Corporation
Los Angeles Aircraft Division
5701 West Imperial Highway
Los Angeles, California 90009

Kulkarni, Satish V.
Materials Sciences Corporation
Blue Bell Office Campus
1777 Walton Road
Blue Bell, Pennsylvania 19422

Lackman, Lester
Rockwell International Corporation
Los Angeles Aircraft Division
5701 West Imperial Highway
Los Angeles, California 90009

McDonough, Thomas B.
Aeronautical Research Associates
of Princeton, Inc.
50 Washington Road
Princeton, New Jersey 08540

Mar, James W.
Dept. of Aeronautic & Astronautics
Massachusetts Institute of Technology
Cambridge, Massachusetts 02139

Morris, Donald
Mechanical Engineering Dept.
Drawer ME
Mississippi State University
Mississippi State, Mississippi 39762

Murphy, Michael
Dept. of Engineering & Technology
Norwich University
Northfield, Vermont 05663

Quinn, Brian
AFOSR/NA,
Bolling Air Force Base, DC 20332

Rehfield, Lawrence W.
School of Aerospace Engineering
Georgia Institute of Technology
Atlanta, Georgia 30332

Reifsnider, Kenneth L.
Virginia Polytechnic Institute &
State University
College of Engineering
Engineering Science & Mechanics
Blacksburg, Virginia 24061

Rodini, Benjamin T.
General Dynamics Convair
Aerospace Division
P. O. Box 748
Fort Worth, Texas 67101

Rose, Joseph L.
Dept. of Mechanical Engineering
Drexel University
Philadelphia, Pennsylvania 19104

Ryder, James T.
Lockheed Aircraft Corporation
Lockheed California Company
Burbank, California 91520

Sachse, Wolfgang H.
Dept. of Theoretical &
Applied Mechanics
Cornell University
Ithica, New York 14853

Schapery, Richard A.
Mechanics & Materials
Research Center
Texas A&M University
College Station, Texas 77843

Sih, George C.
Lehigh University
Institute of Fracture and Solid
Mechanics
Bethlehem, Pennsylvania 18015

Springer, George S.
University of Michigan
Mechanical Engineering Dept.
Ann Arbor, Michigan 48104

Starnes, James H.
NASA Langley Research Center
Hampton, Virginia 23665

Stinchcombe, Wayne
Virginia Polytechnic Institute &
State University
College of Engineering
Engineering Science & Mechanics
Blacksburg, Virginia 24061

Verrette, Ralph
Northrop Corporation
3901 West Broadway
Hawthorne, California 90250

Vinson, Jack R.
Center for Composite Materials
University of Delaware
Newark, Delaware 19711

Viswamatham, A. B.
Boeing Aerospace Corporation
P. O. Box 3999
Seattle, Washington 98124

Walker, William
AFOSR/NA
Bolling Air Force Base, DC 20332

Whiteside, James B.
Grumman Aerospace Corporation
South Oyster Bay Road
Bethpage, New York 11714

Yang, Jann N.
George Washington University
Washington, DC 20052

ADDENDUM TO LIST OF ATTENDEES

Baumgartner, Walter
Lockheed Aircraft Corporation
Lockheed California Company
Burbank, California 91520

Garrett, Ray
McDonnell Douglas Corporation
Astro East, Bldg 106, Box 516
Dept E-452
St. Louis, Missouri 63066

Hays, Charles
AFOSR/NA
Bolling Air Force Base, DC 20332

Jones, Robert E.
Aerospace Group
Seattle, Washington 98124

Lo, Him
Materials Research Laboratory
Washington University
St. Louis, Missouri 63130

Nguyen, Nhan
Materials Research Laboratory
Washington University
St. Louis, Missouri 63130

Pao, Yih Hsing
Dept. of Theoretical & Applied
Mechanics
Cornell University
Ithaca, New York 14853

Rousseau, Charles
Space Division Rockwell International
12214 Lakewood Blvd., Mail Stop AB 70
Downey, California 90241

Sun, C.T.
Purdue University
School of Aeronautics, Astronautics
& Engineering Sciences
LaFayette, Indiana 47907

Wu, Edward M.
Materials Engineering Division
Lawrence Livermore Laboratories
University of California
P.O. Box 808
Livermore, California 94550

DAYTON LIST

Aeronautical Systems Division

Goodman, John
King, Troy T.
Tipps, Daniel

Air Force Flight Dynamics Laboratory

Davidson, Edward
Demuts, Edwin
Garrison, Jan
Parmley, Philip
Sendeckyj, George P.
Shirrell, David
Waggoner, Gary

Air Force Materials Laboratory

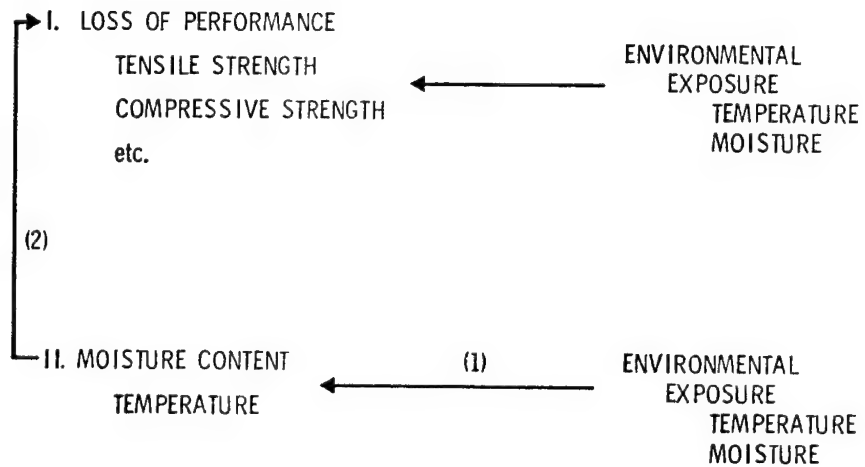
Awerbuch, Jonathan
Duhl, Michael
Erikson, Jan
Jones, William B.
Kelble, Jerome M.
Kelley, Frank N.
Knight, Marvin
Pagano, Nicholas J.
Rhodehamel, John
Tsai, Stephen W.
Watson, David
Weitsman, Yechiel
Whitney, James M.

University of Dayton Research Institute

Hahn, H. Thomas
Kim, Ran Y.

MOISTURE EFFECTS ON EPOXY-MATRIX COMPOSITES

George S. Springer
Department of Mechanical Engineering
The University of Michigan



"MOISTURE PROBLEM"

I GIVEN

Ambient Moisture Content
Ambient Temperature

Find

Material

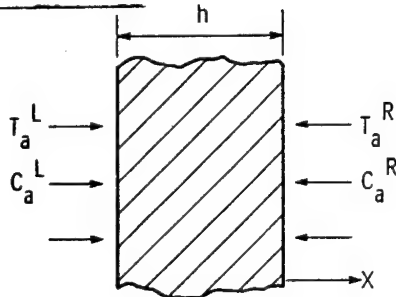
- a) Moisture Content
- Weight Gain
- Moisture Distribution
- b) Temperature Distribution

II SINGLE LAYER - Steady State Solution

III EXPERIMENTAL PROCEDURES

IV MULTILAYER - Unsteady (numerical) Solution

SINGLE LAYER - STEADY



$$1. T_a^L = T_a^R = \text{CONST}$$

$$C_a^R = C_a^R = \text{CONST}$$

(STEADY)

$$2. \text{INITIALLY } (t < 0)$$

C, T UNIFORMLY
DISTR. BUTED

$$3. K = K(T) \text{ ONLY}$$

$$4. \text{TEMP. DISTR. CONSTANT (INDEP. OF TIME)}$$

$$5. D = D(T) \text{ ONLY}$$

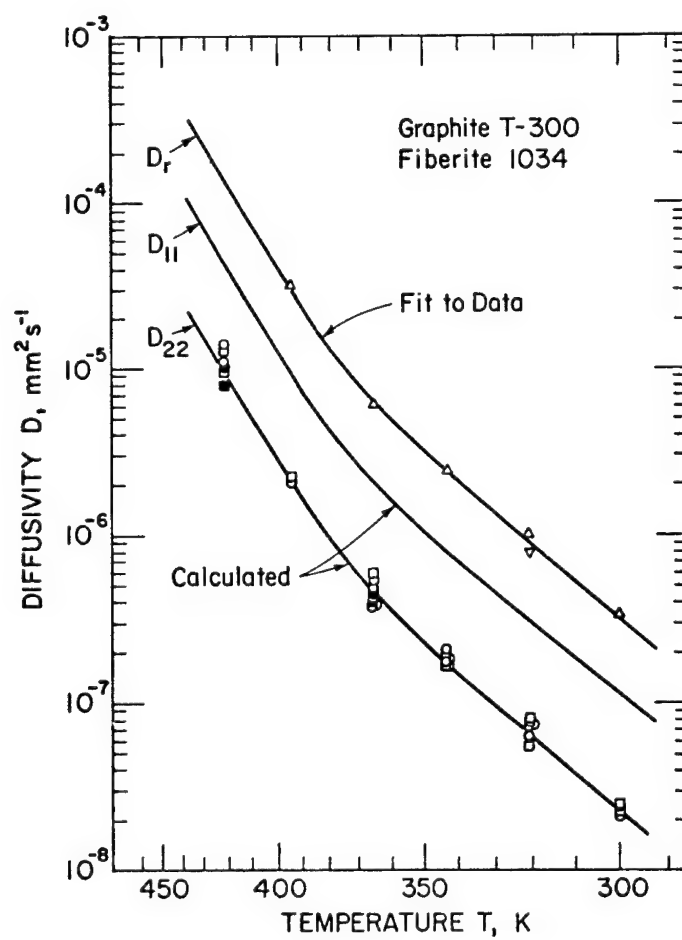
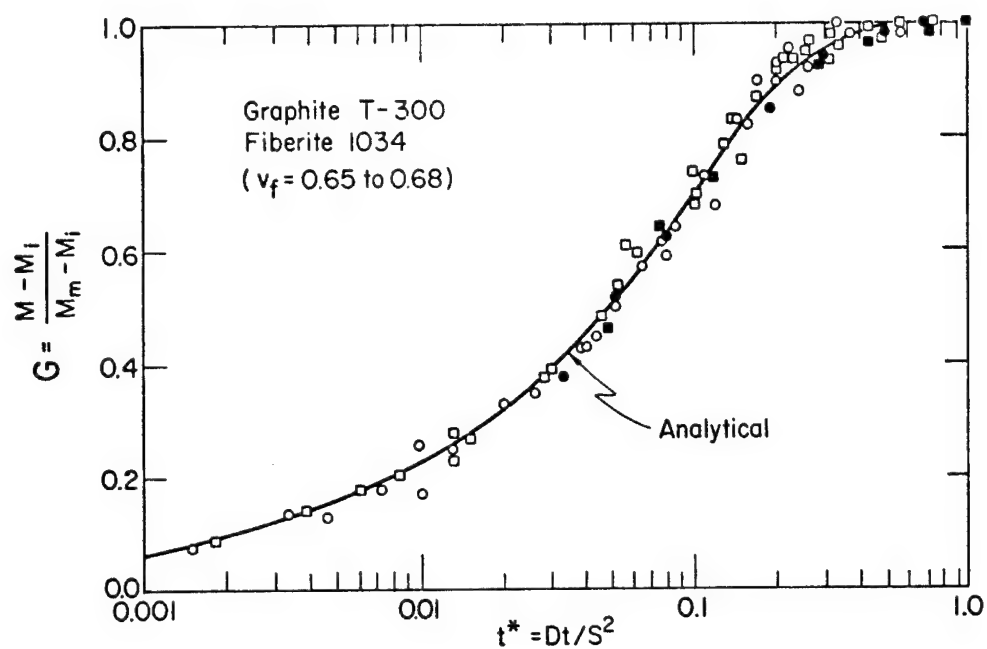
MOISTURE CONTENT (% WEIGHT GAIN)

$$M(t) = G(M_m - M_i) + M_i$$

\swarrow t \swarrow h \swarrow D

ABSORPTION

DESORPTION

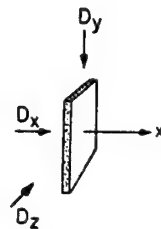


EXPERIMENTS

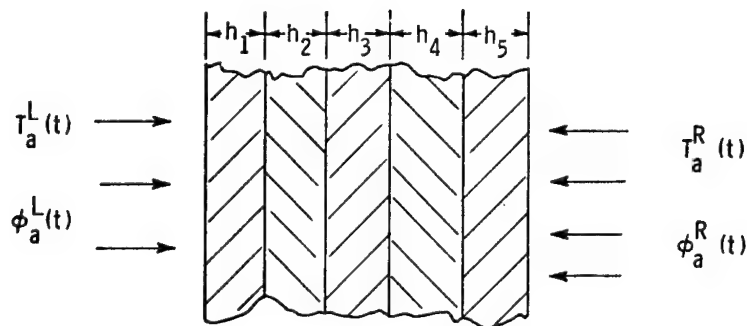
NEEDED: a) Diffusion Coefficient
 b) Maximum Saturation Level

PRESENT PROGRAM

- 1) Simple Apparatus for Large Number of Tests
- 2) Edge Corrections
- 3) Accelerated Test Procedures
- 4) Generate Data

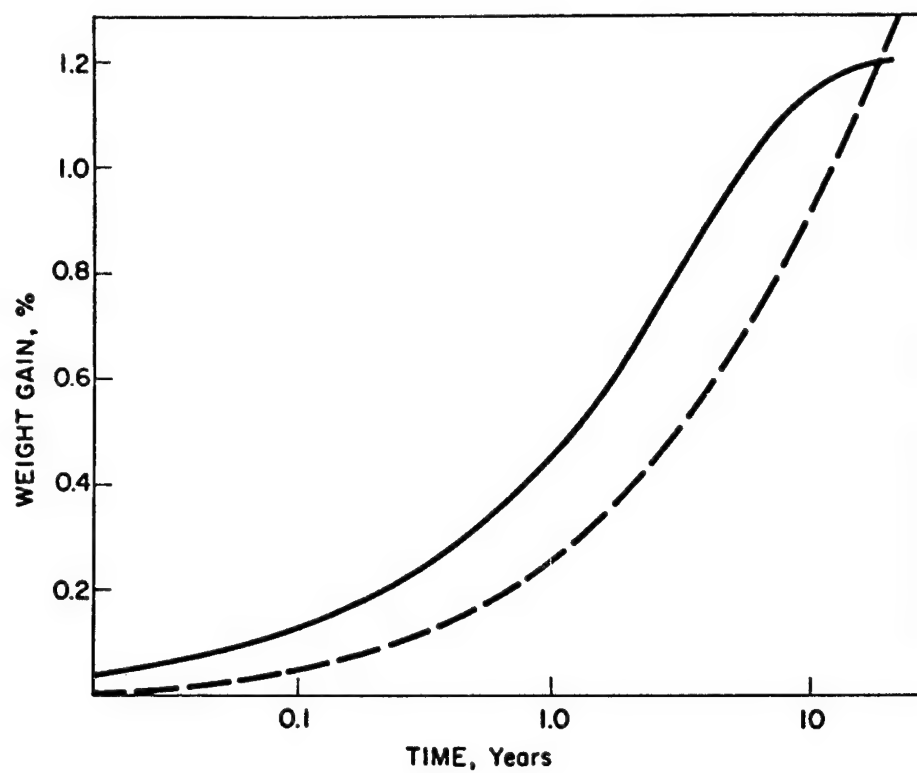


GENERAL PROBLEM



Material Specified By: $K(T)$, $D(T)$, $M_m(\phi)$, P

- RESULTS:
- 1) Total Moisture Content (Wt Gain) as a Function of Time
 - 2) Moisture Content (Wt Gain) of each Layer as a Function of Time
 - 3) Moisture Distribution in Each Layer
 - 4) Temperature Distribution in Each Layer



SUMMARY - MOISTURE PROBLEM

- 1) Exact Steady State Solution
- 2) Experimental Procedures
- 3) Test Facility
- 4) Fully Operational Computer Code for
General-Multilayered-Unsteady Problems

TENSILE STRENGTH

ENVIRONMENTAL DEPENDENCE

- 1) Moisture
- 2) Temperature
- 3) Combined Moisture and Temperature

MATERIAL DEPENDENCE

- 1) Composition
- 2) Fiber Orientation

NEEDED : COMPREHENSIVE SET OF DATA

- 1) For "Absolute" Values
- 2) For Showing Trends
- 3) For Extracting Information from Existing Data
- 4) For Guidance in Future Tests

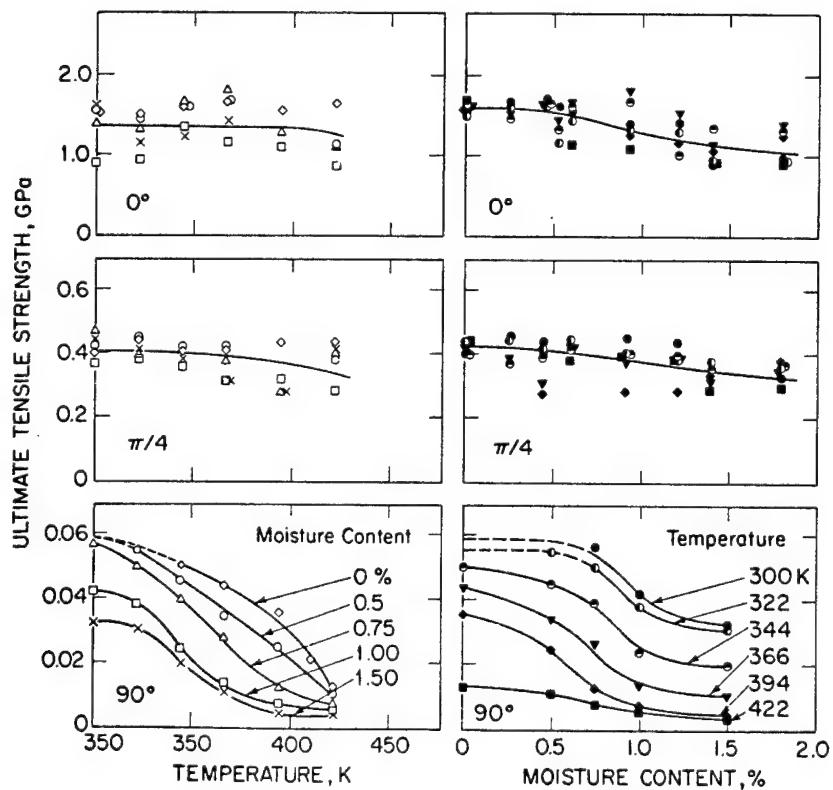
DATA

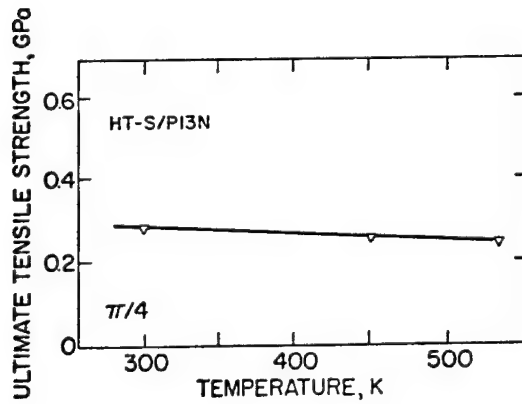
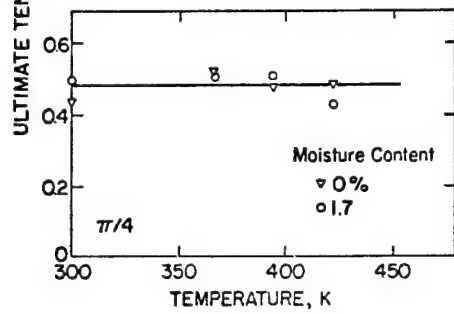
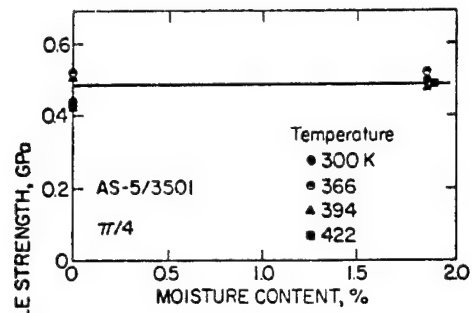
THORNEL 300 / FIBERITE 1034

SPECIMEN : 8 Ply 4" x 1/2" x 0.036"

MOISTURE CONTENT	TEMPERATURE °F					
	77	120	160	200	250	300
Dry						
33% Saturated						
50% Saturated						
67% Saturated						
100% Saturated						

FIBER ORIENTATION $\begin{cases} 0 \\ 90 \\ \pi/4 \end{cases}$





		0°		$\pi/4$		90°	
		M	T	M	T	M	T
Thornel 300/Fiberite 1034	Shen-Springer	X	X	X	X	X	X
Hercules AS-5/3501	Browning et al	X	X	X	X	X	X
	Verette	X	X	X	-	X	X
	Kerr et al	-	X	-	X	-	X
	Kim-Whitney	-	-	X	X	-	-
	Hofer et al	X	X	X	X	X	X
Thornel 300/Narmco 5208	Husman	-	-	-	-	X	X
Modmor II / Narmco 5206	Hofer et al	X	X	X	X	X	X
Courtaulds HMS / Hercules 3002M	Hofer et al	X	X	X	X	X	X
HT-S/ERLA-4617	Browning	-	-	X	X	-	-
HT-S/Fiberite X-911	Browning	-	-	X	X	-	-
HT-S/UCC X-2546	Browning	-	-	X	X	-	-
PRD-49/ERLB-4617	Hanson	-	X	-	-	-	-
HT-S/(8183/137-NDA-BF ₃ : MEA)	Hertz	-	-	-	-	X	X
HT-S/HYSOL ADX-516	Browning	-	-	X	X	-	-
Hercules HT-S/710	Kerr et al	-	X	-	X	-	X
HT-S/P13N	Browning	-	-	-	X	-	-
Boron/AVCO 5505	Hofer et al	X	X	X	X	X	X
Boron/Narmco 5505	Kaminski	-	X	-	-	-	X
	Browning	-	-	X	X	-	-

GENERAL CONCLUSIONS - ULTIMATE TENSILE STRENGTH

A. Temperature

- 1) 0° and $\pi/4$ → Negligible Effects
- 2) 90° → Significant Effects
 - a) Moisture Dependent
 - b) 60-90% Max. Loss in Strength

B. Moisture

- 1) 0° and $\pi/4$ → Small Effects
 - a) Negligible Below 1%
 - b) Small (20-30% Max. Strength Loss) Above 1%
- 2) 90° → Significant Effects
 - a) Temperature Dependent
 - b) 60-90% Max. Loss in Strength

SUMMARY - ULTIMATE TENSILE STRENGTH

- 1) Extensive Set of Data for Thornel 300 / Fiberite 1034
- 2) Summary of Existing Data
- 3) Interpretation of Existing Data
- 4) General Trends Due to Moisture and Temperature
- 5) Guidelines for Future Tests

ENVIRONMENTAL EXPOSURE EFFECTS ON COMPOSITE MATERIALS

AFOSR 72-2214F

**Principal Investigator: Lawrence J. Broutman
Illinois Institute of Technology**

OBJECTIVES:

- 1. To Study the Impact Behavior of Advanced Fiber Composites.**
- 2. To Study the Influence of Fiber-Resin Interface Strength on Impact Energy Absorption.**
- 3. To Study the Effects of Moisture Content on Performance of Carbon Fiber Composites. Determine the Relative Roles of the Interface and Matrix.**
 - 3.1 Characterize Moisture Diffusion as a Function of Applied Stress and Temperature.**
 - 3.2 Characterize Interfacial Moisture Diffusion.**
 - 3.3 Determine Effect of Moisture on Strength and Impact Behavior by Measuring Current and Residual Properties.**
 - 3.4 Analyze the Long Term Degradation (11 Years) of Carbon Fiber Reinforced Epoxy Resins.**

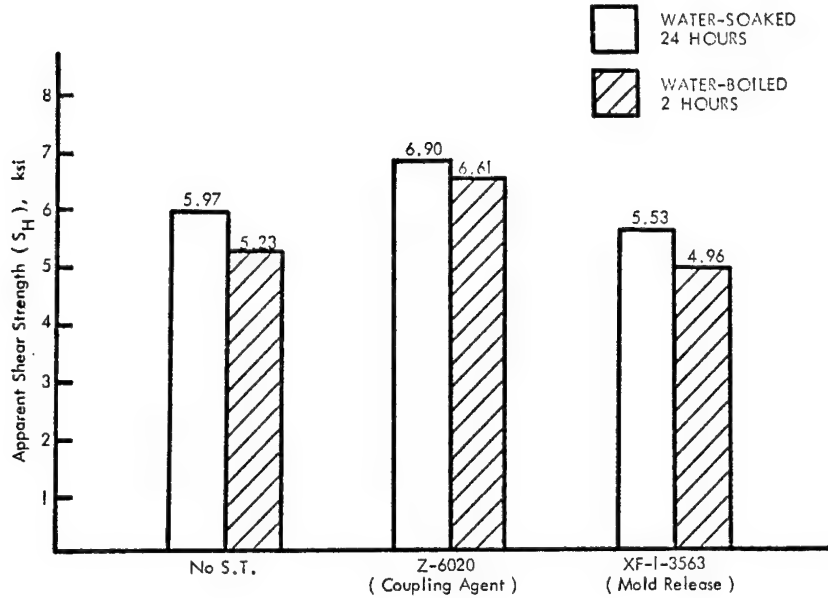


Figure 23. Effects of Enviromental Degradation on the Apparent Shear Strength of Fiberglass-Epoxy Laminates

64

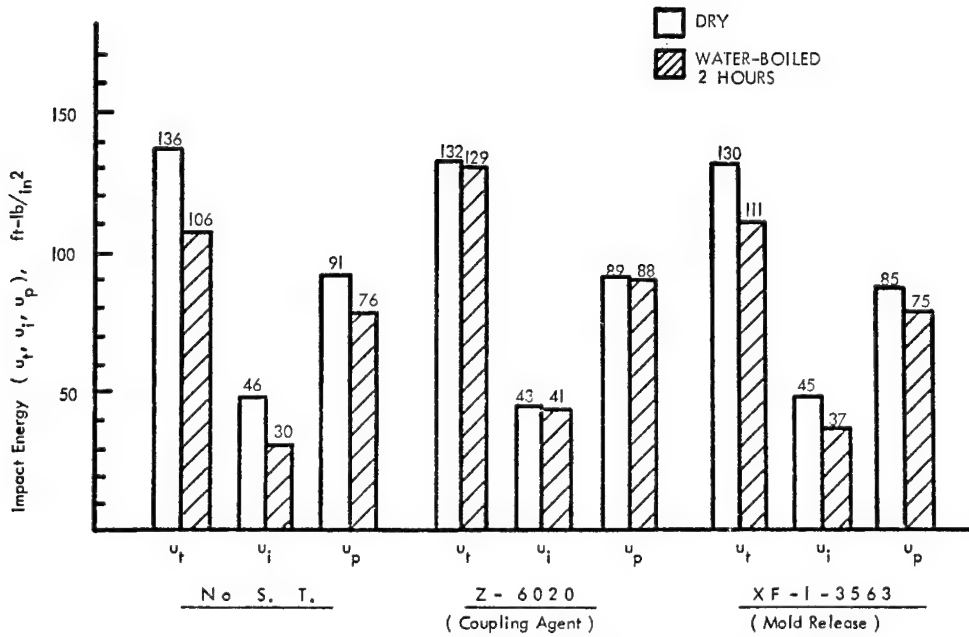


Figure 24. Effects of Enviromental Degradation on Impact Strength of Fiberglass-Epoxy Laminates

65

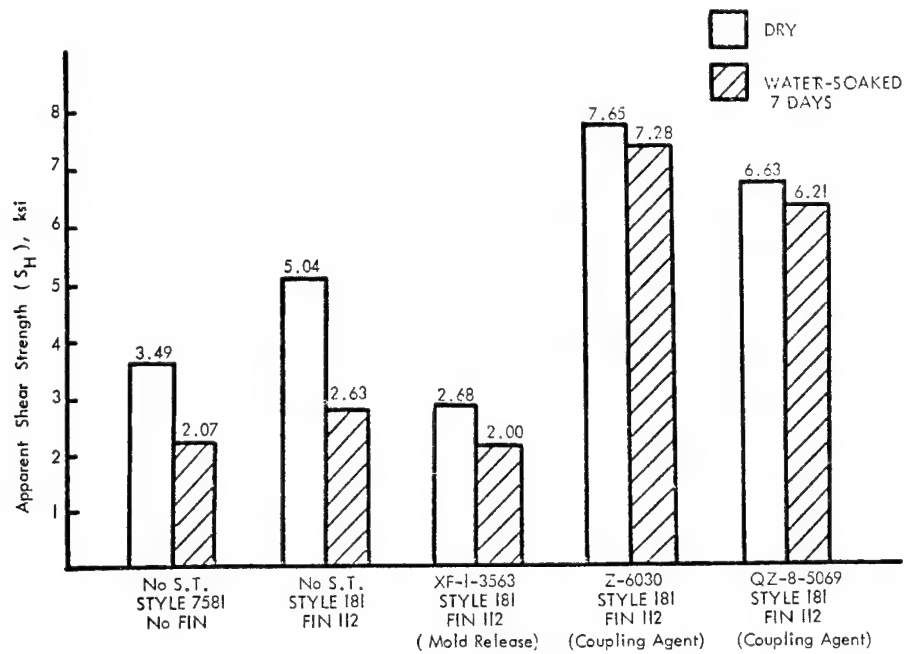


Figure 27. Effects of Enviromental Degradation on the Apparent Shear Strength of Fiberglass-Polyester Laminates

73

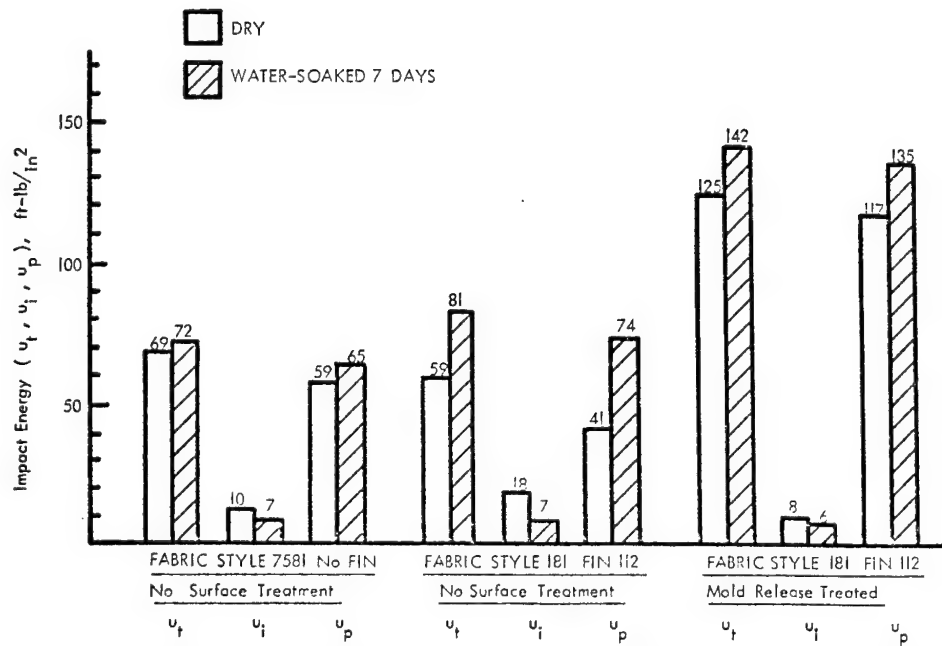


Figure 29. Effects of Enviromental Degradation on Impact Strength of Poorly-Bonded Fiberglass-Polyester Laminates

75

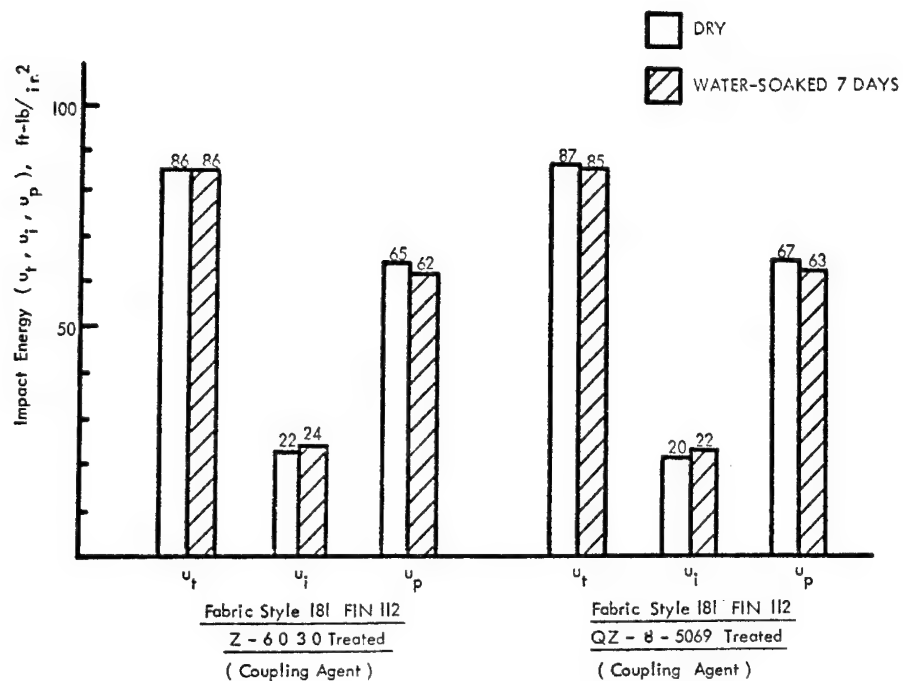


Figure 30. Effects of Environmental Degradation on Impact Strength Of Strongly-Bonded Fiberglass-Polyester Laminates

76

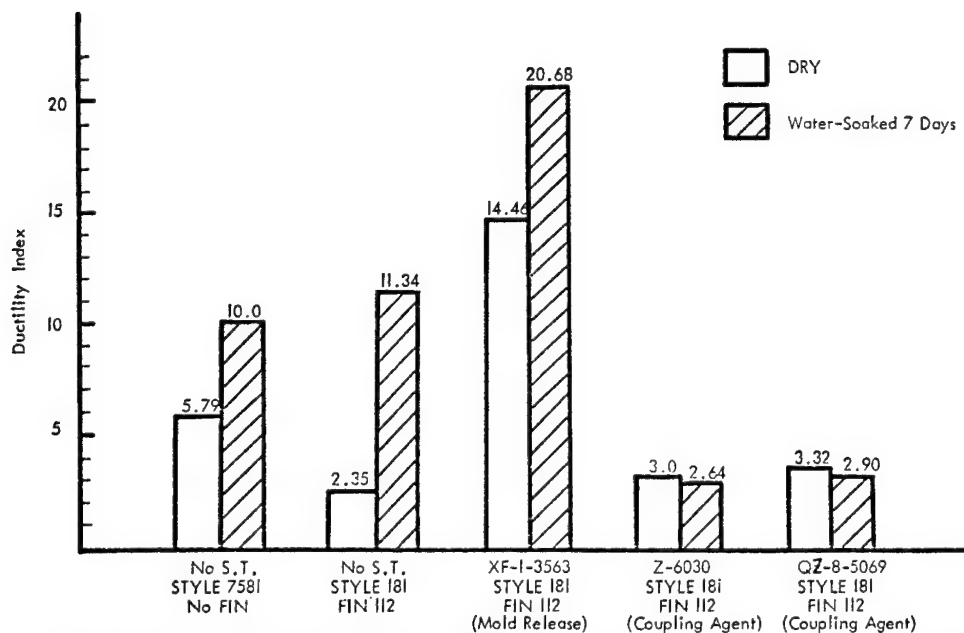
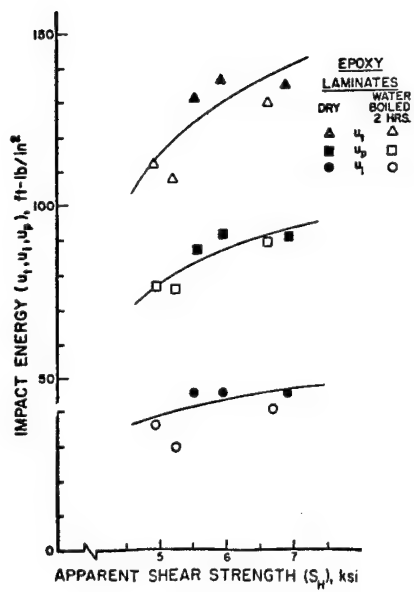
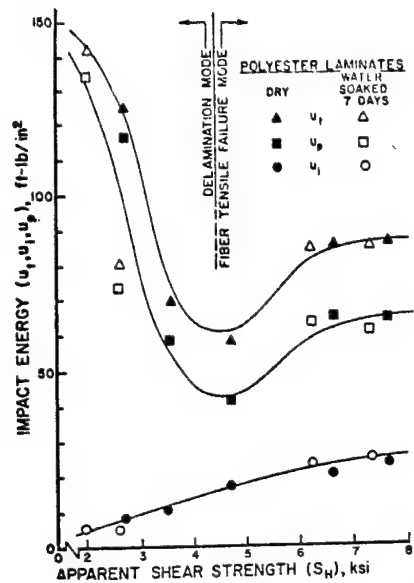
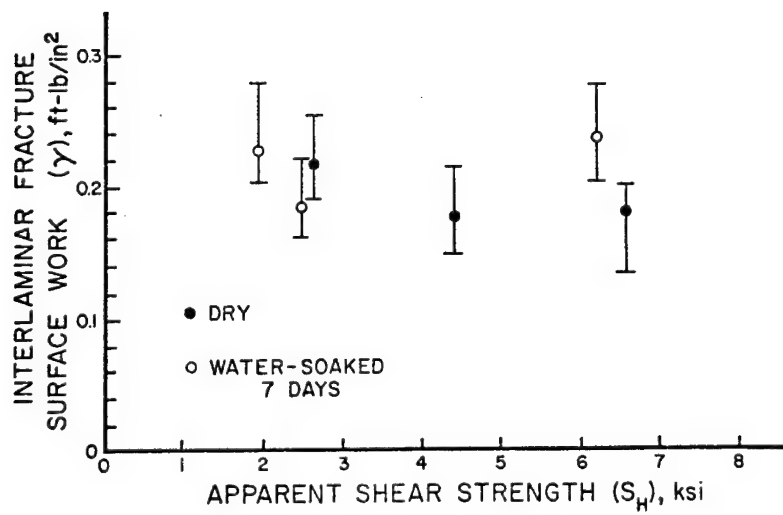
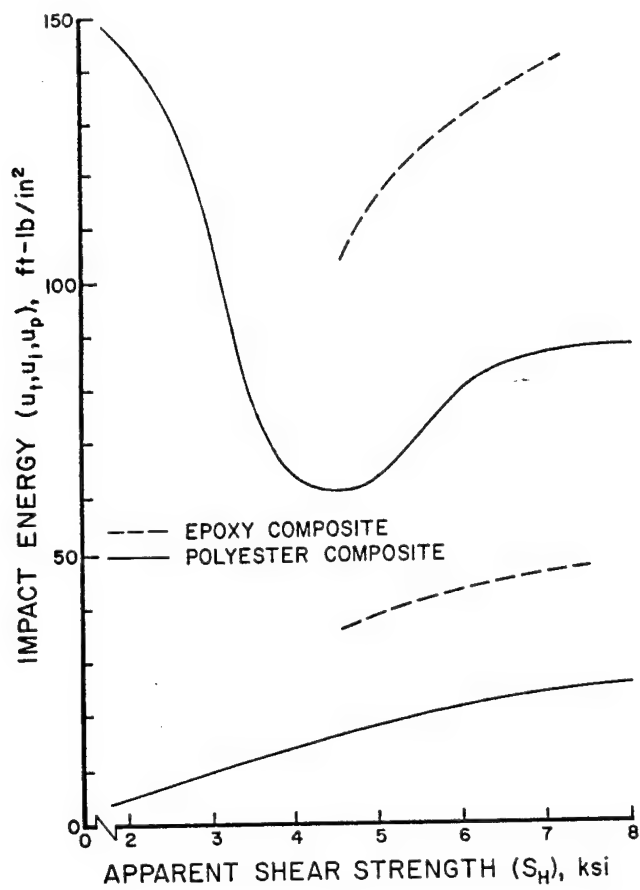


Figure 32. Effects of Environmental Degradation on the Ductility Index of Fiberglass-Polyester Laminates in Impact

79





MOISTURE SORPTION OF CARBON FIBERS

Measured Fiber Density (VVB 105-1/5) : $M_D = 1.57$

Theoretical Graphite Density : $M_T = 2.24$

Practical Fiber Density : $M_P = 1.76 - 1.78$ (Thorne 50 - Thorne 300)

$$\text{Practical Void Content, } v\% = \frac{M_P - M_D}{M_P} = 11.3\%$$

$$\text{Theoretical Void Content, } v\% = \frac{M_T - M_D}{M_T} = 29.9\%$$

$$\left(\frac{\Delta W}{W}\right)_f = \frac{v \times \rho_{\text{water}}}{M_D}$$

$$\text{Practical : } \frac{\Delta W}{W} = \frac{11.3}{1.57} = 7.2\%$$

$$\text{Theoretical : } \frac{\Delta W}{W} = \frac{29.9}{1.57} = 19.0\%$$

CALCULATED VALUE OF COMPOSITE MOISTURE SORPTION

$$\left(\frac{\Delta W}{W}\right)_{\text{max}} = AR + \left(\frac{v \times \rho}{M_d}\right)_{\text{comp}} + \left(\frac{v \times \rho}{M_D}\right)_{\text{fiber}} (1 - R)$$

$$\begin{aligned} \left(\frac{\Delta W}{W}\right)_{\text{max}} &= 4.2 \times 0.46 + \frac{4.3 \times 1}{1.32} + \frac{29.9}{1.57} \times 0.54 \\ &= 1.93 + 3.26 + 10.3 = 15.5\% \end{aligned}$$

RESULTS OF DTA TESTS

Material	Exposure Conditions for 11 years	Test Conditions	T _g (°C)	Moisture Desorption Peak
Epoxy	-	Dry	151	-
Epoxy	-	Water at 60°C to equilibrium	142	153 - 158
Carbon-epoxy	Dry	Dry	140	-
Carbon-epoxy	Sea Water	Dried at 60°C	128	-
Carbon-epoxy	Distilled Water	Wet	115	152 - 156
Graphite-epoxy	Dry	Dry	134	-
Graphite-epoxy	Distilled Water	Wet	133	172 - 177



A



B

Interlaminar Shear Surfaces for (A) Carbon Fiber and (B) Graphite Fiber Specimens Stored in Sea Water for 11 Years (2000X)

Table 7. Diffusion Coefficients* of Carbon-Epoxy Reexposed to Humid Environments After 11 Years
Environmental History $[10^{-10} \text{ cm}^2/\text{sec}]$

Material Designation	11 Years History	Re-exposure Conditions					
		Distilled Water, 60°C			98% R.H., 60°C		
		D_M	D_C	$\frac{D_M - D_C}{D_C} \times 100$	D_M	D_C	$\frac{D_M - D_C}{D_C} \times 100$
CD	Dry	89.04	90.06	-1.13%	88.24	87.4%	+0.89%
CW _D	Distilled water	114.81	84.55	+35.79%	125.99	82.11	+53.44%
CW _S	Sea water	122.36	84.55	+44.72%	133.17	82.11	+62.18%

* D_M - measured coefficient

D_C - calculated coefficient, equation (5)

Table 8. Diffusion Coefficients of Carbon-Epoxy Laminates

Fiber/Resin	Orientation	Environmental	D [10^{-10} cm ² /sec]	References
		Conditions		
T300/5208	0 ₂ /± 45	R. H. 60°C	32	(2)
T300/5208	0 ₂ /± 45	80% R. H., 60°C	9	(3)
T300/1031	0 ₂ /± 45	80% R. H., 60°C	83.4	(3)
HMS/1034	0 ₂ /± 45	80% R. H., 60°C	93.5	(3)
T300/1034	± 45; 0	water, 60°C	11.3	(1)

Table 9. Interlaminar Shear Strength of Carbon-Epoxy Composites Exposed for 11 Years to Environmental Conditions ($\times 10^3$ psi)

Reference ¹ Value	Test Mode	Environmental History		
		Dry	Distilled Water	Sea Water
10.2 ± .1	Current ²	9.48 ± .10	6.21 ± .20	7.04 ± .05
	Partial drying ³	9.58 ± .20	6.31 ± .20	7.63 ± .10
	Residual ⁴	9.81 ± .10	7.24 ± .10	7.83 ± .10

¹Tested by Union Carbide in 1965²Tested in 1970, "immediately" after removing the specimens from the environmental conditions³Tested after a drying period of 10 days, at 60°C under vacuum. The water content in each case is shown in Figures 1-5.⁴Tested after complete drying.Table 11. Interlaminar Shear Strength of Graphite-Epoxy Specimens Exposed for 11 Years to Environmental Conditions ($\times 10^3$ psi)

Reference* Value	Test Mode*	Environmental History		
		Dry	Distilled Water	Sea Water
3.3 ± .1	Current	2.59 ± .20	3.68 ± .05	3.60 ± .10
	Residual	2.61 ± .05	3.34 ± .05	3.27 ± .05

* See notes in Table 9.

Table 12. Flexural Strength of Carbon and Graphite Epoxy Composites
[10³ psi]

Specimen	"Dry" History	Distilled Water History	Sea Water History
<u>Carbon</u>			
Current 1	---	81.40	73.67
2	---	75.30	76.35
Average	---	78.35	75.01
Residual 1	83.74	84.90	75.65
2	80.60	78.56	77.23
Average	82.17	81.73	76.44
<u>Graphite</u>			
Current 1	---	66.98	62.49
2	---	68.83	64.51
Average	---	67.50	63.50
Residual 1	60.24	66.98	66.76
2	64.79	67.61	64.56
Average	62.51	67.30	65.65

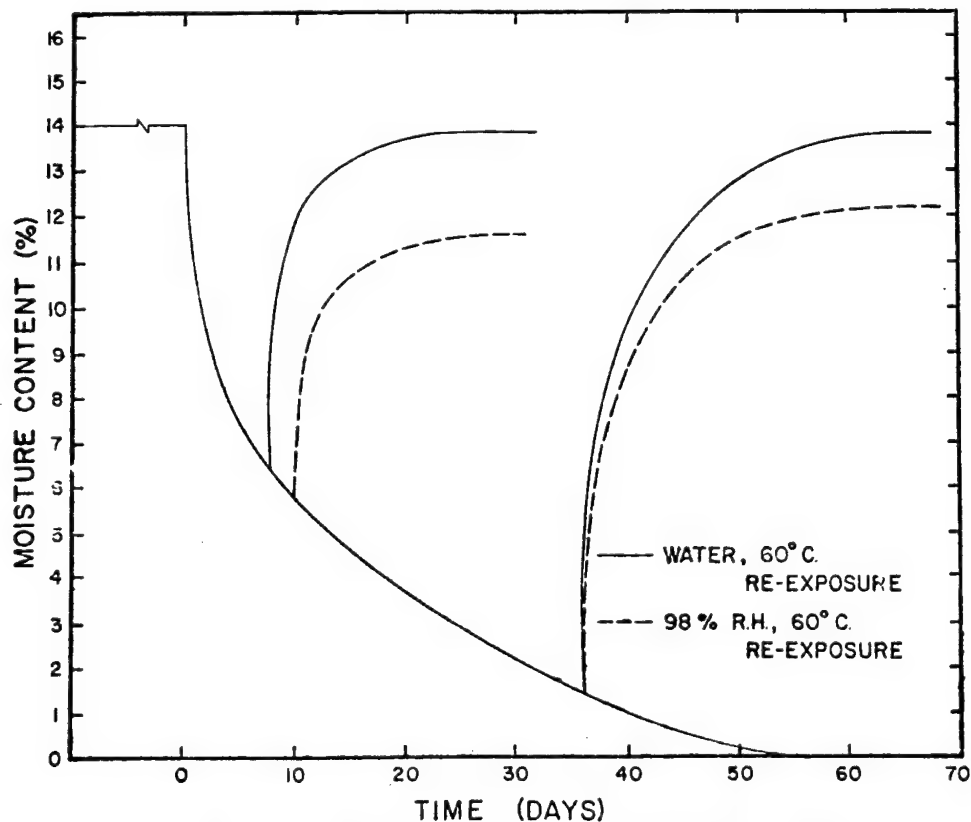


Figure 2. Moisture Desorption of Carbon Epoxy Specimens Exposed to 11 Years Sea Water, and Moisture Absorption Upon Reexposure to Humid Environment

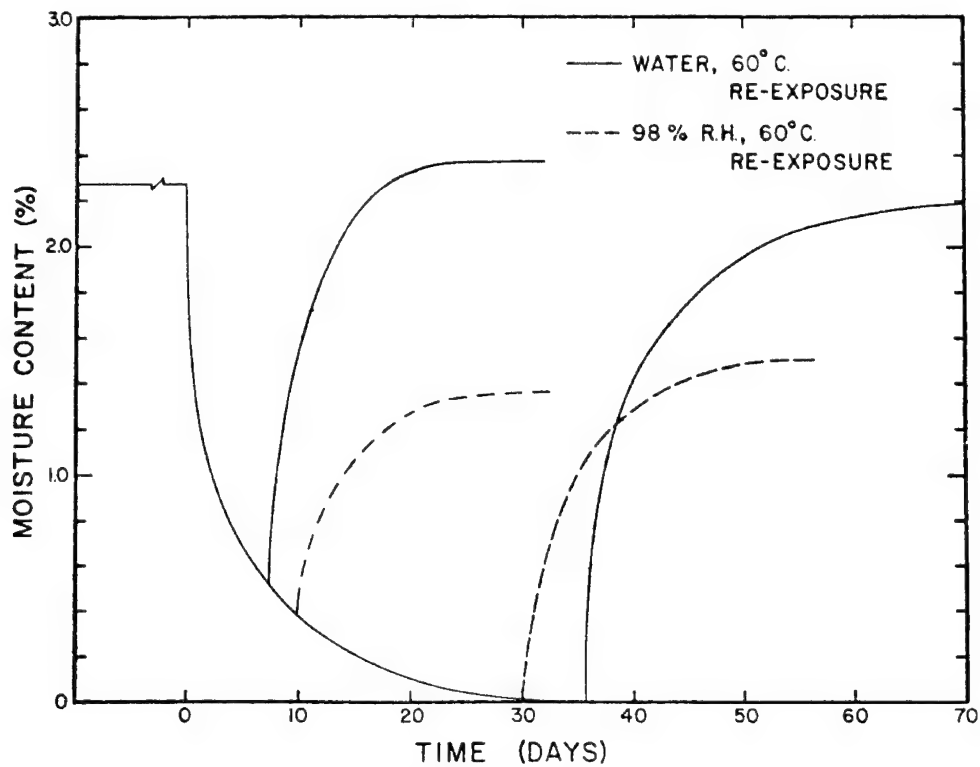


Figure 3. Moisture Desorption of Graphite Epoxy Specimens Exposed to 11 Years Distilled Water, and Moisture Absorption Upon Reexposure to Humid Environments

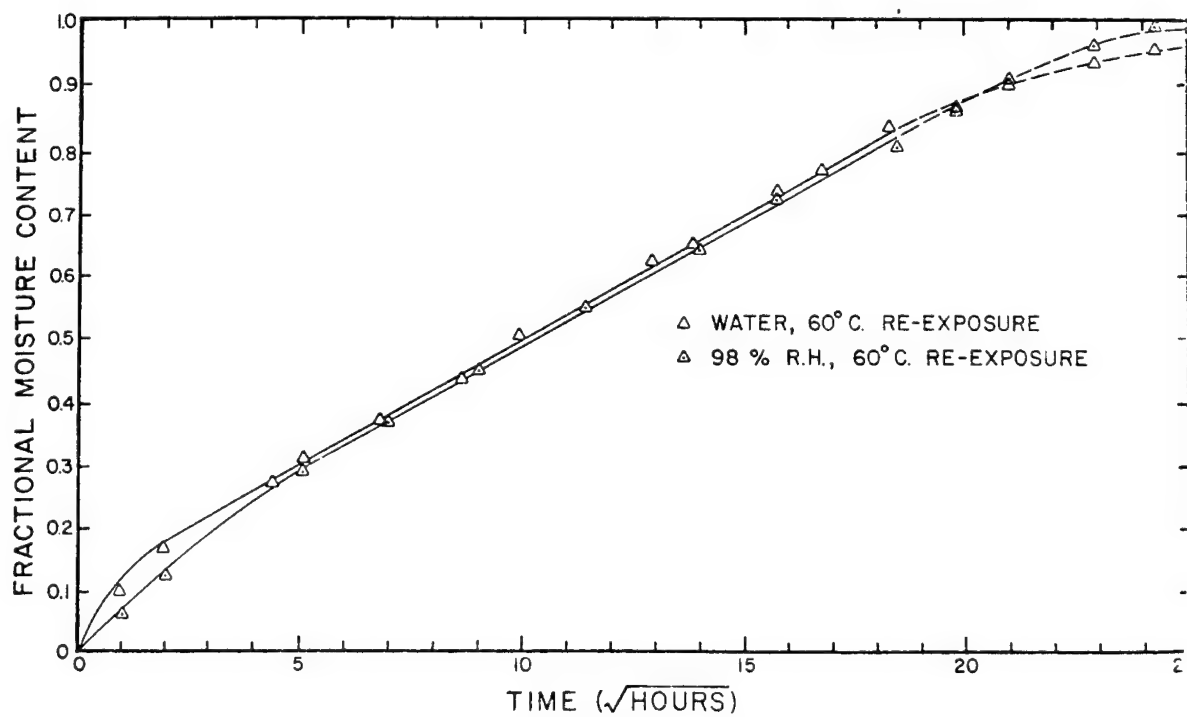


Figure 4. Fractional Weight Gain of Carbon-Epoxy Specimens Exposed to 11 Years of Dist. Environment Upon Reexposure to Humid Environments.

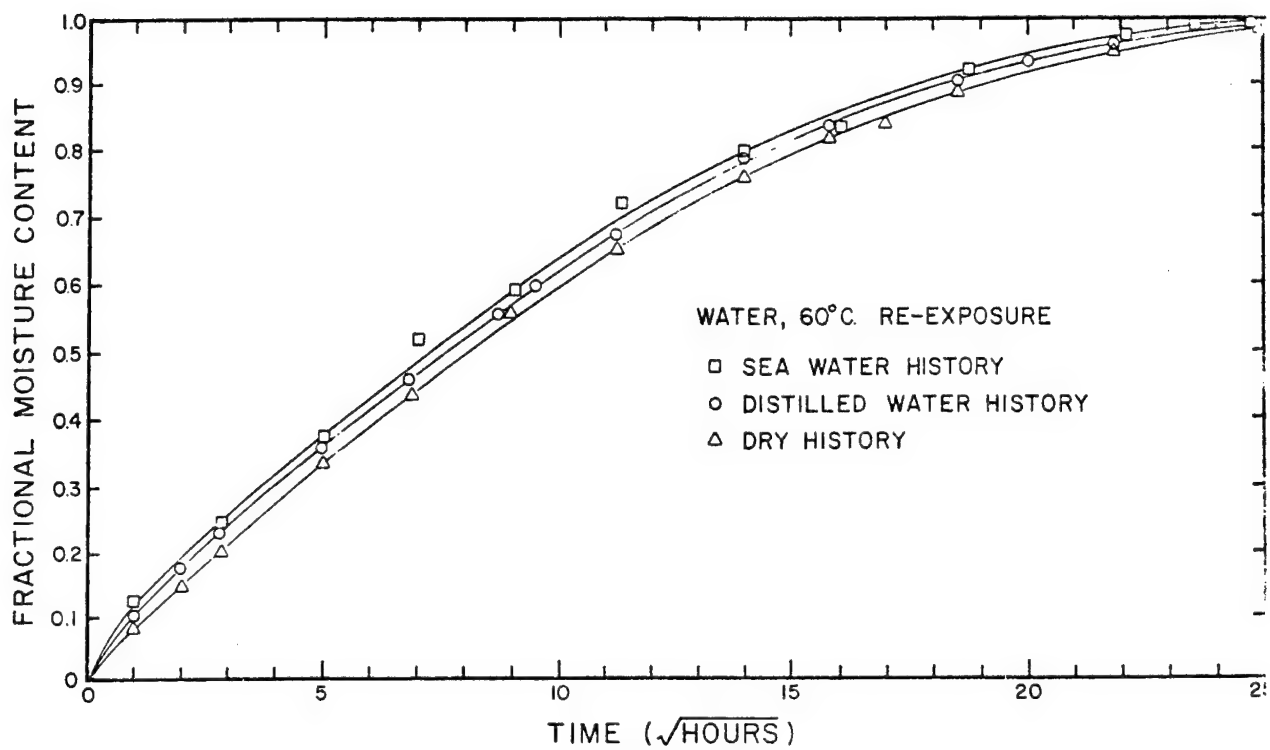


Figure 11. Fractional Weight Gain of GFRP-Epoxy Specimens Having Different Environmental Histories Upon Reexposure to Distilled Water

PRINCIPAL CONCLUSIONS

- 1. The Initiation Impact Energy (Unnotched Charpy Test) Increases with Increasing Values of Interlaminar Shear Strength for Glass-Epoxy and Glass-Polyester Laminates.**
- 2. It has been found that a critical value of interlaminar shear strength (ILSS) can be defined. Below this value the impact propagation energy increases with decreasing ILSS. Above this value, the propagation energy increases with increasing ILSS. Epoxy-glass laminates are always above this critical value of ILSS while polyester laminates can be either above or below depending upon the glass surface treatment. Carbon-epoxy laminates will also always be above this critical value.**
- 3. A study on the effects of 11 years of exposure to dry and wet (full immersion in sea water and distilled water) environments for filament wound carbon fiber reinforced epoxy NOL rings has shown:**
 - 3.1 The 11 years immersion in wet environments considerably affected the initial moisture weight gain and the diffusion coefficients upon reexposure to humid environments.**
 - 3.2 A considerable shear strength reduction (current and residual) was found for carbon-epoxy specimens having 11 years of humid exposure.**
 - 3.3 The shear strength degradation has been qualitatively correlated and interpreted with the moisture absorption characteristics.**
 - 3.4 No irreversible damage in the fiber properties was observed as concluded from flexural strength results.**
 - 3.5 The shear strength of graphite-epoxy specimens exposed to humid conditions was greater than the shear strength of dry specimens.**
- 4. In the case of Thorne 300-epoxy composites the following can be concluded:**
 - 4.1 The equilibrium content for complete immersion in water is greater than for 98% relative humidity.**
 - 4.2 The quality of the exposed surface has an influence on moisture diffusion rate.**
 - 4.3 The exposure temperature has an effect on equilibrium moisture content.**
 - 4.4 The moisture diffusion coefficient parallel to the fiber axes is at least 3 times greater than the coefficient perpendicular to the fibers.**
 - 4.5 The initial moisture absorption for a unidirectional lamina subjected to a transverse tensile stress (50% of ultimate strength) was at least 2 times greater than for an unstressed specimen.**

DURABILITY OF FIBER
REINFORCED RESIN MATRIX COMPOSITES

JAMES M. WHITNEY
AIR FORCE MATERIALS LABORATORY
In-House Work Unit

DURABILITY OF COMPOSITES

OBJECTIVE: TO DEVELOP ANALYTICAL AND EXPERIMENTAL METHODOLOGY FOR PREDICTING FAILURE AND FATIGUE LIFE IN CONJUNCTION WITH ENVIRONMENTAL EFFECTS. CONSIDERABLE EMPHASIS IN THE NEAR TERM IS PLACED ON ENVIRONMENTAL EFFECTS.

APPROACH: ANALYTICAL MODELS BASED ON THEORETICAL CONSIDERATIONS AND EXPERIMENTAL OBSERVATIONS. INTERDISCIPLINARY APPROACH BETWEEN MECHANICS AND MATERIALS SCIENCE. EMPHASIS ALSO PLACED ON DEVELOPING HIGH QUALITY EXPERIMENTAL METHODS AND PROCEDURES.

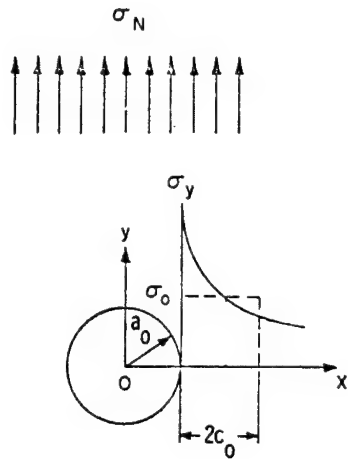
DURABILITY OF COMPOSITES

CURRENT ACTIVITIES

- I. FAILURE AND FATIGUE
 - A. STRESS CONCENTRATIONS
 - B. FATIGUE OF UNIDIRECTIONAL COMPOSITES
- II. ENVIRONMENTAL EFFECTS
 - A. DIFFUSION STUDIES FOR ACCELERATED TESTING, INCLUDING THERMAL SPIKE EFFECTS
 - B. EXPANSIONAL STRAINS IN COMPOSITE LAMINATES
 - C. EFFECT ON MECHANICAL PROPERTIES OF UNIDIRECTIONAL AND LAMINATED COMPOSITES
 - D. EFFECT ON COMPRESSION LOADING
 - E. EFFECT ON NOTCH STRENGTH

TOPICS OF DISCUSSION

- I. STRESS CONCENTRATIONS - ANGLE CRACKS
- II. DIFFUSION STUDIES FOR ACCELERATED TESTING, INCLUDING THERMAL SPIKE EFFECTS
- III. EXPANSIONAL STRAINS IN COMPOSITE LAMINATES
- IV. EFFECT OF ENVIRONMENT ON MECHANICAL PROPERTIES OF UNIDIRECTIONAL AND LAMINATED COMPOSITES



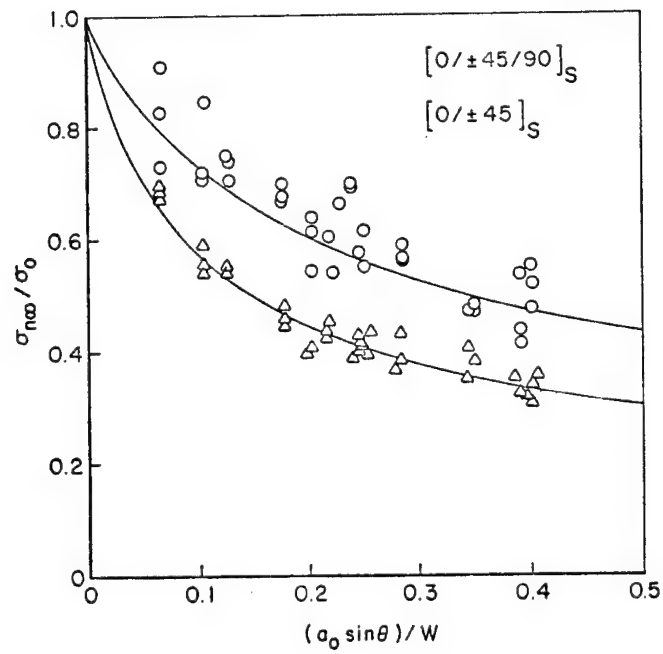
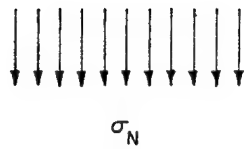
AVERAGE STRESS CRITERION

$$\frac{1}{2c_0} \int_{a_0}^{a_0+2c_0} \sigma_y(x, 0) dx = \sigma_0$$

FOR CENTER CRACK

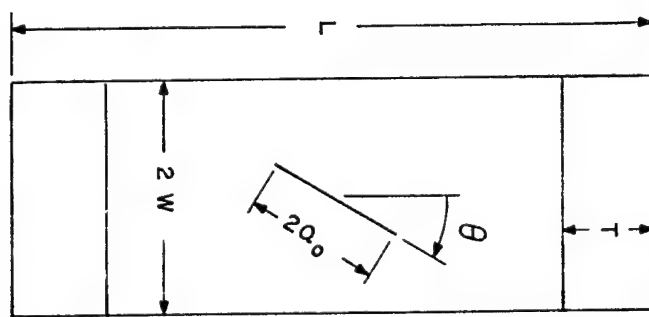
$$\frac{\sigma_{n\infty}}{\sigma_0} = \sqrt{\frac{c_0}{a_0+c_0}}$$

$$K_Q = \sigma_{n\infty} \sqrt{\pi(a_0+c_0)}$$

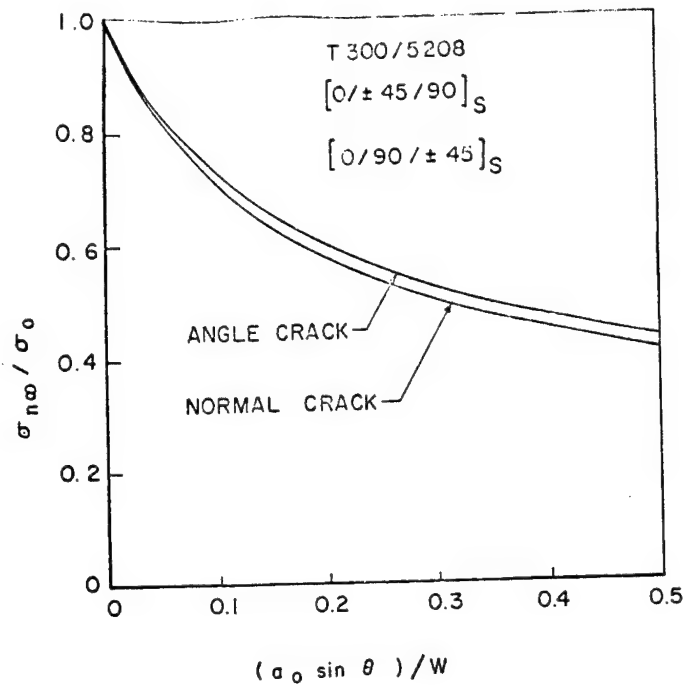


Theory versus experiment - average stress criterion.

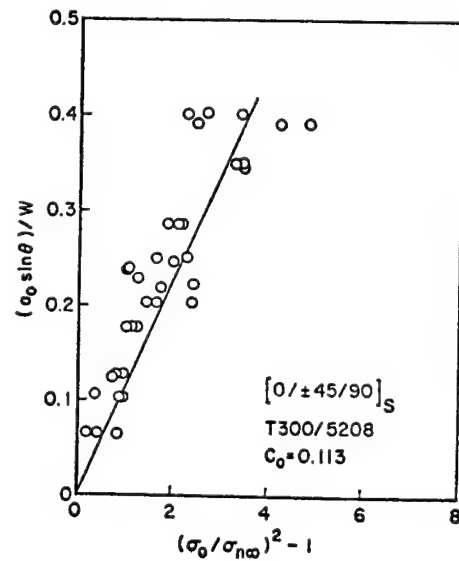
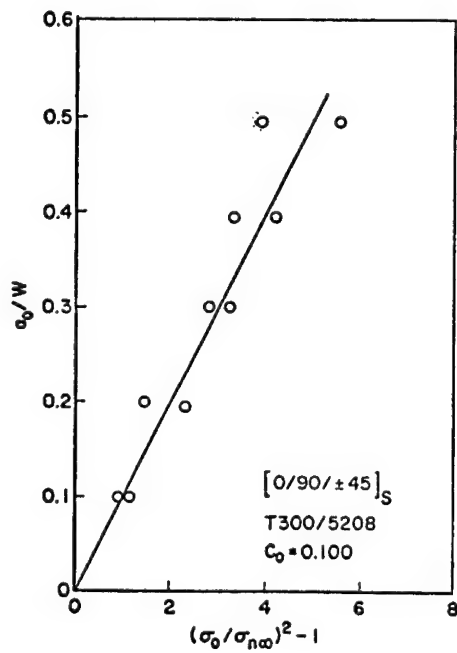
I. STRESS CONCENTRATIONS - ANGLE CRACKS



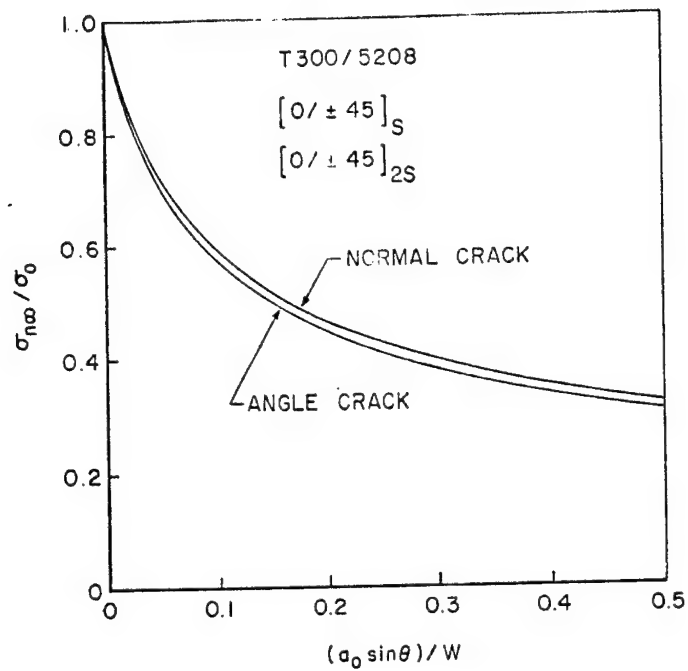
Angle crack specimen, $W = 1"$, $a_0 = 0.25"$, $0.4"$, $\theta = 15^\circ, 30^\circ, 45^\circ, 60^\circ, 75^\circ, 90^\circ$,
T300 / 5208.



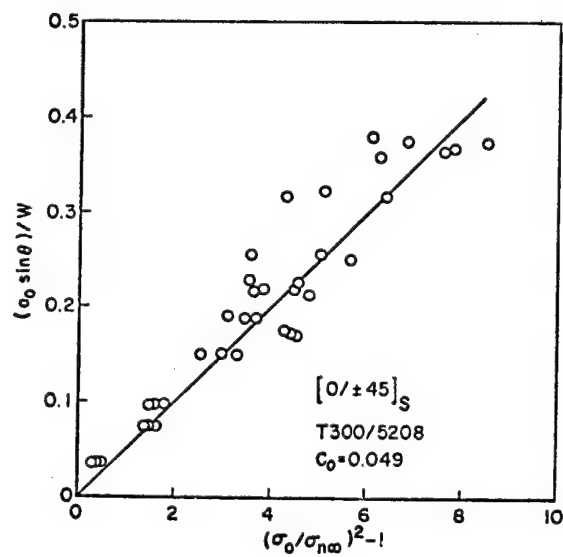
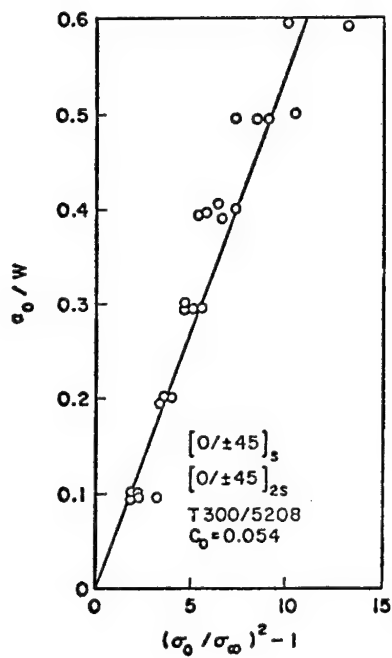
Comparison of angle crack to normal crack, average stress criterion.



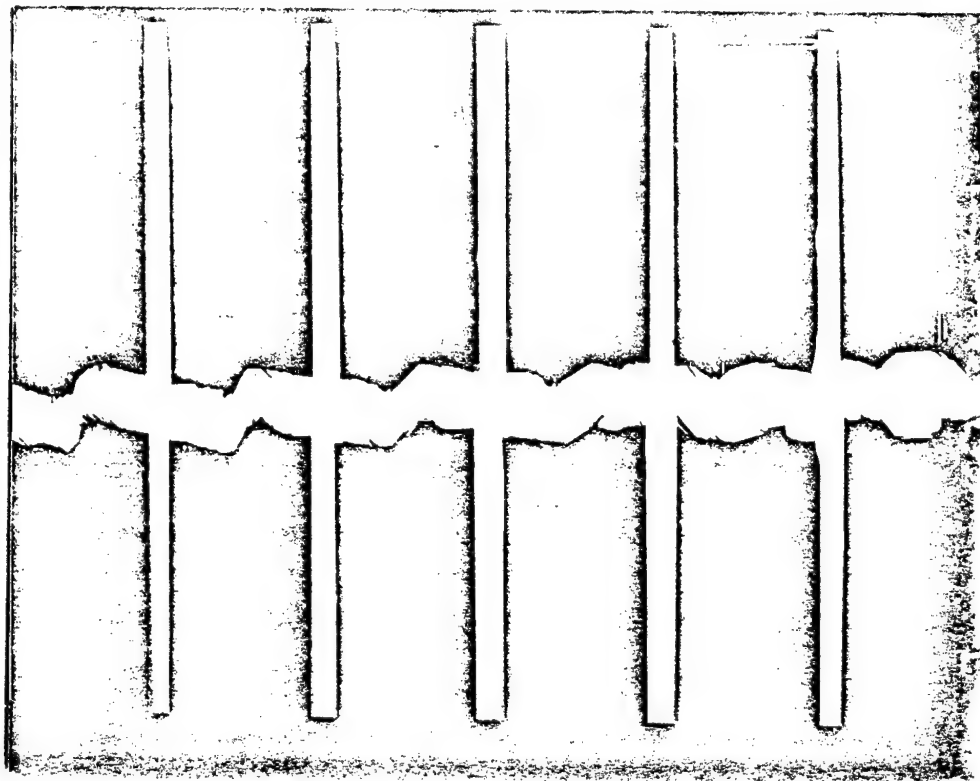
Least squares fit for c_0



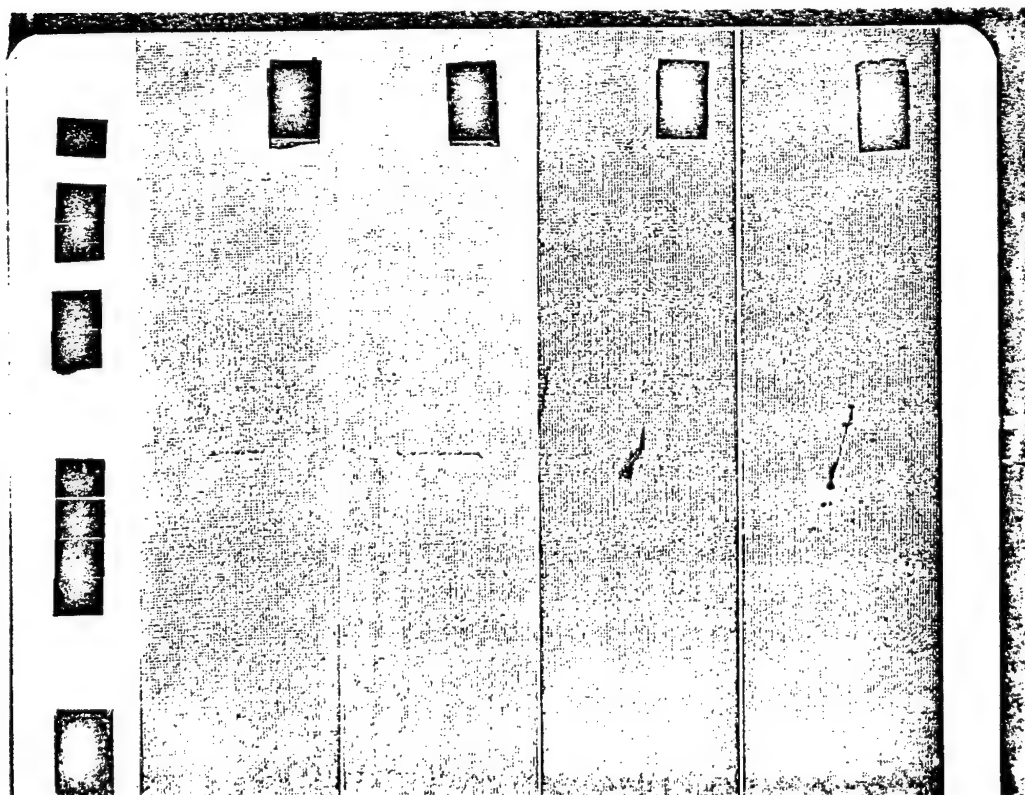
Comparison of angle crack to normal crack, average stress criterion.



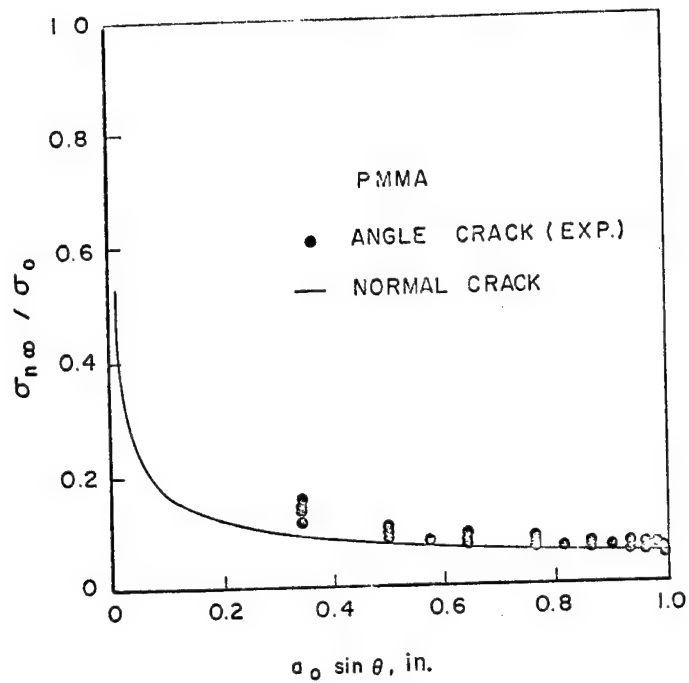
Least squares fit for c_0



Failure Modes



X-Ray photographs at 95% of average ultimate for notched specimens.



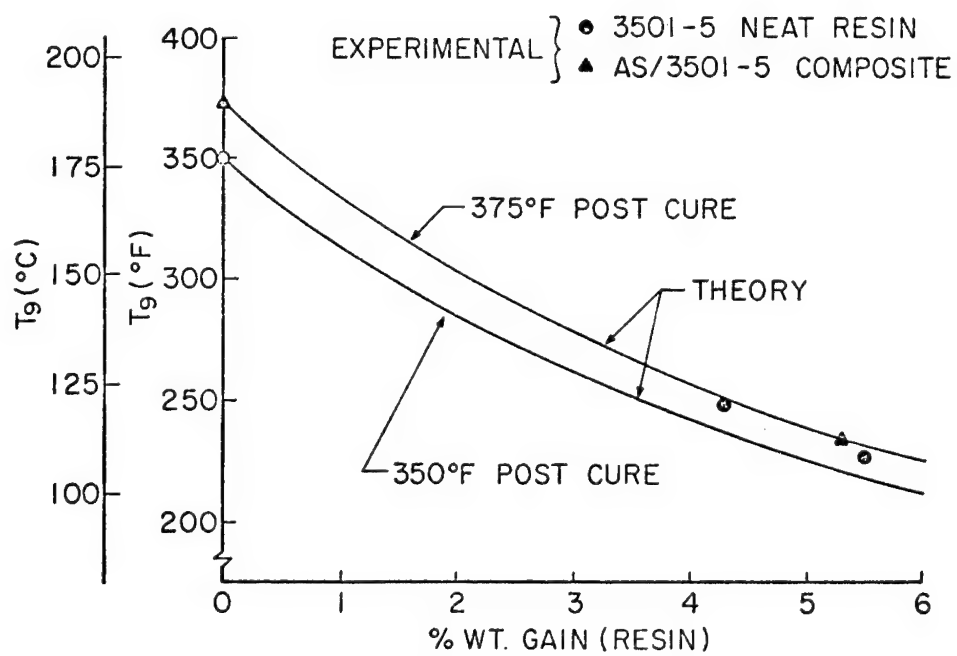
Angle crack compared to normal crack for plexiglass.

STRESS - CONCENTRATIONS - ANGLE CRACKS

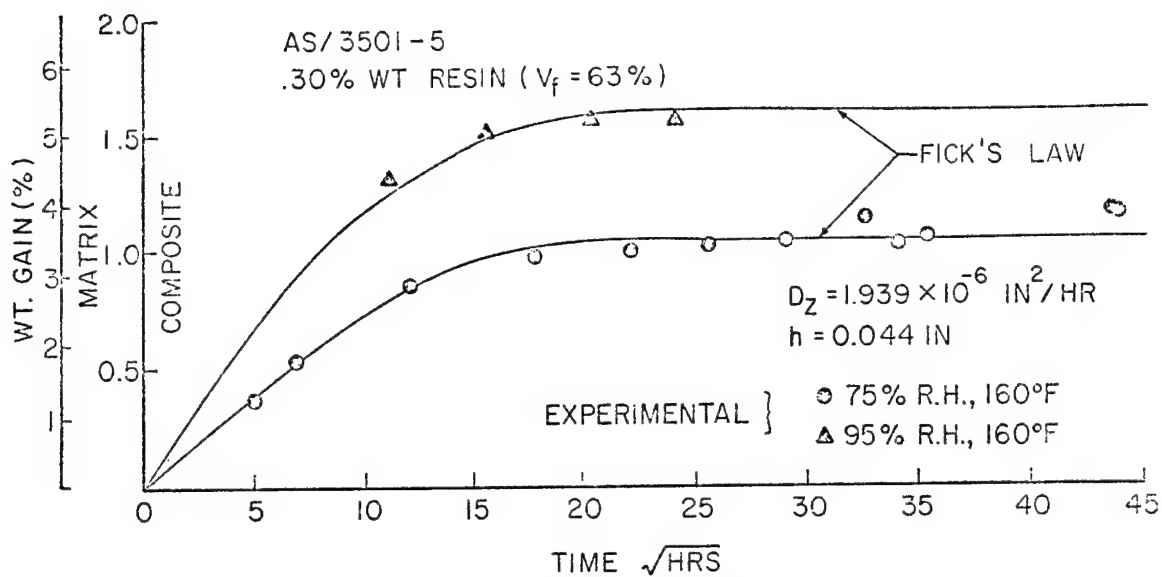
CONCLUSION

AN ANGLE CRACK IN A LAMINATED COMPOSITE CAN BE TREATED AS AN EQUIVALENT NORMAL CRACK HAVING A LENGTH EQUAL TO THE PROJECTION OF THE ANGLE CRACK ON TO THE NORMAL DIRECTION.

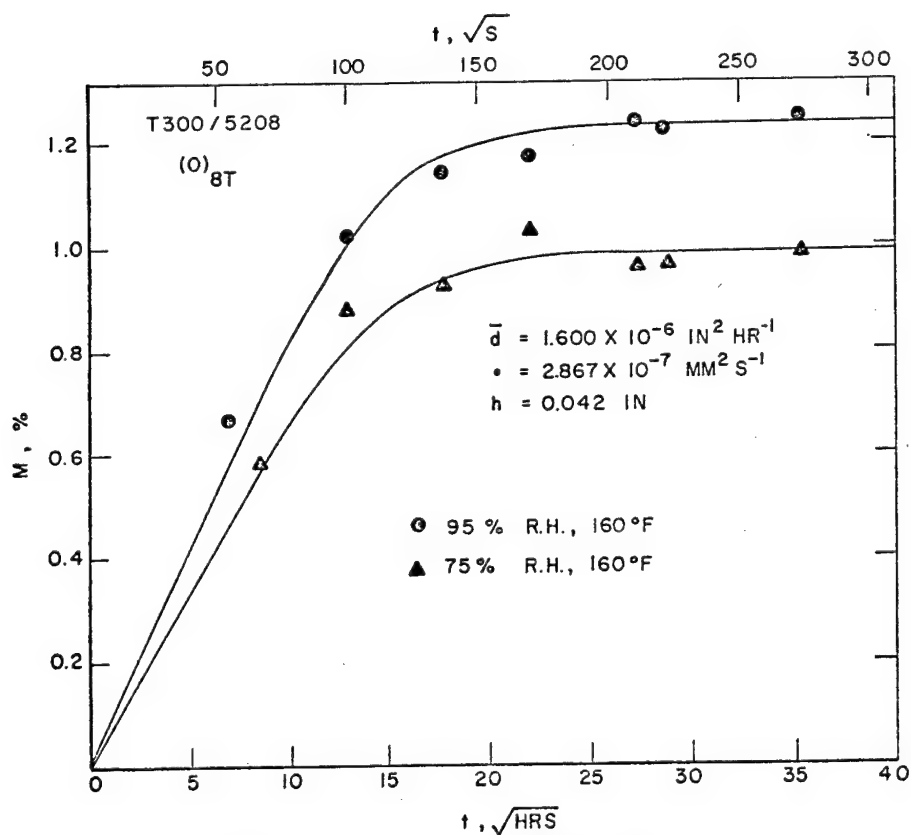
II. DIFFUSION STUDIES FOR ACCELERATED TESTING



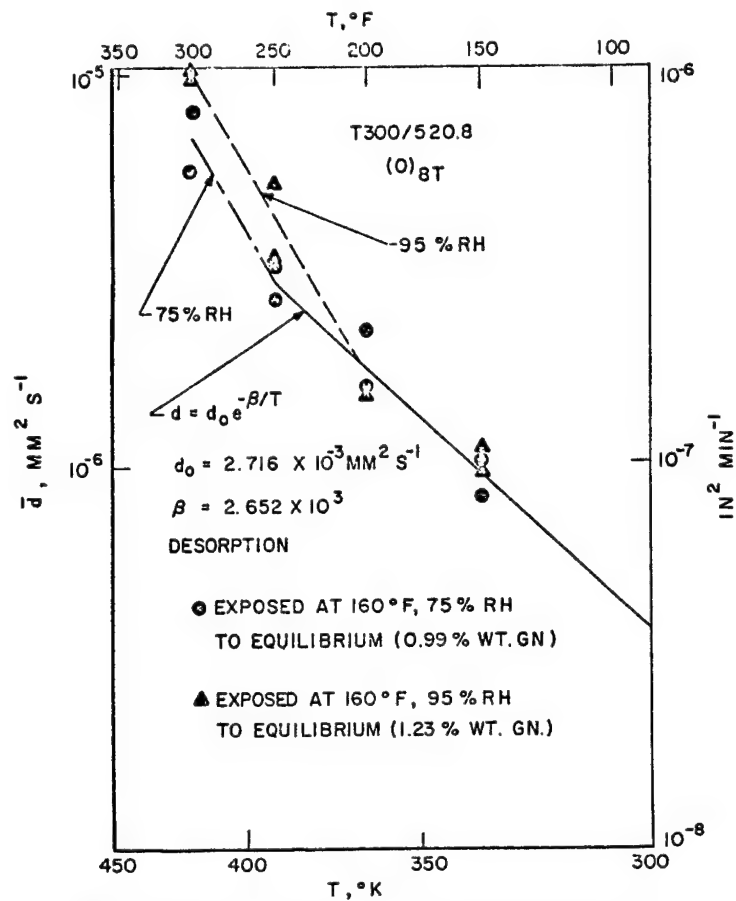
Kelley-Bueche Theory for glass temperature as a function of moisture content.



Fick's Law for total weight gain, AS / 3501-5.



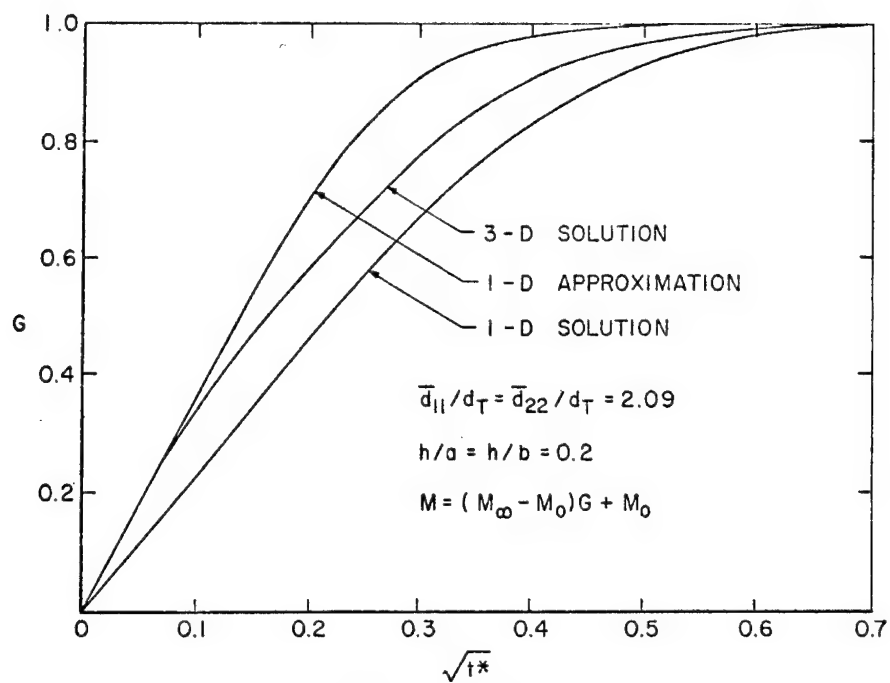
Fick's Law for total weight gain, T300 / 5208.



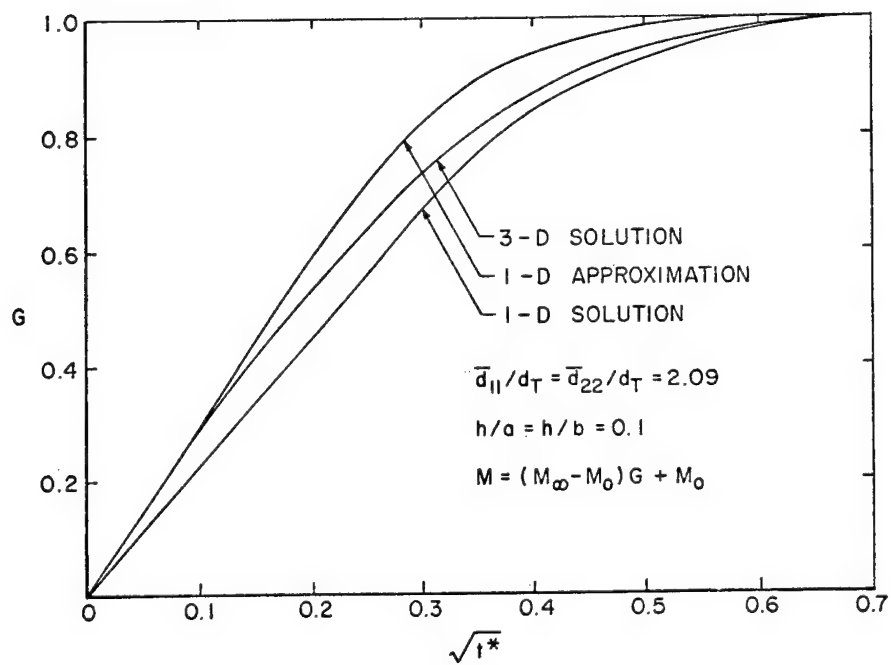
Diffusion coefficient for desorption as a function of temperature.

T300 / 5208

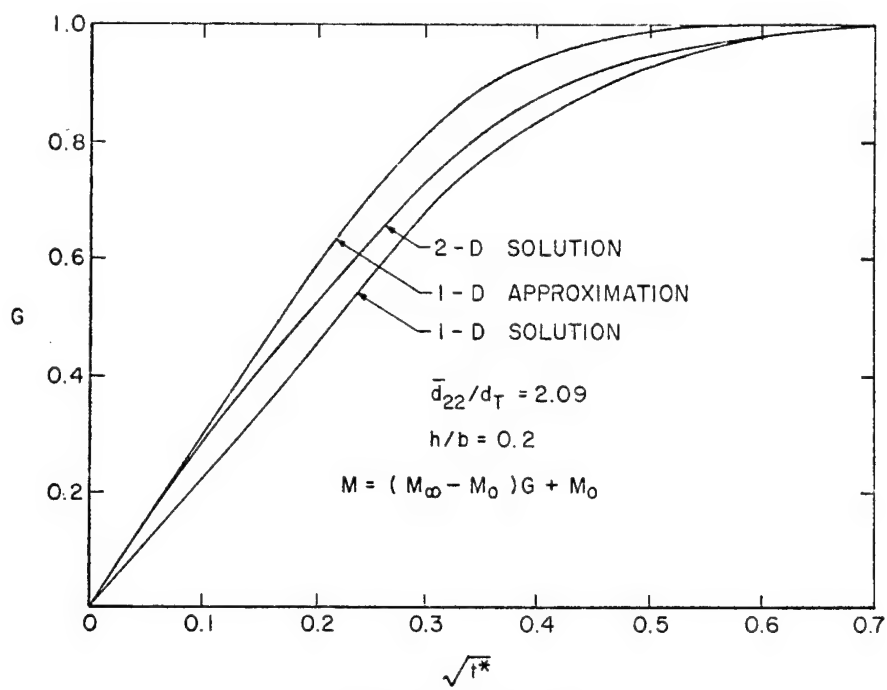
60 DAYS IN WATER		90 DAYS IN WATER	
T, °F	M, %	T, °F	M, %
120	1.55	120	1.73
160	1.90	160	2.06
180	2.23	180	2.36



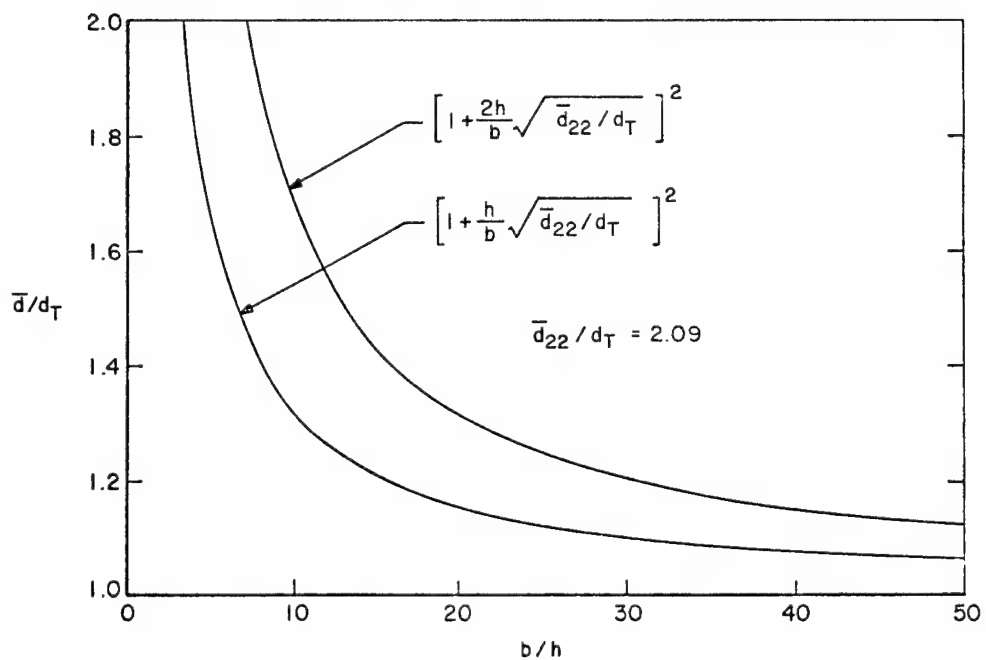
Fick's Law for 3-dimensions.



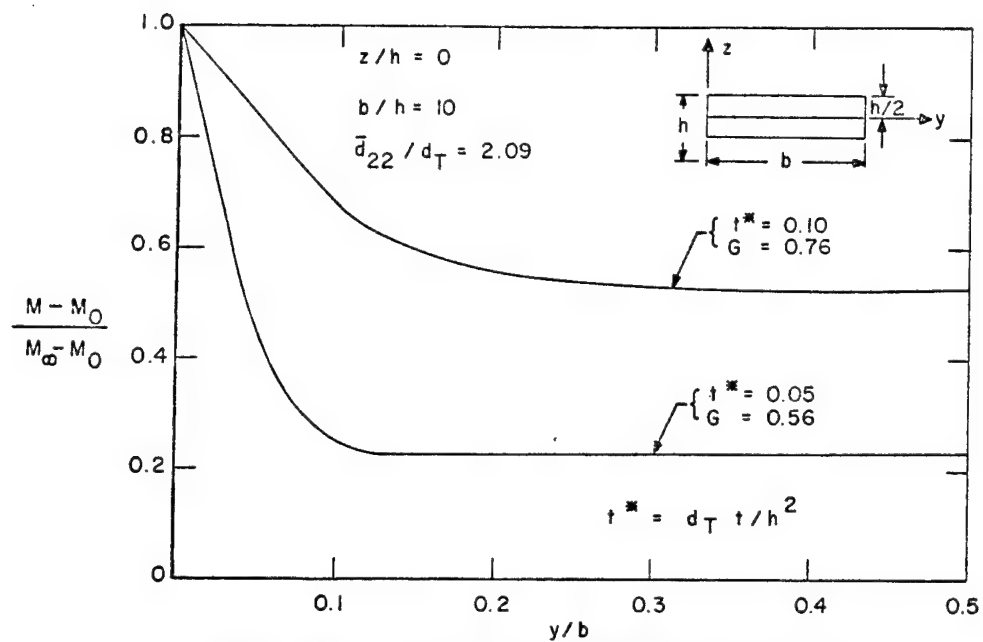
Fick's Law for 3-dimensions.



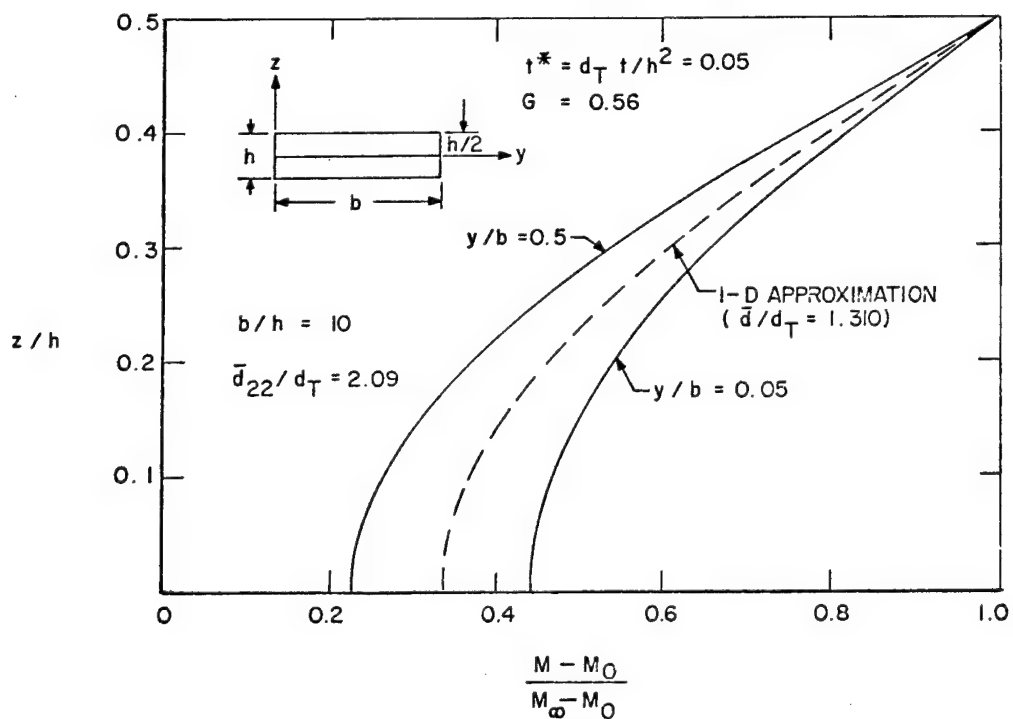
Fick's Law for 2-dimensions.



Edge adjustment factors for one-dimensional diffusion in laminates with quasi-isotropic expansional properties.

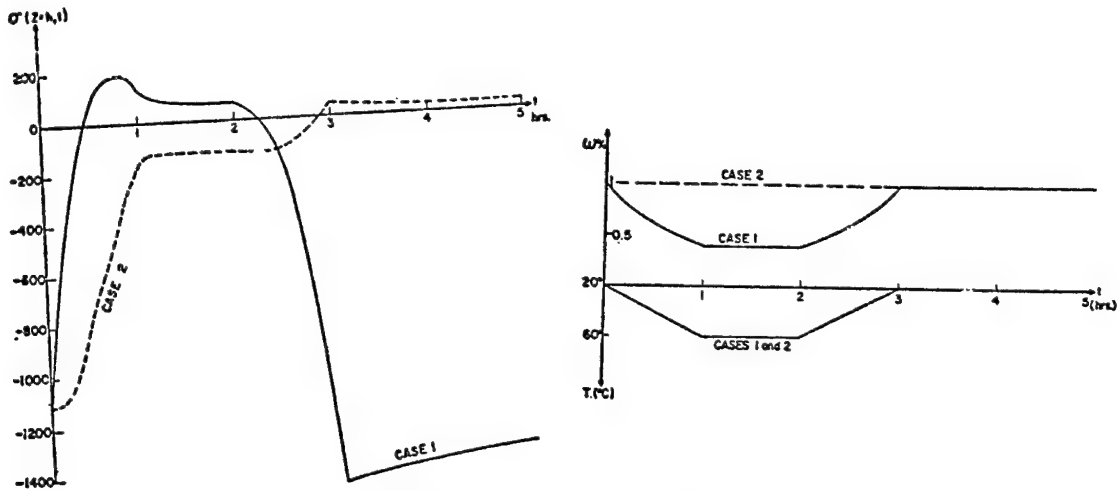


Moisture gradient along centerline of laminate with quasi-isotropic expansional properties.

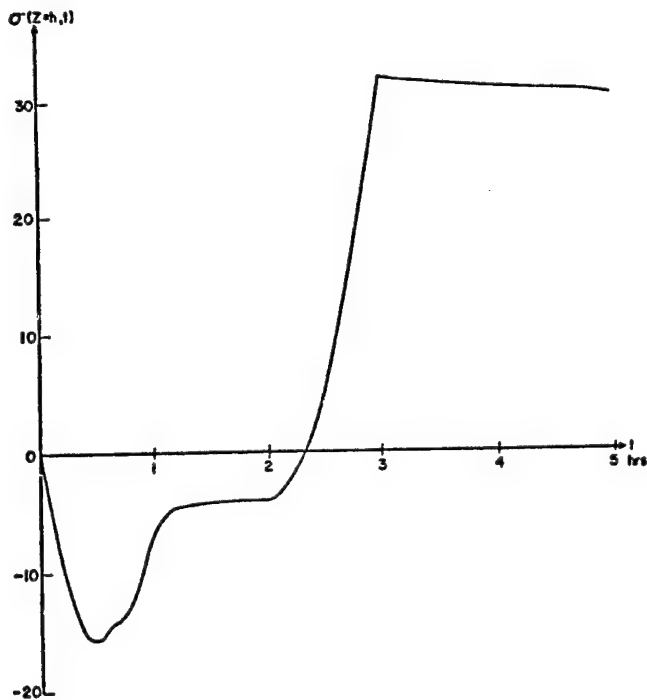


Moisture gradient through the thickness for laminate with quasi-isotropic expansional properties.

TIME - DEPENDENT RESPONSE OF A RESIN - SLAB SUBJECTED TO A THERMAL SPIKE



The stress response at the boundary, $(z=h,t)$ for a 'Thermal-Spike' and the Ensuing Fluctuation in Moisture (case 1) and for the Same Thermal Spike with a Fixed Level of Moisture (case 2), vs. time.



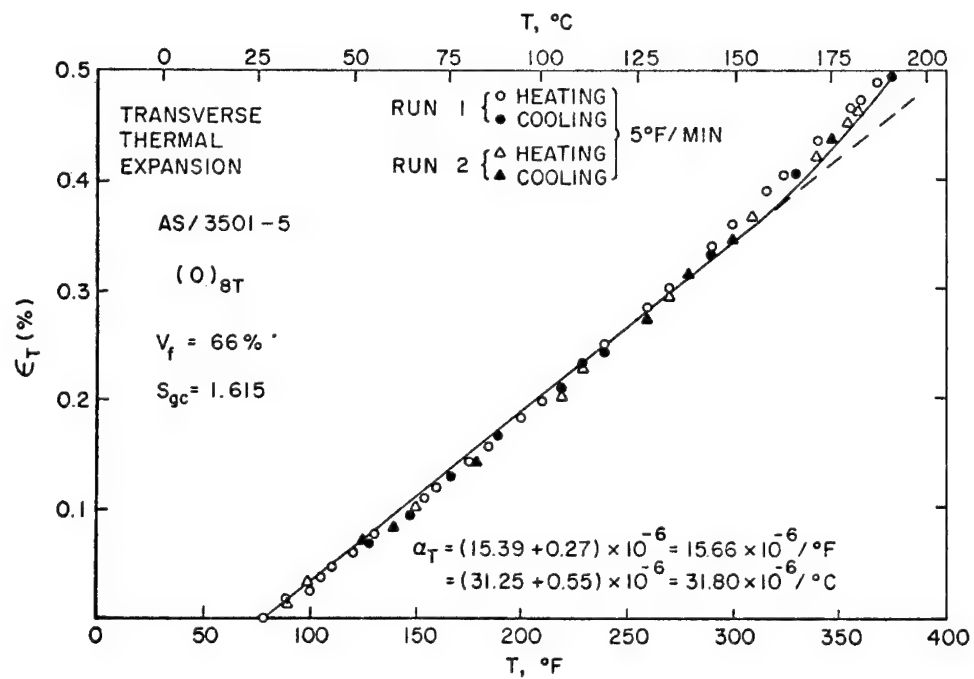
The Stress-Response at the Boundary, $\sigma(z=h,t)$, Due to the 'Thermal Spike' and with $w=0$ for all Times.

DIFFUSION STUDIES FOR ACCELERATED TESTING

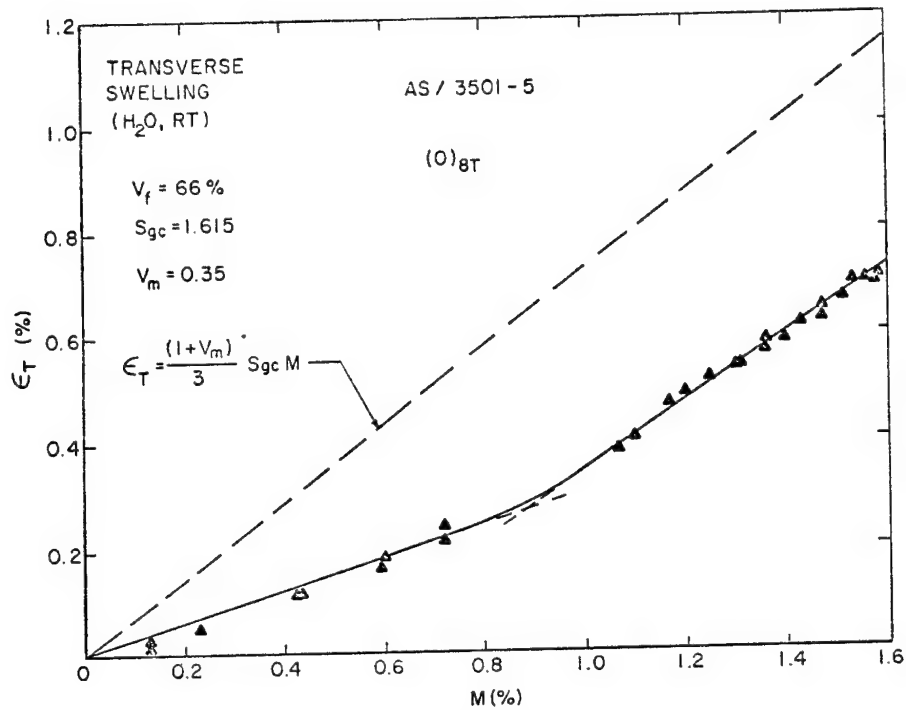
CONCLUSIONS

1. MOISTURE LOWERS THE GLASS TRANSITION TEMPERATURE OF EPOXY RESINS. THIS ABSORPTION APPARENTLY DOES NOT LEAD TO ANY SIGNIFICANT CHEMICAL DEGRADATION, ALTHOUGH MECHANICAL DAMAGE CAN OCCUR IN THE FORM OF CRAZING OR CRACKING.
2. FICK'S LAW ADEQUATELY PREDICTS TOTAL MOISTURE GAIN IN RESINS AND COMPOSITES.
3. TWO AND THREE DIMENSIONAL DIFFUSION CAN BE ESTIMATED BY USING A MODIFIED ONE DIMENSIONAL APPROXIMATION FOR A WIDE RANGE OF LAMINATE DIMENSIONS.
4. PRESENT DATA INDICATES THAT THE DIFFUSION PROCESS IN COMPOSITES CAN INDUCE MATRIX CRAZING. THUS IT IS IMPORTANT THAT ACCELERATED MOISTURE CONDITIONING TECHNIQUES ARE NOT USED WHICH ARE MORE SEVERE THAN REAL LIFE CONDITIONS.
5. PRESENT DATA INDICATES THAT THERMAL SPIKES ABOVE THE GLASS TRANSITION TEMPERATURE IN CONJUNCTION WITH RAPID COOL DOWN RATES CAN INDUCE MATRIX CRACKING.

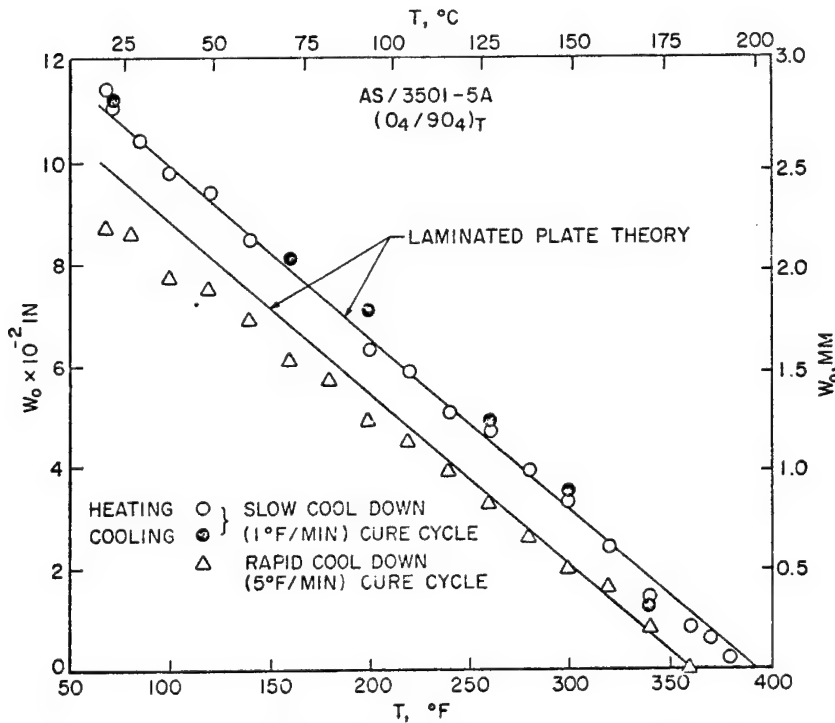
III. EXPANSIONAL STRAINS IN COMPOSITE LAMINATES



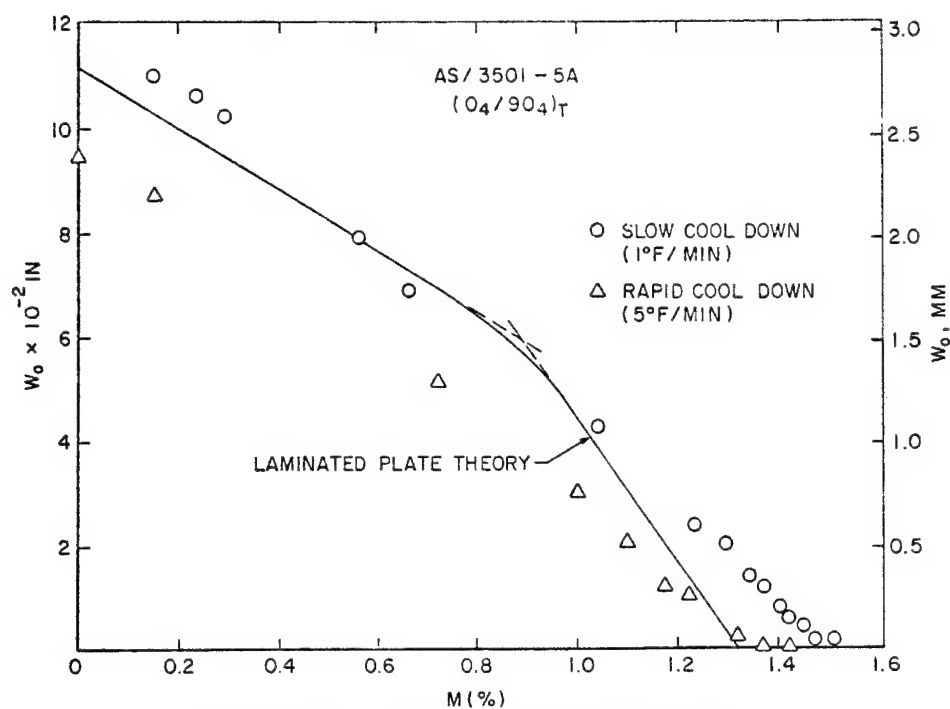
Transverse coefficient of thermal expansion.



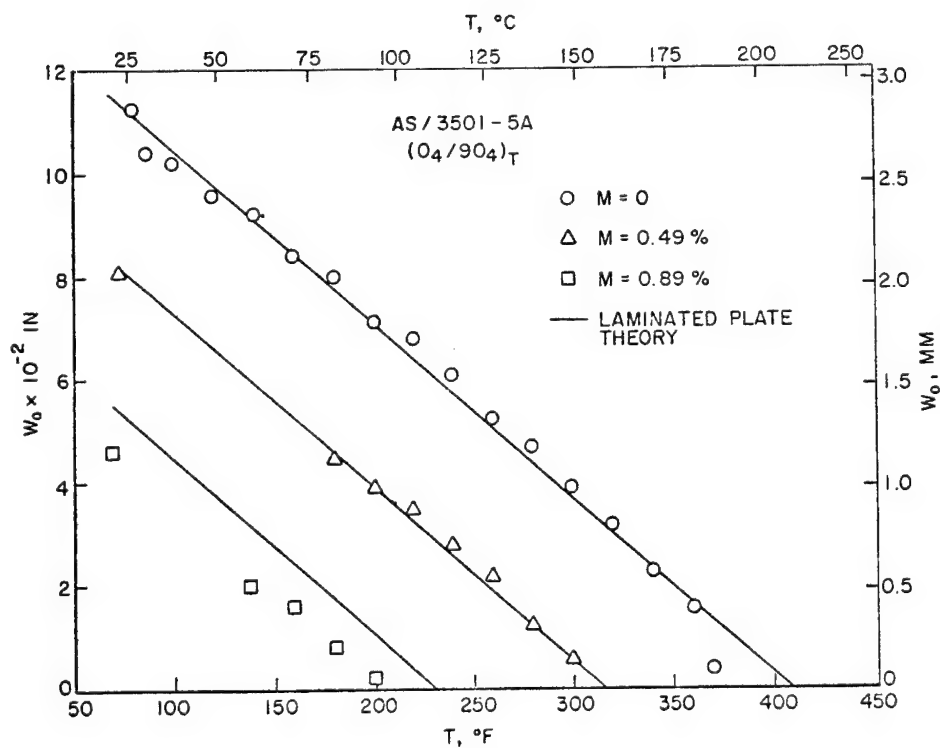
Transverse swelling strain as a function of moisture content.



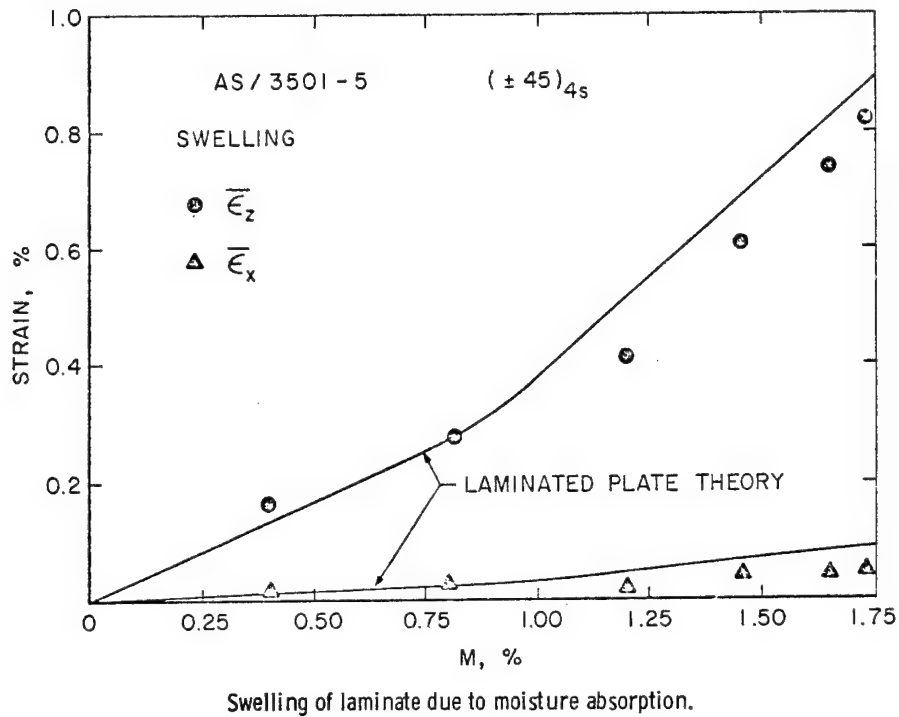
Warping of unsymmetric laminate due to curing temperature.



Effect of moisture on warping of an unsymmetric laminate.



Effect of temperature and moisture on the warping of an unsymmetric laminate.

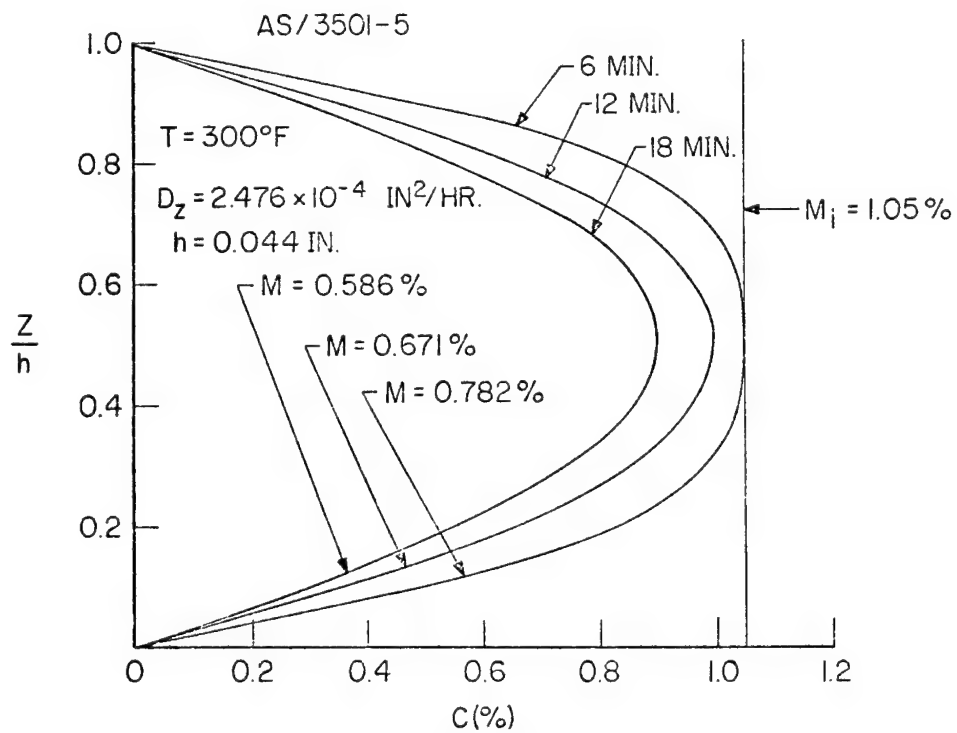


EXPANSIONAL STRAINS IN COMPOSITE LAMINATES

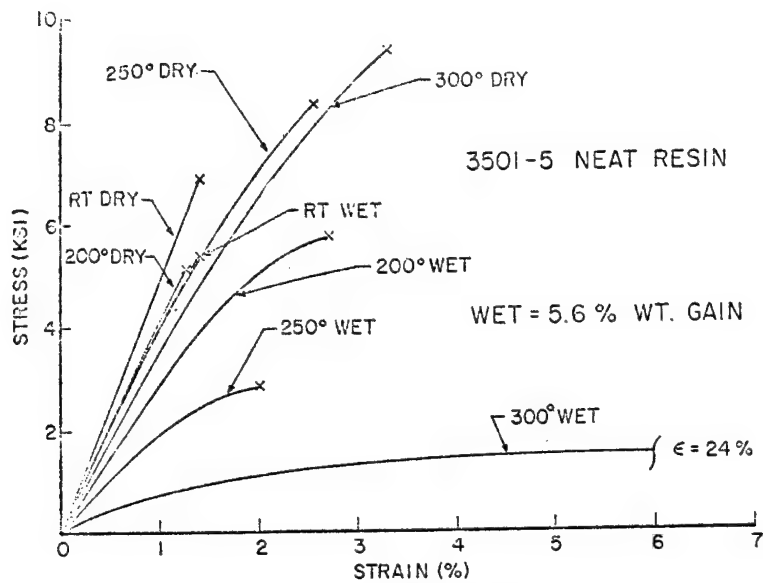
CONCLUSIONS

1. MOISTURE ABSORPTION CAN INDUCE SIGNIFICANT DIMENSIONAL CHANGES IN GRAPHITE / EPOXY COMPOSITES.
2. CURRENT DATA INDICATES THAT DIMENSIONAL CHANGES INDUCED IN COMPOSITE LAMINATES BY TEMPERATURE AND MOISTURE CAN BE PREDICTED BY CLASSICAL LAMINATED PLATE THEORY.

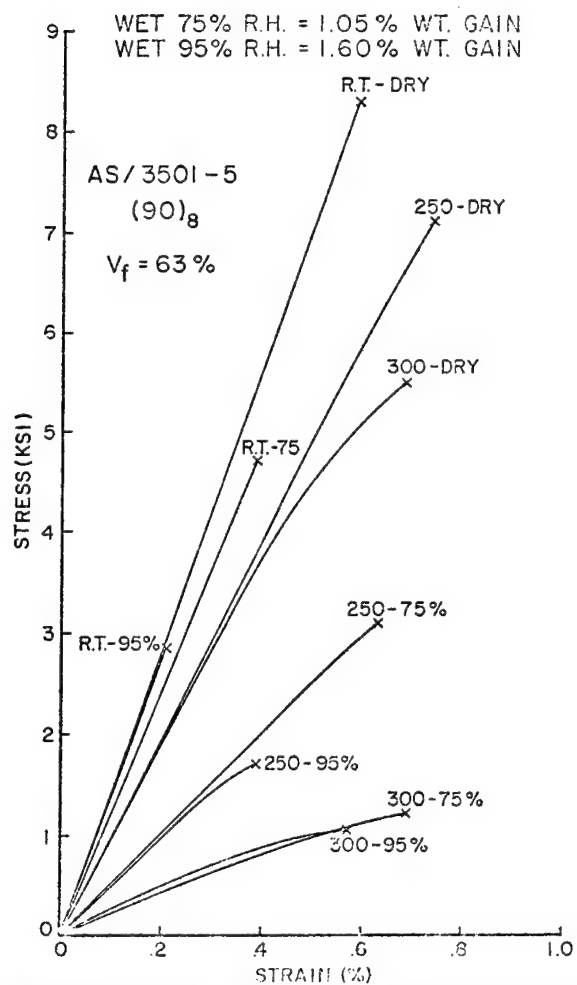
IV. EFFECT OF ENVIRONMENT ON MECHANICAL PROPERTIES



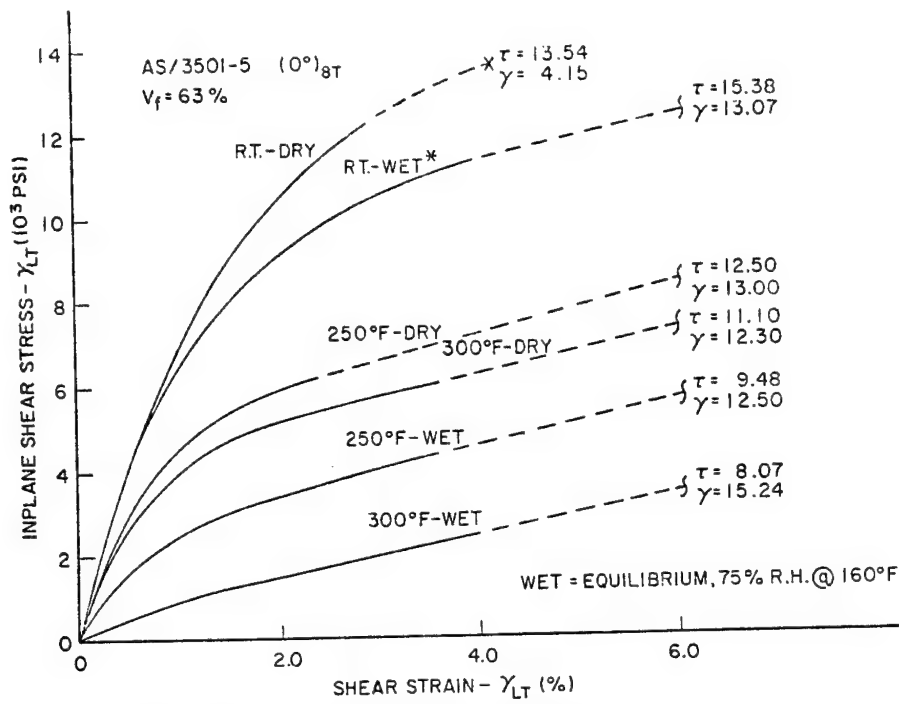
Moisture gradient through-the-thickness of laminate after various drying-out times.



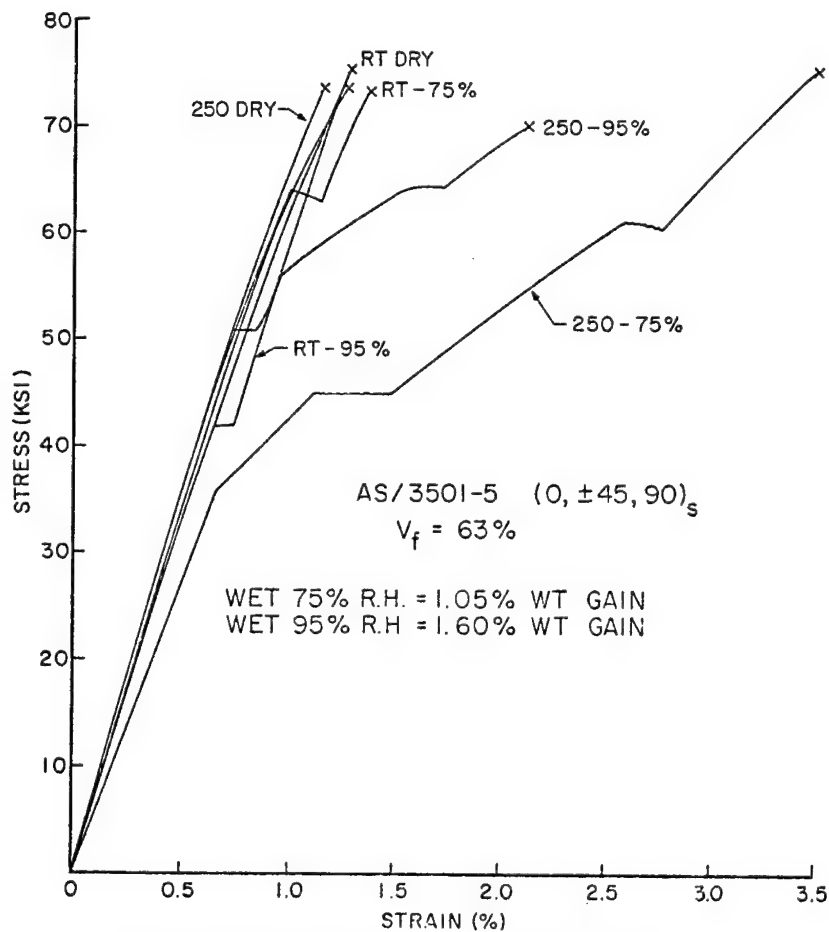
Stress-strain curves for neat resin.



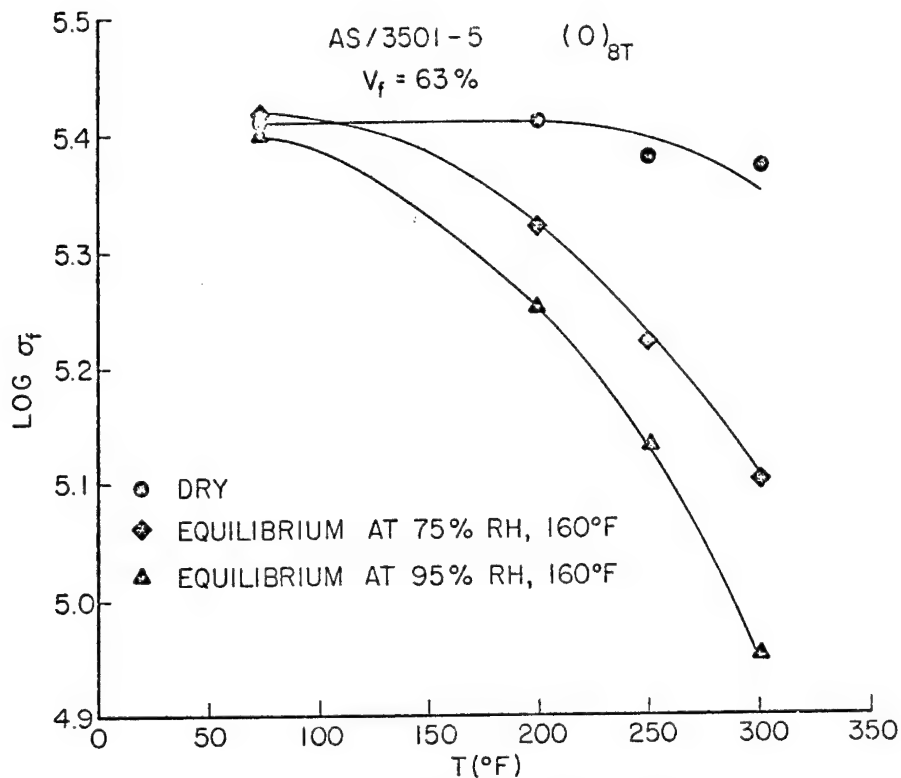
Stress-strain curves for transverse tension of a unidirectional composite.



Inplane shear stress-strain curves for unidirectional composite.



Stress-strain curves for quasi-isotropic laminate in tension.



Flex strength for unidirectional composite as a function of temperature and moisture.

EFFECT OF ENVIRONMENT ON MECHANICAL PROPERTIES OF UNIDIRECTIONAL AND LAMINATED COMPOSITES

CONCLUSIONS

1. PARTICULAR CARE MUST BE EXERCISED IN EXPERIMENTAL METHODOLOGY WHEN PERFORMING MECHANICAL TESTS ABOVE THE WET GLASS TRANSITION TEMPERATURE OF THE COMPOSITE.
2. MATRIX DOMINATED COMPOSITE PROPERTIES (E.G. TRANSVERSE UNIDIRECTIONAL TENSION, UNIDIRECTIONAL SHEAR, ETC.) ARE REDUCED AT ELEVATED TEMPERATURE BY THE PRESENCE OF MOISTURE.
3. MOISTURE AT ELEVATED TEMPERATURES CAN INDUCE A CHANGE IN FAILURE MODE FROM FILAMENT DOMINATED TO MATRIX DOMINATED. CLASSIC EXAMPLE IS THE 0 DEGREE FLEX TEST.

FUTURE EMPHASIS

1. DIFFUSION STUDIES - CONDITIONS WHICH PRODUCE MATRIX CRAZING AND CRACKING.
2. EFFECT OF ENVIRONMENT ON LAMINATE COMPRESSION STRENGTH.
3. DIMENSIONAL CHANGES DUE TO MOISTURE ABSORPTION.
4. USE OF FLEX TEST FOR EVALUATING MOISTURE EFFECTS IN COMPOSITES.
5. EFFECT OF ENVIRONMENT ON LAMINATE NOTCH STRENGTH (HOLES AND CRACKS).
6. UNIDIRECTIONAL FATIGUE - PURSUE CONCEPT OF FATIGUE LIMIT.
7. STRESS CONCENTRATIONS - MATRIX DOMINATED LAMINATES.

ENVIRONMENTAL EFFECTS ON THE THERMOMECHANICAL BEHAVIOR OF COMPOSITES

**T. S. COOKE
SOUTHWEST RESEARCH INSTITUTE**

Overall Objective

Determine the influence of the environment on the moisture content and the mechanical properties of a resin base composite.

Specific Goals

Determine the effect of temperature and humidity on water absorption by the composite .

Investigate the interaction of the environment with the composite parameters and the resulting effect on mechanical properties.

Test Parameters

To carry out this program, the following parameters will be investigated

Composite Parameters
Ply Configuration
Thickness
Volume Fraction

Environmental Parameters
Temperature
Relative Humidity
Spiking

Basic Equations of Diffusion

Flow of a substance,

$$F = -D \frac{\partial C}{\partial x}$$

F - diffusion flow, $g/cm^2/sec$

D - diffusivity, cm^2/sec

C - concentration, g/cm^3

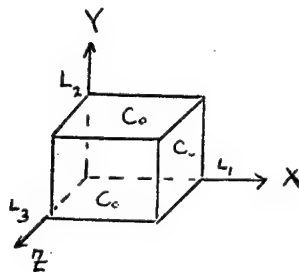
Change in a unit volume,

$$\frac{\partial C}{\partial t} = -\frac{\partial F}{\partial x}$$

If D is not a function of position,

$$\frac{\partial C}{\partial t} = D \frac{\partial^2 C}{\partial x^2}$$

Anisotropic 3D cases



Initial Condition

$$C_0 = C \text{ at } t = 0$$

$$\frac{\partial C}{\partial t} = \frac{\partial}{\partial x} \left(D_x \frac{\partial C}{\partial x} \right) + \frac{\partial}{\partial y} \left(D_y \frac{\partial C}{\partial y} \right) + \frac{\partial}{\partial z} \left(D_z \frac{\partial C}{\partial z} \right)$$

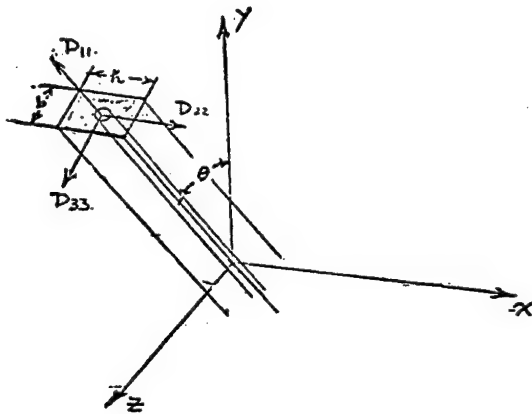
One solution is

$$C = C_0 - \frac{64}{\pi^3} (C_0 - C_s) \sum_{l,m,n} \frac{1}{lmn} \sin \frac{l\pi x}{L_1} \sin \frac{m\pi y}{L_2}$$

$$\otimes \sin \frac{n\pi z}{L_3} \exp \left[-\pi^2 t \left(D_x \frac{l^2}{L_1^2} + D_y \frac{m^2}{L_2^2} + D_z \frac{n^2}{L_3^2} \right) \right]$$

For short time, t , an alternate solution, in terms of the error function is preferable.

For a unit cell, the coefficients of diffusivity are:



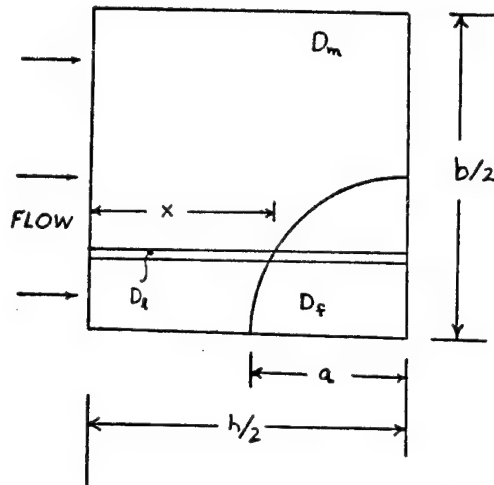
$$D_x = D_{22}$$

$$D_y = D_{11} \cos^2 \theta + D_{33} \sin^2 \theta$$

$$D_z = D_{11} \sin^2 \theta + D_{33} \cos^2 \theta$$

For flow in the x -direction, no effect of stacking sequence.

Effective Diffusion Coefficient in a Composite System with Rectangular Packing Array



Series-Parallel approximation

$$B_D = 2 \left(\frac{D_m}{D_f} - 1 \right)$$

$$V_f = \pi a^2 / bh$$

$$f = h/b$$

$$\frac{D_{SP}}{D_m} = 1 - 2 \sqrt{\frac{V_f f}{\pi}} + \frac{f}{B_D} \left[\pi - \frac{4}{\sqrt{1 - \frac{V_f}{f\pi} B_D^2}} \right] \quad (*)$$

$$(*) \tan^{-1} \left[\frac{\sqrt{1 - \sqrt{\frac{V_f}{f\pi} B_D^2}}}{\sqrt{1 + \sqrt{\frac{V_f}{f\pi} B_D^2}}} \right], \quad 1 - \frac{V_f}{f\pi} B_D^2 > 0$$

$$\frac{D_{SP}}{D_m} = 1 - 2 \sqrt{\frac{V_f f}{\pi}} + \frac{f}{B_D} \left[\pi - \frac{2}{\sqrt{\frac{V_f}{f\pi} B_D^2 - 1}} \right] \quad (*)$$

$$(*) \ln \left\{ \sqrt{\frac{V_f}{f\pi} B_D^2} + \sqrt{\frac{V_f}{f\pi} B_D^2 - 1} \right\}, \quad \frac{V_f}{f\pi} B_D^2 - 1 > 0$$

For a laminated composite

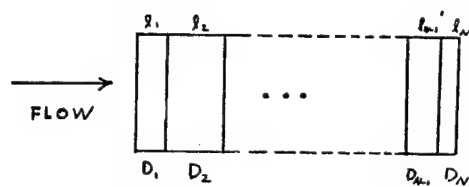
$$D_x = \frac{\sum_{i=1}^N h_i}{\sum_{i=1}^N \frac{h_i}{F_{2i} D_{22}^i}}$$

$$D_y = \frac{\sum_{i=1}^N h_i F_{1i} D_{11}^i \cos^2 \theta_i}{\sum_{i=1}^N h_i} + \frac{\sum_{i=1}^N h_i F_{3i} D_{33}^i \sin^2 \theta_i}{\sum_{i=1}^N h_i}$$

$$D_z = \frac{\sum_{i=1}^N h_i F_{1i} D_{1i} \sin^2 \theta_i}{\sum_{i=1}^N h_i} + \frac{\sum_{i=1}^N h_i F_{3i} D_{3i} \cos^2 \theta_i}{\sum_{i=1}^N h_i}$$

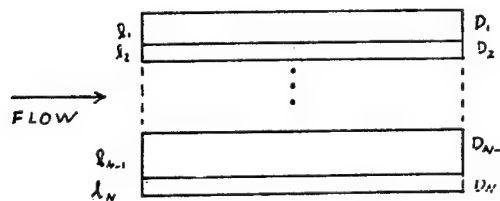
where F_{ji} are interface coefficients reflecting any changes in diffusivity at the interface between two layers.

Effective Diffusion Coefficients for Layer Composites.



SERIES

$$\frac{l_1}{D_1} + \frac{l_2}{D_2} + \dots + \frac{l_N}{D_N} = \frac{L}{D}$$



PARALLEL

$$l_1 D_1 + l_2 D_2 + \dots + l_N D_N = LD$$

Once D_i is known, we compute concentration distribution or total moisture content.

$$C = C_0 - \frac{64}{\pi^3} (C_0 - C_i) \sum_{l,m,n} \frac{1}{l m n} \sin \frac{l \pi x}{L_1} \sin \frac{m \pi y}{L_2} \quad (4)$$

$$\otimes \sin \frac{n \pi z}{L_3} e^{-\lambda_{lmn} \tau}$$

$$\frac{M - M_i}{M_\infty - M_i} = 1 - \frac{8}{\pi^6} \sum_{l,m,n \text{ (odd)}} \frac{e^{-\lambda_{lmn} \tau}}{l m n}$$

$$\text{where } \lambda_{lmn} = \pi^2 \left(D_x \frac{l^2}{L_1^2} + D_y \frac{m^2}{L_2^2} + D_z \frac{n^2}{L_3^2} \right)$$

Moisture experiments usually measure total weight gain

5 picking

D diffusivity is temperature dependent,

$$D = D_0 e^{-B/\theta(\tau)} = D_0 h(\tau)$$

where θ is the absolute temperature, is an empirical relation. Following Weitzman,

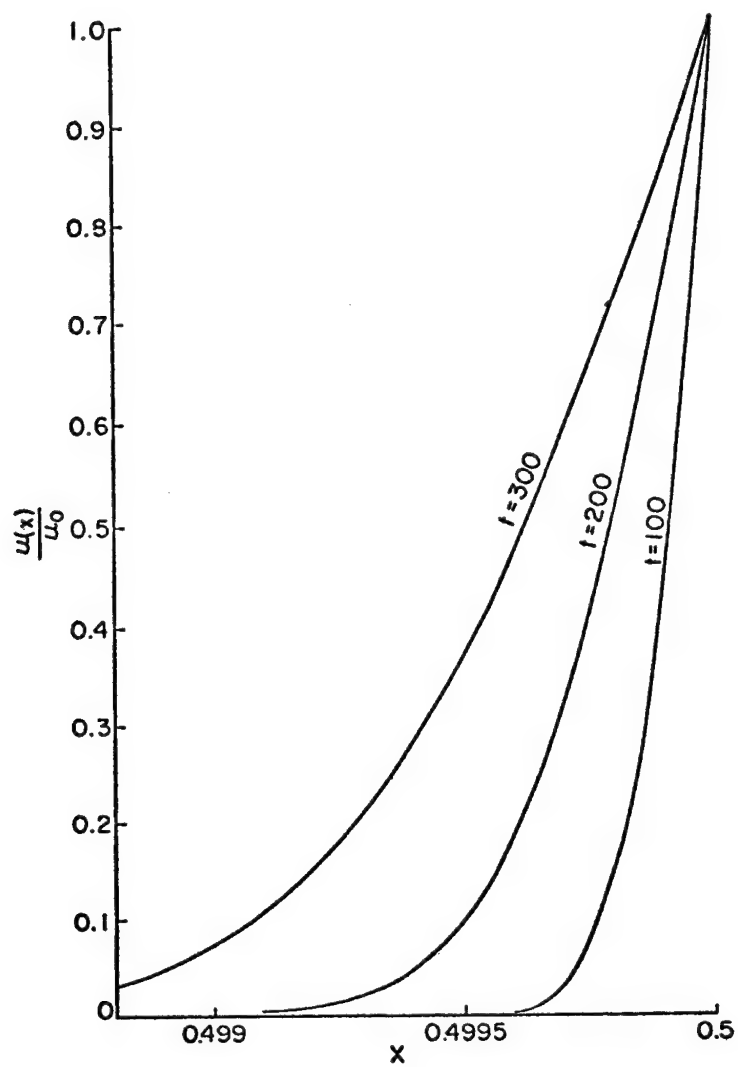
$$Z^* = D_0 \int_0^{\tau} h(s) ds$$

For any known solution, replace τ by τ^* .

This allows the computation of moisture distribution as well as total content. Can be used to determine whether or not spiking matches the desired environmental conditions. For NARMCO 5208 Hms, Weitzman provided distribution curves for a thermal spike

$$\theta = 303 + \frac{117}{300} \tau$$

from 303°K to 422°K over 300 seconds.



Moisture Profiles at times $t = 100, 200, 300$ secs.
for the "Ramp-Temperature" case. \bar{r}_{Rom} WEITSMAN.

ANALYSIS AND DESIGN OF COMPOSITE
BONDED JOINTS UNDER A DYNAMIC TYPE LOAD

JACK R. VINSON

R. BYRON PIPES

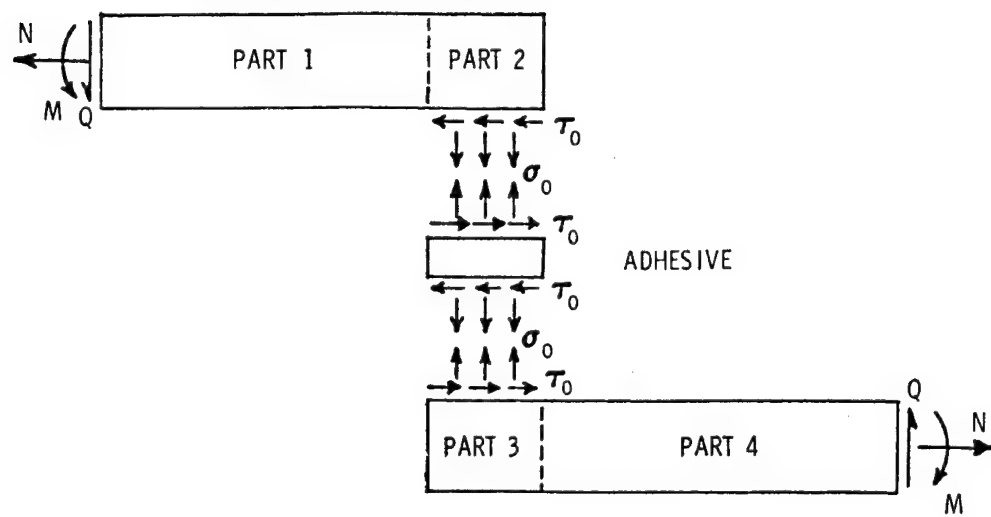
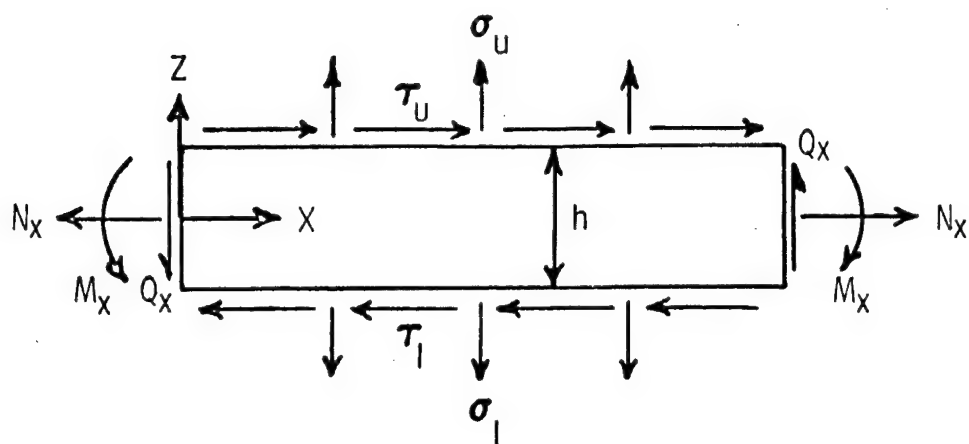
THE CENTER FOR COMPOSITE MATERIALS AND
THE DEPARTMENT OF MECHANICAL AND AEROSPACE ENGINEERING
UNIVERSITY OF DELAWARE

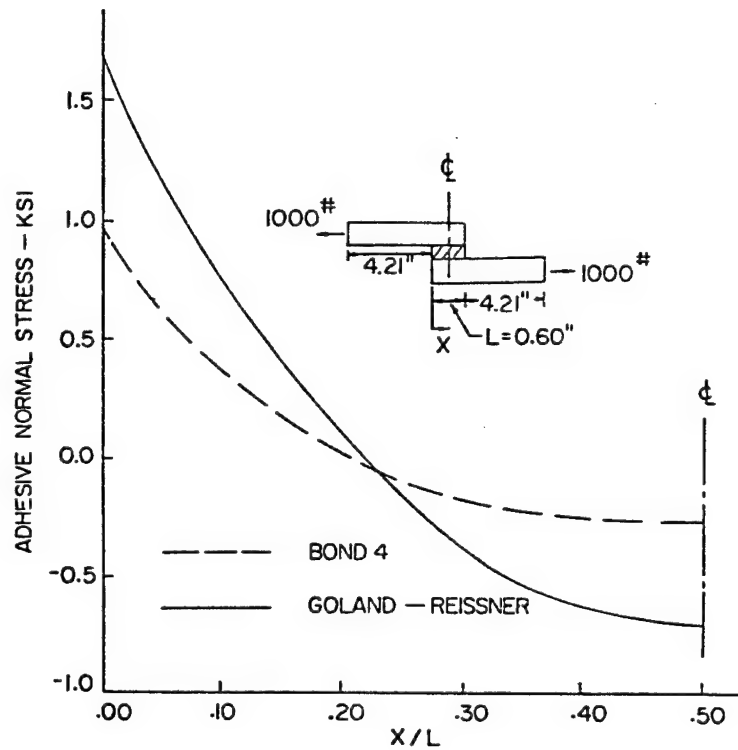
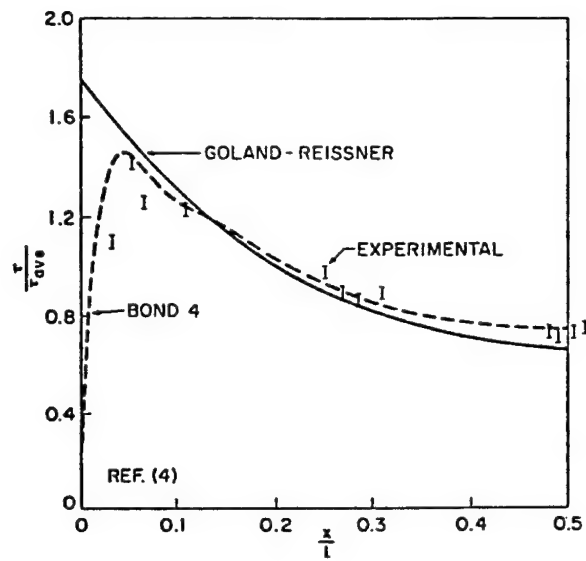
OBJECTIVE: Phase IV

TO SYSTEMATICALLY CHARACTERIZE PROMISING
ADHESIVES AT BOTH ROOM AND ELEVATED TEMPERATURE
USING THE UNIQUE SHEAR AND TENSILE TESTS DEVELOPED
AT DELAWARE.

OBJECTIVE: Phase V

INVESTIGATING THE EFFECTS OF COMBINED HIGH
TEMPERATURE AND HIGH HUMIDITY (HYGROTHERMAL
EFFECTS) UPON BONDED JOINTS BETWEEN STRUCTURAL
COMPONENTS OF COMPOSITE MATERIALS.





TYPICAL ADHESIVE SHEAR AND NORMAL STRESS DISTRIBUTIONS

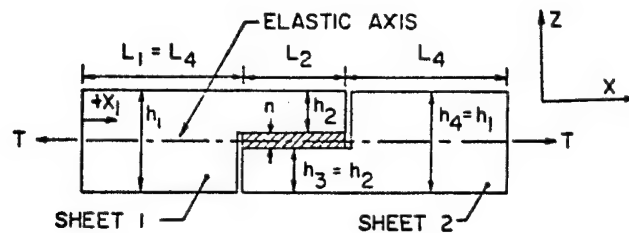


Figure (6)

Assuming that Parts (2) and (3) are identical, reference [2] shows that the governing equations are:

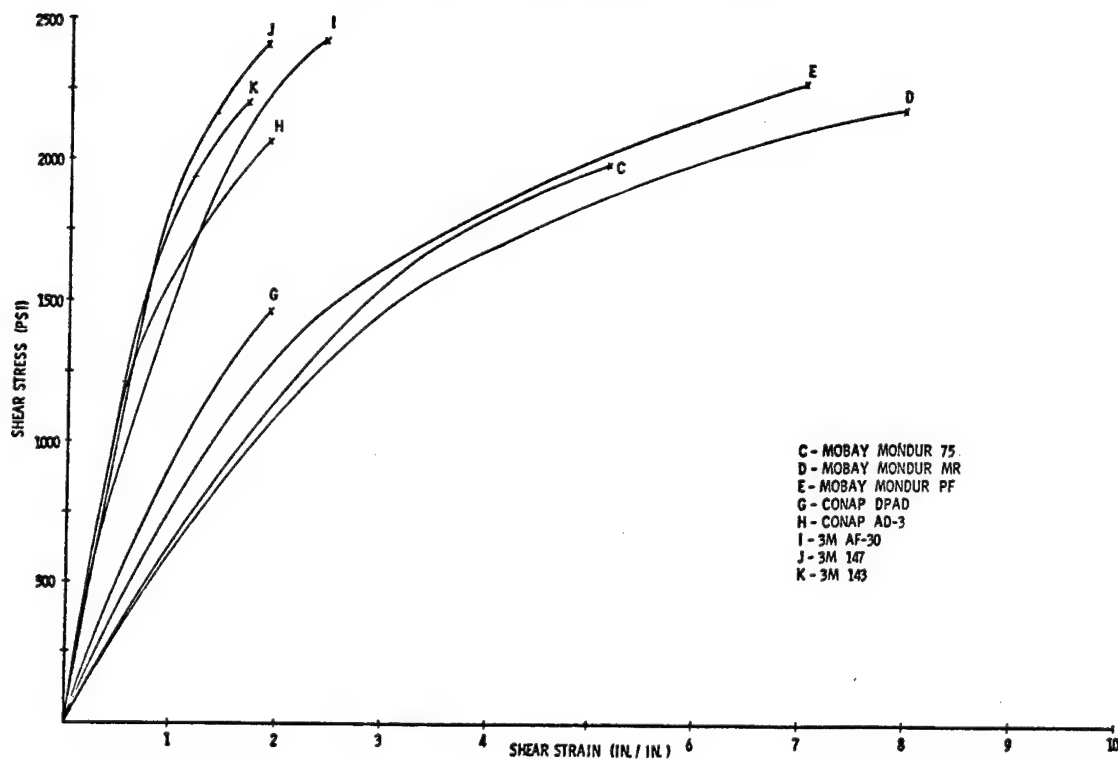
$$A_1 \frac{d^4 \tau_o}{dx^4} + A_2 \frac{d^2 \tau_o}{dx^2} + A_3 \tau_o = f(x)$$

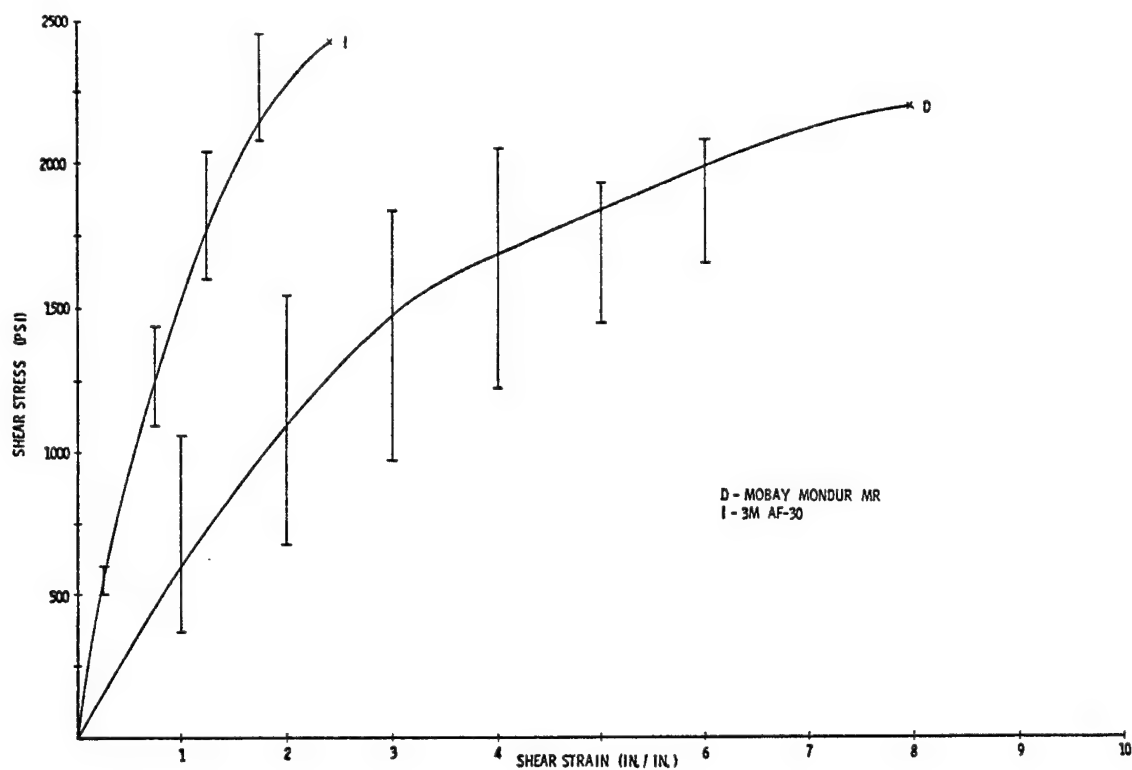
$$B_4 \frac{d^4 \sigma_o}{dx^4} + B_5 \frac{d^2 \sigma_o}{dx^2} - \frac{2\sigma_o}{D_{11}} = 0$$

where $f(x)$ is a function of the uniform temperature distribution and all constants are functions of material properties and geometry and are given explicitly in reference [2].

The adhesive shear and normal stresses are again of the form:

$$\tau_o(x) = S_i e^{\lambda_i x} + \text{(Particular Solution)} \quad i=1,4$$





	MANUFACTURER ULT. SHEAR STRESS(PSI)/STD. DEV.	UNIV. OF DELAWARE ULT. SHEAR STRESS(PSI)/STD. DEV.
MOBAY MONDUR 75	1989 / 7.5	1622 / 43
MOBAY MONDUR MR	2182 / 92	2512 / 189
MOBAY MONDUR PF	2273 / 67	2379 / 74
CONAP DPAD	1459 / 86	-----
CONAP AD-3	2061 / 98	-----
3M AF-30	2426 / 239	2080 / 125
3M 147	2405 / 107	2560 / 63
3M 143	2171 / 37	2175 / 282
3M AF-55	-----	2239 / 196

	MANUFACTURER ULT. SHEAR STRAIN/STD. DEV.	UNIV. OF DELAWARE ULT. SHEAR STRAIN/STD. DEV.
MOBAY MONDUR 75	5.137 / .932	6.651 / 2.931
MOBAY MONDUR MR	7.976 / 3.741	1.808 / .868
MOBAY MONDUR PF	7.037 / 1.484	>2.229 / -
CONAP DPAD	1.911 / .431	-----
CONAP AD-3	1.902 / .3	-----
3M AF-30	>2.451 / -	>2.918 / -
3M 147	1.858 / .831	1.558 / .378
3M 143	1.681 / .663	1.392 / .633
3M AF-55	-----	1.715 / .536

	MANUFACTURER SHEAR MODULUS (PSI) /STD. DEV.	UNIV. OF DELAWARE SHEAR MODULUS (PSI) /STD. DEV.
MOBAY MONDUR 75	813 / 152	630/213
MOBAY MONDUR MR	750 / 330	3624 / 1516
MOBAY MONDUR PF	768 / 210	2965 / 586
CONAP DPAD	992 / 209	-----
CONAP AD-3	2614 / 758	-----
3M AF-30	2351 / 213	1522 / 242
3M 147	2566 / 869	3251 / 1083
3M 143	2469 / 737	3717 / 1547
3M AF-55	-----	2575 / 697

TEST MATRIX - PHASE V

3 REPETITIVE TESTS

1 ADHEREND SYSTEM (Graphite-Epoxy)

2 ADHESIVE SYSTEMS

5 TIMES IN SOAK: 0, 1, 3, 5, 7 Months

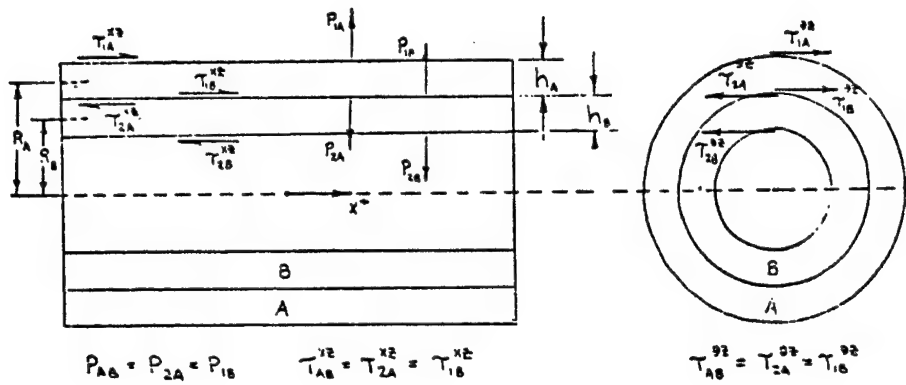
3 TESTS: Static, HC-LL Fatigue; LC-HL Fatigue

2 TEST ENVIRONMENTS: Room Temp. , Elevated Temp.

180 TEST PIECES

OTHER RESEARCH COMPLETED

- BUCKLING OF COMPOSITE PLATES DUE TO IN-PLANE LOADS FOR MANY BOUNDARY CONDITIONS
- INTERLAMINAR STRESSES IN COMPOSITE CYLINDRICAL SHELLS
- HYGROTHERMAL EFFECTS IN COMPOSITE LAMINATES
- PLANE STRAIN FINITE ELEMENT INCLUDING HYGROTHERMAL EFFECTS
- PARAMETRIC STUDIES OF STRUCTURAL ADHESIVE JOINTS



FORCES ON A TWO LAMINA COMPOSITE SHELL

BORON EPOXY

$$E_{11} = 32.5 \times 10^6 \text{ PSI}$$

$$H = 0.25''$$

$$E_{22} = 1.84 \times 10^6 \text{ PSI}$$

$$R = 12.5''$$

$$\nu_{12} = 0.256$$

$$L = 50''$$

$$G_{12} = G_{13} = 0.642 \times 10^6 \text{ PSI}$$

$$P = 100 \text{ PSI}$$

$$G_{23} = 0.361 \times 10^6 \text{ PSI}$$

BENDING BOUNDARY LAYER IN MERIDIONAL DIRECTION

ISOTROPIC MATERIAL

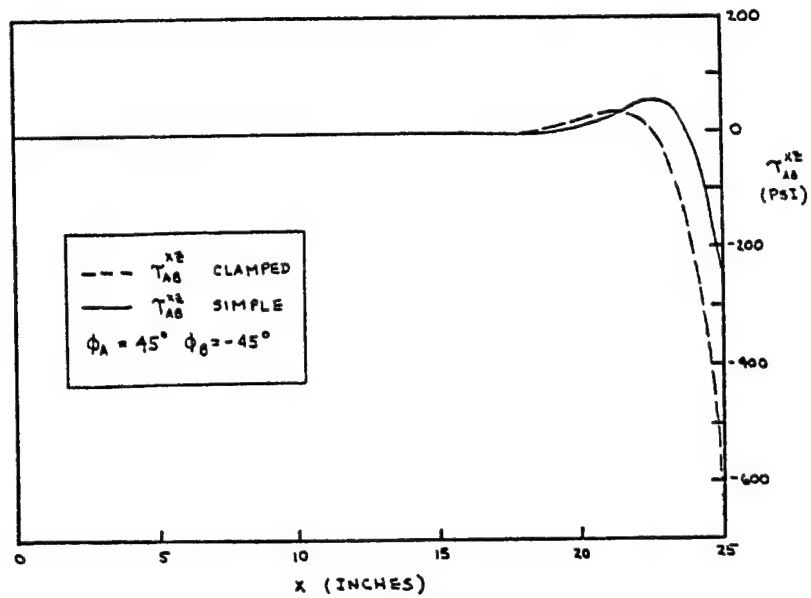
$$L_B = 4 \sqrt{R_\theta h}$$

ORTHOTROPIC MATERIAL

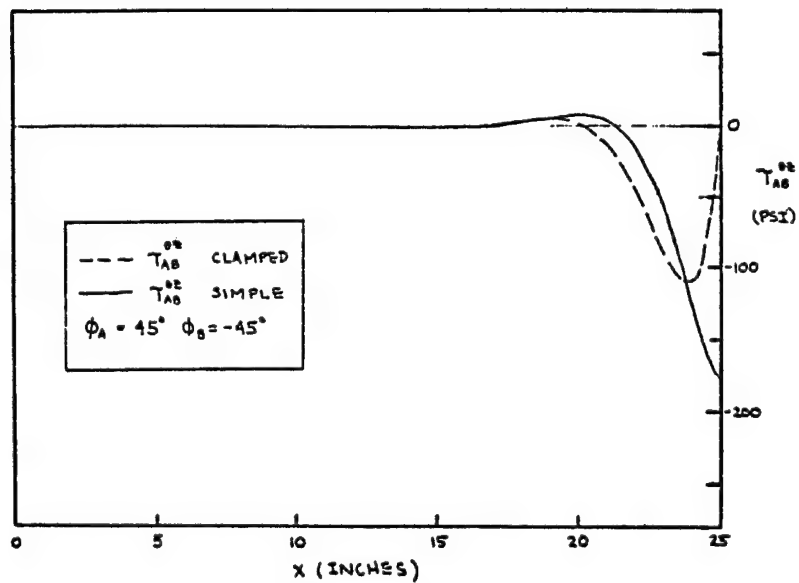
$$L_B = 4 \sqrt{\left(\frac{E_X}{E_\theta}\right)^{1/2} R_\theta h}$$

LAMINATED SHELL

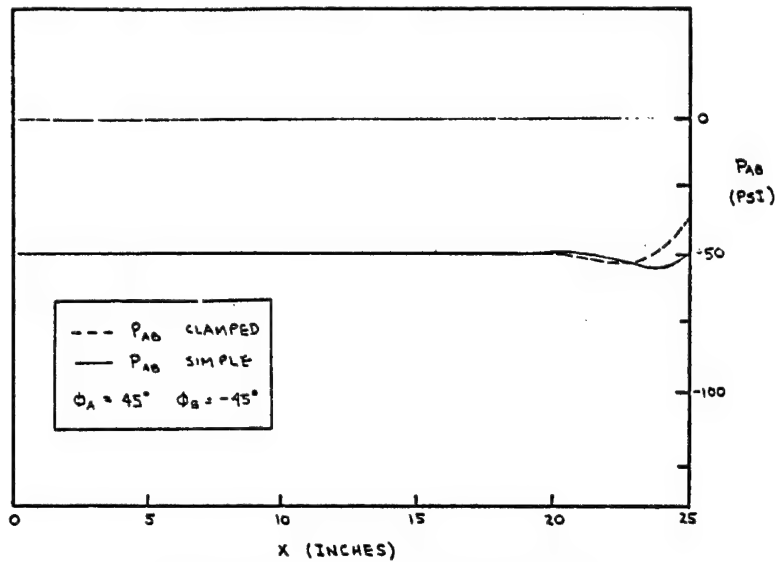
$$L_B = 4 \sqrt{\left(\frac{D_{11}}{D_{22}}\right)^{1/2} R_\theta h}$$



INTERLAMINAR AXIAL SHEAR STRESS DISTRIBUTION FOR BOTH
CLAMPED AND SIMPLY SUPPORTED ENDS

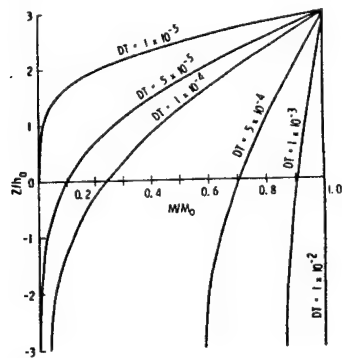


INTERLAMINAR CIRCUMFERENTIAL SHEAR STRESS DISTRIBUTION FOR BOTH
CLAMPED AND SIMPLY SUPPORTED ENDS

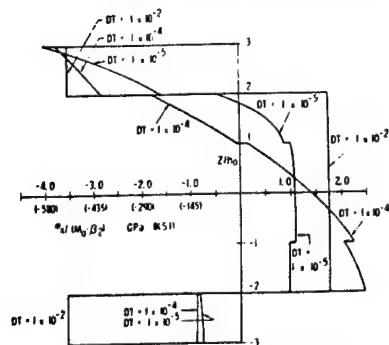


INTERLAMINAR NORMAL STRESS DISTRIBUTION FOR BOTH
CLAMPED AND SIMPLY SUPPORTED ENDS

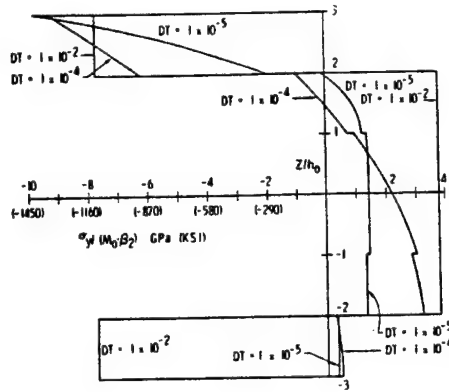
On the Hygrothermal Response of Laminated Composite Systems



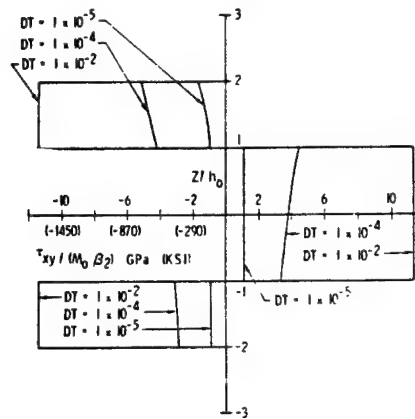
Single Surface Absorption - Moisture Distribution.



Single Surface Absorption - σ_y Stress Distribution



Single Surface Absorption - σ_y Stress Distribution.



Single Surface Absorption - τ_{xy} Stress Distribution.

OTHER RESEARCH IN PROGRESS

- ANALYSIS OF BONDED JOINTS OF SEVERAL CONFIGURATIONS USING THE ANALYTICAL FINITE ELEMENT INCLUDING HYGROTHERMAL EFFECTS
- ANALYSIS OF SINGLE LAP JOINTS WITH LINEARLY TAPERED ADHERENDS
- NEW TECHNIQUES OF SOLUTION FOR COMPOSITE PLATES AND SHELLS USING PERTURBATION TECHNIQUES

AIR FORCE OFFICE OF SCIENTIFIC RESEARCH

AND THE

CENTER FOR COMPOSITE MATERIALS

UNIVERSITY OF DELAWARE

WORKSHOP

ON

THE EFFECTS OF RELATIVE HUMIDITY AND ELEVATED

TEMPERATURE ON COMPOSITE STRUCTURES

MARCH 30-31, 1976

EFFECT OF COMPRESSION ON
FATIGUE OF GRAPHITE/EPOXY COMPOSITES

PRINCIPAL INVESTIGATOR: J. T. RYDER
PROGRAM MANAGER: E. K. WALKER

LOCKHEED-CALIFORNIA COMPANY

PURPOSE

- BUILD STATISTICAL DATA BASE
- EVALUATE WEAROUT MODEL
- EVALUATE EFFECT OF COMPRESSION FATIGUE

PROGRAM DEFINITION

TWO LAMINATES

LAMINATE 1: 25% 0^0 FIBERS
16 PLIES
(0/+45/90/-45₂/90/45/0)₂
QUASI-ISOTROPIC

LAMINATE 2: 66.7% 0^0 FIBERS
24 PLIES
(0/+45/0₂/-45/0₂/+45/0₂/-45/0)₂

PROGRAM DEFINITION (CONT'D)

TESTING

- STATIC TENSION, COMPRESSION
- S-N CURVE, T-T, C-T
- EVALUATE FATIGUE SCATTER
- MINIMUM TWENTY TESTS AT EACH STRESS LEVEL
- RESIDUAL STRENGTH
 - FATIGUE CYCLE 40 COUPONS AT STRESS LEVELS CHOSEN
 - FAIL HALF TENSION & COMPRESSION
 - ORIGINAL STRENGTH DISTRIBUTION

PROGRAM DEFINITION (CONT'D)

MATERIAL: (934/T300)

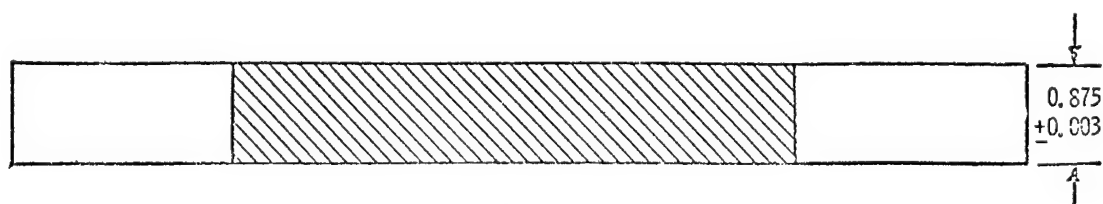
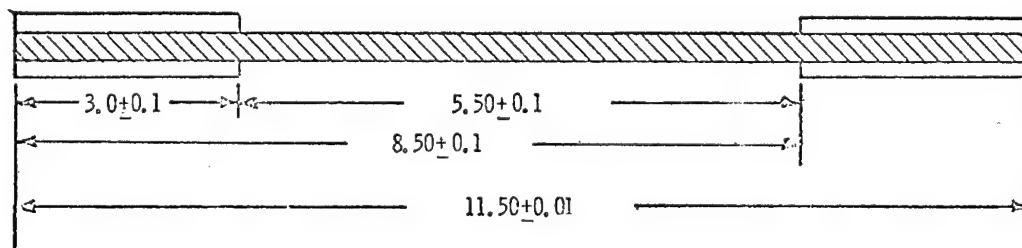
CURE CYCLE: 350 0 F CURE FOR 2 HOURS

CONDITIONING: 72 HOURS AT 72 \pm 2 0 F, 40 \pm 10% R. H.

TEST ENVIRONMENT: 72 \pm 2 0 F, 40 \pm 10% R. H.

COUPON TYPE

- PARALLEL SIDED
- 5-1/2 IN. CENTER SECTION
- NON-TAPERED END TABS



COMPOSITE SPECIMEN GEOMETRY

FABRICATION

VARIATION IN AREA: $\pm 1.5\%$ WITHIN COUPON

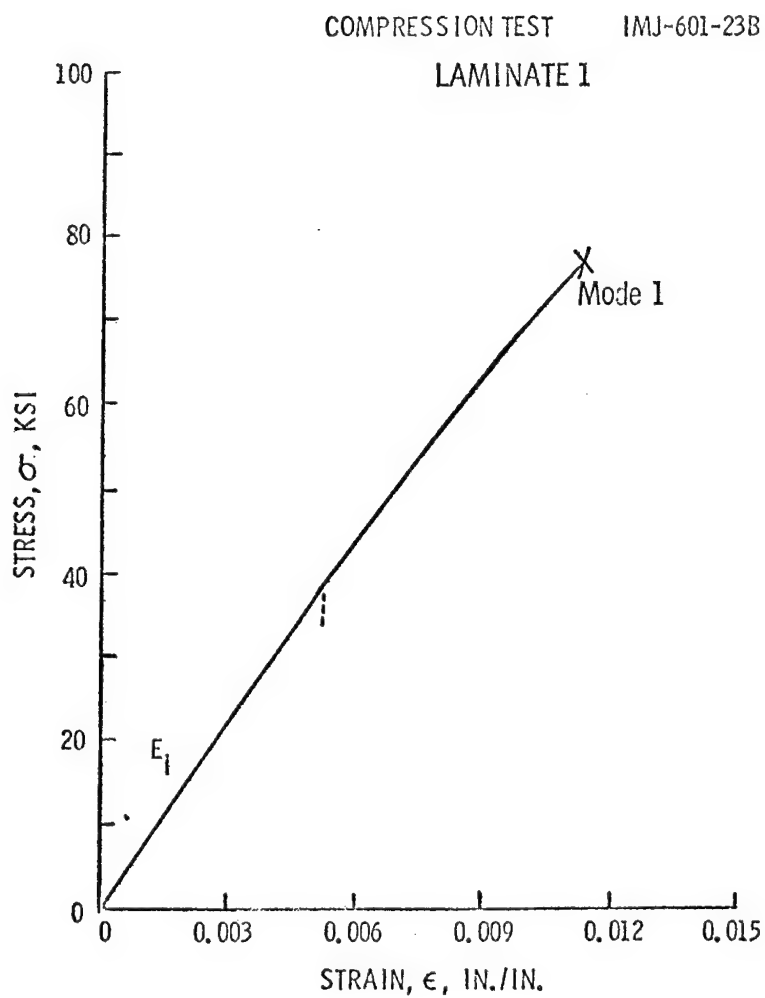
VARIATION IN AREA: $\pm 4\%$ FOR ALL COUPONS

PERCENT VOLUME OF FIBER:

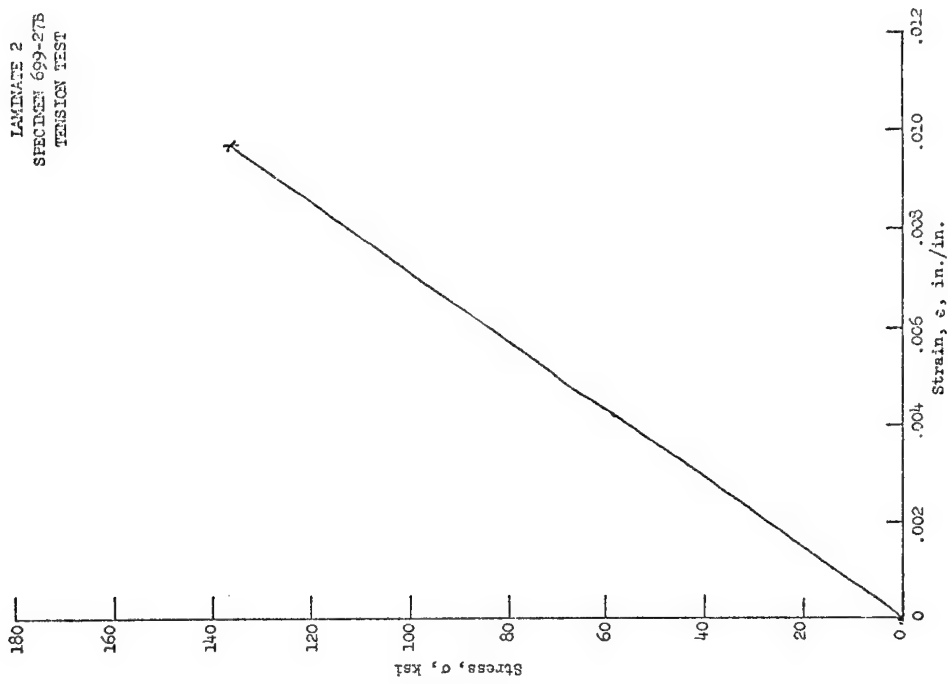
LAMINATE 1: 60.3 - 66.4

LAMINATE 2: 60.0 - 63.1

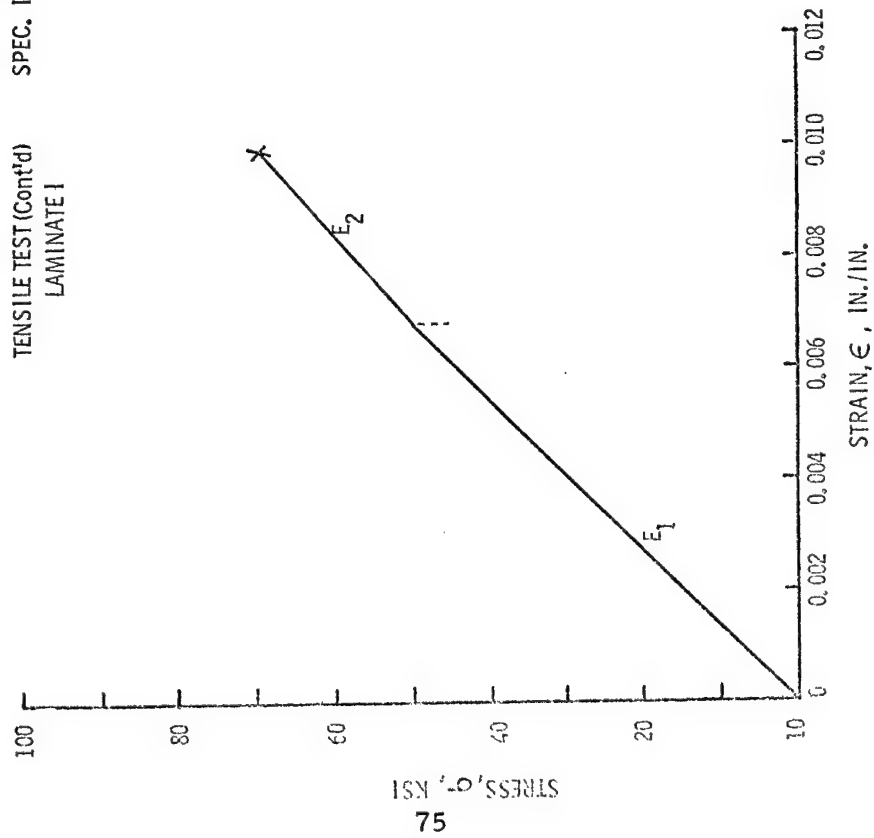
VOIDS: $\ll 1/2\%$



LAMINATE 2
SPECIMEN 699-275
TENSION TEST



TENSILE TEST (Cont'd)
LAMINATE 1
SPEC. IMJ-603-6A



TENSILE TESTS

	ULTIMATE STRESS, σ_{ult} , ksi	ULTIMATE STRAIN ϵ_{ult} , in./in.	APPARENT MODULUS OF ELASTICITY, E_A psi x 10^6
LAMINATE 1	69.2	0.0096	7.64
	+ 6.2, 9%	+0.0011, 11%	+0.54, 7%
	- 7.2, 10%	-0.0010, 10%	-0.69, 9%
LAMINATE 2	141.7	0.0092	15.4
	+20.1, 14%	+0.0009, 10%	+2.9, 19%
	-20.3, 14%	-0.0027, 29%	-1.9, 12%

TENSILE TESTS (CONT'D)

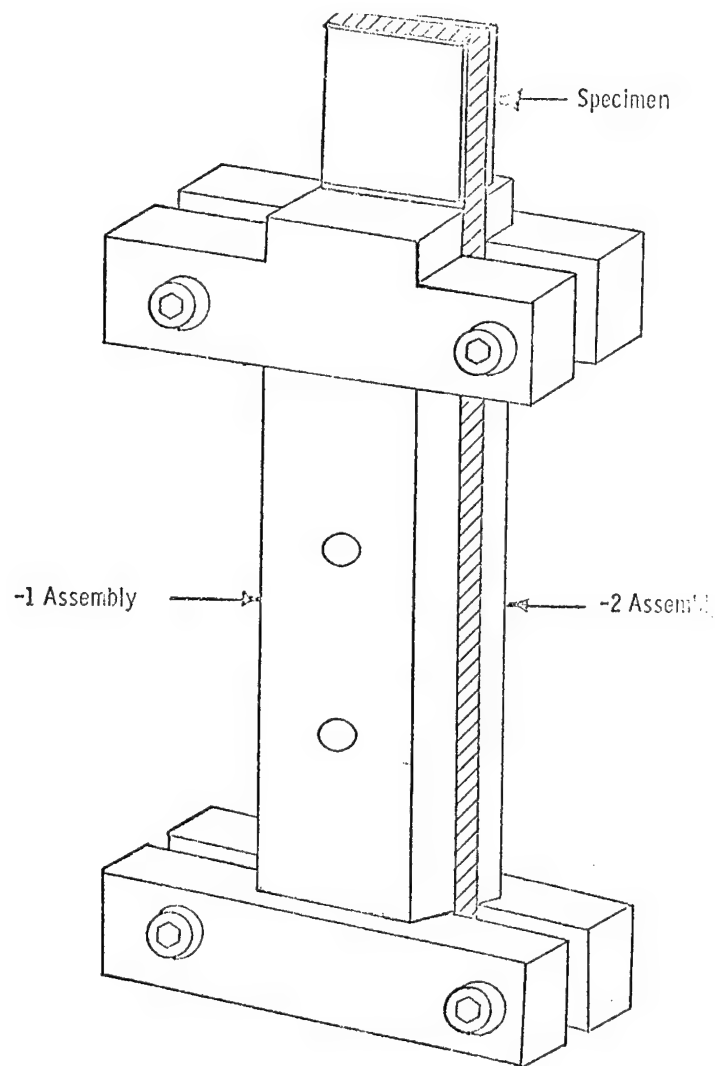
		k	e	v	R & FIT
LAMINATE 1	3 PARAMETER	24.18	-0.0753	70.50	EQUAL
	2 PARAMETER	24.12	0	70.57	
LAMINATE 2	3 PARAMETER	18.87	-0.4304	144.4	EQUAL
	2 PARAMETER	18.76	0	144.8	

$$P(x) = \exp \left[- \left(\frac{x-e}{v-e} \right)^k \right]$$

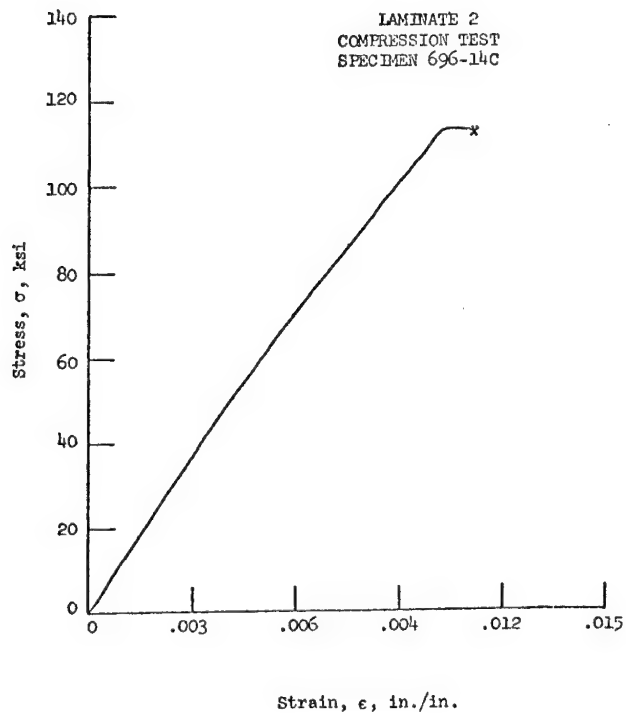
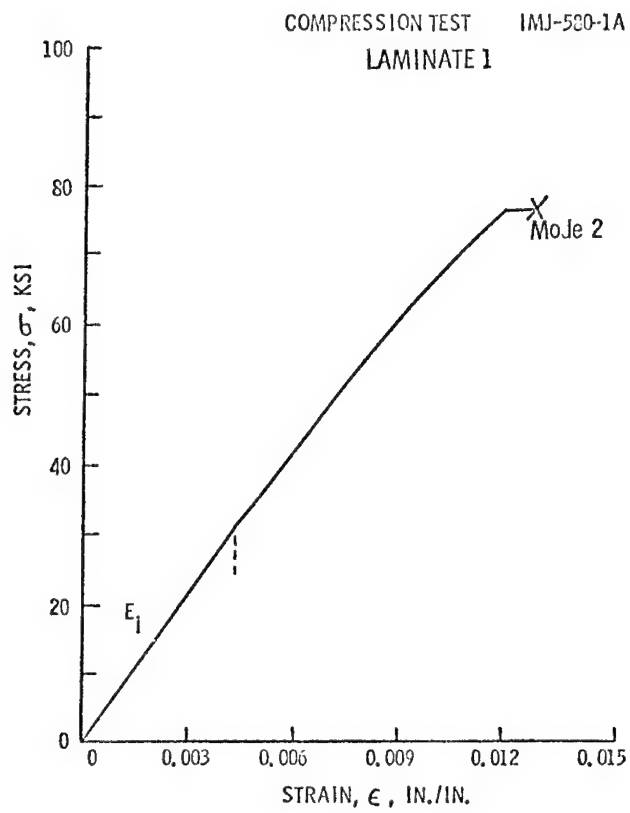
FOR 2 PARAMETER, $\alpha = k$, $\hat{F} = v$

COMPRESSION TESTS

- FULLY SIDE SUPPORTED
- SUPPORTS TAPED WITH TEFLON
- TOP END TABBED
- BOTTOM END UNTABBED, BEARING ON PLATE
- PROCEDURE PREVENTED BUCKLING AND END BROOMING
- FAILURES WERE FRACTURES THROUGH PLYS AT 45° AND 90°



COMPRESSION TESTING FIXTURE



COMPRESSION TESTS (CONT'D)

	ULTIMATE STRESS, σ_{ult} ksi	ULTIMATE STRAIN, ϵ_{ult} in./in.	APPARENT MODULUS OF ELASTICITY, E_A , psi X 10^6
LAMINATE 1	69.7 +11.8, 17% -12.1, 17%	0.0110 +0.0022, 20% -0.0025, 23%	6.95 +0.29, 4% -0.83, 12%
LAMINATE 2	114.2 +15.0, 13% -10.2, 9%	+0.0014, 14% -0.0011, 11%	+0.8, 7% -0.5, 4%

COMPRESSION TESTS (CONT'D)

		k	e	v	R & FIT
LAMINATE 1	3 PARAMETER	12.09	-0.4572	72.19	EQUAL
	2 PARAMETER	11.94	0	72.53	
LAMINATE 2	3 PARAMETER	25.01	-0.2592	115.82	EQUAL
	2 PARAMETER	24.91	0	116.07	

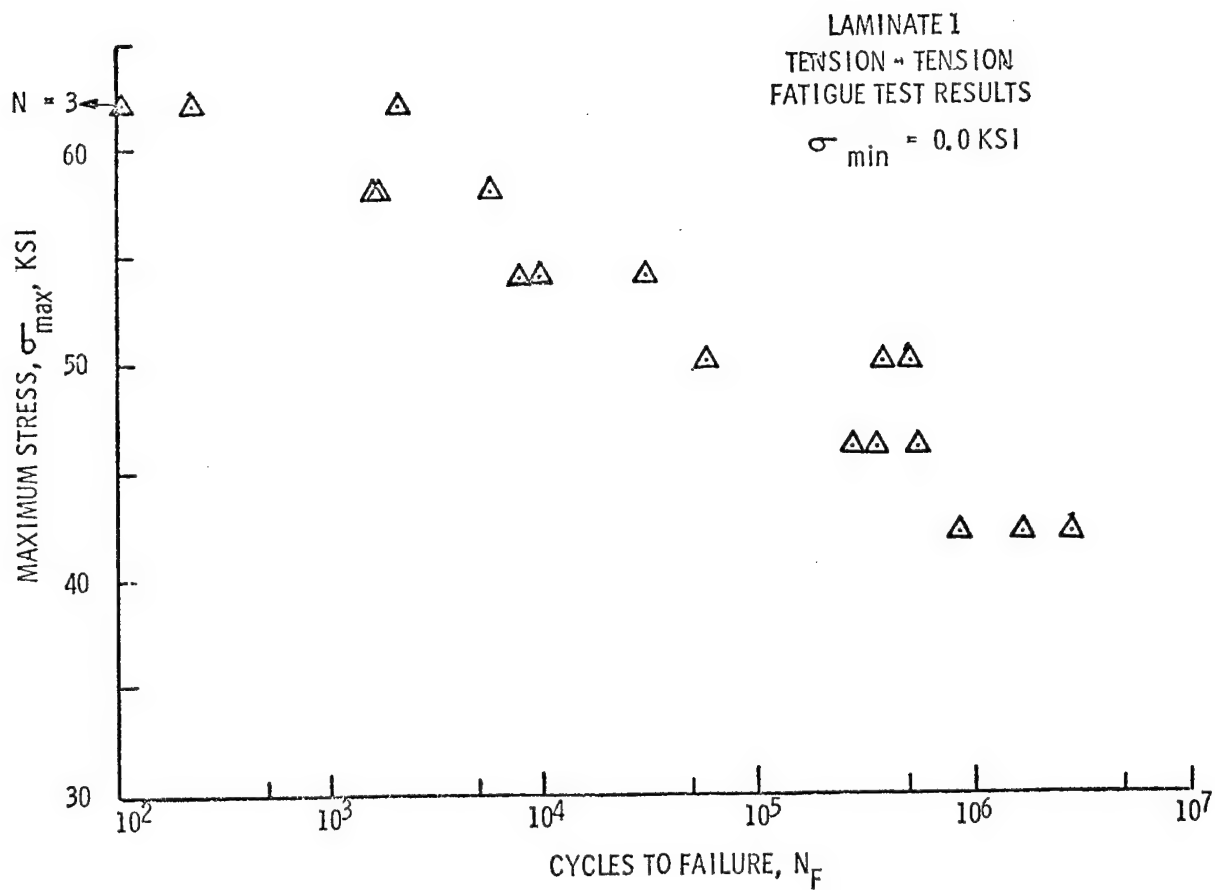
S-N CURVE SCAN

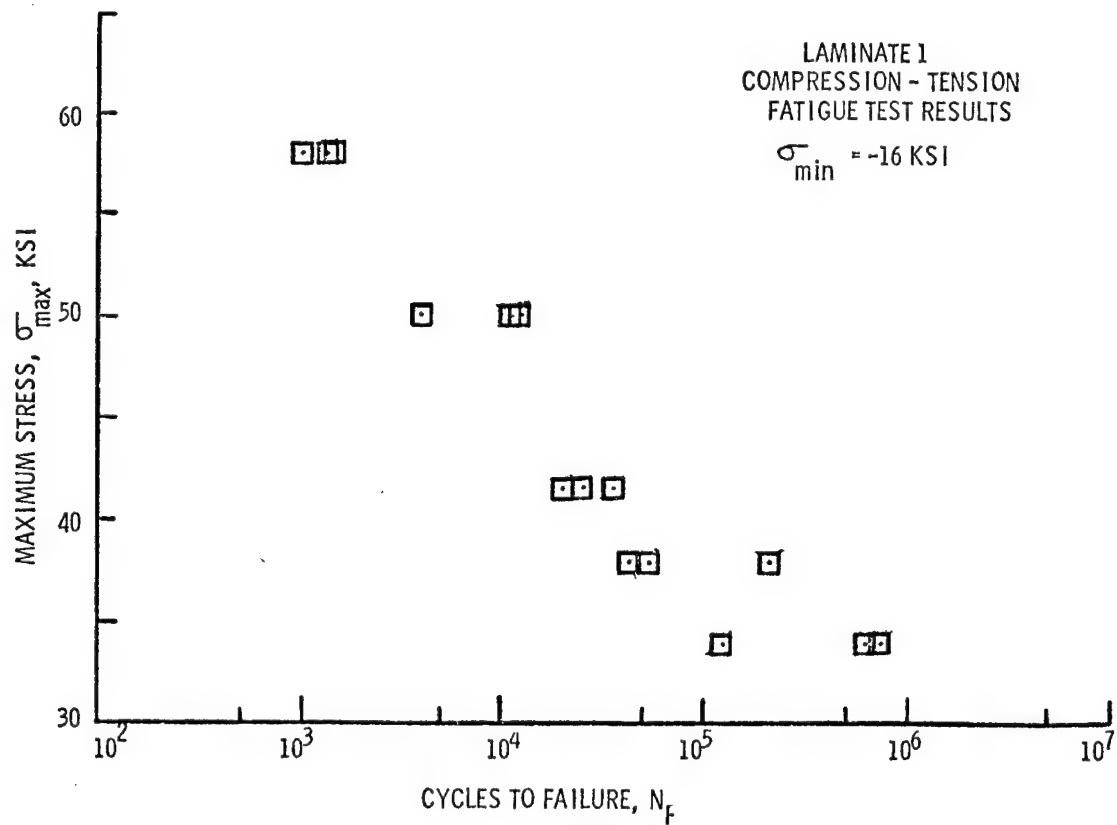
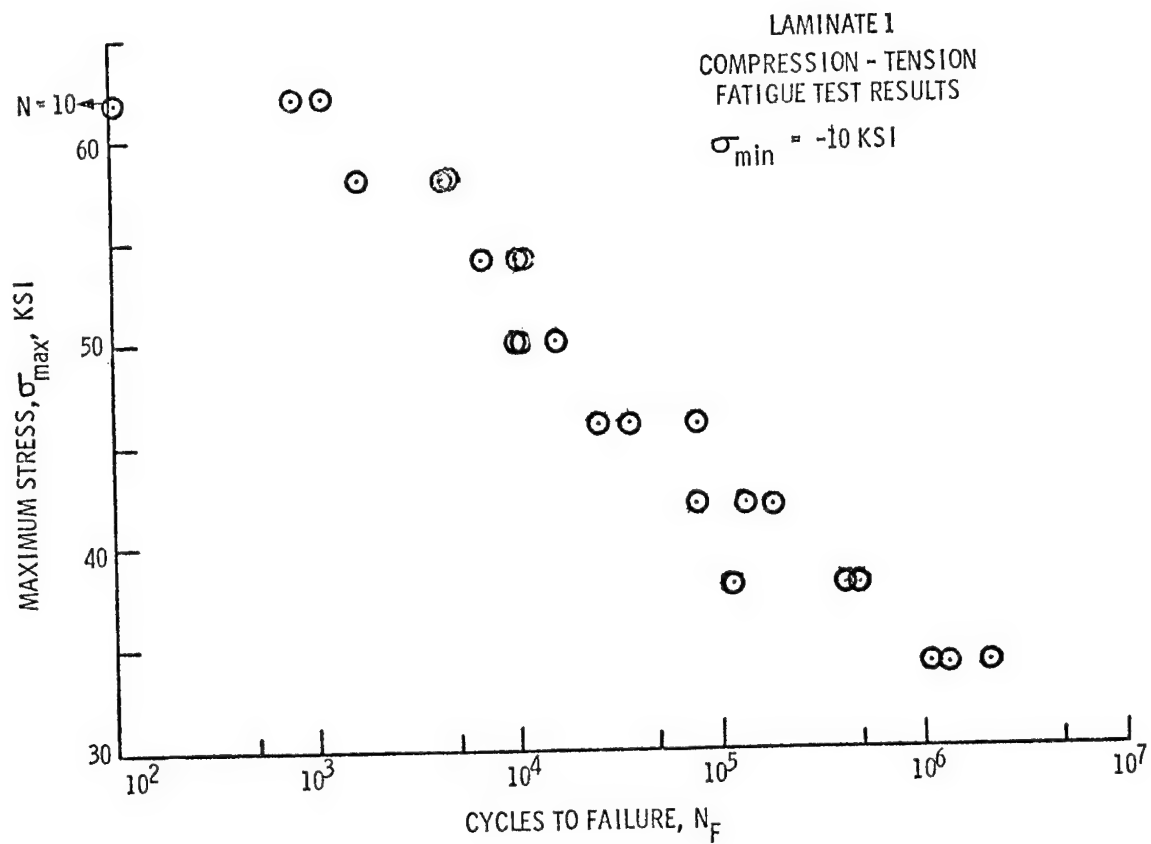
THREE COUPONS AT EACH STRESS LEVEL

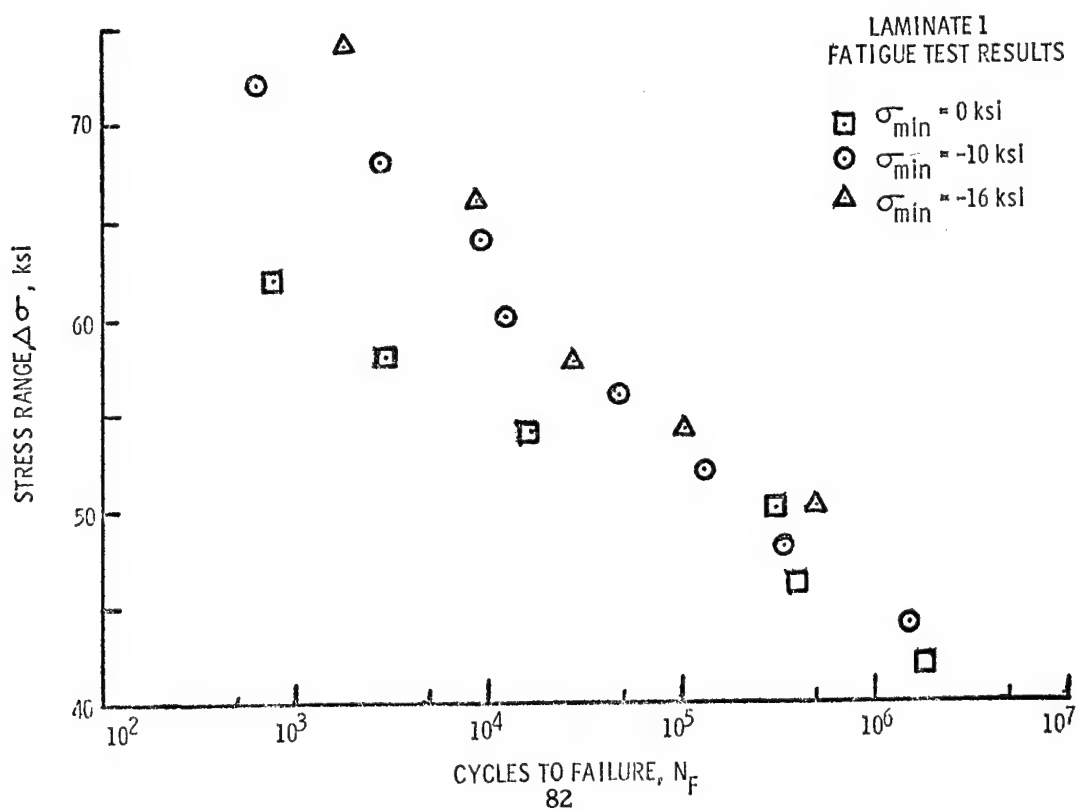
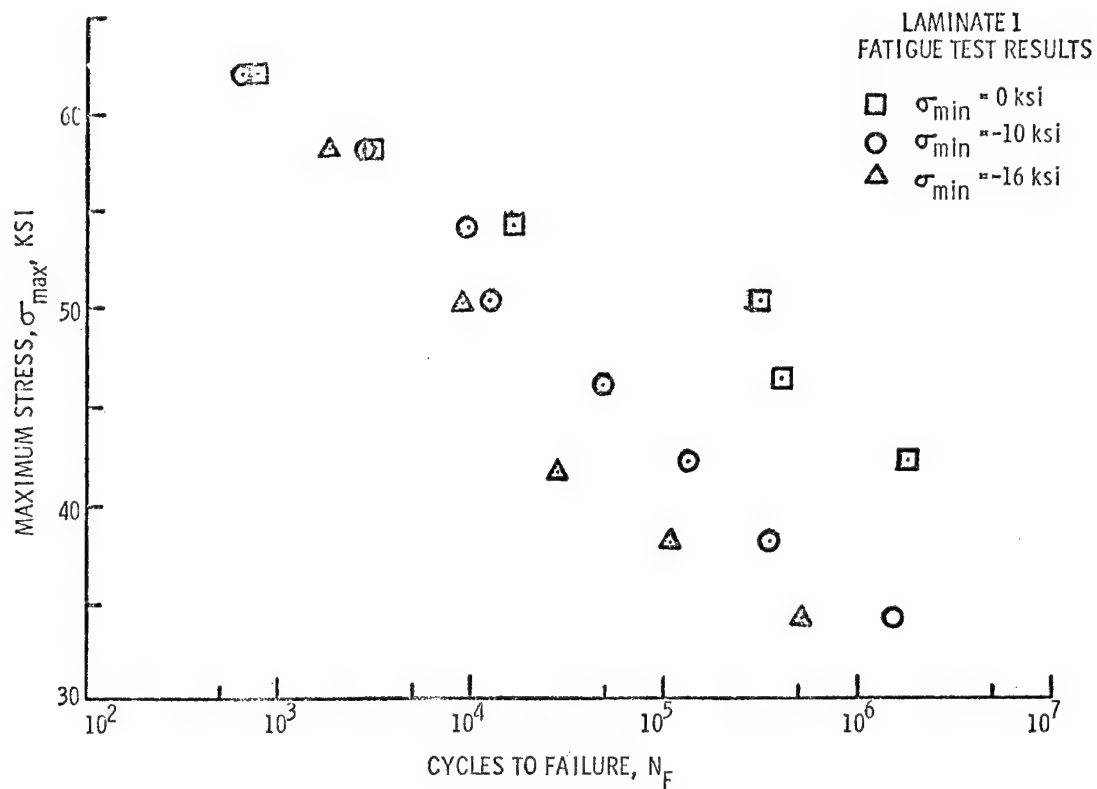
CHOSE σ_{\min} CONSTANT, VARIED σ_{\max}

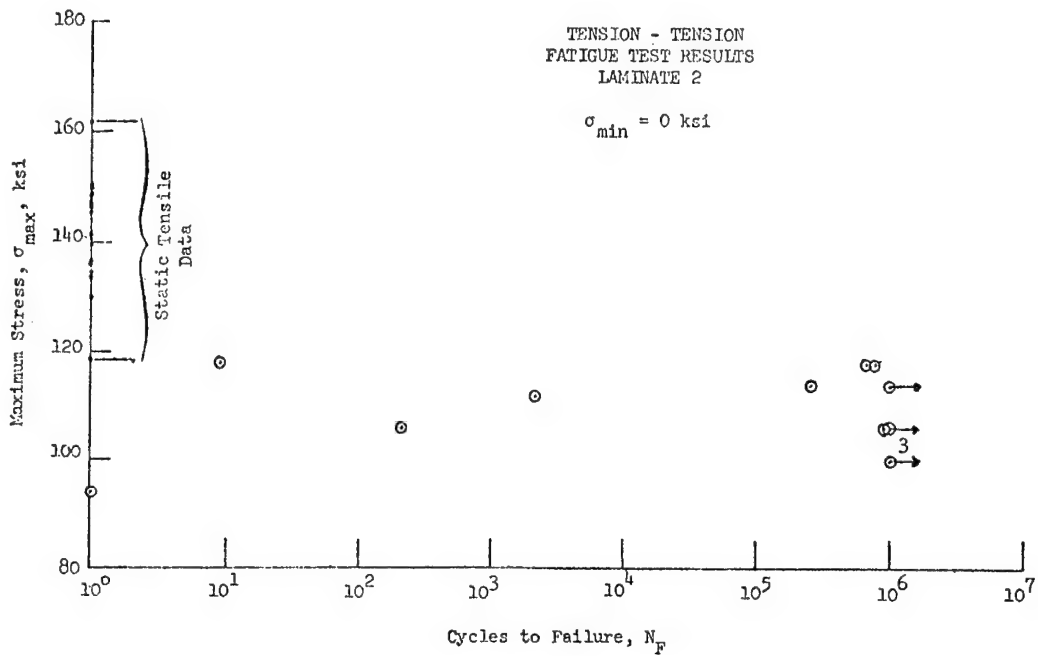
ALLOWED COMPARISON BY $\Delta\sigma$ AND σ_{\max}

TEST FREQUENCY, 10 Hz



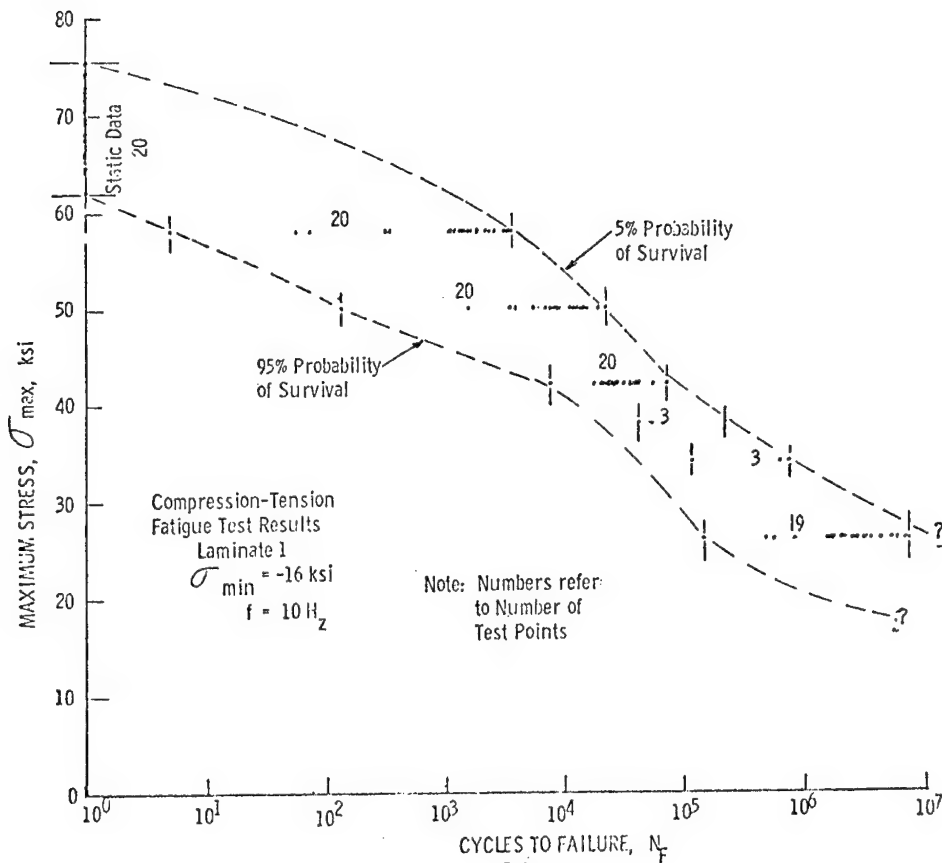
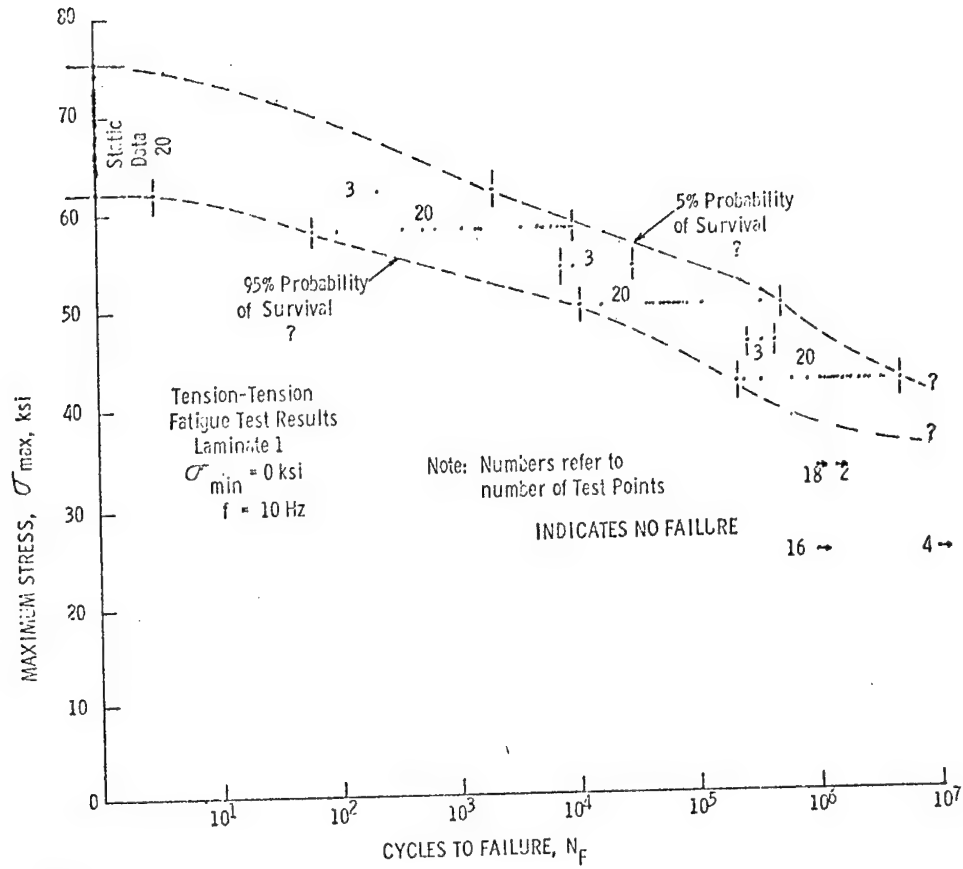


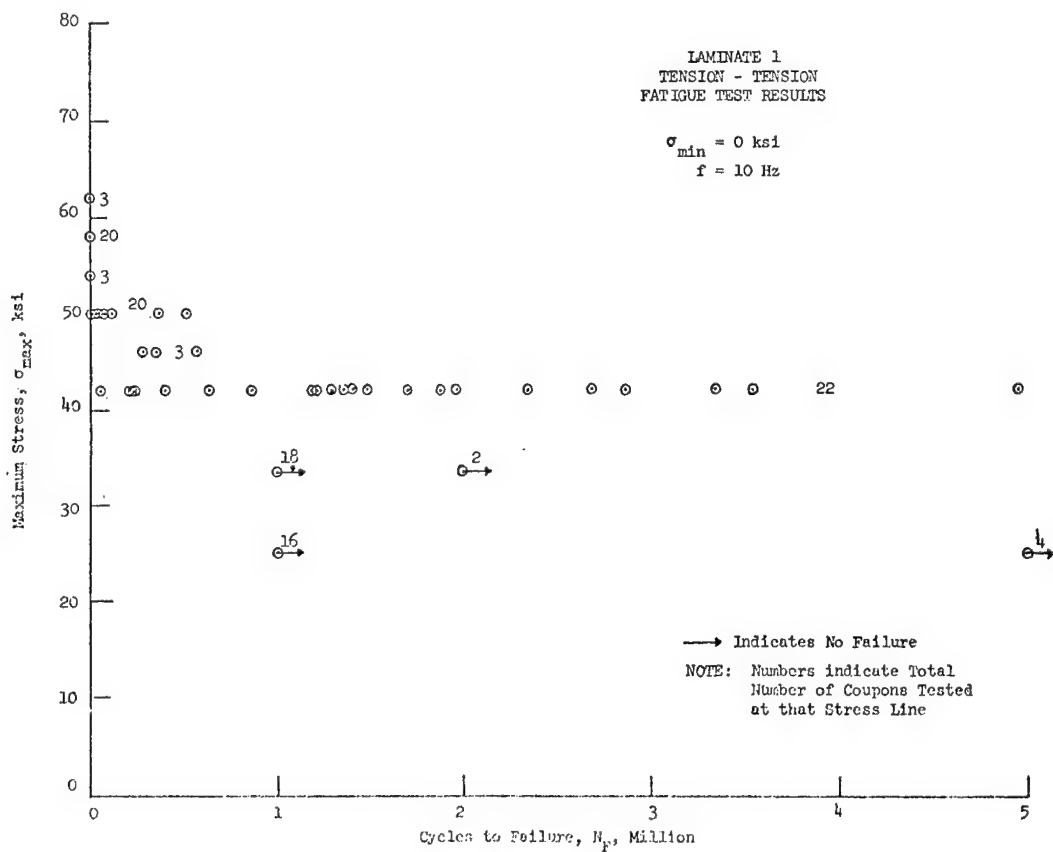
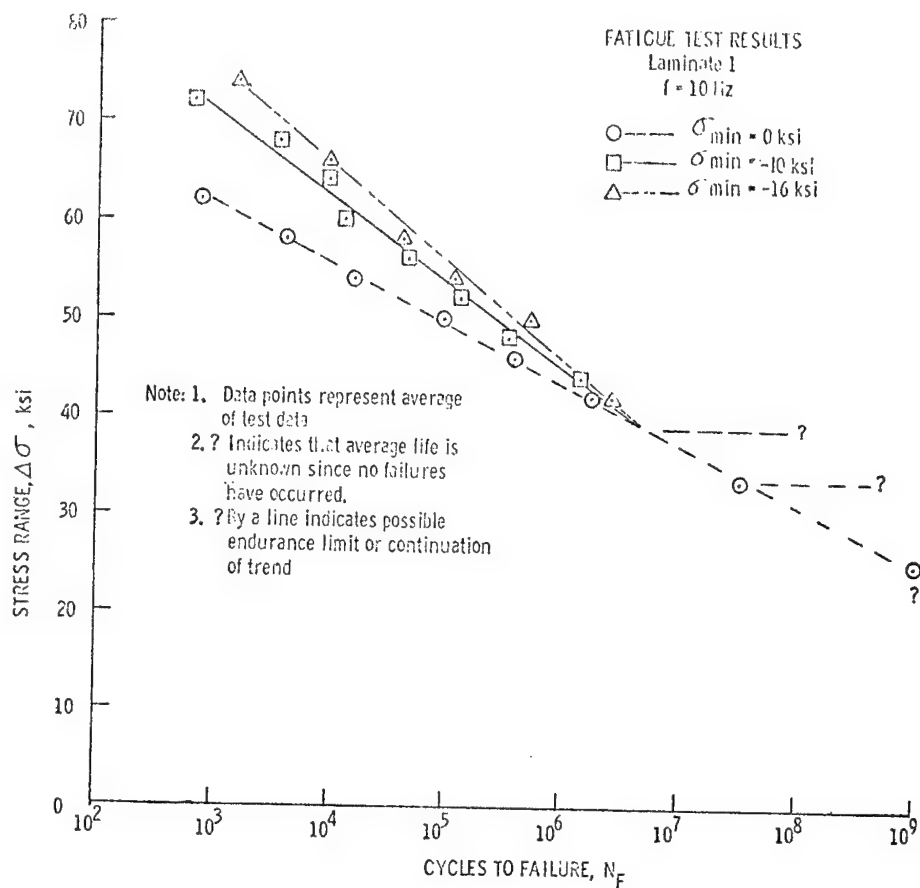


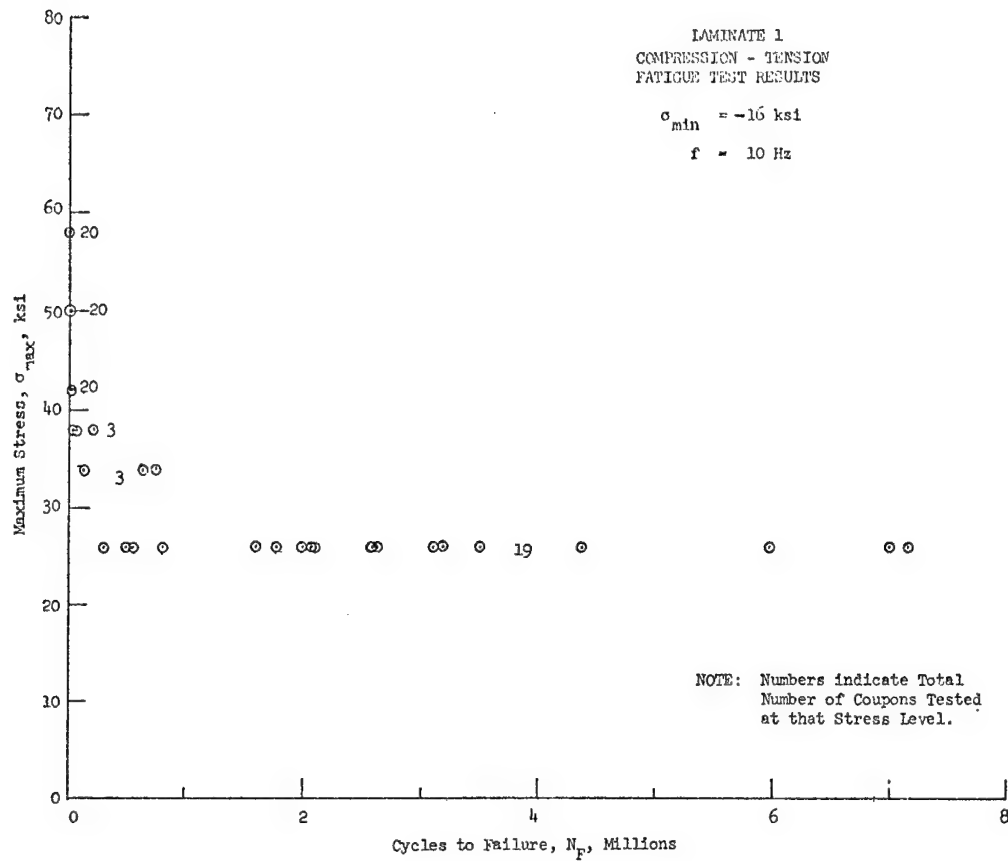


FATIGUE RESULTS

- CHOSE SPECIFIC σ_{\max} LEVELS
- TWENTY COUPON / σ LEVEL
- PICKED SPECIFIC STRESS LEVELS FOR RESIDUAL STRENGTH STUDY

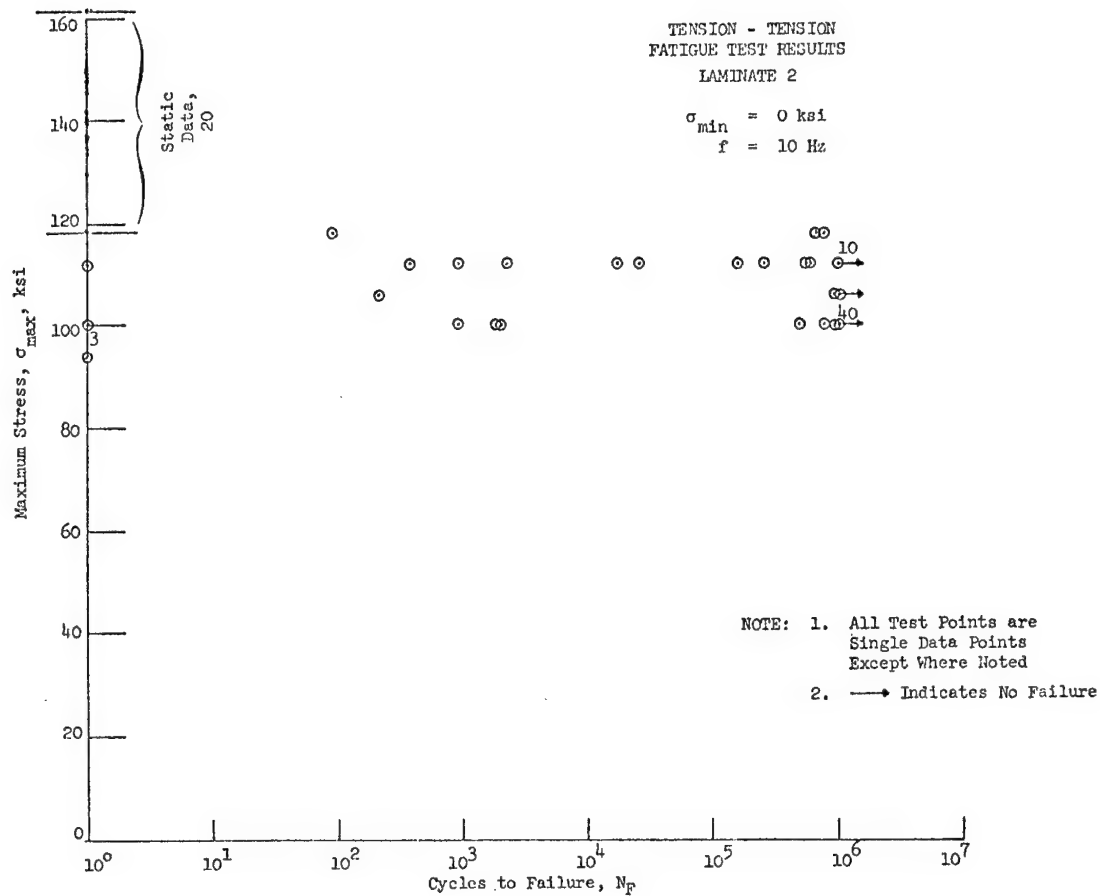


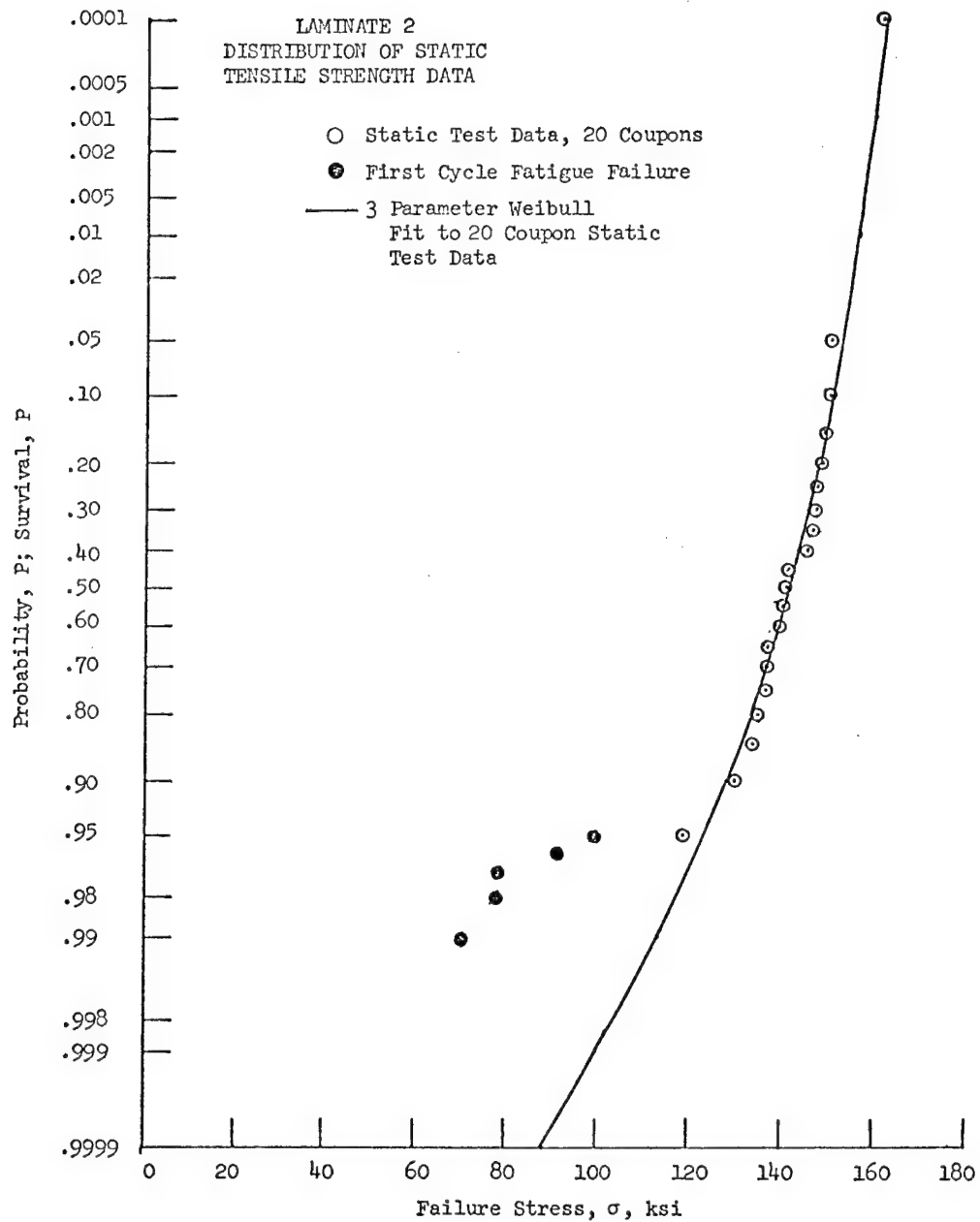




WEIBULL PARAMETERS
LAMINATE 1

Stress ksi		k	e	v
max	min			
58	0	1.988	- 2,030	4,899
50	0	4.564	- 20,711	64,621
42	0	1.846	-280,781	1,900,898
58	-16	2.409	- 1,015	1,979
50	-16	2.796	- 4,973	10,964
42	-16	2.915	- 3,040	33,806
26	-16	1.214	+ 74,246	2,892,580





RESIDUAL STRENGTH STUDY - LAMINATE 1

- COUPONS FATIGUED TO $P_{.90}$ AT EACH σ LEVEL
- FAILED COUPONS REPLACED
- 40 COUPONS/ σ LEVEL, 1/2 T AND 1/2 C
- FAILURE MODE SAME AS PREVIOUS T AND C, DISSIMILAR TO FATIGUE

RESIDUAL STRENGTH STUDY LAMINATE 1

FATIGUE STRESS LEVEL, KSI	LOWEST TENSILE FAILURE STRESS, KSI	MODE, KSI	AVERAGE TENSILE STRENGTH KSI
0 TO 42	49.2	64.1	62.4
0 TO 50	54.6	66.7	65.1
-16 TO 42	59.0	68.2	67.2
-16 TO 50	58.3	69.0	67.7
STATIC TENSILE TEST	62.0	70.3	69.2

COUPONS FAILED IN FATIGUE NOT INCLUDED - FAILURE MODES DIFFER

SUMMARY OF RESIDUAL STRENGTH TESTS - LAMINATE 1
TENSILE

Fatigue Stress Level, ksi	Weibull Parameters			Average Ultimate Stress, σ_{avg} , ksi	Average Ultimate Strain, ϵ_{avg} , in./in.	Average Initial Slope, E_{avg} , psi x 10 ⁶
	k	e	v			
Tensile Test Results Before Fatigue	24.18 24.12	-0.0753 0	70.50 70.57	69.2	0.0096	7.64
0 to 42	12.12 11.88	-0.6276 0	64.52 65.04	62.4	0.0090	6.84
0 to 50	12.85 12.78	-0.1688 0	67.31 64.45	65.1	0.0093	7.01
-16 to 42	18.51 18.48	-0.0608 0	68.43 68.49	67.2	0.0094	7.17
-16 to 50	18.34 18.27	-0.1326 0	69.26 69.38	67.7	0.0095	7.13

SUMMARY OF RESIDUAL STRENGTH TESTS - LAMINATE 1
COMPRESSIVE

Fatigue Stress Levels, ksi	Weibull Parameters			Average Ultimate Stress, σ_{avg} , ksi	Average Ultimate Strain, ϵ_{avg} , in./in.	Average Initial Slope, E_{avg} , psi x 10 ⁶
	k	e	v			
Compressive Test Results Before Fatigue	12.09 11.94	-0.4572 0	72.19 72.53	69.7	0.0110	6.95
0 to 42	7.22 7.07	-0.6574 0	60.15 60.52	57.2	0.0098	6.37
0 to 50	13.02 12.94	-0.2053 0	65.62 65.79	63.7	0.0111	6.64
-16 to 42	12.54 12.46	-0.2387 0	67.25 67.45	65.3	0.0108	6.66
-16 to 50	14.74 14.52	-0.5418 0	70.34 70.82	68.6	0.0110	6.66

RESIDUAL STRENGTH STUDY - LAMINATE 2

- T-T COUPONS CYCLED TO 10^6 AT 0 TO 100 ksi
- C-T COUPONS CYCLED TO 10^6 AT -30 TO 70 ksi
- 40 COUPONS AT EACH CONDITION, 1/2 T & 1/2 C
- FAILED COUPONS REPLACED
- FAILURE MODE SAME AS PREVIOUS T & C

RESIDUAL STRENGTH STUDY - LAMINATE 2

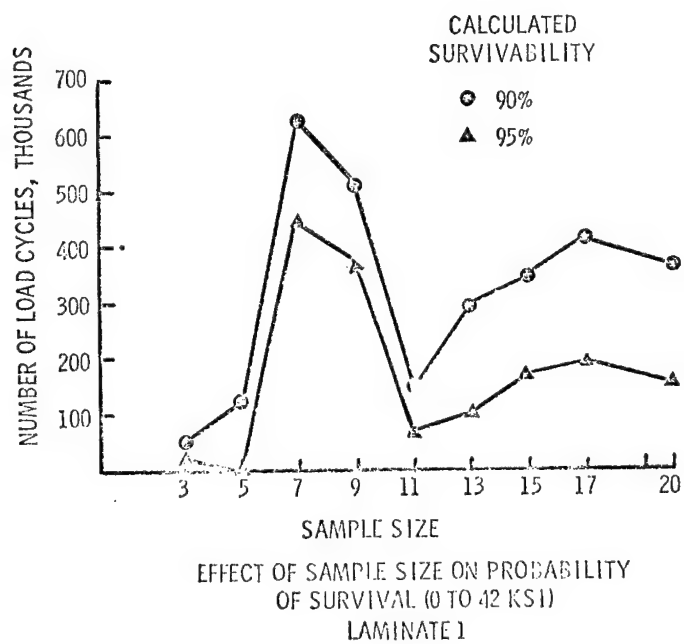
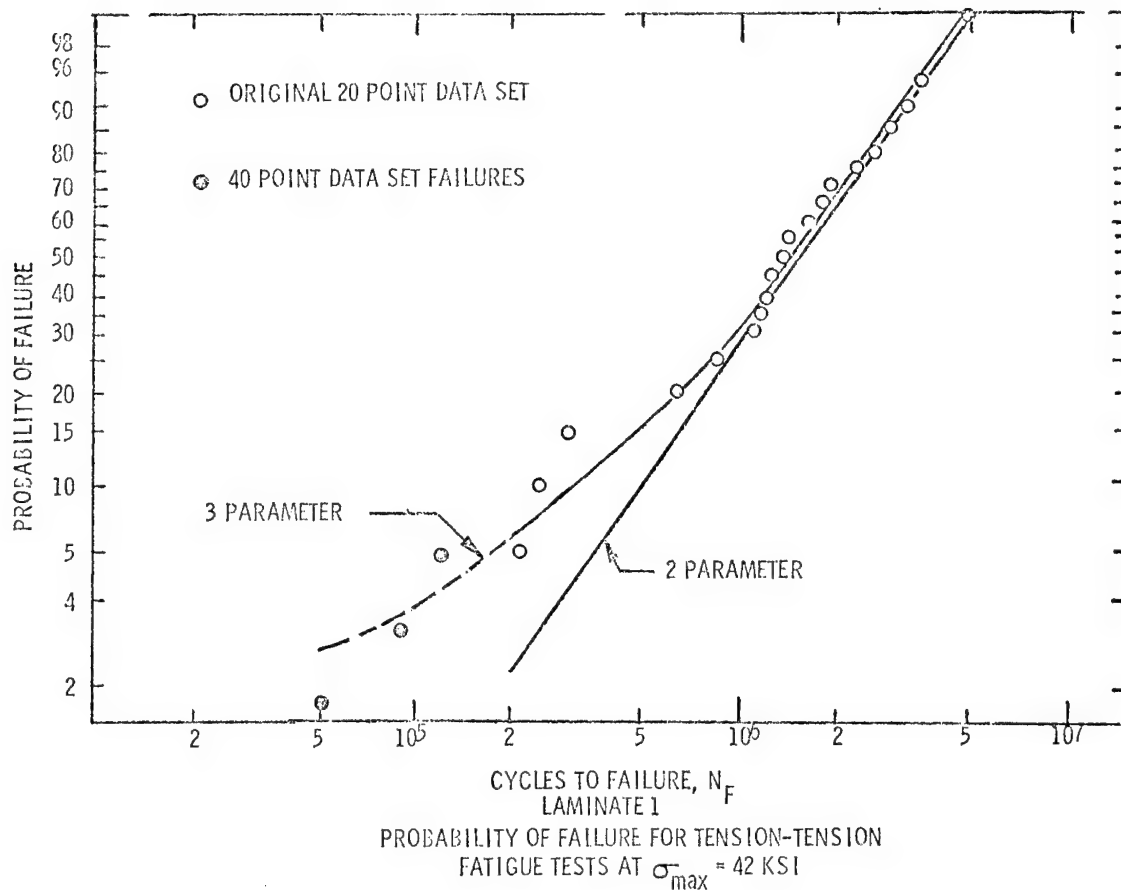
TYPE OF STATIC TEST T - TENSILE C - COMPRESSION	FATIGUE STRESS LEVEL ksi	WEIBUL PARAMETERS			AVERAGE ULTIMATE STRESS σ_{avg} , ksi	AVERAGE ULTIMATE STRAIN ϵ_{avg} , in./in.	AVERAGE INITIAL SLOPE E_{avg} , psi $\times 10^6$
		k	e	v			
T	TENSILE TEST RESULTS BEFORE FATIGUE	18.87	-0.4304	144.41	141.7	.0092	15.4
	0 to 100	17.19	-0.3926	146.81	143.5	.0092	15.7
	-30 to 70	21.57	-0.1409	146.42	143.7	.0094	15.3
C	COMPRESSION TEST RESULTS BEFORE FATIGUE	25.02	-0.2592	115.82	114.2	.0098	11.5
	0 to 100						
	-30 to 70						

LAMINATE 1
COMPARISON OF ACTUAL AND PREDICTED FAILURE
RATES AT P_{.90}
(THREE PARAMETER WEIBULL ANALYSIS)

TOTAL SAMPLE SIZE	240
FAILURES	24
PREDICTED FAILURES	23

LAMINATE 1
COMPARISON OF ACTUAL AND PREDICTED FAILURE
RATES AT P_{.95}

TOTAL SAMPLE SIZE	240
FAILURES	12
PREDICTED FAILURES	12 (3 PARAMETER FIT)
PREDICTED FAILURES	19 (2 PARAMETER FIT)



SUMMARY

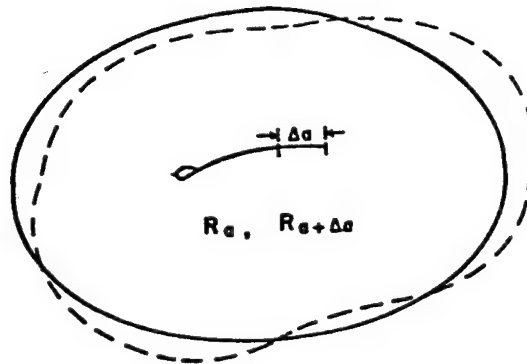
1. STATIC COMPRESSION SCATTER LARGER THAN TENSION
2. LARGE FATIGUE DATA SCATTER
3. COMPRESSION LOWERS FATIGUE LIFE
4. STATIC AND FATIGUE FAILURE MODES DIFFER
5. EFFECTS OF σ_{\max} AND $\Delta\sigma$ UNCLEAR, NEITHER CORRELATE WELL
6. LAMINATES 1 AND 2 DIFFER IN STATIC AND FATIGUE RESPONSE
7. FIRST CYCLE FATIGUE FAILURES OCCUR FOR LAMINATE 2; INDICATES LARGE STATIC STRENGTH SCATTER?
8. FOR LAMINATE 1, AT σ LEVELS WHERE FATIGUE FAILURE OCCURS, WEAROUT OCCURS
9. FOR LAMINATE 2, NO WEAROUT AT σ LEVELS WHERE FATIGUE FAILURE OCCURS
10. THREE PARAMETER FITS SHOULD BE USED FOR FATIGUE
11. SAMPLE SIZE TWENTY OR LARGER
12. CAN RESULTS BE EXTENDED TO LARGE COUPONS OR PANELS?

COMPOSITE STRUCTURE OPTIMAL
DESIGN BY ENERGY METHODS

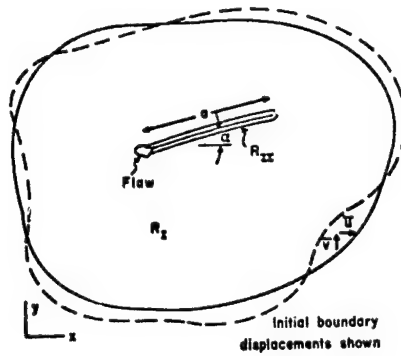
M. Murphy
Norwich University

OBJECTIVES: To formulate and test appropriate optimization criteria for the design of fail-safe aerospace composite structures. Since design criteria are based on failure modes and many composites of interest in aerospace applications fail by fracture, a specific research objective is the development of criteria predicting fracture onset, fracture path and fracture arrest.

ACCOMPLISHMENTS: A theory of fracture has been developed for a quasistatic, adiabatic fracture process based on the principle of maximum rate of entropy production. New minimum principles have been developed from the Calculus of Variations for predicting the crack path and crack initiation. Specifically, these developments lead to a theory of crack movement, a numerical procedure for crack initiation, conditions for crack arrest, and conditions for instability in the running crack. The numerical results for fracture in isotropic media are in agreement with results of other investigators. Presently, numerical methods applying these minimum principles to simple composite fracture are being developed and evaluated. A new test method for measuring the environmentally sensitive fiber-matrix interface fracture parameters is under evaluation also.



AN INCREMENT OF CRACK LENGTH



TWO REGIONS

$$dS = \frac{dQ}{\theta_0} + \frac{dW_{rev} - dW_{act}}{\theta_0} \geq 0$$

$$dS = - \frac{dI}{\theta_0} - \frac{Gda}{\theta_0} \geq 0$$

$$\frac{dS}{dt} = - \frac{1}{\theta_0} \frac{dI}{da} \frac{da}{dt} - \frac{G}{\theta_0} \frac{da}{dt} \geq 0$$

$$\frac{dS}{dt} = \frac{I}{\theta_0} \frac{da}{dt} \geq 0$$

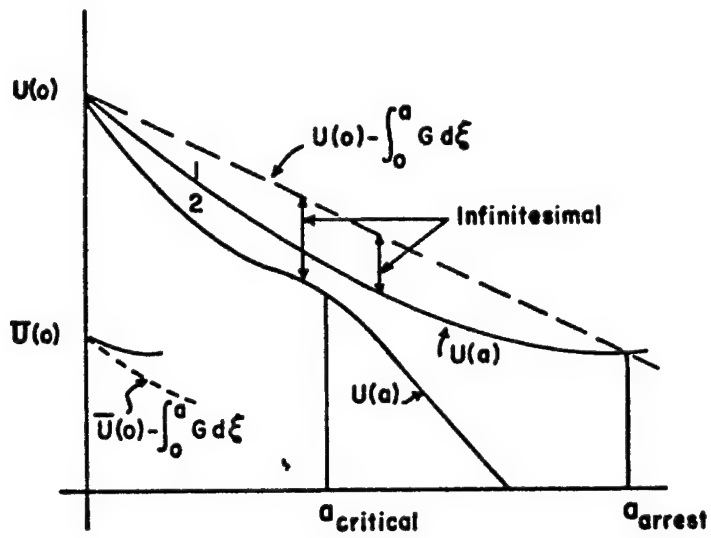
$$I \geq 0$$

$$I(\bar{a}, a) \geq I(a, a)$$

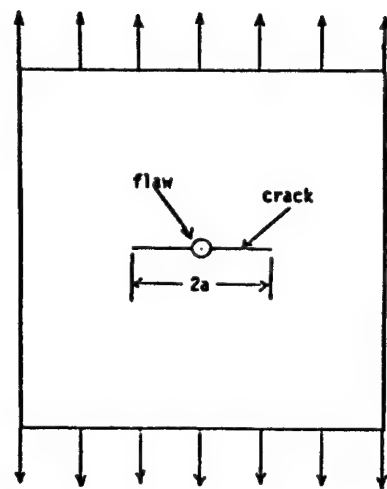
$$- \frac{\partial U(\bar{a}, a)}{\partial a} - \frac{\partial W_{ac}(\bar{a}, a)}{\partial a} \geq - \frac{\partial U(a, a)}{\partial a} - \frac{\partial W_{act}(a, a)}{\partial a}$$

$$U(\bar{a}, a) \leq U(a, a) + \int_0^a (G(a, \xi) - G(\bar{a}, \xi)) d\xi$$

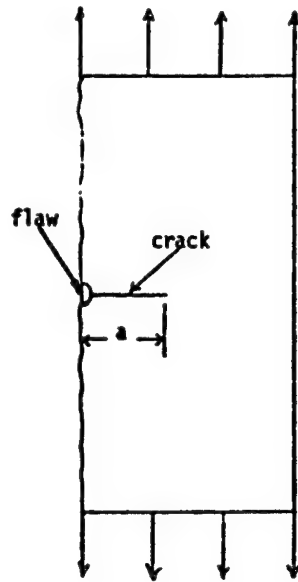
$$U(\bar{a}, a) \leq U(a, a)$$



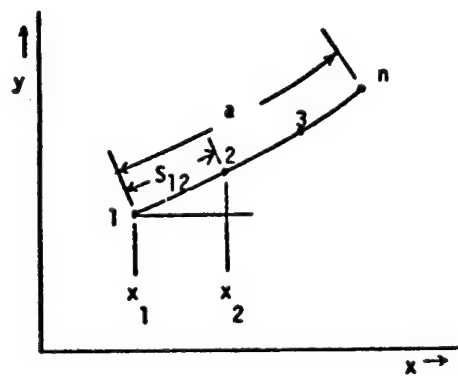
SUMMARY OF CONCEPTS



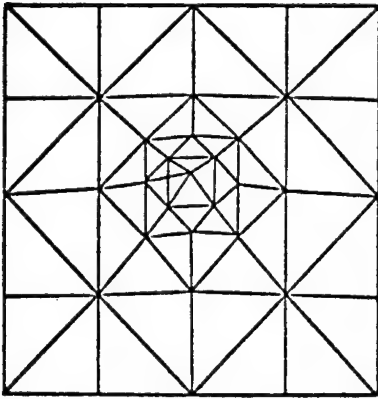
Crack in a Test Specimen



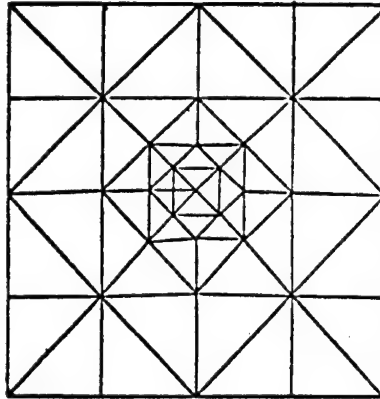
Actual Model to be Analyzed
Due to Symmetry



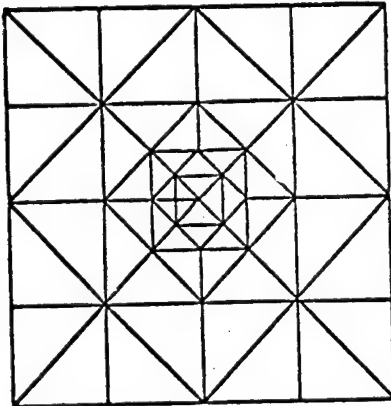
Crack Path Description.



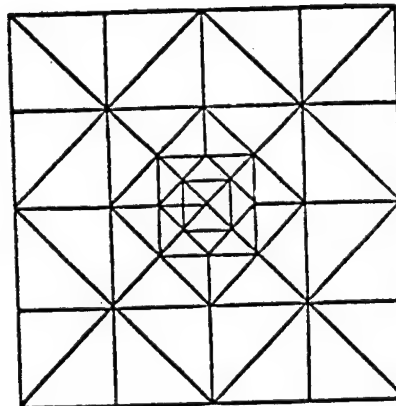
Initial Position of Crack



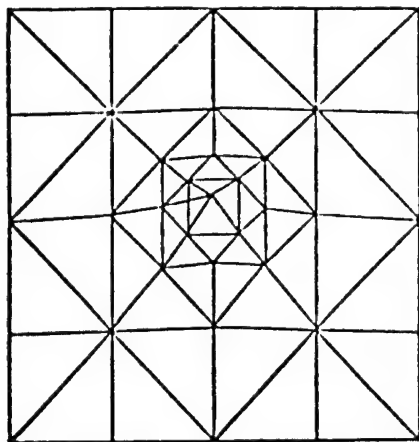
Final Position of Crack



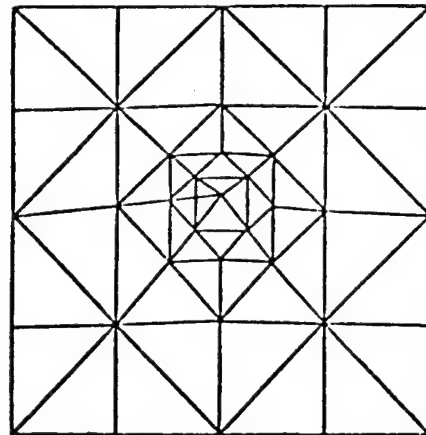
Initial Position of Crack



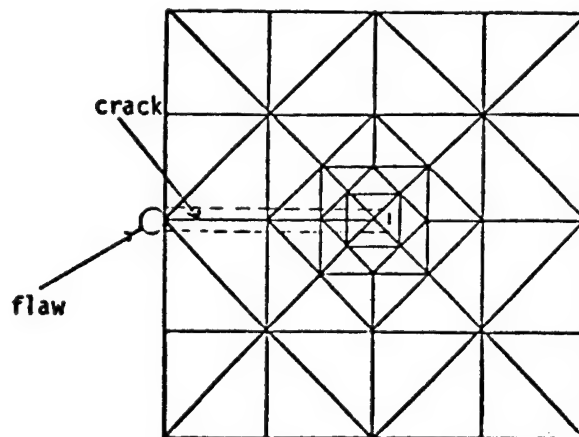
Final Position of Crack



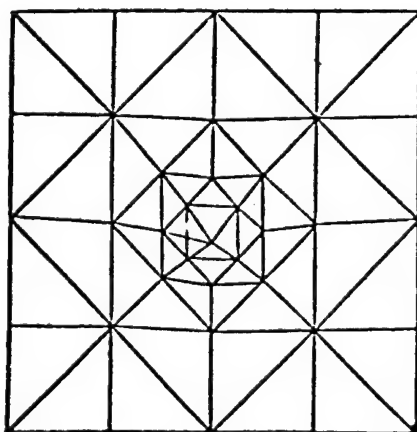
d



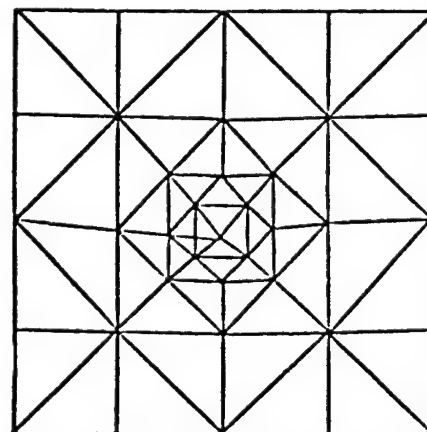
b



a

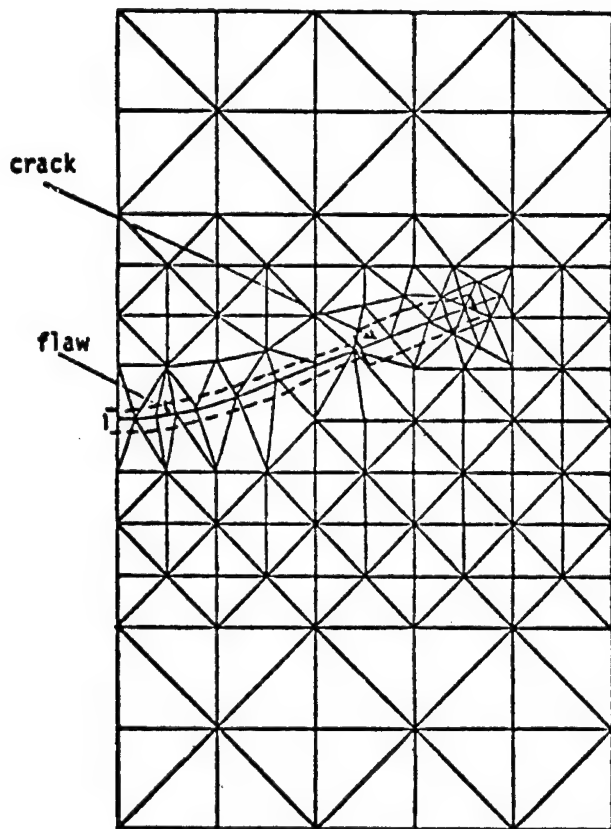


e

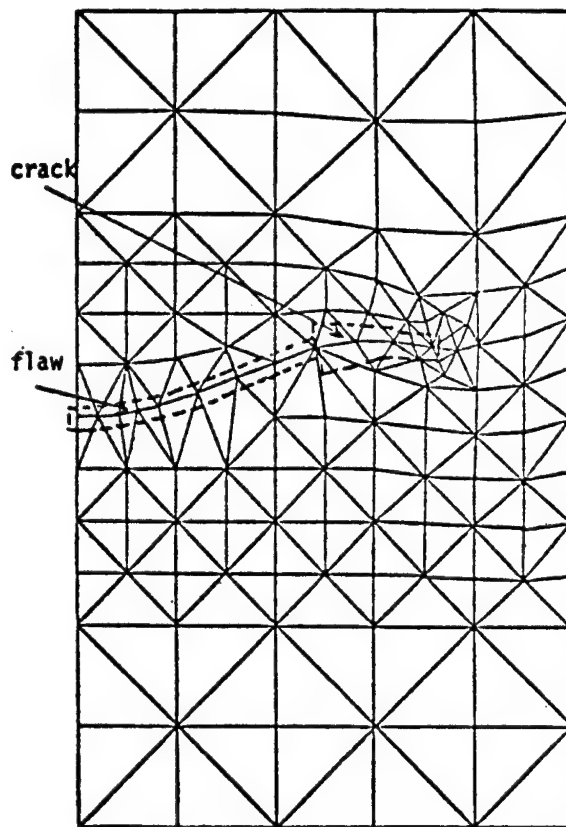


c

Mesh Used and Crack Movement in the Test Specimen.-



Initial Position of Crack



Final Position of Crack

	$\sigma_{\text{Extension}}$	Percent error
Model Results	$5.7 \times 10^3 \sqrt{G}$	-5%
Griffith Solution	$6 \times 10^3 \sqrt{G}$	-
Energy Difference Solution	$8.1 \times 10^3 \sqrt{G}$	+35%

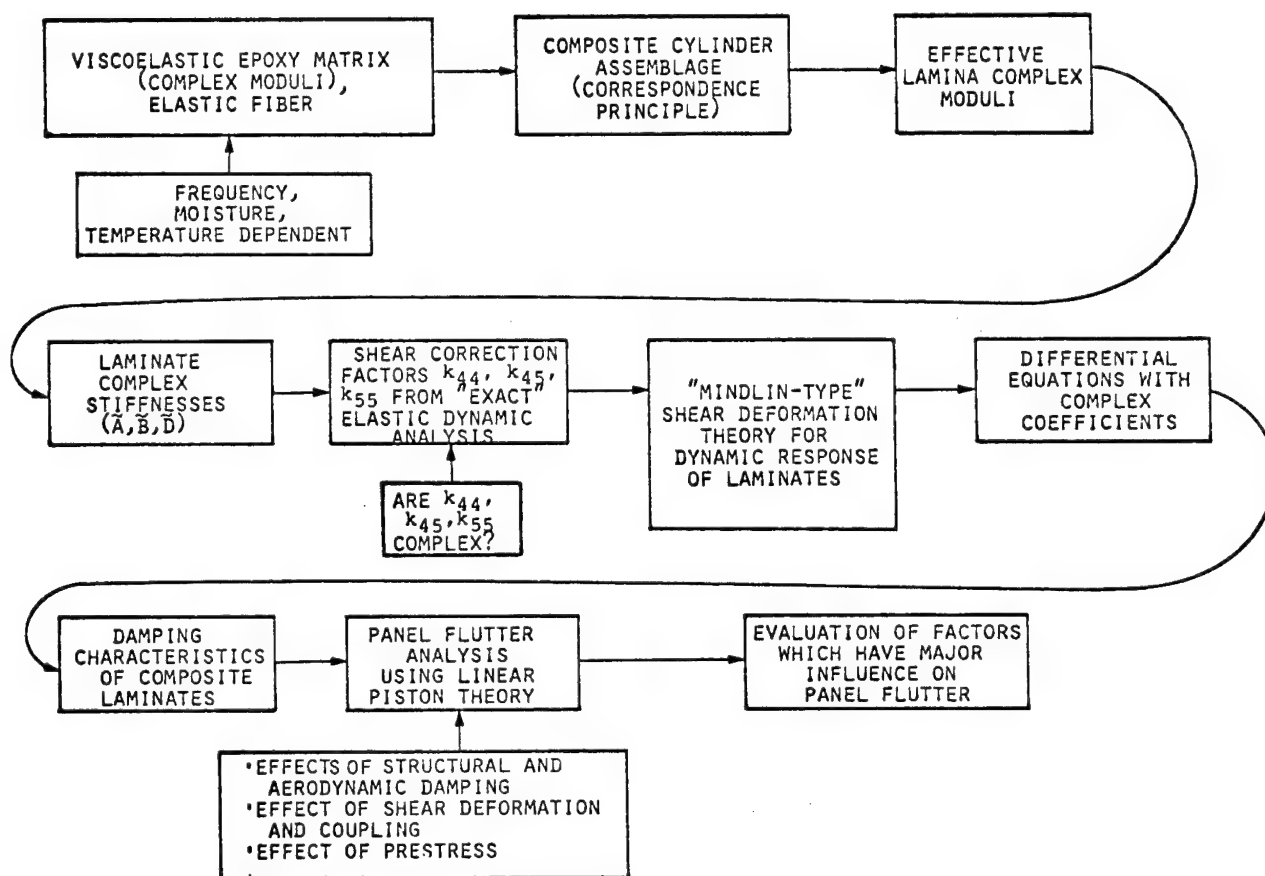
Griffith Solution Results

MATERIALS SCIENCES CORPORATION

EFFECTS OF ENVIRONMENT, AND DAMPING AND COUPLING PROPERTIES OF COMPOSITE LAMINATES ON PANEL FLUTTER (AFOSR CONTRACT F44620-76-C-0080)

OBJECTIVES

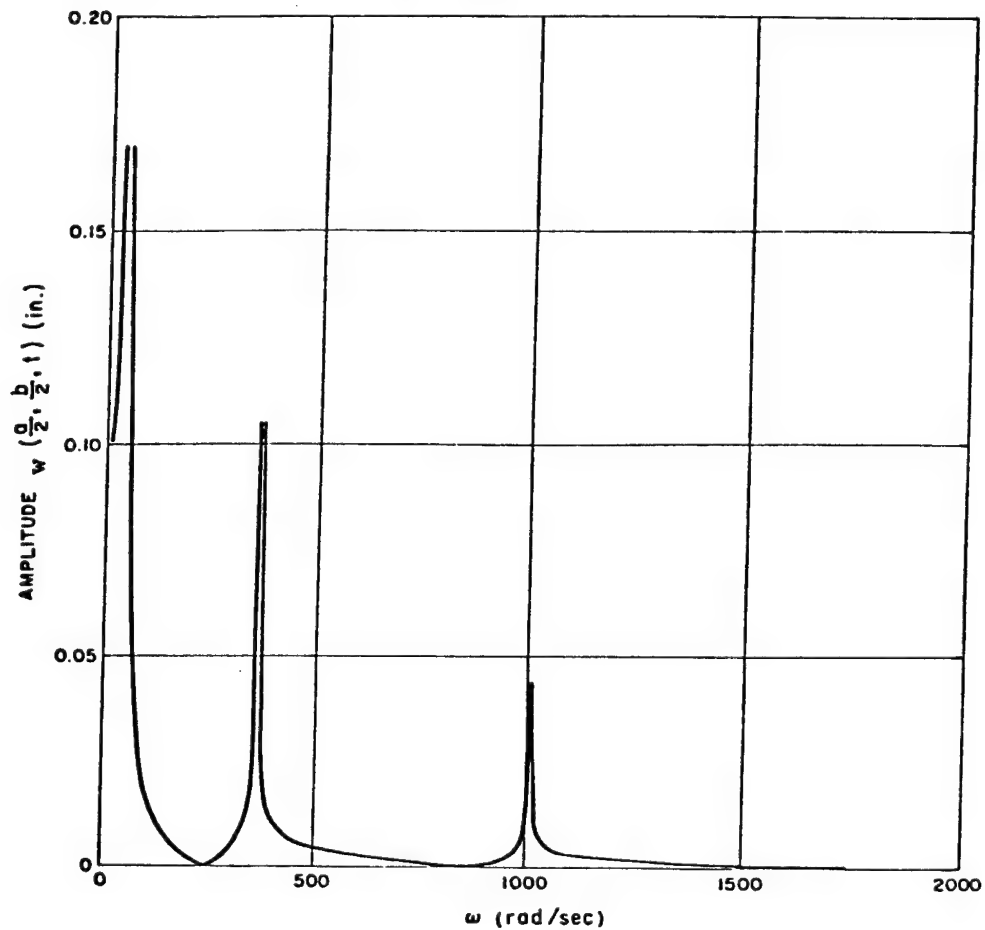
- I. DEVELOP EPOXY-MATRIX COMPOSITE LAMINATE CONSTITUTIVE RELATIONS WHICH ACCOUNT FOR THE EFFECTS OF LAMINAE STACKING SEQUENCE, TRANSVERSE SHEAR DEFORMATION, AND TIME-DEPENDENT BEHAVIOR IN A FORM THAT IS APPLICABLE TO STRUCTURAL DYNAMICS.
- II. EXTEND CONSTITUTIVE RELATIONS UNDER "I." TO CONSIDER EFFECTS OF MOISTURE ABSORPTION AND ELEVATED TEMPERATURE ON EPOXY-MATRIX ADVANCED COMPOSITES.
- III. EVALUATE DAMPING CHARACTERISTICS OF COMPOSITE PANELS USING CONSTITUTIVE THEORY DEVELOPED.
- IV. PERFORM PANEL FLUTTER ANALYSIS USING LINEAR PISTON THEORY AERODYNAMICS AND THE CONSTITUTIVE THEORY DEVELOPED. QUANTITATIVELY EVALUATE COMPOSITE MATERIAL AND DESIGN FACTORS WHICH HAVE MAJOR INFLUENCE ON PANEL FLUTTER.



I. LAMINATE CONSTITUTIVE RELATIONS

OBSERVATIONS

- DAMPING IS AN INHERENT PROPERTY IN FIBER-REINFORCED EPOXY-MATRIX COMPOSITES.
- BENEFICIAL EFFECT IS THE ATTENUATION OF PEAKS AT RESONANCE (PARTICULARLY AT HIGHER FREQUENCIES).



AMPLITUDE OF LATERAL DEFLECTION OF A VISCOELASTIC PLATE AS A
FUNCTION OF FREQUENCY

APPROACH

EFFECTIVE COMPLEX MODULI OF LAMINA

- CONSTITUTIVE RELATIONS FOR CONSTITUENTS ARE KNOWN FROM DYNAMIC EXPERIMENT
- EPOXY-MATRIX IS VISCOELASTIC; FIBER IS ELASTIC
- DYNAMIC CORRESPONDENCE PRINCIPLE IS USED FOLLOWING HASHIN; PARTICULARLY SUITABLE WHEN ELASTIC MODULI ARE OF A FORM EXPLICIT IN TERMS OF THE MODULI OF THE CONSTITUENT MATERIAL

$$\tilde{E}_A^* = v^f \tilde{E}_A^f + v^m \tilde{E}_A^m + \frac{4(\tilde{v}_A^f - \tilde{v}_A^m)^2 v^f v^m}{\frac{v^m}{\tilde{K}^f} + \frac{v^f}{\tilde{K}^m} + \frac{1}{\tilde{G}_T^m}}$$

(~ indicates complex moduli)

$$\tilde{v}_A^* = v^f \tilde{v}_A^f + v^m \tilde{v}_A^m + \frac{v^f v^m (\tilde{v}_A^f - \tilde{v}_A^m) (\frac{1}{\tilde{K}^m} - \frac{1}{\tilde{K}^f})}{\frac{v^m}{\tilde{K}^f} + \frac{v^f}{\tilde{K}^m} + \frac{1}{\tilde{G}_T^m}}$$

$$\tilde{G}_A^* = \tilde{G}_A^m \frac{v^m \tilde{G}_A^m + (1 + v^f) \tilde{G}_A^f}{(1 + v^f) \tilde{G}_A^m + v^m \tilde{G}_A^f}$$

$$\tilde{K}^* = \frac{v^m \tilde{K}^m (\tilde{K}^f + \tilde{G}_T^m) + v^f \tilde{K}^f (\tilde{K}^m + \tilde{G}_T^m)}{v^m (\tilde{K}^f + \tilde{G}_T^m) + v^f (\tilde{K}^m + \tilde{G}_T^m)}$$

$$\tilde{G}_T^* = \tilde{G}_T^m \frac{C_1}{C_2}$$

$$\tilde{E}_T^* = \frac{4\tilde{K}^* \tilde{G}_T^*}{\tilde{K}^* + (1 + \frac{4\tilde{K}^* \tilde{V}_A^* \tilde{V}_A^*}{\tilde{E}_A^*}) \tilde{G}_T^*}$$

$$\tilde{V}_T^* = \frac{\tilde{E}_T^*}{2\tilde{G}_T^*} - 1$$

where V^m and V^f are the volume fractions of matrix and fibers in the fiber bundle, respectively,

$$C_1 = (\frac{\gamma + \beta^m}{\gamma - 1} + \beta^m V^f) (1 + (\frac{\beta^m - \gamma \beta^f}{1 + \gamma \beta^f}) (V^f)^3) - 3V^f (V^m)^2 (\beta^m)^2 ,$$

$$C_2 = (\frac{\gamma + \beta^m}{\gamma - 1} - V^f) (1 + \frac{\beta^m - \gamma \beta^f}{1 + \gamma \beta^f} (V^f)^3) - 3V^f (V^m)^2 (\beta^m)^2$$

$$\gamma = \frac{\tilde{G}_T^f}{\tilde{G}_T^m} ,$$

$$\beta^m = \frac{1}{1 + \frac{2\tilde{G}_T^m}{\tilde{K}^m}} \quad \text{and} \quad \beta^f = \frac{1}{1 + \frac{2\tilde{G}_T^f}{\tilde{K}^f}}$$

LAMINATE COMPLEX STIFFNESSES

- OBTAINED FROM LAMINA EFFECTIVE COMPLEX MODULI AND ASSUMED DISPLACEMENT FIELD

$$(\tilde{A}_{ij}, \tilde{B}_{ij}, \tilde{D}_{ij}) = \int_{-h/2}^{h/2} \tilde{Q}_{ij} (1, z, z^2) dz \quad (i, j = 1, 2, 6)$$

$$\tilde{Q}_{ij} = \tilde{C}_{ij} - \frac{\tilde{C}_{i3}}{\tilde{C}_{33}} \tilde{C}_{3\alpha} \quad (\text{PLANE STRESS REDUCED STIFFNESSES})$$

$$\tilde{A}_{ij} = k_{ij} \int_{-h/2}^{h/2} \tilde{C}_{ij} dz \quad (i, j = 4, 5)$$

\tilde{C}_{ij} = LAMINA COMPLEX STIFFNESS MATRIX

k_{ij} = SHEAR CORRECTION FACTORS FOR TRANSVERSE SHEAR (REAL)

- CAN k_{ij} BE COMPLEX?

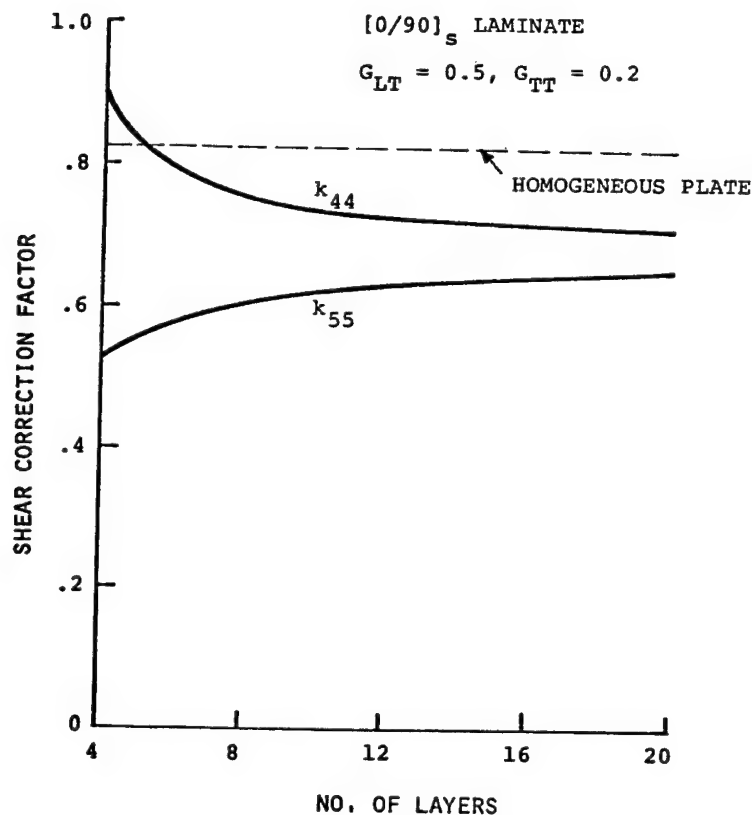
EXAMPLE

$$\tilde{A}_{ij}^R(\omega) = A_{ij}^R(\omega) + i A_{ij}^I(\omega) = A_{ij}^R(\omega) \left\{ 1 + i \frac{A_{ij}^I(\omega)}{A_{ij}^R(\omega)} \right\}$$

$$\frac{A_{ij}^I(\omega)}{A_{ij}^R(\omega)} = \text{LOSS FACTOR}$$

TRANSVERSE SHEAR DEFORMATION EFFECTS

- RATIOS OF E_L/G_{LT} OR E_L/G_{TT} FOR COMPOSITES HIGHER THAN ISOTROPIC MATERIALS.
- "SOFTER" MATERIAL IN SHEAR INCREASES THE IMPORTANCE OF SHEAR DEFORMATION.
- SINCE STRUCTURAL DAMPING IN VIBRATING LAMINATED BEAM/PLATES ARISES PRIMARILY DUE TO INTERLAMINAR SHEAR, THE COUPLED EFFECT OF SHEAR DEFORMATION AND DAMPING MAY BE IMPORTANT.
- UTILIZE A SHEAR DEFORMATION THEORY WHICH CONSIDERS SHEAR CORRECTION FACTORS FOR OBTAINING LAMINATE DYNAMIC VISCOELASTIC CONSTITUTIVE EQUATIONS.
- DETERMINE THE SHEAR CORRECTION FACTORS AS A FUNCTION OF STACKING SEQUENCE AND LAMINATE CONSTRUCTION FROM "EXACT" ELASTIC ANALYSIS.



SHEAR CORRECTION FACTOR
VS. NO. OF LAYERS

II. MOISTURE/TEMPERATURE EFFECTS

OBSERVATIONS

- EFFECT OF MOISTURE/TEMPERATURE IS TO ALTER LAMINA/LAMINATE COMPLEX MODULI (PARTICULARLY THOSE WHICH ARE MATRIX CONTROLLED).
- PLASTICIZING EFFECT OF MOISTURE/TEMPERATURE REDUCES THE STORAGE MODULUS AND INCREASES THE LOSS FACTOR (FOR EXAMPLE, MECHANICAL DAMPING INDEX PEAKS WHEN THE RELATIVE RIGIDITY DROPS AT $T = T_g$ FOR AN EPOXY; HOWEVER, DATA FOR COMPLEX DYNAMIC PROPERTIES OF EPOXIES/LAMINA FOR DIFFERENT MOISTURE CONTENTS AND TEMPERATURES ARE LACKING).

APPROACH

- DETERMINE LAMINA DIFFUSIVITIES FROM CONSTITUENT DIFFUSIVITIES (USING CONDUCTIVITY ANALOGY AND COMPOSITE CYLINDER ASSEMBLAGE RESULTS).
- DETERMINE THE THROUGH-THE-THICKNESS TRANSIENT/STEADY-STATE MOISTURE DISTRIBUTION IN A LAMINATE FROM THE 1-D DIFFUSION EQUATION.
- FOR THE TRANSIENT/STEADY STATES, DETERMINE EFFECT OF MOISTURE DISTRIBUTION ON LAMINATE PROPERTIES (USE APPROPRIATE KNOCK-DOWN FACTORS FOR STORAGE AND LOSS MODULI; ALSO, CONSIDER THE SITUATION WHEN SYMMETRIC LAMINATES MAY BEHAVE AS ASYMMETRIC LAMINATES WHEN MOISTURE DISTRIBUTION IS NOT SYMMETRIC).

III. DAMPING CHARACTERISTICS OF COMPOSITE PANELS

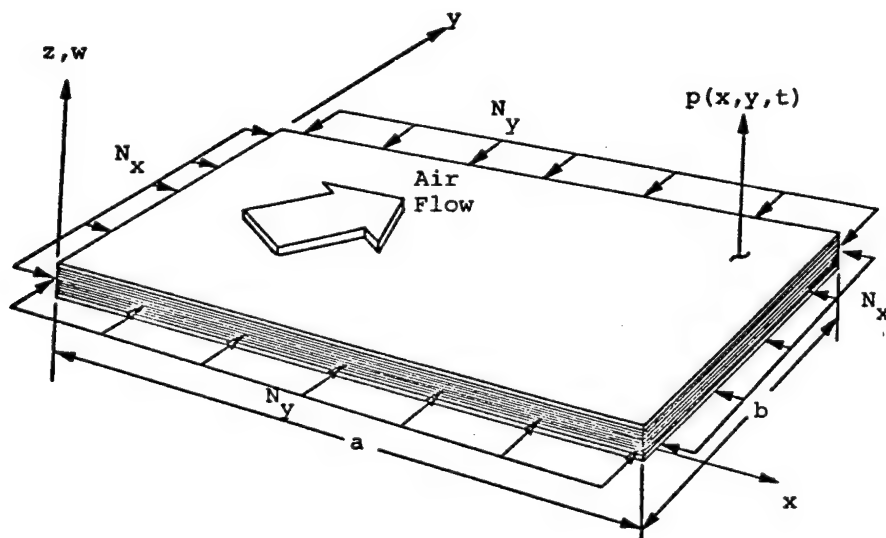
APPROACH

- INTEGRATE THE ANALYSES FOR THE DETERMINATION OF (A) DYNAMIC VISCOELASTIC PROPERTIES OF LAMINATES FROM CONSTITUENT PROPERTIES, (B) SHEAR (ELASTIC CASE) CORRECTION FACTORS FOR DIFFERENT LAMINATES, AND (C) MOISTURE/TEMPERATURE EFFECTS INTO A SINGLE PREDICTIVE TOOL (COMPUTER PROGRAM).
- COMPARE THE LAMINATE DYNAMIC COMPLEX MODULI AS A FUNCTION OF FREQUENCY OBTAINED FROM THE COMPUTER PROGRAM WITH EXPERIMENTAL DATA.
- DETERMINE THE DYNAMIC RESPONSE CHARACTERISTICS (PEAK AMPLITUDE VS. FREQUENCY; NO AERODYNAMIC LOADING) FOR LAMINATES.

IV. PANEL FLUTTER

APPROACH

- SOLVE THE CYLINDRICAL BENDING AND A FINITE SIZE PLATE FLUTTER PROBLEM USING GALERKIN PROCEDURE.
- INVESTIGATE THE EFFECTS OF:
 - STRUCTURAL DAMPING (DYNAMIC VISCOELASTIC LAMINATE PROPERTIES)
 - AERODYNAMIC DAMPING
 - PRESTRESS
 - SHEAR DEFORMATION WITH SHEAR CORRECTION FACTOR OBTAINED AS A FUNCTION OF STACKING SEQUENCE AND LAMINATE CONSTRUCTION.
 - BENDING/EXTENSION, BENDING/TWISTING COUPLING
 - MOISTURE/TEMPERATURE
- QUANTITATIVELY EVALUATE FACTORS WHICH HAVE MAJOR INFLUENCE ON PANEL FLUTTER.



PANEL CONFIGURATION AND COORDINATE SYSTEM

VARIOUS PLATE GEOMETRIES

- $y \rightarrow \infty$, S.S. ($x = 0, a$)
- $y \rightarrow \infty$, clamped ($x = 0$); free ($x = a$)
- S.S. ($x = 0, a$), ($y = 0, b$)

- SHEAR DEFORMATION THEORY FOR LAMINATED PLATES (AFTER WHITNEY & PAGANO) WITH COMPLEX, PLANE STRESS REDUCED STIFFNESSES AND THE SHEAR CORRECTION FACTORS k_{ij} INTRODUCED DIRECTLY INTO THE GOVERNING EQUATIONS.
- k_{ij} CALCULATED FOR EACH LAMINATE FROM THE THICKNESS SHEAR MODE CUT-OFF FREQUENCIES.
- FROM PISTON-THEORY AERODYNAMICS,

$$\text{AERODYNAMIC LOAD} = -\frac{2q}{\beta} (w_{,x} \cos \theta + w_{,y} \sin \theta) - \rho c w_{,t}$$

$$q = \text{FREE-STREAM DYNAMIC PRESSURE, } \frac{1}{2} \rho U^2$$

$$U = \text{FREE-STREAM AIR VELOCITY}$$

$$\beta = \text{COMPRESSIBILITY FACTOR, } \sqrt{M^2 - 1} \text{ (M IS THE MACH NUMBER)}$$

$$\theta = \text{FLOW ANGLE wrt X-AXIS}$$

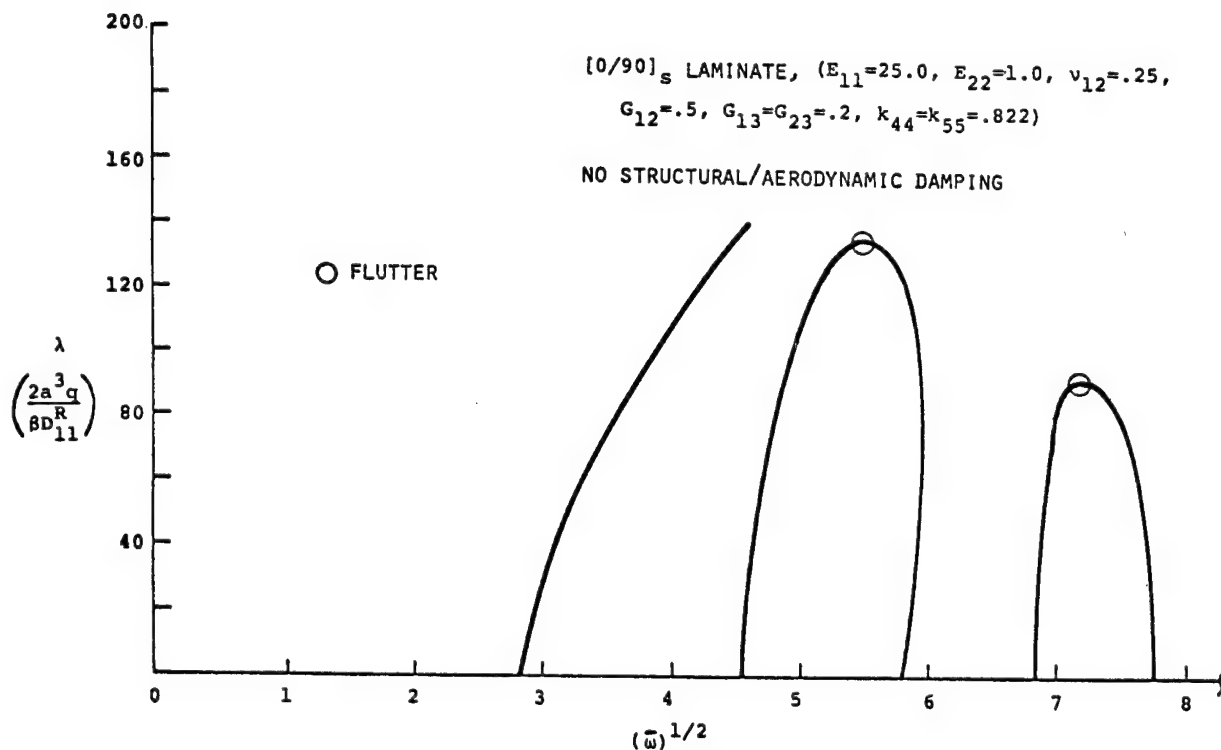
$$c = \text{FREE-STREAM SPEED OF SOUND}$$

$$\rho = \text{FREE-STREAM AIR DENSITY}$$

SO

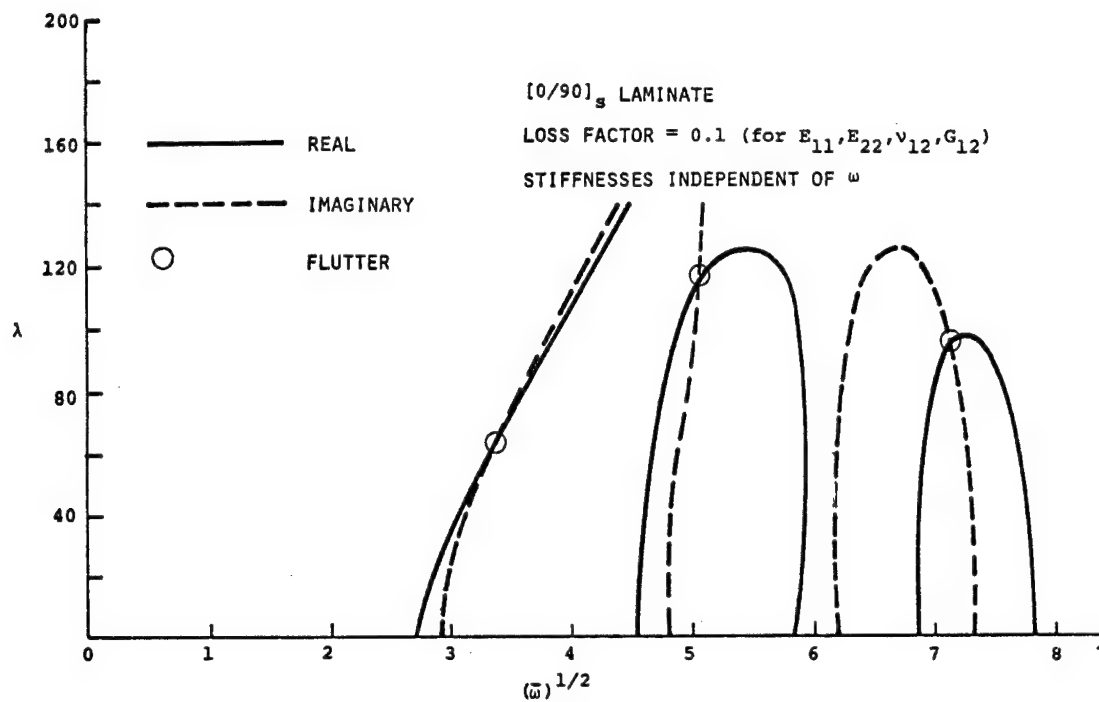
$$p(x,y,t) = -\rho_{\text{panel}} w_{,tt} + \text{AERODYNAMIC LOAD}$$

"FREQUENCY LOOPS" IN THE $\lambda, (\bar{\omega})^{1/2}$ PLANE (FOR FIRST FIVE MODES)

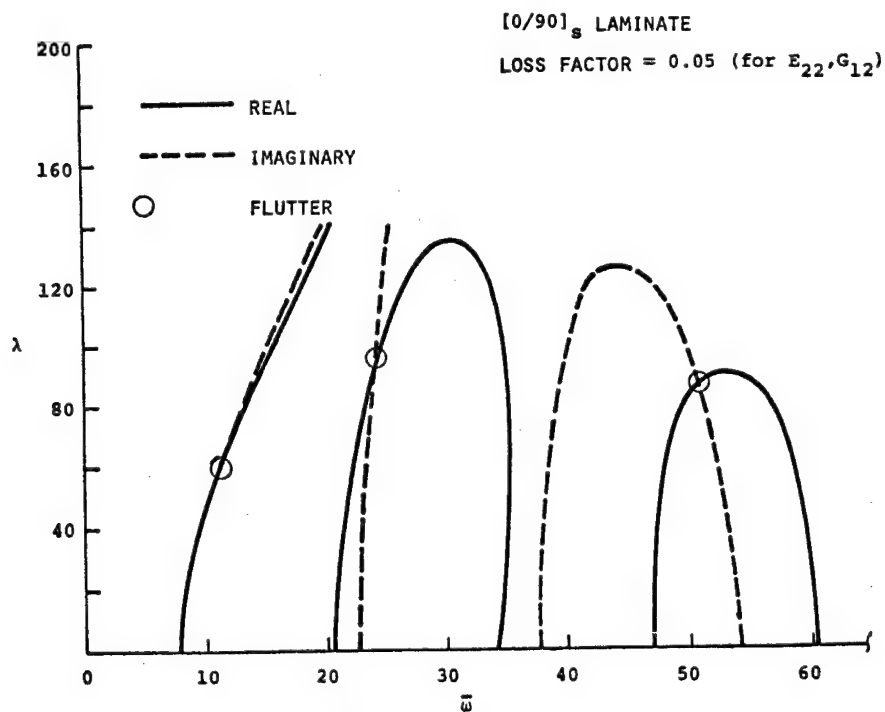


$$\left[\left(\frac{P}{D_{11}^R} \right)^{1/2} \omega a^2 \right]^{1/2}, P = \int \rho_{\text{lamina}} dz$$

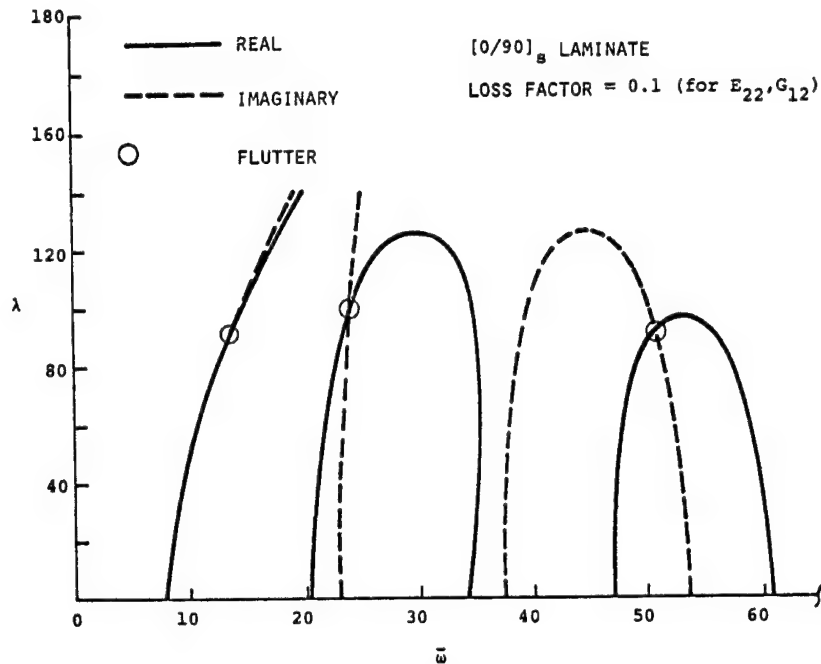
"FREQUENCY LOOPS" IN THE $\lambda, (\bar{\omega})^{1/2}$ PLANE



"FREQUENCY LOOPS" IN THE $\lambda, \bar{\omega}$ PLANE



"FREQUENCY LOOPS" IN THE $\lambda, \bar{\omega}$ PLANE



PRELIMINARY OBSERVATIONS

- CRITICAL VALUE OF FLUTTER PARAMETER λ IS REDUCED WHEN DAMPING IS CONSIDERED (TENDS TO CONFIRM EARLIER OBSERVATIONS THAT INSTABILITY LOAD IS LOWERED FOR NON-CONSERVATIVE SYSTEMS WITH DAMPING).
- FURTHER STUDY OF THIS PHENOMENON REQUIRED BY INVESTIGATING BEHAVIOR OF THE COMPLEX FREQUENCIES IN THE VICINITY OF FLUTTER POINTS (WHICH CORRESPOND TO REAL FREQUENCIES) AND INCLUSION OF THE FREQUENCY DEPENDENCE OF COMPLEX STIFFNESSES.

FRACTURE AND FATIGUE OF BI-MATERIALS

J. W. Mar

Massachusetts Institute of Technology

- FRACTURE
- FATIGUE
 - MECHANISMS
 - CORRELATION WITH
FRACTURE
MECHANICS

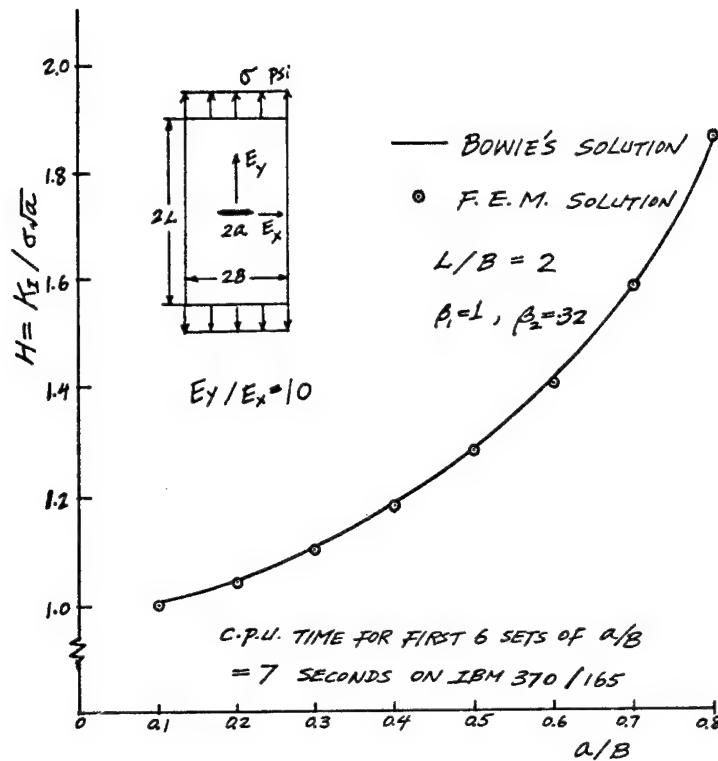


Fig. 1 COMPARISON OF F.E.M. SOLUTION WITH BOWIE'S SOLUTION FOR A CENTRAL CRACK IN AN ORTHOTROPIC STRIP.

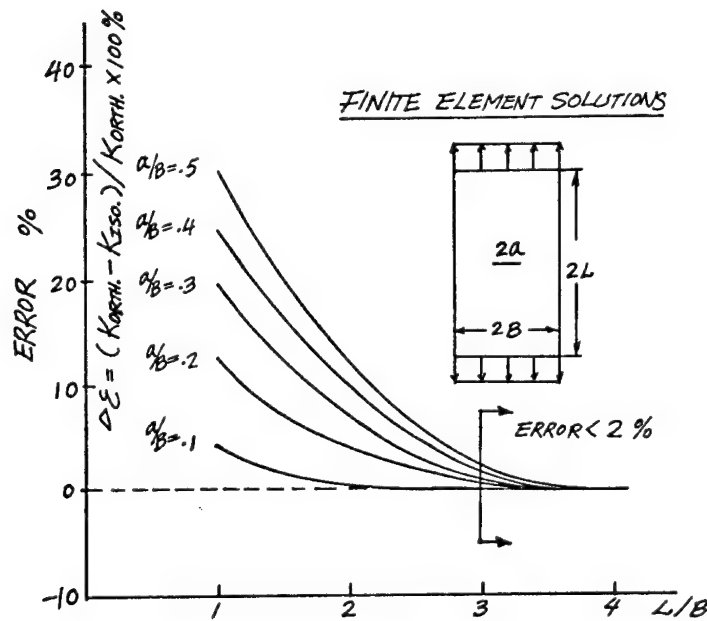


Fig. 2 ERRORS V.S. L/B FOR GRAPHITE/EPOXY [0] (CENTER CRACK)

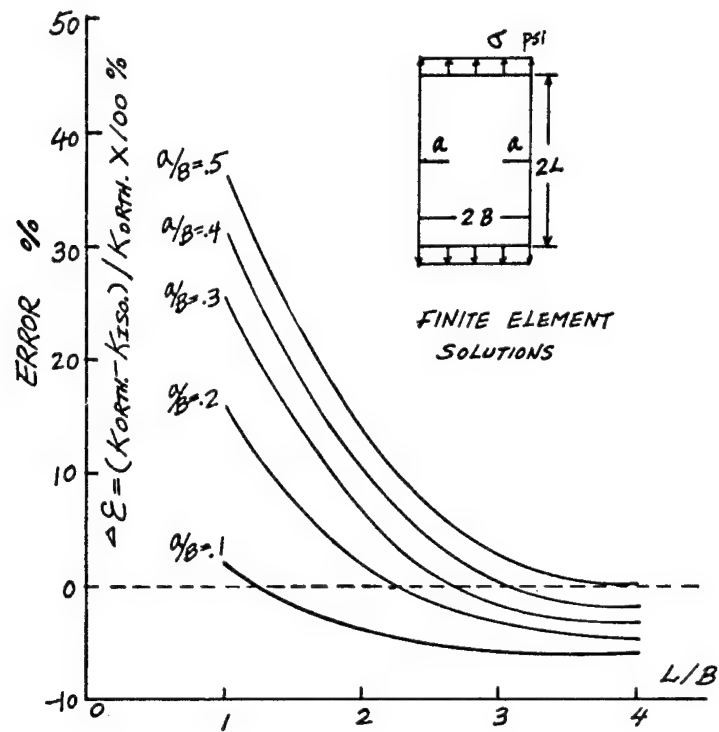


Fig. 3 ERRORS ΔE V.S. L/B
FOR GRAPHITE/EPOXY [0]
(DOUBLE EDGE CRACK)

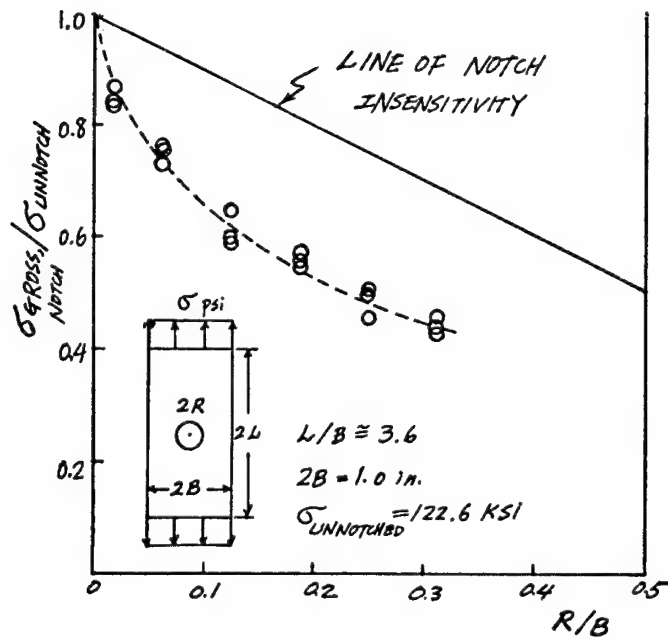


Fig. 4 B/AL ($\pm 45/0_2$)_s, CCN
NOTCH SENSITIVITY V.S. R/B

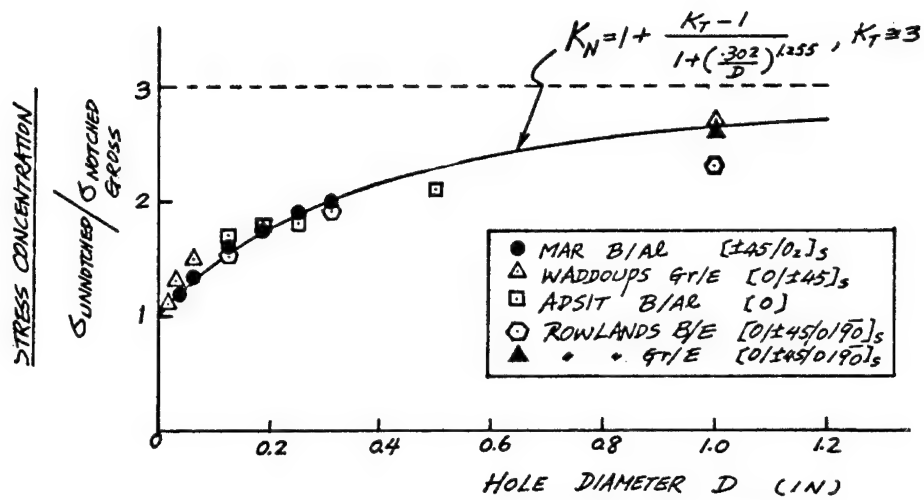


Fig. 5 COMPOSITES DATA CORRELATION WITH
 "MODIFIED NEUBER" EMPIRICAL MODEL

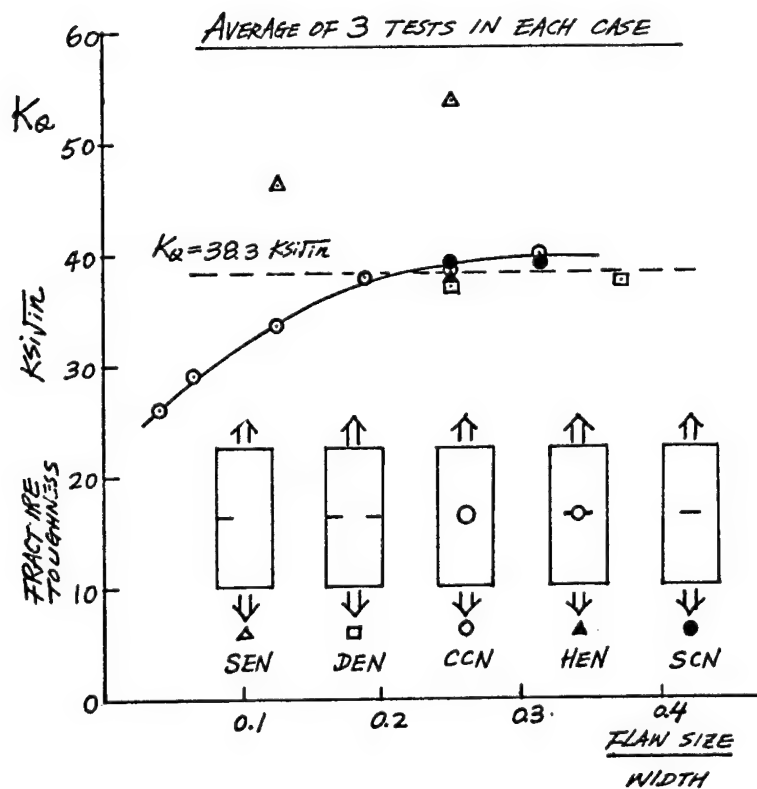


Fig. 6 K_Q V.S. FLAW SIZE FOR
 VARIOUS NOTCH GEOMETRIES

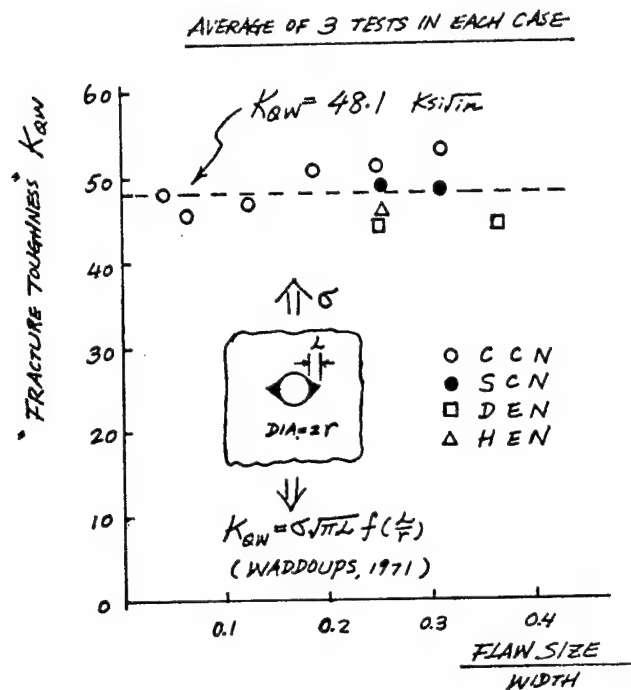


Fig. 7 "FRACTURE TOUGHNESS" WITH
INHERENT FLAW CONCEPT FOR
B/AL [$\pm 45/0_2$]_S

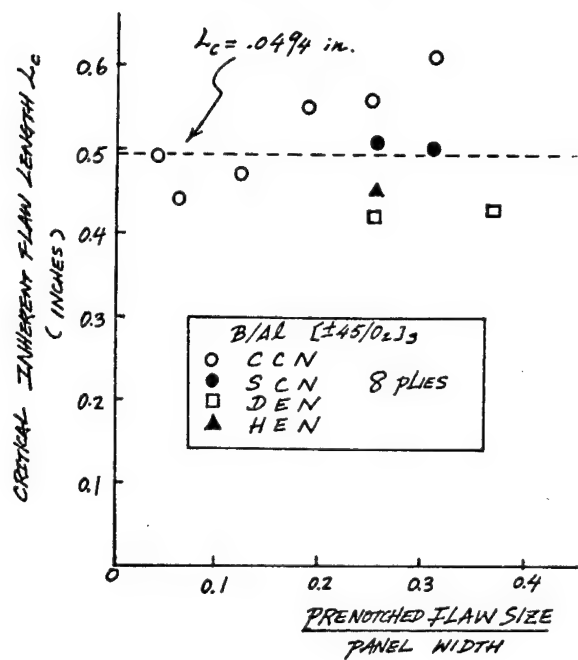


Fig. 8. CRITICAL INHERENT FLAW LENGTH
 L_c V.S. PRENOTCHED FLAW
SIZE FOR VARIOUS NOTCH
GEOMETRIES

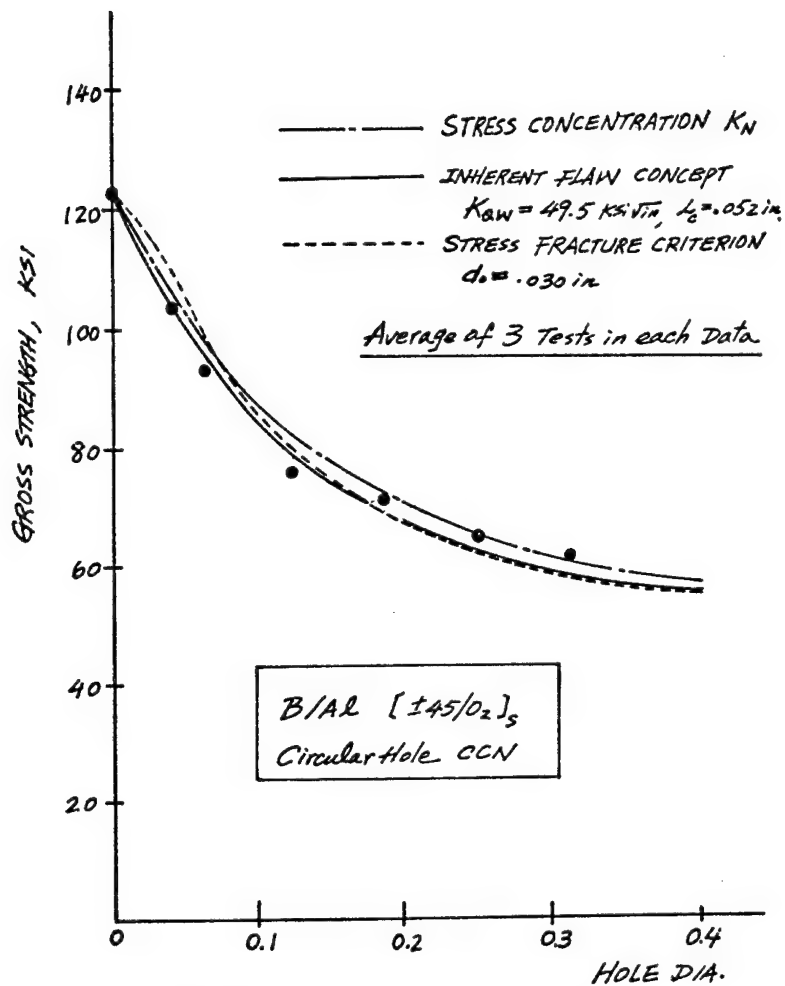


Fig. 9. STRENGTH PREDICTION FOR
 CCN NOTCH USING VARIOUS
 FRACTURE CRITERIA

BIAXIAL TESTING OF GRAPHITE/EPOXY
COMPOSITES CONTAINING STRESS CONCENTRATIONS

BY

I.M. DANIEL
IIT RESEARCH INSTITUTE
CHICAGO, ILLINOIS 60616

OBJECTIVE

DETERMINE EFFECT OF BIAXIAL LOADING ON DEFORMATION
AND FAILURE OF FLAT GRAPHITE/EPOXY LAMINATES WITH CIRCULAR
HOLES AND THROUGH THE THICKNESS CRACKS.

INVESTIGATE ALSO NOTCH SIZE EFFECT.

SCOPE

MATERIAL: SP-286T300 (3M COMPANY)

LAMINATE ORIENTATIONS: $[0/\pm 45/90]_s$, $[0_2/\pm 45]_s$

TESTS

- UNNOTCHED UNIAXIAL
- NOTCHED UNIAXIAL
- UNNOTCHED BIAXIAL
- NOTCHED BIAXIAL
- NOTCHED UNIAXIAL WITH INCLINED CRACKS
(EFFECT OF NORMAL STRESS IN DIRECTION OF CRACK)

PROCEDURE

- USE STRAIN GAGES, PHOTOELASTIC COATINGS AND MOIRÉ TO MEASURE STRAINS IN VICINITY OF DISCONTINUITY AND IN FAR FIELD
- DETERMINE STRAIN CONCENTRATIONS, STRAIN DISTRIBUTIONS, FAILURE MODES AND STRENGTH REDUCTION RATIOS
- CORRELATE EXPERIMENTAL RESULTS WITH EXISTING THEORY

Determine:

- Moduli: E_{11} , E_{22} , G_{12}
- Poisson's ratios: ν_{12} , ν_{21}
- Strengths: S_{11T} , S_{22T} ,
 S_{11C} , S_{22C} , S_{12}
- Ultimate strains: ϵ_{11T}^u , ϵ_{22T}^u ,
 ϵ_{11C}^u , ϵ_{22C}^u , ϵ_{12}^u

PROPERTIES OF UNIDIRECTIONAL GRAPHITE/EPOXY
SP-286T300

Property	Value
Ply Thickness	0.130 mm (0.0051 in.)
Longitudinal Modulus, E_{11}	151 GPa (21.9×10^6 psi)
Transverse Modulus, E_{22}	10.6 GPa (1.53×10^6 psi)
Shear Modulus, G_{12}	6.6 GPa (0.96×10^6 psi)
Major Poisson's Ratio, ν_{12}	0.31
Minor Poisson's Ratio, ν_{21}	0.014
Longitudinal Tensile Strength, S_{11T}	1401 MPa (203 ksi)
Ultimate Longitudinal Tensile Strain, ϵ_{11T}^u	0.00925
Longitudinal Compressive Strength, S_{11C}	1132 MPa (164 ksi)
Ultimate Longitudinal Compressive Strain, ϵ_{11C}^u	0.01040
Transverse Tensile Strength, S_{22T}	54 MPa (7.8 ksi)
Ultimate Transverse Tensile Strain, ϵ_{22T}^u	0.00541
Transverse Compressive Strength, S_{22C}	211 MPa (30.6 ksi)
Ultimate Transverse Compressive Strain, ϵ_{22C}^u	0.02565
In-plane Shear Strength, S_{12}	72 MPa (10.5 ksi)
Ultimate Shear Strain, ϵ_{12}^u	0.0110

UNNOTCHED UNIAXIAL TESTS

SPECIMENS: STANDARD 2.54 cm x 23 cm (1 in x 9 in)
COUPONS OF $[0/\pm 45/90]_s$ LAMINATE

TESTS: TWO TESTS EACH IN 0-DEG. AND 90-DEG.
DIRECTIONS

RESULTS:

Layup	Modulus E_{xx} GPa (10^6 psi)	Poisson's Ratio ν_{xy}	Strength S_{xxT} MPa (ksi)	Ultimate Strain ϵ_{xxT}^u ($10^{-3}\epsilon$)
$[0/\pm 45/90]_s$	57 (8.3)	0.31	502 (73)	10.0
$[90/\pm 45/0]_s$	55 (7.9)	0.30	541 (78)	10.3

STATIC TENSILE PROPERTIES OF UNNOTCHED [0₂/±45]_s GRAPHITE/EPOXY LAMINATES

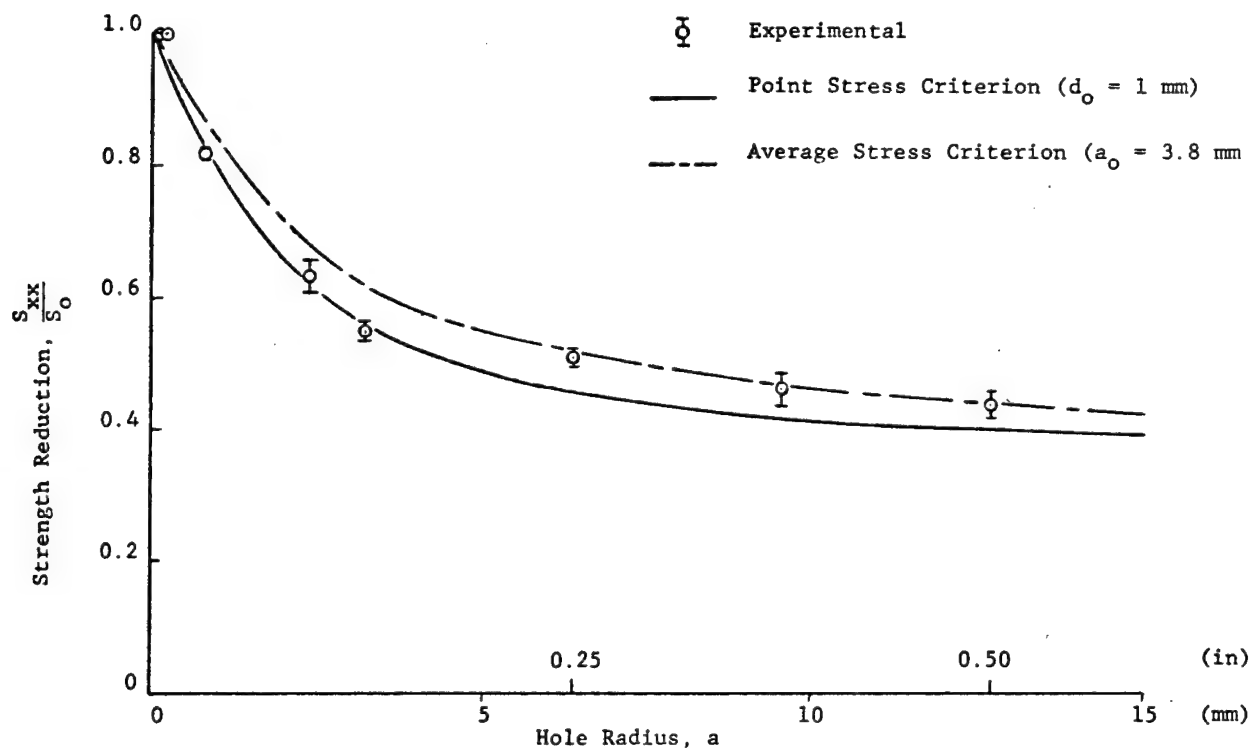
Direction Loading	Modulus E_{xx} GPa (10^6 psi)	Poisson's Ratio, ν_{xy}	Strength S_{xxT} MPa (ksi)	Ultimate Strain ϵ_{xxT}^u ($10^3\epsilon$)
0-deg	82 (11.8)	0.65	805 (116)	10.0
22.5-deg	73 (10.6)	0.33	290 (42)	4.0
45-deg	49 (7.1)	0.11	356 (52)	>9.0
90-deg	24 (3.46)	0.20	139 (20)	7.5

NOTCHED UNIAXIAL TESTS

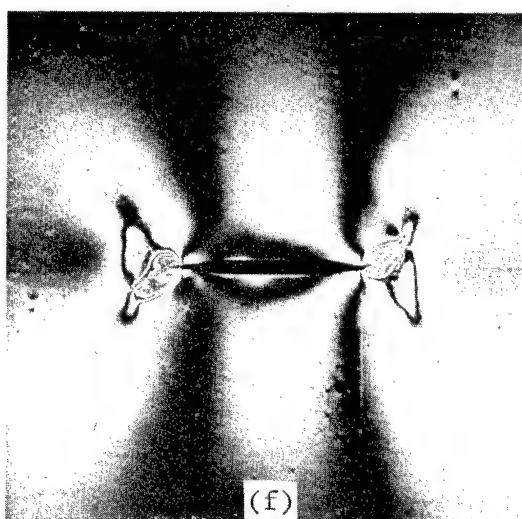
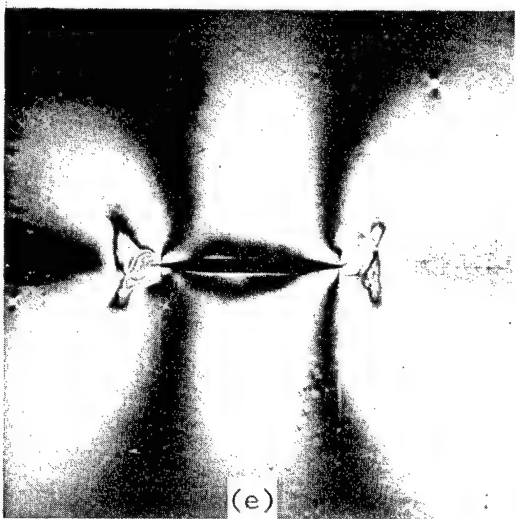
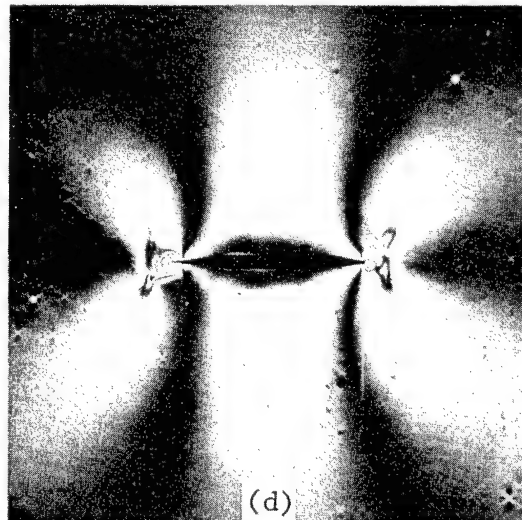
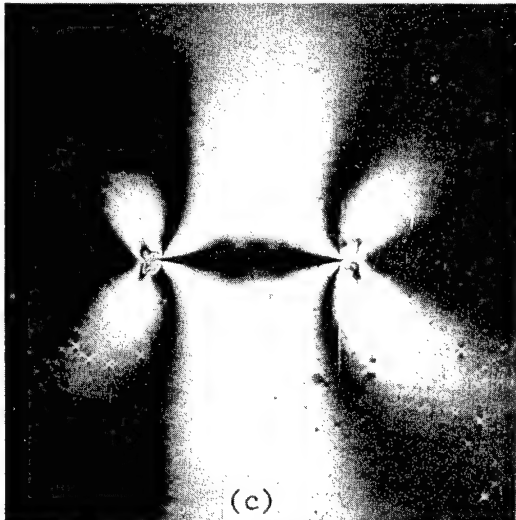
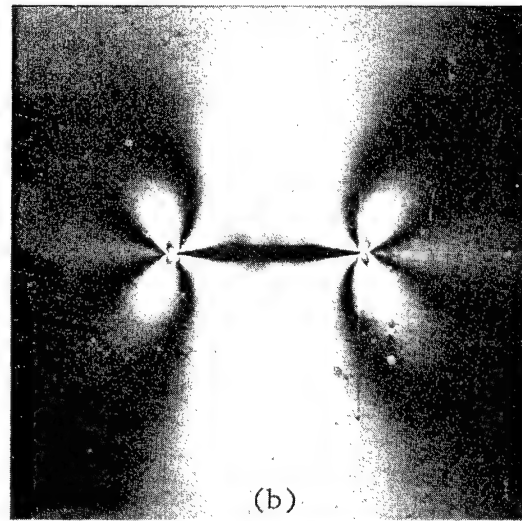
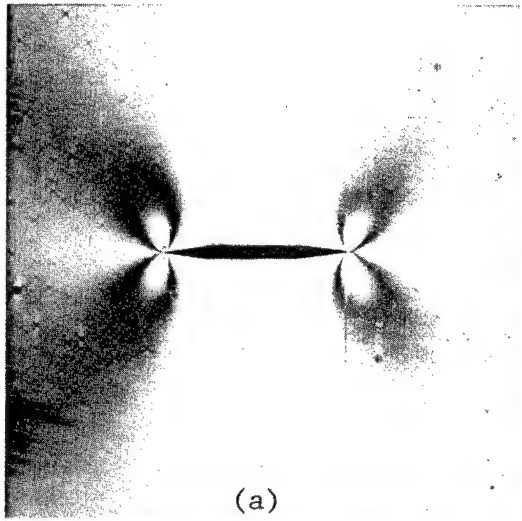
	$[0/\pm 45/90]_s$	$[0_2/\pm 45]_s$
	2a, cm (in)	2a, cm (in)
<p>Diagram of a rectangular specimen with a circular hole. The specimen is subjected to uniaxial tension σ_1. The hole has a diameter of $2a$. The width of the specimen is 12.7 cm (5 in).</p>	<p>2.54 (1.00)</p> <p>1.91 (0.75)</p> <p>1.27 (0.50)</p> <p>0.64 (0.25)</p>	<p>2.54 (1.00)</p> <p>1.91 (0.75)</p> <p>1.27 (0.50)</p> <p>0.64 (0.25)</p>
<p>Diagram of a rectangular specimen with a diamond-shaped hole. The specimen is subjected to uniaxial tension σ_1. The hole has a width of $2a$. The width of the specimen is 12.7 cm (5 in).</p>	<p>2.54 (1.00)</p> <p>1.91 (0.75)</p> <p>1.27 (0.50)</p> <p>0.64 (0.25)</p>	

UNIAXIAL $[0/\pm 45/90]_s$ LAMINATES WITH CIRCULAR HOLES

Spec. No.	Hole Diameter $2a$ cm (in)	Modulus E_{xx} GPa (10^6 psi)	Poisson's Ratio ν_{xy}	Strain Conc. Factor k_ϵ	Strength S_{xx} MPa (ksi)	Maximum Strain at Failure ($10^{-3}\epsilon$)	Strength Reduction, S_{xx}/S_o
4-11	2.54 (1.00)	56 (8.1)	0.30	3.00	229 (33)	> 22	0.455
4-12	2.54 (1.00)	54 (7.9)	0.30	3.00	209 (30)	11.5	0.416
4-9	1.91 (0.75)	56 (8.1)	0.28	2.85	243 (35)	18.5	0.482
4-10	1.91 (0.75)	53 (7.6)	0.29	2.90	219 (32)	-	0.436
4-3	1.27 (0.50)	54 (7.9)	0.31	2.96	247 (36)	18.6	0.493
4-4	1.27 (0.50)	56 (8.2)	0.30	2.64	263 (38)	-	0.521
4-1	0.64 (0.25)	54 (7.9)	0.30	-	271 (39)	> 9.4	0.534
4-2	0.64 (0.25)	56 (8.1)	0.25	2.96	282 (41)	19	0.562
4-17	0.48 (0.187)				309 (45)		0.658
4-18	0.48 (0.187)				286 (41)		0.608
4-19	0.16 (0.062)				381 (55)		0.811
4-20	0.16 (0.062)				388 (56)		0.825
4-21	0.04 (0.016)				463 (67)		1
4-22	0.04 (0.016)				434 (63)		1
4-23	0.02 (0.008)				505 (73)		1
4-24	0.02 (0.008)				478 (69)		1



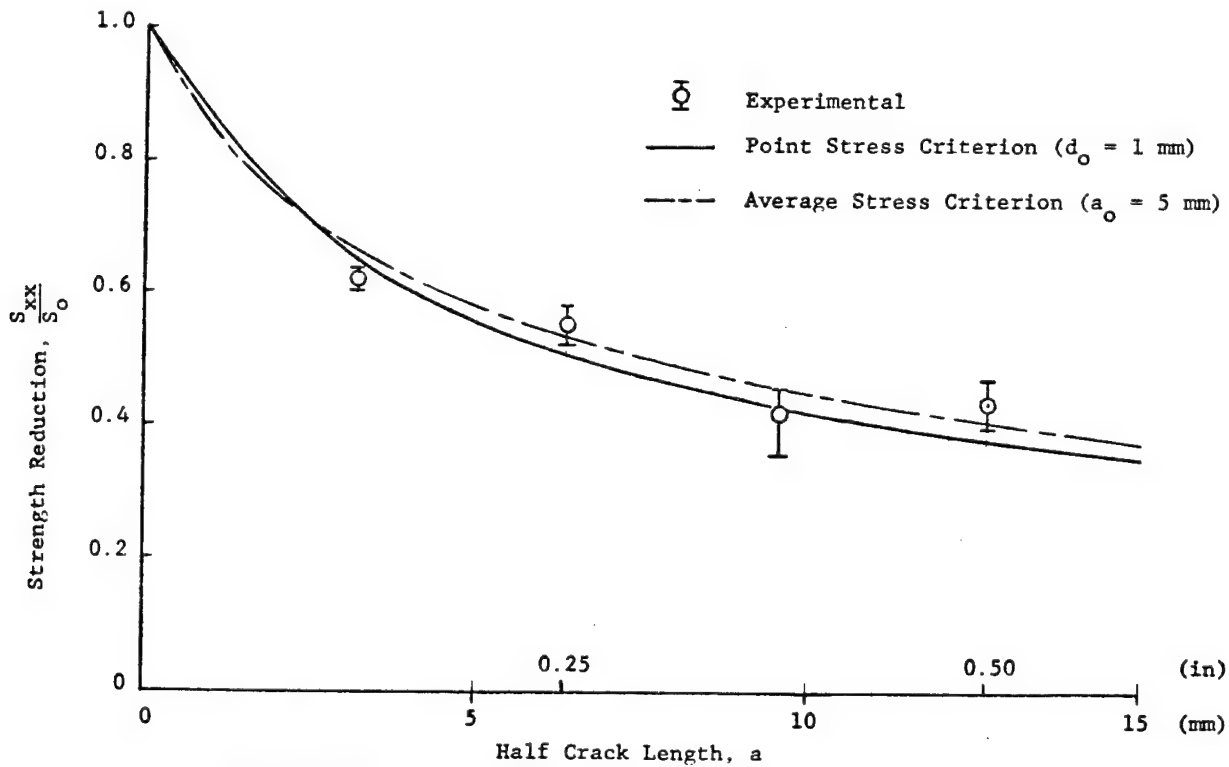
STRENGTH REDUCTION AS A FUNCTION OF HOLE RADIUS FOR $[0/\pm 45/90]_s$ GRAPHITE/EPOXY PLATES WITH CIRCULAR HOLES UNDER UNIAXIAL TENSILE LOADING



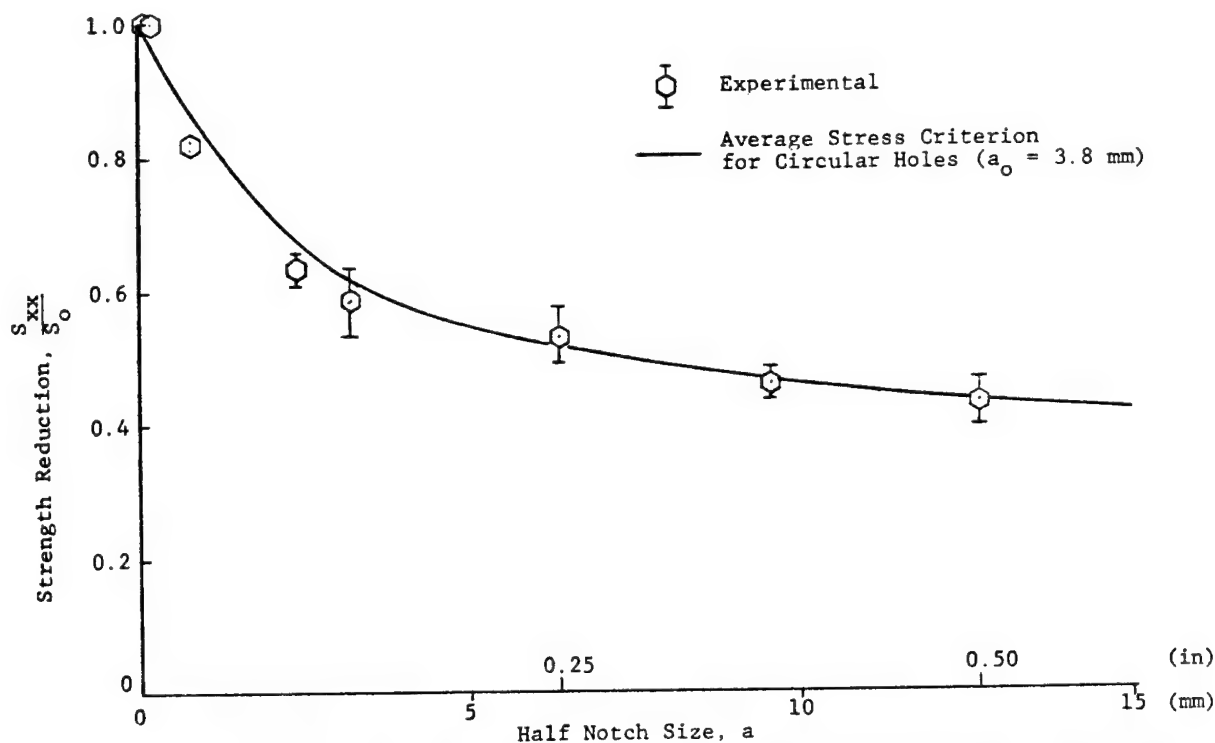
ISOCHROMATIC FRINGE PATTERNS IN PHOTOELASTIC COATING AROUND CRACK OF SPECIMEN NO. 4-6 AT APPLIED STRESS LEVELS: (a) 121 MPa (17.6 ksi), (b) 152 MPa (22.0 ksi), (c) 172 MPa (24.9 ksi), (d) 192 MPa (27.9 ksi) (e) 212 MPa (30.8 ksi) and (f) 223 MPa (32.3 ksi).

UNIAXIAL $[0/\pm 45/90]_s$ LAMINATES WITH CRACKS

Spec. No.	Crack Length $2a$ cm (in)	Modulus E_{xx} GPa (10^6 psi)	Poisson's Ratio ν_{xy}	Strain Ratio $\epsilon_{max}/\epsilon_o$ at y/a		Strength S_{xx} MPa (ksi)	Strength Reduction S_{xx}/S_o
4-5	2.54 (1.00)	52 (7.5)	0.27	3.95	1.02	202 (29)	0.397
4-6	2.54 (1.00)	55 (7.9)	0.29	3.25	1.03	233 (34)	0.466
4-7	1.91 (0.75)	53 (7.7)	0.30	2.72	1.06	180 (26)	0.356
4-8	1.91 (0.75)	55 (7.9)	0.30	2.53	1.06	231 (33)	0.452
4-25	1.91 (0.75)	-	-	-	-	224 (32)	0.445
4-13	1.27 (0.50)	57 (8.3)	0.28	2.25	1.08	293 (42)	0.578
4-14	1.27 (0.50)	55 (7.9)	0.28	2.33	1.08	261 (38)	0.521
4-15	0.64 (0.25)	58 (8.3)	0.27	2.51	1.06	320 (46)	0.637
4-16	0.64 (0.25)	56 (8.1)	0.30	1.85	1.14	304 (44)	0.602



STRENGTH REDUCTION AS A FUNCTION OF CRACK LENGTH FOR $[0/\pm 45/90]_s$ GRAPHITE/EPOXY PLATES WITH HORIZONTAL CRACKS UNDER UNIAXIAL TENSILE LOADING



STRENGTH REDUCTION AS A FUNCTION OF NOTCH SIZE FOR $[0/\pm 45/90]_s$ GRAPHITE/EPOXY PLATES WITH CIRCULAR HOLES AND CRACKS UNDER UNIAXIAL TENSILE LOADING

CONCLUSIONS

UNIAXIAL TESTS - STRAINS

1. IN THE ELASTIC RANGE, THE MEASURED STRESS CONCENTRATION IS CLOSE TO THE THEORETICAL VALUE OF 3 FOR THE UNIAXIAL PLATES WITH CIRCULAR HOLES.
2. STRAINS NEAR THE DISCONTINUITY BECOME NONLINEAR AT A STRAIN LEVEL OF APPROXIMATELY 0.006ϵ CORRESPONDING TO FIRST-PLY FAILURE OF THE 90-DEG. PLIES. THE ULTIMATE TRANSVERSE TENSILE STRAIN IS 0.0054ϵ .
3. THE STRAINS NEAR THE CRACK TIP SHOW AN ADDITIONAL POINT OF RATE CHANGE OCCURRING AT A STRAIN LEVEL OF APPROXIMATELY 0.002ϵ .
4. MAXIMUM STRAINS AT FAILURE ON THE HOLE BOUNDARY OR NEAR THE CRACK TIP HAVE EXCEEDED TWICE THE ULTIMATE STRAIN OF THE UNNOTCHED MATERIAL.

CONCLUSIONS

UNIAXIAL TESTS - STRENGTH

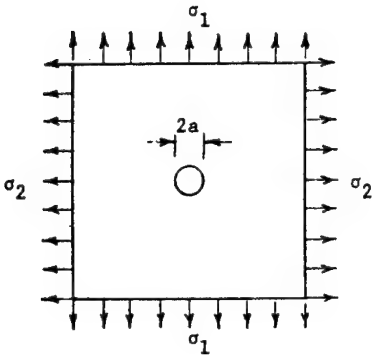
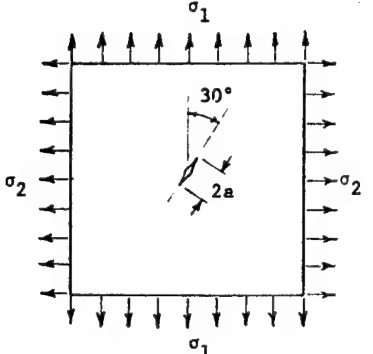
1. THE STRENGTH REDUCTION RATIO, RATIO OF NOTCHED TO UNNOTCHED STRENGTH, RANGES BETWEEN 0.40 AND 0.64 FOR NOTCHES BETWEEN 2.5 cm and 0.6 cm IN SIZE.
2. STRENGTH REDUCTION RESULTS FOR UNIAXIAL SPECIMENS ARE IN AGREEMENT WITH OTHER EXPERIMENTAL DATA ON GRAPHITE/EPOXY, BORON/EPOXY AND GLASS/EPOXY.
3. THE EFFECT OF NOTCH SIZE CAN BE SATISFACTORILY DESCRIBED BY USING THE STRESS, POINT OR AVERAGE, NEAR THE BOUNDARY OF THE DISCONTINUITY AS A CRITERION. THE AVERAGE STRESS OVER A DISTANCE OF 3.8 TO 5 mm SEEMS TO GIVE THE BEST FIT.
4. THE STRENGTH REDUCTION IS INDEPENDENT OF NOTCH GEOMETRY. SPECIMENS WITH HOLES AND CRACKS OF THE SAME SIZE GAVE THE SAME STRENGTH REDUCTION.
5. THERE IS A CRITICAL NOTCH SIZE BELOW WHICH FRACTURE IS AS LIKELY TO OCCUR THROUGH THE UNNOTCHED SECTION AS THROUGH THE NOTCHED SECTION.

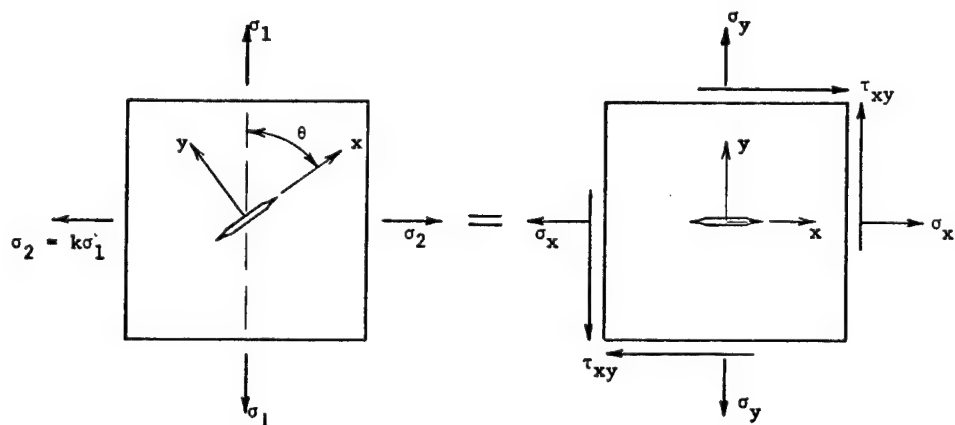
CONCLUSIONS

UNIAXIAL TESTS - FAILURE MODES

1. IN THE SPECIMENS WITH CIRCULAR HOLES, FAILURE INITIATES OFF THE HORIZONTAL AXIS AT POINTS WHERE THE INTERLAMINAR AND MEMBRANE SHEAR STRESSES REACH MAXIMUM VALUES.
2. NO CRACK EXTENSION WAS VISIBLE. FAILURE IN THE FORM OF CRACKING AND DELAMINATION INITIATED OFF THE VERY TIP OF THE CRACK AND PROPAGATED AT AN ANGLE TO THE CRACK.
3. FINAL FAILURE OCCURS WHEN THE DAMAGED AREA AROUND THE TIP OF THE CRACK REACHES SOME CRITICAL SIZE.

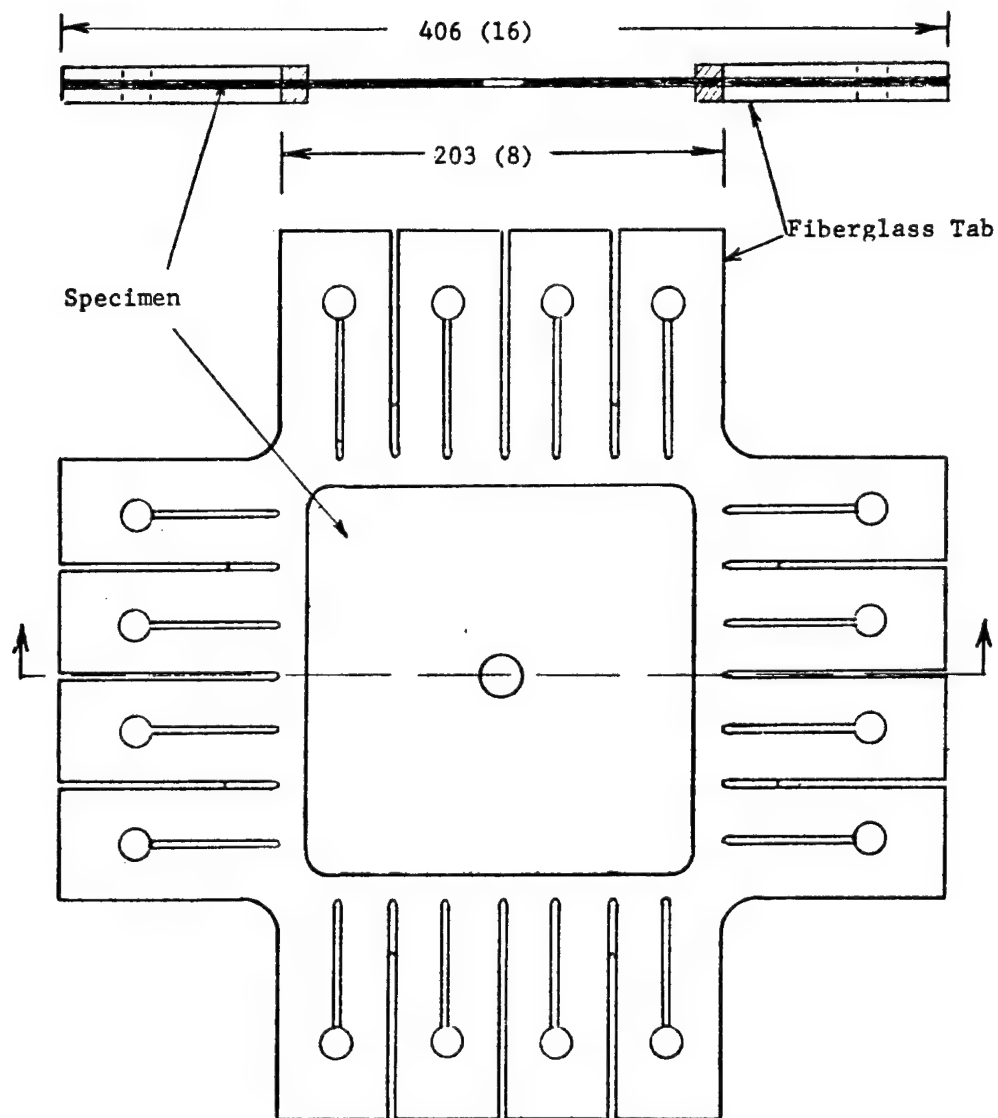
NOTCHED BIAXIAL SPECIMENS

	$[0/\pm 45/90]_s$	$[0_2/\pm 45]_s$
	2a, cm(in) σ_1/σ_2	2a, cm(in) σ_1/σ_2
		
	2.54 (1.00) 1	2.54 (1.00) 2
	1.91 (0.75) 1	1.91 (0.75) 2
	1.27 (0.50) 1	1.27 (0.50) 2
	0.64 (0.25) 1	0.64 (0.25) 2
		
	2.54 (1.00) 2	
	1.91 (0.75) 2	
	1.27 (0.50) 2	
	0.64 (0.25) 2	

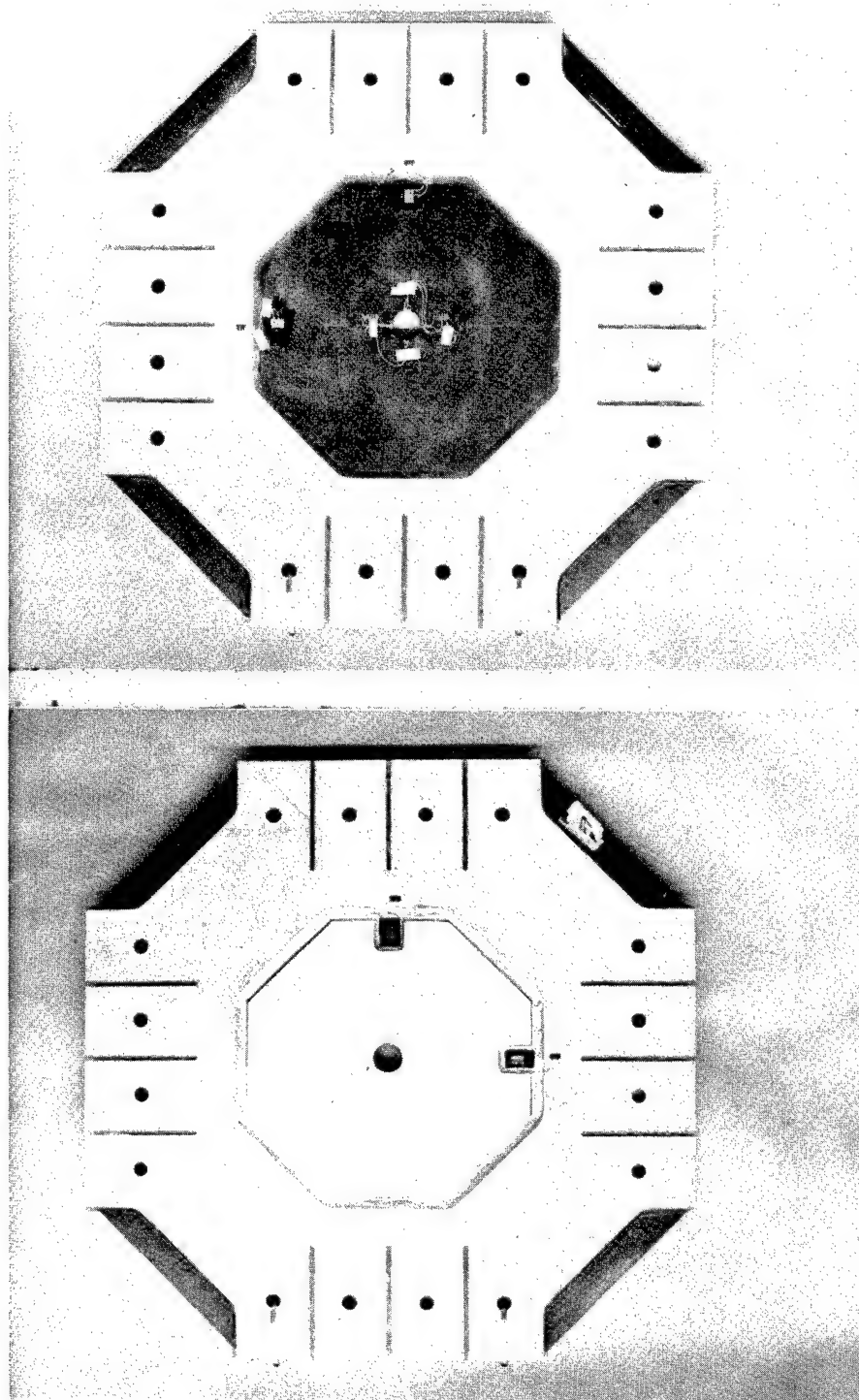


$$\frac{\sigma_y}{\tau_{xy}} = \frac{1 + k - (1-k)\cos 2\theta}{(1-k)\sin 2\theta}$$

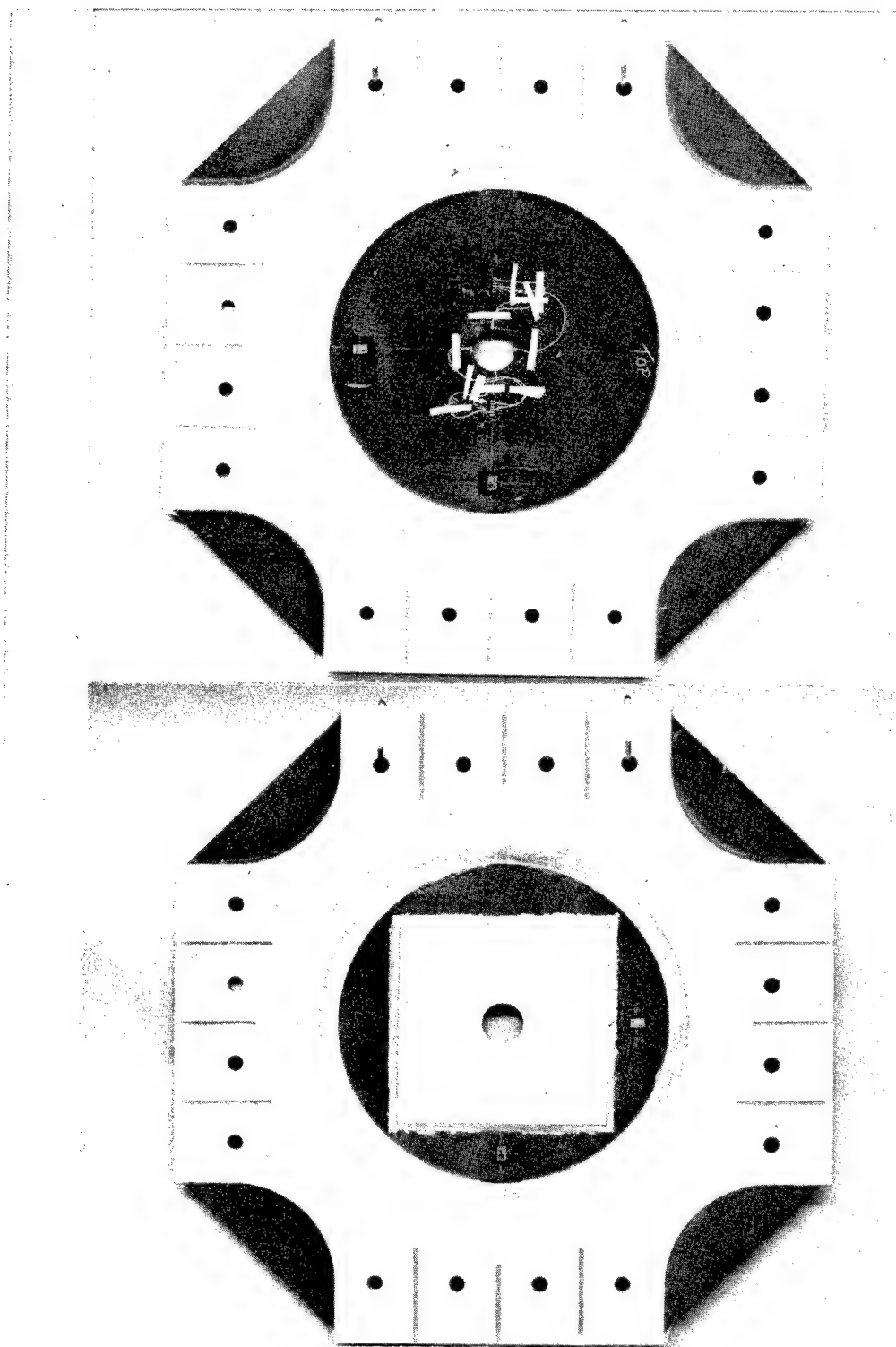
STRESS TRANSFORMATIONS OF THE FAR-FIELD BIAXIAL STATE OF STRESS AROUND A CRACK



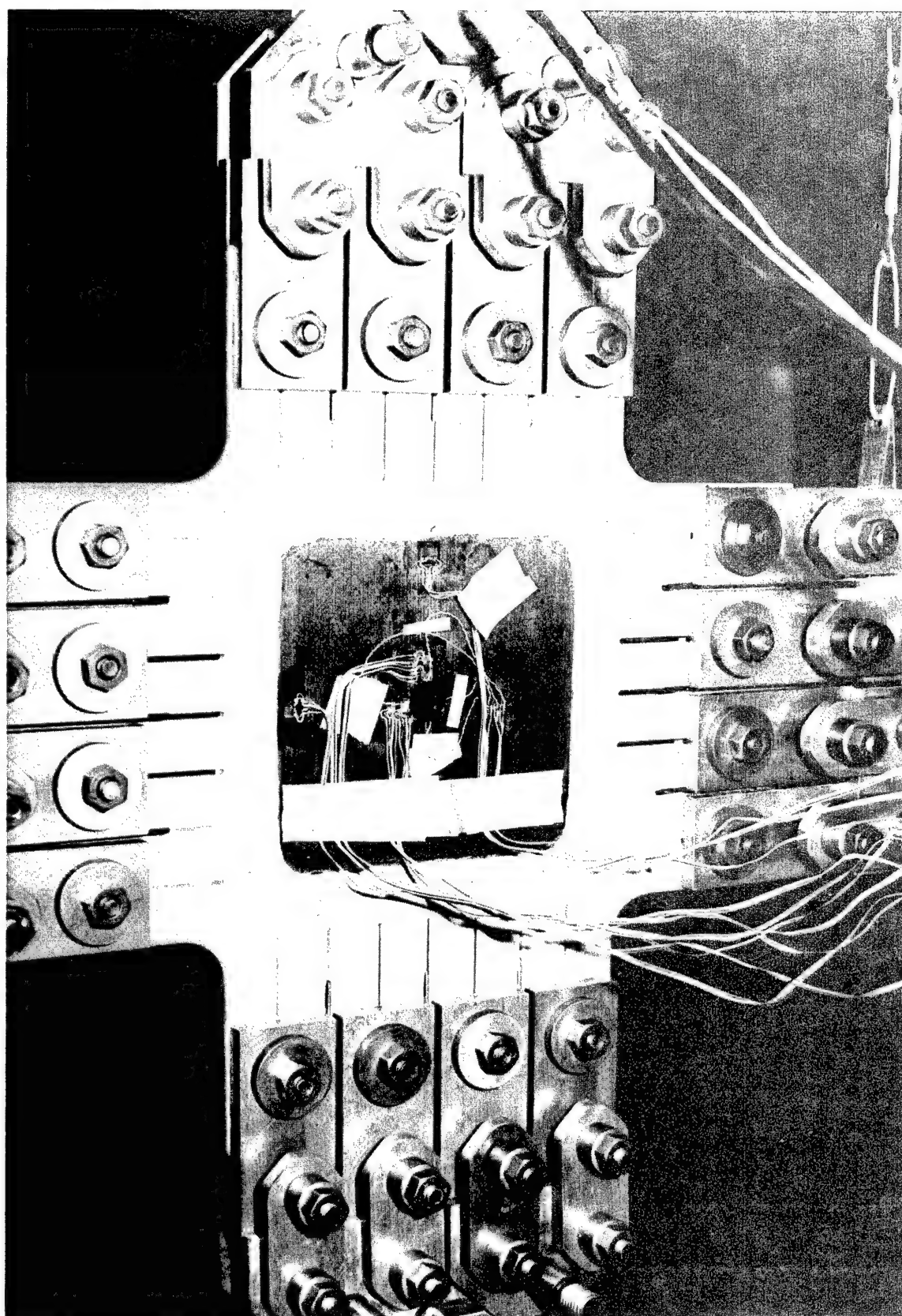
SKETCH OF BIAXIAL COMPOSITE SPECIMEN
(Dimensions are in millimeters and inches)



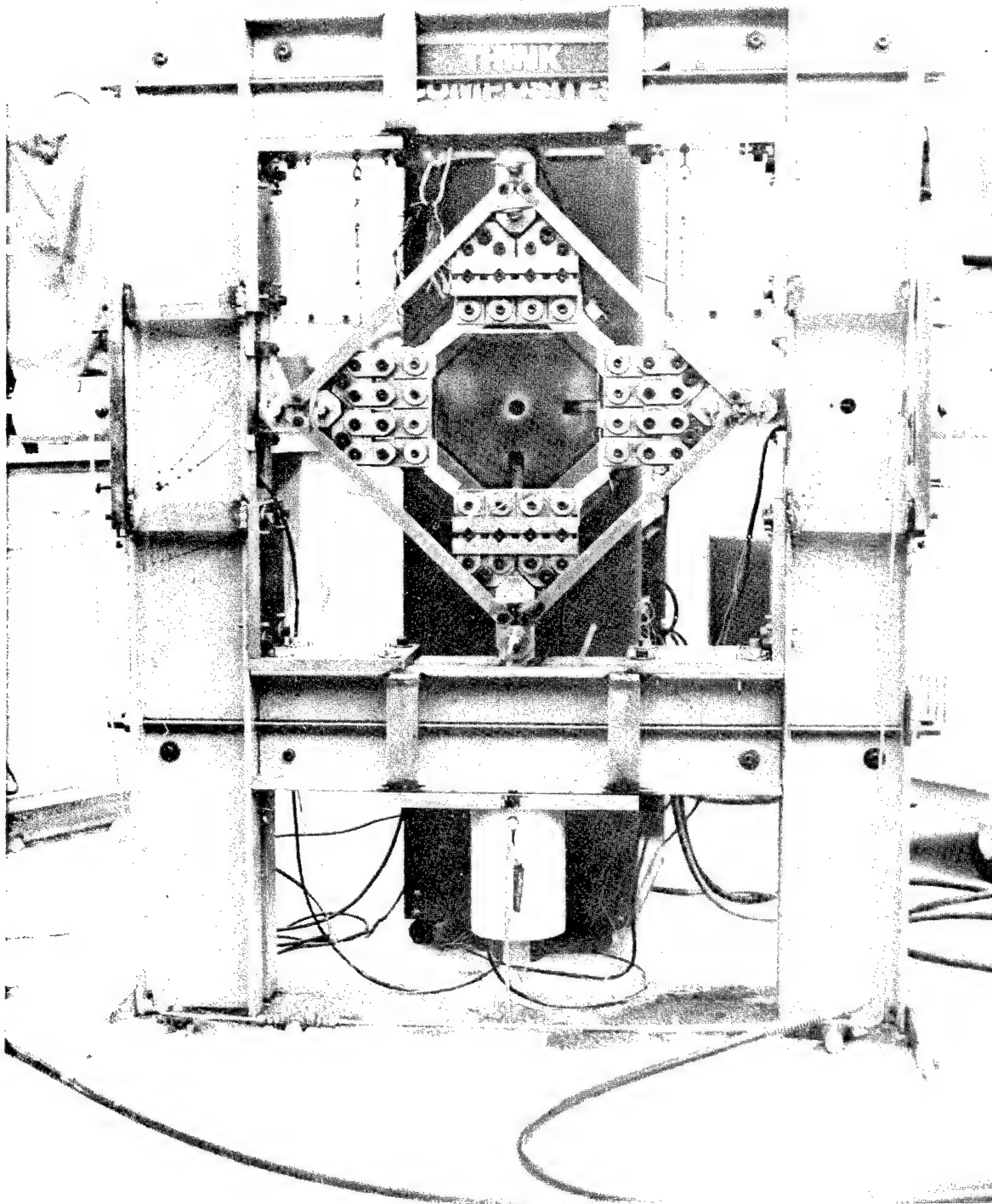
BIAXIAL SPECIMEN NO. 6-6 WITH 1.91 cm (0.75 in.)
DIAMETER HOLE.



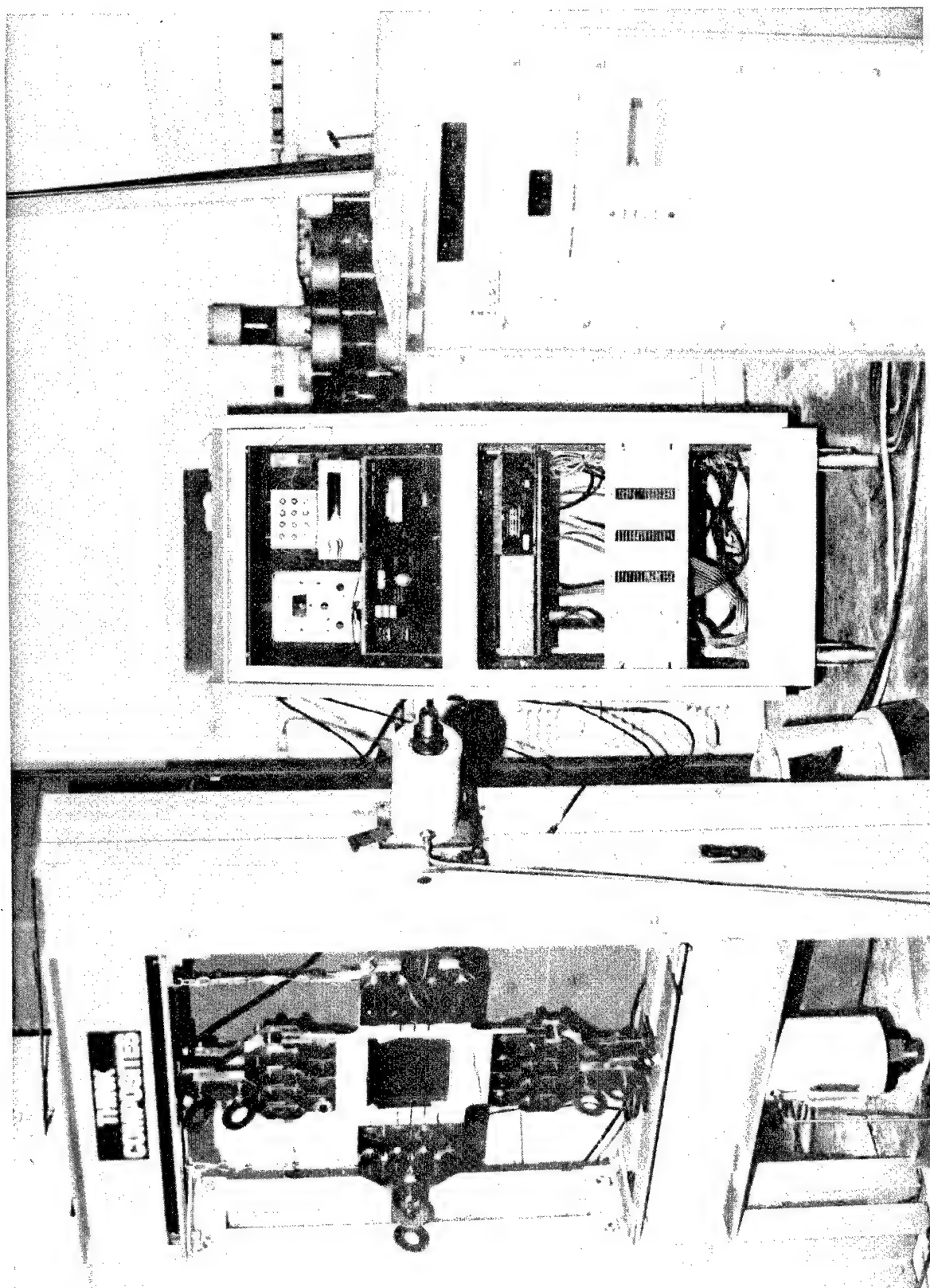
BIAXIAL SPECIMEN NO. 6-7 WITH 2.54 cm (1 in.) DIAMETER HOLE.



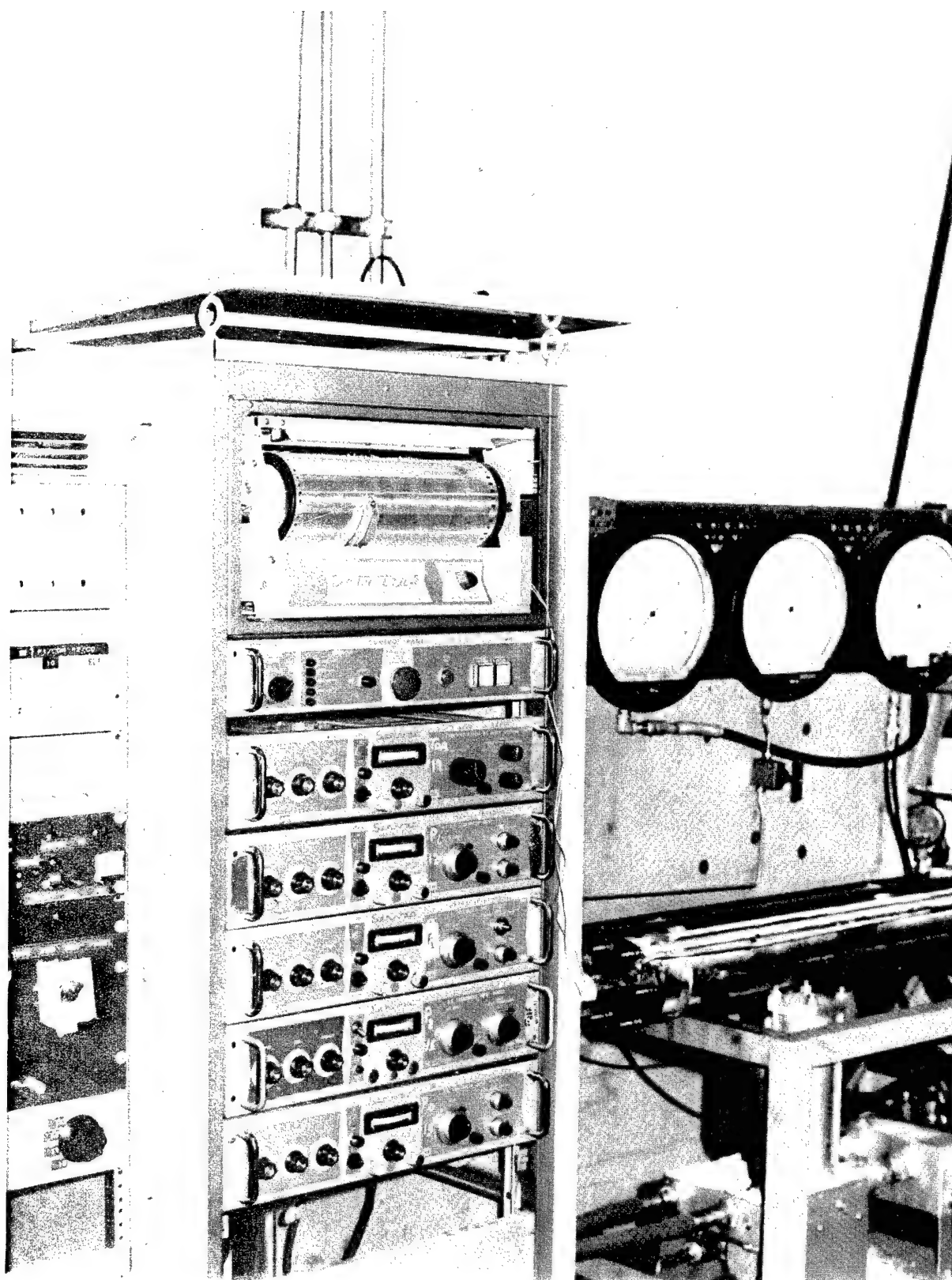
BIAXIAL SPECIMEN WITH HOLE MOUNTED IN LOADING FRAME



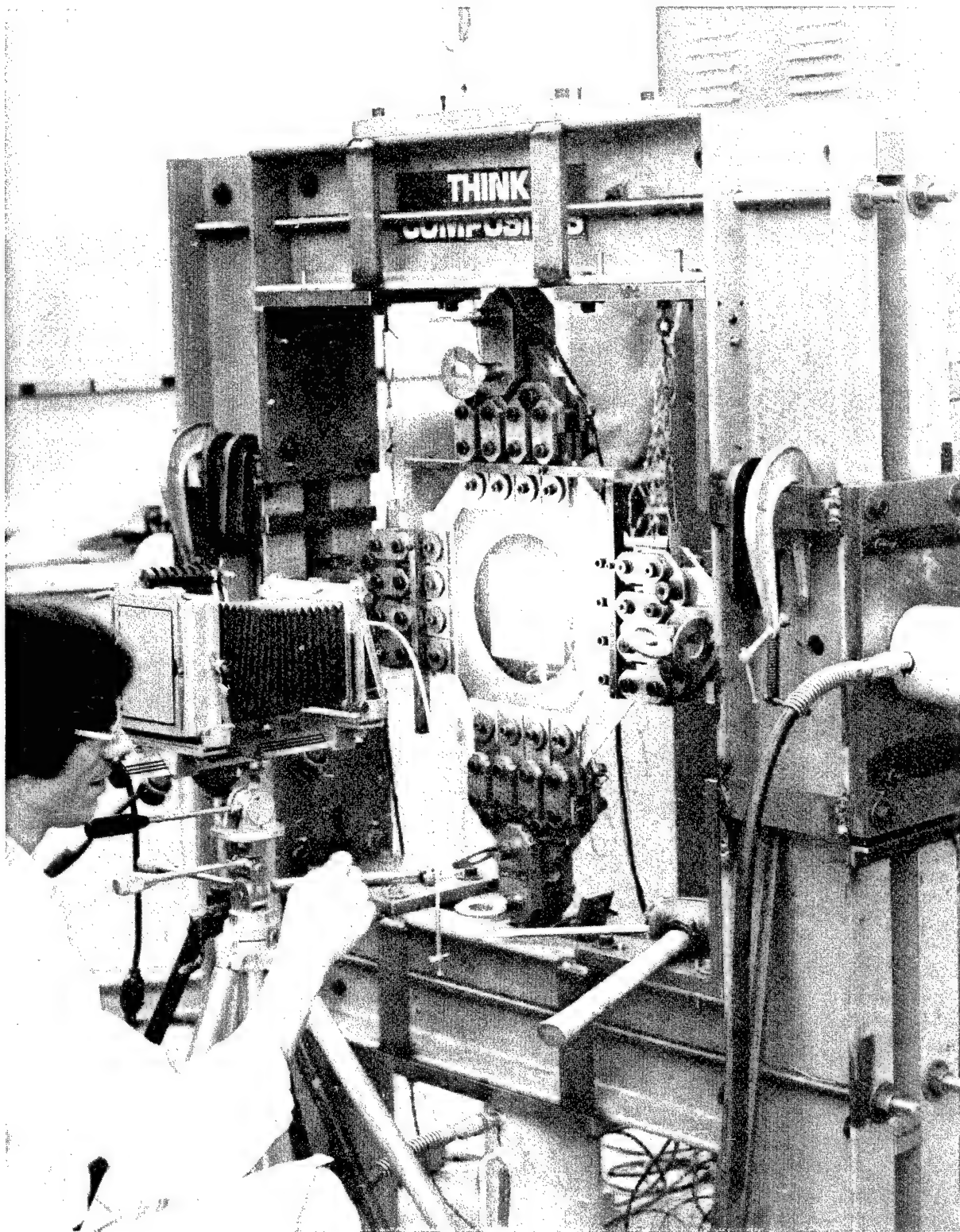
BIAXIAL SPECIMEN WITH ALIGNMENT FIXTURE IN LOADING FRAME



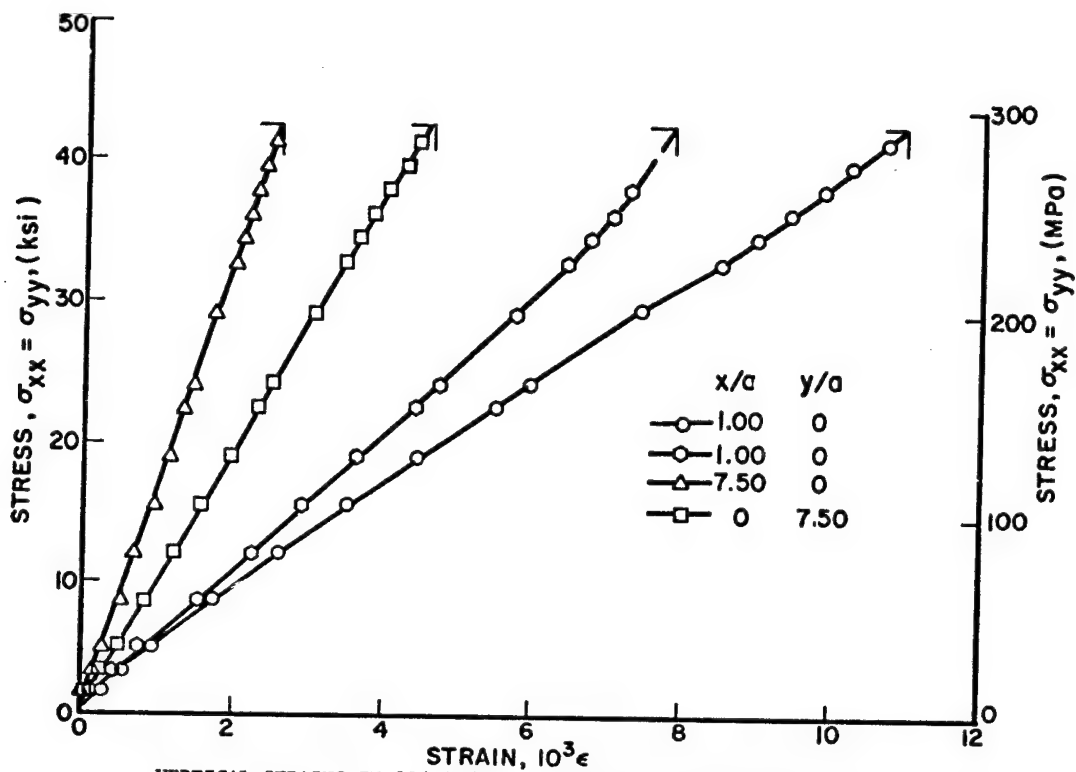
LOADING FRAME FOR BIAXIAL TESTING OF FLAT LAMINATES AND ASSOCIATED STRAIN RECORDING INSTRUMENTATION



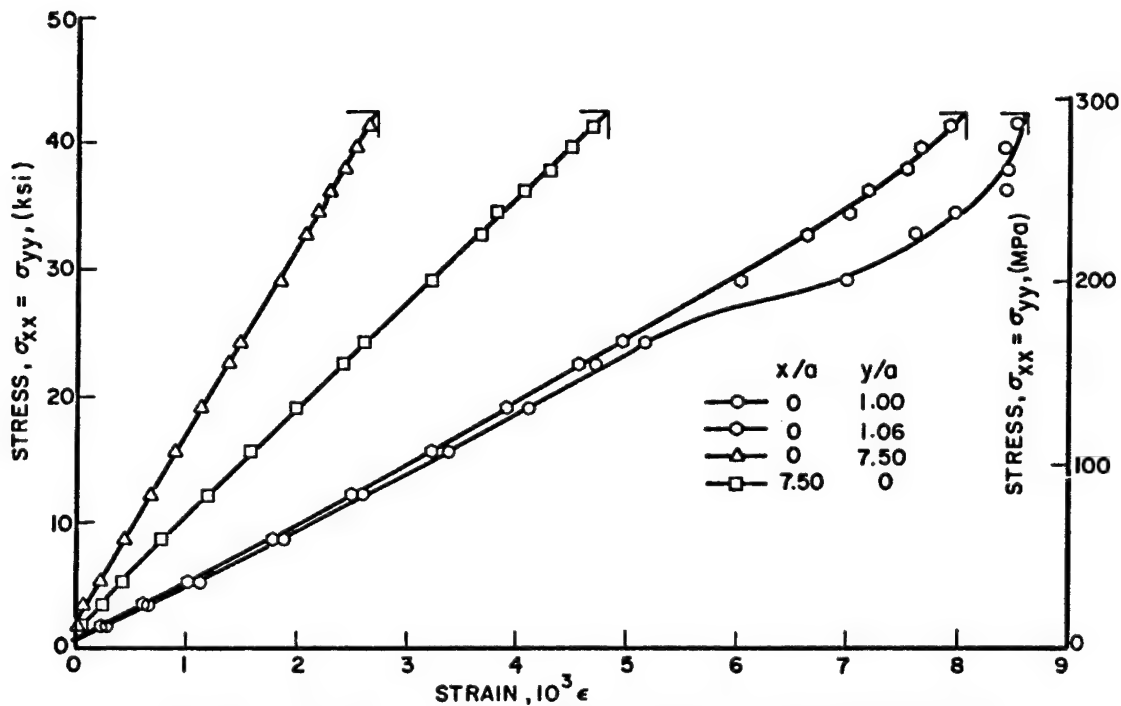
PRESSURE CONTROL INSTRUMENTATION FOR BIAXIAL LOADING
OF SPECIMENS



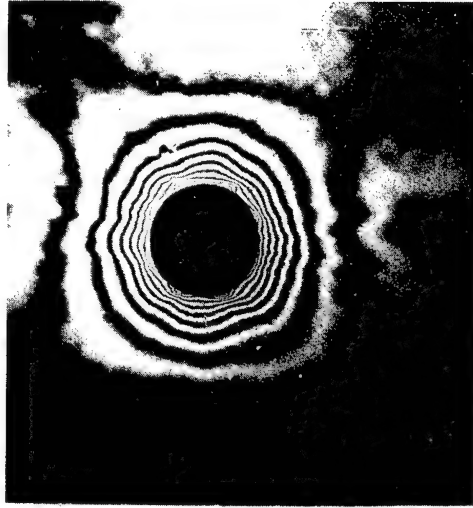
RECORDING FRINGE PATTERNS IN PHOTOELASTIC COATING OF
BIAXIAL SPECIMEN



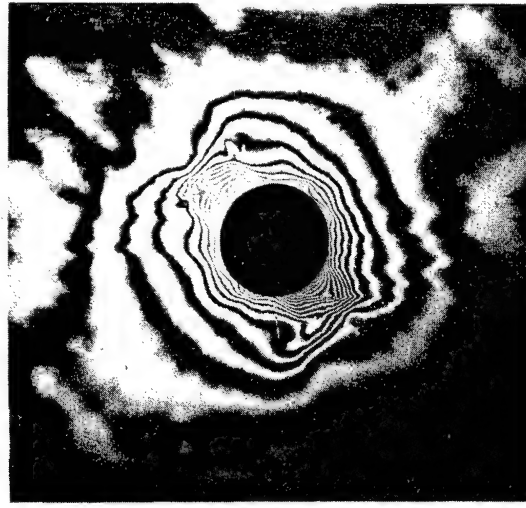
VERTICAL STRAINS IN $[0/\pm 45/90]_s$ GRAPHITE/EPOXY SPECIMEN WITH 2.54 cm (1 in.) DIAMETER HOLE UNDER EQUAL BIAXIAL LOADING (Spec. No. 6-7).



HORIZONTAL STRAINS IN $[0/\pm 45/90]_s$ GRAPHITE/EPOXY SPECIMEN WITH 2.54 cm (1 in.) DIAMETER HOLE UNDER EQUAL BIAXIAL LOADING (Spec. No. 6-7).



266 MPa (39 ksi)



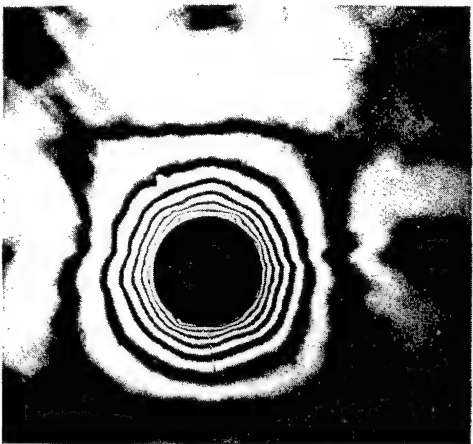
293 MPa (42 ksi)



247 MPa (36 ksi)



284 MPa (41 ksi)

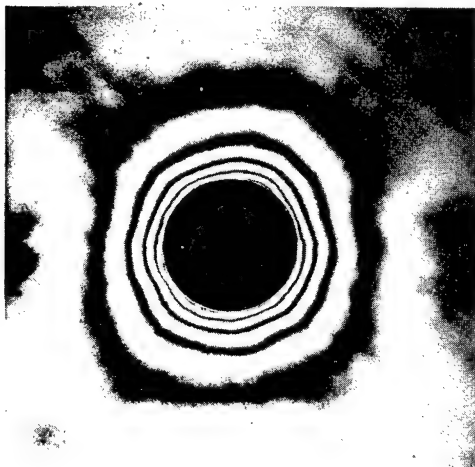


229 MPa (33 ksi)



275 MPa (40 ksi)

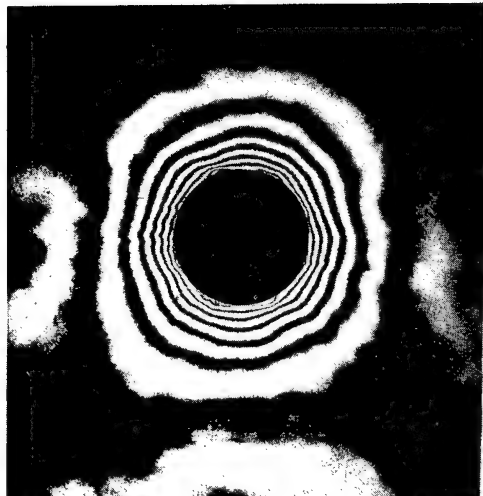
ISOCROMATIC FRINGE PATTERNS IN PHOTOELASTIC COATING OF $[0/+45/90]_s$ GRAPHITE/EPOXY SPECIMEN UNDER EQUAL BIAXIAL LOADING (Spec. No. 6-6; far-field biaxial stress marked).



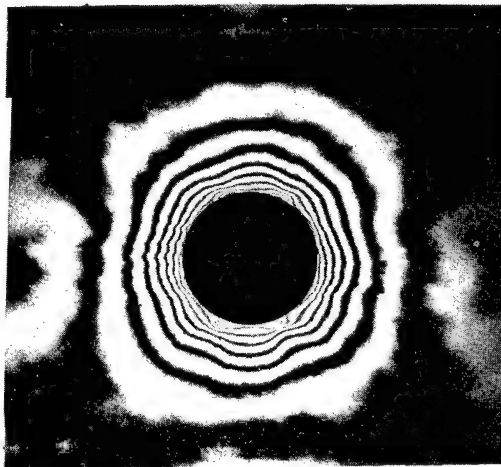
166 MPa (24 ksi)



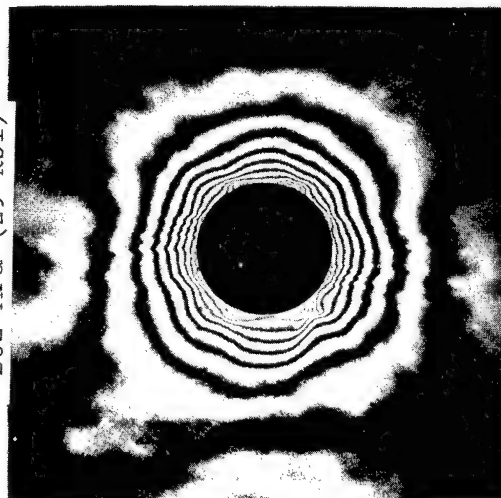
202 MPa (29 ksi)



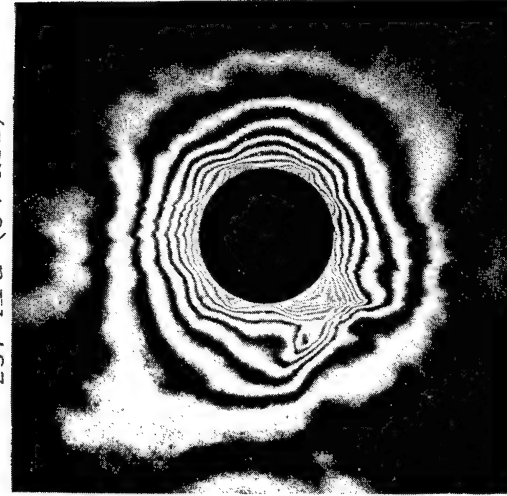
237 MPa (34 ksi)



261 MPa (38 ksi)

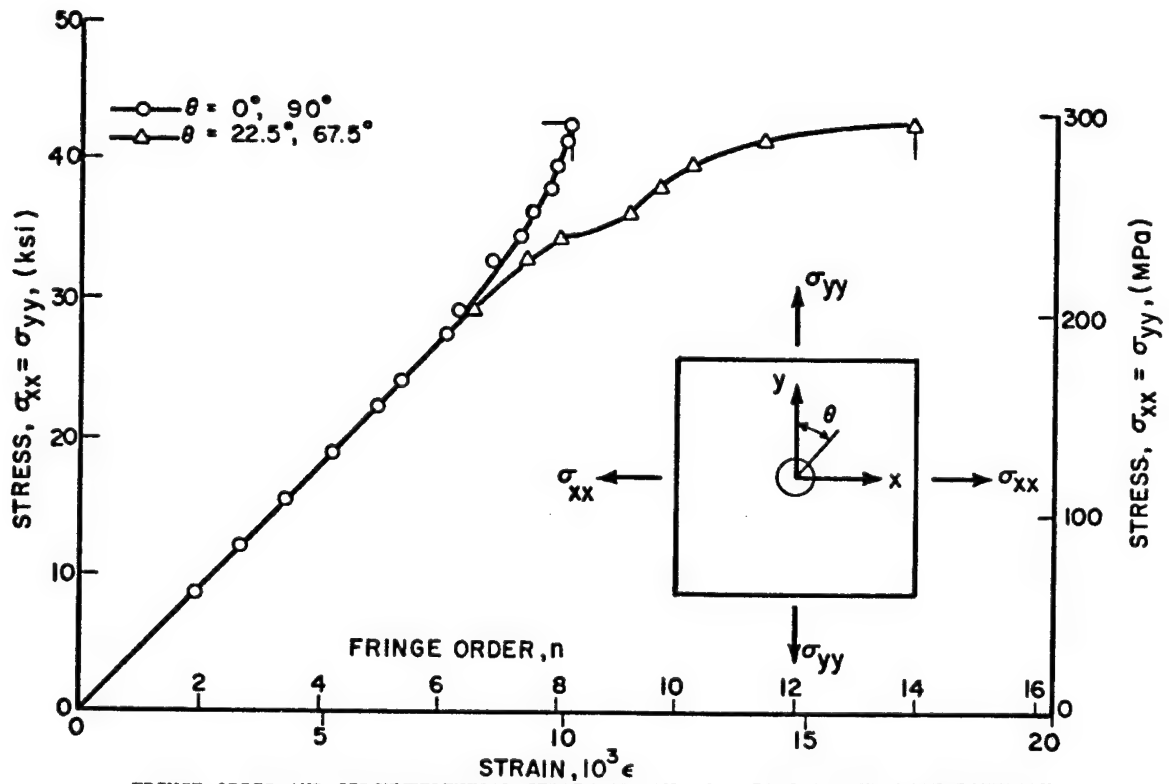


285 MPa (41 ksi)

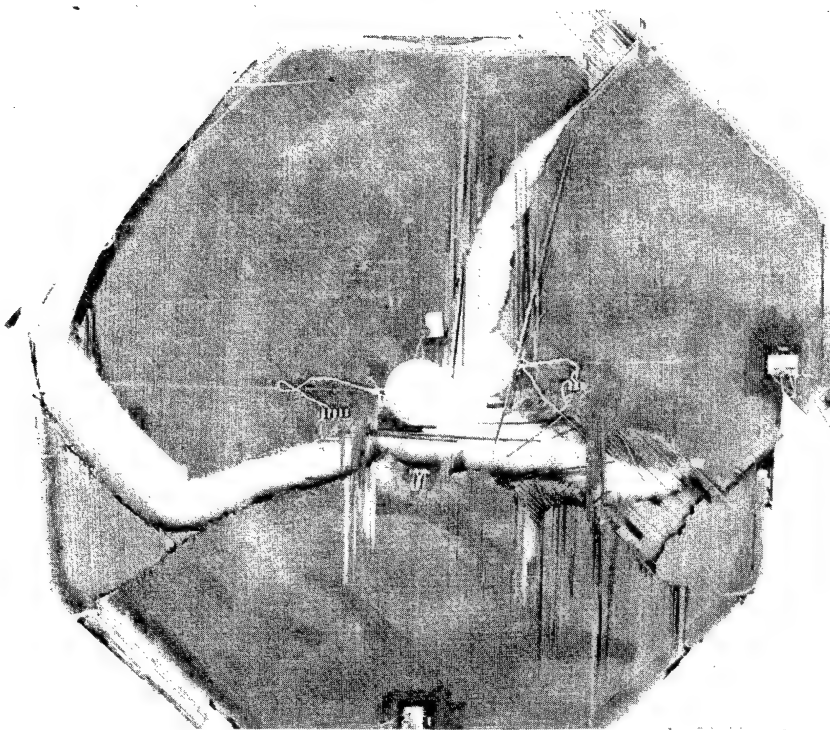


293 MPa (42 ksi)

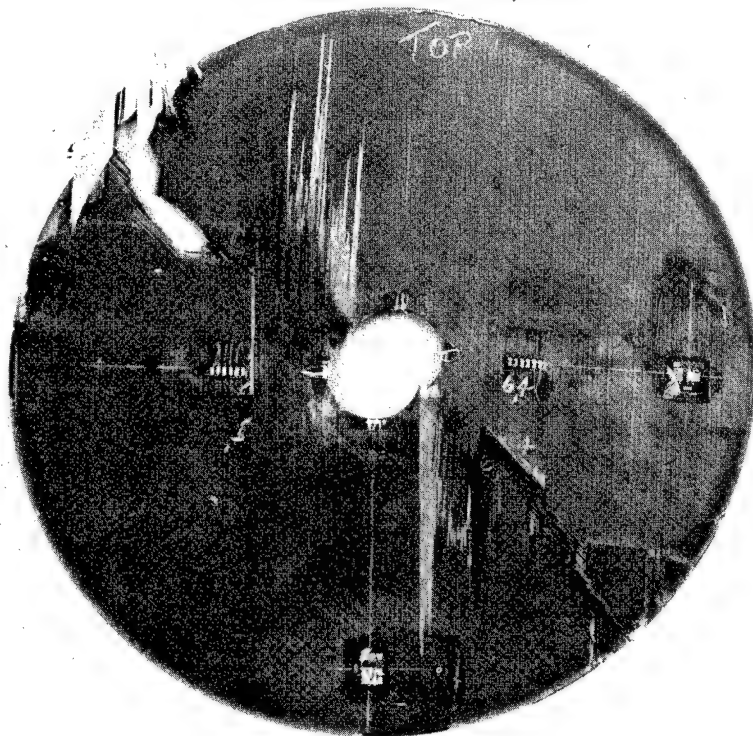
ISOCHROMATIC FRINGE PATTERNS IN PHOTOELASTIC COATING OF
SPECIMEN NO. 6-7 (Far-Field Biaxial Stress Marked).



FRINGE ORDER AND CIRCUMFERENTIAL STRAIN AT TWO LOCATIONS ON THE HOLE BOUNDARY FOR $[0/+45/90]_s$ GRAPHITE/EPOXY SPECIMEN WITH 2.54 cm (1 in.) DIAMETER HOLE UNDER EQUAL BIAXIAL LOADING (Spec. No. 6-7).



FAILURE PATTERN IN $[0/+45/90]_s$ GRAPHITE/EPOXY SPECIMEN WITH 1.91 cm (0.75 in.) DIAMETER HOLE UNDER EQUAL BIAXIAL LOADING (Spec. No. 6-6)

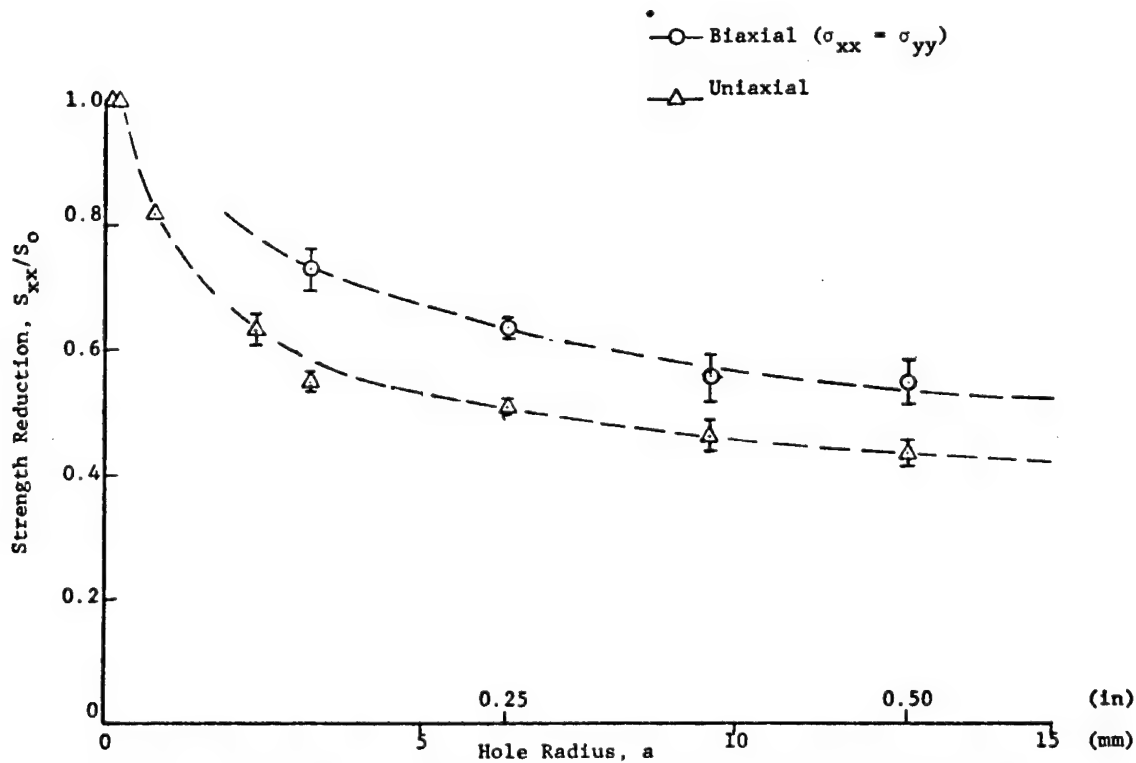


FAILURE PATTERN IN $[0/\pm 45/90]_s$ GRAPHITE/EPOXY SPECIMEN WITH 2.54 cm (1 in.) DIAMETER HOLE UNDER EQUAL BIAXIAL LOADING (Spec. No. 6-7).

Table 1

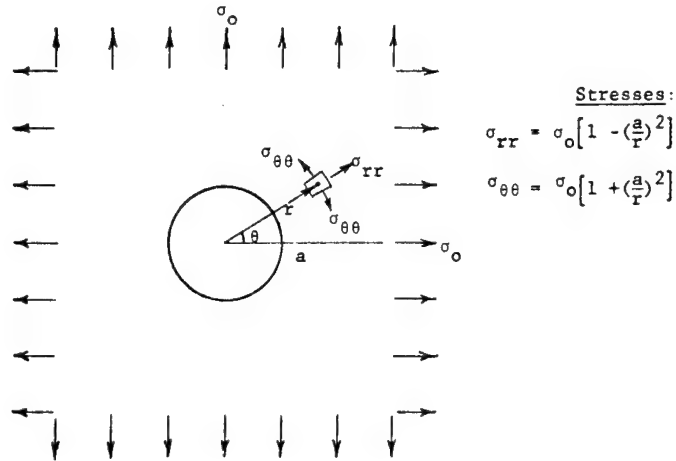
BIAXIAL $[0_2/\pm 45/90]_s$ LAMINATES WITH CIRCULAR HOLES

Spec. No.	Hole Diam. $2a$ cm (in.)	Failure Stress $S_{xxT} = S_{yyT}$ MPa (ksi)	Maximum Strain at Failure ($10^{-3}\epsilon$)		Strength Reduction Ratio S_{xx}/S_o
			$\theta=0^\circ$	$\theta=22.5^\circ$	
6-7	2.54 (1.00)	293 (42)	10.0	17.5	0.582
6-8	2.54 (1.00)	258 (37)	10.2	10.7	0.512
6-6	1.91 (0.75)	299 (43)	10.0	19.5	0.593
6-9	1.91 (0.75)	261 (38)	10.3	11.8	0.518
6-10	1.27 (0.50)	312 (45)	12.2	-	0.619
6-11	1.27 (0.50)	328 (48)	12.0	14.9	0.651
6-15	0.64 (0.25)	383 (56)	15.0	18.5	0.761
6-22	0.64 (0.25)	349 (51)	14.3	17.3	0.693



STRENGTH REDUCTION AS A FUNCTION OF HOLE RADIUS FOR $[0/\pm 45/90]_s$ GRAPHITE/EPOXY PLATES WITH CIRCULAR HOLES UNDER UNIAXIAL AND 1:1 BIAXIAL LOADING

CIRCULAR HOLE IN BIAXIAL STRESS FIELD



Average Stresses (In annulus $r = a$ to $r = r_1$)

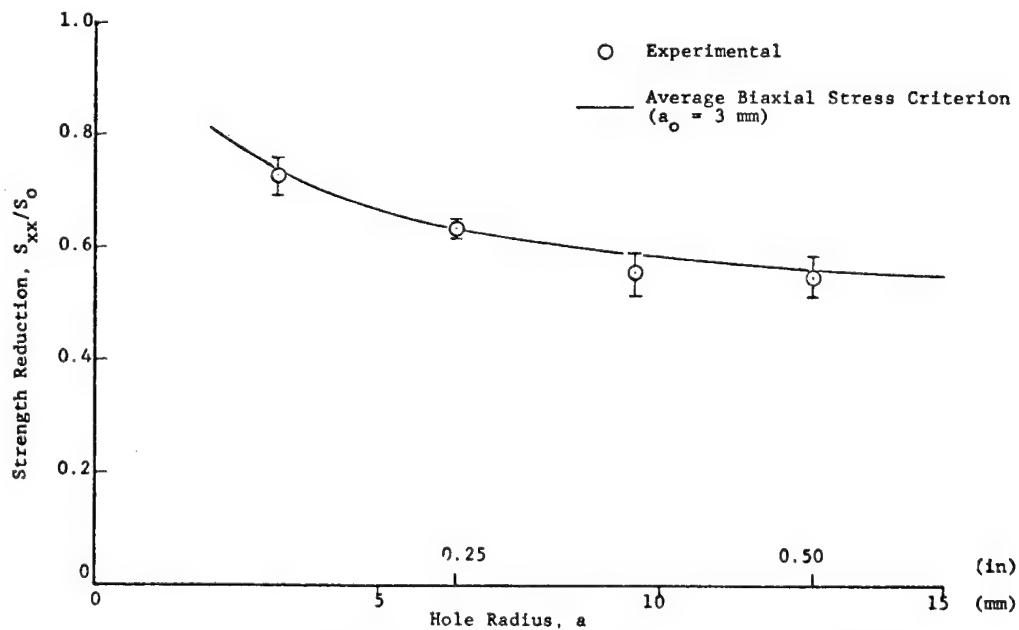
$$\bar{\sigma}_{rr} = \sigma_o \left[1 - \frac{2}{r_1^2 - 1} \log \rho_1 \right]$$

$$\bar{\sigma}_{\theta\theta} = \sigma_o \left[1 + \frac{2}{r_1^2 - 1} \log \rho_1 \right]$$

$$\rho_1 = \frac{r_1}{a}$$

Failure Criterion

- Failure occurs when $\bar{\sigma}_{rr}$ and $\bar{\sigma}_{\theta\theta}$ fall on failure envelope for laminate
- $(r_1 - a) = \text{characteristic dimension}$



STRENGTH REDUCTION AS A FUNCTION OF HOLE RADIUS FOR $[0/+45/90]_s$ GRAPHITE/EPOXY PLATES WITH CIRCULAR HOLES UNDER 1:1 BIAXIAL TENSILE LOADING

CONCLUSIONS

[0/+45/90]_s LAMINATES WITH HOLES UNDER EQUAL BIAXIAL TENSION

STRAINS AND FAILURE

1. STRAINS ON THE BOUNDARY OF THE HOLE BECOME NONLINEAR AT APPLIED STRESSES OF $\sigma_{xx} = \sigma_{yy} \approx 120 \text{ MPa (17.5 ksi)}$ CORRESPONDING TO A STRAIN LEVEL OF APPROXIMATELY $4 \times 10^{-3} \epsilon$. THIS IS THE STRAIN LEVEL AT WHICH THE RESPONSE OF THE UNIAXIAL UNNOTCHED SPECIMENS BECOMES NONLINEAR.
2. INITIALLY, THE CIRCUMFERENTIAL STRAIN IS UNIFORM AROUND THE BOUNDARY OF THE HOLE. SUBSEQUENTLY, WITH INCREASING LOAD, REGIONS OF HIGH STRAIN CONCENTRATION WITH NON-LINEAR RESPONSE DEVELOP AT EIGHT CHARACTERISTIC LOCATIONS 22.5-DEG. OFF THE FIBER AXES.
3. MAXIMUM STRAINS AT FAILURE ON THE HOLE BOUNDARY REACH VALUES UP TO 19.5×10^{-3} COMPARED TO THE ULTIMATE STRAIN 10^{-2} OF THE UNNOTCHED LAMINATE.
4. FAILURE INITIATES ON THE HOLE BOUNDARY AT POINTS 22.5 DEG. OFF THE HORIZONTAL AND VERTICAL AXES.

CONCLUSIONS

[0/+45/90]_s LAMINATES WITH HOLES UNDER EQUAL BIAXIAL TENSION

STRENGTH

1. THE STRENGTH REDUCTION RATIO OF NOTCHED TO UNNOTCHED STRENGTH RANGES BETWEEN 0.55 AND 0.73 FOR HOLES BETWEEN 2.54 cm and 0.64 cm IN DIAMETER.
2. THE STRENGTH REDUCTION RATIOS ARE HIGHER THAN CORRESPONDING VALUES FOR UNIAXIAL LOADING BY 26 TO 33 PERCENT.
3. THE VARIATION OF STRENGTH REDUCTION RATIO WITH HOLE DIAMETER CAN BE SATISFACTORILY DESCRIBED BY USING AN AVERAGE BIAXIAL STRESS CRITERION OVER A RADIAL DISTANCE OF 3 mm.
4. THE STRENGTH REDUCTION RATIOS FOR UNIAXIAL AND EQUAL BIAXIAL LOADING REPRESENT LOWER AND UPPER BOUNDS. THE STRENGTH REDUCTION RATIO FOR ANY OTHER BIAXIALITY RATIO WOULD FALL BETWEEN THESE TWO EXTREMES.

DESIGN RECOMMENDATION

QUASI-ISOTROPIC COMPOSITE PANELS WITH CIRCULAR CUTOUTS CAN BE DESIGNED CONSERVATIVELY BY ASSUMING STRENGTH REDUCTION RATIOS CORRESPONDING TO UNIAXIAL LOADING.

RESPONSE OF GRAPHITE COMPOSITES
TO LASER RADIATION
(F44620-76-C-0030)

K. G. KIBLER

Materials Research Laboratory
GENERAL DYNAMICS
Ft. Worth, TX 76101

OBJECTIVE: DEVELOP A BASIC UNDERSTANDING OF THE PHYSICAL BEHAVIOR
OF GRAPHITE-EPOXY COMPOSITE MATERIALS EXPOSED TO
CW CO₂ LASER RADIATION

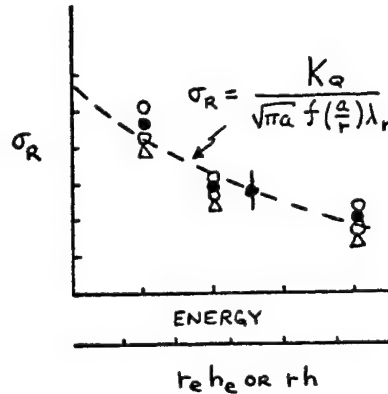
- SCOPE:**
1. DETERMINE PENETRATION RATE, THERMAL RESPONSE,
AND STRENGTH DEGRADATION OF COMPOSITES
 2. IDENTIFY THERMOPHYSICAL MECHANISMS OF
DEGRADATION, OTHER THAN COMPLETE PENETRATION
 3. FORMULATE SIMPLE MODELS TO PREDICT PENETRATION
RATE AND STRENGTH DEGRADATION IN COMPOSITES
 4. COMPARE EFFECTS ON COMPOSITES WITH EFFECTS
ON ALUMINUM

1. ENVIRONMENT

- LASER IRRADIATE (0/+45/90)_S 5208/T300
at 200 w/ 0.2 - 1.0 cm²
(PARTIAL PENETRATION)
- CHARACTERIZE DAMAGE
- MEASURE RESIDUAL STRENGTH

2. RESULTS

- σ_R DEPENDS MONOTONICALLY ON E
- DEPENDENCE RESEMBLES CIRCULAR HOLE EFFECTS

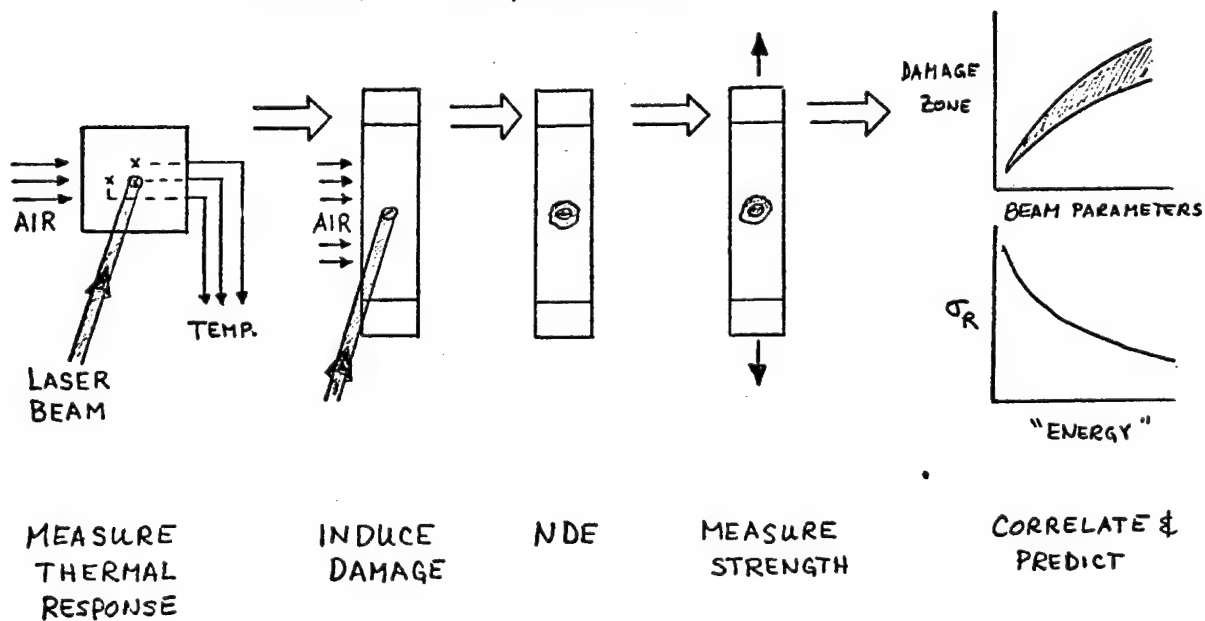


3. ANALYSIS

- CALCULATE σ_R FOR CIRCULAR HOLES
- DESCRIBE DAMAGE BY

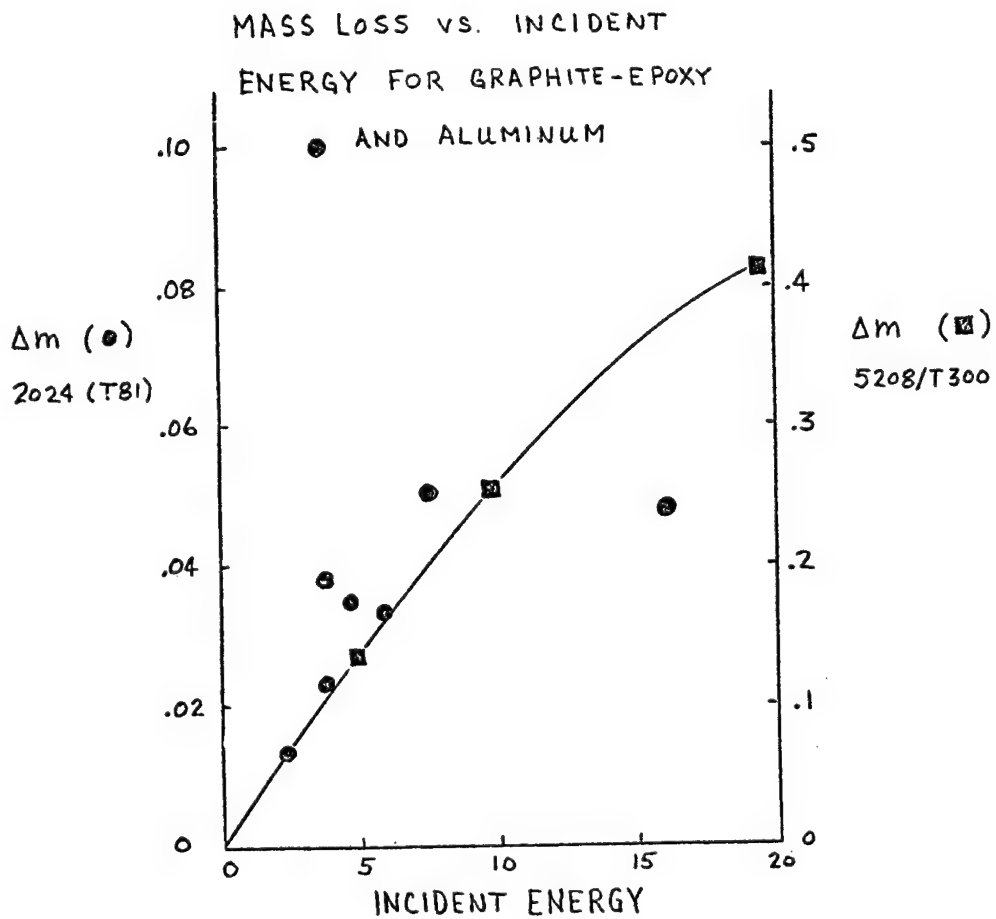
$$r_e h_e \approx \Delta m / \rho r_e$$

CHARACTERIZATION OF STRENGTH DEGRADATION

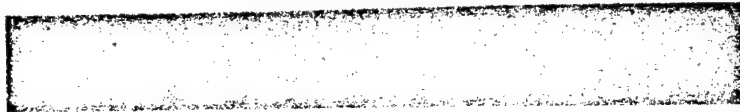


TEST SPECIMEN SUMMARY

	LASER TEST SPECIMENS	CONTROL SPECIMENS	LASER EXPERIMENTS
			TIME
			POWER
			BURN DEPTH
			THERMAL RESPONSE
			PRELOAD
			MOISTURE
			(SPOT SIZE)
THICKNESS EFFECTS	(0/±45) ₅ ----- U, 1/8"(T), 1/4"(T)		
	(0/±45) ₄₅ ----- U, 1/8"(T), 1/4"(T), 1/8"(I), 1/4"(I)		
	(0/±45) ₂₅ ----- U, 1/8"(T), 1/4"(T)		
	LONG. VS. TRANSV. STRENGTH		
STACKING EFFECTS	(90/±45) ₂₅ ----- U		
	(±45/90) ₂₅ ----- U		
	2024 (T81) ----- U, 1/8"(T), 1/4"(T), 1/8"(I), 1/4"(I)		



LASER DAMAGE IN 5208/T300 (0/+45)_{2S}
 INCIDENT BEAM 750 w / 0.5 cm²



2

25.6 sec.
 (Burnthrough)



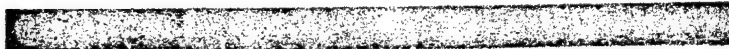
5

12.8 sec.

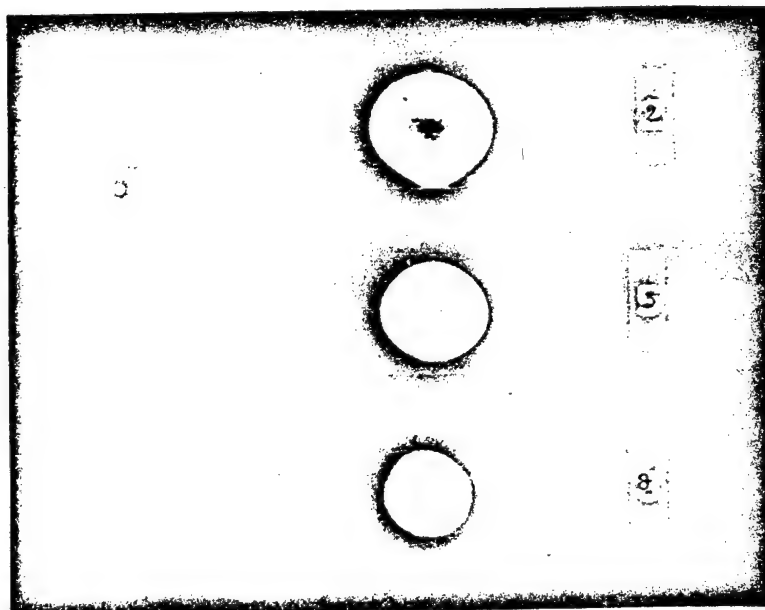


8

6.4 sec.



LASER DAMAGE IN 5208/T300 (0/+45)_{2S}
 INCIDENT BEAM 750 w / 0.5 cm²
 X-RAY WITH TBE



2

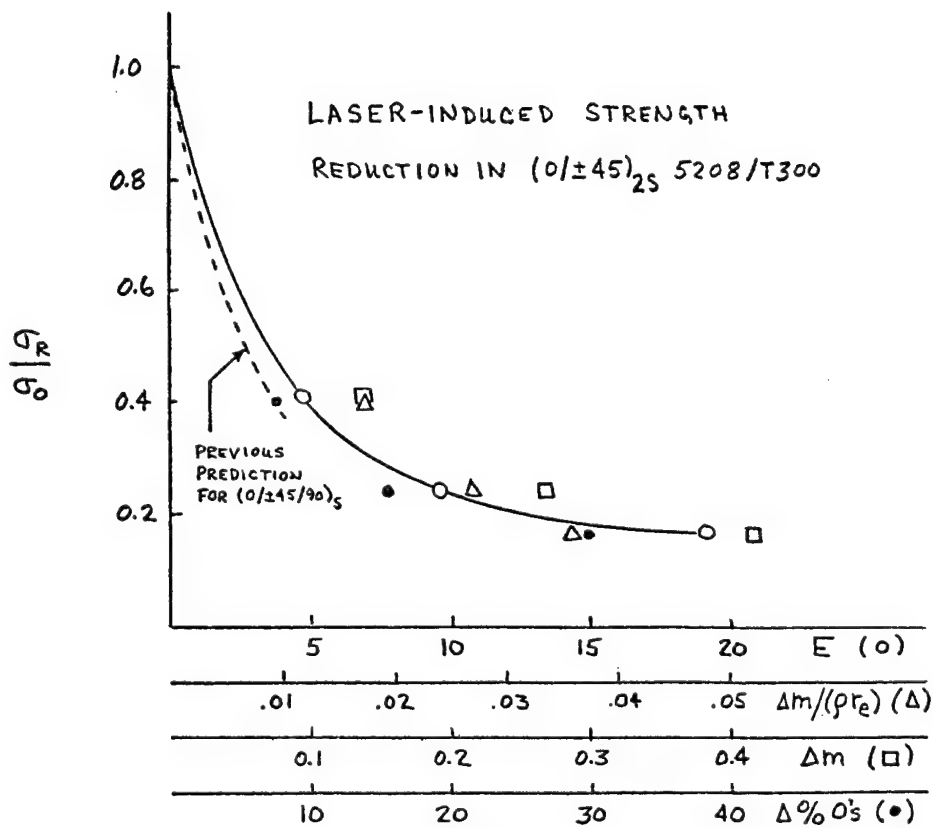
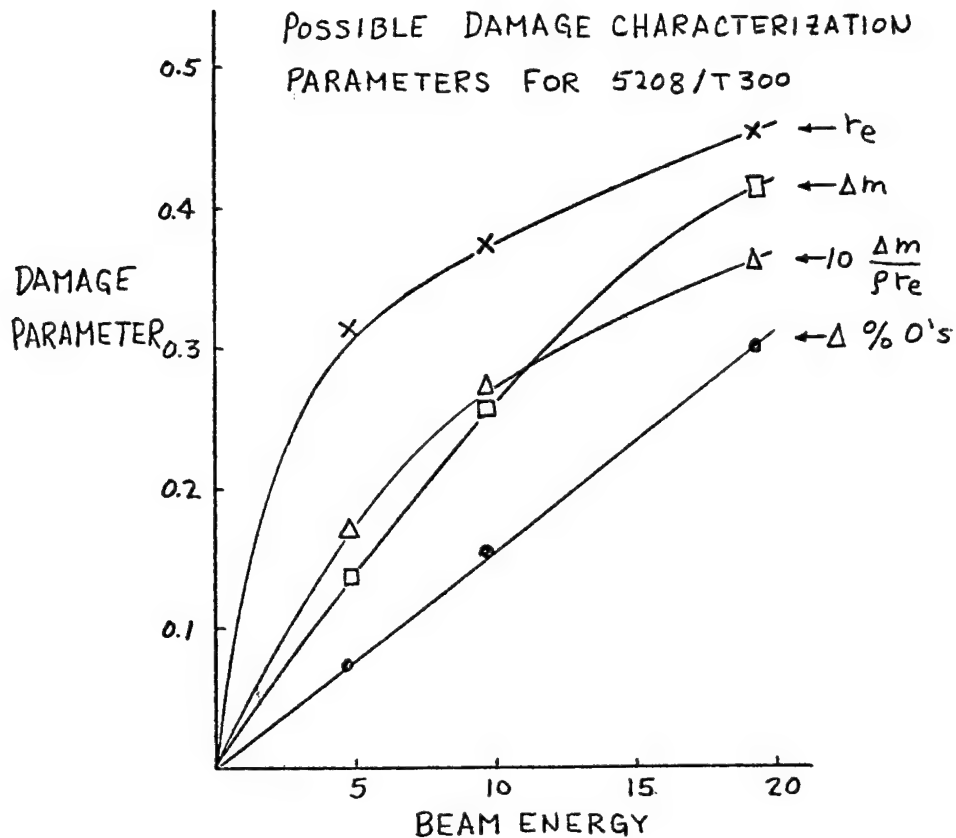
25.6 sec.

5

12.8 sec.

8

6.4 sec.



PRINCIPAL RESULTS TO DATE (1 SEPT 1976)

- o REQUIRED BURNTHROUGH ENERGY FOR ALUMINUM ABOUT 1/3
THAT FOR GRAPHITE-EPOXY
- o ROUGH CALCULATION FOR EFFECTIVE HEAT OF ABLATION GIVES
VALUE UNREALISTICALLY HIGH - - SIGNIFICANT CONDUCTION
LOSS IN G/E ?
- o CONSIDERABLE DATA SCATTER FOR Al -- NOT SO FOR G/E
- o NO EFFECT OF STACKING SEQUENCE ON MASS LOSS OR
PENETRATION DEPTH - -
SLIGHT THICKNESS EFFECT
- o STRENGTH REDUCTION IN G/E APPEARS PREDICTABLE
USING "SIMPLE" PARAMETERS

DEFECT - PROPERTY RELATIONSHIPS IN COMPOSITE MATERIALS

INVESTIGATORS

E. G. HENNEKE II, K. L. REIFSNIDER, W. W. STINCHCOMB
VIRGINIA POLYTECHNIC INSTITUTE & STATE UNIVERSITY
BLACKSBURG, VIRGINIA

OBJECTIVES:

1. To IDENTIFY THE PRECISE NATURE OF DAMAGE DEVELOPMENT IN QUASI-ISOTROPIC GRAPHITE-EPOXY LAMINATES UNDER VARIOUS LOAD HISTORIES.
2. To DETERMINE THE PHYSICAL PARAMETERS WHICH LEAD TO A LOSS OF STRENGTH AND/OR LIFE.
3. To ESTABLISH THE MECHANICS OF THE INDIVIDUAL AND COMBINED ACTION OF THESE PARAMETERS AS THEY INFLUENCE MECHANICAL RESPONSE.
4. To ADDRESS THE QUESTION OF HOW THESE FINDINGS CAN BEST BE DESCRIBED BY ANALYSIS.

FIGURE 1

INVESTIGATIVE PROGRAM:

TYPE I MATERIAL - $[0, \pm 45, 90]_s$, AS3501 GRAPHITE-EPOXY

INSTRUMENTED TENSILE TESTS
LAMINATE THEORY CALCULATIONS - FAILURE PREDICTIONS
SEM AND LIGHT MICROSCOPE STUDIES
ACOUSTIC EMISSION AND ULTRASONIC ATTENUATION STUDIES
FATIGUE LOADING
VIDEO AND THERMOGRAPHIC STUDIES
SECTIONING STUDIES

TYPE II MATERIALS - $[0, 90, \pm 45]_s$, AS3501 GRAPHITE-EPOXY

INSTRUMENTED TENSILE TESTS
LAMINATE ANALYSIS AND 3-D FEM - FAILURE PREDICTIONS
SEM AND LIGHT MICROSCOPE STUDIES
ACOUSTIC EMISSION AND ULTRASONIC ATTENUATION STUDIES
INSTRUMENTED FATIGUE LOADING
VIDEO, CINE, AND THERMOGRAPHIC STUDIES
SECTIONING STUDIES

GENERAL

LOAD HISTORY STUDIES
TRANSVERSE CRACK AND DELAMINATION INVESTIGATION - INITIATION, GROWTH AND FRACTURE
TECHNIQUE DEVELOPMENT - ULTRASONIC ATTENUATION, THERMOGRAPHY, REPLICATION
ANALYSIS EVALUATION AND DEVELOPMENT

TABLE III
SUMMARY OF PROPERTIES *
FOR AS-3501

Elastic Stiffness Properties	Tensile Value	Compression Value
E_1	20.2×10^6 psi	17×10^6 psi
E_2	1.4×10^6 psi	1.6×10^6 psi
ν_{12}	0.28	0.28
G_{12}	0.65×10^6 psi	0.65×10^6 psi
Strength Properties		
X	235,000 psi	180,000 psi
Y	8,200 psi	25,000 psi
S	17,900 psi	17,900 psi

Other Properties

Thermal expansion coefficients:

α_1 (fiber direction) = -0.2×10^{-6} in/in/°F

α_2 (transverse direction) = 13.0×10^{-6} in/in/°F

Fiber volume fraction 0.62

Ply thickness 0.0052 ± 0.0004 in.

Void content 2%

Density 0.057 lb/in^3

Stress-free temperature 278°F

* Data supplied by Hercules, Inc.

FIGURE 3

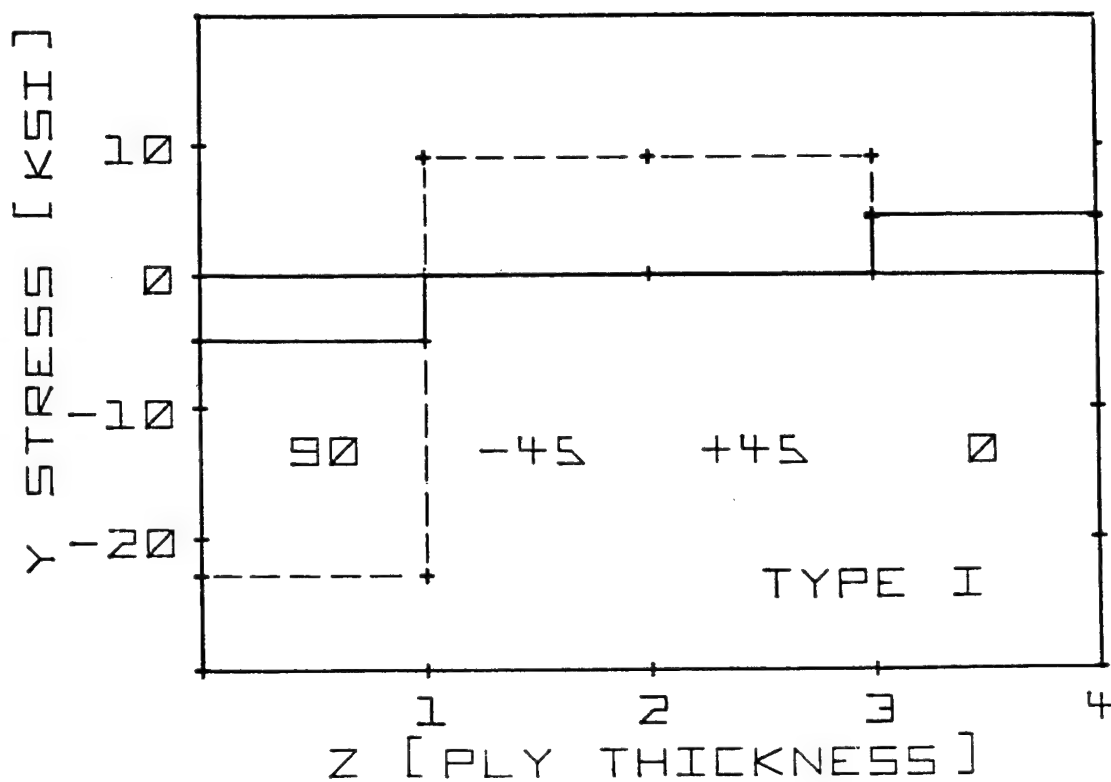


FIG. 4 - TRANSVERSE STRESS DISTRIBUTION THROUGH THE THICKNESS FOR TYPE I MATERIAL

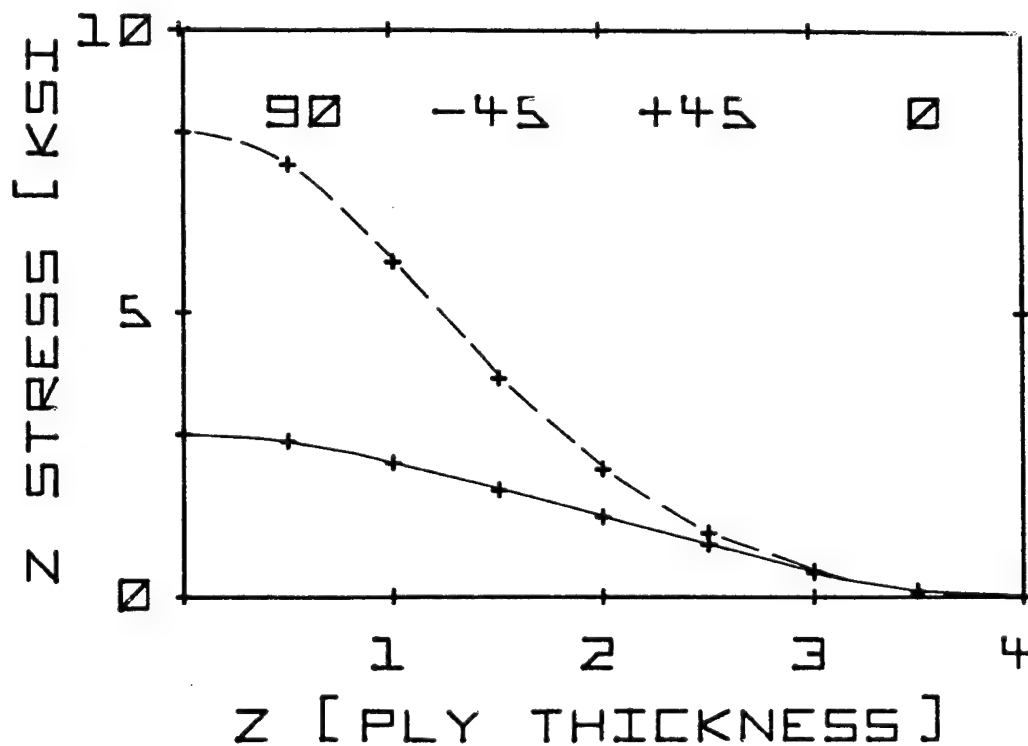


FIG. 5 - INTERLAMINAR NORMAL STRESS DISTRIBUTION THROUGH THE THICKNESS FOR TYPE I MATERIAL

APPENDIX

FOR A STRESS FREE TEMPERATURE WHICH DIFFERS FROM ROOM TEMPERATURE THE MIDPLANE STRAINS ARE GIVEN BY

$$[\epsilon^0] = [A]^{-1} [N + N^T] \quad (A)$$

WHERE $[\epsilon]$ IS THE MATRIX OF MIDPLANE STRAINS, $[A]^{-1}$ IS THE INVERSE OF THE PLATE STIFFNESS MATRIX IN THE ABSENCE OF BENDING, $[N]$ IS THE COLUMN MATRIX OF APPLIED IN-PLANE RESULTANTS, AND $[N^T]$ IS THE AMBIENT TEMPERATURE RESULTANTS DUE TO THERMAL RESIDUAL STRESSES GIVEN BY

$$[N^T] = \int [\bar{Q}] [\alpha] \Delta T dz \quad (B)$$

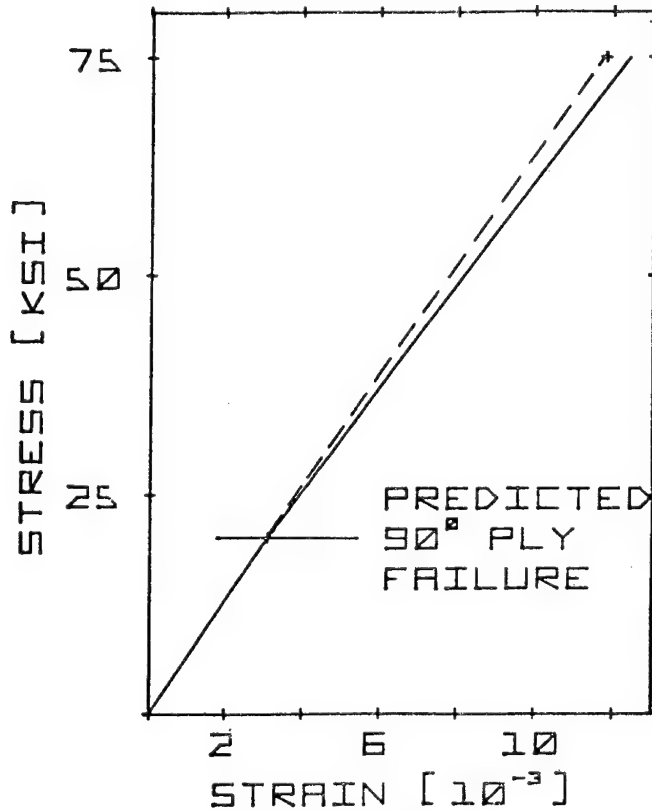
WHERE $[\alpha]$ ARE THE THERMAL EXPANSION COEFFICIENTS, LISTED IN TABLE III. THE STRESSES IN A GIVEN LAYER ARE THEN

$$[\sigma]^K = [\bar{Q}]^K [[\epsilon^0] - [\alpha] \Delta T]^K \quad (C)$$

THE PERTINENT MAXIMUM STRAIN CONDITION IS,

$$\sigma_X^{90^\circ} \leq \frac{Y}{\sin^2 \theta - \nu_{21} \cos^2 \theta} \quad (D)$$

FIG. 6 - SUMMARY OF MAXIMUM STRAIN CRITERIAN INCLUDING THERMAL STRESSES



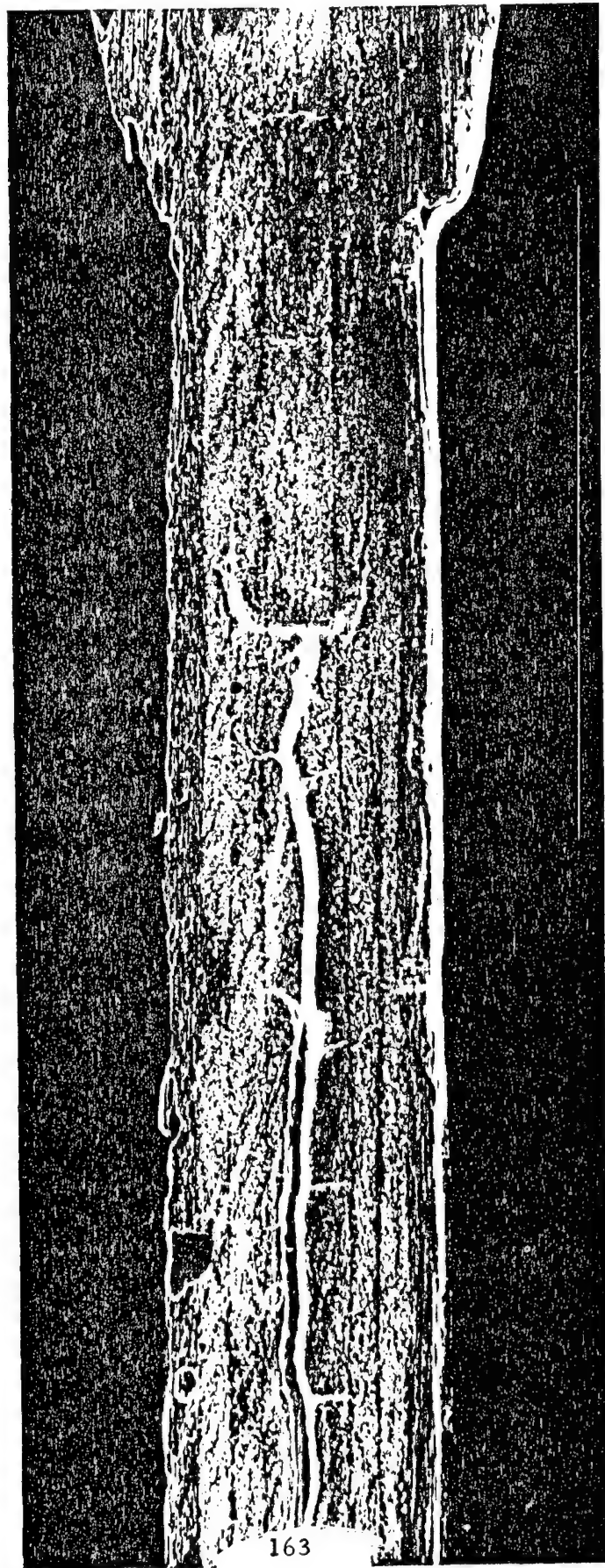
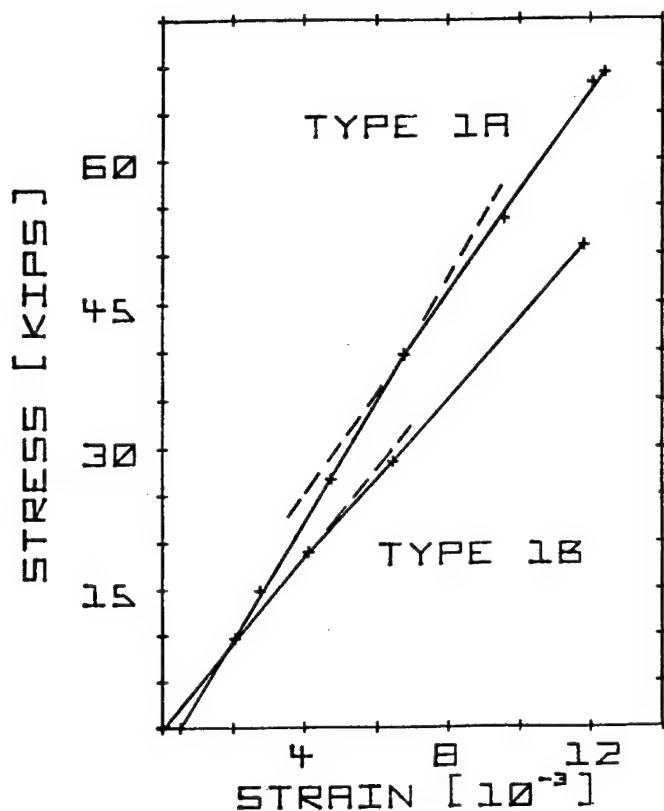


FIG. 8 - DELAMINATION AND TRANSVERSE CRACKING IN TYPE I MATERIAL AT 2700 LB.

FIG. 9 - TYPICAL OBSERVED STRESS-STRAIN CURVES FOR TYPE I MATERIAL



VIDEO-THERMOGRAPHY STUDY

1. CYCLED TYPE ONE SPECIMEN AT 30 HZ AT 82% OF STATIC FAILURE LOAD. SPECIMEN HAD 1/4 IN. CENTER HOLE. BROKE AFTER A FEW HUNDRED CYCLES. VERY LITTLE HEAT GENERATION OR CHANGE.
2. SIMILAR TO 1. AT 70% OF FAILURE LOAD. NO SUBSTANTIAL PATTERN CHANGE.
3. RAN SOME BEP AND BAL FOR COMPARISON. BAL IS SIMILAR IN HEAT OUTPUT.
4. INTRODUCED VARIABLE FREQUENCY EXCITATION - "VIBRO-THERMOGRAPHY", AND IDENTIFIED DAMAGE MORE READILY IN:
 - I) 0° GEP AFTER STATIC LOADING
 - II) NOTCHED UNIDIRECTIONAL GEP AFTER STATIC LOADING
 - III) QUASI-ISOTROPIC LAMINATE WITH HOLE
 - IV) $\pm 60^{\circ}$ GEP
 - V) 90° GEP UNIDIRECTIONAL
 - VI) TYPE I AND II GEP WITHOUT HOLE
5. IDENTIFIED GRIP REGION AS A SPECIAL PROBLEM.

FIG. 10 - SUMMARY OF VIDEO-THERMOGRAPHY STUDY

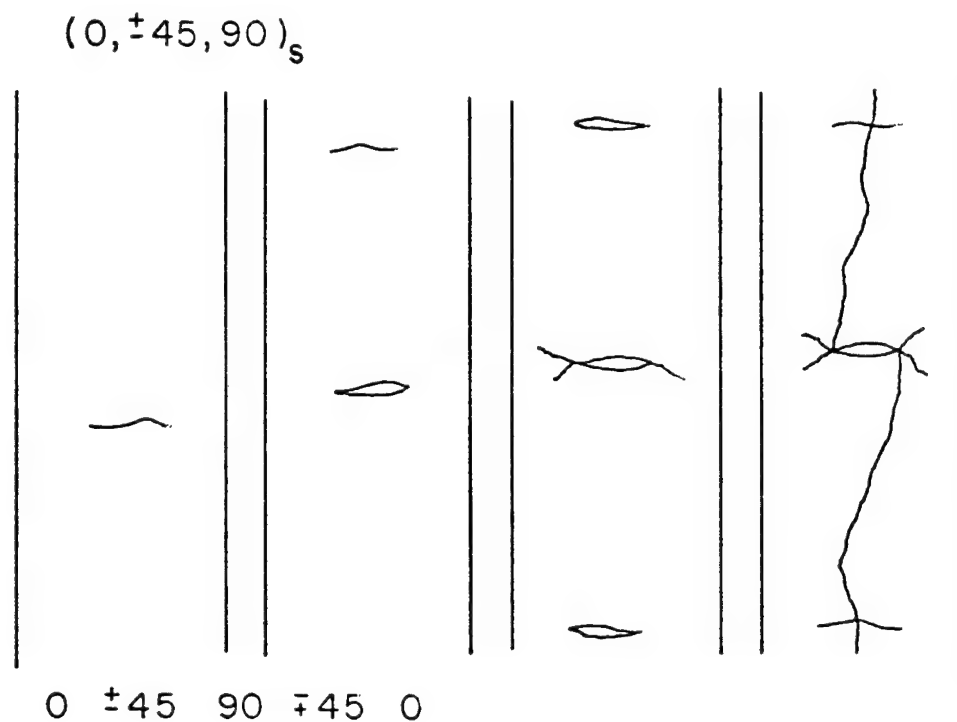


FIG. 11 - SCHEMATIC DIAGRAM OF DAMAGE DEVELOPMENT IN TYPE I MATERIAL

TYPE I

TRANSVERSE CRACKING OF 90° PLIES:

1. COMMONLY OBSERVED AT 1500-1800 LB UNDER LOAD.
2. CRACKS PROPAGATE THROUGH THICKNESS, FIRST THROUGH 90° PLIES, THEN INTO $\pm 45^\circ$ PLIES.
3. BRANCHING IN 45° PLIES IS COMMON, USUALLY AT 2500-2700 LB.
4. DELAMINATION OCCURS BEGINNING AT TRANSVERSE CRACKS AND RELAXES THE BRANCHES OF THE PRIMARY CRACK.

FIG. 12 - SUMMARY OF DAMAGE PROCESS IN TYPE I MATERIAL

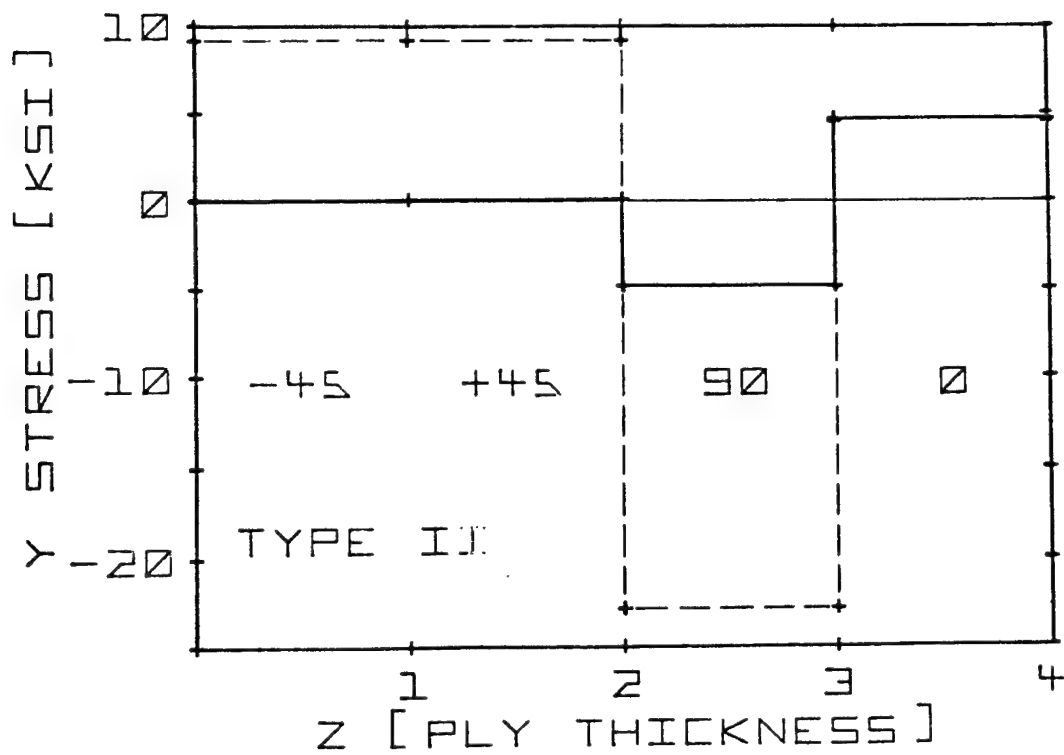


FIG. 13 - TRANSVERSE STRESS DISTRIBUTION THROUGH THE THICKNESS FOR TYPE II MATERIAL

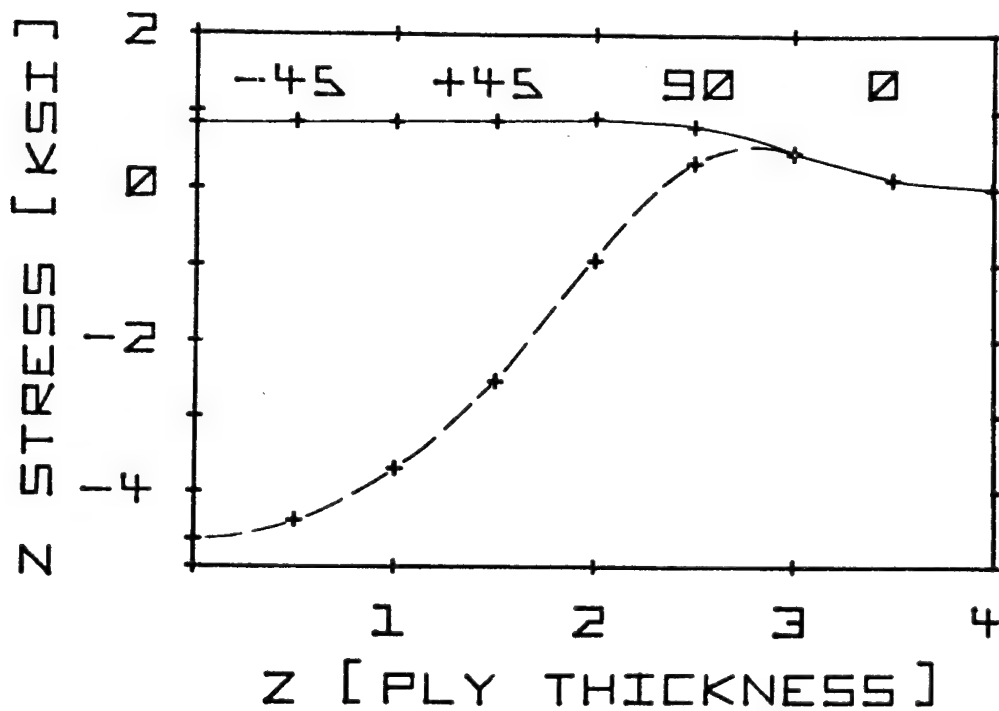


FIG. 14 - INTERLAMINAR NORMAL STRESS DISTRIBUTION THROUGH THE THICKNESS FOR TYPE II MATERIAL

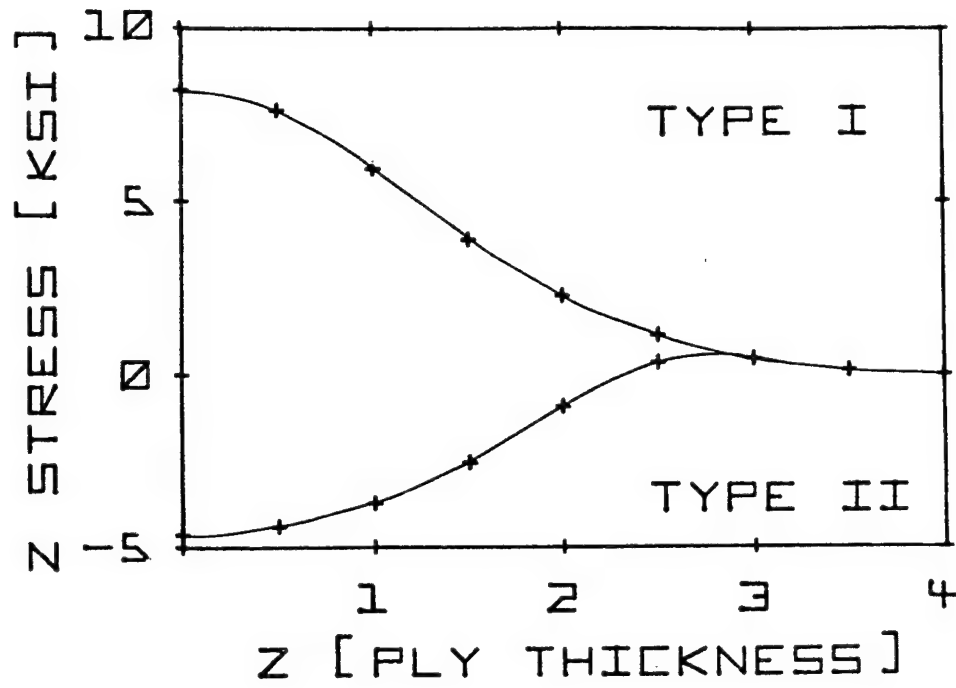


FIG. 15 - COMPARISON OF INTERLAMINAR NORMAL STRESS DISTRIBUTIONS IN TYPE I & TYPE II MATERIALS

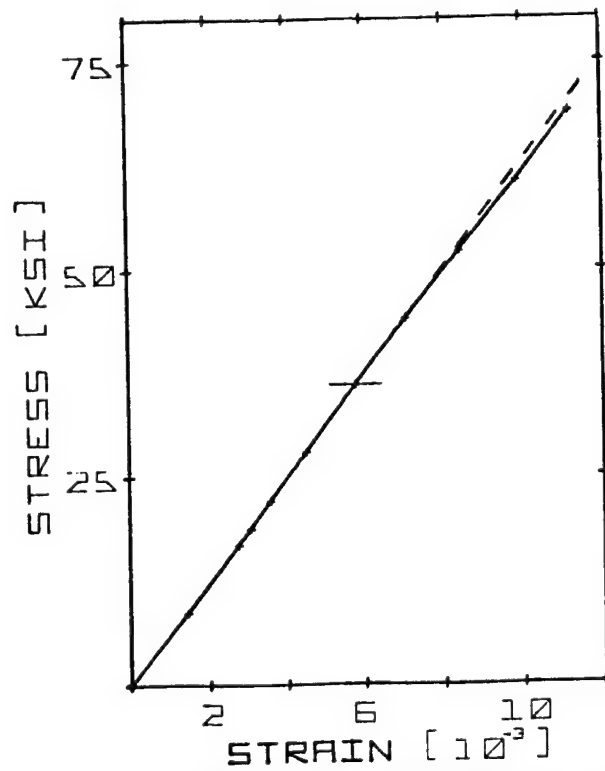


FIG. 16 - TYPICAL OBSERVED STRESS-STRAIN CURVE FOR TYPE II MATERIAL

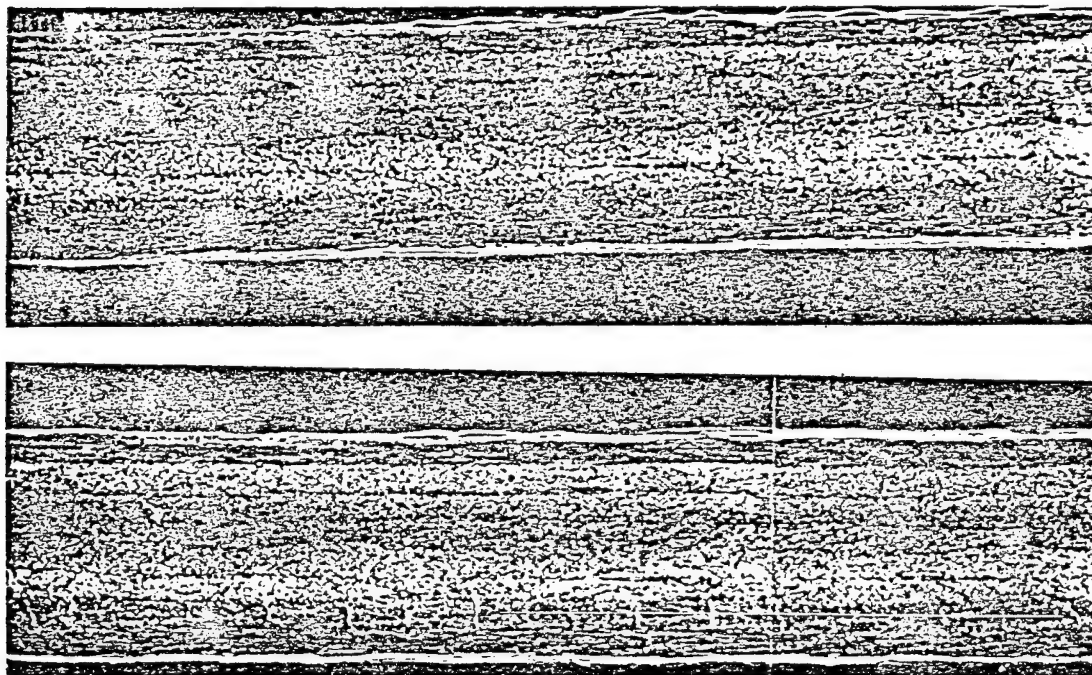


FIG. 17 EDGE REPLICAS OF TYPE II SPECIMENS AT 200 LB. AND 2700 LB.

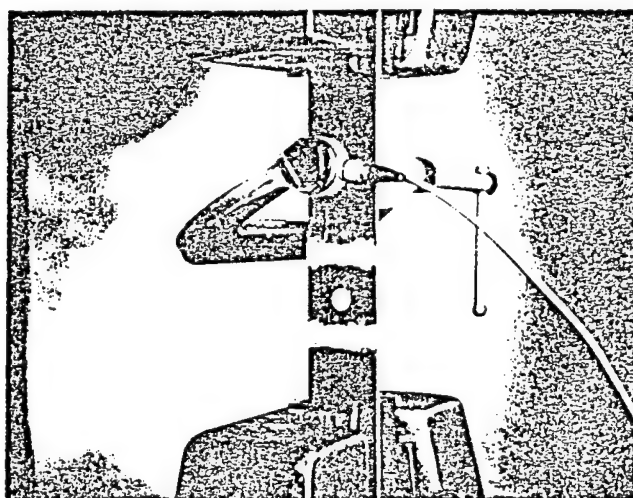


Figure18- Ultrasonic transducer clamped to a composite specimen mounted in testing grips.

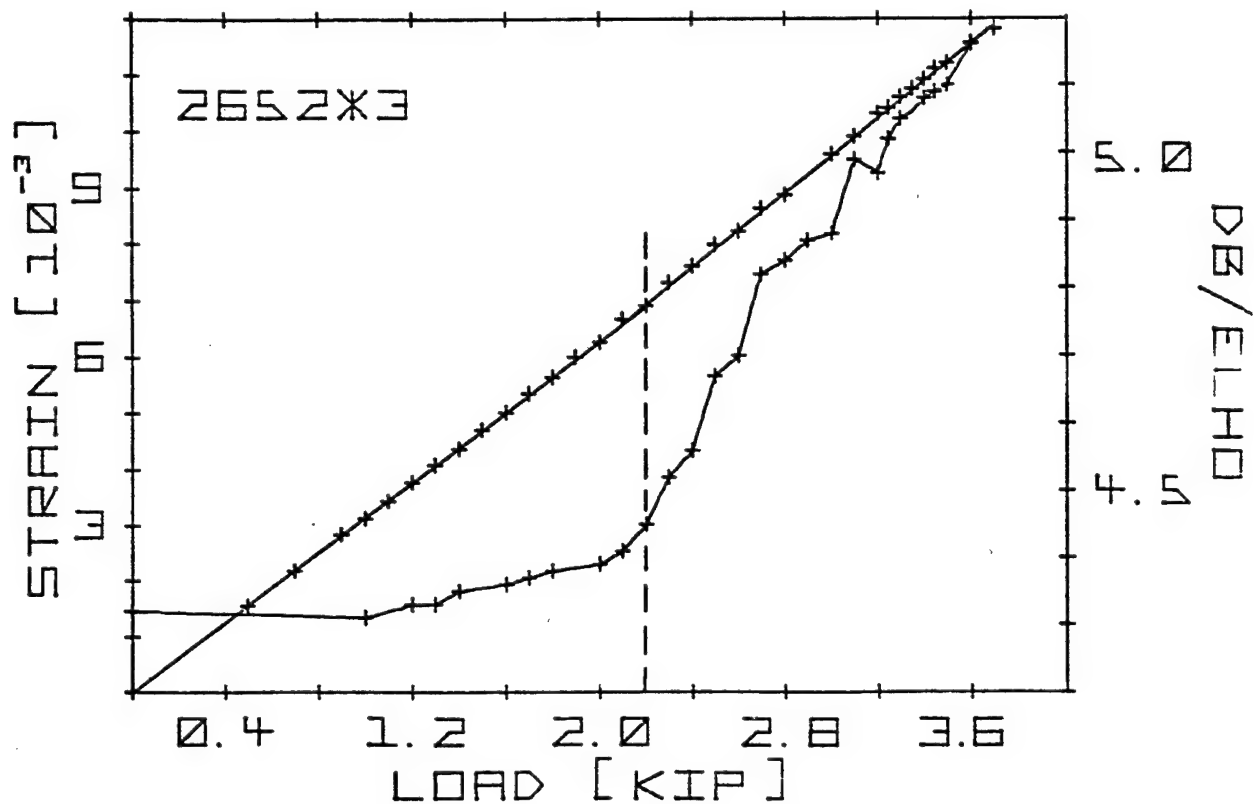


FIG. 19 - REAL-TIME ATTENUATION AND STRAIN VERSES LOAD FOR A TEST OF TYPE II MATERIAL

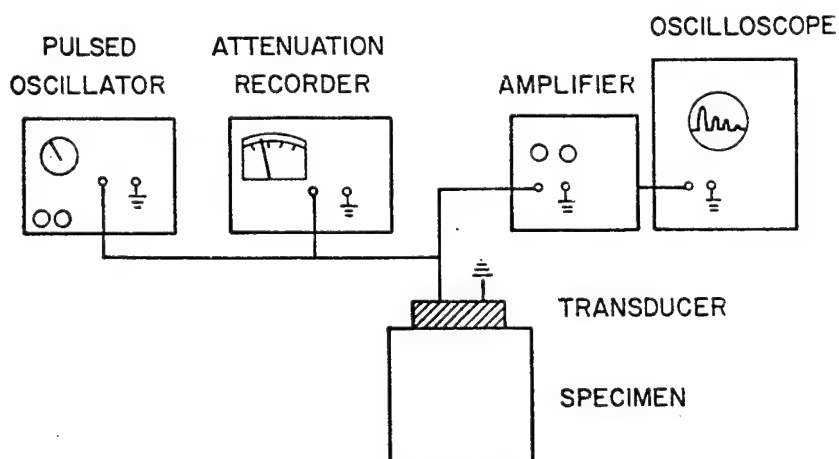


FIG. 20 - SCHEMATIC OF REAL-TIME ATTENUATION APPARATUS

FIG. 21 - TYPICAL ATTENUATION VERSES LOAD DATA FOR TYPE II MATERIAL

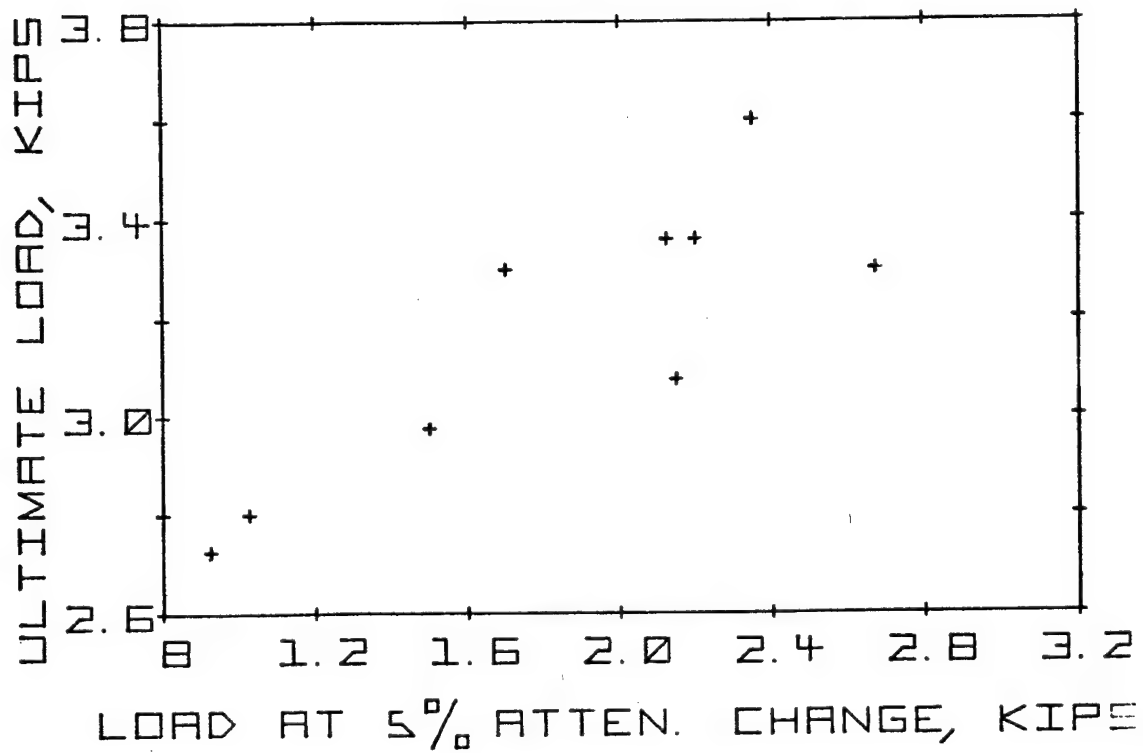
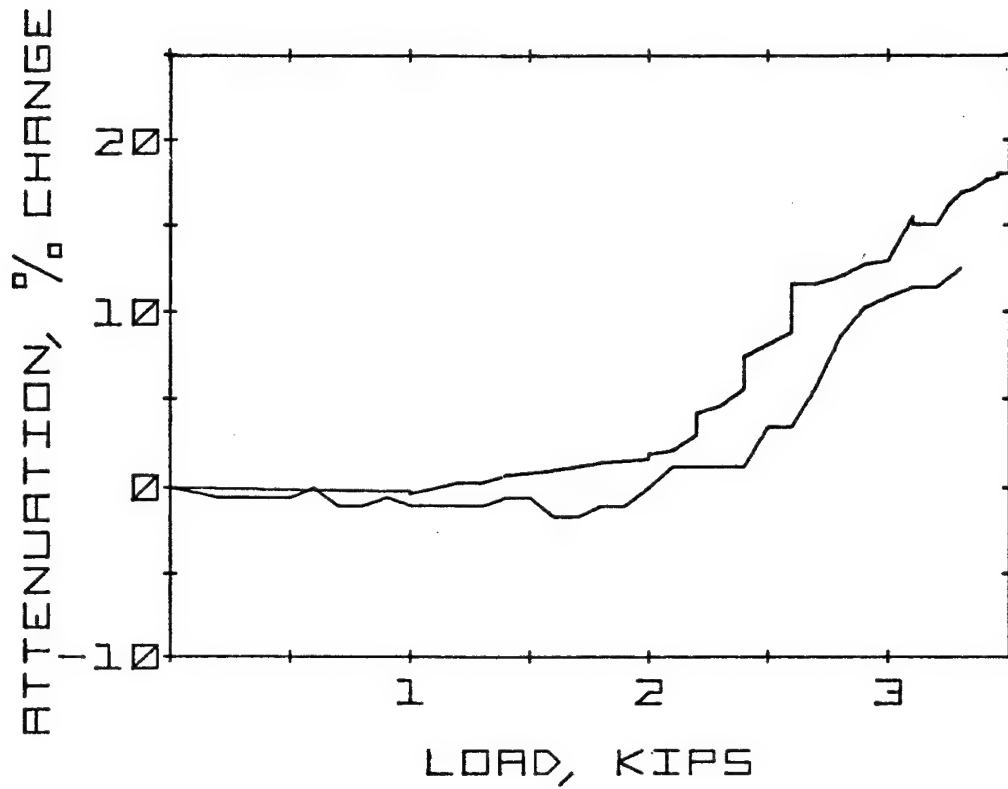


FIG. 22 - COMPARISON OF ULTIMATE LOAD AND LOAD VALUES AT WHICH A FIVE PERCENT ATTENUATION OCCURRED IN SEVERAL TESTS OF TYPE II MATERIAL

STRAIN GAGE STUDY:

1. OBSERVED AS MUCH AS 12% DIFFERENCE IN READINGS FROM EDGE TO CENTERLINE.
2. DIFFERENCES CAN BE CAUSED BY VARIATIONS IN TAB THICKNESSES, IMPRECISE ALIGNMENT OF GRIP FACES, OR NONUNIFORM GRIP PURCHASE.
3. FRACTURE INITIATED FROM HIGH STRAIN REGION.
4. OBTAINED DATA WHEREIN FRACTURE OCCURRED THROUGH THE GAGES - STRAINS WERE ESSENTIALLY IDENTICAL TO FRACTURE - NO EVIDENCE OF PREMATURE RELAXATION AT EDGES OR CENTER.
5. TEMPERATURE WAS FOUND TO INFLUENCE STRAIN GAGE READINGS.

FIG. 23 - SUMMARY OF RESULTS OF STRAIN GAGE STUDY

CENTERLINE SECTIONING SERIES:

1. TYPE I SPECIMEN LOADED TO 1500 LB
 - A. ESSENTIALLY SAME NUMBER OF MAJOR TRANSVERSE CRACKS ON INTERIOR & EXTERIOR EDGES IN 90° LAYERS
 - B. MORE CRACKS IN 45° LAYERS IN INTERIOR
 - C. MANY MORE ANGULAR AND MINOR CRACKS IN INTERIOR - LARGEST SINGLE CRACK FOUND IN INTERIOR
 - D. 90° CRACKS MORE VISIBLE AT 100X ON LIGHT MICROSCOPE UNDER LOAD THAN AT 400X ON SEM, UNLOADED
 - E. CRACKS IN 45° LAYERS MORE VISIBLE IN SEM (UNLOADED) THAN UNDER LOAD WITH LIGHT MICROSCOPE
 - F. NO CRACKS ON OUTSIDE EDGE OBSERVED ON SEM
2. TYPE I SPECIMEN LOADED TO 1000 LB
 - A. TRANSVERSE CRACKS WERE FOUND IN INTERIOR WITH SEM
 - B. NO CRACKS WERE FOUND ON EXTERIOR EDGE WITH SEM
 - C. CRACKS IN 45° LAYERS IN INTERIOR ARE FREQUENTLY ANGULAR
 - D. TRANSDUCER REGION DOES NOT SHOW ANY IRREGULARITIES
 - E. AT-LOAD LIGHT MICROSCOPE STUDY SHOWED LARGER NUMBER OF CRACKS ON INTERIOR THAN EXTERIOR EDGE. RESULTS ON TWO HALVES SHOWED GOOD REPRODUCIBILITY

FIG. 24 - SUMMARY OF RESULTS OF CENTERLINE SECTIONING SERIES

3. TYPE II SPECIMEN LOADED TO 1000 LB STRESS AMPLITUDE FOR 850,000 CYCLES
 - A. LIGHT MICROSCOPE EXAMINATION AT-LOAD SHOWED LARGER NUMBER OF TRANSVERSE CRACKS THAN FOR THE SPECIMEN LOADED STATICALLY
 - B. MANY MORE TRANSVERSE CRACKS WERE FOUND IN THE INTERIOR EDGE THAN ON THE EXTERIOR EDGE
 - C. MORE INTERFACIAL AND IRREGULAR CRACK FORMATION BEHAVIOR WAS NOTED THAN FOR THE STATIC LOADING CASES
 - D. THE LARGEST CRACKS, ESPECIALLY IN THE ANGLE PLIES, WERE FOUND IN THE INTERIOR EDGE
4. TYPE I SPECIMEN LOADED AT 1000 LB LOAD AMPLITUDE FOR 850 THOUSAND CYCLES
 - A. TRANSVERSE CRACK COUNT WAS 36 ON ONE EXTERIOR EDGE (WHICH DELAMINATED) AND 20 ON THE OTHER. INTERIOR EDGE COUNT WAS 24.
 - B. DELAMINATION OCCURRED AT ONE END AND NEAR THE CENTER ON ONE EDGE ONLY
 - C. STIFFNESS APPEARS TO DECREASE WITH DAMAGE BUT INCREASE WITH CYCLES WHEN DAMAGE IS NOT DEVELOPING
5. TYPE I SPECIMEN IN AS-RECEIVED CONDITION
 - A. OBSERVED NINE OR TEN INITIAL CRACKS WHICH HAVE THE APPEARANCE OF SMALLER VERSIONS OF WHAT WE FIND IN LOADED SPECIMENS
 - B. INTERIOR AND EXTERIOR EDGES APPEAR TO BE ESSENTIALLY IDENTICAL
 - C. THE INITIAL CRACKS THAT ARE SEEN DO NOT ALWAYS APPEAR WITH ORIENTATIONS TRANSVERSE TO THE SPECIMEN LONGITUDINAL AXIS
 - D. A PREDOMINANT PROPORTION OF THOSE INITIAL CRACKS WHICH WERE OBSERVED WERE FOUND TO BE LOCATED IN A REGION WITHIN 1 CM OR SO FROM THE TABS

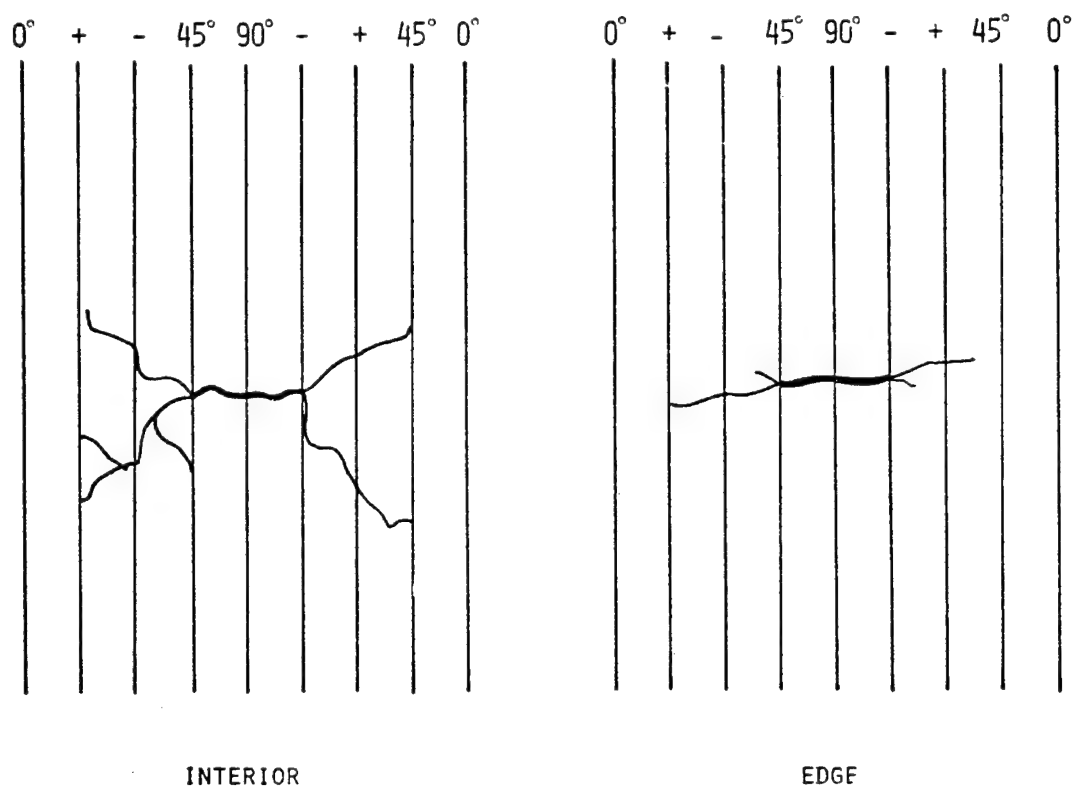


FIG. 25 - SCHEMATIC DIAGRAM OF CRACK BRANCHING ON INTERIOR AND EXTERIOR SURFACES

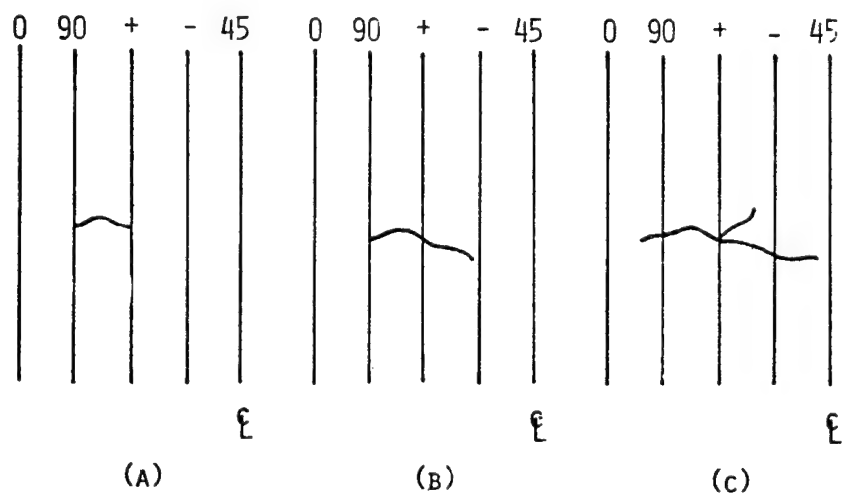


FIG. 26- THROUGH-THE-THICKNESS DAMAGE SEQUENCE IN TYPE II SPECIMENS (EDGE VIEW).

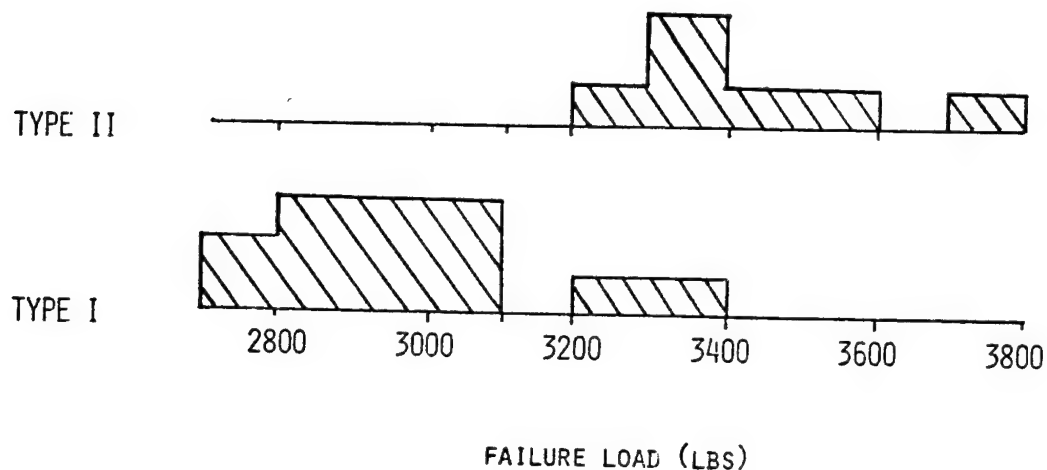


FIG. 27 - DISTRIBUTION OF FAILURE LOADS FOR TYPE I AND TYPE II SPECIMENS

TYPE II

1. "KNEE" IN STRESS-STRAIN CURVE NEARLY IMPERCEPTIBLE - MORE LIKE A GENTLE CURVE.
2. TRANSVERSE CRACKING MORE DIFFICULT TO SEE - FIRST OBSERVE AT 1800-2300 LB.
3. THE GROWTH OF TRANSVERSE CRACKS IS SLOWER THAN IN TYPE I. SPREAD INTO 45° PLIES OCCURS BETWEEN 3000-3200 LB.
4. DELAMINATION DOES NOT STOP THE TRANSVERSE PROPAGATION, BUT A COMPLETE TRANSVERSE CRACK THROUGH-THE-THICKNESS FORMS ONLY IN A FEW INSTANCES.
5. FORMATION OF A THROUGH-THE-THICKNESS TRANSVERSE CRACK OCCURS QUITE CLOSE TO THE FINAL FAILURE LOAD, USUALLY IMMEDIATELY PRECEEDING IT.

FIG. 28 - SUMMARY OF DAMAGE PROCESS IN TYPE II MATERIAL

DAMAGE CHARACTERIZATION:

1. ULTRASONIC ATTENUATION AND ACOUSTIC EMISSION INDICATE DAMAGE DEVELOPMENT BEFORE VISUAL CRACK OBSERVATION OF "KNEE" IN σ - ϵ CURVE, AT LEVEL QUITE CLOSE TO PREDICTED ONE.
2. CRACKS DO NOT APPEAR ON BOTH EDGES AT THE SAME TIME \Rightarrow IN PLANE GROWTH.
3. NO EVIDENCE THAT CRACKS GROW FROM EDGE TO CENTER.
4. NEED TO UNDERSTAND GROWTH PROCESS TO CHARACTERIZE DAMAGE CORRECTLY, AND THEREBY ESTABLISH CONTROLLING PARAMETERS FOR STRENGTH AND LIFE.

Fig. 29 - GENERAL DAMAGE CHARACTERIZATION

PRINCIPAL FINDINGS AND CONCLUSIONS

1. IN QUASI-ISOTROPIC LAMINATES IT WOULD APPEAR THAT "FIRST-PLY FAILURE" IS MORE CORRECTLY INTERPRETED AS THE INITIATION OF A PROCESS THAN THE DISCRETE OCCURRENCE OF A SINGLE EVENT.
2. IF THERMAL RESIDUAL STRESSES ARE INCLUDED IN THE CALCULATIONS, LAMINATE THEORY PREDICTIONS ARE WITHIN ABOUT 5% OF THE LEVEL AT WHICH OUR NDT&E TECHNIQUES INDICATE DAMAGE INITIATION.
3. THE "KNEE" IN THE STRESS-STRAIN CURVE IS MORE OR LESS WELL DEFINED DEPENDING UPON THE CONSTRAINT IN THE REGION OF CRACK FORMATION IN THE 90° PLIES AND IS, THEREFORE, A FUNCTION OF STACKING SEQUENCE. OUR OBSERVATIONS OF THE KNEE GENERALLY OCCUR AT HIGHER STRESS LEVELS THAN DO THE FIRST INDICATIONS AND OBSERVATIONS OF MICRO-DAMAGE, SOMETIMES AS MUCH AS 50-75% HIGHER.
4. BRANCHING OF TRANSVERSE CRACKS FROM THE 90° PLIES INTO THE ADJACENT PLIES. GENERAL CRACKING OF THE ANGLE PLIES APPEARS TO BE MORE EXTENSIVE IN THE INTERIOR OF THE SPECIMEN THAN AT THE EDGE. TRANSVERSE CRACKS COMPLETELY THROUGH THE THICKNESS APPEAR TO FORM AT THE EDGE.
5. THE STRENGTH OF THE $[0^\circ, 90^\circ, \pm 45^\circ]_S$ LAMINATES IS SOMEWHAT GREATER THAN THE $[0^\circ, \pm 45^\circ, 90^\circ]_S$ LAMINATES.
6. THESE MATERIALS DO EXHIBIT MEMORY EFFECTS IN SOME CASES, TIME DELAYED FRACTURE AT CONSTANT ELONGATION HAS BEEN OBSERVED.
7. ULTRASONIC ATTENUATION CHANGE APPEARS TO BE A CLEAR, PRECISE, CONSISTENT AND REPRODUCIBLE INDICATION OF DAMAGE INITIATION AND GROWTH. IT CORRELATES WELL WITH MICRO-SCOPE OBSERVATIONS.

FIGURE 30

FATIGUE IN ADHESIVELY BONDED LAMINATES

J. A. ALIC

DEPARTMENT OF MECHANICAL ENGINEERING
WICHITA STATE UNIVERSITY

OBJECTIVES

CRACK INITIATION (7075-T6)

ISOLATION OF FATIGUE DAMAGE

S-N PERFORMANCE, WITH AND
WITHOUT STRESS CONCENTRATION

CRACK PROPAGATION

EFFECT OF LAMINA THICKNESS
(7075-T6)

7075-T6(51) BONDED TO 2024-T3(51)

LAMINA TYPES

THIN LAYERS

8 LAYERS, 0.032 INCH THICK

22 LAYERS, 0.011 INCH THICK

THICK LAYERS

2 LAYERS, $\frac{1}{4}$ INCH THICK

4 LAYERS, $\frac{1}{8}$ INCH THICK

CRACK PROPAGATION

COMPACT SPECIMEN, $R=0.1$

MONOLITHIC 7075-T6(51) AND
2024-T3(51)

THIN LAMINAE (7075-T6)

8 LAYER

22 LAYER

THICK LAMINAE (7075-T651)

2 LAYER

4 LAYER

COMBINED 7075/2024

2 LAYER

4 LAYER

CRACK INITIATION AND S-N

CYCLIC TENSION, $R=0.1$

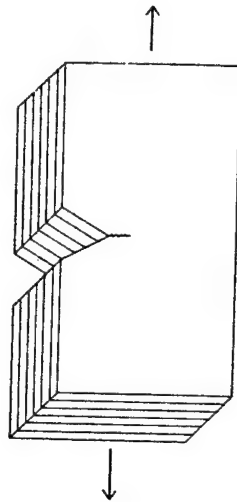
UNNOTCHED AND NOTCHED (CENTRAL
HOLE, $1T_t=2.5$)

MONOLITHIC, $\frac{1}{4}$ INCH THICK

8 LAYER

22 LAYER

BACKGROUND



CRACK DIVIDER

THICKNESS EFFECT
ON CRACK GROWTH



CRACK ARRESTOR

DISCONTINUITY
AT INTERFACE

MECHANISM

REAL STRUCTURE MAY BE INTERMEDIATE SITUATION

PRELIMINARY RESULTS

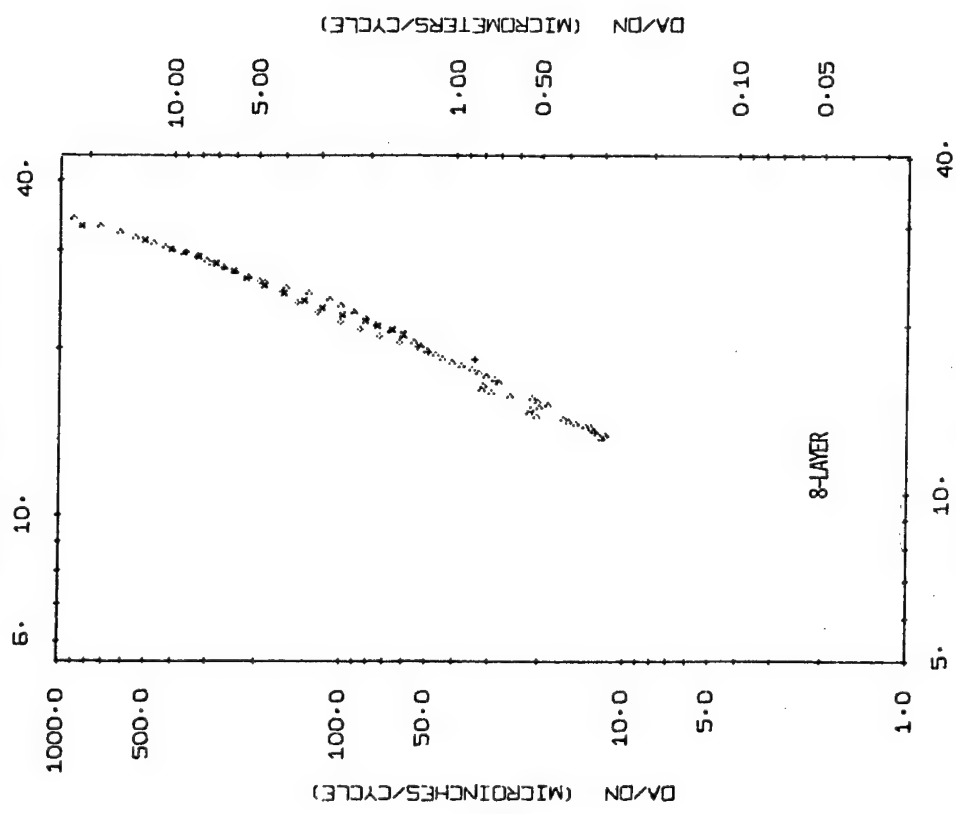
THIN LAMINAE
(8 OR 22 LAYERS)

ADHESIVE: HYSOL EA 9410

TENSILE PROPERTIES

	YS (KSI)	TS (KSI)	ELONG. (%)	K_{IC} (KSI/IN)
8-LAYER	74	82	15	~55
22-LAYER	72	79	16	52

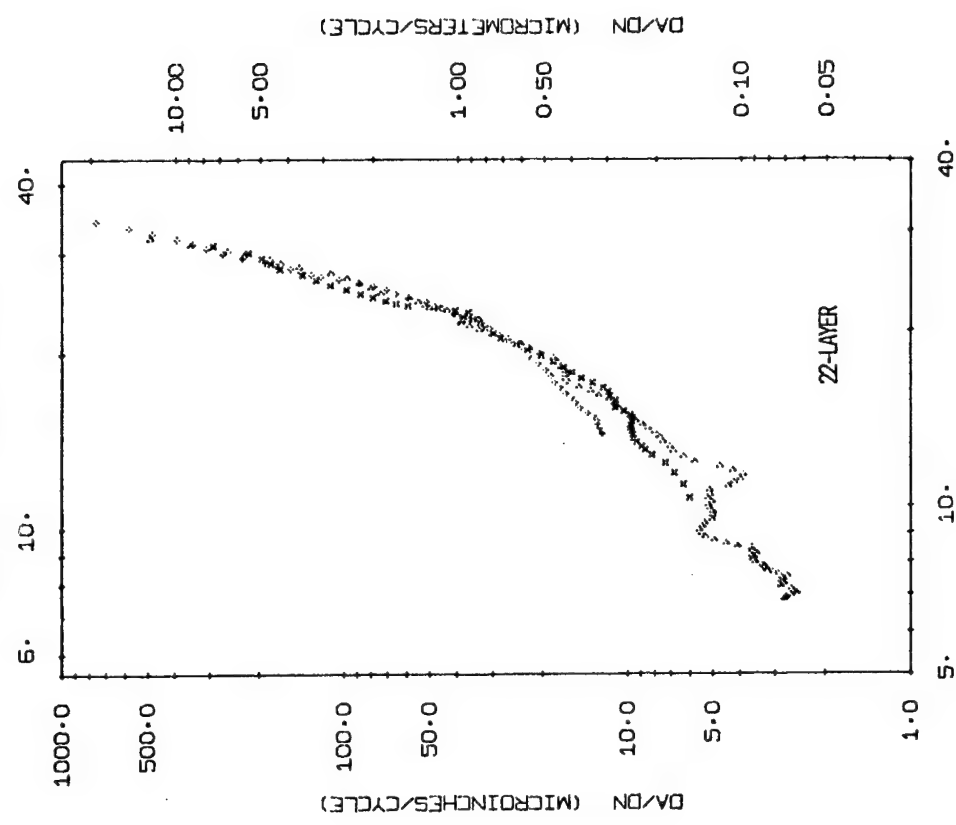
DELTA K (MPA(M)**1/2)



DELTA K (KSI(IN)**1/2)

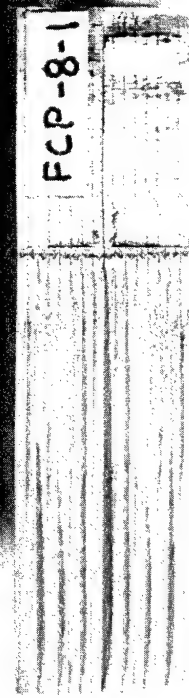
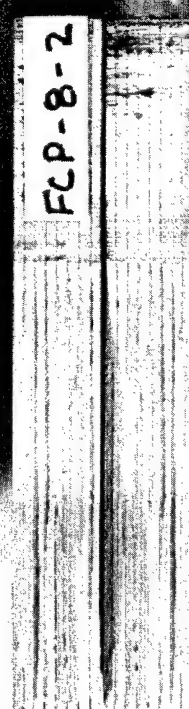
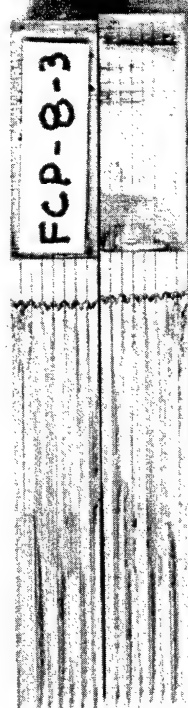
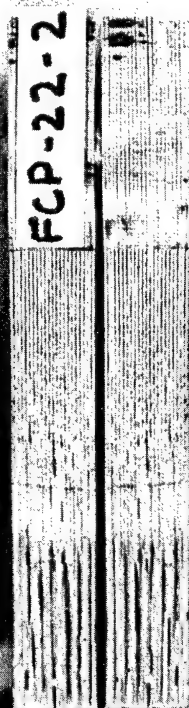
SPECIMEN FCP-8-2 IS +
SPECIMEN FCP-8-3 IS X
SPECIMEN FCP-8-4 IS ▴

DELTA K (MPA(M)**1/2)



DELTA K (KSI(IN)**1/2)

SPECIMEN FCP-22-1 IS +
SPECIMEN FCP-22-2 IS X
SPECIMEN FCP-22-3 IS ▴ (TOP POINT)



CONCLUSIONS

- SOMEWHAT LOWER GROWTH RATES IN 22-LAYER LAMINATES AT INTERMEDIATE LOAD LEVELS.
- PROPAGATION ERRATIC IN LAMINATES AT LOW GROWTH RATES.

FAILURE MECHANISMS AND CRITERIA IN COMPOSITE MATERIALS

N. J. PAGANO
AIR FORCE MATERIALS LABORATORY
In-House Work Unit

FAILURE MODES IN COMPOSITES AND ADHESIVE JOINTS

Three-Dimensional Stress Analysis, Delamination	Curing Stress	Identification of Damage	First Ply Failure
N. J. Pagano	H. T. Hahn	M. Knight	VPISU
P. W. Hsu	N. J. Pagano	H. T. Hahn	SWRI
	R. Y. Kim	VPISU	J. Erikson
			H. T. Hahn
Structural Failure Analysis	Analysis of Rosettes	C / C Modeling	
R. L. Foye	N. J. Pagano	P. W. Hsu	
N. J. Pagano		N. J. Pagano	

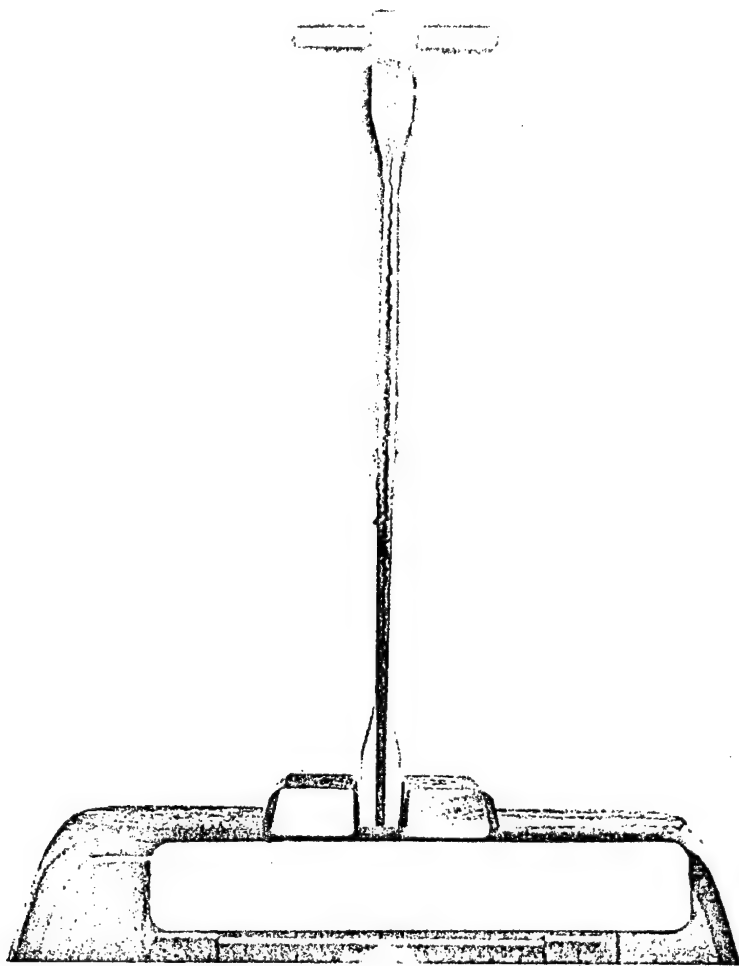


Figure 2. Static Delamination

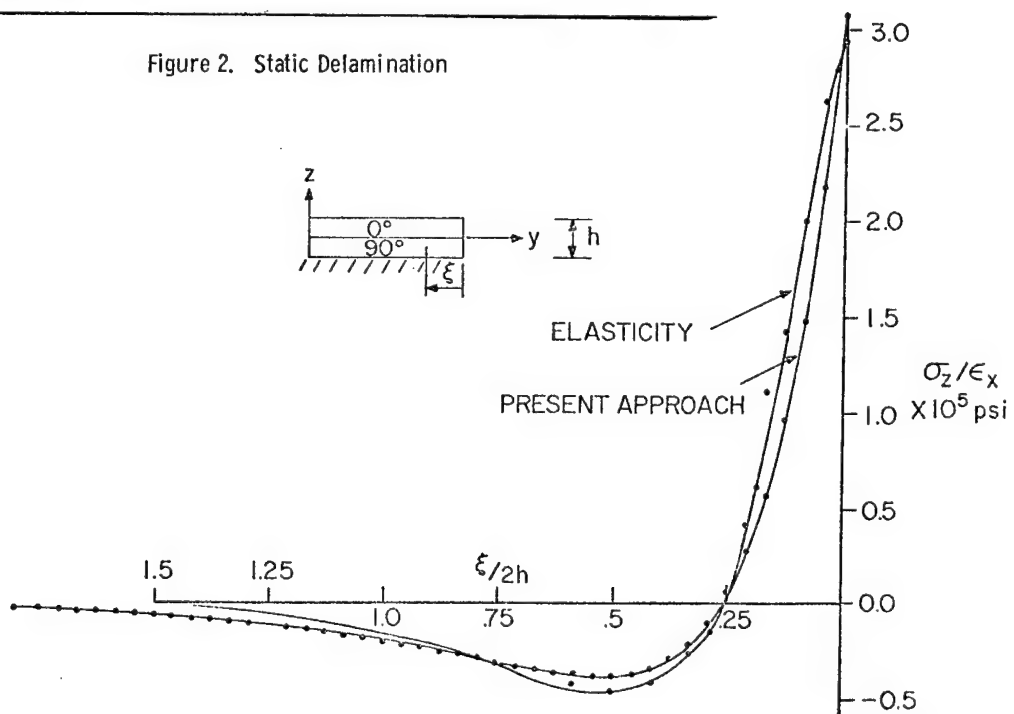


Figure 3. Interlaminar Normal Stress Distribution.

VARIATIONAL PRINCIPLE FOR LAMINATES

$$\text{Let } \delta Q = 0$$

$$\text{where } Q = \int_V F dV - \int_{S'} P_i U_i dS$$

S' = Traction boundary surface

$$F = \frac{\sigma_{ij}}{2} (U_{i,j} + U_{j,i}) - W$$

W = Complementary energy = $W(\sigma_{ij}, e_{ij})$

e_{ij} = expansional strain tensor

P_i = prescribed tractions

For a body with interfaces, we get

$$\begin{aligned} \delta Q = & \sum_{K=1}^N \int_{V_K} \left[\left(\frac{U_{i,j} + U_{j,i}}{2} - W, \sigma_{ij} \right) \delta \sigma_{ij} - \sigma_{ij,j} \delta U_i \right]^{(K)} dV_K + \int_{S'} (\tau_i - P_i) \delta U_i dS \\ & + \int_{S''} \tau_i \delta U_i dS + \sum_{K=1}^{N-1} \int_{I_K} \left(\tau_i^{(K)} \delta U_i^{(K)} + \tau_i^{(K+1)} \delta U_i^{(K+1)} \right) dI_K = 0 \end{aligned}$$

Curing Stresses

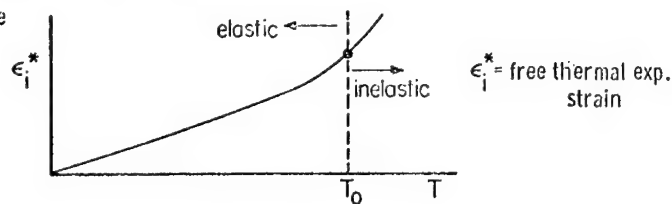
Curing Stresses caused by

- Non-uniform inelastic deformation of resin (microstresses)
- Thermal deformations of "hard" layers (Effective Modulus theory applies)

For the latter, we assume

$$\sigma_i(T) = Q_{ij}(T) [\epsilon_j(T) - e_j(T)]$$

where



$$\text{and } e_j(T) = \epsilon_j^*(T) - \epsilon_j^*(T_0) \quad (T < T_0)$$

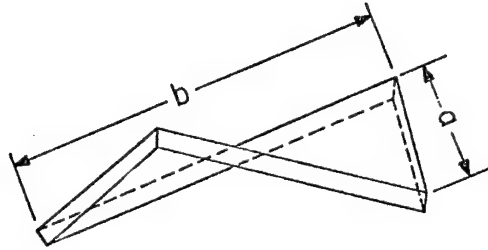
$$\sigma_i(T_0) = 0$$

As a first approx., we may put $e_j(T) = \alpha_j(T)(T - T_0)$. Then only

R.T. measurements are required.

EXPERIMENTAL CHECK

Unsymmetric angle - ply ($\pm\theta$)



$$W_{\max} = 2\kappa_6 ab$$

where

$$\kappa_6 = \frac{4e_6}{h} \left[1 - \frac{Q_{66}(Q_{11}Q_{22} - Q_{12}^2)}{D} \right]$$

and

$$D = 4Q_{66}(Q_{11}Q_{22} - Q_{12}^2) - 3(Q_{11}Q_{26}^2 + Q_{22}Q_{16}^2) + 6Q_{12}Q_{16}Q_{26}$$

TABLE 1 PREDICTED AND OBSERVED PLATE DEFLECTIONS

MATERIAL $\pm\theta$ w, in.	GLASS/EPOXY		T300/5208	
	PREDICTED	OBSERVED	PREDICTED	OBSERVED
15°	.104	.111	.229	.269
30°	.173	.198	.306	.311
45°	.201	.236	.329	.298*

* Evidence of damage

MAXIMUM STRAIN CRITERION

TRANSVERSE LAYER

$$\epsilon_f = \frac{S}{E_T} + \epsilon_T$$

LAMINATE STRENGTH

$$\sigma_f = \frac{(A_{11}A_{22} - A_{12}^2)}{A_{22}h} \left(\frac{S}{E_T} + \epsilon_T - \bar{\epsilon} \right)$$

TABLE 3 PREDICTED APPLIED STRESS AT FIRST PLY FAILURE (psi)

LAMINATE/CRITERION	WITH CURING STRESS		WITHOUT CURING STRESS	
	MAX. σ	MAX. ϵ	MAX. σ	MAX. ϵ
$[90,0,+45]_s$	20,530	19,150	41,480	37,680
$[0,90]_s$	25,605	26,100	51,730	51,370
$[90,\pm30]_s$	20,530	19,150	41,480	37,680
$[90,\pm45]_s$	11,470	7,890	20,390	18,530

SWELLING STRAINS

$$e_T^{(m)} \cong \frac{1}{2} m s_c$$

FOR T300/5208:

$$e_T^{(T)} = -2167 \times 10^{-6}$$

AND $s_c = 1.6$

THUS $e_T^{(m)} = / e_T^{(T)} /$

WHEN $m = .27 \%$

TABLE III.- CURING STRAINS AND CURING STRESSES

	$-e_0^{oT}, \%$		$-e_{90}^{oT}, \%$		$-e_{45}^{oT}, \%$		$\frac{\sigma_T^R}{X_T}$	$\frac{\sigma_{LT}^R}{X_{LT}}$
	EXP.	CAL.	EXP.	CAL.	EXP.	CAL.		
B/Ep	0.123	0.109	0.234	0.259	0.171	0.184	0.99	0.13
B/PI	0.100	0.075	0.214	0.186	0.163	0.131	4.09	0.33
Gr/Ep	-0.018 (-0.009)	-0.019	0.104 (0.068)	0.122	0.036 (0.026)	0.052	1.09	0.11
Gr/PI	0.002	-0.004	0.031	0.051	0.017	0.028	1.20	0.11
GI/Ep	0.105	0.117	0.260	0.361	0.182	0.239	1.39	0.65
Remarks: Numbers inside the parentheses for Gr/Ep are measured during the cooling stage of curing and the heating stage of postcuring.								

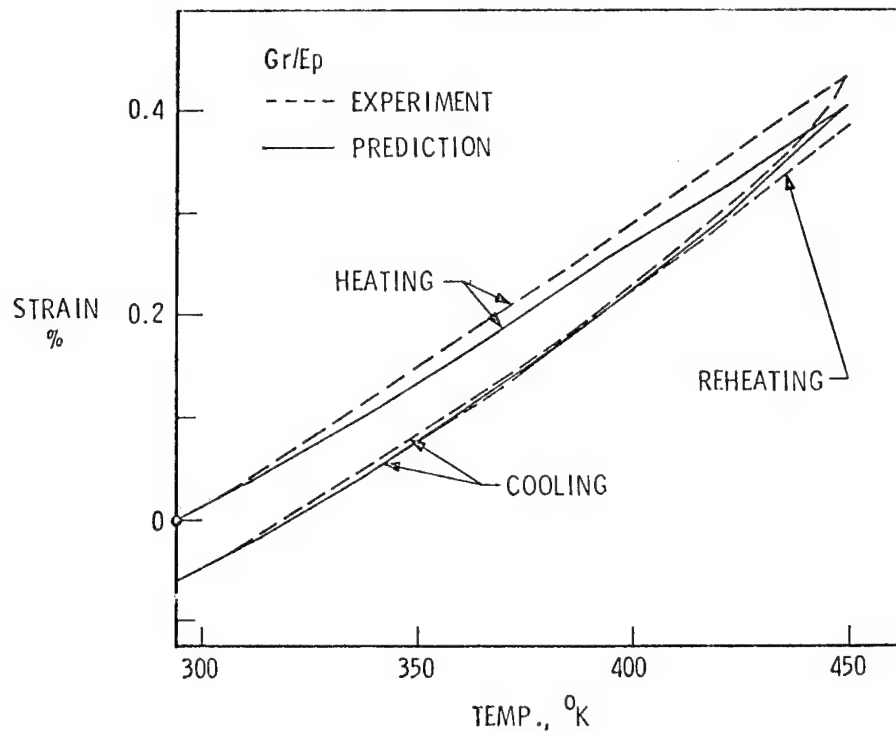


Figure 12. Transverse Strain During Thermal Cycling

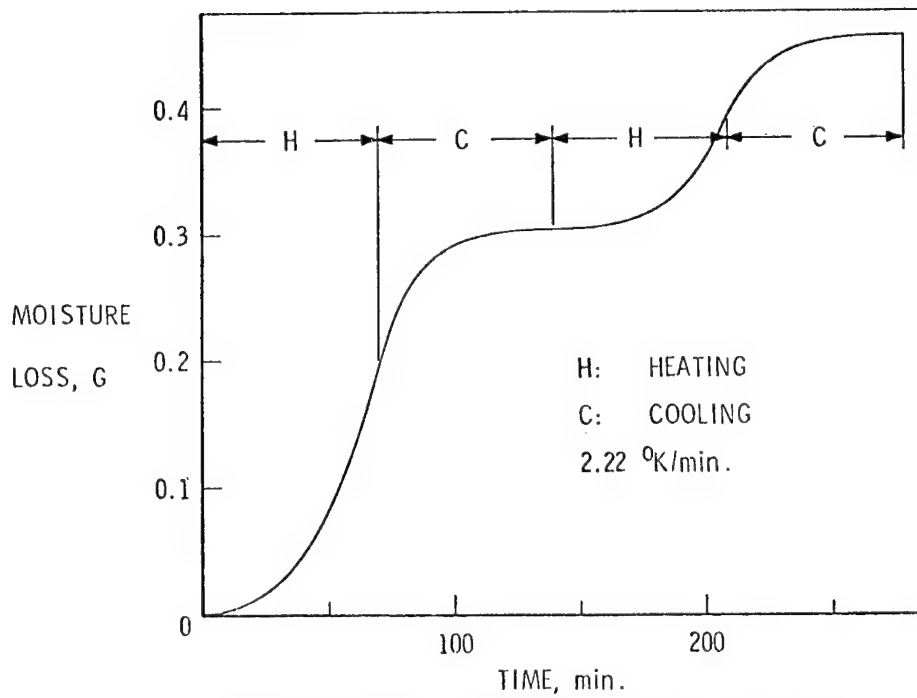


Figure 13. Moisture Desorption During Thermal Cycling

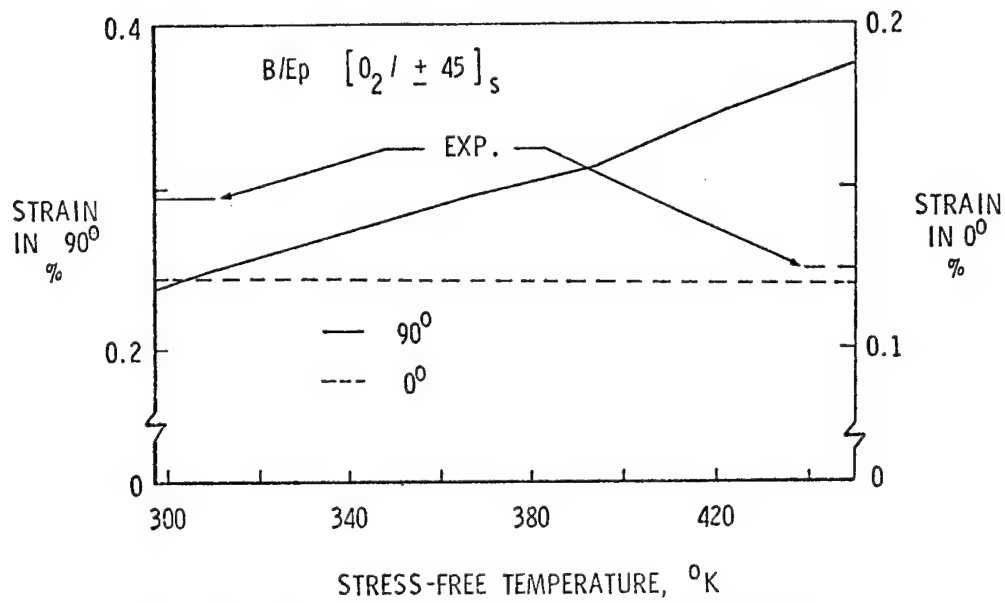


Figure 14. Effect of Stress-Free Temperature on Laminate Thermal Strain Between Room Temperature and $450^{\circ}K$

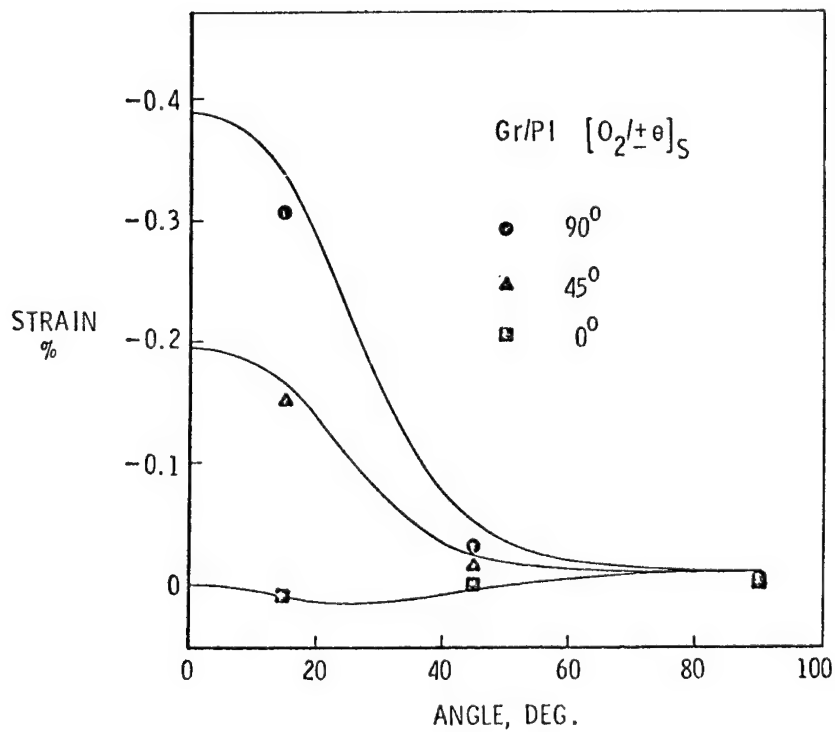


Figure 15. Curing Strains of $[0_2 / \pm \theta]_s$ Gr/PI Laminates

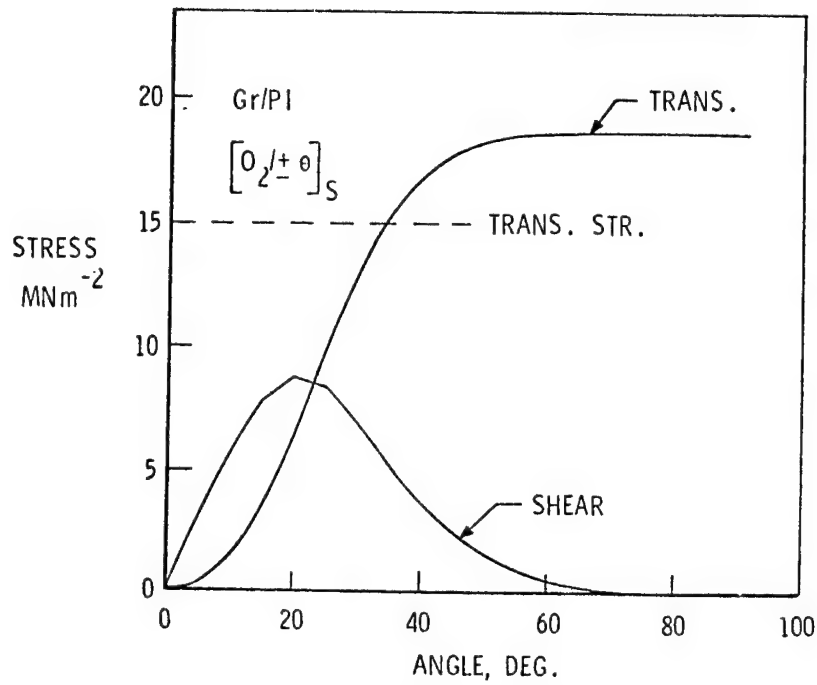


Figure 16. Curing Stresses Within θ° Plies of $[0_2/\pm\theta]_s$ Gr/PI Laminates

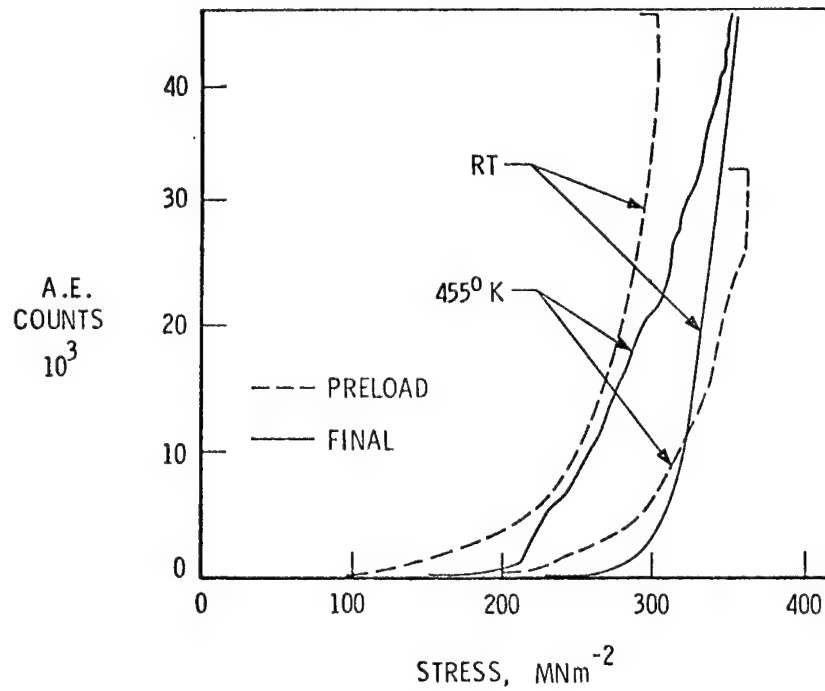
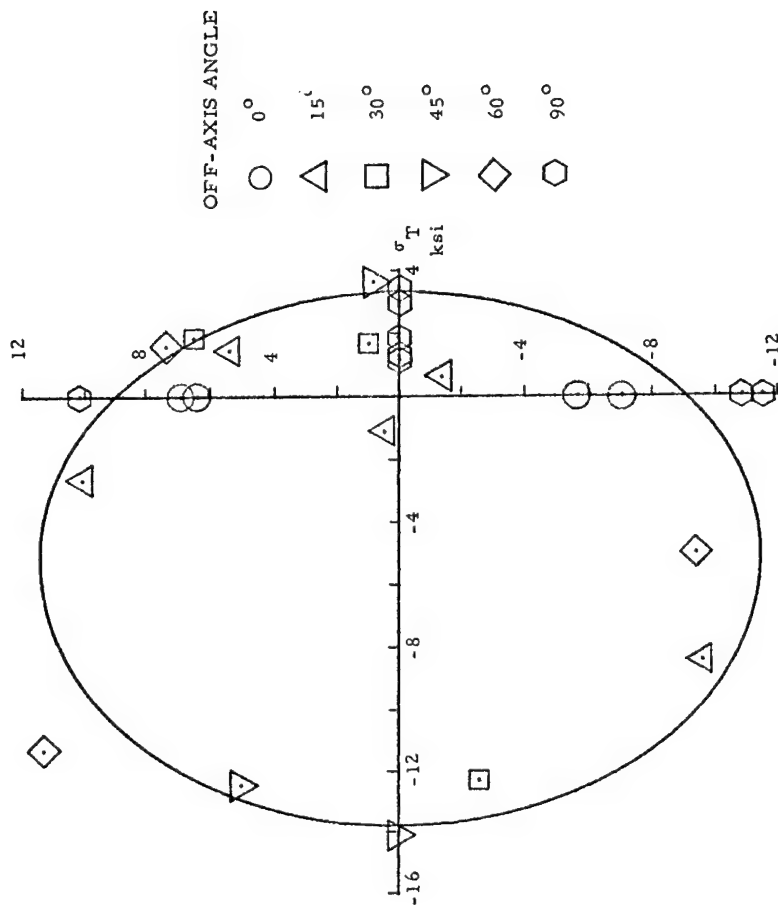


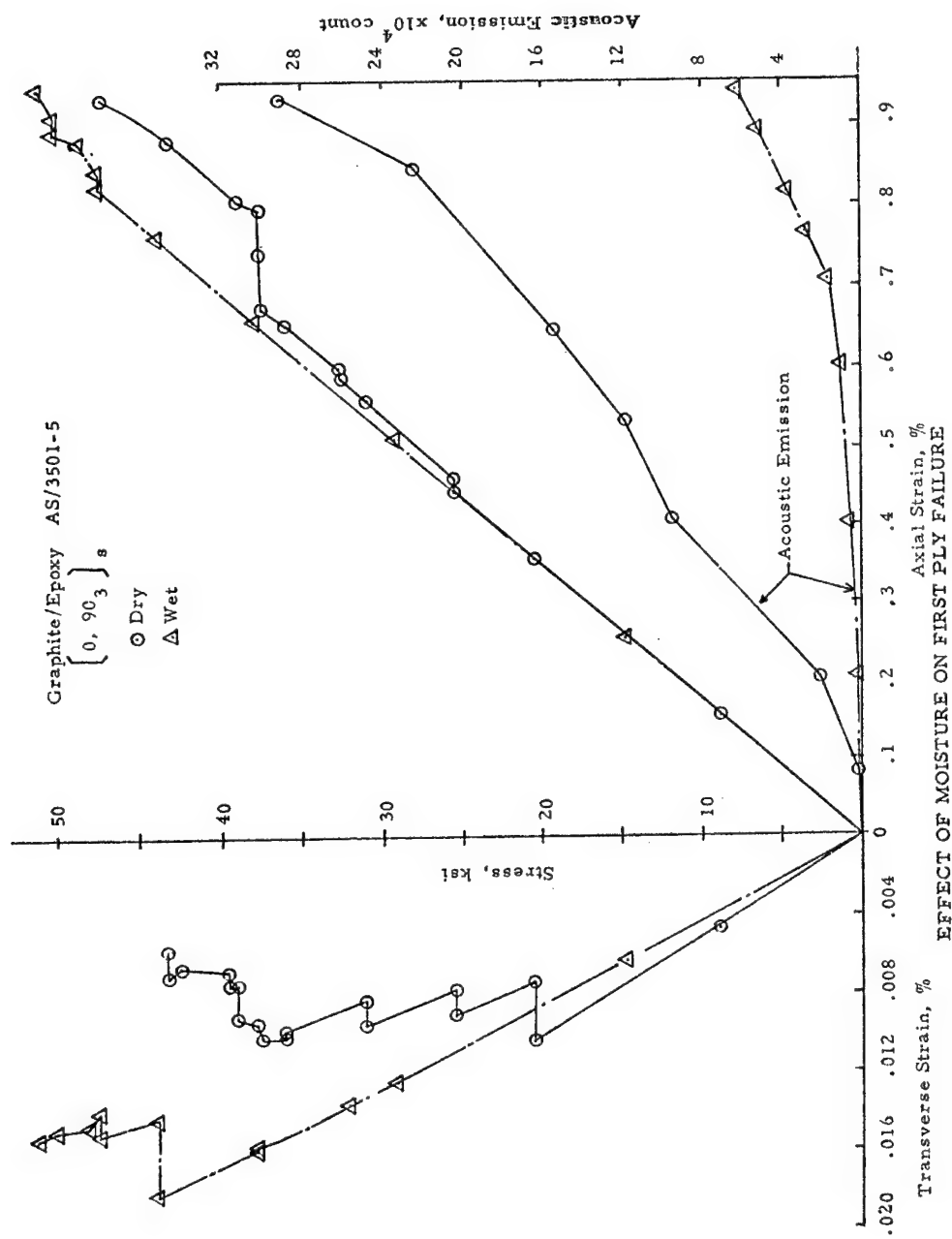
Figure 17. Effect of Preloading on Total Number of A.E. Counts at Two Different Temperatures

FAILURE SURFACE IN σ_T - σ_{LT} PLANE



PLY FAILURE UNDER COMBINED LOADING

- UNIDIRECTIONAL TUBES
 - $S_{11}^+ = S_{11}^-$ EXCEPT IN ONE CASE (0°)
 - $S_{12}^+ = S_{12}^-$
 - $S_{66}^+ = S_{66}^-$
 - $S_{16} = S_{61}$
 - APPLICATION OF INVARIANTS
 - STRENGTH DATA
- ANGLE-PLY TUBES ($[\pm\theta]_{4T}$)
 - FIRST-PLY FAILURE
 - BEHAVIOR AFTER FPF
 - FINAL FAILURE
 - EFFECT OF PLY FAILURE ON INITIAL MODULI



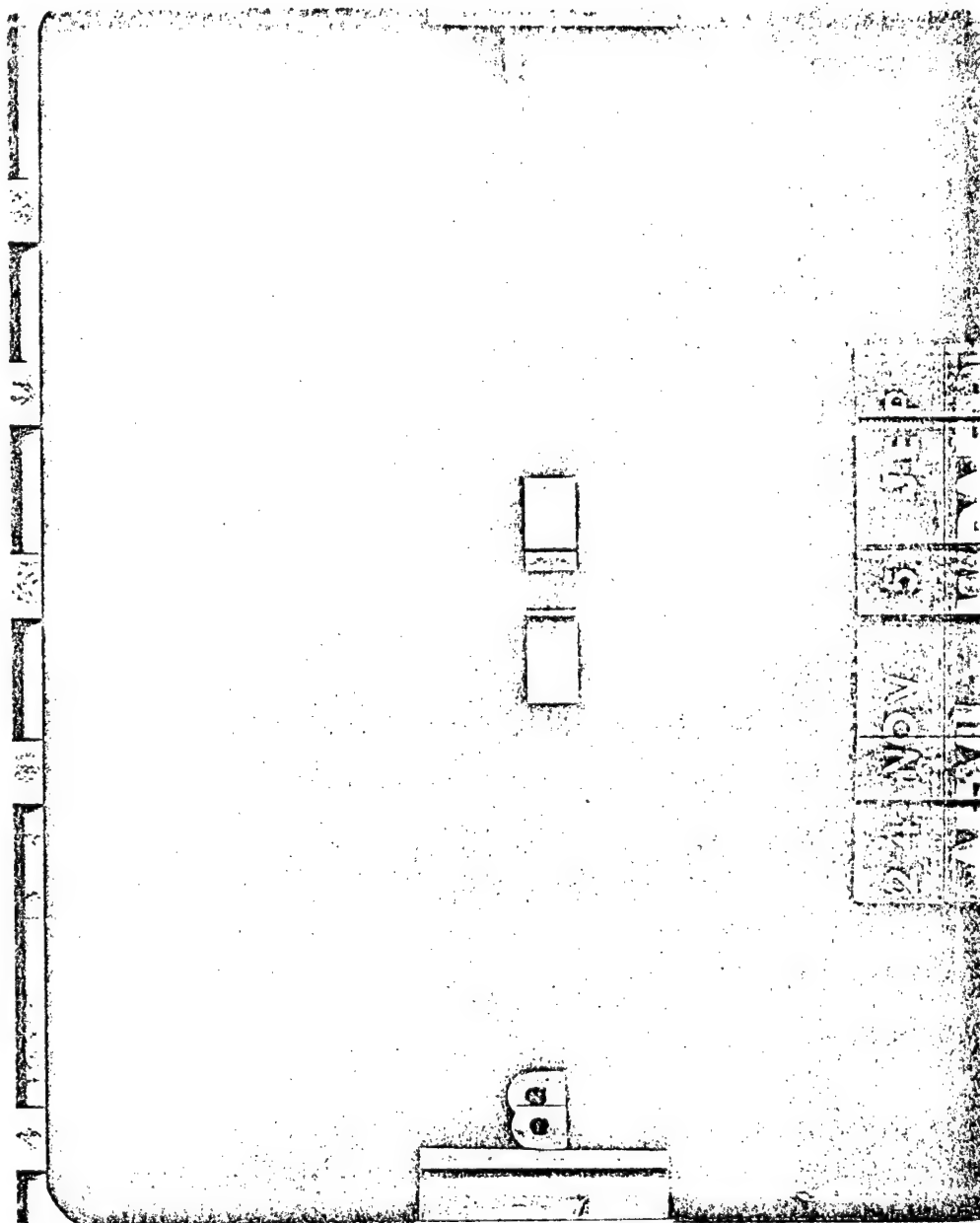
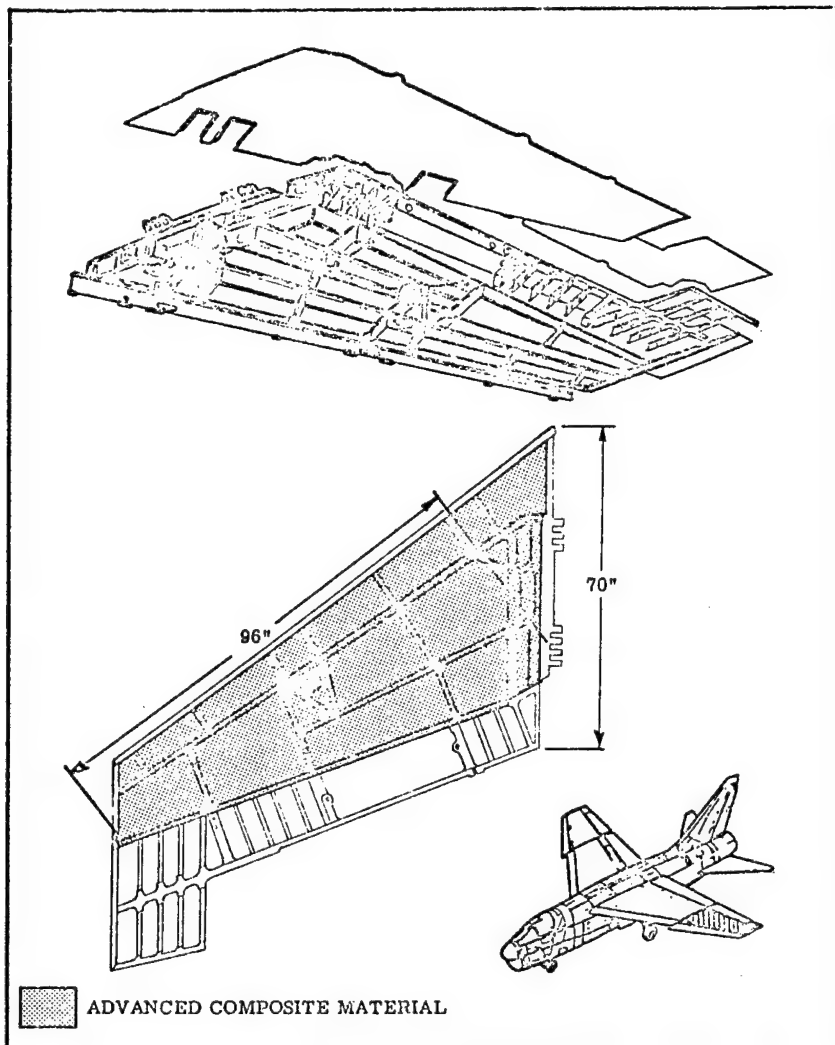
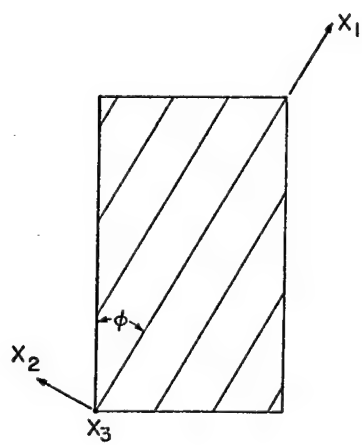


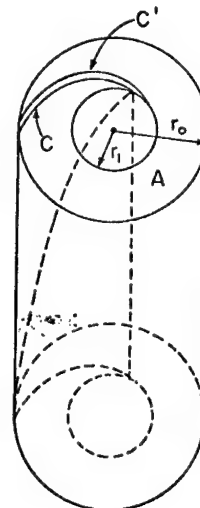
Figure 21. Laminate Damage



A7D OUTER WING PANEL



(a)



(b)

$$\begin{pmatrix} \sigma_\theta \\ \sigma_r \\ \sigma_z \\ \tau_{rz} \\ \tau_{z\theta} \\ \tau_{r\theta} \end{pmatrix} = \begin{pmatrix} c_{11} & c_{12} & c_{13} & c_{14} & c_{15} & c_{16} \\ & c_{22} & c_{23} & c_{24} & c_{25} & c_{26} \\ & & c_{33} & c_{34} & c_{35} & c_{36} \\ \text{symm.} & & & c_{44} & c_{45} & c_{46} \\ & & & & c_{55} & c_{56} \\ & & & & & c_{66} \end{pmatrix} \begin{pmatrix} \epsilon_\theta - e_\theta \\ \epsilon_r - e_r \\ \epsilon_z - e_z \\ \gamma_{rz} - e_{rz} \\ \gamma_{z\theta} - e_{z\theta} \\ \gamma_{r\theta} - e_{r\theta} \end{pmatrix}$$

For axisymmetric loadings

$$u = U(r) \quad v = V(r) + Arz \quad , w = W(r) + \epsilon z$$

$$\epsilon_\theta = U/r \quad \gamma_{rz} = W, r$$

$$\epsilon_r = U, r \quad \gamma_{z\theta} = Ar$$

$$\epsilon_z = \epsilon \quad \gamma_{r\theta} = V, r - V/r$$

Equilibrium Equations

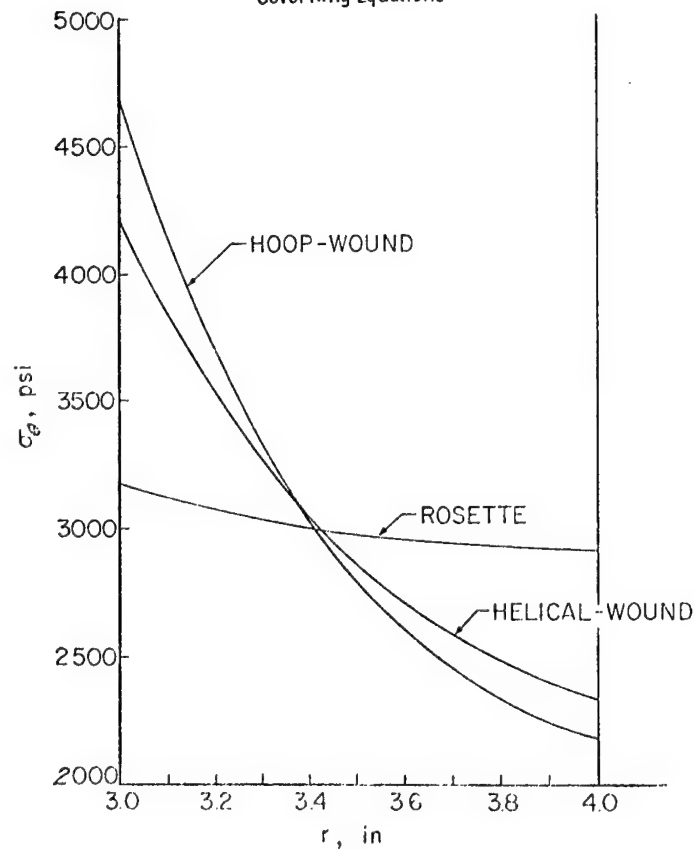
$$(r\sigma_r), r - \sigma_\theta = 0$$

$$\tau_{rz} = B/r$$

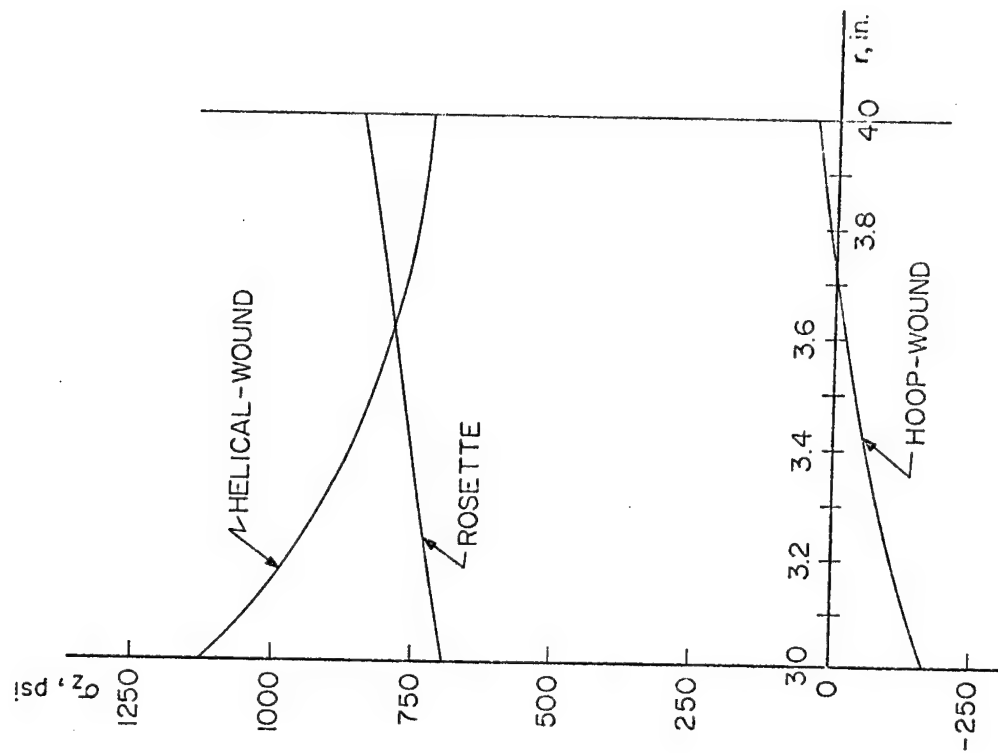
$$\tau_{r\theta} = D/r^2$$

This yields 3 D.E. with variable coefficients in U, V, W.

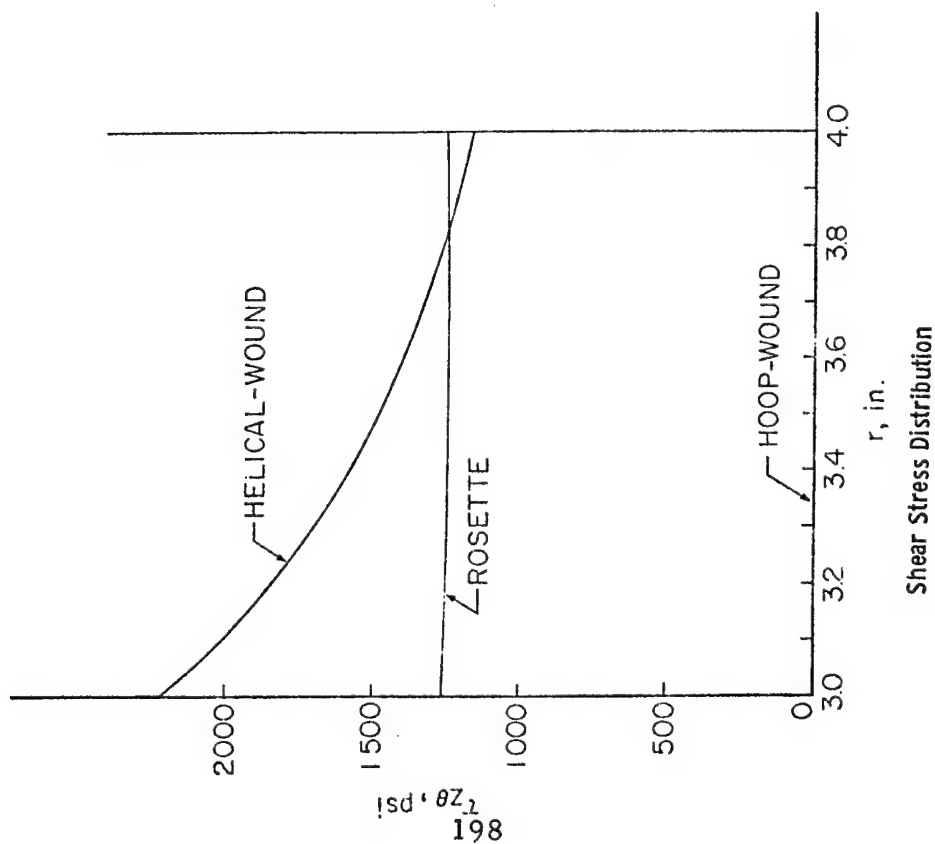
Governing Equations



Hoop Stress Distribution



Axial Stress Distribution



Shear Stress Distribution

AF76-2992

ULTRASONIC NON-DESTRUCTIVE TESTING
OF COMPOSITE MATERIALS

W. SACHSE AND Y.H. PAO
DEPARTMENT OF THEORETICAL AND APPLIED MECHANICS
CORNELL UNIVERSITY
ITHACA, N.Y. 14853

(April 1, 1976 - March 31, 1977)

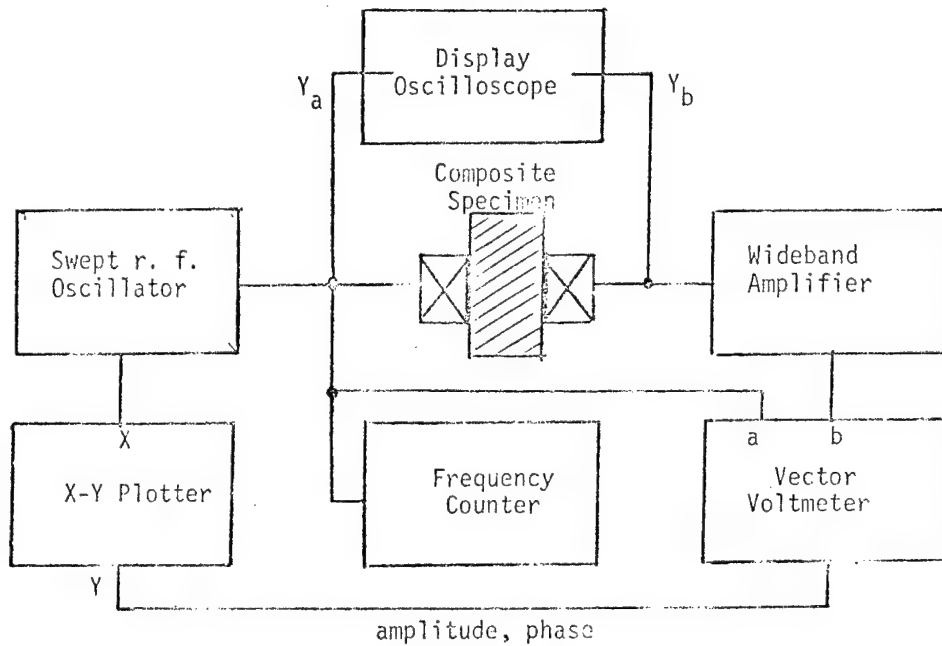
ACCOMPLISHMENTS (AS OF OCTOBER, 1976)

1. PROCURED COMPOSITE SPECIMENS AND FABRICATED TEST SPECIMENS OF VARIOUS FIBER ORIENTATIONS, GRAPHITE-EPOXY ($0/\pm 45$), BORON-EPOXY (UNIDIRECTIONAL)
2. SET UP PULSED ULTRASONIC EQUIPMENT AND ANALOG AND DIGITAL SIGNAL PROCESSING SYSTEMS.
3. DEVELOPED AND TESTED TECHNIQUES FOR THE EXPERIMENTAL DETERMINATION OF THE DISPERSIVE BEHAVIOR OF COMPOSITE MATERIALS.
4. COMPLETED PRELIMINARY ULTRASONIC DISPERSION MEASUREMENTS FOR ARBITRARY ANGLES OF INCIDENCE TO THE REINFORCING FIBERS IN UNFLAWED COMPOSITE SPECIMENS.
5. FORMULATED A METHOD BASED ON THE SCATTERING MATRIX (T-MATRIX) TO STUDY THE EFFECTIVE PROPERTIES OF A FIBER-REINFORCED COMPOSITE. THE STUDY INVOLVES THE MULTIPLE SCATTERING OF SH- WAVES INCIDENT NORMAL TO THE FIBERS WHICH MAY BE OF ANY ARBITRARY CROSS SECTION.
6. EXTENDED THE T-MATRIX FORMULATION OF ELASTIC WAVES (P AND S) TO THE MULTIPLE SCATTERING SITUATION OF NORMAL INCIDENT WAVES ON PARALLEL CYLINDERS OF ARBITRARY CROSS SECTION.

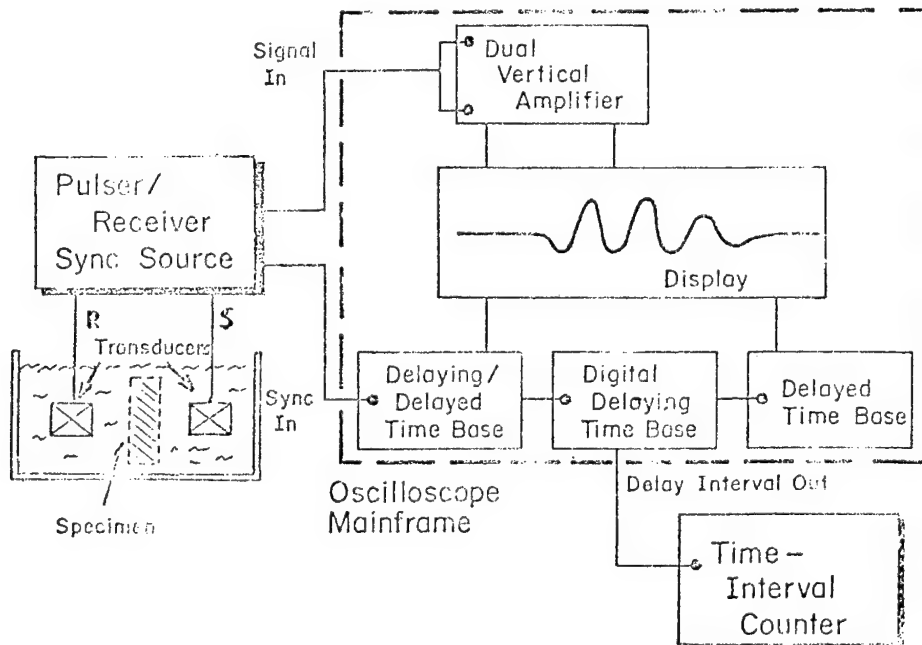
FREQUENCY-DEPENDENT VELOCITY MEASUREMENTS

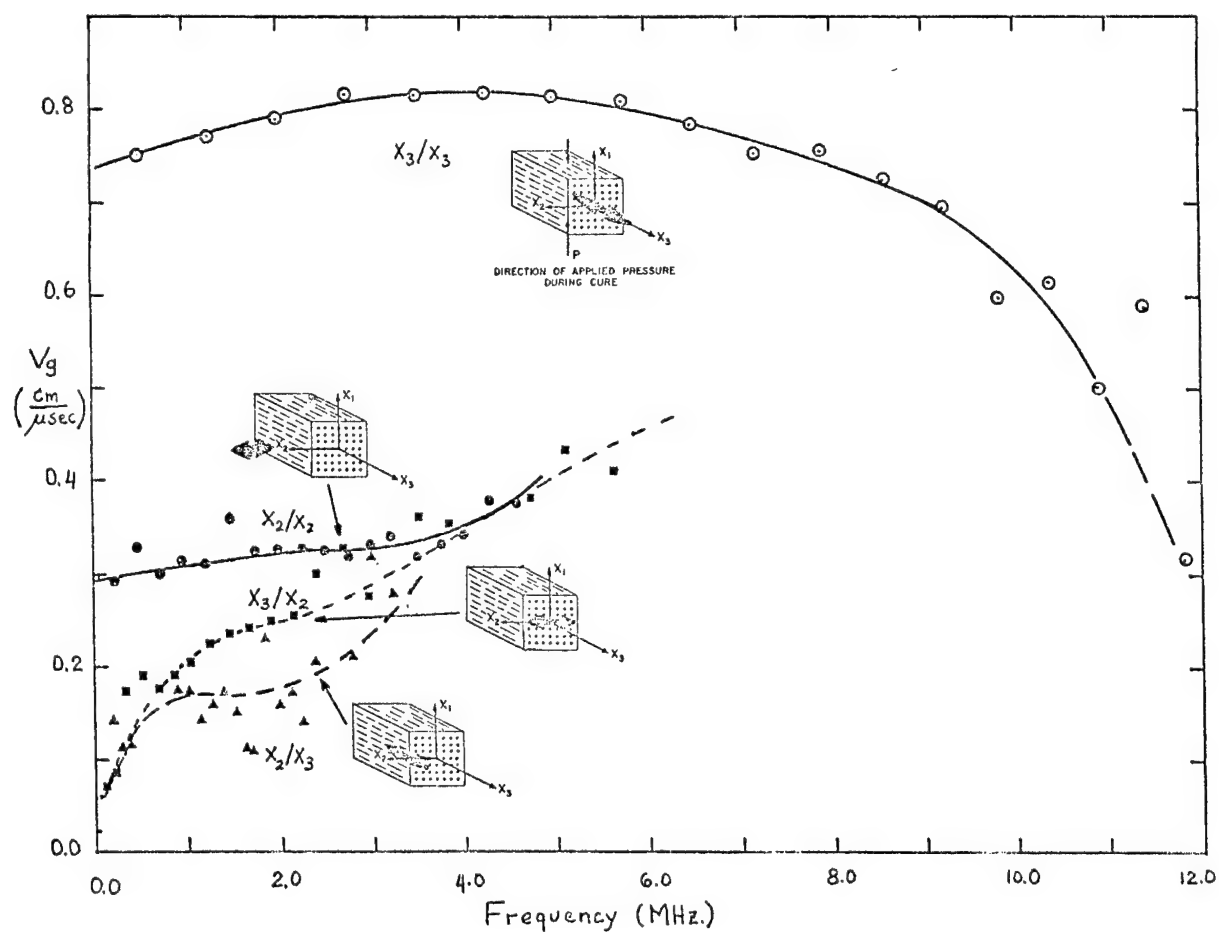
A. ANALOG TECHNIQUES

1. Harmonic Wave: π - phase difference measurements



2. Pulse: group, delay-time measurements

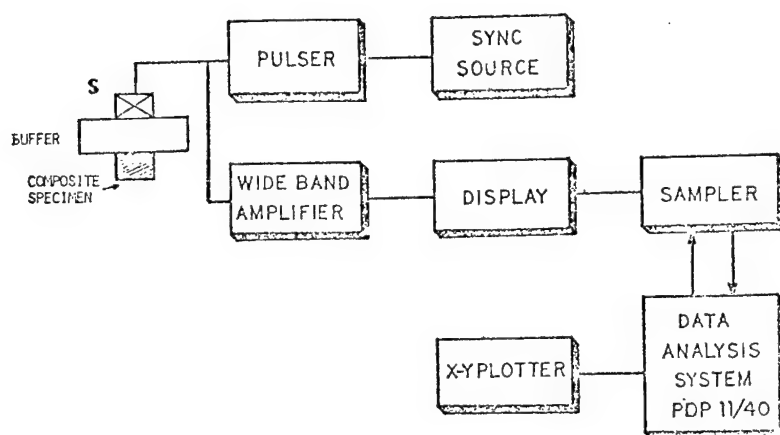




FREQUENCY-DEPENDENT VELOCITY MEASUREMENTS

B. ANALOG/DIGITAL TECHNIQUES

1. Pulse: reflection coefficient measurements

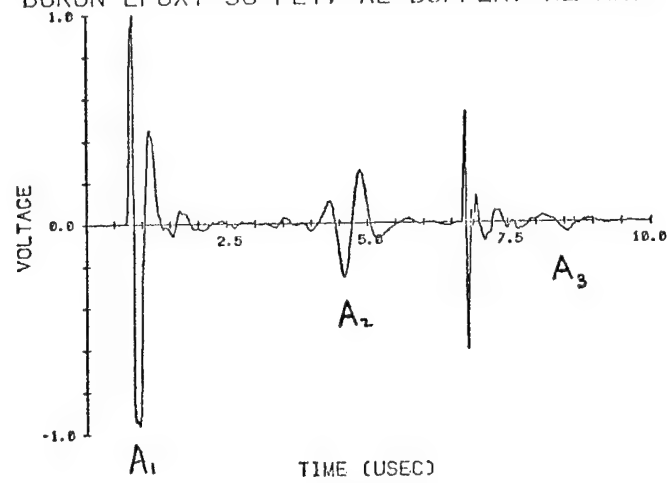


$$R(f) = \left[\frac{A_1(f) A_3(f)}{A_1(f) A_3(f) - A_2^2(f)} \right]^{1/2}$$

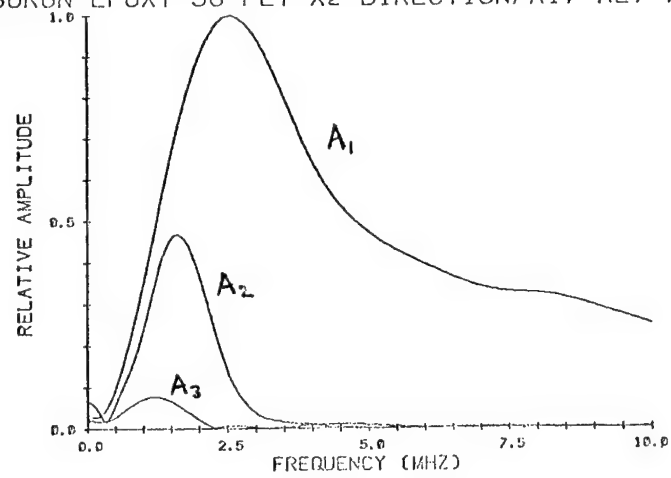
$$\alpha(f) = \frac{1}{2l} \ln \frac{R A_2(f)}{A_3(f)}$$

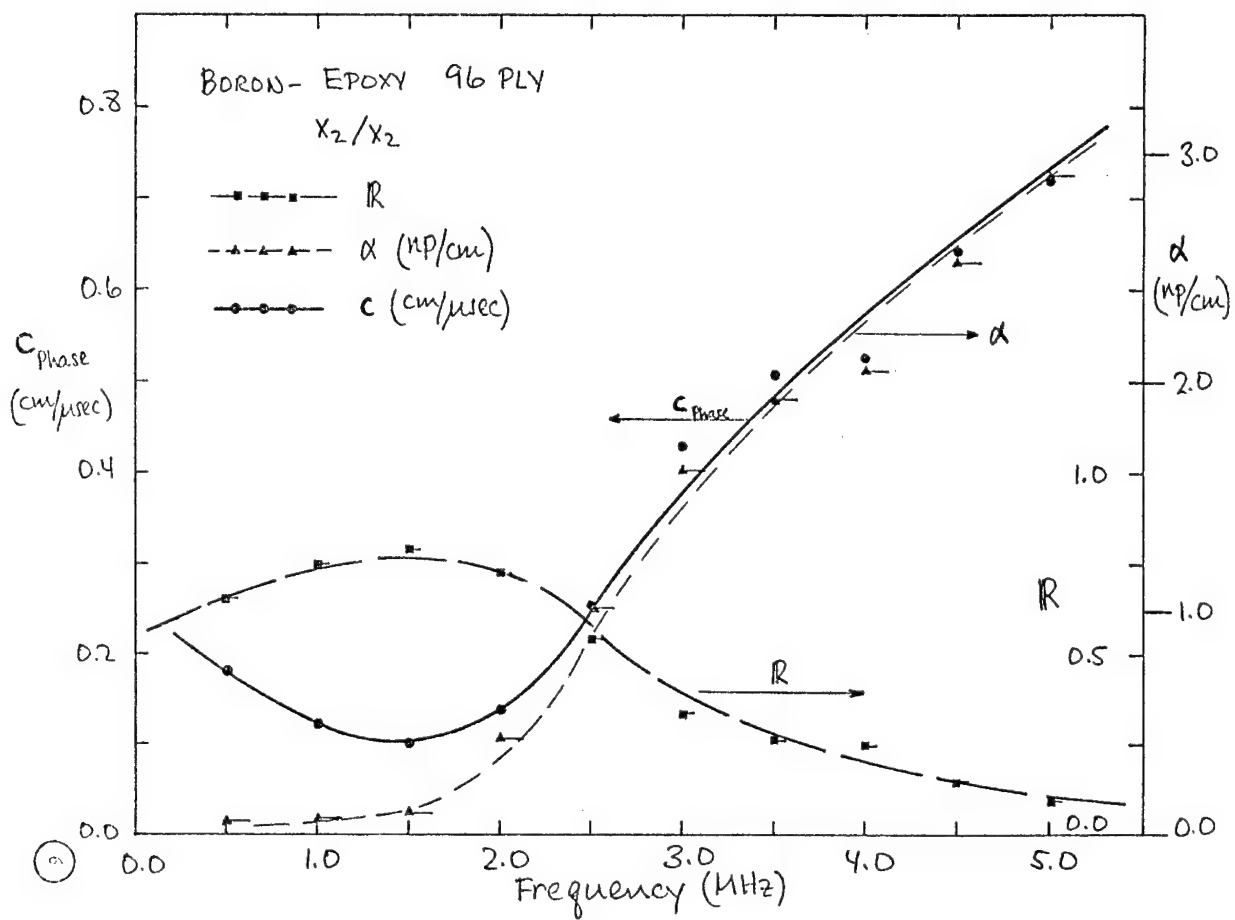
$$c(f) = \frac{z_{buff}}{\rho_{comp}} \cdot \frac{1 - R(f)}{1 + R(f)}$$

BORON-EPOXY 96-PLY, AL BUFFER, X1-AXIS



BORON-EPOXY 96-PLY X2-DIRECTION/A1, A2, A3





Integral Formula for the Scattering of Elastic Waves

$$\nabla \cdot \underline{\underline{u}} + \rho \omega^2 \underline{\underline{u}} = 0$$

$$\underline{\underline{T}} = \lambda \mathbf{I} \nabla \cdot \underline{\underline{u}} + \mu (\nabla \underline{\underline{u}} + \underline{\underline{u}} \nabla)$$

$$\nabla \cdot \underline{\underline{\Sigma}} + \rho \omega^2 \underline{\underline{G}} = -4\pi \delta(\underline{\underline{r}} - \underline{\underline{r}}')$$

$$\Sigma_{ijk} = \lambda \delta_{ij} \partial_k G_{lk} + \mu (\partial_i G_{jk} + \partial_j G_{ik})$$

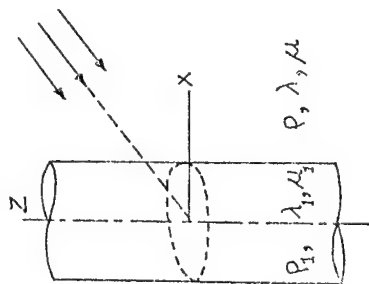
$$\underline{\underline{u}} = \underline{\underline{u}}_1 \quad \text{inside } S$$

$$\underline{\underline{u}} = \underline{\underline{u}}^0 + \underline{\underline{u}}^S \quad \text{outside } S$$

$$\int [\underline{\underline{u}}(\underline{\underline{x}}') \cdot \underline{\underline{n}}' \cdot \underline{\underline{\Sigma}}(\underline{\underline{x}}|\underline{\underline{x}}') - \underline{\underline{n}}' \cdot \underline{\underline{T}}' \cdot \underline{\underline{G}}] ds = \begin{cases} \underline{\underline{u}}(\underline{\underline{x}}), \underline{\underline{x}} \text{ outside } S \\ -\underline{\underline{u}}^0(\underline{\underline{x}}), \underline{\underline{x}} \text{ inside } S \end{cases}$$

Boundary conditions

$$\left. \begin{aligned} \underline{\underline{u}}(\underline{\underline{x}}') &= \underline{\underline{u}}_1(\underline{\underline{x}}') \\ \underline{\underline{n}}' \cdot \underline{\underline{T}}(\underline{\underline{x}}') &= \underline{\underline{n}}' \cdot \underline{\underline{T}}_1'(\underline{\underline{x}}') \end{aligned} \right\} \underline{\underline{x}}' \text{ on } S$$



Transition Matrix for Scattering by a Cylinder

$$\underline{\underline{u}}^0(\underline{\underline{x}}) = \sum_n (a_n^{\sigma} \text{Re } \phi_n^{\sigma} + b_n^{\sigma} \text{Re } \psi_n^{\sigma} + c_n^{\sigma} \text{Re } \chi_n^{\sigma})$$

$$\underline{\underline{u}}^S(\underline{\underline{x}}) = \sum_n (\alpha_n^{\sigma} \phi_n^{\sigma} + \beta_n^{\sigma} \psi_n^{\sigma} + \gamma_n^{\sigma} \chi_n^{\sigma})$$

$$\underline{\underline{u}}_1(\underline{\underline{x}}) = \sum_n (A_n^{\sigma} \text{Re } \phi_{n1}^{\sigma} + B_n^{\sigma} \text{Re } \psi_{n1}^{\sigma} + C_n^{\sigma} \text{Re } \chi_{n1}^{\sigma})$$

$$\int [\underline{\underline{u}}' \cdot \underline{\underline{n}}' \cdot \underline{\underline{\Sigma}} - \underline{\underline{n}}' \cdot \underline{\underline{T}}' \cdot \underline{\underline{G}}] ds = \begin{cases} \underline{\underline{u}}^S(\underline{\underline{x}}) \\ -\underline{\underline{u}}^0(\underline{\underline{x}}) \end{cases}$$

$$\begin{pmatrix} \alpha \\ \beta \\ \gamma \end{pmatrix} = - \begin{bmatrix} T^{11} & T^{12} & T^{13} \\ T^{21} & T^{22} & T^{23} \\ T^{31} & T^{32} & T^{33} \end{bmatrix} \begin{pmatrix} a \\ b \\ c \end{pmatrix}$$

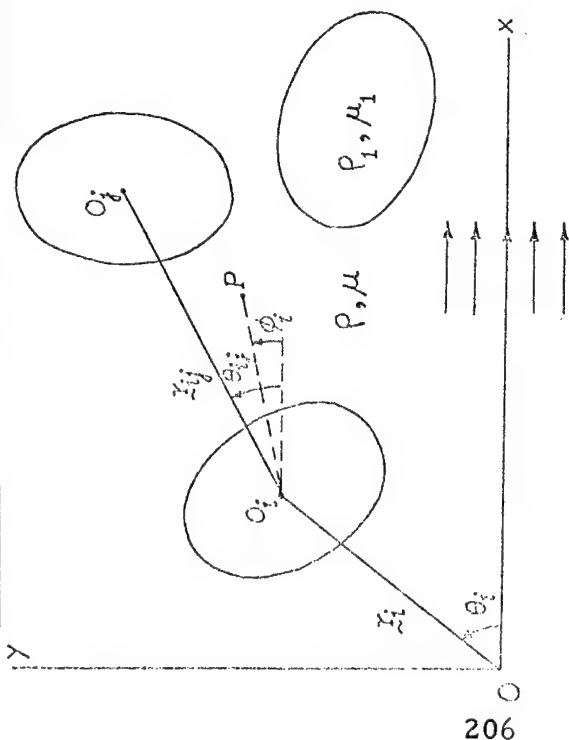
Obliquely Incident Elastic Waves

$$\underline{\underline{u}}^0(\underline{\underline{x}}) = \nabla e^{i(\underline{\underline{k}}^0 \cdot \underline{\underline{x}} - \omega t)} \quad ; \quad |\underline{\underline{k}}^0| = k_p, \underline{\underline{p}}\text{-wave}$$

$$\underline{\underline{u}}^0(\underline{\underline{x}}) = \nabla \times \underline{\underline{z}} e^{i(\underline{\underline{k}}^0 \cdot \underline{\underline{x}} - \omega t)} + \frac{1}{k_s} \nabla \times \nabla \times \underline{\underline{z}} e^{i(\underline{\underline{k}}^0 \cdot \underline{\underline{x}} - \omega t)} \quad |\underline{\underline{k}}^0| = k_s, \underline{\underline{s}}\text{-wave}$$

Normally incident shear waves - SH waves

$$\chi_n^{\sigma} = \underline{\underline{z}} \sqrt{\epsilon_n} H_n(k_s r) \quad \begin{matrix} \cos n\theta & ; & \sigma=1 \\ \sin n\theta & ; & \sigma=2 \end{matrix}$$



$$w_i^E(x) = w_i^O(x) + \sum_{j \neq i}^N w_j^S(x - r_j)$$

$$w_i^E = \sum_n a_n^i \operatorname{Re} \psi_n(x - r_i) ; w_i^S(x) = \sum_n b_n^i \psi_n(x - r_j)$$

$$w_i^O(x) = \sum_n i^n \operatorname{Re} \psi_n(x - r_i) e^{ik \cdot r_i}$$

$$b_n^i = \sum_m T_{nm}^i a_m^i$$

$$\langle a_n^i \rangle = i^n e^{ik \cdot r_i} + \frac{N-1}{V} \sum_{\ell} \sum_m (-i)^\ell T_{\ell m} \int_{|r_{ij}| > 2a} \langle a_m^j \rangle \psi_{\ell-n}(r_i) d\vec{r}_j$$

Lax's approximation

$$\langle a_m^i \rangle_{ij} = \langle a_m^j \rangle_j$$

Propagation characteristics of the medium

Plane wave solution

$$\langle a_m^i \rangle_i = i^m X_m e^{iK r_i \cos \theta_i}$$

$$i^n X_n = n_0 \frac{2\pi a}{k^2 - K^2} \sum_t \sum_m i^{(m-t)} X_m T_{t+n,m}$$

$$\left[J_t(2ka) 2k H'_t(2ka) - H_t(2ka) 2k J'_t(2ka) \right]$$

$$n_0 = \frac{N}{V}$$

Rayleigh limit - circular cylinders ($r=a$)

$$T_0 = -i \frac{\pi}{4} (ka)^2 (d-1) \quad ; \quad d = \frac{\rho_1}{\rho}$$

$$T_1 = T_{-1} = i \frac{\pi}{4} (ka)^2 \frac{m-1}{m+1} \quad ; \quad m = \frac{\mu_1}{\mu}$$

$$T_{|n|} = 0 \quad \text{for } n \geq 2$$

$$\left(\frac{c}{k}\right)^2 = \left[\frac{1+c(d-1)}{1+c} \right] \frac{1-c \frac{m-1}{m+1}}{\frac{m-1}{m+1}} \quad ; \quad c = n_0 \pi a^2$$

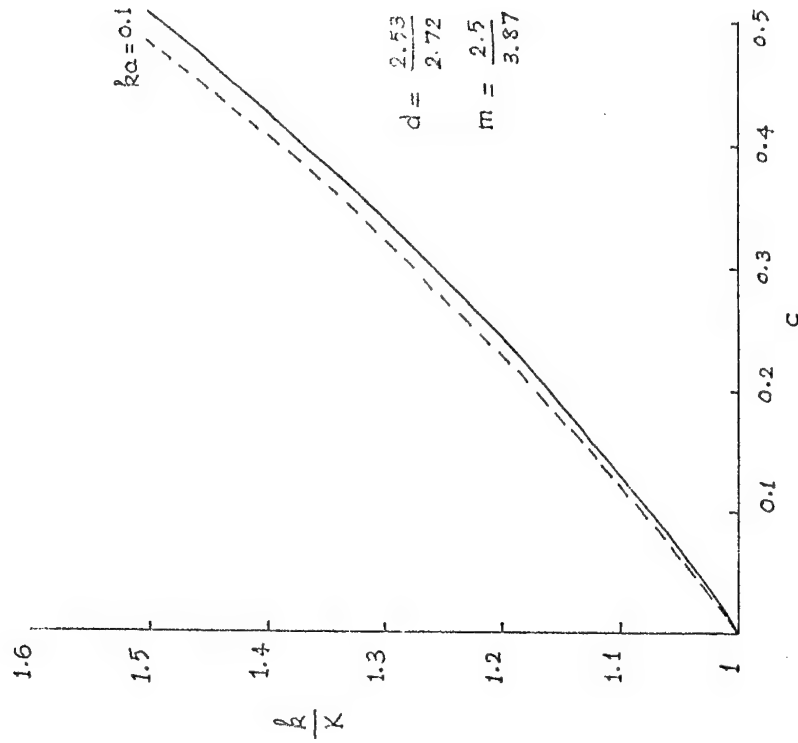
Define an average shear modulus

$$\langle \mu \rangle = \omega^2 \langle \rho \rangle / k^2$$

$$\text{where } \langle \rho \rangle = c \rho_1 + (1-c) \rho$$

Effective shear modulus of the inhomogeneous media

$$\frac{\langle \mu \rangle}{\mu} = \frac{1 + c \frac{m-1}{m+1}}{1 - c \frac{m-1}{m+1}}$$



BIAXIAL FATIGUE OF COMPOSITES

P. H. Francis

Southwest Research Institute

PROGRAM OBJECTIVES

Determine the characteristics of first ply failure (FPF) of laminated Gr/Ep composites under combined states of plane stress (static & fatigue).

SUMMARY OF PRINCIPAL FINDINGS

1. FPF--localized, uniformly distributed matrix failures of a ply--is a real phenomenon. Both matrix tension and shear FPF mechanisms have been observed using two techniques.
2. FPF predictions can be very sensitive to input property data.
3. FPF generally occurs outside predicted envelopes, suggesting laminate theory is conservative in predicting FPF.
4. FPF is a precursor to laminate failure, i.e., measured ultimate strength always exceeds predicted FPF.
5. FPF data so far suggest only weak interaction between matrix shear, tensile modes.

ORGANIZATION OF TALK

1. Tubular specimens for characterizing mechanical performance of laminated composites.
2. Analytical results - FPF.
3. Experimental results - FPF.
4. Conclusions.

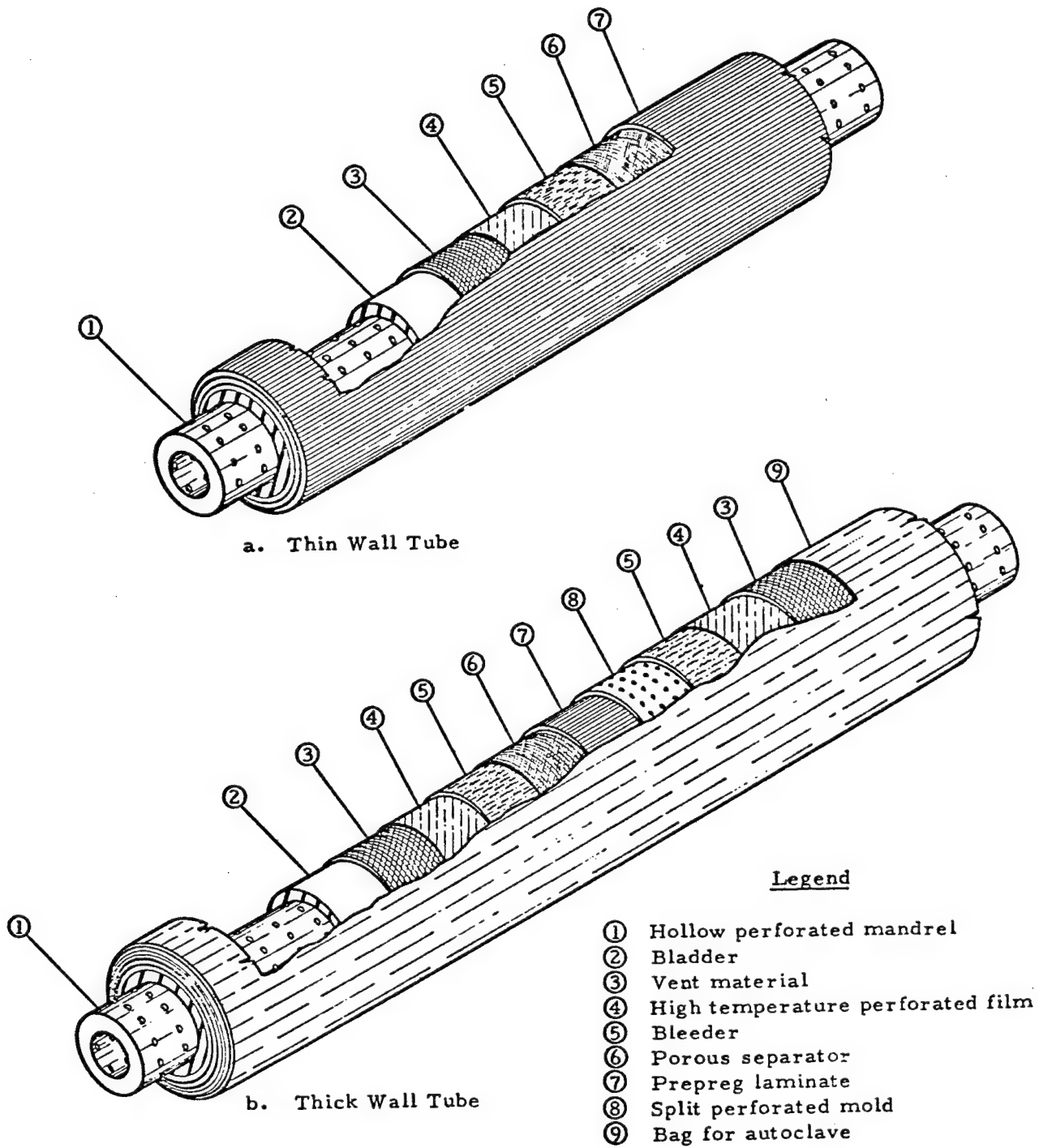


Figure 3

Exposed View of Fabrication Assembly
for Thin and Thick Walled Tubes

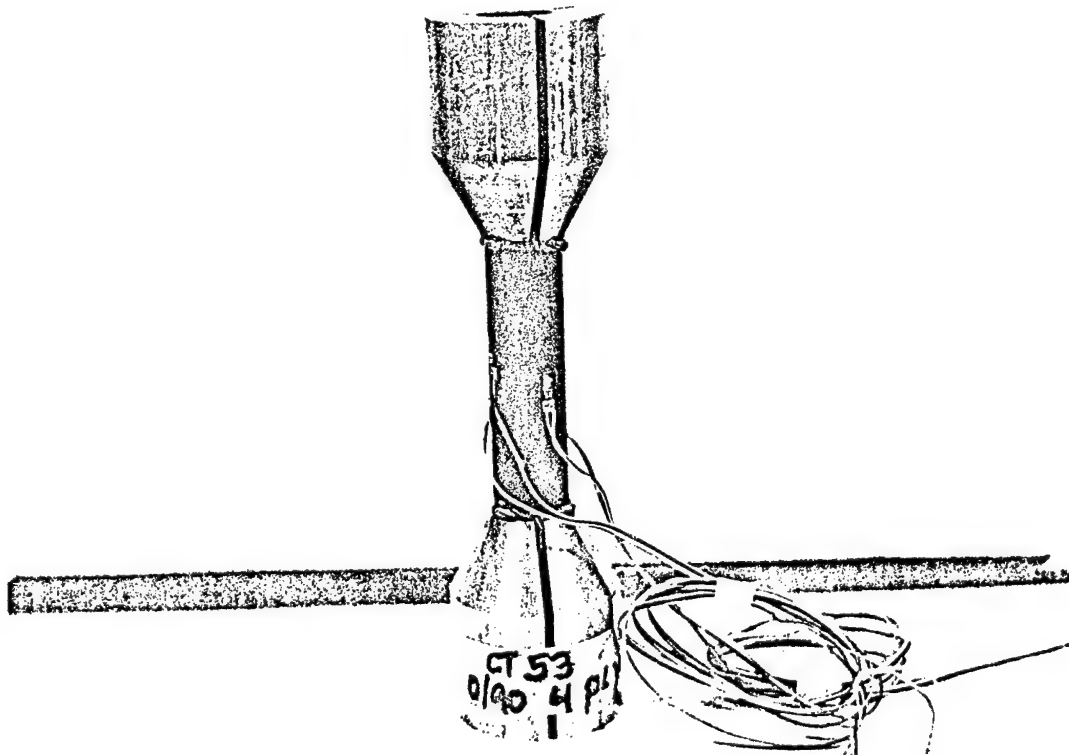
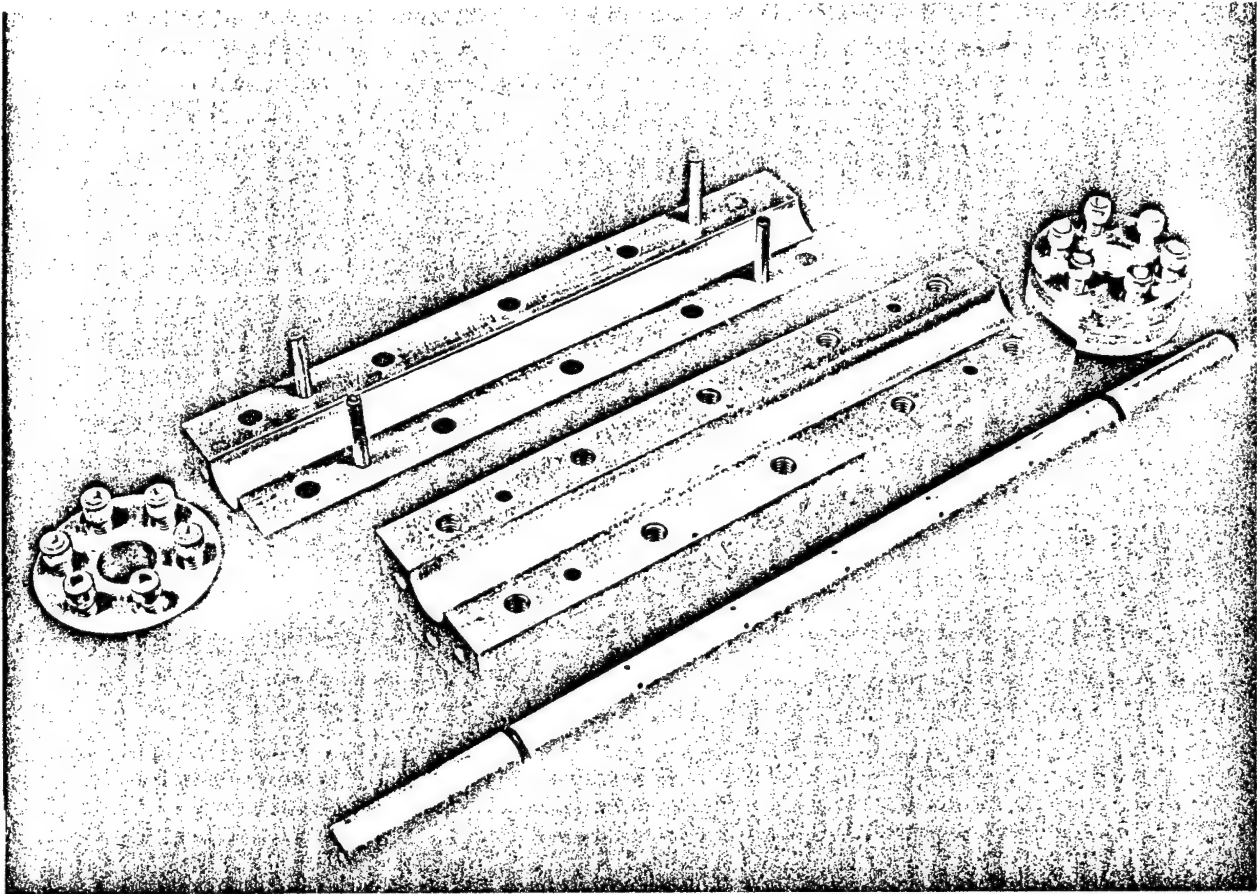


FIGURE 15. GAGED TUBE SPECIMEN (1/4 INCH, 350Ω GAGES)

**TUBES VIS-A-VIS FLAT COUPONS FOR CHARACTERIZING COMPOSITES:
RELATIVE ADVANTAGES**

	<u>COUPON</u>	<u>TUBE</u>
Geometric Aspects	- - -	"thin" ($R/t \geq 10$)
Edge Effects	influence strength	absent
Grip Aspects	conventional tabs	rigid tabs compensation
Data Value/Test	limited	full orthotropic good shear specimen
Cost to Mfg. + Tab	inexpensive: ~10% cost of tube	costly

A DEFINITION OF TUBE "THINNESS" REQUIREMENT

<u>Loading Mode</u>	<u>R/t for given % stress gradient in wall</u> *	
	<u>5%</u>	<u>10%</u>
Axial	4	2
Hoop	23	13
Torsion	20	10

*Based on a 16-ply (0/+ 45) Layup.

COMPARISON OF AVERAGE LAMINATE PROPERTIES
MEASURED USING TUBES AND COUPONS

PROPERTY	(0) ₄ TUBE DATA	COUPON DATA	
E_{xx}	19.3	23.0	} (0) ₆
S_x^{ut}	---	214	
u_{xy}	0.35	0.34	
E_{yy}	1.44	1.6	} (90) ₈
S_y^{ut}	3.5	6.8	
u_{yx}	0.03	0.03	
G_{xy}	0.94	0.87	} (\pm 45) _s
S_{xy}^{us}	11.1	10.8	

Fiberite hy-E 1034C graphite/epoxy (T-300 fiber)

Strength values in ksi

Modulus values in 10³ ksi

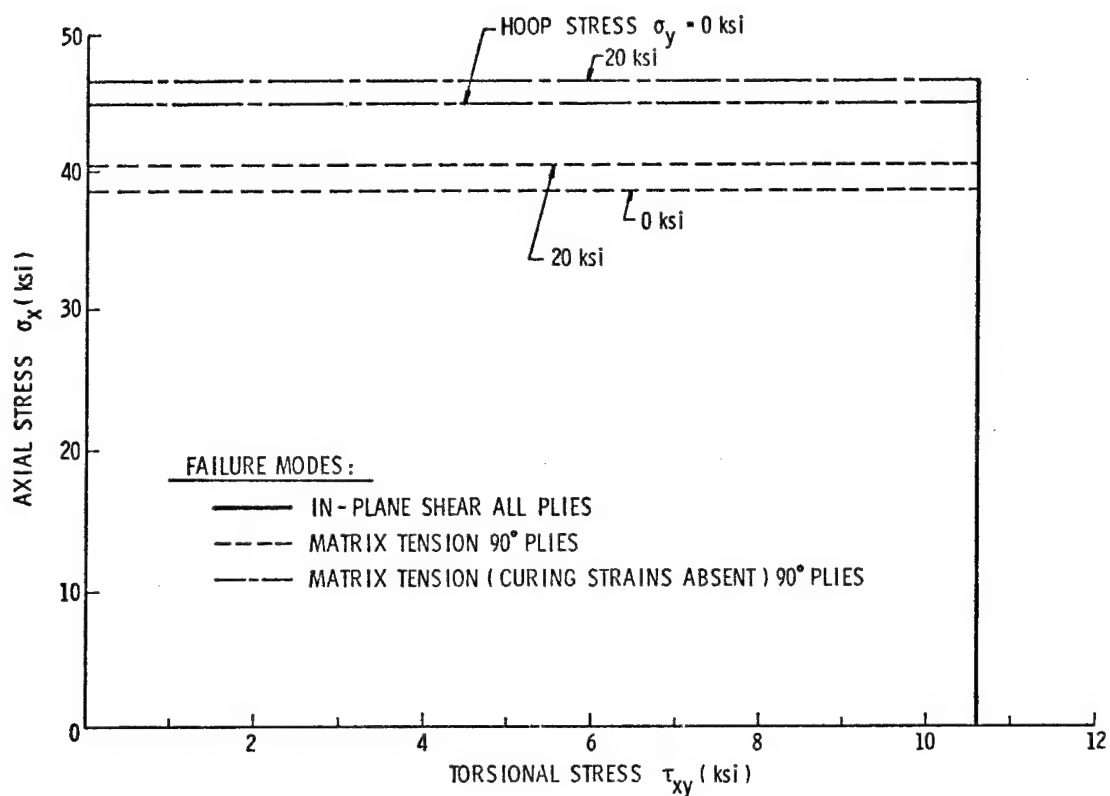


Figure Predicted First Ply Failure Surfaces of $(0/90)_5$ Tubes by Laminate Analysis

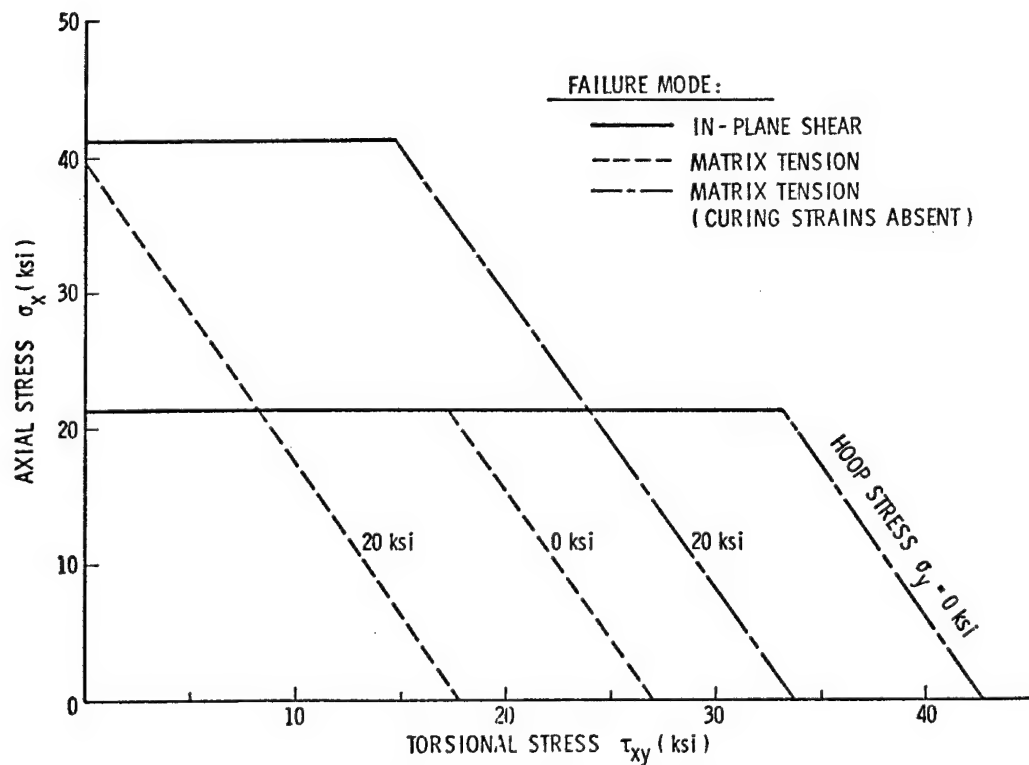


Figure Predicted First Ply Failure Surfaces of $(\pm 45)_5$ Tubes by Laminate Analysis

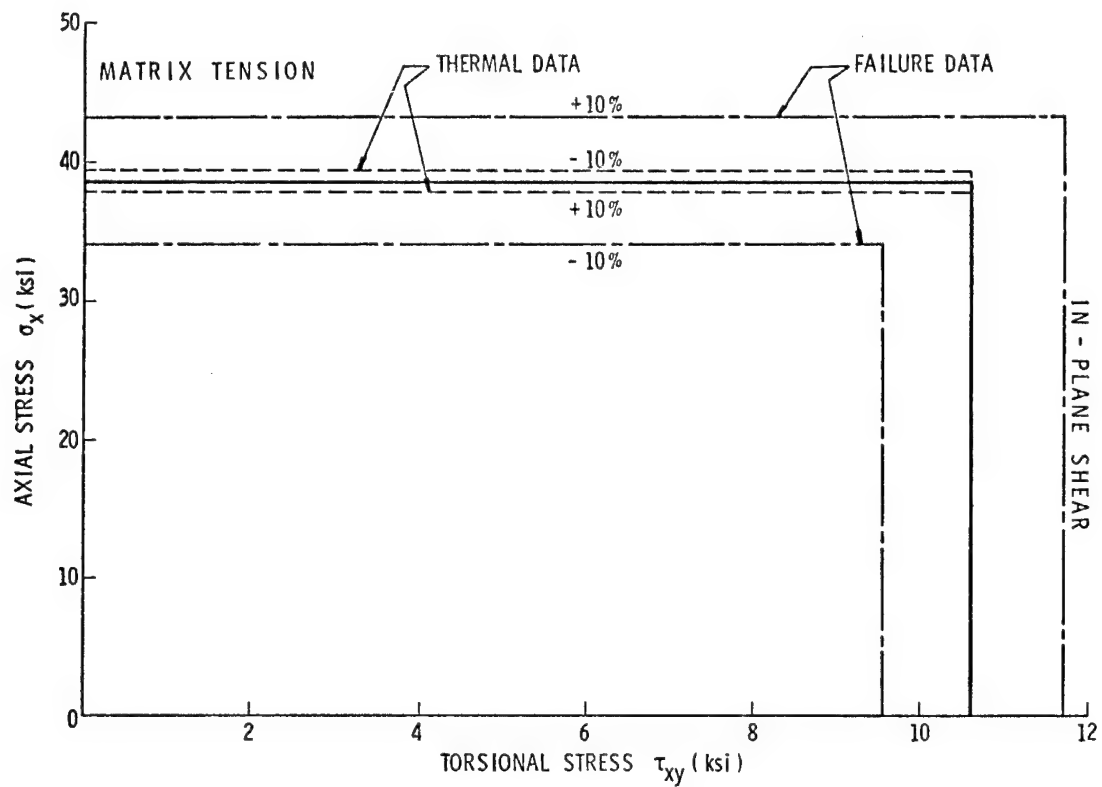


Figure FPF Prediction Input Data Variation (0/90)_S

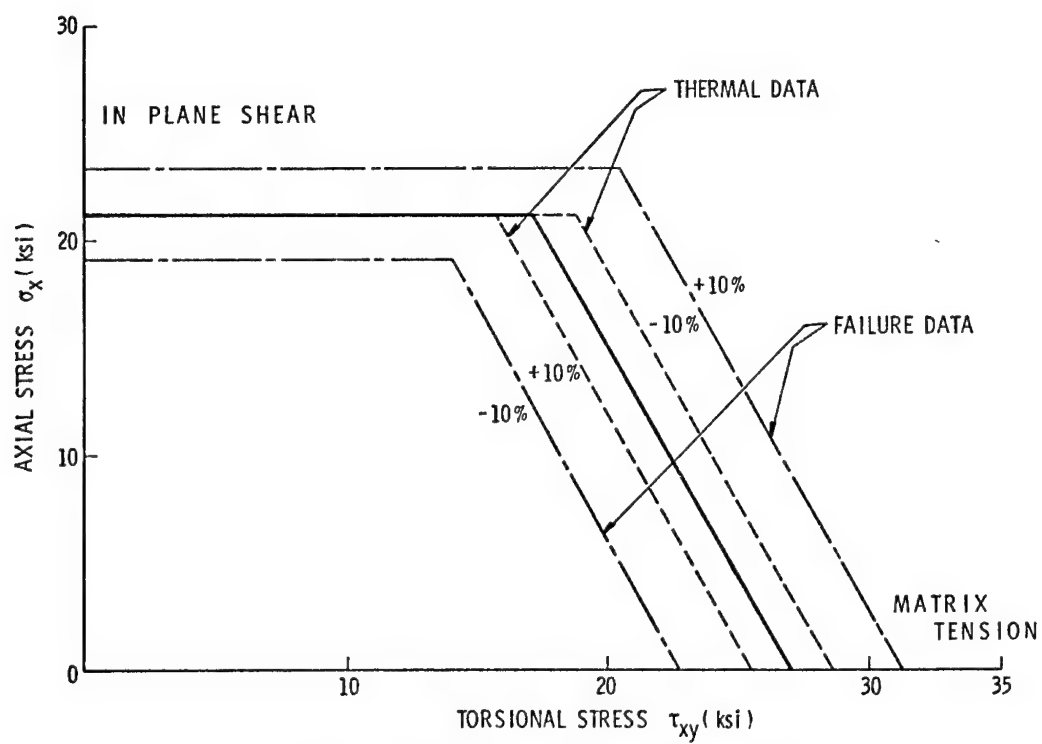
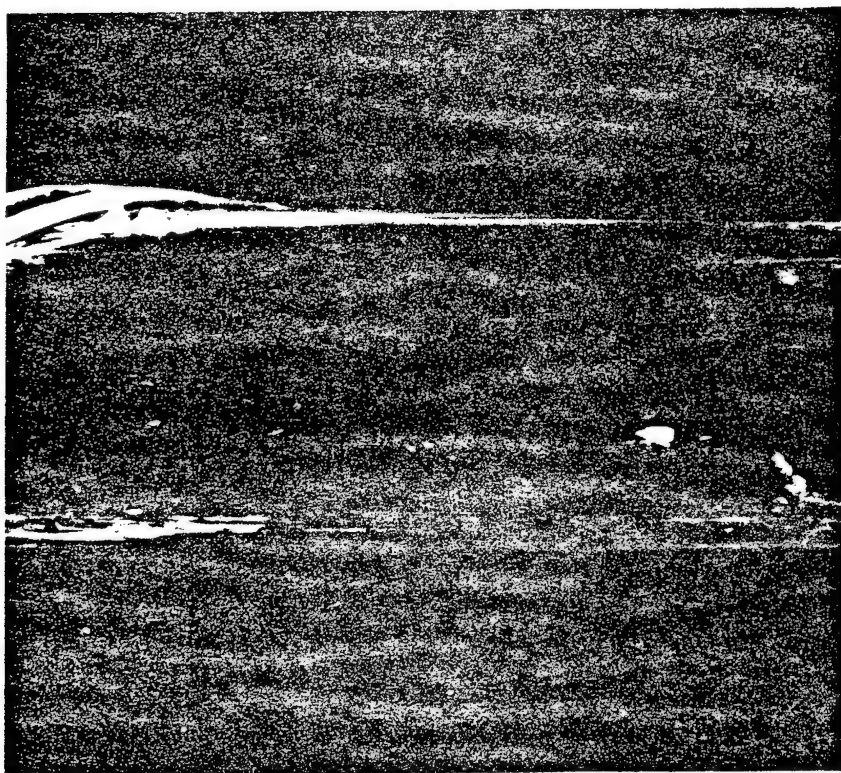
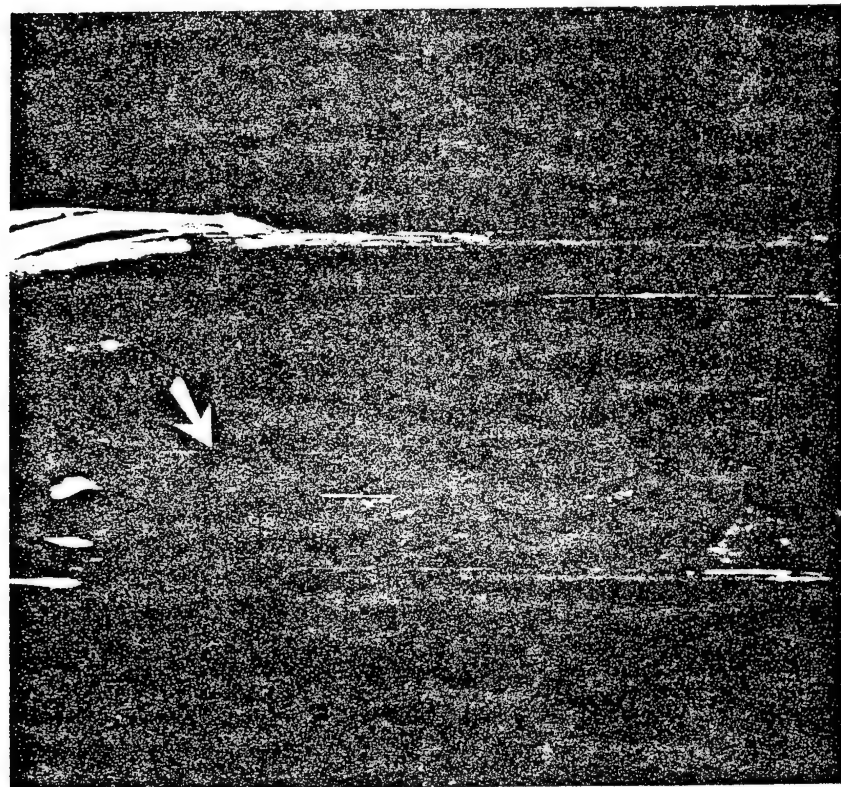


Figure FPF Prediction Input Data Variation (± 45)_S
215

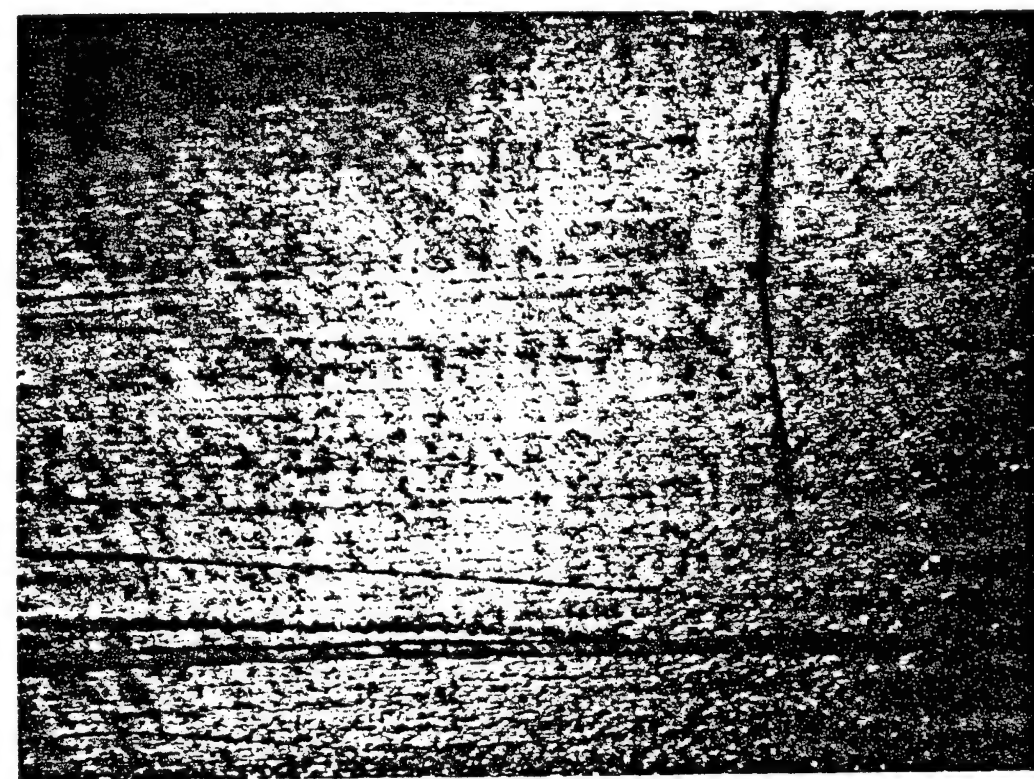


BEFORE

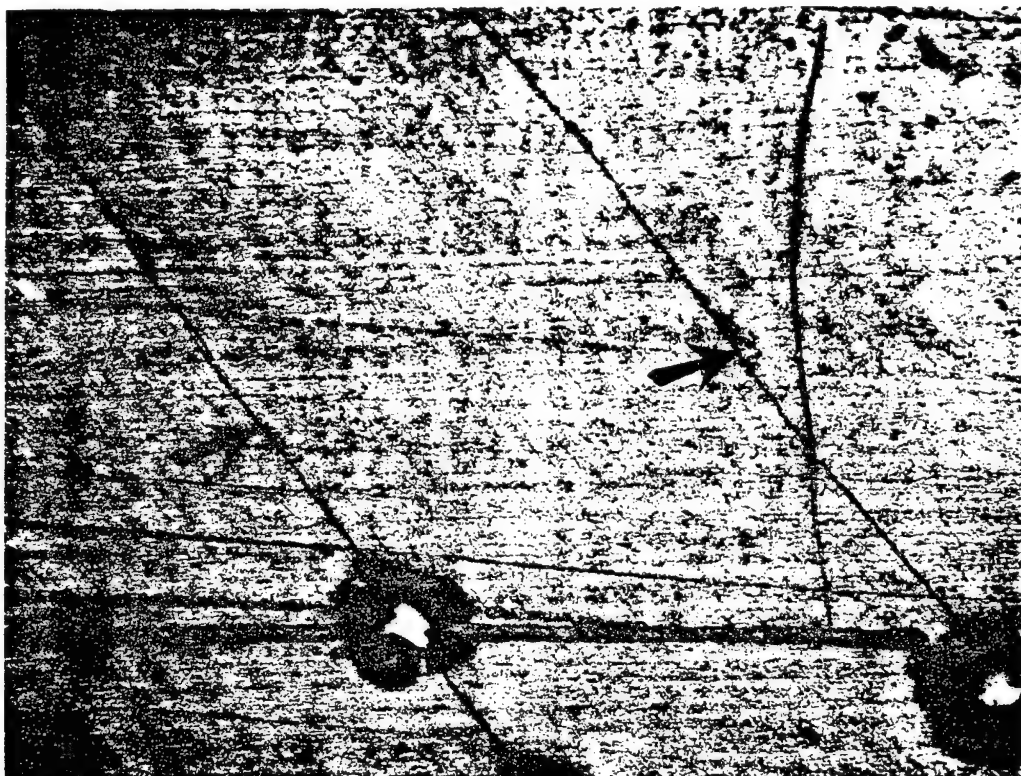


AFTER

FPF by Dye Penetrant



BEFORE

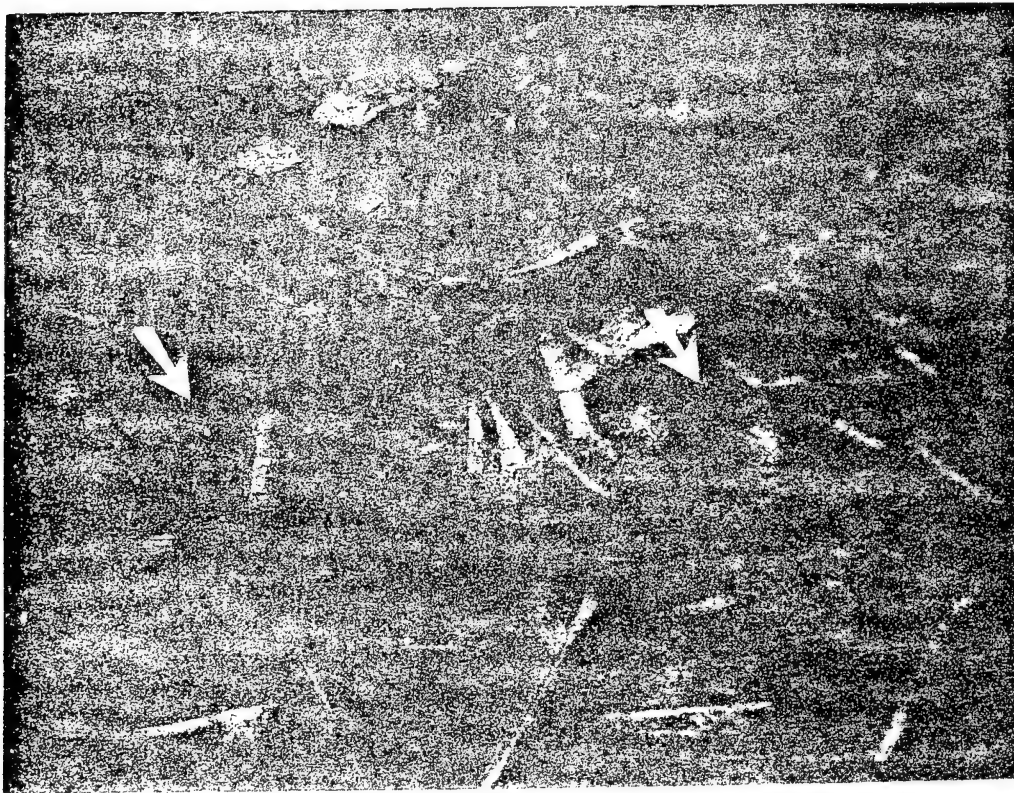


AFTER

FPF by Replication Microscopy



BEFORE



AFTER

FPF by Replica Microscopy

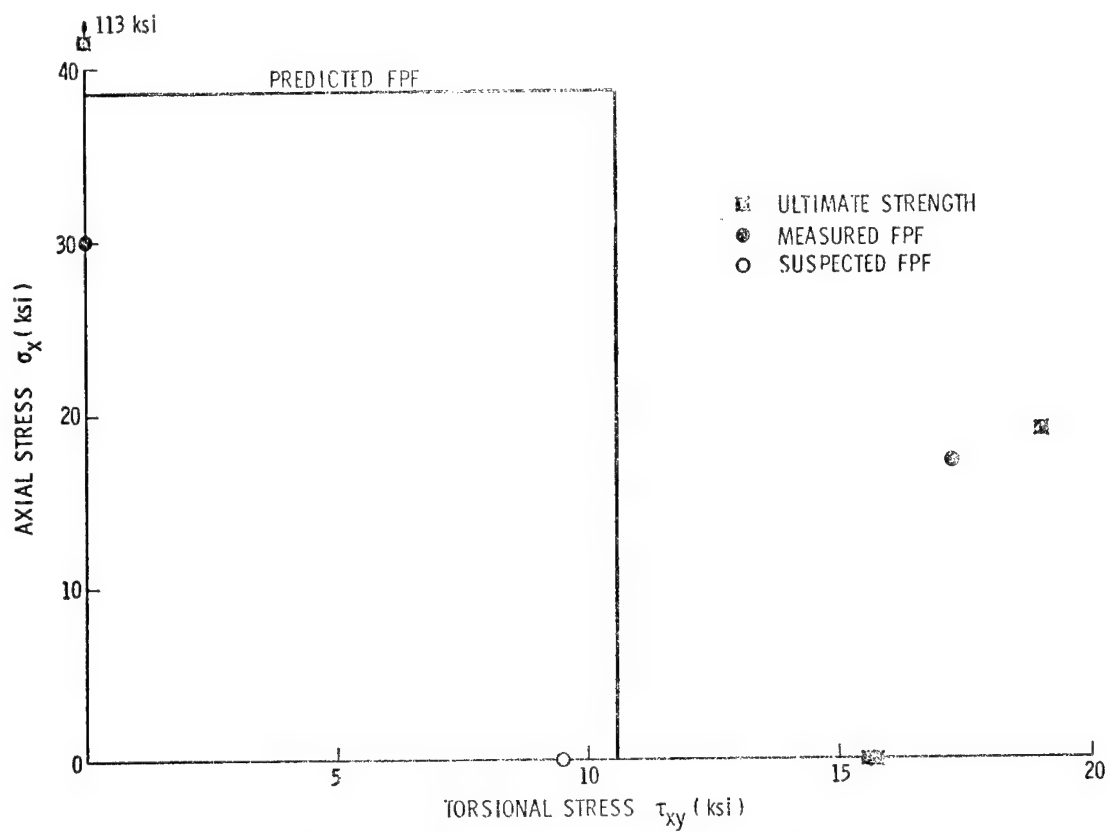


Figure Experimental FPF Measurements on (0/90)₅ Tubes

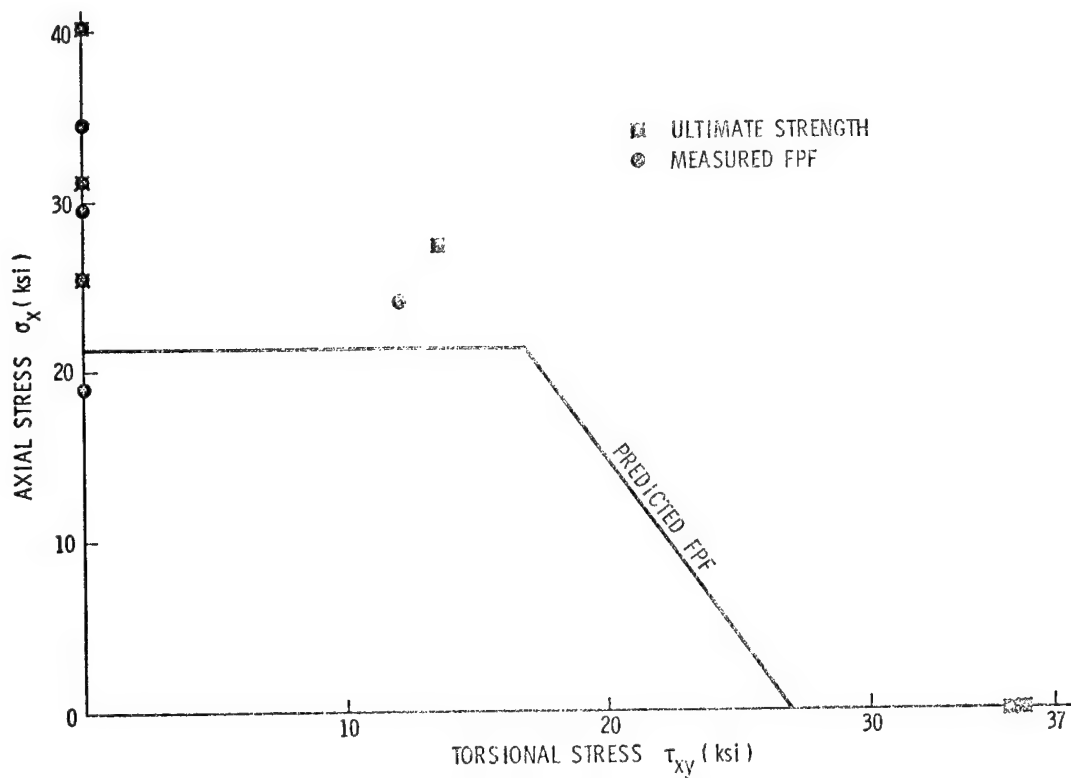
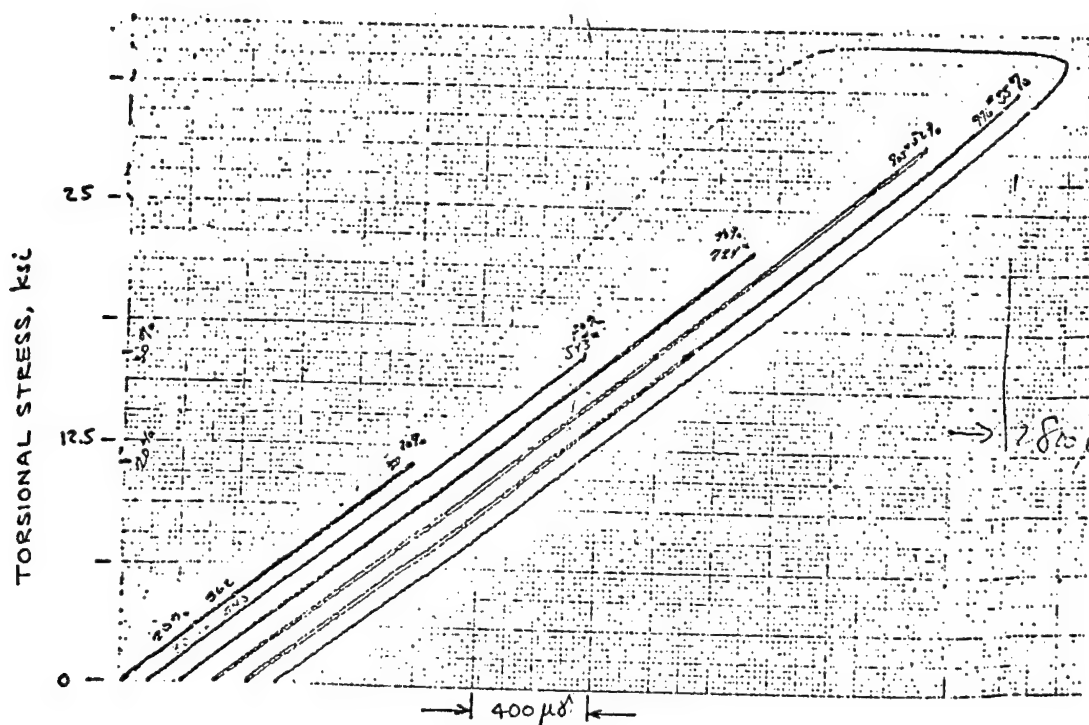
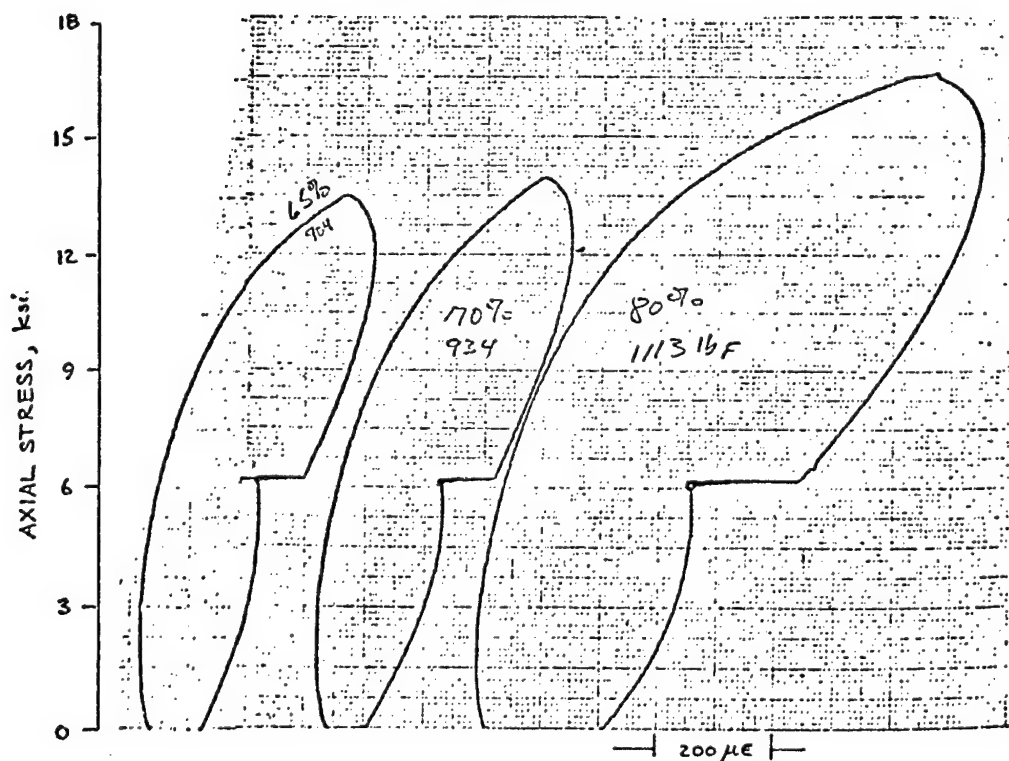


Figure Experimental FPF Measurements on (±45)₅ Tubes



$(\pm 45)_s$ TUBE UNDER TORSIONAL LOADING

$(\tau_u = 33.4 \text{ ksi})$



$(\pm 45)_s$ TUBE UNDER TENSILE LOADING

$(\sigma_t = 28.4 \text{ ksi})$

TIME-DEPENDENT FRACTURE OF COMPOSITES

R. A. Schapery

RECENTLY COMPLETED STUDIES

- "Some Viscoelastic Crack Growth Relations for Orthotropic and Prestrained Media"
- "A Theory of Time-Dependent Bonding for Viscoelastic Media"
(For analyzing healing of flaws in solid propellant and the adhesion component of sliding friction)

CURRENT RESEARCH

- Approximate Method of Analysis of Time-Dependent Cracking and Healing for Problems in which the Extended Correspondence Principle does not Apply. (E.g., dynamic problems & problems involving temperature & moisture gradients)
- Numerical Determination of Stress Intensity Factors using Nodal Point Force & Displacement from F.E. & Fast Fourier Transform Solutions.

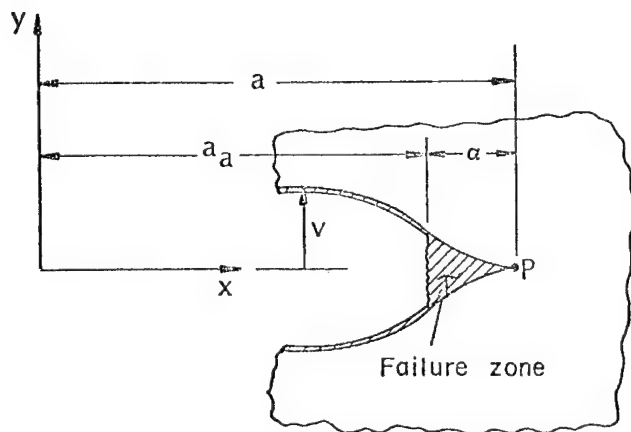


Figure 1. Cross-section of an idealized crack.

CRACKS IN ORTHOTROPIC MEDIA

Crack Speed; \dot{a}

$$K_{22}^v \left(\frac{\alpha}{3\dot{a}} \right) K_I^2 + K_{11}^v \left(\frac{\alpha}{3\dot{a}} \right) K_{II}^2 = 4\Gamma$$

Calculation of α :

$$F(K_I, K_{II}, \dot{a}, \alpha) = 0$$

Initiation Time, t_i

$$K_{22}^v \rightarrow (K_I^2)^{-1} \int_0^{t_i} K_{22}^v(t_i - \tau) \frac{dK_I^2}{d\tau} d\tau$$

$$K_{11}^v \rightarrow (K_{II}^2)^{-1} \int_0^{t_i} K_{11}^v(t_i - \tau) \frac{dK_{II}^2}{d\tau} d\tau$$

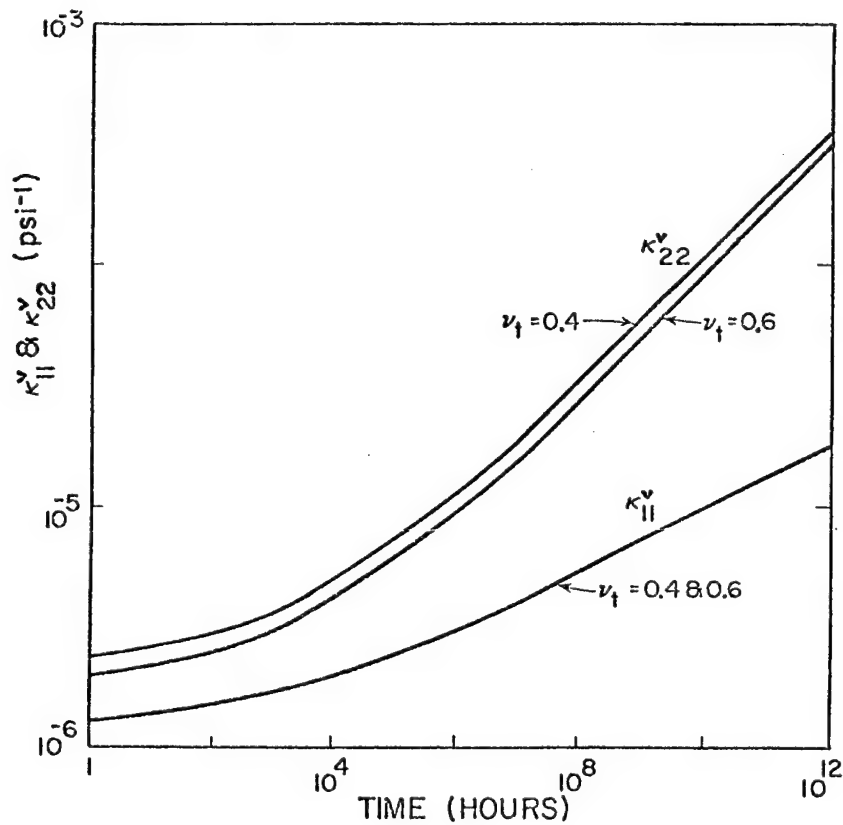


Figure 2. Viscoelastic functions κ_{11}^v and κ_{22}^v for a glass fiber-reinforced plastic.

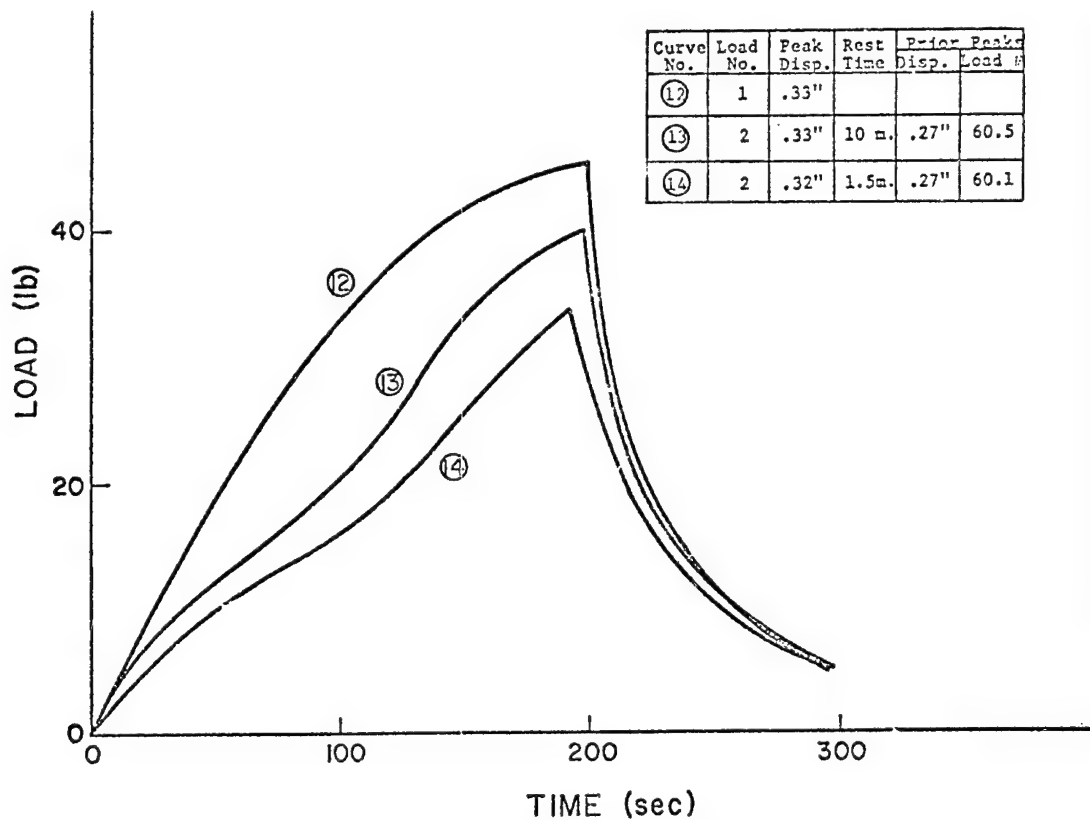


Figure 3. Ramp test with varying rest times
(Solid Propellant)

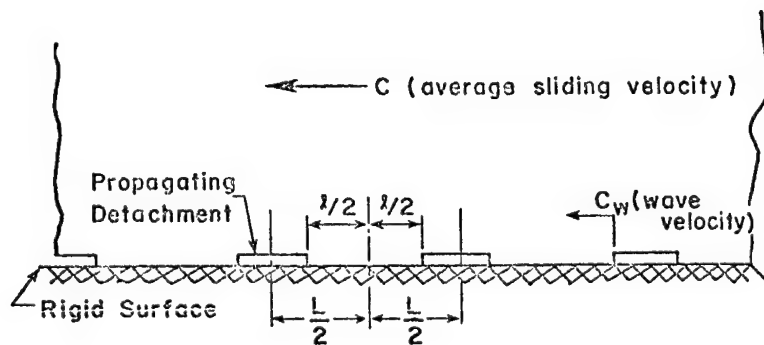


Fig. 4 - Assumed mode of discontinuous sliding with adhesion.

TIME-DEPENDENT BONDING

Bonding Speed, \dot{a}_b

$$\frac{1}{8} D_I^2 C_V^{-1} \left(\frac{P}{3\dot{a}_b} \right) = \Gamma_b$$

Calculation of β

$$\beta = 32\pi \frac{\Gamma_b^2}{S_m^2 J_1^2} D_I^{-2}$$

Bonding Criteria

$$\dot{a}_b = 0 \quad \text{if} \quad K_I \geq [8\Gamma_b / C_V(\infty)]^{1/2}$$

$$\dot{a}_b = \infty \quad \text{if} \quad K_I \leq [8\Gamma_b / C_V(\infty)]^{1/2} [C_V(0) / C_V(\infty)]^{1/2}$$

$0 < \dot{a}_b < \infty$ whenever K_I is between these limits

EXPLORATORY DEVELOPMENT OF PROBABILISTIC CHARACTERIZATION
AND TESTING TECHNIQUES FOR FATIGUE BEHAVIOR
OF COMPOSITE LAMINATES

CONTRACT No. F33615-75-C-5112

BY

ROBERT A. HELLER

JANN N. YANG

JOHN J. MCGOWAN

DEPARTMENT OF ENGINEERING SCIENCE AND MECHANICS
VIRGINIA POLYTECHNIC INSTITUTE AND STATE UNIVERSITY
BLACKSBURG, VIRGINIA

PURPOSES:

EXAMINATION OF THE STATISTICAL DISTRIBUTIONS OF STATIC STRENGTH AND STIFFNESS
FOR GRAPHITE/EPOXY COMPOSITES AND THEIR EFFECTS ON:

1. CONSTANT AMPLITUDE FATIGUE LIFE
2. RANDOM FATIGUE LIFE
3. RESIDUAL STRENGTH REDUCTION
4. STIFFNESS CHANGES
5. CREEP AND CREEP RUPTURE
6. PERIODIC PROOF TESTS

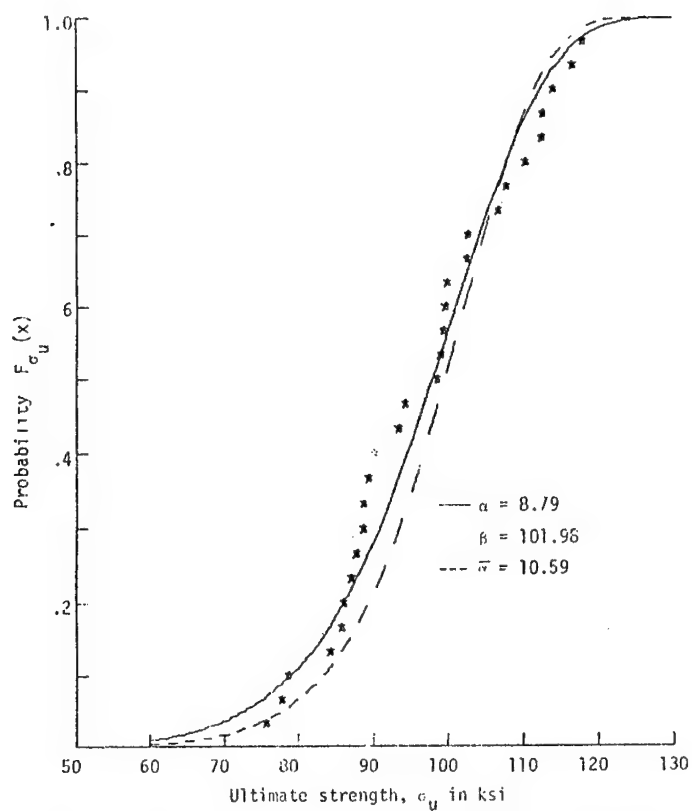


Fig. 2 Distribution of ultimate strength for G/E 0, ± 45 , 0/s specimens (Table 4).

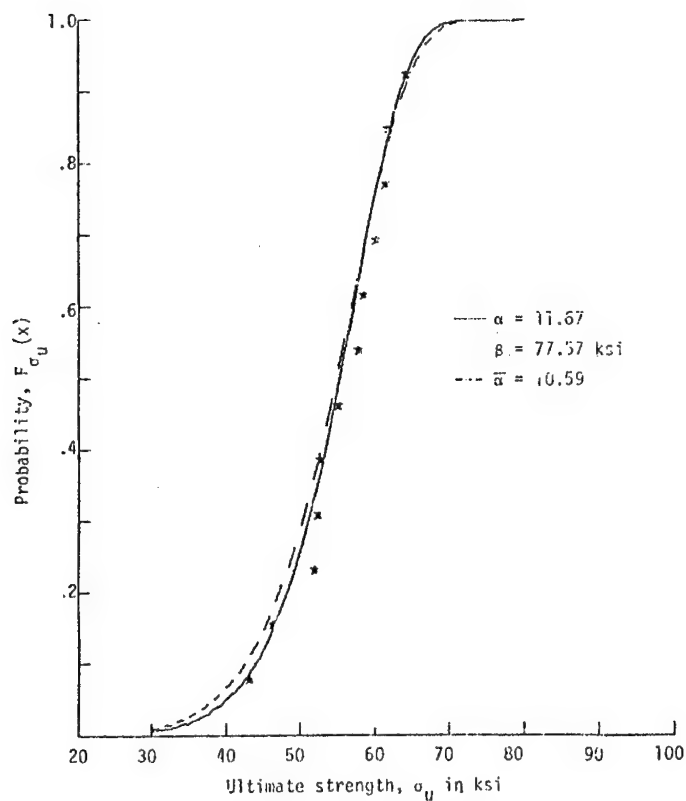


Fig. 3 Distribution of ultimate strength for G/E 0, 90, ± 45 /s specimens (Table 9).

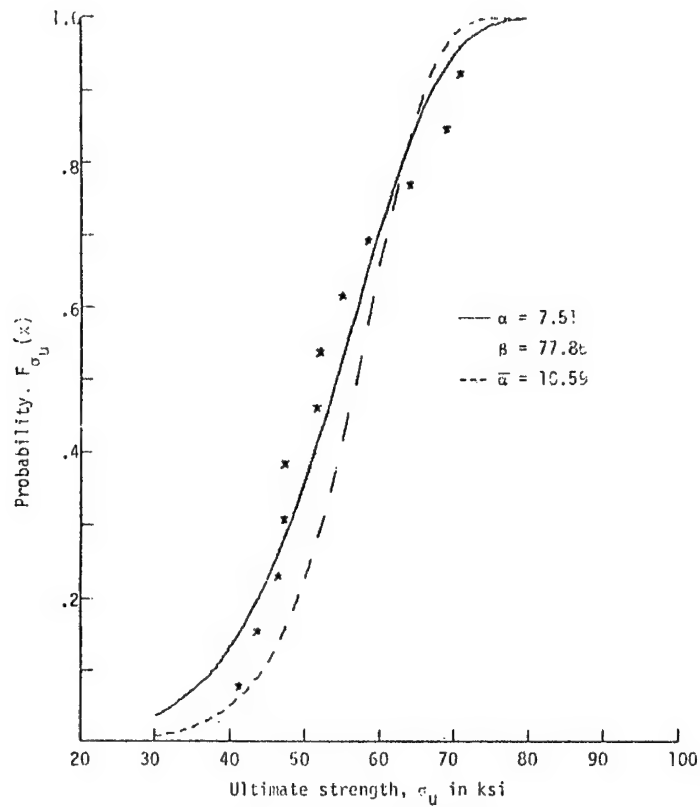


Fig. 4. Distribution of ultimate strength for G/E 90,0,+45/s specimens (Table 10).

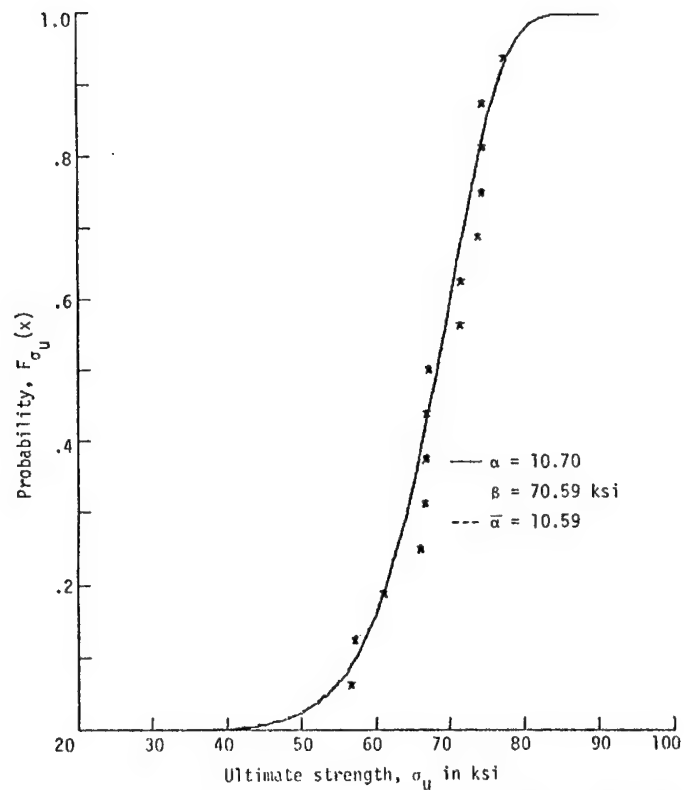


Fig. 5. Distribution of ultimate strength for G/E 0,+45,90/s specimens (Table 13).

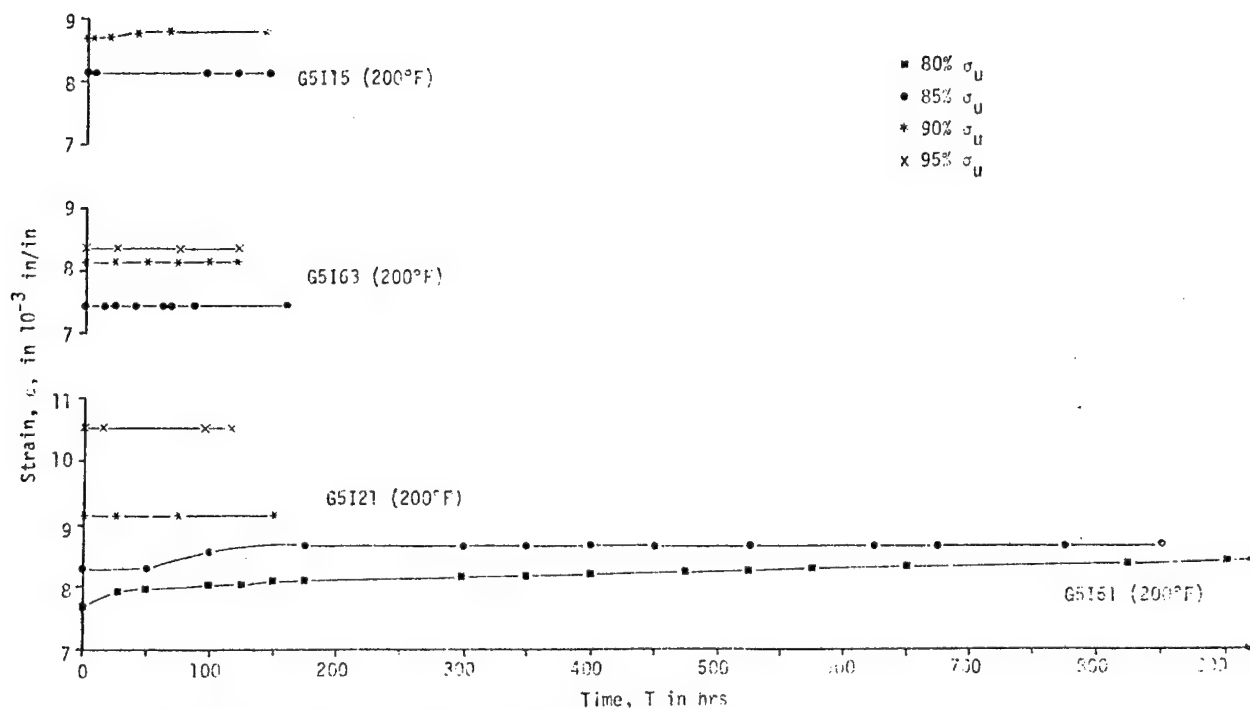


Fig. 6. Creep tests on G/E 0, ±45, 0/5 specimens ($\sigma_U = 98$ KSI)

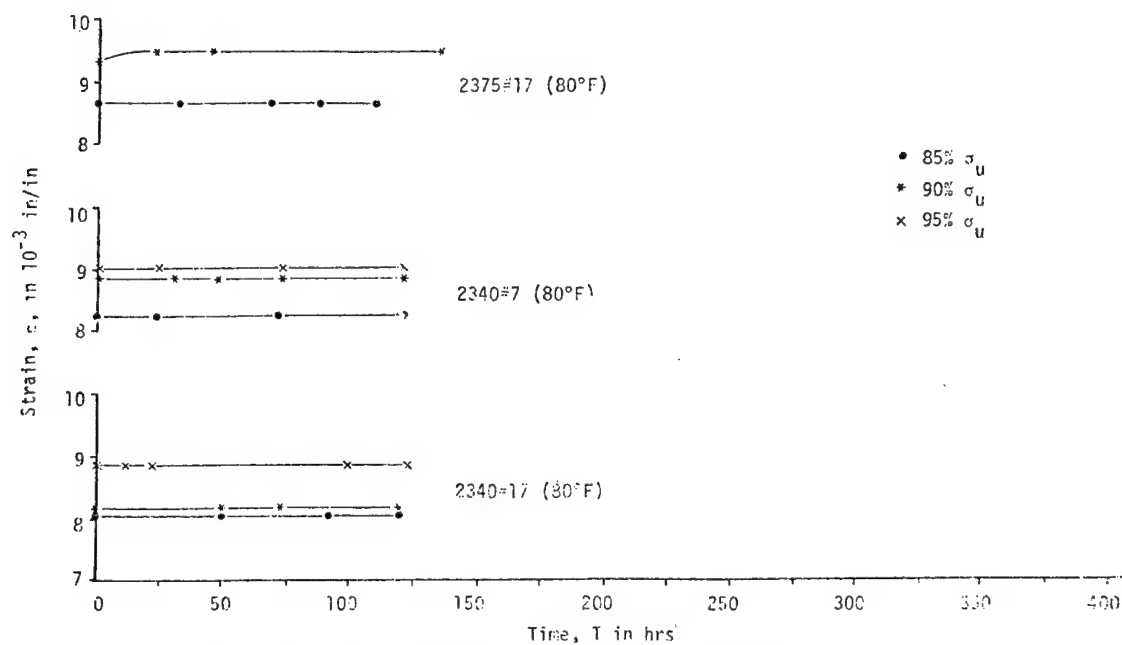


Fig. 7. Creep tests on G/E 0, ±45, 90/5 specimens ($\sigma_U = 68.33$ KSI)

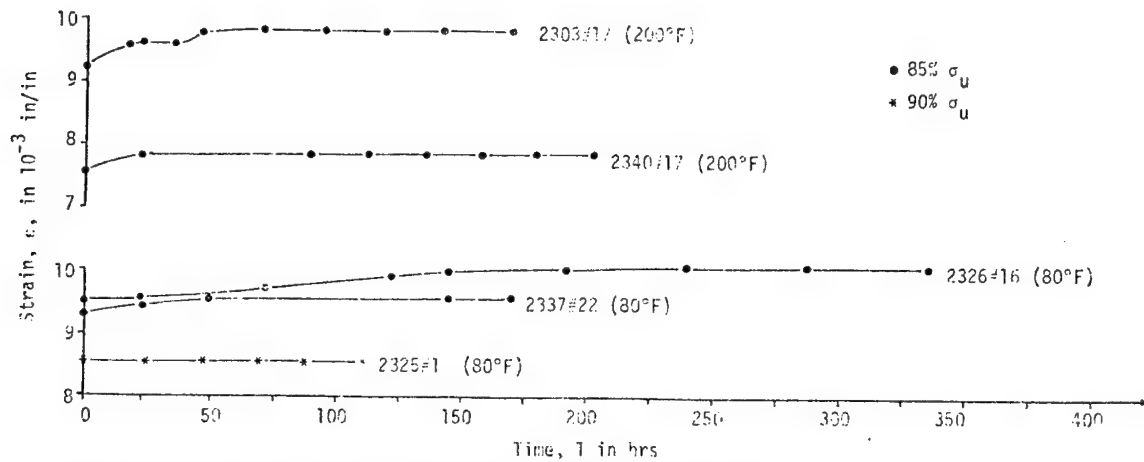


Fig. 8 Creep tests on G/E 0, +15, 90° specimens ($\sigma_u = 68.33$ KSI)

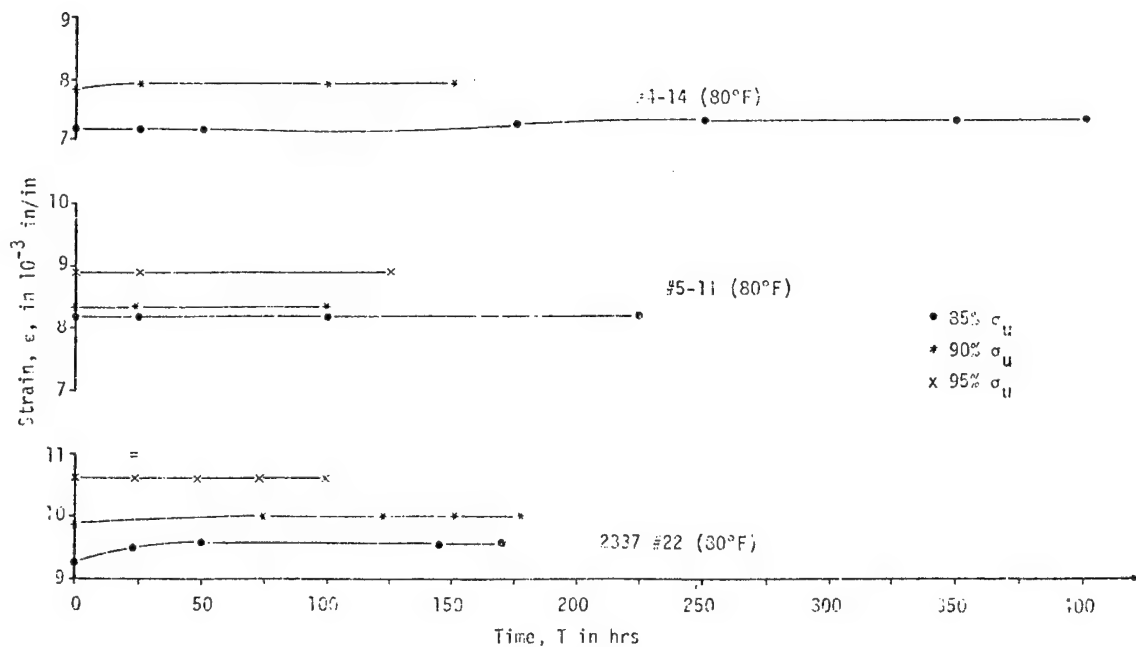


Fig. 9. Creep tests on G/E 0, +15, 90° and C, 0, 45° specimens ($\sigma_u = 62.32$ KSI and 59.57 KSI respectively).

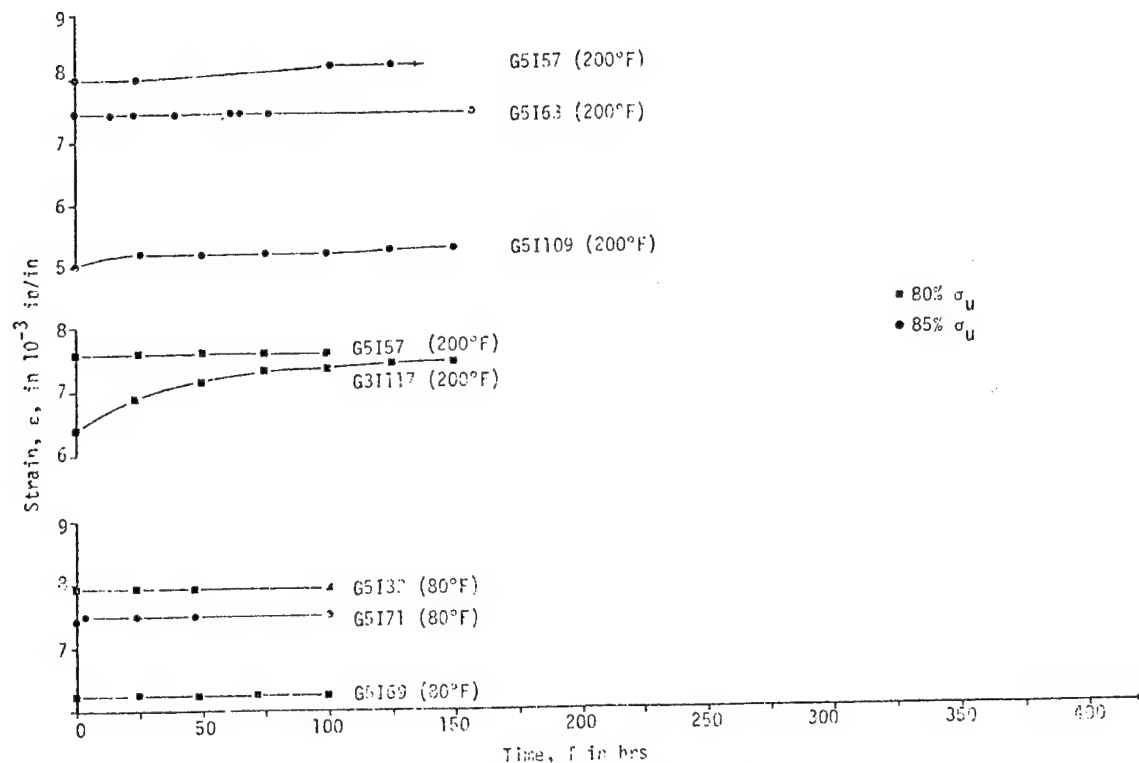


Fig. 10. Creep test results on G/F 0, $\pm 45.0/s$ specimens ($\sigma_u = 88$ KSI)

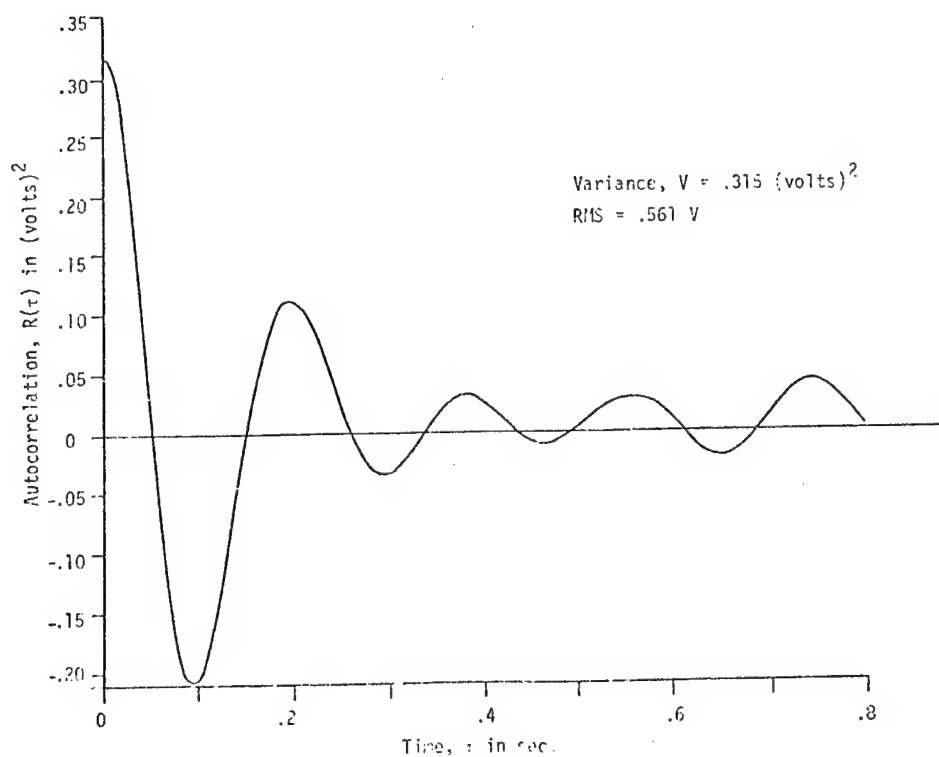


Fig. 11. Autocorrelation of the narrow band load spectrum (closed loop control system input).

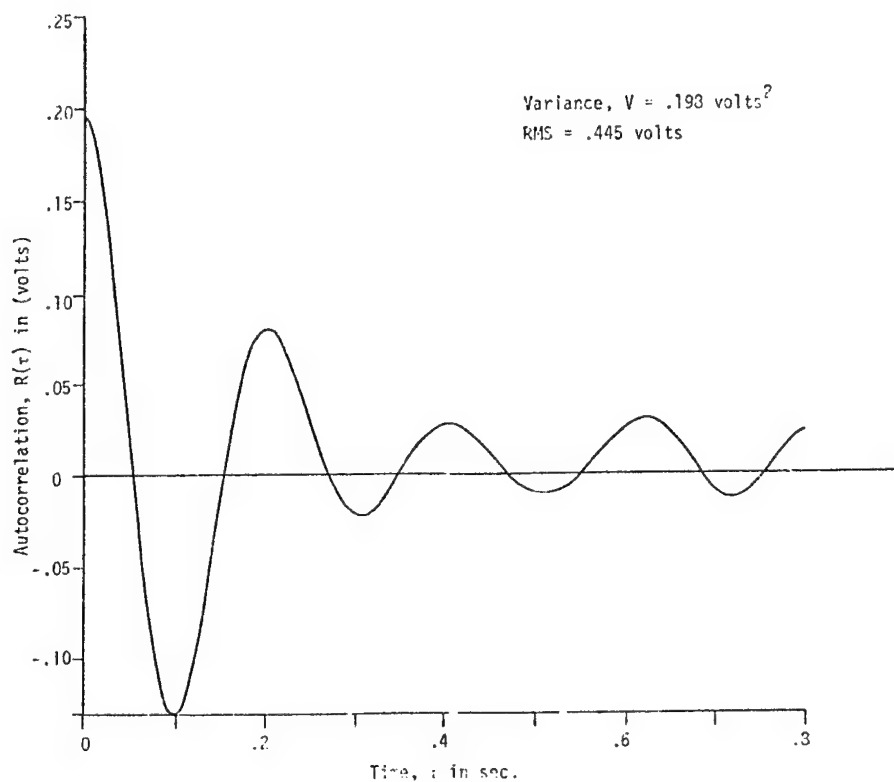


Fig. 12 Autocorrelation of the narrow band load spectrum (load cell output).

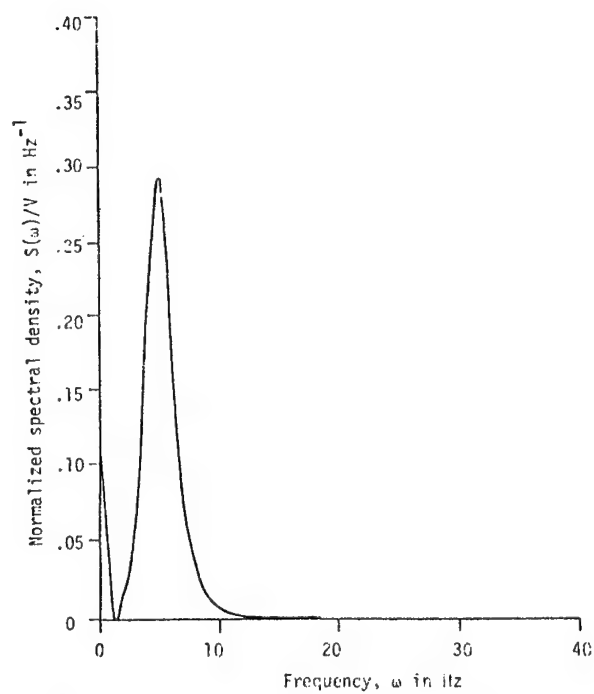


Fig. 13. Input spectral density (narrow band).

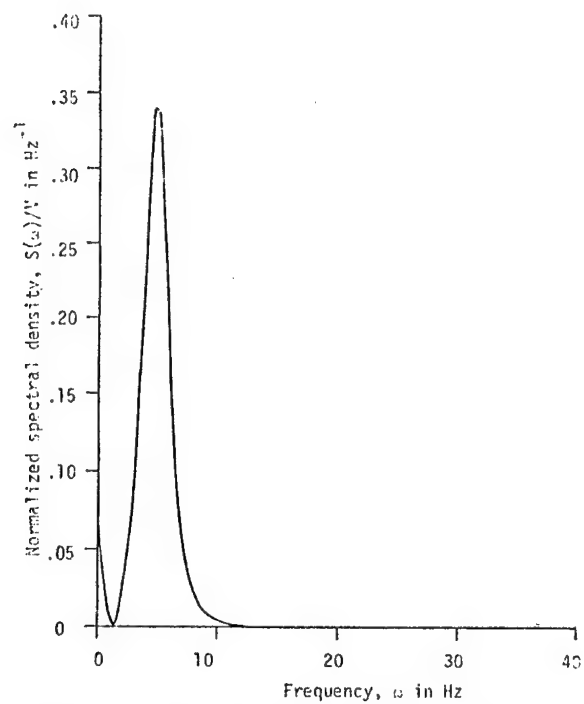


Fig. 14. Output spectral density (narrow band).

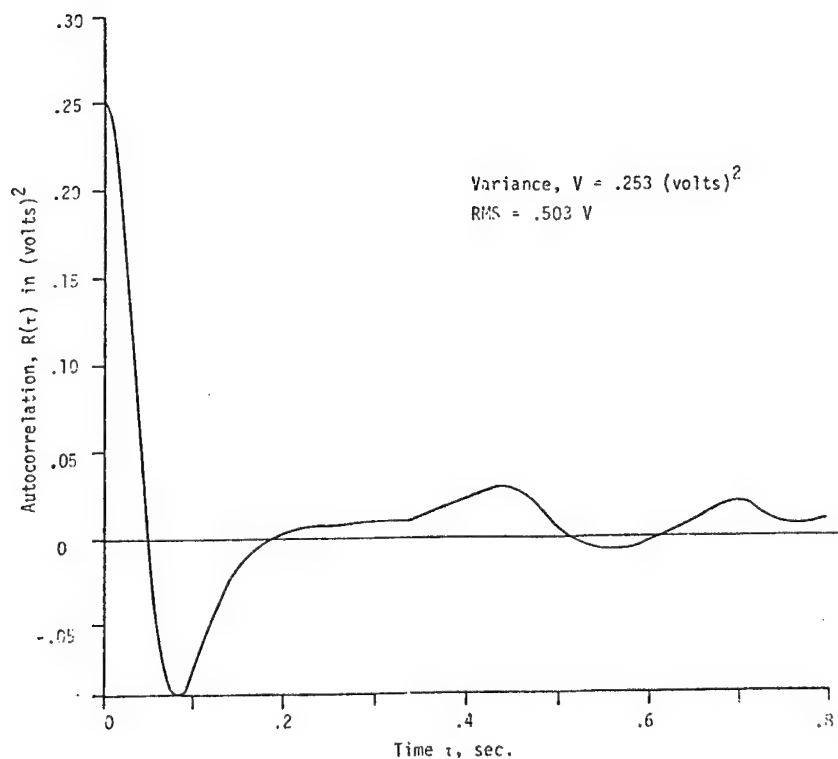


Fig. 15 Autocorrelation of the wide band load spectrum (closed loop control system input).

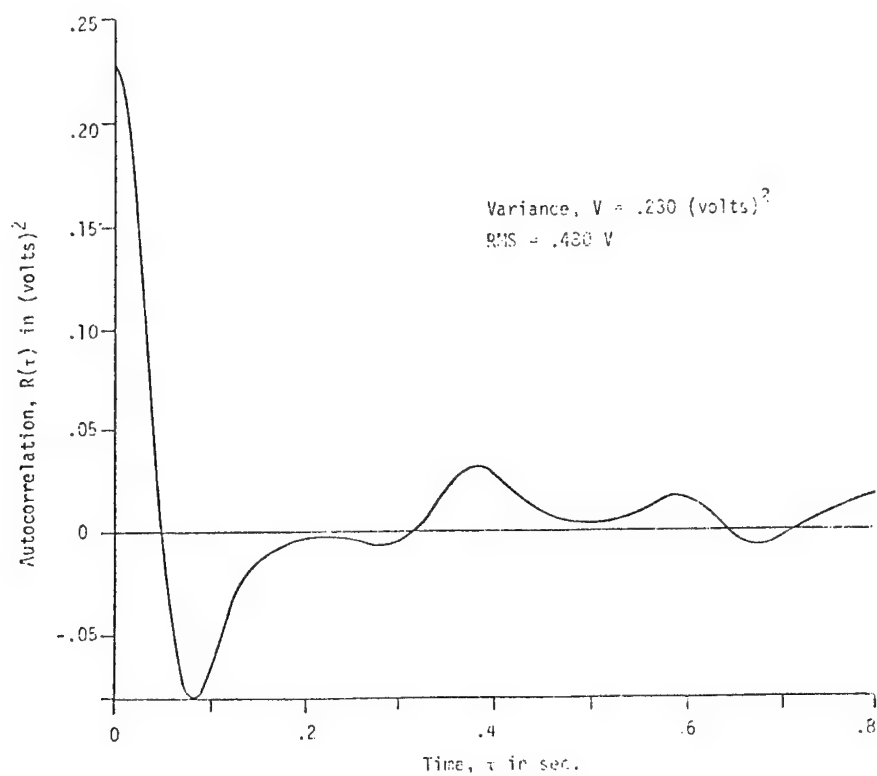


Fig. 16. Autocorrelation of the wide band load spectrum (load cell output).

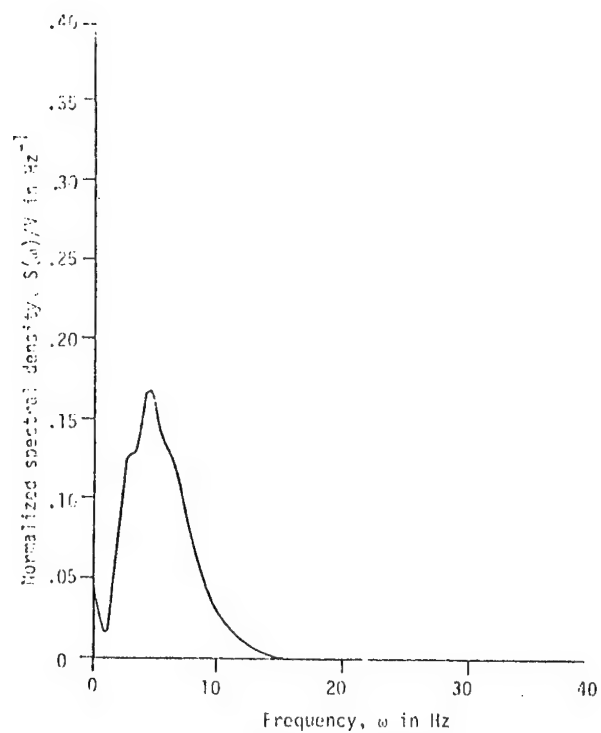


Fig. 17. Input spectral density (wide band).

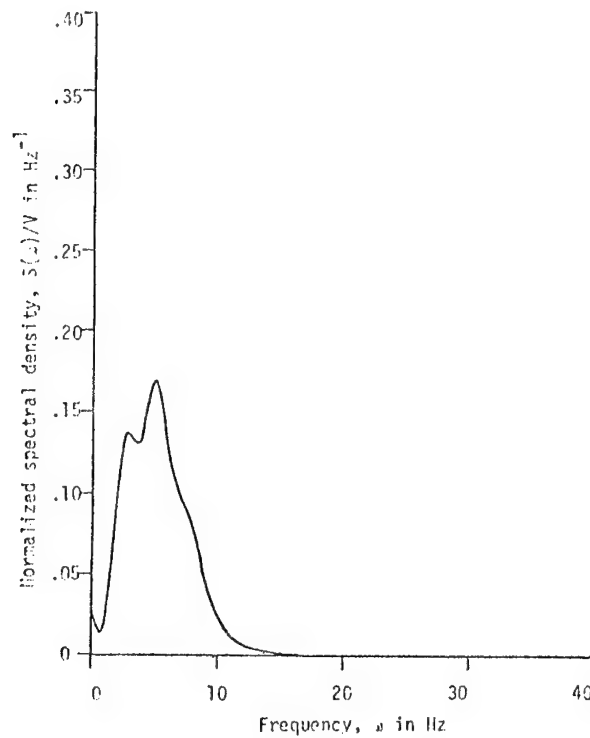


Fig. 18. Output spectral density (wide band).

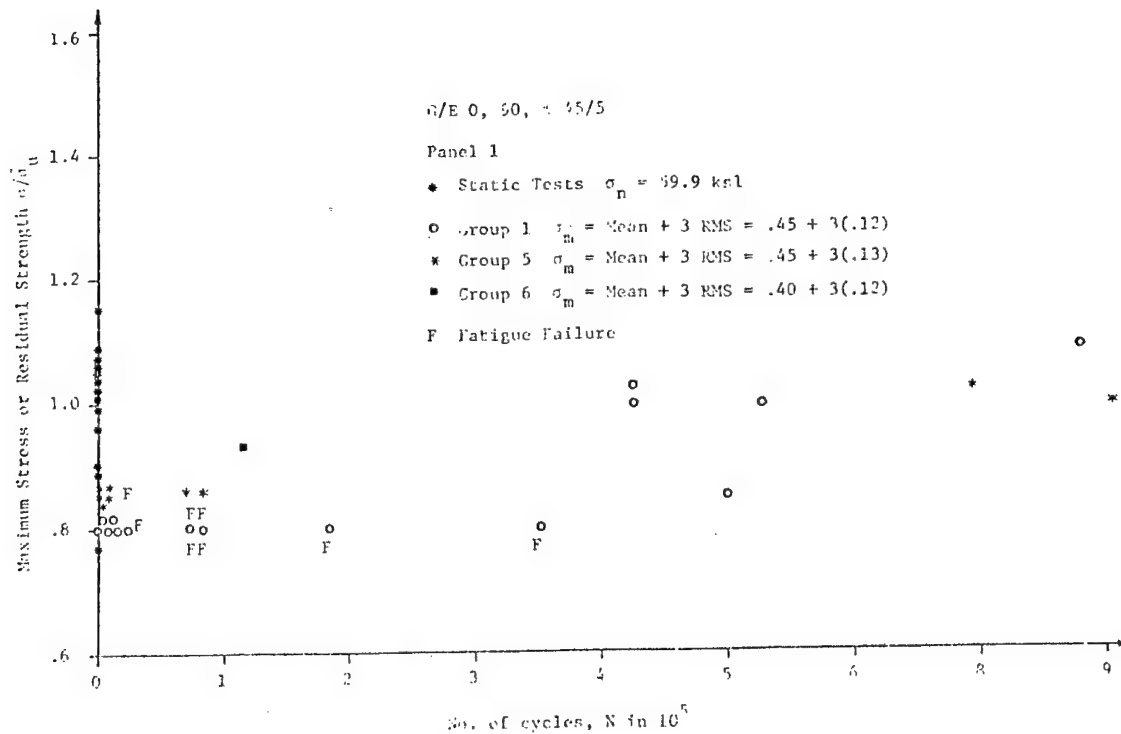


Fig. 19. Random Fatigue Test Results

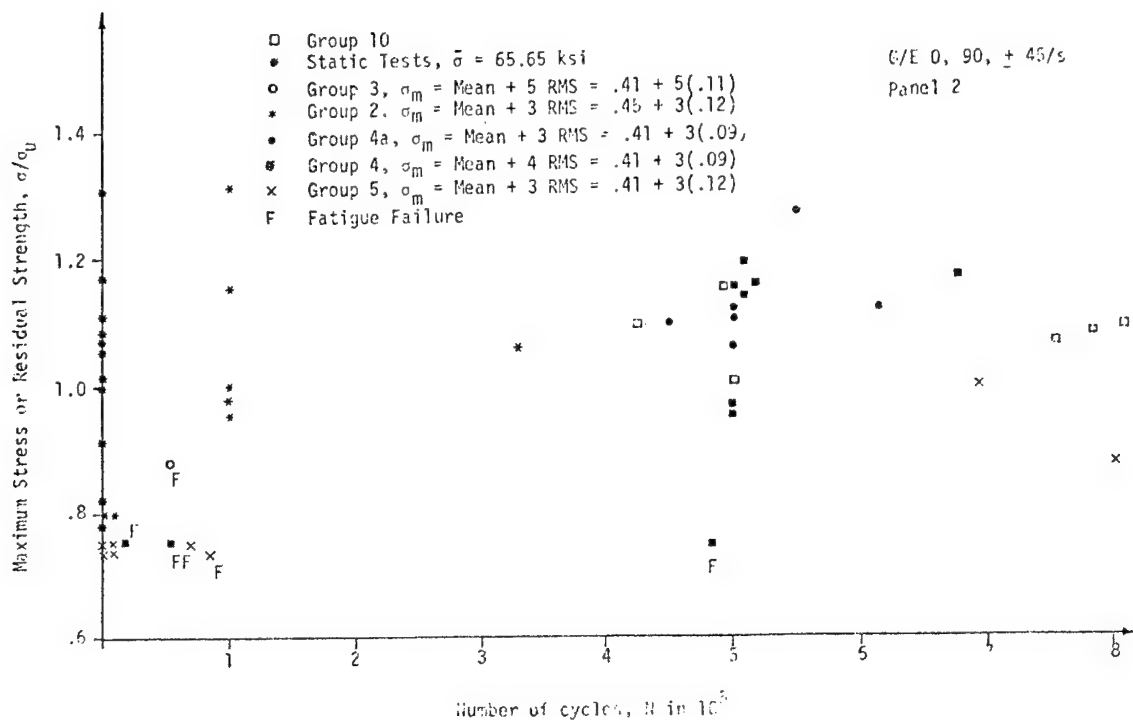


Fig. 20 Random Fatigue Test Results

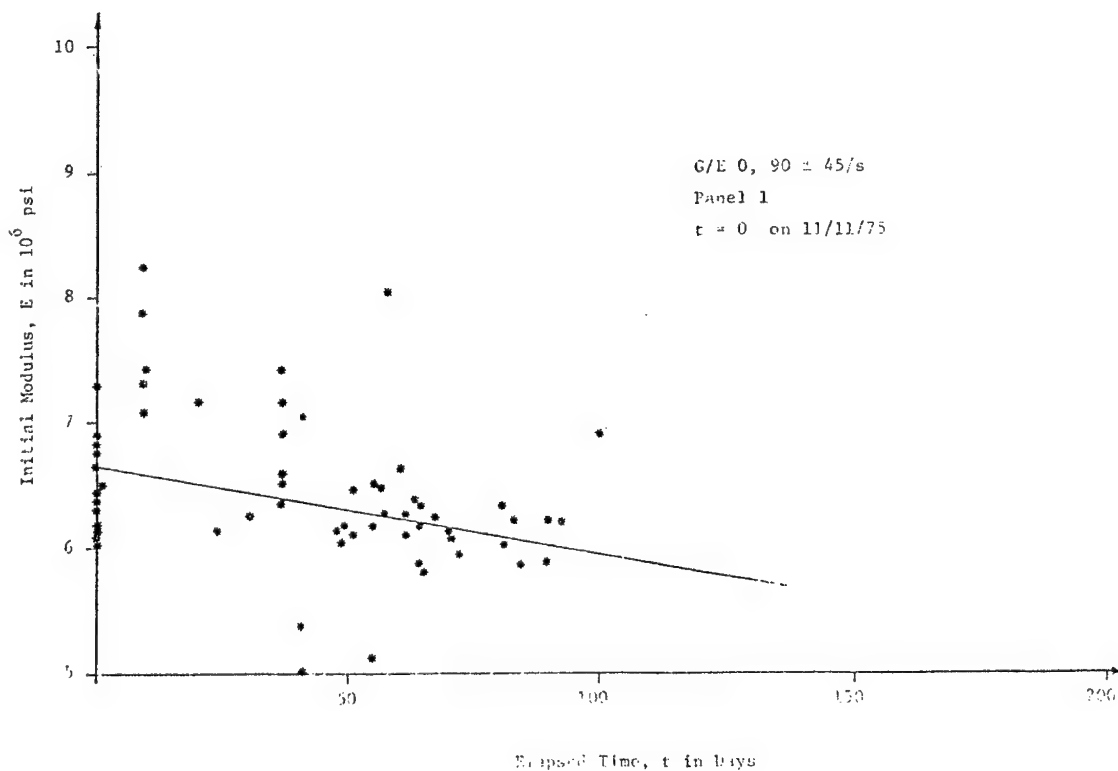


Fig. 21 Initial Modulus as a function of Date of Test

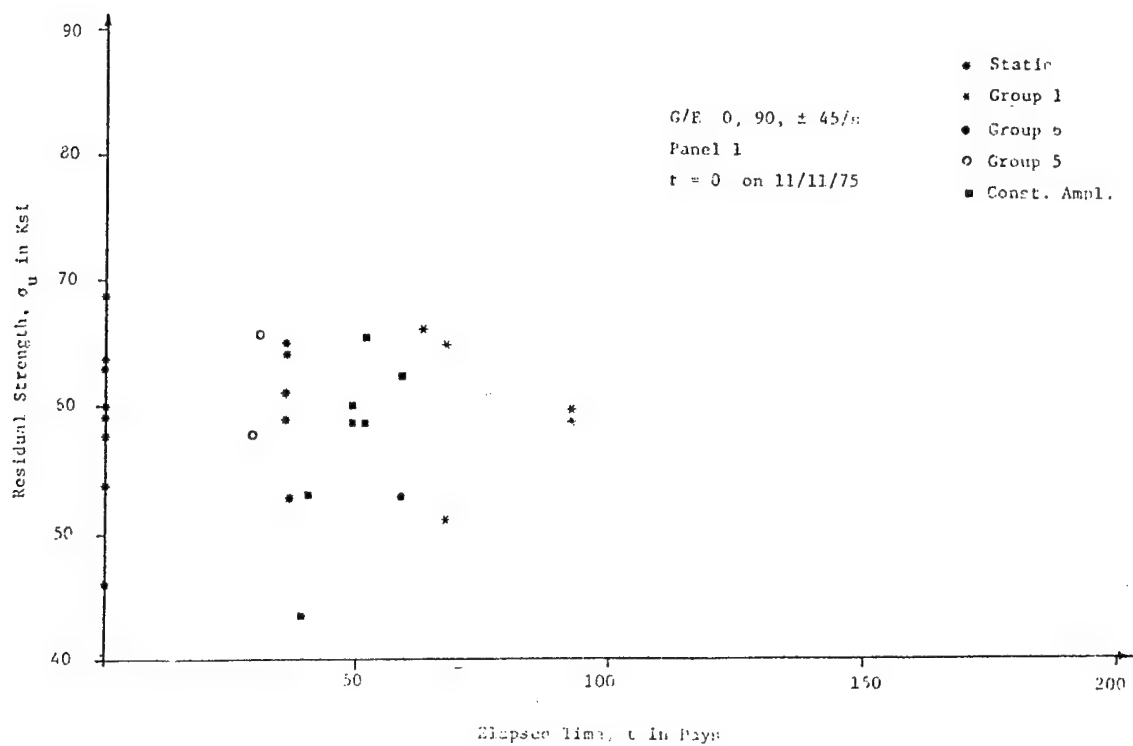


Fig. 22 Residual Strength as a Function of Date of Test

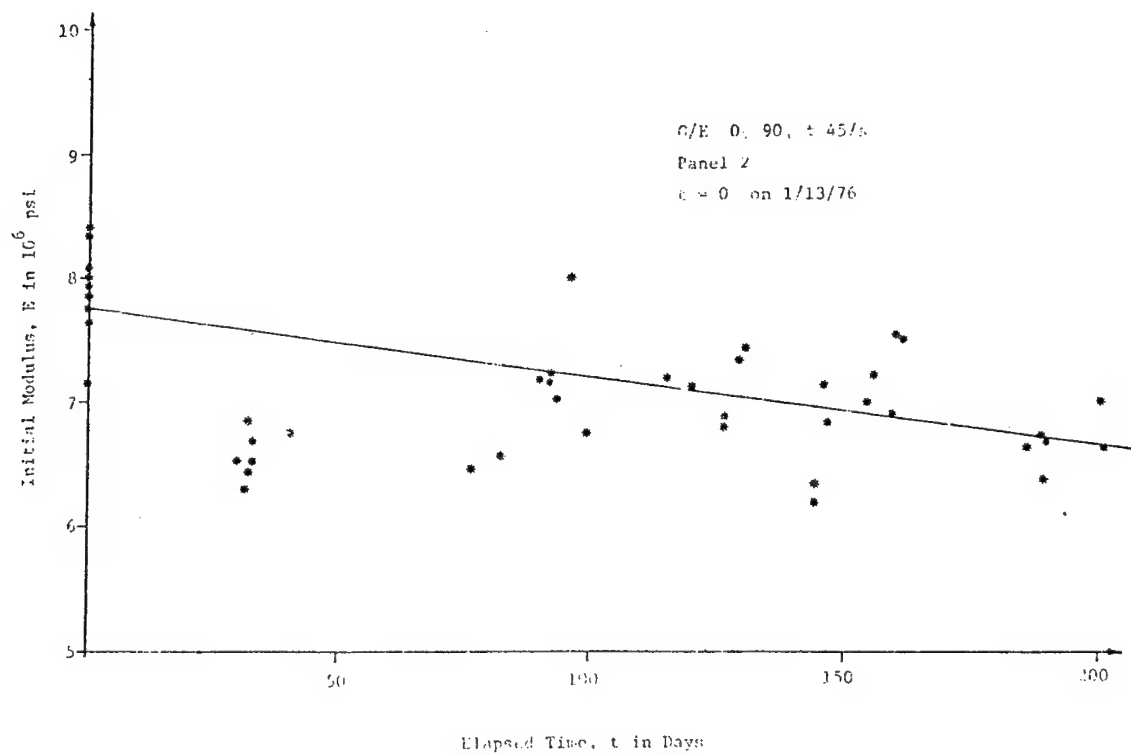


Fig. 23 Initial Modulus as a Function of Date of Test

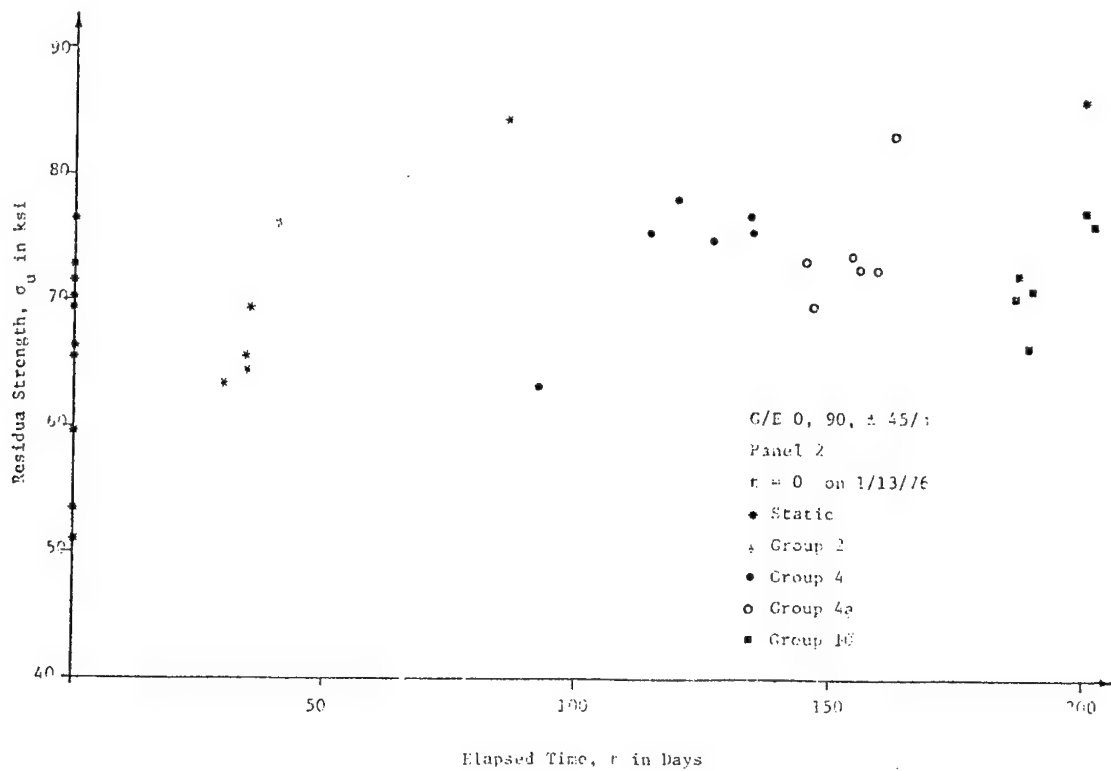


Fig. 24 Residual Strength as a Function of Date of Test

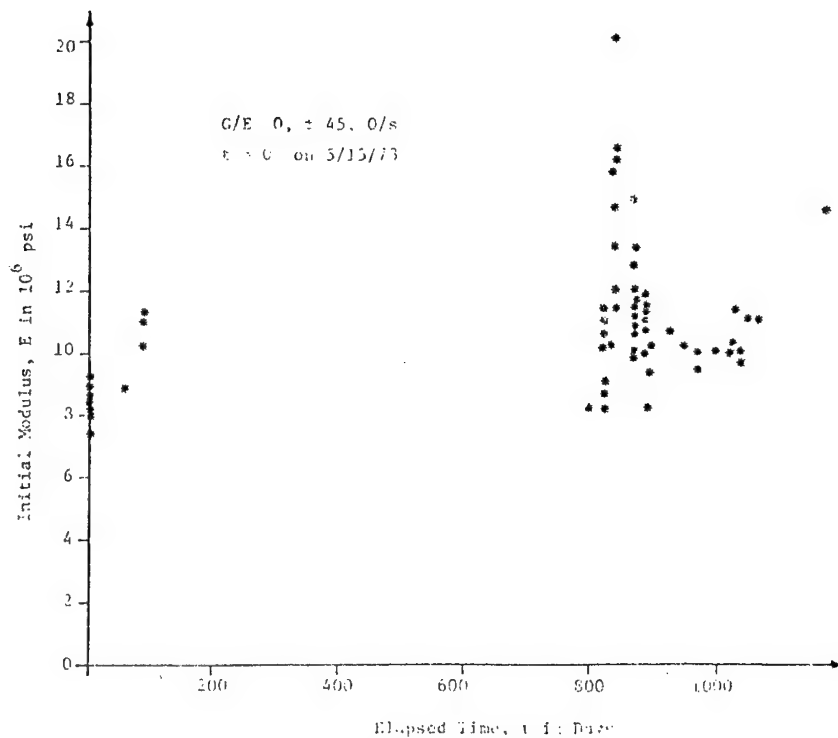


Fig. 25 Initial Modulus as a Function of Date of Test



Table 1. Creep Tests on
G/E 0,+45, 0/_s Specimens, $\sigma_u = 98.00$ KSI

DATE	SPECIMEN NO.	STRESS KSI	STRESS % OF σ_u	E loading x 10 ⁶ psi	E unloading x 10 ⁶ psi	Temperature °F	REMARKS
8/12/75	G31117		80	8.35		200	
9/4/75	G31109		85	10.26		200	
10/27/75	G5169	78.00	80	10.86		80	
10/27/75	G5133	78.00	80	10.00		80	
11/7/75	G51128		85	8.15		80	Broke during loading
11/10/75	G51133	88.20	90	10.00		80	
11/10/75	G51150	88.20	90	10.00		30	
11/12/75	G5171	83.30	85	10.16		80	
11/19/75	G5161	78.40	80	9.34		200	Temperature controls incorrect
12/16/75	G5157	78.40	80	10.74		200	
1/14/76	G5121	83.30	85	10.19	10.19	200	
2/4/76	G5121	88.20	90	10.00	10.00	200	Stress increased to 90%
3/23/76	G5121	93.10	95	10.00	10.00	200	Stress increased to 95%
2/4/76	G5122	83.30	85	9.52		200	Temperature controls incorrect
2/25/76	G5146	83.30	85	10.00		200	Temperature controls incorrect
3/30/76	G5115	83.30	85	10.13	10.13	200	
4/7/76	G5115	88.20	90	9.88	9.88		Stress increased to 90%
4/5/76	G5163	83.30	85	11.54	11.18	200	
4/19/76	G5163	88.20	90	11.33	11.32	200	Stress increased to 90%
4/27/76	G5163	93.10	95	11.15		200	Stress increased to 95%

Table 2. Creep Tests on
G/E 0,+45,90/_s Specimens, $\sigma_u = 68.38$ KSI
Proof Stress = 63 KSI

DATE	SPECIMEN NO.	STRESS KSI	STRESS % OF σ_u	E loading x 10 ⁶ psi	E unloading x 10 ⁶ psi	Temperature °F	REMARKS
1/26/76	2340#7	58.13	85	7.5	7.5	80	
2/5/76	2340#7	61.55	90	7.5	7.5	80	Stress increased to 90%
2/10/76	2340#7	64.97	95	7.5	7.5	80	Stress increased to 95%
1/27/76	2336#10					80	Broke during loading
1/29/76	2374#2					80	Broke during loading
2/7/76	2340#17	58.13	85	7.35	7.35	80	
2/24/76	2340#17	61.97	90	7.35	7.35	80	Stress increased to 90%
3/23/76	2340#17	64.96	95	7.31	7.31	80	Stress increased to 95%
2/10/76	2361#5	54.71	80	6.10		80	Broke after one day
3/29/76	2337#22	58.13	85	6.54	6.36	80	
4/18/76	2337#20	61.55	90	6.27	6.10	80	
5/5/76	2337#20	64.97	95	6.20		80	Stress increased to 95%
5/3/76	2336#7			5.88		80	Broke during proof loading
5/14/76	2374#3			6.71		80	Broke during proof loading
5/17/76	2303#17	58.13	85	5.63	5.58	200	Proof loaded at 80°F. E=5.69
5/19/76	2326#16	58.13	85	5.27	6.27	80	
6/10/76	2335#19	58.13	85	6.25		200	Proof loaded at 80°F. E=6.98
6/8/76	2375#17	58.13	85	6.92	6.90	80	
7/27/76	2375#17	61.55	90	6.90	6.74	80	Stress increased to 90%
5/10/76	2325#1	61.55	90	7.00	6.85	80	
7/18/76	2325#1	64.97	95			80	Broke during load increase
6/10/76	2340#17	58.13	85	7.40	7.15	200	Proof loaded at 80°F. E=7.17
7/27/76	2325#20	58.13	85	6.43		80	Broke during loading
7/27/76	2375#13	58.13	85	6.0		80	Broke during loading

Table 3 . Creep Tests on
G/E 0, 90, $\pm 45^\circ$ Specimens. Panel 1
 $\sigma_u = 59.57$ KSI

DATE	SPECIMEN NO.	STRESS KSI	STRESS % OF σ_u	E loading x 10^6 psi	E unloading x 10^6 psi	Temperature $^{\circ}\text{F}$	REMARKS
12/29/75	5-11	50.63	85	6.11	6.11	80	
1/15/76	5-11	53.61	90	6.11	6.11	80	Stress increased to 90%
1/21/76				6.20	6.20	80	Specimen broke during load increase
12/22/75	4-14	50.63	85	7.06	7.06	80	
1/16/76	4-14	53.61	90	6.92	6.92	80	Stress increased to 90%

TABLE 4 RANDOM FATIGUE TEST RESULTS
G/E 0,90,+45/ Panel No. 1 Group No. 1
Mean Stress = 26.80 ksi
RMS Stress = 6.95 ksi
Clipping at Mean +3 RMS

Date	Specimen No.	Residual Stress (ksi)	Applied Cycles x 10 ³	E ₀ (Initial) x 10 ⁶ psi	E ₁ x 10 ⁶ psi at x 10 ³ cycles	E ₂ x 10 ⁶ psi at x 10 ³ cycles	E ₃ x 10 ⁶ psi at x 10 ³ cycles	E ₄ x 10 ⁶ psi at x 10 ³ cycles	E ₅ x 10 ⁶ psi at x 10 ³ cycles	Remarks (FAILURE MODE)
2-11-76	4-11	58.48	526.30	6.21	6.00 at 1.00	5.89 at 5.00	5.79 at 10.00	5.79 at 56.49	5.79 at 100.00	5.69 x 10 ⁶ at 526.3 x 10 ³ cycles. Broke in middle during tension test
2-10-76	3-8	-		5.89						Broke while proof tested
2-3-76	5-6	-	73.00	6.32	6.18 at 2.00	5.97 at 8.62	5.75 at 50.00			Broke in middle during fatigue
2-5-76	2-1	-	12.40	5.89	5.89 at 1.00	5.89 at 5.00	5.80 at 10.00			Broke in lower tab during fatigue
2-4-76	1-10	59.43	427.50	6.22	6.20 at 1.00	6.04 at 5.00	5.88 at 10.00	5.84 at 84.90	5.77 at 427.50	Broke in middle during tension test
2-3-76	6-13	-	2.00	6.02						Broke in middle (doubtful data) during fatigue
1-18-76	2-3	64.96	787.00	6.22	5.90 at 1.00	5.90 at 5.00	5.73 at 50.00	5.72 at 787.00		Broke in middle during tension test
1-23-76	5-5	-	.640	5.95						Broke near lower tab during fatigue
1-22-76	6-12	-	80.59	6.09	6.01 at 1.00	6.01 at 5.00	5.82 at 10.00			Broke in top grip during fatigue
1-21-76	6-11	51.11	500.00	6.14	5.89 at 10.00	5.80 at 50.00	5.76 at 100.00	5.54 at 500.00		Broke in top grip during tension test
1-19-76	1-13	-	11.34	6.31	5.98 at 1.00	5.98 at 5.07				Broke in top grip during fatigue
1-16-76	1-14	-	353.70	5.81	5.66 at 3.00	5.66 at 20.00	5.38 at 50.00	5.28 at 100.00		Broke in top grip during fatigue
1-15-76	5-8	-	184.70	5.83	5.61 at 6.02	5.47 at 50.00	5.30 at 100.00			Broke in middle during fatigue
1-14-76	2-5	65.03	423.10	6.37	6.07 at 1.00	6.01 at 6.36	5.88 at 70.93	5.87 at 423.00		Broke in lower grip during tension test
1-13-76	6-10	-	4.07	6.10	5.88 at 2.00					Broke in top grip during fatigue
11-13-76	4-3	-	1.12							Broke in top grip during fatigue

TABLE 5 RANDOM FATIGUE TEST RESULTS
 G/E 0,90,+45/ Panel No. 2 Group No. 2
 Mean Stress = 29.54 ksi
 RMS Stress = 7.66 ksi
 Clipping at Mean ± 3 RMS

Date	Specimen No.	Residual Stress (ksi)	Applied Cycles $\times 10^3$	E_0 (Initial) $\times 10^6$ psi	$E_1 \times 10^5$ psi at $\times 10^3$ cycles	$E_2 \times 10^6$ psi at $\times 10^3$ cycles	$E_3 \times 10^6$ psi at $\times 10^3$ cycles	$E_4 \times 10^6$ psi at $\times 10^3$ cycles	$E_5 \times 10^5$ psi at $\times 10^3$ cycles	Remarks (FAILURE MODE)
3-30-76	9-5	84.37	100.00	7.01	6.88 at 1.00	6.80 at 5.00	6.50 at 10.00	6.50 at 50.00	6.50 at 100.00	broke in middle during tension test
2-24-76	12-1	76.88	100.00	6.74	6.74 at 1.00	6.74 at 5.00	6.74 at 10.00	6.74 at 50.00	6.74 at 100.00	Broke in top grip during tension test
2-19-76	12-3	64.45	100.00	6.69	6.52 at 1.00	6.52 at 5.00	6.52 at 10.00	6.52 at 50.00	6.52 at 100.00	Broke in lower grip during tension test
2-17-76	1-4	-	11.64	6.43	6.27 at 1.00	6.03 at 5.00	6.03 at 10.00			Broke in top grip during fatigue
2-18-76	13-5	69.50	330.00	6.49	6.33 at 1.00	6.30 at 5.00	6.30 at 10.00	6.30 at 50.00	6.30 at 330.00	Broke in middle during tension test
2-17-76	14-1	-	.85	6.30						Broke in middle Specimen damaged in loading
2-16-76	7-6	65.41	100.00	6.85	6.66 at 1.00	6.44 at 5.00	6.44 at 10.00	6.34 at 50.00	6.27 at 100.00	Broke in middle during tension test
2-12-76	4-2	63.47	100.00	6.51	6.39 at 1.00	6.30 at 5.00	6.42 at 10.00	6.27 at 50.00	6.27 at 100.00	Broke in middle during tension test

TABLE 6 RANDOM FATIGUE TEST RESULTS
 G/E 0,90,+45/ Panel No. 2 Group No. 3
 Mean Stress = 22.93 ksi
 RMS Stress = 7.02 ksi
 Clipping at Mean ± 5 RMS

Date	Specimen No.	Residual Stress (ksi)	Applied Cycles $\times 10^3$	E_0 (Initial) $\times 10^6$ psi	$E_1 \times 10^5$ psi at $\times 10^3$ cycles	$E_2 \times 10^6$ psi at $\times 10^3$ cycles	$E_3 \times 10^6$ psi at $\times 10^3$ cycles	$E_4 \times 10^6$ psi at $\times 10^3$ cycles	$E_5 \times 10^5$ psi at $\times 10^3$ cycles	Remarks (FAILURE MODE)
4-1-76	1-6	-	53.00	6.47	6.28 at 1.00	6.28 at 5.00	6.28 at 10.00	6.28 at 50.00		Broke in middle during fatigue

TABLE 7 RANDOM FATIGUE TEST RESULTS

G/E 0,90,+45/ Panel No. 2 Group No. 4
 Mean Stress = 26.80 ksi
 RMS Stress = 5.96 ksi
 Clipping at Mean ± 4 RMS

Date	Specimen No.	Residual Stress (ksi)	Applied Cycles $\times 10^3$	E_0 (Initial) $\times 10^6$ psi	$E_1 \times 10^6$ psi at $\times 10^3$ cycles	$E_2 \times 10^6$ psi at $\times 10^3$ cycles	$E_3 \times 10^6$ psi at $\times 10^3$ cycles	$E_4 \times 10^6$ psi at $\times 10^3$ cycles	$E_5 \times 10^6$ psi at $\times 10^3$ cycles	Remarks (FAILURE MODE)
5-27-76	13-1	76.98	677.00	7.33	7.13 at 1.00	7.13 at 5.00	7.09 at 10.00	6.94 at 50.00	7.17 at 677.00	Broke in middle during tension test
5-20-76	11-5	75.15	508.70	6.89	7.22 at 1.00	7.05 at 5.00	7.05 at 10.00	7.05 at 50.00	7.05 at 96.50	7.05×10^6 at 508.7×10^3 cycles Broke in top tab during tension test
5-20-76	2-5	-	18.00	6.88	6.88 at 1.00	6.88 at 5.00	6.88 at 10.00			Broke near top tab during fatigue
5-13-76	11-3	78.10	511.00	7.13	6.90 at 1.00	6.81 at 5.00	6.90 at 10.00	6.81 at 50.00	6.97 at 100.00	6.97×10^6 at 511×10^3 cycles Broke in lower tab during tension test
4-29-76	5-6	75.45	517.50	7.43	7.10 at 1.00	7.10 at 5.00	7.31 at 10.00	6.99 at 50.00	6.96 at 81.00	6.91×10^6 at 517.5×10^3 cycles Broke in middle during tension test
5-8-76	9-2	75.76	501.00	7.20	7.16 at 1.00	7.21 at 5.00	7.01 at 10.00	7.01 at 50.00	7.06 at 100.00	7.06×10^6 at 501×10^3 cycles Broke in top tab during tension test
4-22-76	5-5	-	500.00	6.76	6.76 at 1.00	6.76 at 5.00	6.76 at 10.00	6.76 at 50.00	6.76 at 100.00	6.49×10^6 at 500×10^3 cycles Broke accidentally Doubtful data
4-16-76	12-4	63.47	500.00	7.03	7.03 at 1.00	7.33 at 5.00	7.18 at 10.00	7.18 at 50.00	7.03 at 100.00	7.03×10^6 at 500×10^3 cycles Broke in lower tab during tension test
4-15-76	10-3	-	86.50	7.22	6.99 at 1.00	6.99 at 5.00	6.99 at 10.00	6.99 at 50.00		Possible machine malfunction
4-15-76	10-3	-	86.50	7.22	6.99 at 1.00	6.99 at 5.00	6.99 at 10.00	6.99 at 50.00		Broke in middle Machine malfunction during fatigue
4-13-76	9-1	-	486.00	7.20	6.90 at 1.00	6.90 at 5.00	6.90 at 10.00	6.90 at 50.00	6.90 at 100.00	Broke at bottom grip during fatigue
4-8-76	13-2	-	54.70	6.59	6.59 at 1.00	6.47 at 5.00	6.40 at 10.00	6.30 at 50.00		Broke in lower tab during fatigue

TABLE 8 RANDOM FATIGUE TEST RESULTS

G/E 0,90,+45/ Panel No. 2 Group No. 4A

Mean Stress = 26.80 ksi

RMS Stress = 5.96 ksi

Clipping at mean ± 3 RMS

Date	Specimen No.	Residual Stress (ksi)	Applied Cycles $\times 10^3$	E_0 (Initial) $\times 10^6$ psi	$E_1 \times 10^6$ psi at $\times 10^3$ cycles	$E_2 \times 10^6$ psi at $\times 10^3$ cycles	$E_3 \times 10^6$ psi at $\times 10^3$ cycles	$E_4 \times 10^6$ psi at $\times 10^3$ cycles	$E_5 \times 10^6$ psi at $\times 10^3$ cycles	Remarks (FAILURE MODE)
6-9-76	8-2	73.71	500.00	7.16	7.45 at 1.00	7.31 at 5.00	7.18 at 10.00	7.36 at 50.00	7.37 at 500.00	Broke in top grip during tension test
6-7-76	2-4	-	64.90	6.33	6.27 at 1.20	6.43 at 5.00	6.38 at 13.80			Broke in lower tab due to twisted torque cell during fatigue
6-8-76	3-5	69.65	503.00	6.87	6.93 at 1.00	6.71 at 5.20	6.60 at 10.00	6.64 at 50.00	6.08 at 100.00	6.64×10^6 at 503×10^3 cycles Broke in top tab during tension test
6-15-76	11-1	73.54	614.00	7.00	6.81 at 2.60	6.81 at 5.00	6.62 at 10.00	6.62 at 329.00	6.62 at 614.00	Broke in middle during tension test
6-17-76	11-6	72.82	500.00	7.27	6.70 at 1.00	6.82 at 5.00	6.72 at 10.00	6.92 at 50.00	6.90 at 100.00	6.90×10^6 at 500×10^3 cycles Broke in lower tab during tension test
6-21-76	6-3	-	500.00	7.55	7.17 at 1.00	7.17 at 5.00	6.79 at 14.70	6.79 at 53.80	6.79 at 102.00	6.85×10^6 at 500×10^3 cycles Broke accidentally Doubtful data
6-22-76	9-4	72.47	452.00	6.91	7.11 at 1.00	7.10 at 5.00	7.10 at 14.90	7.02 at 452.00		Broke in top tab during tension test
6-25-76	4-3	83.22	555.00	7.53	7.53 at 1.00	7.21 at 5.00	7.13 at 10.00	7.33 at 66.90	7.45 at 109.00	7.13×10^6 at 555×10^3 cycles Broke near lower tab during tension test

TABLE 9 RANDOM FATIGUE TEST RESULTS

G/E 0,90,+45/ Panel No. 1 Group No. 5

Mean Stress = 26.80 ksi

RMS Stress = 7.94 ksi

Clipping at Mean +3 RMS

Date	Specimen No.	Residual Stress (ksi)	Applied Cycles x 10 ³	E ₀ (Initial) x 10 ⁶ psi	E ₁ x 10 ⁶ psi at x 10 ³ cycles	E ₂ x 10 ⁶ psi at x 10 ³ cycles	E ₃ x 10 ⁶ psi at x 10 ³ cycles	E ₄ x 10 ⁶ psi at x 10 ³ cycles	E ₅ x 10 ⁶ psi at x 10 ³ cycles	Remarks (FAILURE MODE)
1-15-76	5-4	-	0.05	6.13						Broke in top tab during fatigue
11-12-75	2-10	-	2.80	6.48						Broke in lower tab during fatigue
11-11-75	3-2	-	1.68	6.30						Broke in top tab during fatigue
11-11-75	3-13	-	3.18	6.12	5.94 at 1.68					Broke in top tab during fatigue
12-5-75	4-4	-	0.10	6.11						Broke in middle during fatigue
12-10-75	4-5	57.79	803.00		5.30 at 803.00					Broke in top tab during tension test
12-12-75	6-3	65.41	693.00	6.27	6.00 at 1.11	5.75 at 32.00	5.73 at 693.00			Broke in middle during tension test
11-10-75	6-7	-	70.00	6.08						Broke in top tab during fatigue
11-11-75	4-6	-	85.00	6.3	6.04 at 1.00					Broke in lower tab during fatigue

TABLE 10 RANDOM FATIGUE TEST RESULTS

G/E 0,90,+45/ Panel No. 1 Group No. 6

Mean Stress = 23.83 ksi

RMS Stress = 6.95 ksi

Clipping at Mean +3 RMS

Date	Specimen No.	Residual Stress (ksi)	Applied Cycles x 10 ³	E ₀ (Initial) x 10 ⁶ psi	E ₁ x 10 ⁶ psi at x 10 ³ cycles	E ₂ x 10 ⁶ psi at x 10 ³ cycles	E ₃ x 10 ⁶ psi at x 10 ³ cycles	E ₄ x 10 ⁶ psi at x 10 ³ cycles	E ₅ x 10 ⁶ psi at x 10 ³ cycles	Remarks (FAILURE MODE)
1-8-76	2-7	55.93	116.00	8.03	8.03 at 2.40	8.03 at 116.00				Broke in top tab during tension test

TABLE 11 RANDOM FATIGUE TEST RESULTS

G/E 0,90,+45/ Panel No. 2 Group No. 10
 Mean Stress = 26.80 ksi
 RMS Stress = 7.4 ksi
 Clipping at Mean ± 3 RMS

Date	Specimen No.	Residual Stress (ksi)	Applied Cycles $\times 10^3$	E_0 (Initial) $\times 10^6$ psi	$E_1 \times 10^6$ psi at $\times 10^3$ cycles	$E_2 \times 10^6$ psi at $\times 10^3$ cycles	$E_3 \times 10^6$ psi at $\times 10^3$ cycles	$E_4 \times 10^6$ psi at $\times 10^3$ cycles	$E_5 \times 10^6$ psi at $\times 10^3$ cycles	Remarks (FAILURE MODE)
7-20-76	10-4	72.05	424.00	6.73	6.73 at 1.00	6.73 at 5.00	6.73 at 10.00	6.73 at 423.59		Broke in middle during tension test
7-19-76	7-1	70.21	759.00	6.62	6.43 at 1.00	6.62 at 5.00	7.00 at 10.00	7.00 at 759.00		Broke in middle during tension test
7-21-76	7-2	66.22	500.00	6.37	6.37 at 1.00	6.37 at 5.00	6.58 at 10.00	6.74 at 47.00	6.37 at 500.00	Broke in middle during tension test
7-23-76	9-3	71.63	802.00	6.70	6.70 at 1.00	6.51 at 5.00	6.51 at 10.00	6.51 at 802.00		Broke in middle during tension test
8-5-76	4-5	76.80	500.00	6.65	6.65 at 1.00	6.65 at 5.00	6.54 at 10.00	6.54 at 50.00	6.54 at 500.00	Broke in top tab during tension test
8-3-76	6-6	77.16	784.00	7.02	6.72 at 1.00	6.72 at 5.00	6.50 at 10.00	6.71 at 784.00		Broke near lower tab during tension test

TABLE 12 RANDOM FATIGUE TEST RESULTS

G/E 0,90,+45/ Panel No. 2 Group No. 11 Wide Band
 Mean Stress = 26.80 ksi
 RMS Stress = 5.96 ksi
 Clipping at Mean ± 4 RMS

Date	Specimen No.	Residual Stress (ksi)	Applied Cycles $\times 10^3$	E_0 (Initial) $\times 10^6$ psi	$E_1 \times 10^6$ psi at $\times 10^3$ cycles	$E_2 \times 10^6$ psi at $\times 10^3$ cycles	$E_3 \times 10^6$ psi at $\times 10^3$ cycles	$E_4 \times 10^6$ psi at $\times 10^3$ cycles	$E_5 \times 10^6$ psi at $\times 10^3$ cycles	$E_6 \times 10^6$ psi at $\times 10^3$ cycles	Remarks (FAILURE MODE)
9-1-76	7-4P2	79.78	500	6.65	6.65 at 1	6.96 at 5	6.96 at 10	6.57 at 50	6.49 at 100	6.49 at 500	Broken in middle
9-13-76	10-6P2	85.03	500	6.93	6.93 at 1	6.93 at 5	6.74 at 10	6.74 at 500			Broken in middle
9-9-76	4-1P2	78.23	500	6.84	6.65 at 1	6.65 at 5	6.65 at 10	6.65 at 50	6.65 at 100	6.65 at 500	Broken in middle
9-7-76	12-6P2	79.34	510	6.67	6.64 at 1	6.64 at 5	6.45 at 10	6.82 at 50	6.42 at 510		Broken in middle

TABLE 13 RANDOM FATIGUE TEST RESULTS

G/E 0,90,+45/ Panel No. 2 Group No. 14 (Wide Band)

Mean Stress = 26.80 ksi

RMS Stress = 7.40 ksi

Clipping at Mean \pm 3 RMS

Date	Specimen No.	Residual Stress (ksi)	Applied Cycles $\times 10^3$	E_0 (Initial) $\times 10^6$ psi	$E_1 \times 10^6$ psi at $\times 10^3$ cycles	$E_2 \times 10^6$ psi at $\times 10^3$ cycles	$E_3 \times 10^6$ psi at $\times 10^3$ cycles	$E_4 \times 10^6$ psi at $\times 10^3$ cycles	$E_5 \times 10^6$ psi at $\times 10^3$ cycles	Remarks (FAILURE MODE)
8-10-76	5-1P2	76.40	501	6.79	6.79 at 1	6.94 at 5	6.82 at 10	6.52 at 501		Broken in middle
8-13-76	6-5P2	77.32	501	6.58	6.51 at 1	7.03 at 5	6.66 at 10	6.58 at 7.19	6.51 at 501	Broken in middle
8-18-76	4-4P2	74.00	500	6.63	6.55 at 1	6.63 at 5	6.48 at 50	6.26 at 500		Broken in middle
8-19-76	5-3P2	78.27	461	6.69	6.58 at 1	6.61 at 5	6.69 at 11	6.73 at 461		Broken in middle
8-24-76	13-6P2	65.44	803	6.77	6.39 at 1	6.39 at 5	6.39 at 10	6.39 at 803		Broken in middle
8-26-76	6-2P2	75.21	501	7.03	6.91 at 1	6.91 at 5	6.84 at 104	6.46 at 501		Broken in middle

TABLE 14. CONSTANT AMPLITUDE FATIGUE TEST RESULTS

G/E [0,90+45]_s Panel 1Average Ultimate Strength = 59.566 KSI
Stress Ratio = 0.1, Cyclic Frequency = 10 Hz

Date (Days)	Specimen Number	Mean Stress (KSI)	Maximum Stress (KSI)	Residual Stress (KSI)	Applied Cycles (10 ³)	E ₀ (Initial) (10 ⁶ psi)	E ₁ (10 ⁶ psi)	E ₂ (10 ⁶ psi)	E ₃ (10 ⁶ psi)	Failure Mode
11-11-75 0	5-3	29.03	52.78	0	3.01					End tab
11-20-75 9	5-1	27.85	50.63	0	0.22	8.23				End tab
11-18-75 8	3-9	27.85	50.63	0	0.48					End tab
12-18-75 37	5-13	27.85	50.63	0	0.16	6.35	6.32 n=100			End tab
12-17-75 36	6-4	27.85	50.63	0	0.20					End tab
11-20-75 9	6-1	26.21	47.65	0	0.26	7.89				End tab
1-12-76 61	2-4	26.21	47.65	0	0.54	6.66				End tab
11-20-75 9	6-2	26.21	47.65	0	0.40	7.07				End tab
1-17-76 61	3-10	26.21	47.65	0	0.46	6.27				End tab
11-20-75 9	4-2	24.57	44.67	0	93.63	7.30	7.06 n=5,000	8.28 n=24,100		End tab
11-21-75 10	1-6	24.57	44.67	0	0.92	7.41				End tab
1-2-76 51	2-9	24.57	44.67	0	1.69	6.10				End tab
1-6-76 55	3-3	24.57	44.67	0	27.21	6.51	6.43 n=1,000	6.25 n=4,000		End tab
1-5-76 54	2-8	24.57	44.67	0	527.84	6.18	6.07 n=2,000	5.22 259.240		End tab
1-5-76 54	5-9	24.57	44.67	0	403.17	5.11	4.93 at 5000			End tab
12-21-75 100	2-12	22.93	41.70	0	2.04	6.91				End tab
12-1-75 20	2-11	22.93	41.70	0	2.74	7.14				End tab
1-2-76 51	3-11	22.93	41.70	58.75	945.10	6.45	6.32 n=2,500	6.26 n=5,300	6.26 n=945,100	End tab
1-2-76 51	1-9	22.93	41.70	65.46	1124.88					Near middle
12-30-75 49	1-7	21.30	38.72	59.78	110.00	6.18	6.02 n=5,000	6.02 n=50,000	5.99 n=110,000	End tab
12-30-75 49	2-2	21.30	38.72	58.48	1686.29	6.04	5.72 n=5,000	5.71 n=10,000	5.31 n=66,000	End tab
12-22-75 41	3-12	21.30	38.72	43.76	1000.00	5.36	4.71 n=5,000	4.57 n=85,000	5.61 n=1,000,000	End tab
12-23-75 42	5-12	21.30	38.72	53.25	1000.00	4.92	4.91 n=5,000	6.34 n=1,000,000		End tab
11-8-75 57	6-8	21.30	38.72	0	39.89	6.26	6.00 n=5,000			End tab
11-8-75 57	6-9	21.30	38.72	62.40	1003.50	6.49	6.45 n=5,000	6.42 n=1,003,500		Near middle

TABLE 15 . CONSTANT AMPLITUDE FATIGUE TEST
Type of Specimen $[0, +45, 90]_S$, Stress Ratio=0.1

Date (Days)	Specimen Number	Mean Stress (KSI)	Maximum Stress (KSI)	Residual Stress (KSI)	Applied Cycles (10^3)	E_0 (Initial) (10^6 psi)	E_1 (10^6 psi)	E_2 (10^6 psi)	E_3 (10^6 psi)	Failure Mode
1-26-76	2325#12	22	40	62.68	1,000	7.29	6.95 $n=10^3$	6.56 $n=10^4$	5.34 $n=10^5$	Middle
1-27-76	2325#5	22	40	69.52	1,000	7.90	7.43 $n=10^3$	7.02 $n=10^4$	6.84 $n=117,570$	Middle
1-29-76	2335#6	22	40	69.17	1,000	7.52	8.59 $n=10^3$	7.39 $n=10^4$	8.20 $n=10^5$	End tab
2-3-76	2335#21	22	40	61.36	1,000	7.76	7.33 $n=10^3$	7.35 $n=10^4$	7.44 $n=10^5$	End tab
2-10-76	2337#3	22	40	0	810	8.97	6.32 $n=10^3$	5.67 $n=10^4$	6.64 $n=10^5$	End tab
2-20-76	2339#18	22	40	71.22	1,000	7.05	6.34 $n=10^3$	5.96 $n=10^4$	5.76 $n=10^5$	Middle
2-24-76	2339#22	22	40	69.98	1,000	6.36	6.88 $n=10^3$	6.58 $n=10^4$	6.39 $n=10^5$	End tab
2-25-76	2340#18	22	40	78.91	1,000	7.05	6.75 $n=10^3$	6.68 $n=10^4$	6.64 $n=10^5$	End tab
3-23-76	2375#7	22	40	72.27	1,000	6.71	6.17 $n=10^3$	5.52 $n=10^4$	6. $n=10^5$	Middle
3-25-76	2360#20	22	40	70.24	1,000	6.04	6.88 $n=10^5$	5.95 $n=5 \times 10^5$	5.81 $n=10^6$	End tab
3-21-76	2374#4	22	40	63.96	1,000	7.11	7.57 $n=10^3$	7.11 $n=10^4$	6.52 $n=1.1 \times 10^5$	End tab
3-22-76	2374#18	22	40	60.56	1,000	6.67	6.31 $n=10^3$	6.41 $n=10^4$	6.49 $n=10^5$	End tab
3-20-76	2379#4	22	40	64.21	1,000	6.83	6.78 $n=10^3$	6.36 $n=10^4$	7.52 $n=10^5$	Middle
3-19-76	2379#14	22	40	74.05	1,000	6.33	5.82 $n=10^3$	5.65 $n=10^4$	6.21 $n=10^5$	End tab

TABLE 16. CONSTANT AMPLITUDE FATIGUE TEST

Type of Specimen = G/E [0,+45,0]_s
 Average Ultimate Strength = 100.4 KSI
 Stress Ratio = 0.1 Cyclic Frequency = 10 Hz

Date (Days)	Specimen Number	Mean Stress (KSI)	Maximum Stress (KSI)	Residual Stress (KSI)	Applied Cycles (10 ³)	E ₀ (Initial) (10 ⁶ psi)	E ₁ (10 ⁶ psi)	E ₂ (10 ⁶ psi)	E ₃ (10 ⁶ psi)	Failure Mode
9-3-75 838	G5I26	46.93	85.33	0	0.23					End tab
9-9-75 844	G5I129	42.76	77.74	0	18.79	11.26				End tab
11-10-75 905	G5I113	43.12	78.40	0	1.21	7.81				End tab
11-6-75 901	G5I122	43.12	78.40	108.71	1099.00	11.47	10.78 n=25,000	9.62 n=1,099,000		End tab
12-4-75 929	G5I31	43.12	78.40	122.92	1020.00	14.90	14.25 n=100,000	12.987 n=850,000	13.08 n=1,020,000	
11-24-75 919	G5I30	43.12	78.40	144.15	1071.60	11.63	10.31 n=231,500	9.85 n=1,071,600		
10-27-75 892	G5I81	43.12	78.40	127.00	2283.24	15.31	13.51 n=5,000	13.54 n=2,283,240		End tab
10-23-75 878	G5I85	43.12	78.40		123.01					
11-24-75 879	G5I59	43.12	78.40	108.81	1141.90	9.86	10.37 n=5,000	11.91 n=789,000	10.38 n=1,141,900	
10-31-75 886	G5I70	43.12	78.40	102.90	1065.83	10.59	10.59 n=20,000	10.37 1,065.830		
10-24-75 889	G5I19	43.12	78.40	0	.14	10.51				End tab
9-10-75 845	G5I13	40.08	72.23	81.76	1.57					
9-3-75 838	G5I77	38.65	70.08	97.46	1926.60					

ANALYSIS OF FATIGUE DATA

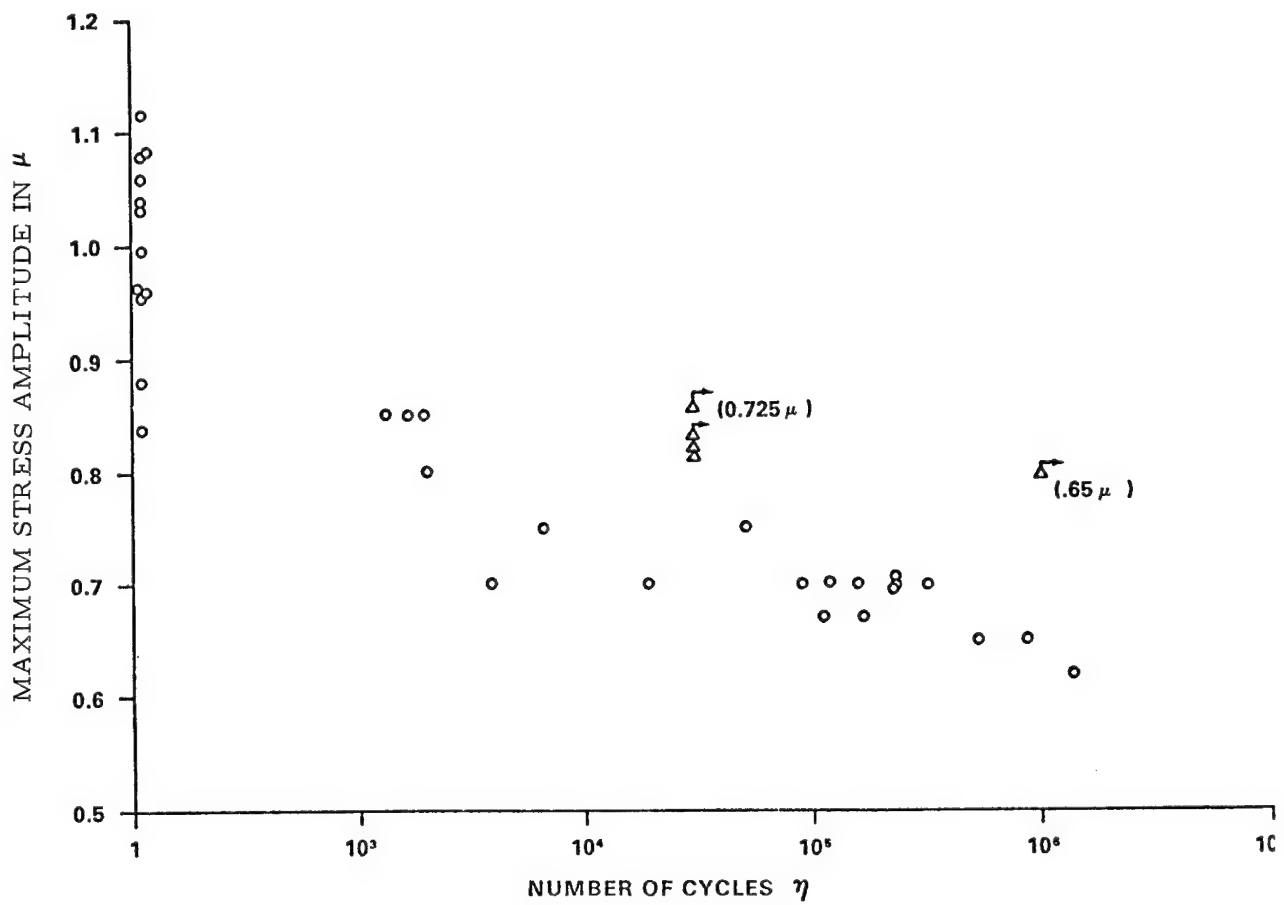
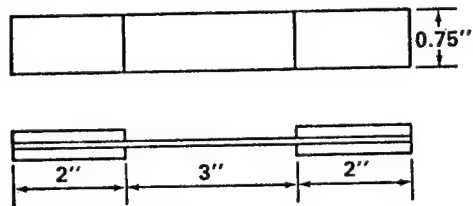
Jann N. Yang
George Washington University
(Formerly Virginia Polytechnic Institute
and State University)

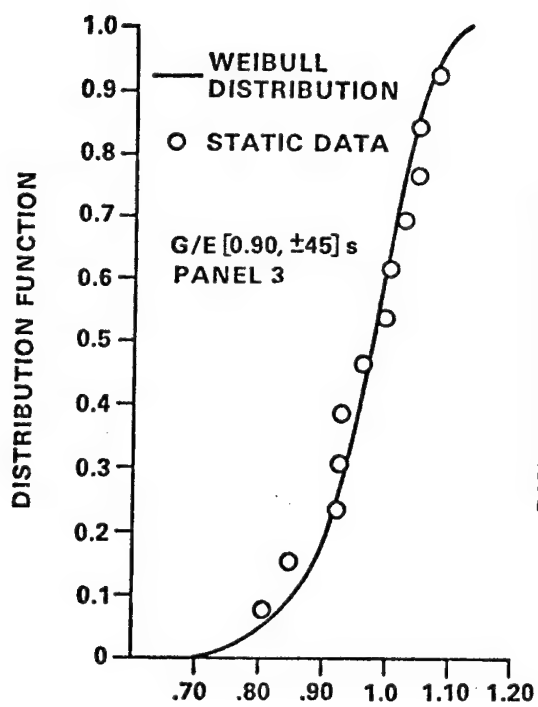
OBJECTIVES

- (1) STRENGTH DEGRADATION MODEL FOR UNNOTCHED COMPOSITE LAMINATES
 - (A) THEORETICAL INVESTIGATION
 - (B) EXPERIMENTAL VERIFICATION
- (2) THEORY OF PERIODIC PROOF TESTS FOR COMPOSITES
 - (A) THEORETICAL INVESTIGATION
 - (B) EXPERIMENTAL VERIFICATION
- (3) RELIABILITY PREDICTION AND COST OPTIMIZATION FOR COMPOSITES UNDER PERIODIC PROOF TESTS IN SERVICE

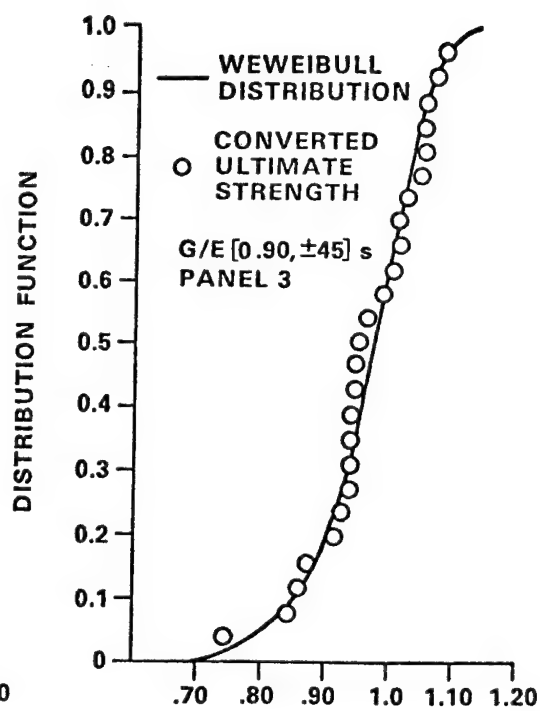
PRINCIPAL FINDINGS AND CONCLUSIONS

- (1) THE THEORETICAL RESIDUAL STRENGTH DEGRADATION MODEL CORRELATES REASONABLY WELL WITH THE EXPERIMENTAL DATA FOR G/E UNNOTCHED LAMINATES
- (2) CORRELATION BETWEEN THE THEORY OF PERIODIC PROOF TESTS FOR COMPOSITES AND THE EXPERIMENTAL DATA IS OUTSTANDING
- (3) DAMAGE TO G/E UNNOTCHED LAMINATES DUE TO REPETITIVE PROOF TESTS APPEARS TO BE NEGLIGIBLE FOR THE PROOF LOAD LEVEL UP TO 90% OF THE MEAN ULTIMATE STRENGTH
- (4) METHODOLOGIES ESTABLISHED FOR THE RELIABILITY PREDICTION OF COMPOSITES UNDER PERIODIC PROOF TESTS IN SERVICE CAN BE USED WITH CONFIDENCE

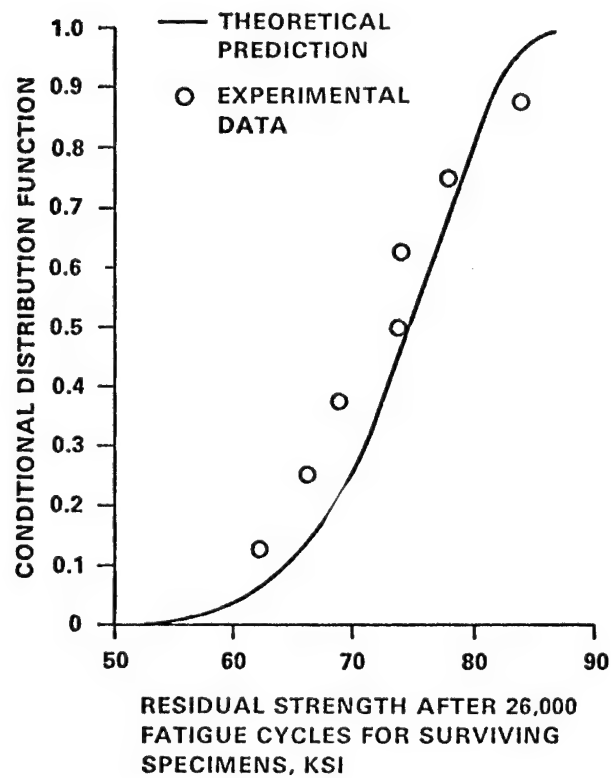
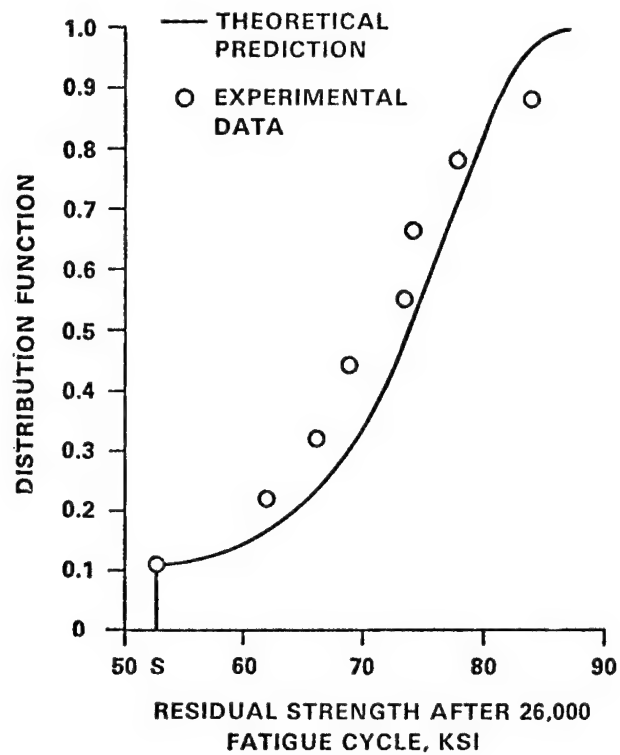


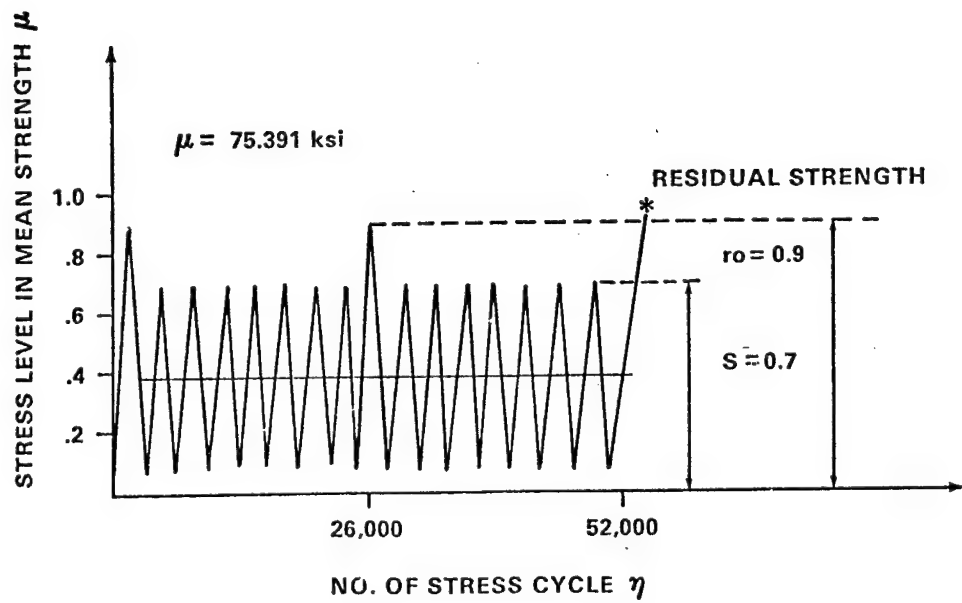
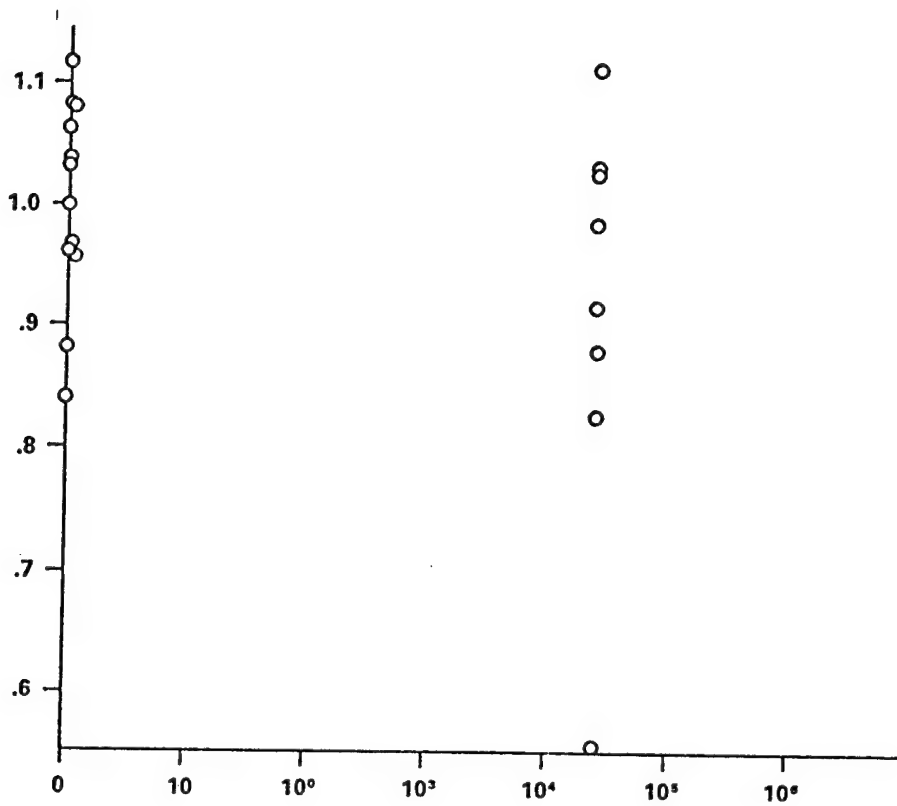


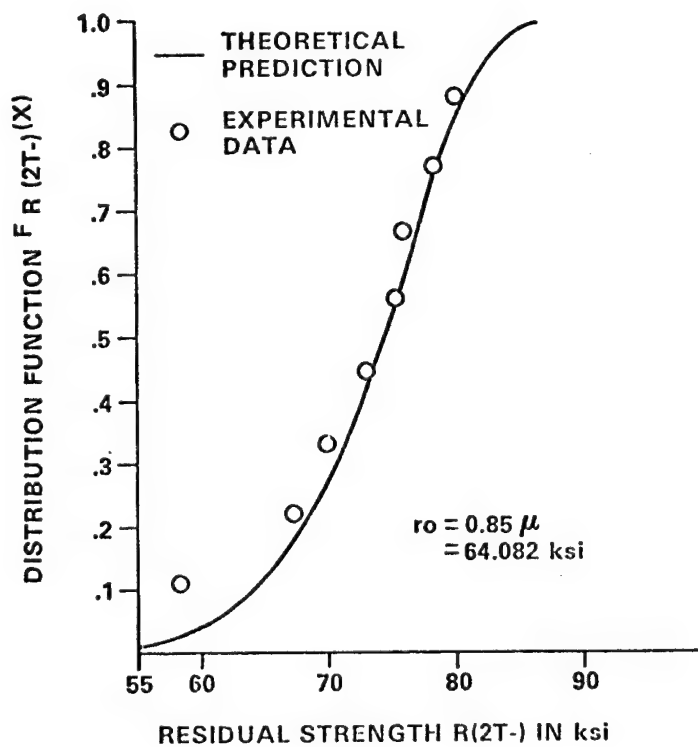
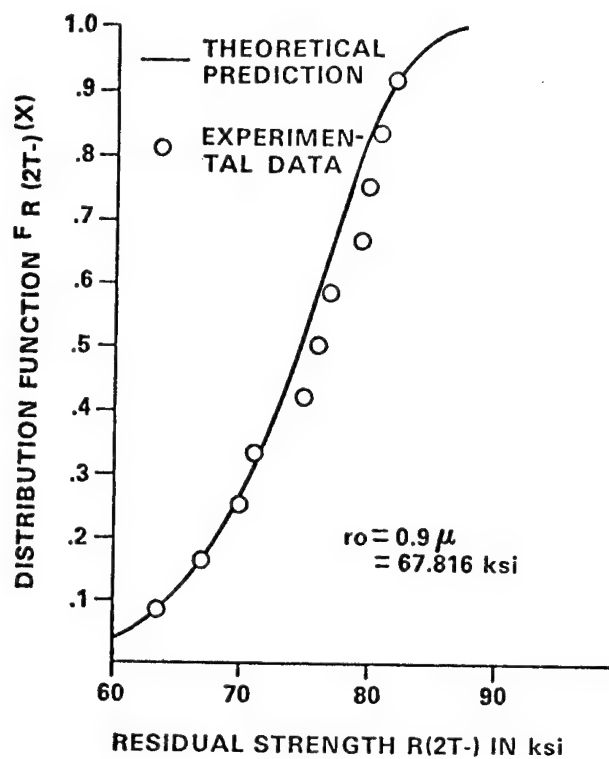
STATIC ULTIMATE STRENGTH IN β

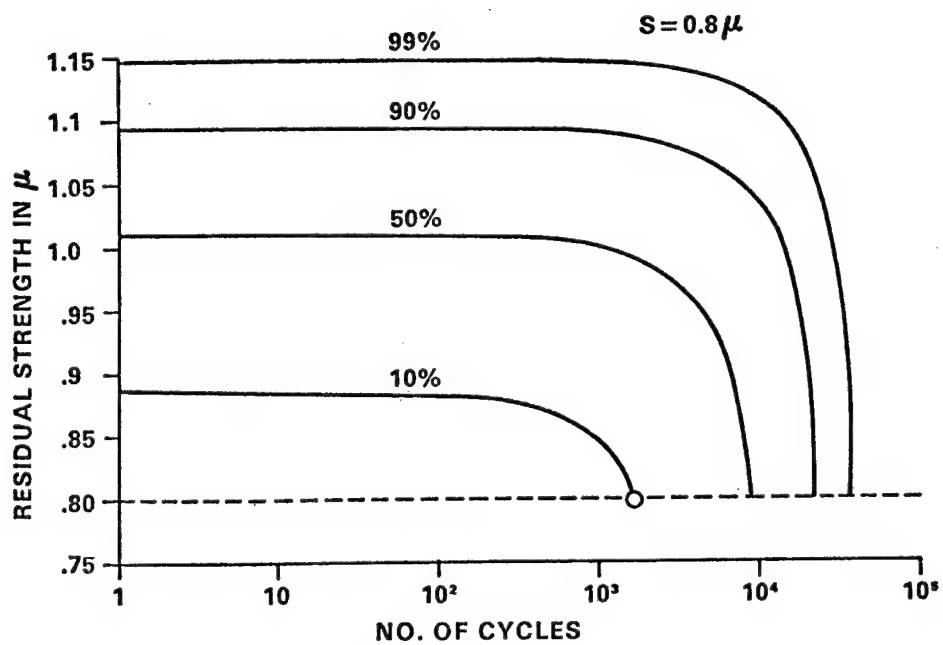
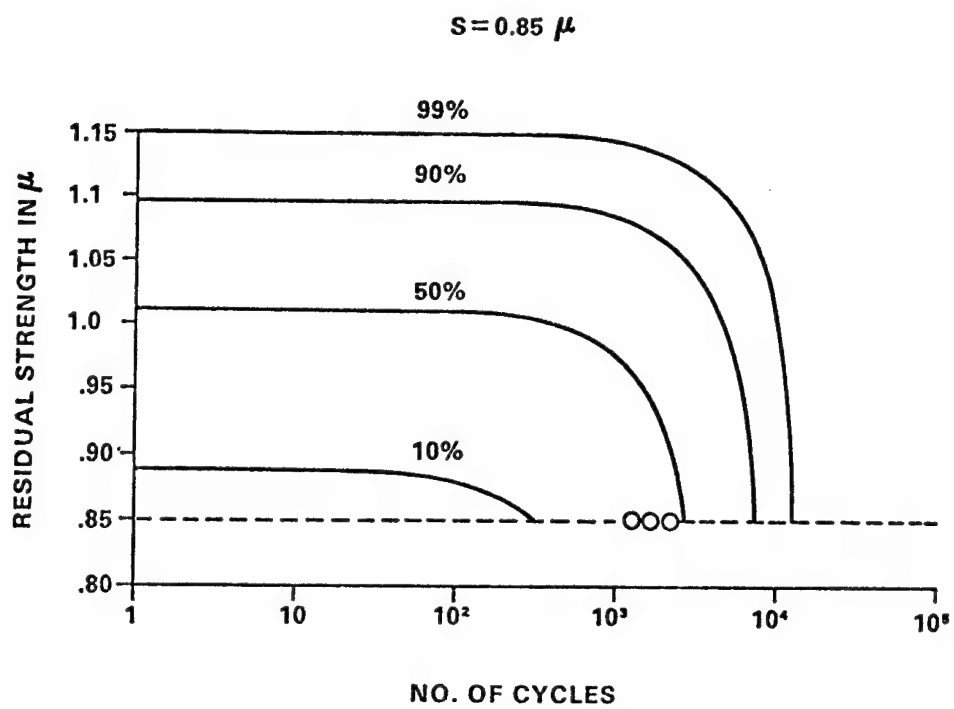


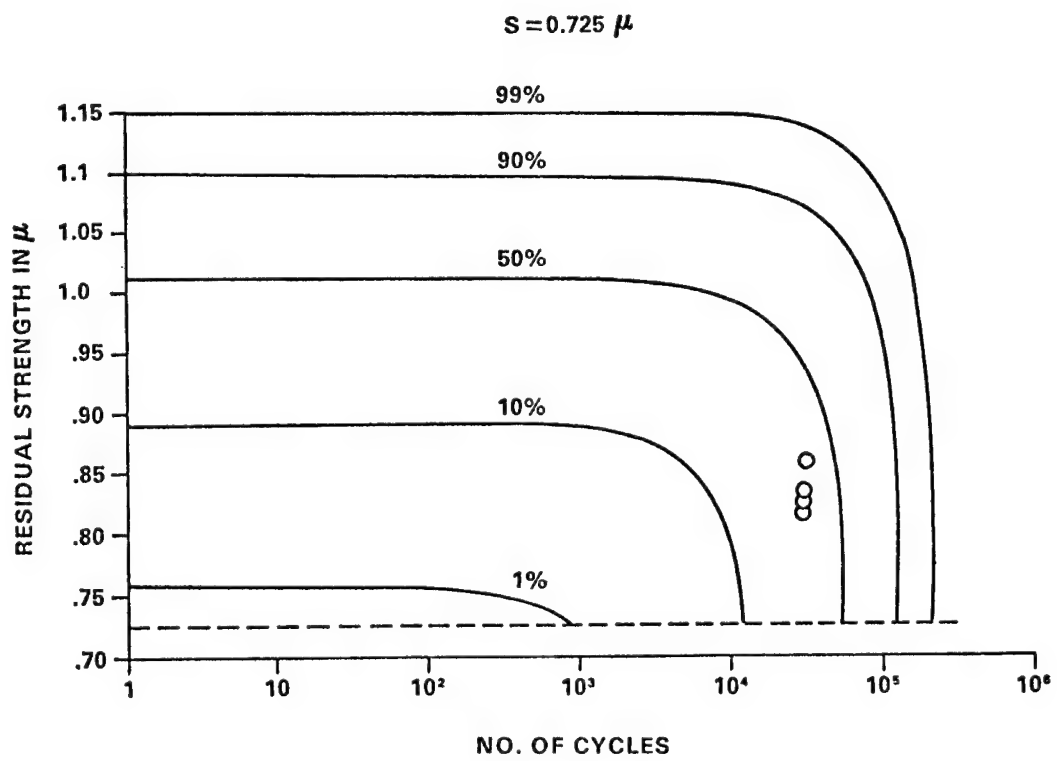
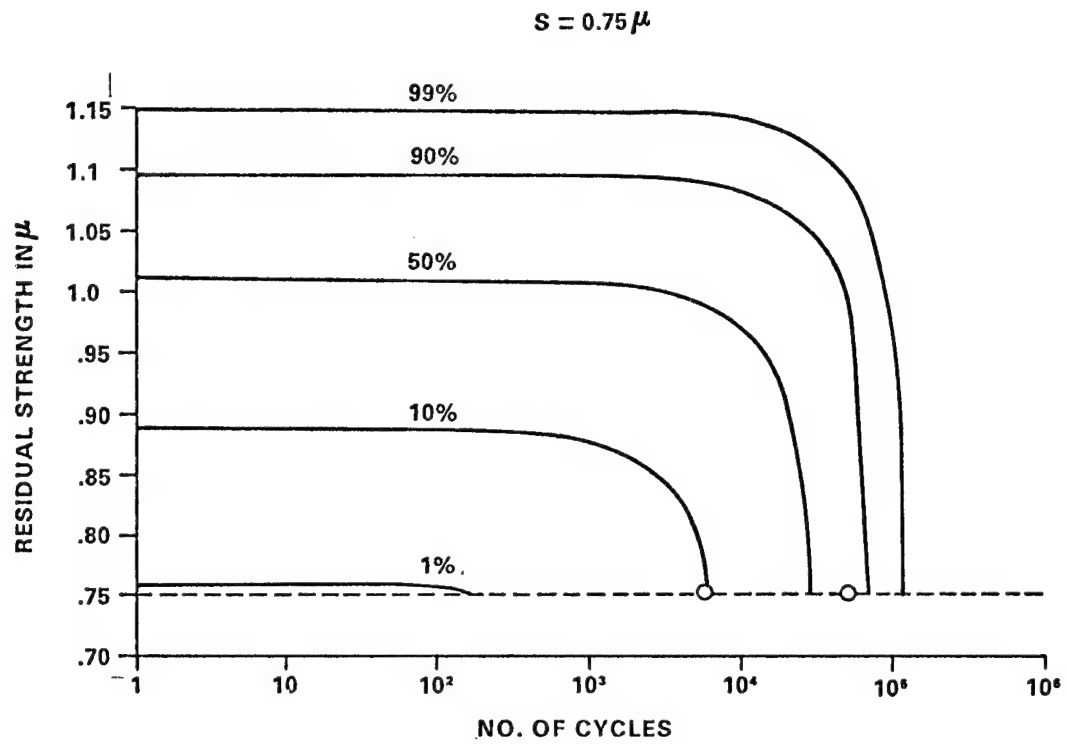
CONVERTED ULTIMATE STRENGTH β

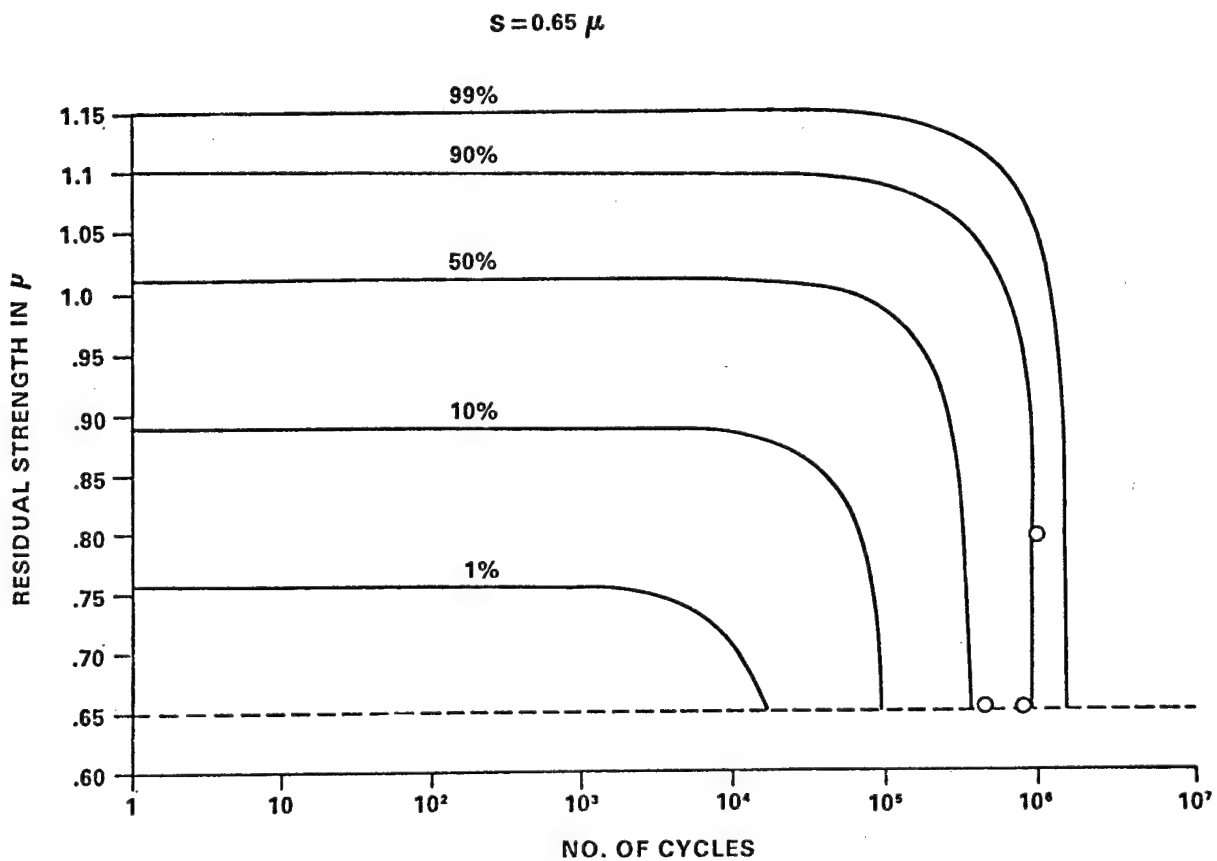
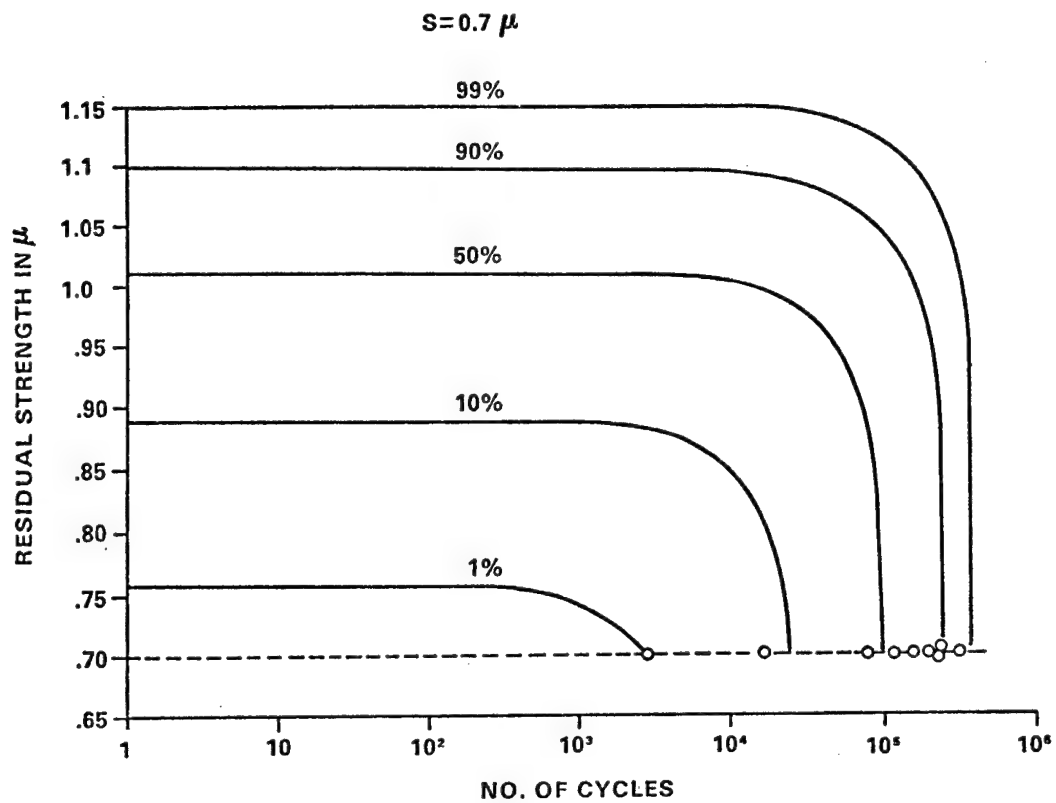












DYNAMICS OF COMPOSITE MATERIALS

by
George Herrmann
Stanford University

Figure Captions

- Fig. 1 Spectral Surface for Harmonic Waves in a Homogeneous Body (i.e. frequency ω as a function of wave numbers K_y, K_z)
- Fig. 2 Laminated Composite
- Fig. 3 Qualitative Representation of Spectral Surface for Laminated Composite for SH-Wave. Frequency Ω as a Function of Wave Number η (in periodic direction) and ζ (singular direction). B_i are Ends of Brillouin zones.
- Fig. 4 Spectral Lines for Constant ζ of Laminated Composite
- Fig. 5 Spectral Lines and Associated Mode Shapes along Ends of Brillouin Zones for Laminated Composite
- Fig. 6 Curves of Constant Frequency (Fermi Lines)
- Fig. 7 Spectral Lines of a Good Conductor
- Fig. 8 Spectral Lines of a Good Insulator
- Fig. 9 Qualitative Dependence of Phase Velocity on Wave Number
- Fig. 10 Qualitative Dependence of Group Velocity on Wave Number
- Fig. 11 Spectral Lines of Six-Parameter MES Theory as an Extension of Effective Stiffness Theory
- Fig. 12 Spectral Lines of Six-Parameter Approximate Theory as an Extension of Kunin Theory
- Fig. 13 Comparison of Mode Shapes at End of First Brillouin Zone. Layer Thicknesses are normalized. Interfaces are at ± 1 Primes refer to Stiffer Layers
- Fig. 14 Equations of Motion and Frequency Equation of Two Approximate Theories

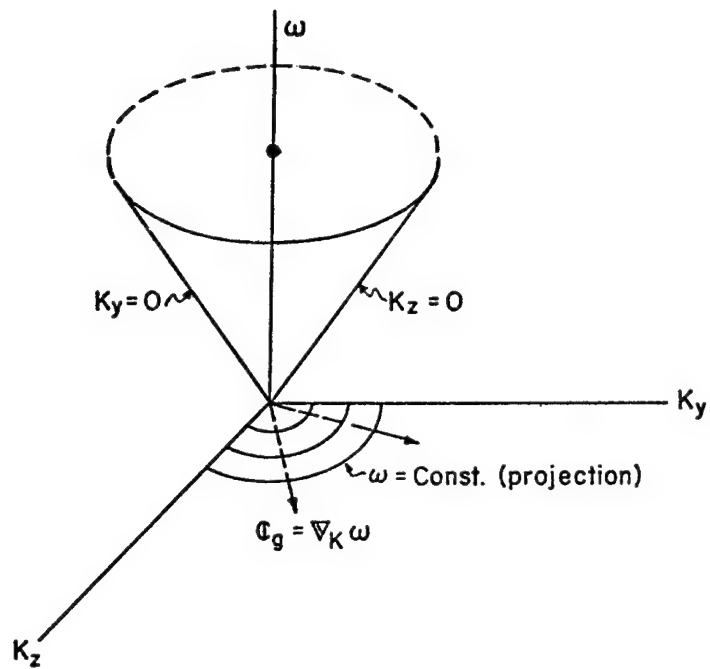


Fig. 1 Spectral Surface for Harmonic Waves in a Homogeneous Body
(i.e. frequency ω as a function of wave numbers K_y, K_z)

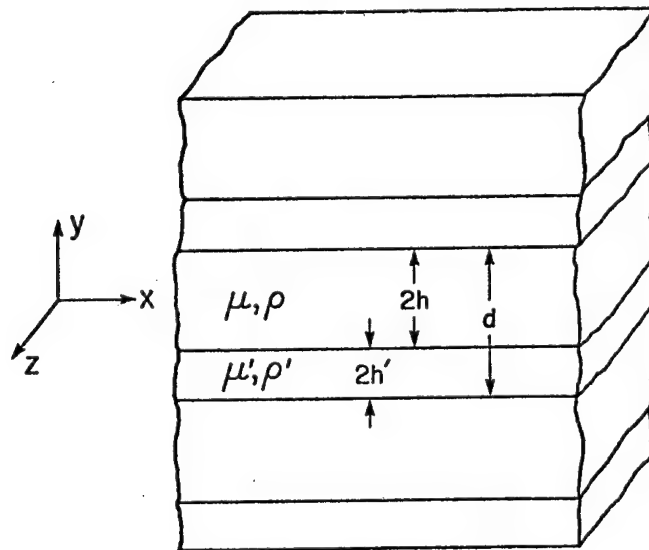


Fig. 2 Laminated Composite 262

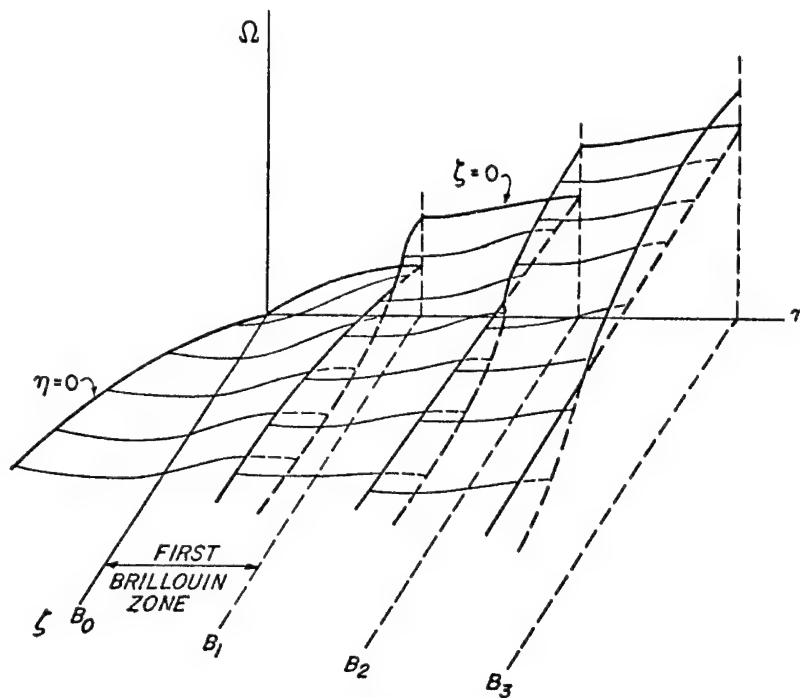


Fig. 3 Qualitative Representation of Spectral Surface for Laminated Composite for SH-Wave... Frequency Ω as a Function of Wave Number η (in periodic direction) and ζ (singular direction). B_i are Ends of Brillouin Zones.

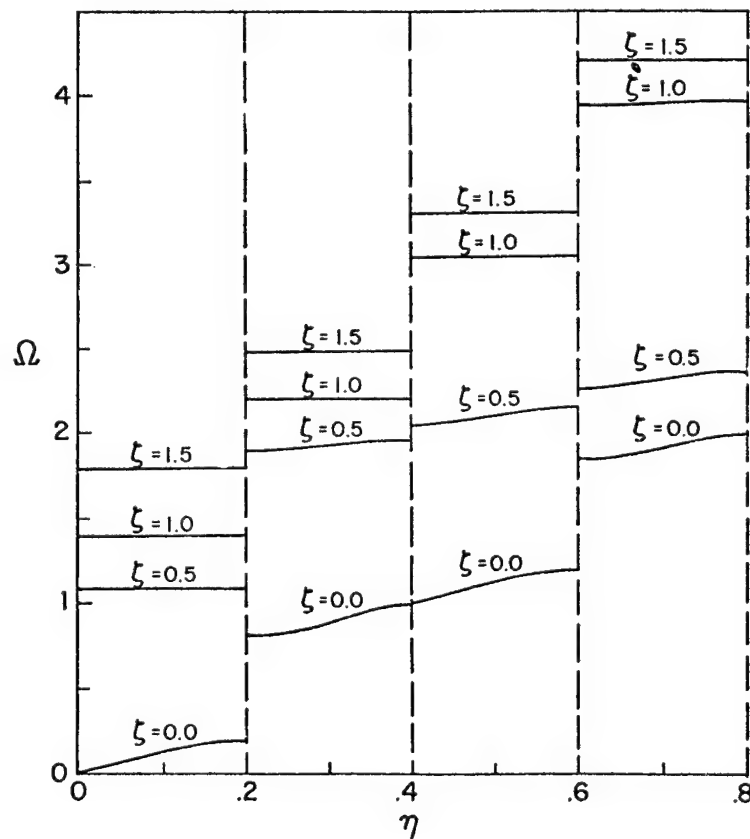


Fig. 4 Spectral Lines for Constant ζ of Laminated Composite

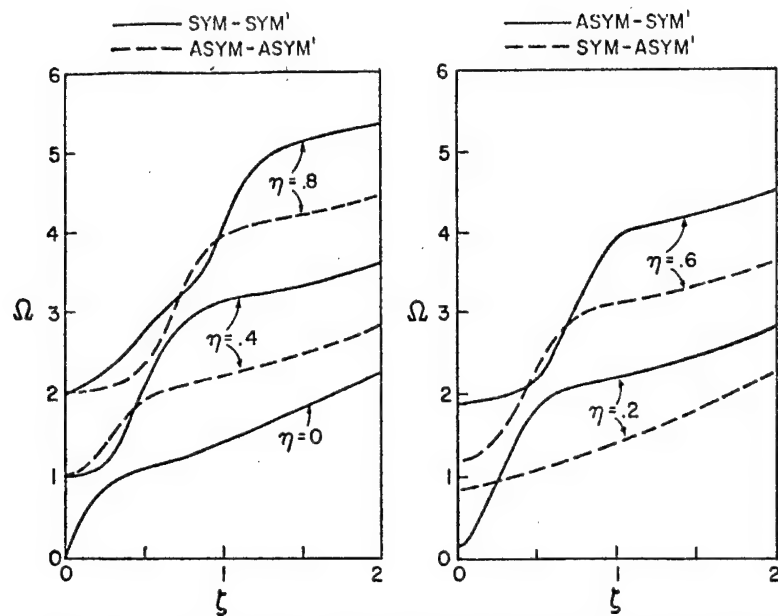


Fig. 5 Spectral Lines and Associated Mode Shapes along Ends of Brillouin Zones for Laminated Composite

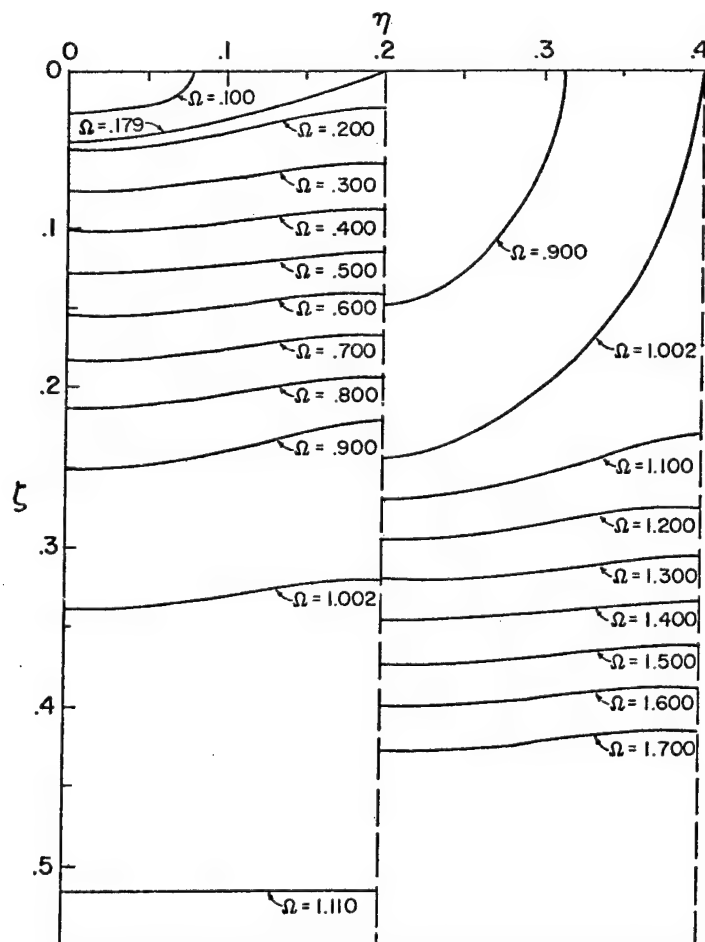


Fig. 6 Curves of Constant Frequency (Fermi Lines)

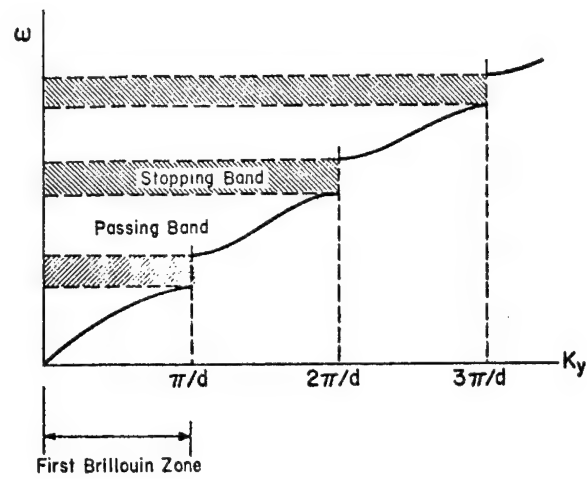


Fig. 7 Spectral Lines of a Good Conductor

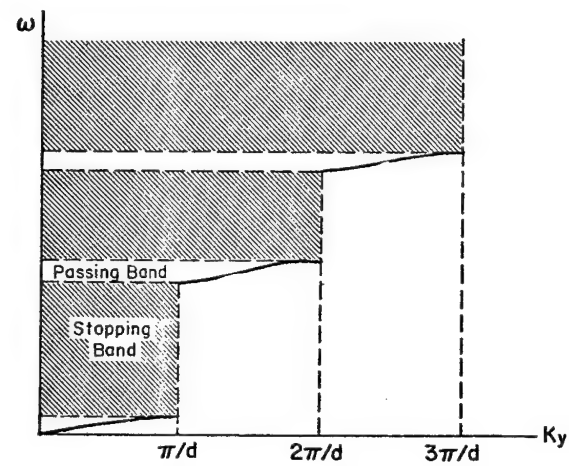


Fig. 8 Spectral Lines of a Good Insulator

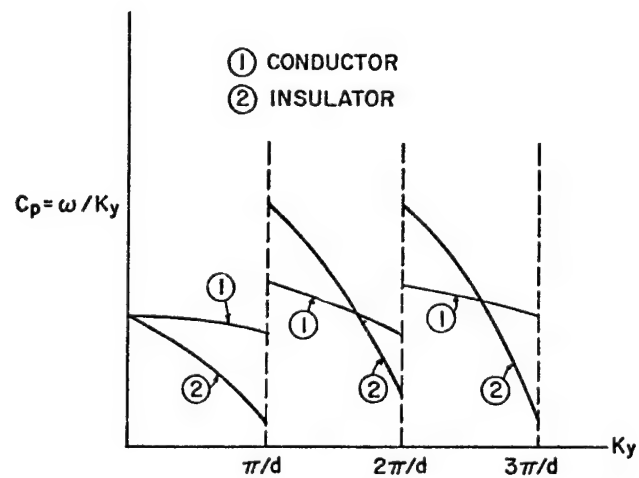


Fig. 9 Qualitative Dependence of Phase Velocity on Wave Number

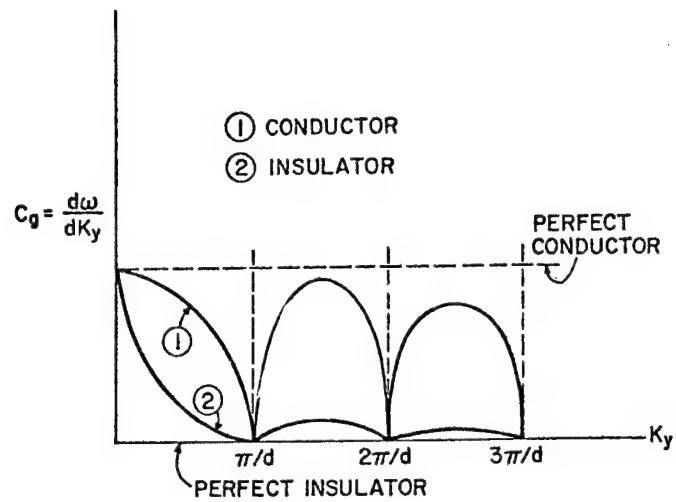


Fig. 10 Qualitative Dependence of Group Velocity on Wave Number

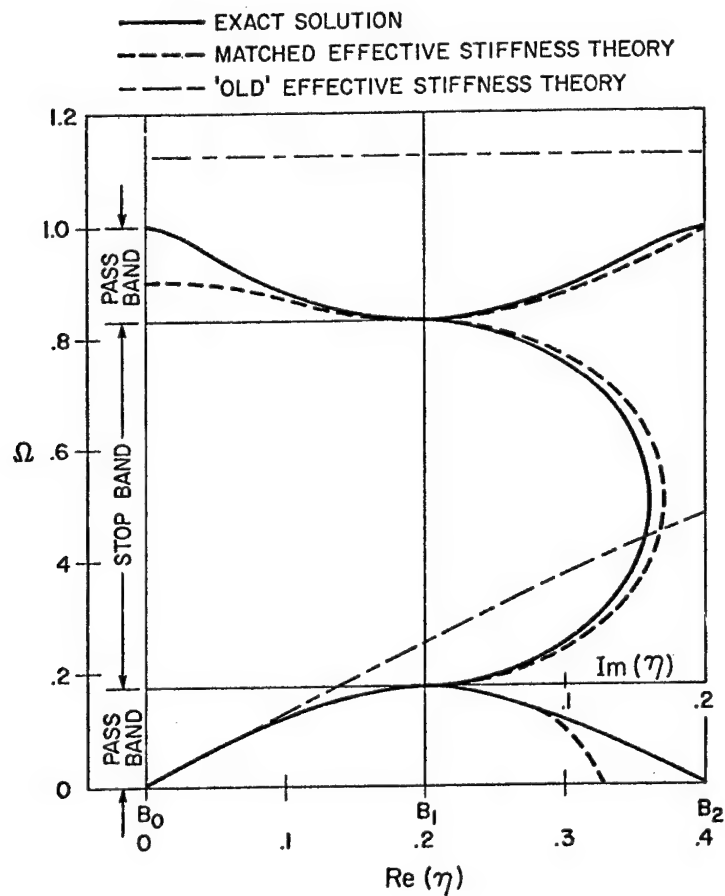


Fig. 11 Spectral Lines of Six-Parameter MES Theory as an Extension of Effective Stiffness Theory

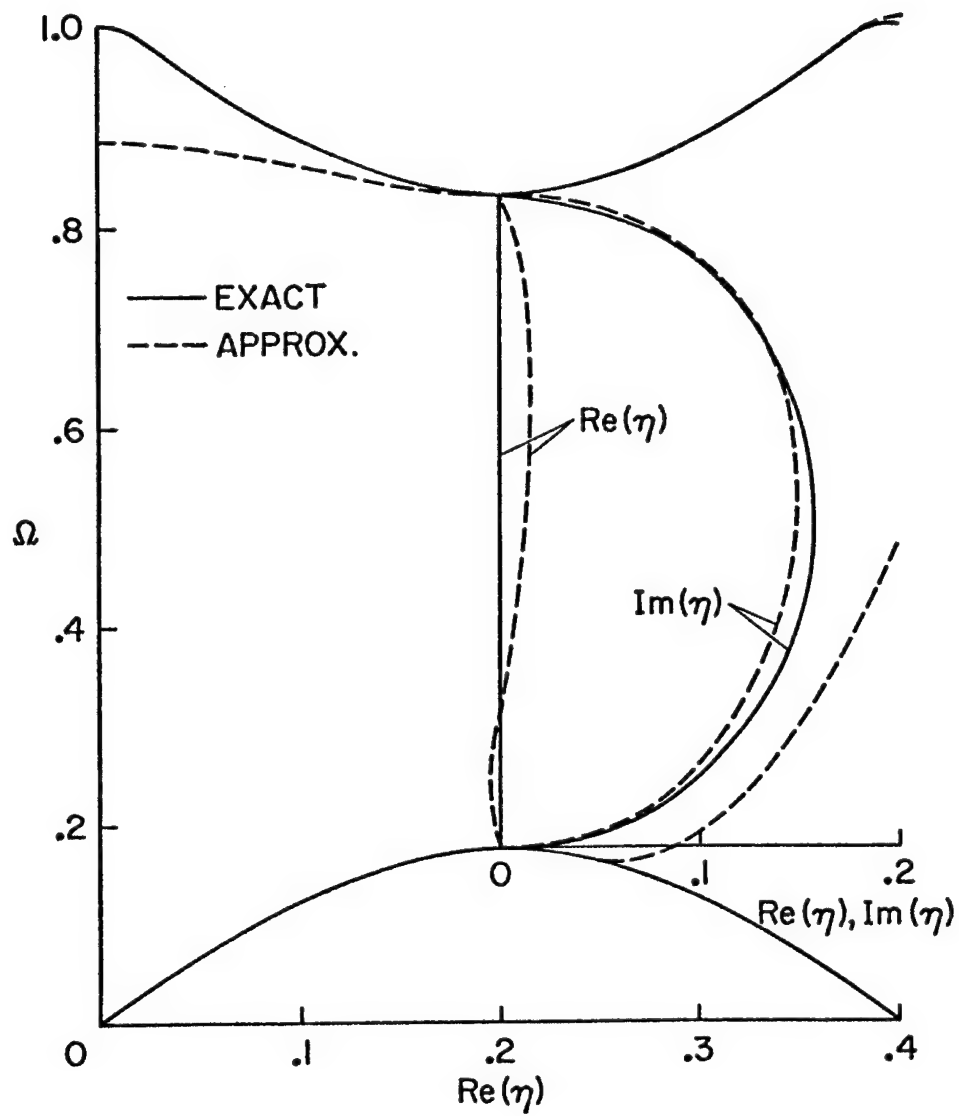


Fig. 12 Spectral Lines of Six-Parameter Approximate Theory as an Extension of Kunin Theory

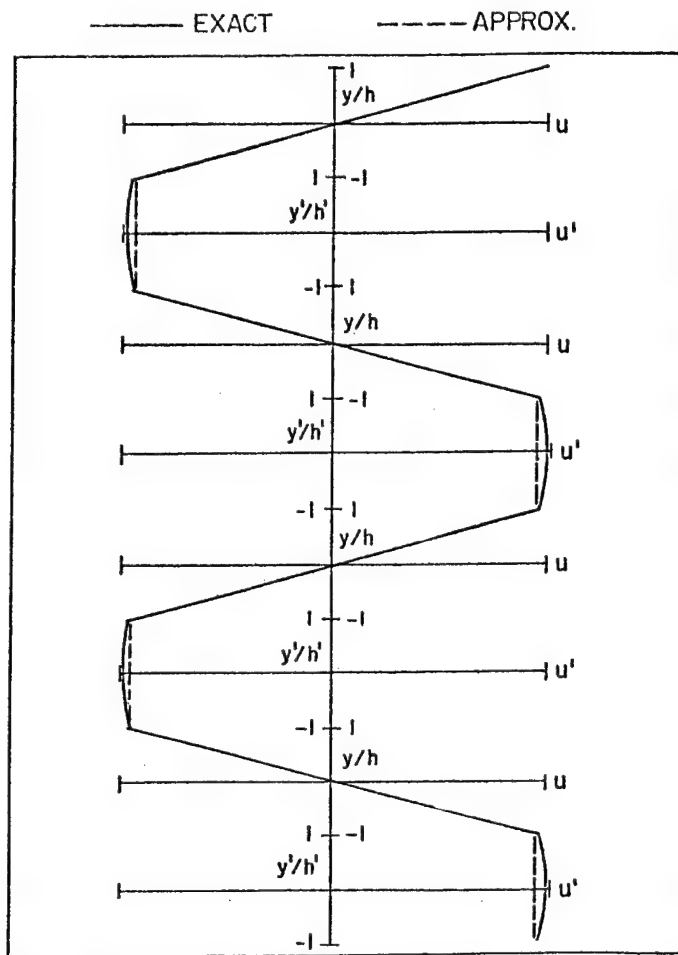


Fig. 13 Comparison of Mode Shapes at End of First Brillouin Zone, Layer Thicknesses are normalized. Interfaces are at ± 1 , Primes Refer to Stiffer Layers

Six Parameter Model (M.E.S.)

$$\begin{aligned} \text{Eqns. of Motion} \quad & \begin{cases} a_1 u_{0,22} - a_2 \Psi_{,2} = -b_1 \ddot{u}_{,22} + b_2 \ddot{u}_0 + b_3 \ddot{\Psi}_{,2} \\ -a_2 u_{0,2} + a_3 \Psi - a_4 \Psi_{,22} = b_3 \ddot{u}_{0,2} - b_4 \ddot{\Psi} \end{cases} \end{aligned}$$

$$(\alpha K^2 + \beta) \omega^4 + (\gamma K^2 + \zeta K^4 + \delta) \omega^2 + \epsilon K^2 + K^4 = 0$$

Six Parameter Model (based on Kuncin)

$$\begin{aligned} \text{Eqns. of Motion} \quad & \begin{cases} a_1 u_{0,22} + a_2 u_{0,2222} - a_3 \Psi_{,2} - a_4 \Psi_{,222} = b_1 \ddot{u}_0 \\ a_3 u_{0,2} + a_4 u_{0,222} - a_5 \Psi - a_6 \Psi_{,22} = b_2 \ddot{\Psi} \end{cases} \end{aligned}$$

$$\alpha \omega^4 + (\beta K^4 + \gamma K^2 + \delta) \omega^2 + \epsilon K^2 + \zeta K^4 + K^6 = 0$$

Fig. 14 Equations of Motion and Frequency Equation of Two Approximate Theories

CONTINUUM THEORY OF FRACTURE

Morton E. Gurtin
Carnegie-Mellon University

I. Fracture

Objectives:

- (a) To develop, within the framework of continuum mechanics, a thermodynamics of fracture.
- (b) To develop constitutive equations for the crack tip.
- (c) To study the effects of temperature on the fracture process [cf. J.G. Williams, J. Matl. Sc. 9 (1974), 1409].
- (d) To develop fracture criteria which are compatible with thermodynamics

II. Diffusion through a deformable solid

Objective: To develop a theory for the diffusion of a fluid through a deformable solid.

Previous work: Biot [J. Appl. Phys. 12 (1941), 155; 26 (1955) 182] developed a linear theory for soils based on concept of pore pressure. This concept may not be applicable for general diffusion.

Preliminary results: Have developed general linear theory

Primitive concepts: u ... displacement

$(E = \frac{1}{2}(\nabla u + \nabla u^T))$... strain, $\vartheta = \text{div} u$... volume change)

S ... stress, c ... fluid concentration

h ... relative mass flux of fluid

Conservation equations:

$$\text{div} S = 0 \quad (\text{equilibrium})$$

$$\dot{c} = -\text{div} h \quad (\text{mass balance})$$

Constitutive assumptions: linearity, homog.,

isotropy, $S = S(E, c)$, $h = h(\underbrace{\nabla c, \nabla E}_{\text{Fick's Law}})$

Results:

$$S = 2\mu E + 2\vartheta I - \alpha c I$$

$$h = -\gamma \nabla c + \beta \nabla \vartheta$$

$$\dot{c} = \kappa \Delta c$$

1. Equations same as uncoupled, quasi-static thermoelasticity:

concentration \leftrightarrow temperature

(Note: $h \leftrightarrow$ ~~heat~~ heat flux)

2. Analogy useful when

c prescribed on boundary

not when

$$h \cdot n = -\gamma \frac{\partial c}{\partial n} + \beta \frac{\partial \vartheta}{\partial n} \text{ prescribed}$$



(except in one space dimension)

3. Define

$$\pi = c - \frac{\alpha}{\beta} \vartheta \quad (\text{flow potential})$$

Then

$$S = 2\mu E + \lambda_0 \theta 1 - \alpha \pi 1$$

$$h = -\gamma \nabla \pi \quad (\text{D'Arcy's law})$$

$$\underbrace{\dot{\pi} + \tau \dot{\vartheta}}_{\uparrow \quad \uparrow} = \gamma \Delta \pi$$

4. Equations same as coupled, quasi-static thermoelasticity

$$\pi \leftrightarrow \text{temperature}$$

$$h \leftrightarrow \text{heat flux}$$

5. Analogy useful when h, n prescribed on boundary.

6. $\pi \sim$ chem. potential, pore pressure

$$S = \frac{\partial \psi}{\partial E}, \quad \pi \sim \frac{\partial \psi}{\partial c}$$

Future work:

(a) Anisotropic materials (more difficult, no analogies, no π).

(b) Study some simple solutions.

(c) Develop the theory within a thermodynamic framework.

(d) Include non-linearities.

LINEAR AND NONLINEAR EFFECTS
IN THE VIBRATION OF
ELASTIC STRUCTURES

Grant AFOSR-73-2479

Lawrence W. Rehfield
Professor
School of Aerospace Engineering
Georgia Institute of Technology
Atlanta, Georgia 30332

NONLINEAR EFFECTS IN
STRUCTURAL VIBRATIONS

- 1) Drift of resonant frequencies with increasing amplitude of the motion.
- 2) Alteration of time history of transient response.
- 3) Jump phenomena.
- 4) Dynamic buckling (oil canning) in the presence of prestress or geometric curvature.
- 5) Subharmonic or superharmonic resonances.
- 6) Bounded limit cycle response.

NONLINEAR MATERIAL EFFECTS IN RESIN MATRIX ADVANCED COMPOSITES

- 1) Different stiffness in tension and compression.
- 2) Nonlinear matrix-dominated shear behavior.
- 3) Accentuating influence of moisture absorption and elevated temperature on the above.

OBJECTIVES

- 1) To determine the nature and extent of the influence of nonlinear material characteristics on vibration behavior of resin matrix composite structures.
- 2) Assess the impact of moisture absorption and elevated temperature on the above.

SCOPE

- 1) Restrict attention to flexural behavior of simple beams.
- 2) Consider $[0]$ and $[\pm 45]$ lay-ups.
- 3) Perform trend analysis.
- 4) Define and perform definitive experiments.

REQUIRED DEVELOPMENTS

- 1) Nonlinear theory and method of analysis.
- 2) Uniaxial nonlinear material model.

$$\sigma = E(\epsilon + \alpha\epsilon^2 + \beta\epsilon^3)$$

- 3) Compressive test method.
- 4) Test method for producing large amplitude structural vibrations.

ANALYTICAL RESULTS FOR FREE VIBRATION OF SIMPLY SUPPORTED BEAMS

$$\frac{\omega_r^2}{\omega_{or}^2} = 1 + B_r \left(\frac{A_r}{\rho} \right)^2$$

r = mode number

If $B_r > 0$, structural response is "hard."

If $B_r < 0$, structural response is "soft."

$$B_r = \frac{3}{16} \left[1 + 4\alpha r^2 \pi^2 \left(\frac{\rho}{L} \right)^2 + (3\beta\mu - 2\alpha^2) r^4 \pi^4 \left(\frac{\rho}{L} \right)^4 \right]$$

ENVIRONMENTAL EFFECTS DUE TO MOISTURE ABSORPTION AND ELEVATED TEMPERATURE ON FIBER DOMINATED BEAM VIBRATIONS

Consider [0] laminates of T300 Narmco 5208 graphite/epoxy with the following room temperature dry properties:

$$E_t = 21.3 \times 10^6 \text{ psi}$$

$$E_c = 18.8 \times 10^6 \text{ psi}$$

$$\epsilon_a = 0.007$$

Under the least favorable environmental conditions, E_c will be reduced by about 25 percent. With this assumption

$$\frac{(w_{or})_w}{(w_{or})_d} = 0.94$$

$$\frac{(B_1)_w}{(B_1)_d} = 1.16, \quad \frac{(B_2)_w}{(B_2)_d} = 1.51 \quad (L/\rho = 100)$$

CONCLUSIONS FROM TREND ANALYSIS

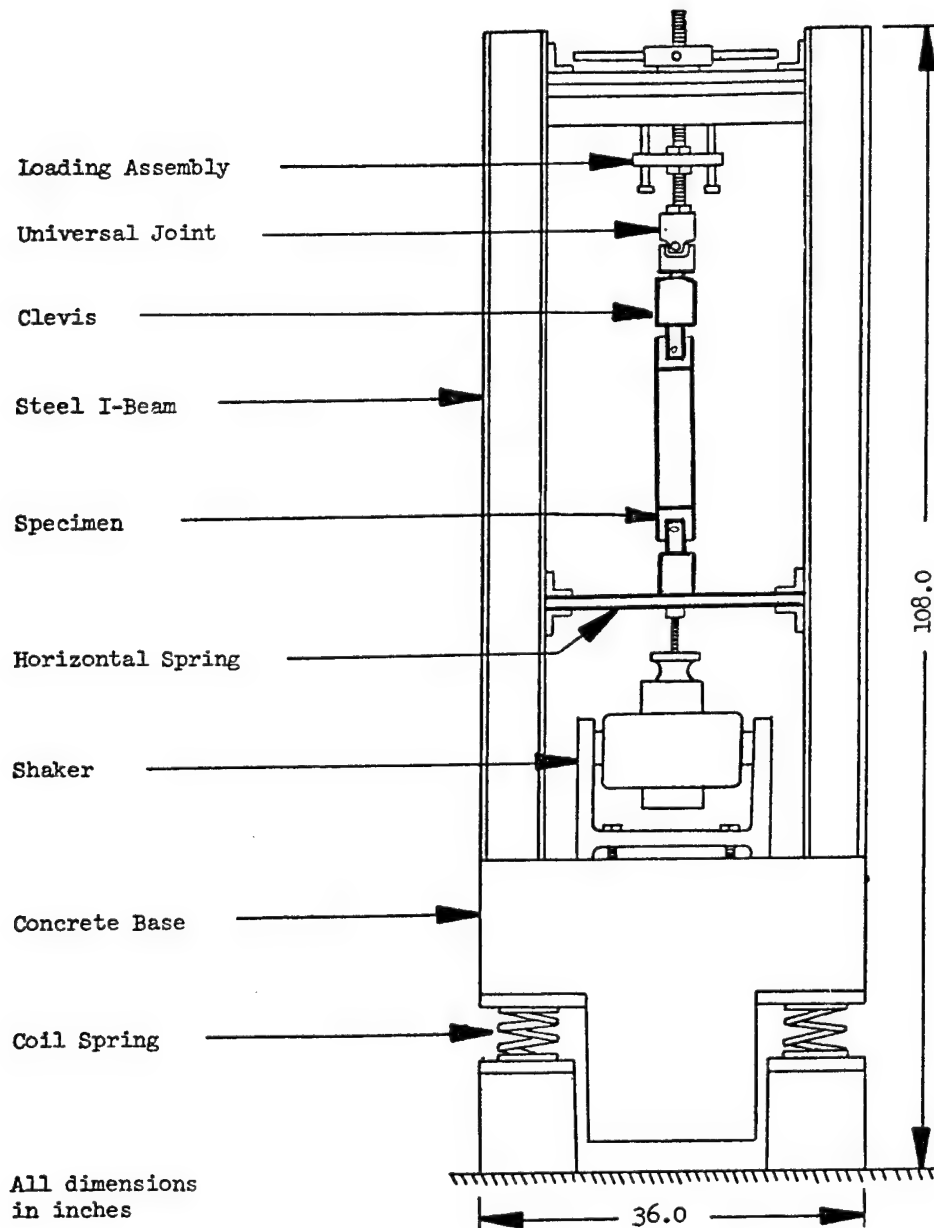
- 1) Nonlinear material effects are increasingly important as
 - a. the slenderness ratio decreases
 - b. the mode number increases
- 2) Graphite/epoxy $[0]$ beams exhibit hardening behavior.
- 3) Boron/epoxy $[0]$ beams exhibit a tendency to softening behavior.
- 4) $[+45]$ laminates exhibit a pronounced tendency to softening behavior.
- 5) Effect of moisture/elevated temperature appears to pose no major problems for fiber dominated flexural vibrations. Matrix dominated vibrations cannot be rationally evaluated at this time.

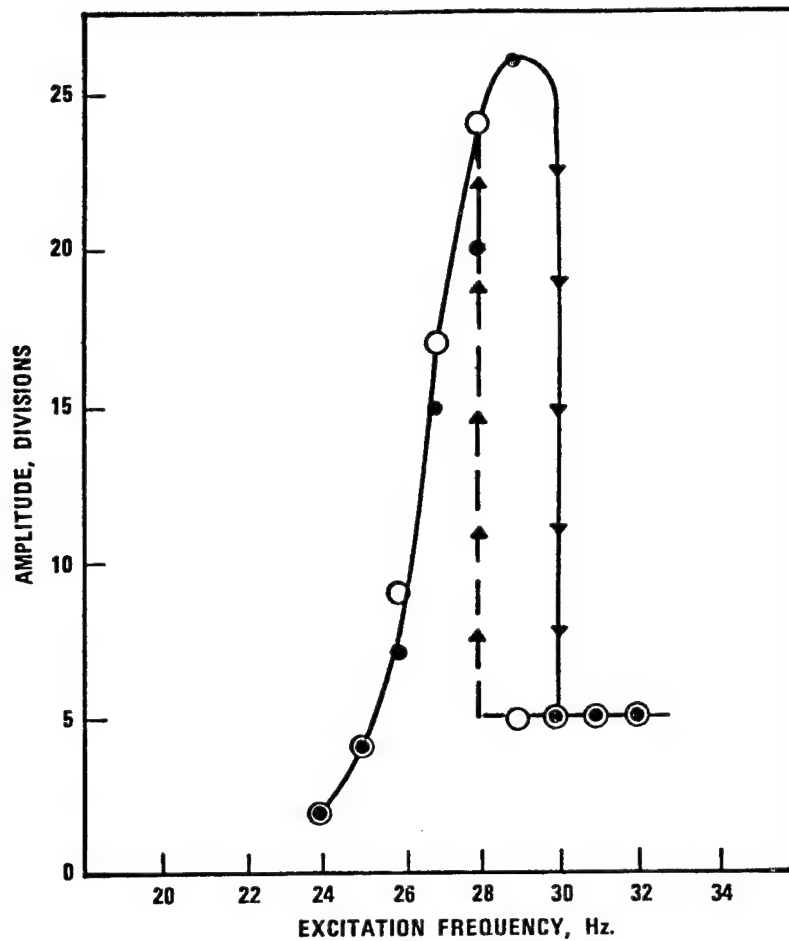
FUTURE THEORY/ANALYSIS WORK

- 1) Material behavioral models for
 - a. two and three dimensional characterization of lamina and laminates.
 - b. realistic description of degradation due to moisture and elevated temperature.
- 2) Flexural vibration of laminated beams accounting for transverse shear and other secondary nonlinear effects, including boundary restraint variation.
- 3) Flexural vibration of angle ply panels.

EXPERIMENTAL RESULTS

- 1) New static compressive test.
- 2) New test method for producing large amplitude structural vibrations
 - a. excite specimen longitudinally rather than laterally.
 - b. extensive metallic specimen data.
 - c. limited composite specimen data.





STIFFENING OVERHANG BEHAVIOR FOR MEAN FORCE, $P_0 = 30$ POUNDS, AND ALTERNATING FORCE, $P_1 = 14$ POUNDS.

DATA FOR INCREASING FREQUENCY - ●
DATA FOR DECREASING FREQUENCY - ○

FUTURE EXPERIMENTAL WORK

- 1) Develop experimental means of quantifying nonlinear effects.
- 2) Environmental simulation of moisture/elevated temperature effects
 - a. material characterization studies.
 - b. large amplitude vibration experiments.
 - c. damping experiments.
- 3) Vibration of angle ply panels.

MECHANICS OF COMPOSITE MATERIALS

G. A. Hegemier
University of California, San Diego

RESEARCH AREAS

1. WAVE PROPAGATION IN COMPOSITE MATERIALS:
PREDICTION OF STRESS, DEFORMATION,
THERMAL FIELDS
2. MICROMECHANICS OF FAILURE:
PREDICTION OF FAILURE MODES, DAMAGE,
DEGRADED PROPERTIES

GEOMETRIES CONSIDERED

1. LAMINATES:

PROPAGATION AT OBLIQUE INCIDENCE

2. FIBROUS COMPOSITES:

1D ARRAYS

2D ARRAYS

COMPLEX 3D ARRAYS

} PROPAGATION AT
0° AND 90°
INCIDENCE

CONSTITUENT BEHAVIOR CONSIDERED

1. LINEAR ELASTIC

2. LINEAR VISCOELASTIC

3. ELASTIC-PERFECTLY PLASTIC

(FINITE DEFORMATIONS, THERMODYNAMICS)

VALIDITY TESTS OF THEORIES

1. COMPARISON OF PHASE VELOCITY SPECTRA
2. COMPARISON OF TRANSIENT PULSE RESULTS

COMPARISON DATA

1. EXACT SPECTRA FOR ELASTIC LAMINATES AT
OBLIQUE INCIDENCE AND ELASTIC FIBERS AT 90°
2. EXACT TRANSIENT PULSE RESULTS FOR ELASTIC
LAMINATES AT 0° INCIDENCE
3. DETAILED NUMERICAL TRANSIENT PULSE RESULTS
FROM 2D NONLINEAR FINITE DIFFERENCE CODES FOR
FINITE AMPLITUDE 90° PROPAGATION IN LAMINATES
AND UNIDIRECTIONAL FIBER ARRAYS
4. EXPERIMENTAL RESULTS ON LAMINATES AND FIBROUS
COMPOSITES (PHASE VELOCITY AND TRANSIENT PULSE)

LINEAR AND NONLINEAR WAVE PROPAGATION IN LAMINATES

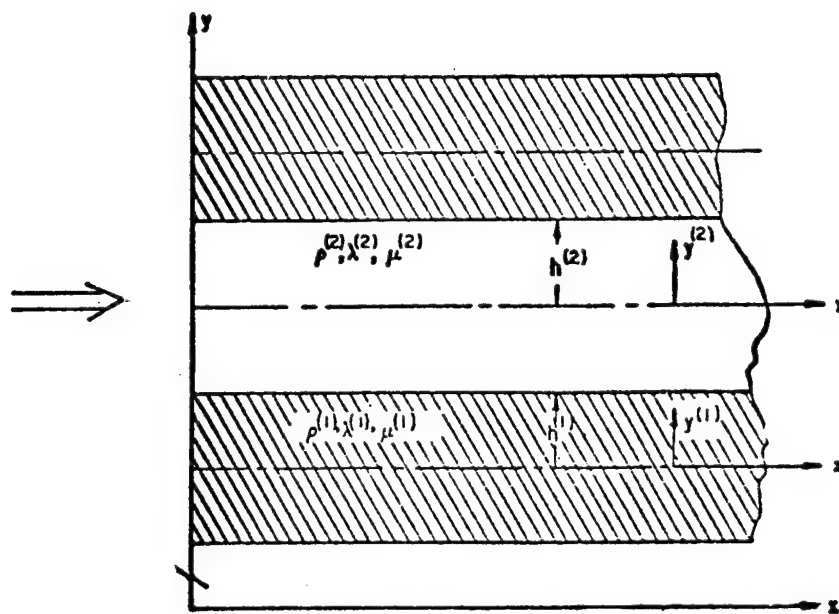


Fig. 1. Geometry and Coordinate System for Wave Guide-type Propagation in Laminates.

TYPICAL MIXTURE FORM FOR LAMINATES

Averages

$$\langle \rangle^{(\alpha a)} \equiv \frac{1}{h^{(\alpha)}} \int_0^{h^{(\alpha)}} \langle \rangle^{(\alpha)} dy^{(\alpha)}$$

Partial stresses, densities, volumes

$$\sigma_{xx}^{(\alpha p)} \equiv n^{(\alpha)} \sigma_{xx}^{(\alpha)}, \quad \rho^{(\alpha p)} \equiv n^{(\alpha)} \rho^{(\alpha)}, \quad n^{(\alpha)} \equiv h^{(\alpha)} / (h^{(1)} + h^{(2)}),$$

Mixture Momentum Equations

$$\partial_x \sigma_{xx}^{(1p)} - \rho^{(1p)} \partial_t^2 u_x^{(1a)} = P, \quad \partial_x \sigma_{xx}^{(2p)} - \rho^{(2p)} \partial_t^2 u_x^{(2a)} = -P, \quad P = \sigma_{xy}^*(x, t)$$

Mixture Constitutive Equations

$$\sigma_{xx}^{(1p)} = C_{11} \partial_x u_x^{(1a)} + C_{12} \partial_x u_x^{(2a)}, \quad \sigma_{xx}^{(2p)} = C_{12} \partial_x u_x^{(1a)} + C_{22} \partial_x u_x^{(2a)}$$

where

$$C_{\alpha\alpha} = n^{(\alpha)} E^{(\alpha)} - \lambda^{(\alpha)^2} / E, \quad C_{\alpha\beta} = \lambda^\alpha \lambda^\beta / E, \quad (\alpha, \beta = 1, 2; \alpha \neq \beta),$$

$$E^{(\alpha)} \equiv (\lambda + 2\mu)^{(\alpha)}, \quad E \equiv \frac{E^{(1)}}{n^{(1)}} + \frac{E^{(2)}}{n^{(2)}}$$

Interaction Terms

$$\partial_x P = \frac{3\mu^{(1)} \mu^{(2)}}{(n^{(1)} \mu^{(2)} + n^{(2)} \mu^{(1)})(h^{(1)} + h^{(2)})^2} (\partial_x u_x^{(1a)} - \partial_x u_x^{(2a)}),$$

$$P = \frac{A - \chi \sigma_{yy}^*}{h^{(1)} + h^{(2)}} \text{sqn}(\partial_x u_x^{(1a)} - \partial_x u_x^{(2a)}), \quad \sigma_{yy}^* = \frac{n^{(1)} \lambda^{(1)} E^{(2)}}{n^{(1)} E^{(2)} + n^{(2)} E^{(1)}} \partial_x u_x^{(1a)}$$

$$+ \frac{n^{(2)} \lambda^{(2)} E^{(1)}}{n^{(1)} E^{(2)} + n^{(2)} E^{(1)}} \partial_x u_x^{(2a)}$$

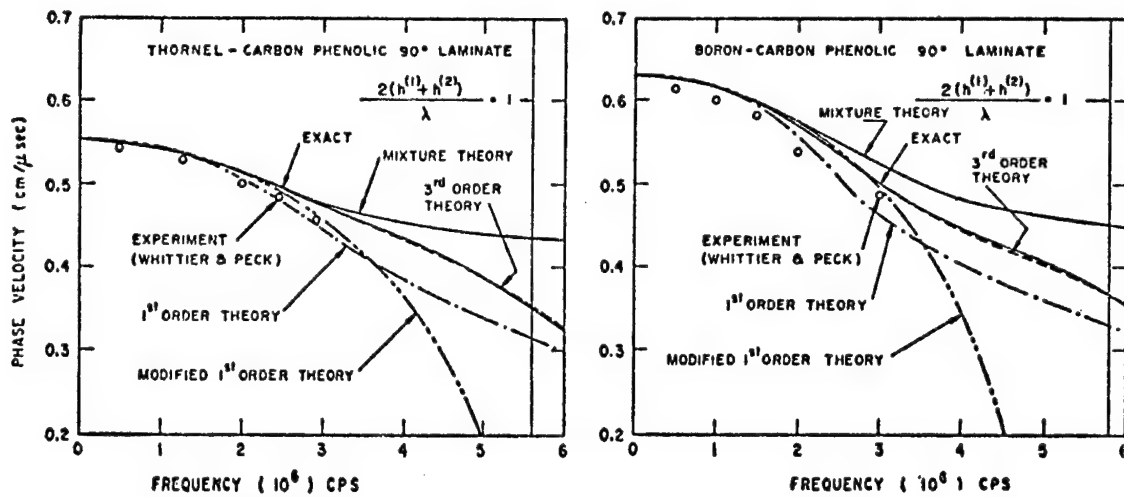


Fig. 2a, b. Lowest symmetric mode of the phase velocity spectrum for typical layered composites.

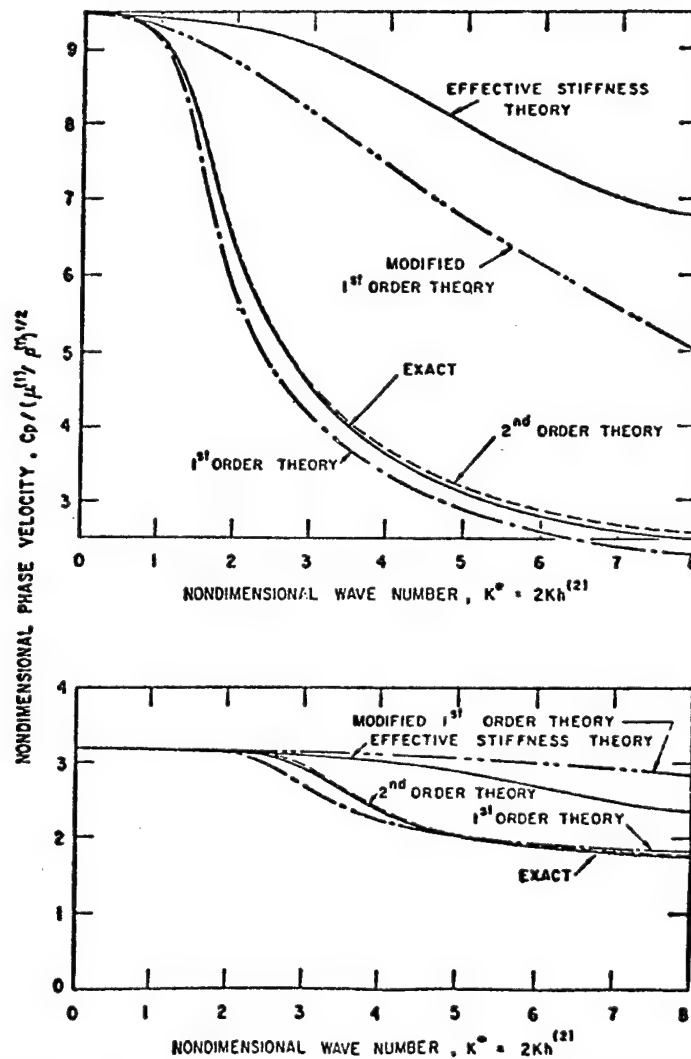


Fig. 3a, b. Phase velocity spectrum comparisons for several theories.

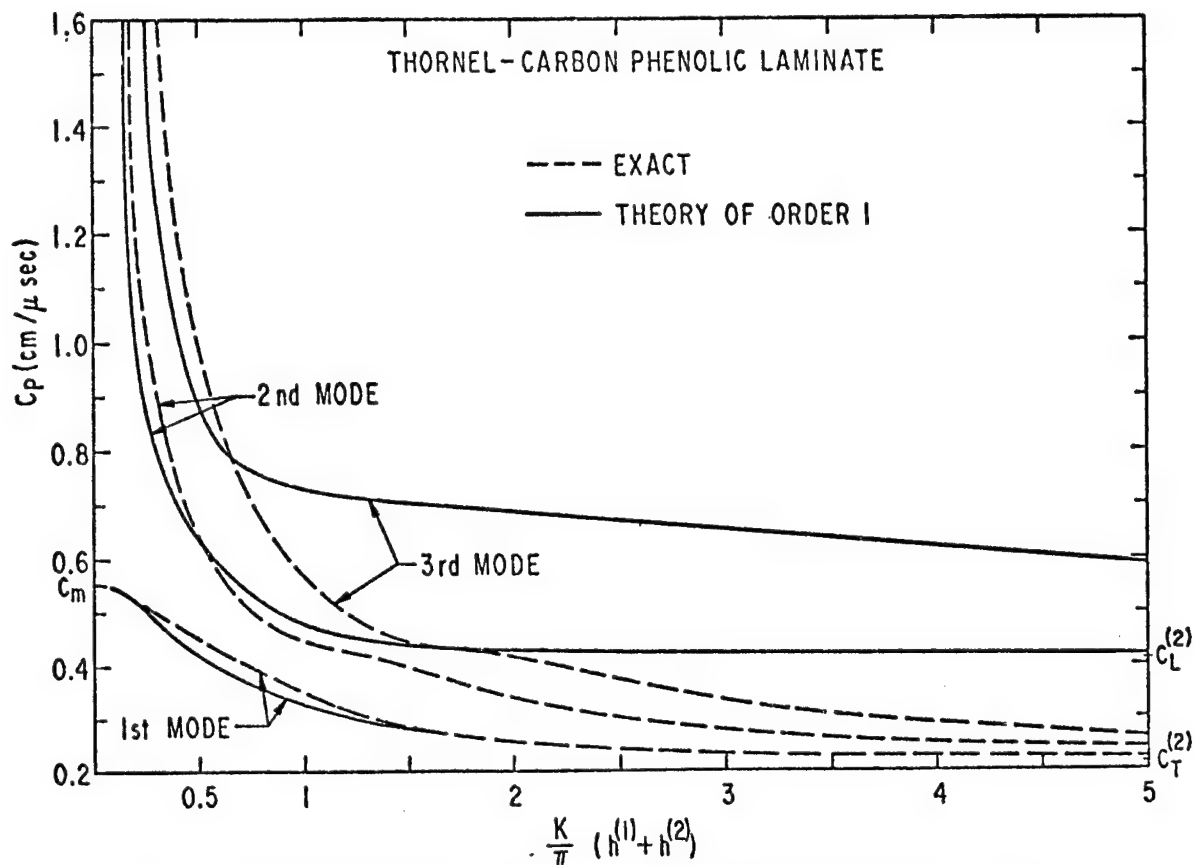


Fig. 4. Phase velocity spectrum--detailed comparison of exact and first-order theories.

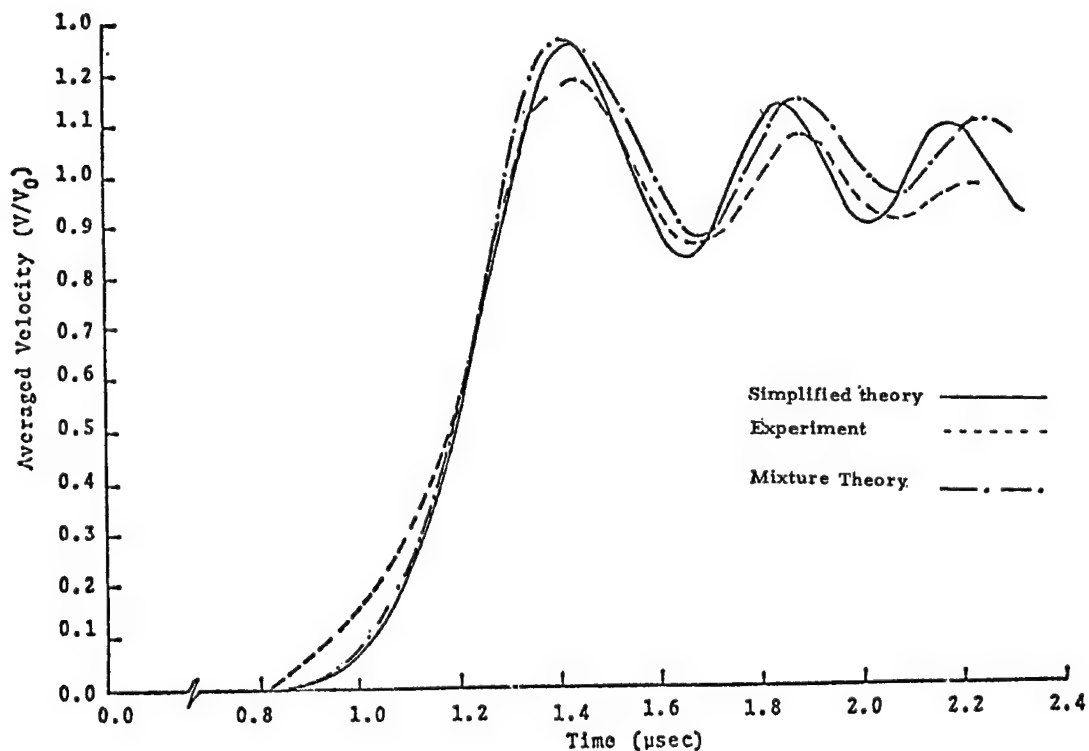


Fig. 5. Comparison of TINC and experimental rear surface velocity results for thornel reinforced carbon phenolic laminates.

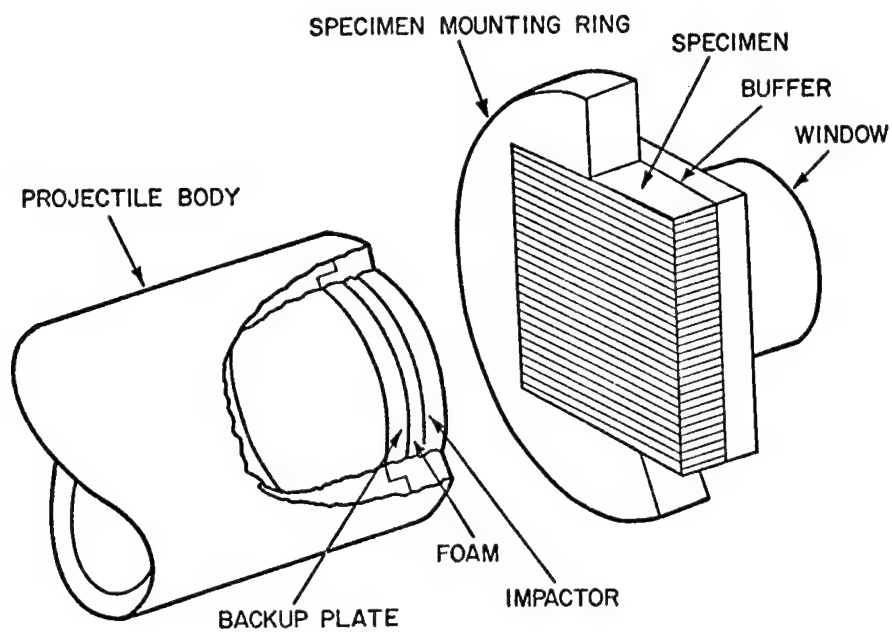


Fig. 6. Experimental arrangement for Sandia experiments.

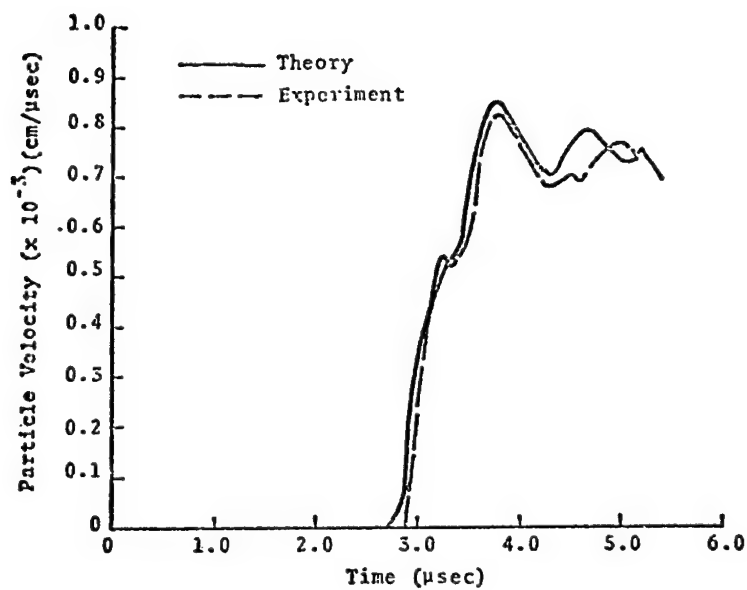


Fig. 7. Comparison of theory with experiment No. 2.

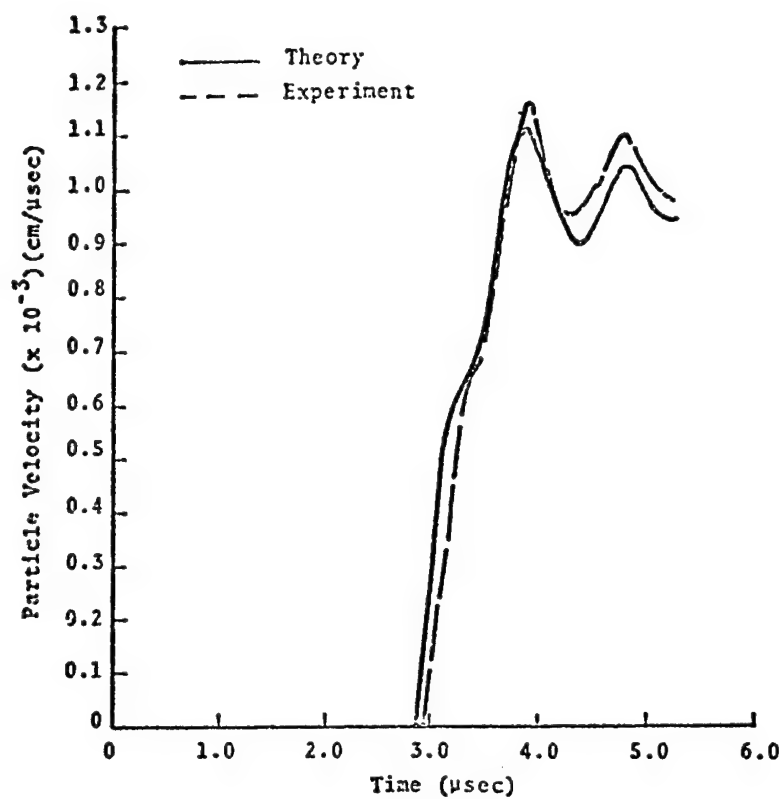


Fig. 8 Comparison of theory with experiment No. 6.

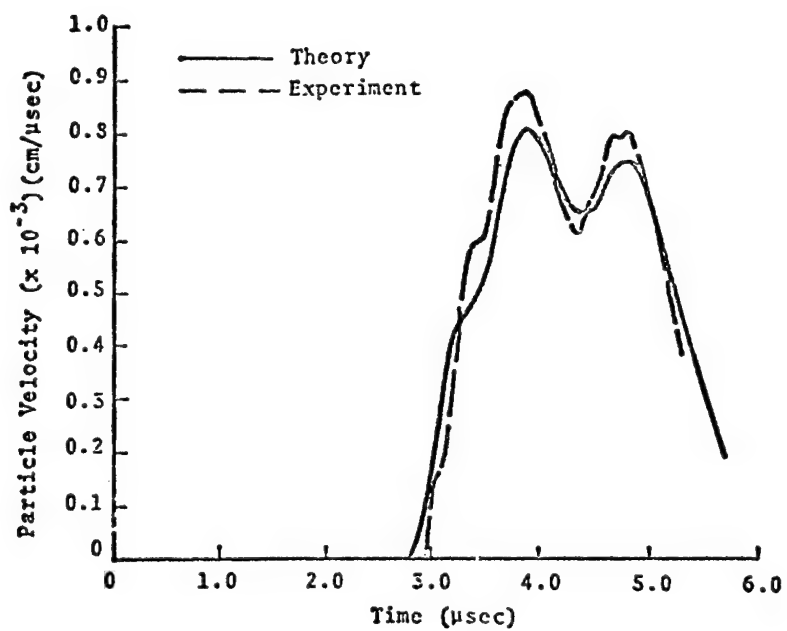


Fig. 9. Comparison of theory with experiment No. 7.

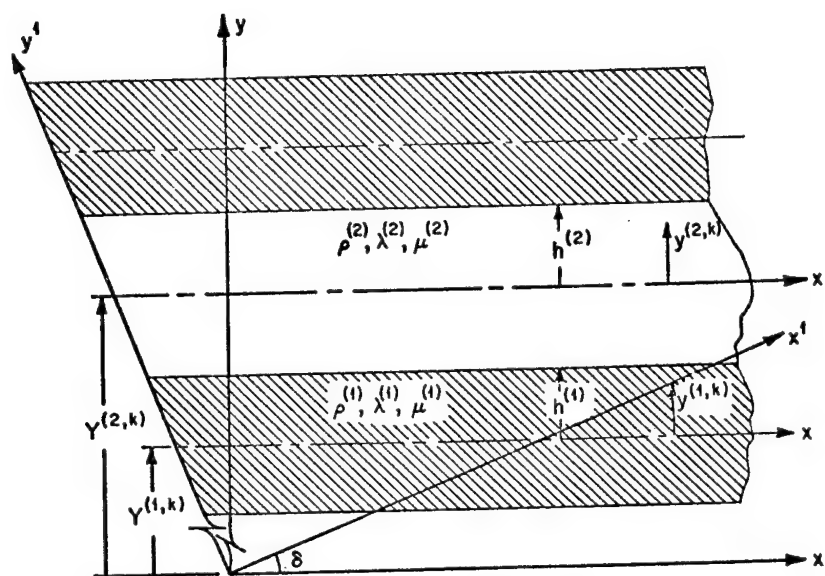


Fig. 10. Geometry and Coordinate System for Oblique Incidence Propagation in Laminates.

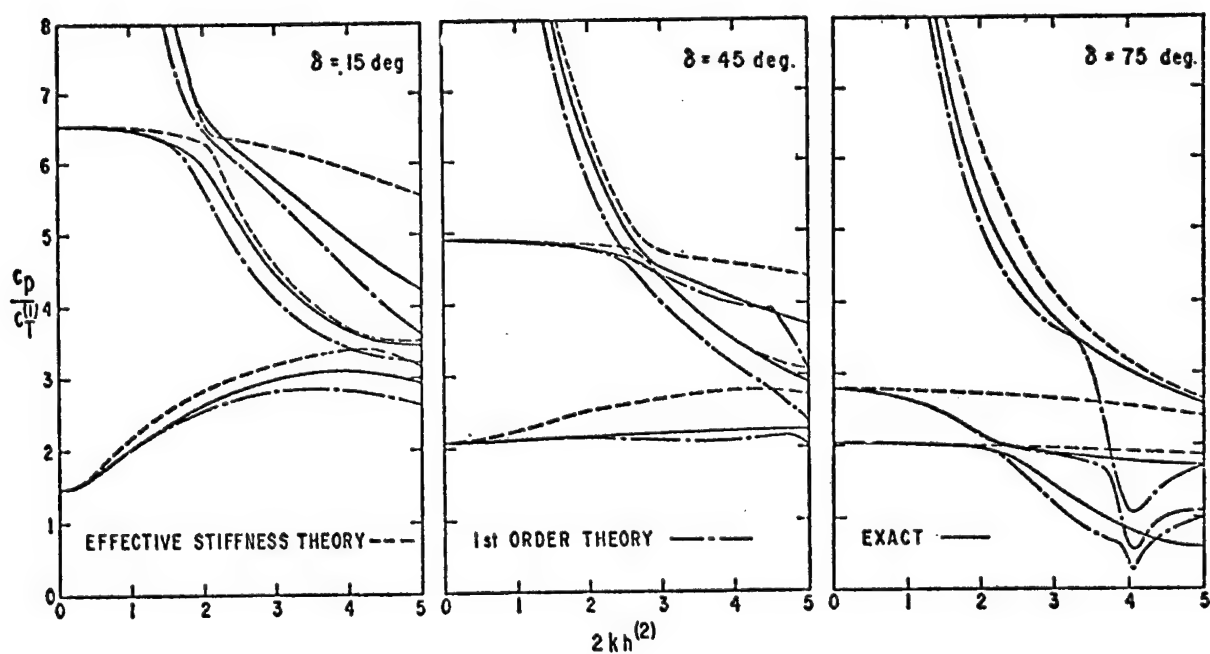


Fig. 11. Phase Velocity vs. Wave Number for Several Propagation Angles.

LINEAR AND NONLINEAR WAVE PROPAGATION IN
UNIDIRECTIONAL FIBROUS COMPOSITES

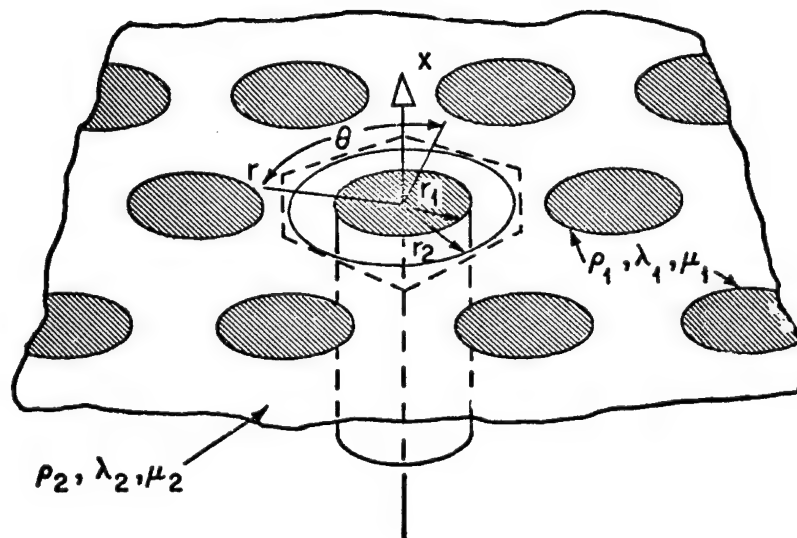


Fig. 12. Unidirectional fiber-reinforced composite with hexagonal array.

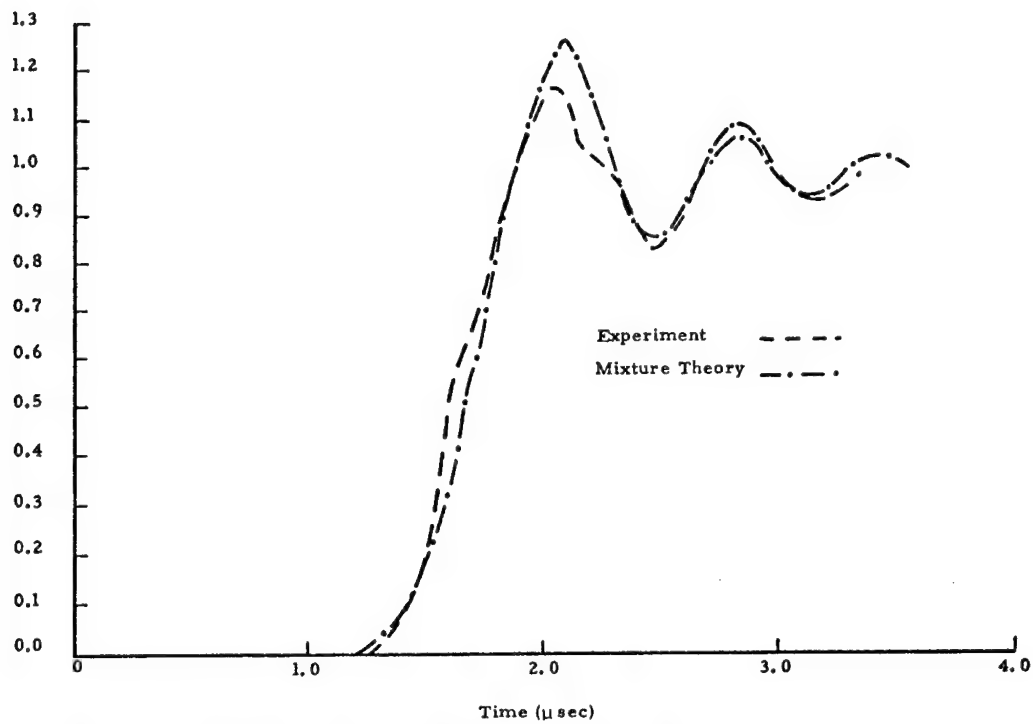


Fig. 13. Comparison of mixture and experimental rear surface velocity results from quartz fiber reinforced phenolic.

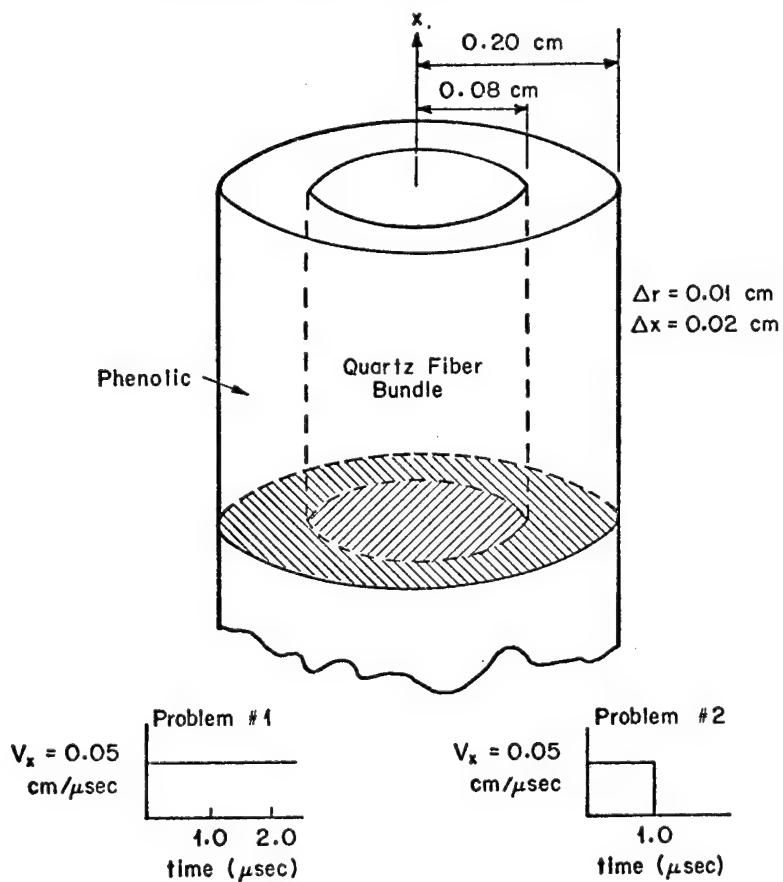


Fig. 14. Geometry for 2D CRAM calculation.

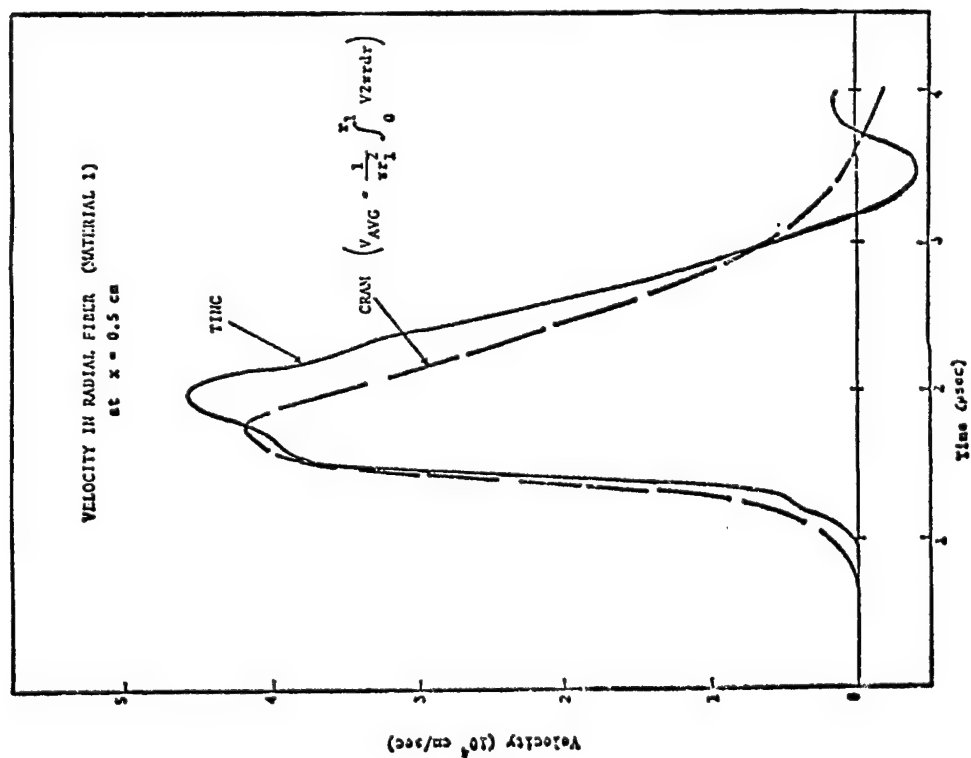


Fig. 15. Comparison of TINC and average GRAM particle velocity histories for radial fiber.

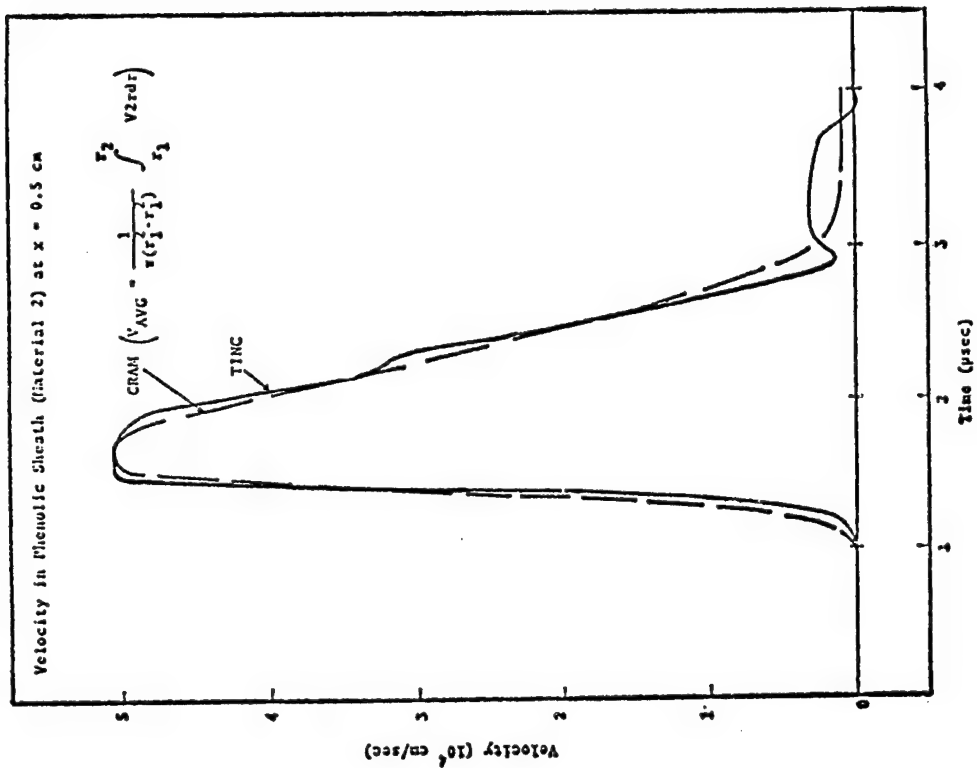


Fig. 16. Comparison of TINC and average GRAM particle velocity histories for sheath.

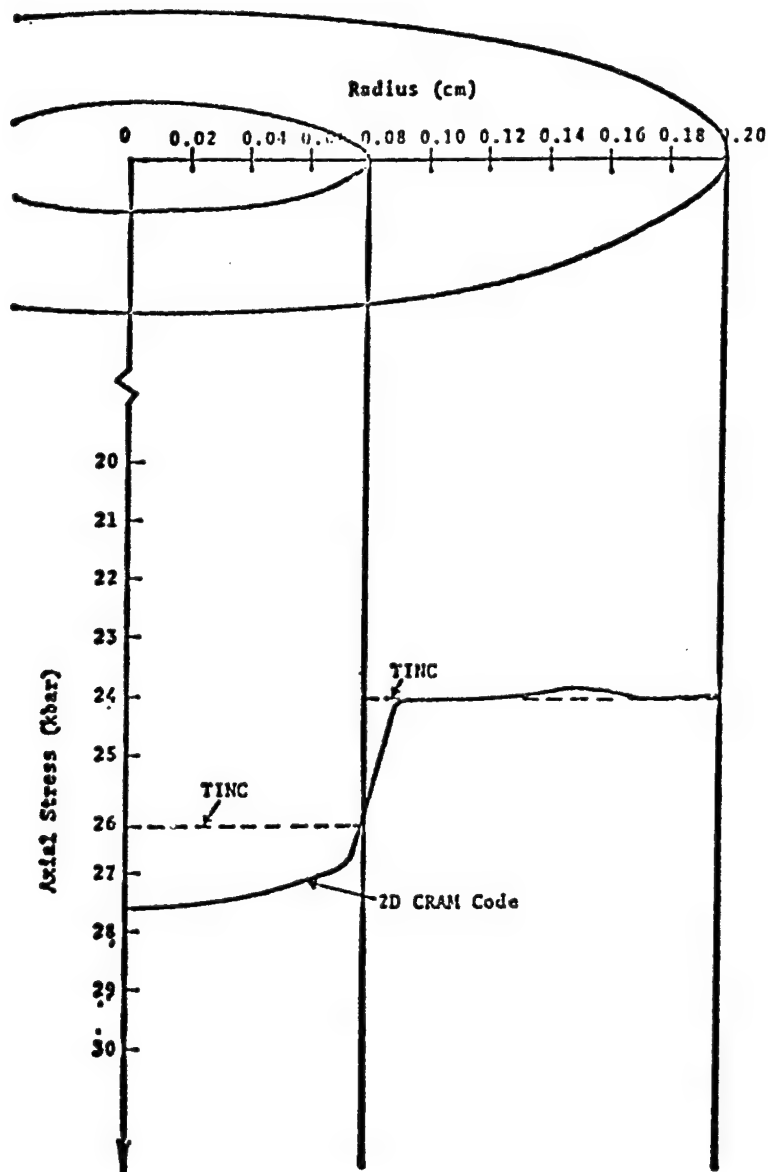


Fig. 17. Comparison of TINC and CRAM predictions of axial stress ($x = 0.2$ cm, $t = 1.0$ μ sec).

LINEAR AND NONLINEAR WAVE-PROPAGATION IN 3D COMPOSITES

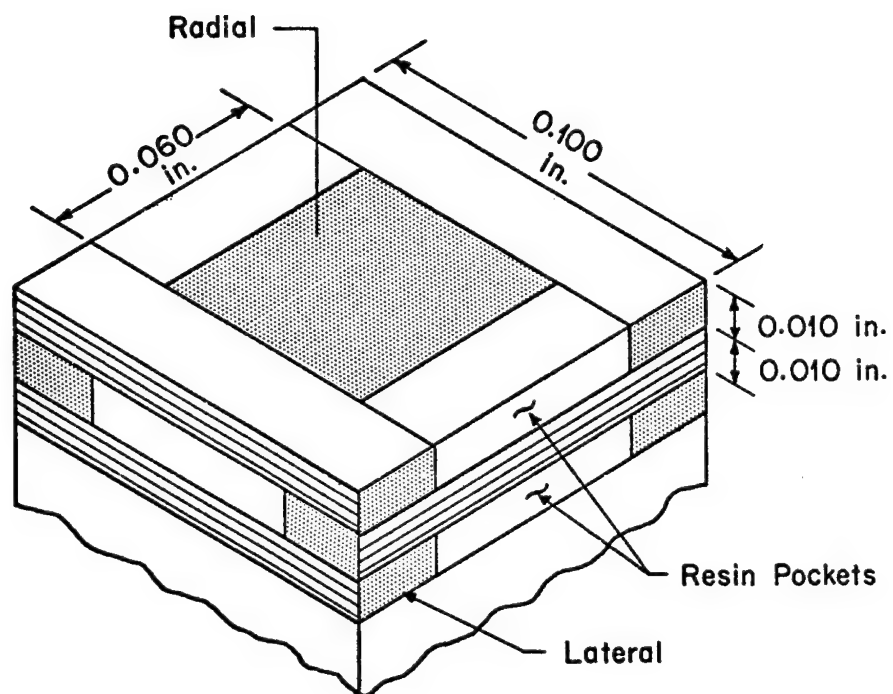


Fig.18. AVCO 3DQP "Black" material.

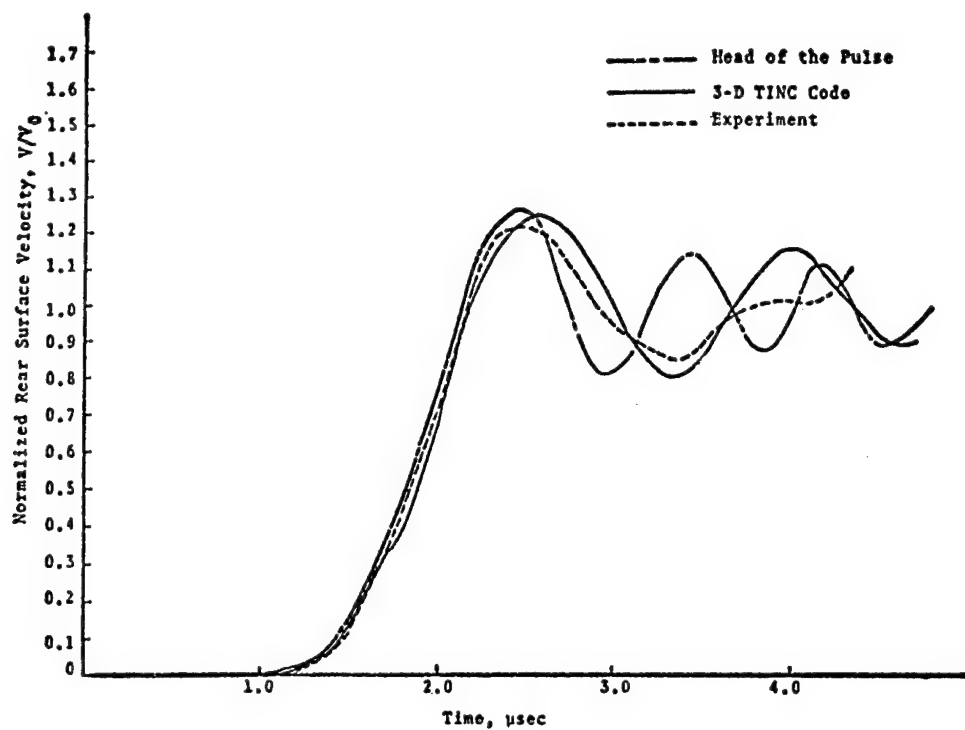


Fig. 19. Comparison of theoretical and experimental results for step pulse in "block" 3DQP ($x = 0.635$ cm).

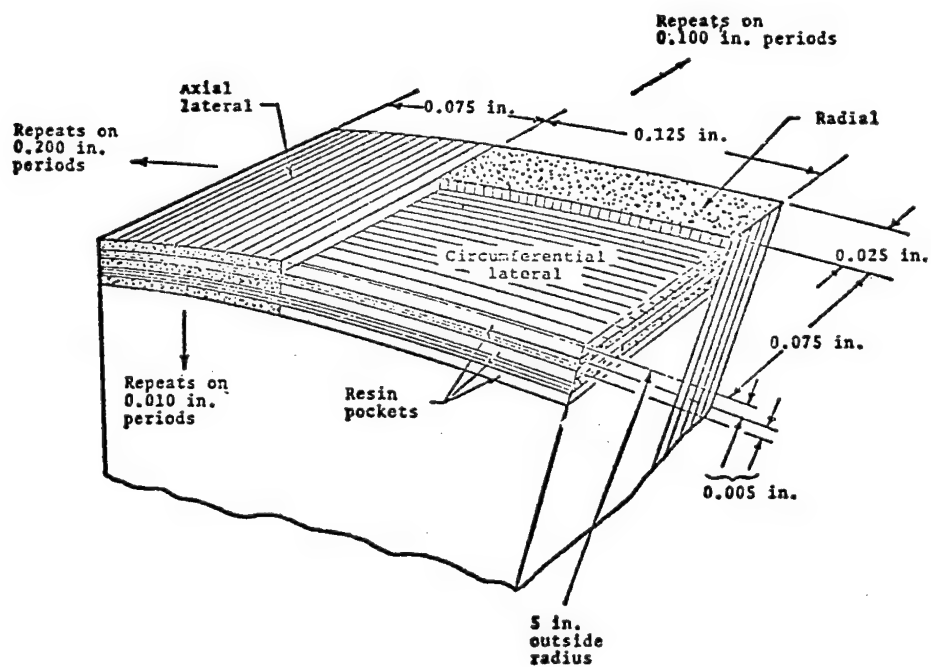


Fig. 20. AVCO 3DQP "shell" material (midspaced).

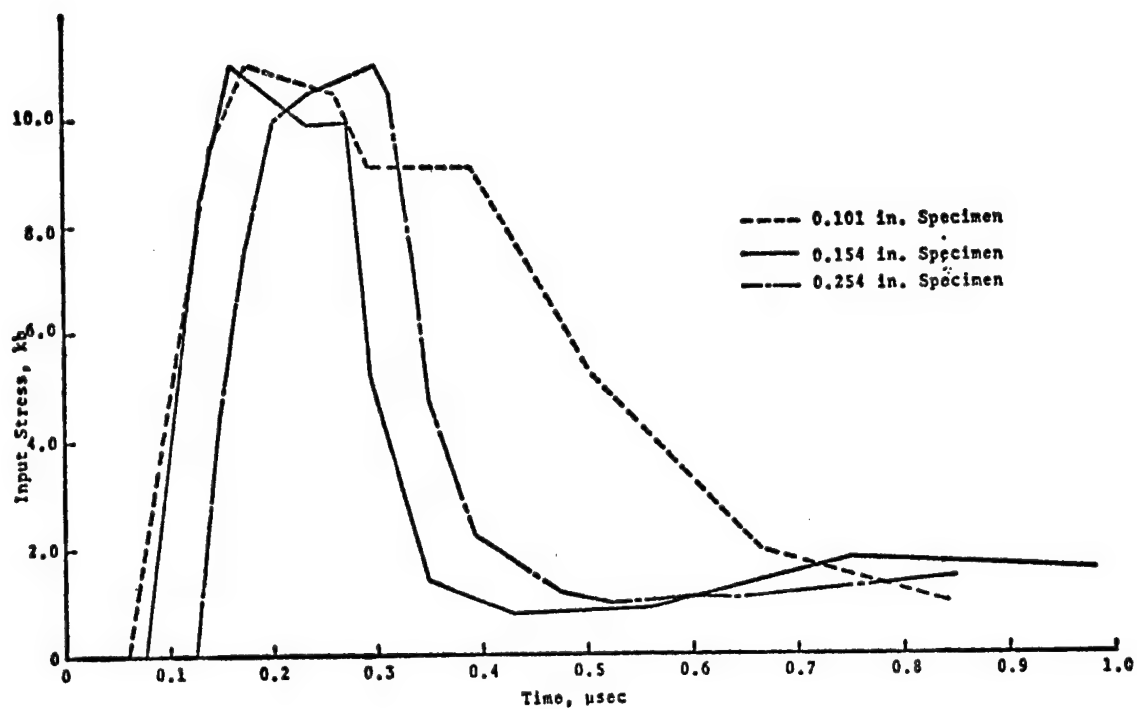


Fig. 21. Input stress profiles for AFWL shot 326.

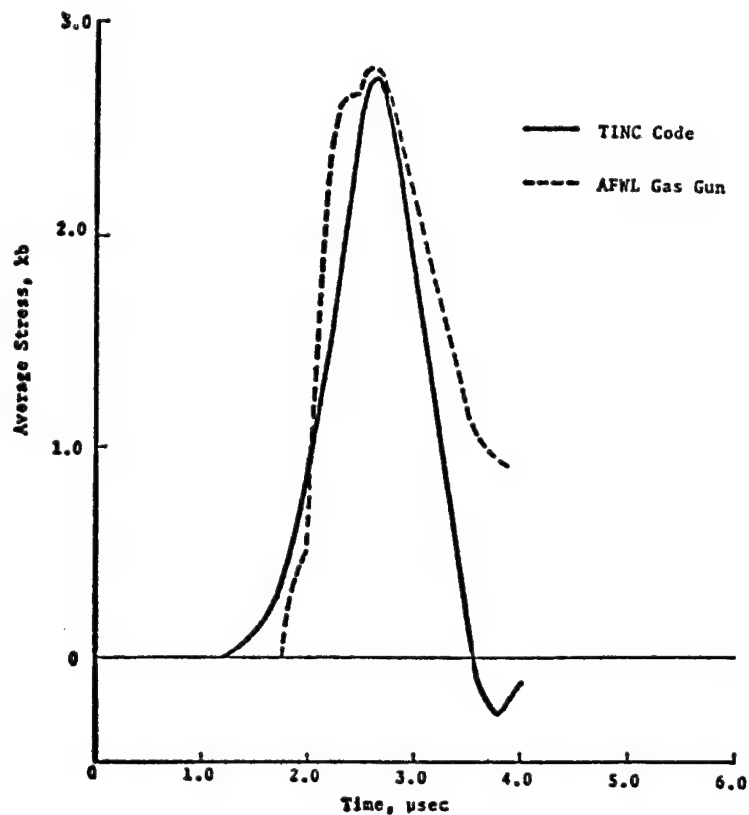


Fig. 22. Stress history at rear of 0.254 in. 3DQP plus 0.060 in. plexiglass (shot 326).

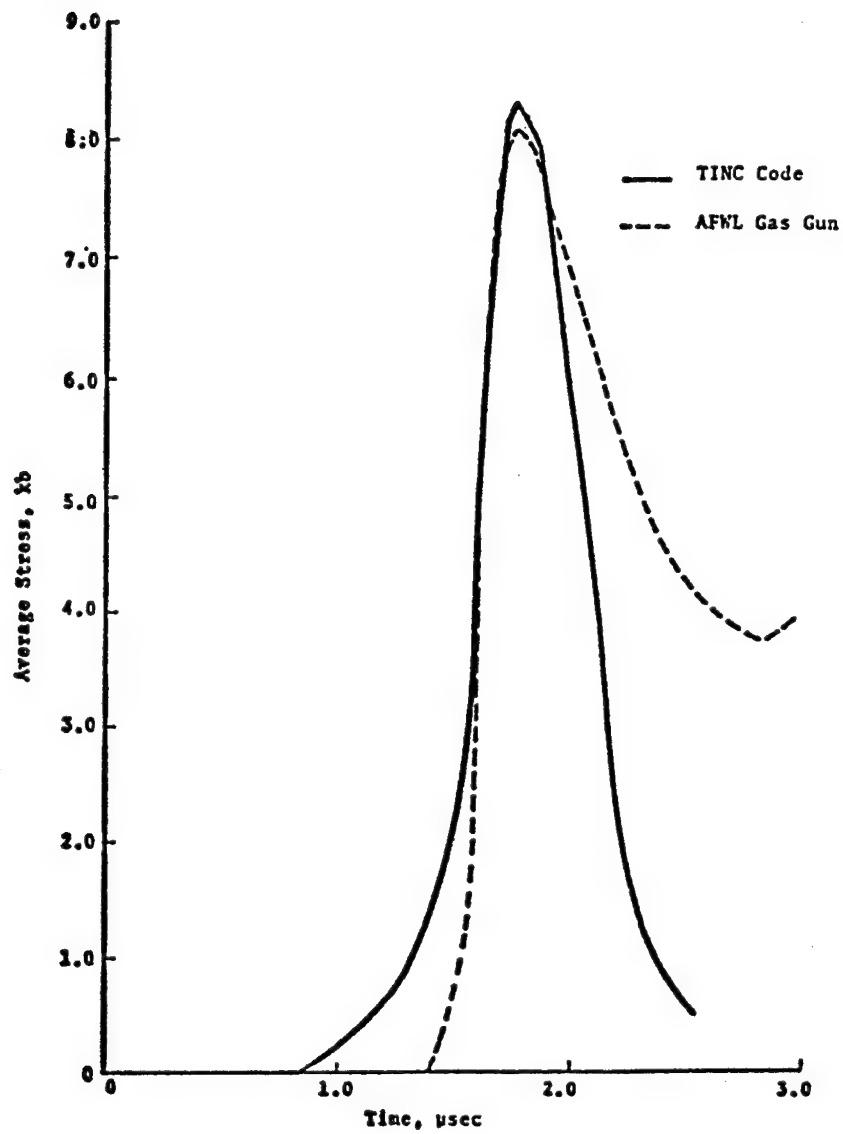


Fig. 23. Stress history at rear of 0.154 in. 3DQP plus 0.060 in. plexiglass (shot 314).

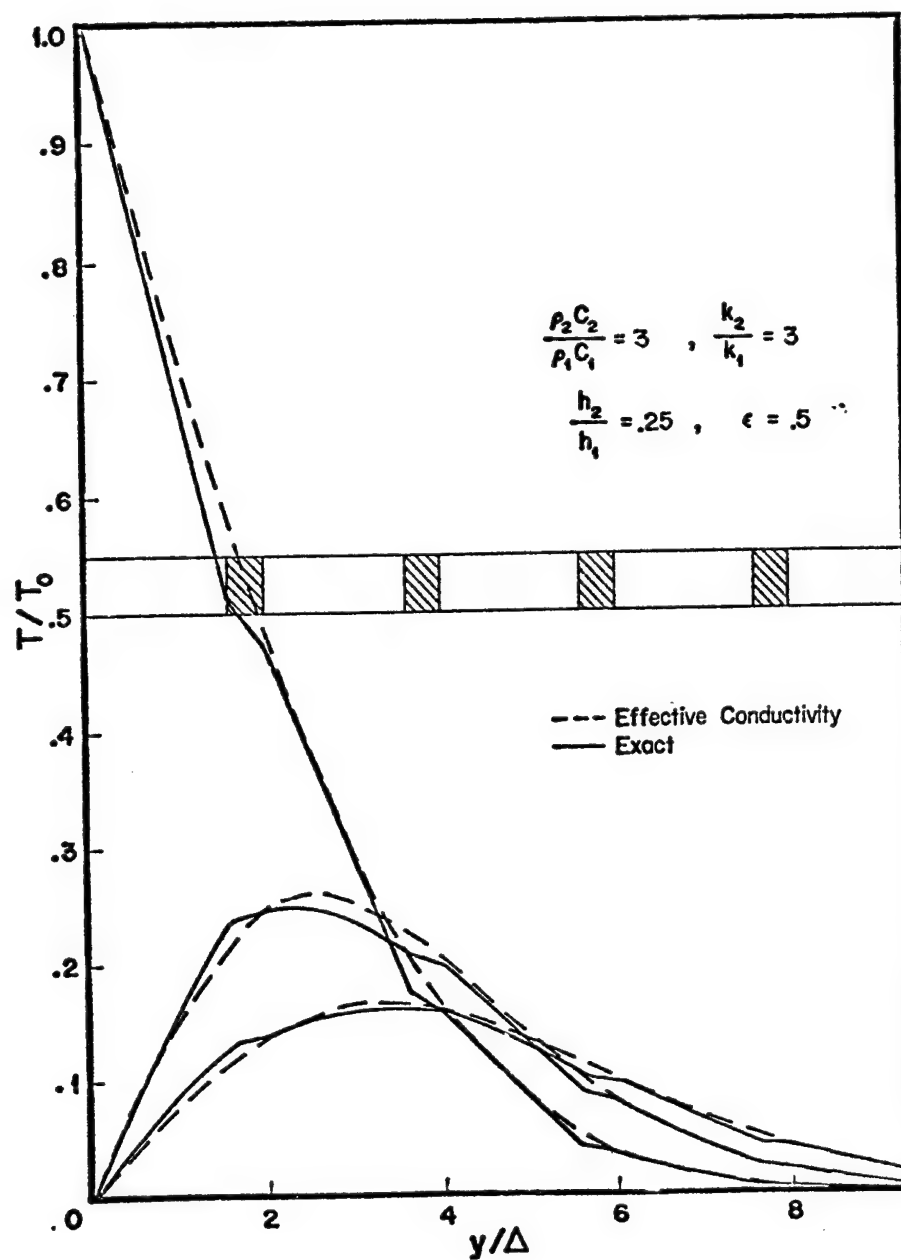


Fig. 24. Temperature distribution at $\tau = 1, 1.5$ and 2 for similar material properties and small duration of input pulse t_0 .

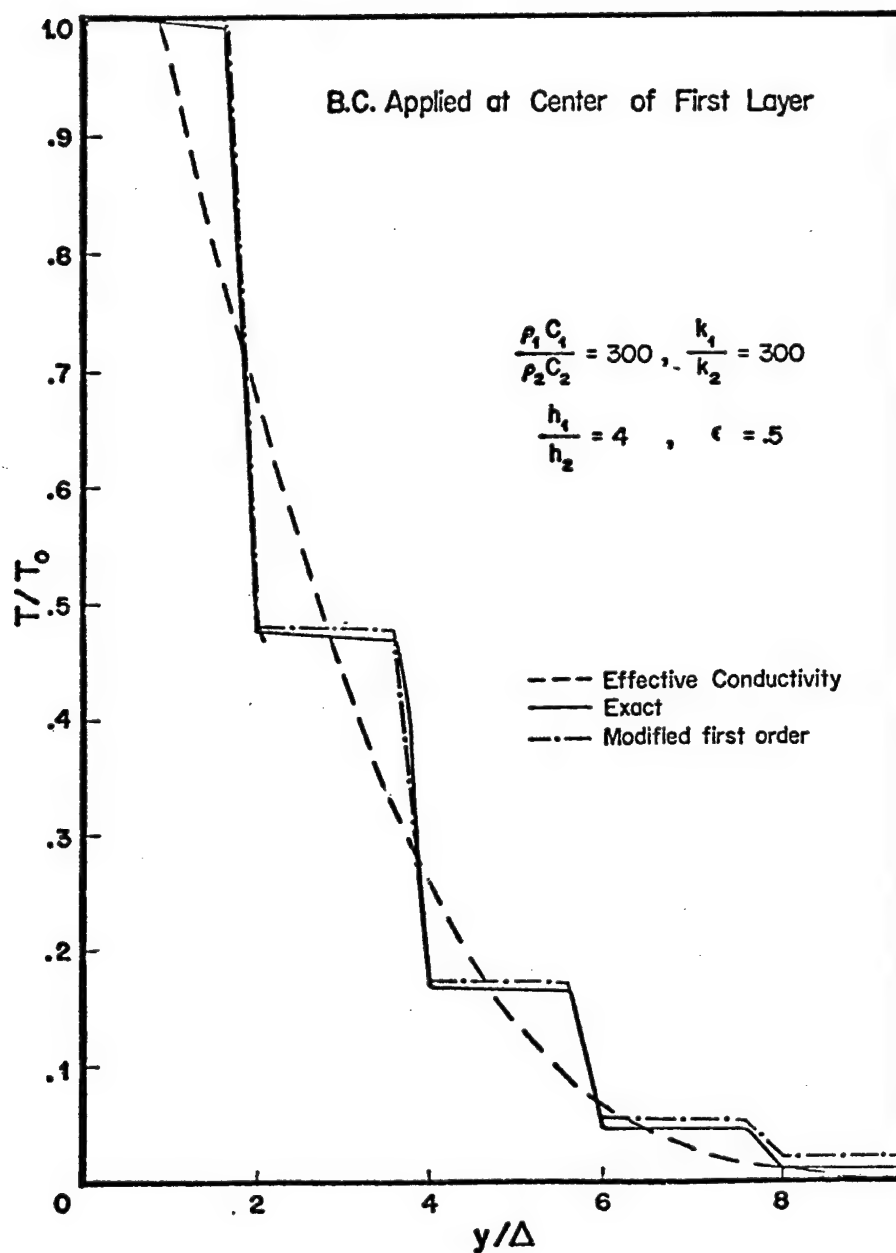


Fig. 25. Temperature distribution at $\tau = 1$ for widely differing material properties and small t_0 .

RESPONSE OF CANTILEVER PLATE (FAN BLADE)
DUE TO IMPACT LOADING

P. C. CHOU

DREXEL UNIVERSITY

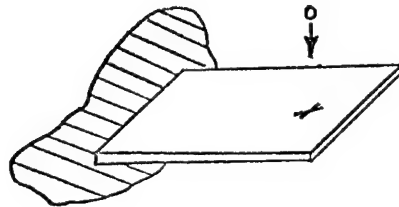
Objectives

1. Design Curve

To obtain a design curve for estimation of peak stress in structural response (in milliseconds).

2. Finite-difference Code

To develop a finite-difference computer code for anisotropic material, for local response (in micro-seconds).



Design Curve

1. Beam - Review of general approach.

Analytical Approach - 5 methods

- Lumped spring energy conserved
- Lumped mass momentum conserved
- Two-degree-of-freedom
- McQuillen solution
- Timoshenko solution

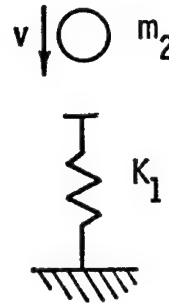
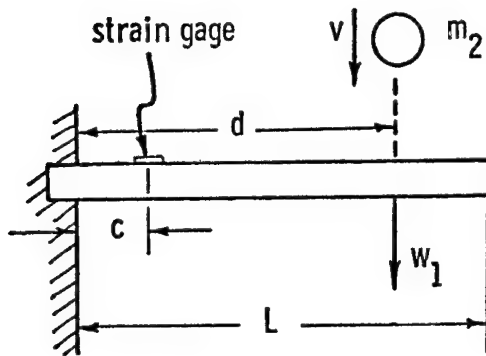
Experimental Approach

- Maximum strain measurement
- Failure experiment

2. Simply Supported Plate

3. Cantilever Plate (Fan blade)

Impact Design Curve for Cantilever Beam



1. Conservation of energy:

impactor kinetic energy = maximum beam strain energy

$$\frac{1}{2} m_2 v^2 = \frac{1}{2} K_1 w_{I\max}^2$$

K_1 = beam spring constant

2. Dynamic deflection curve assumed same as static.

$$K_1 = \frac{2E I}{d^3}$$

$$\epsilon_{x=c} = \frac{h}{d^2} \left(1 - \frac{c}{d}\right) w_{I\max}$$

3. Define generalized strain:

$$\bar{\epsilon} = \epsilon_{x=c} \frac{a^2}{hv}$$

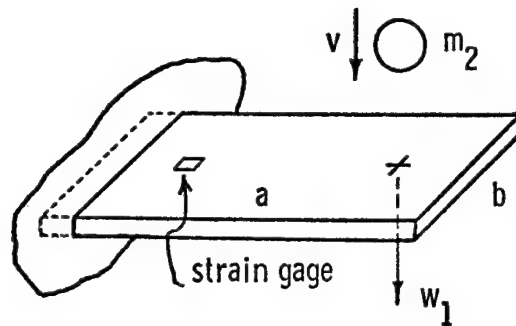
$$\text{where } a^2 = \sqrt{EI/\rho A}$$

Final result:

$$\bar{\epsilon} = \frac{C_1}{\sqrt{M}}$$

$$\text{where } C_1 = \left(1 - \frac{c}{d}\right) \sqrt{\frac{3L}{4d}}$$

Impact Design Curve for Cantilever Plate



1. Conservation of energy:

$$\frac{1}{2} m_2 v^2 = \frac{1}{2} K_1 w_{1\max}^2$$

2. Perform experiments to determine spring constant and relationship between strain and deflection by applying static load at impact point

$$P = K_1 w_1$$

$$P = K_2 \epsilon$$

$$\therefore \epsilon = \frac{K_1}{K_2} w_1$$

3. Define generalized strain:

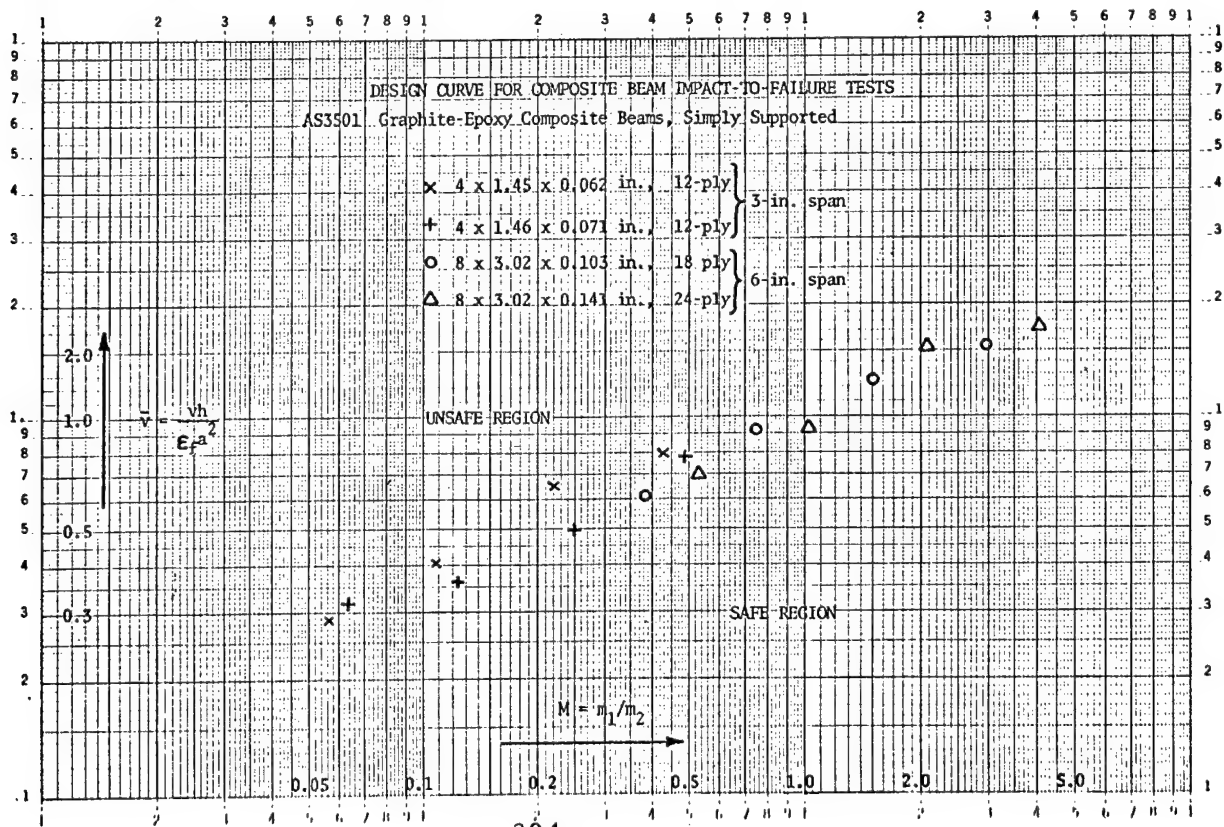
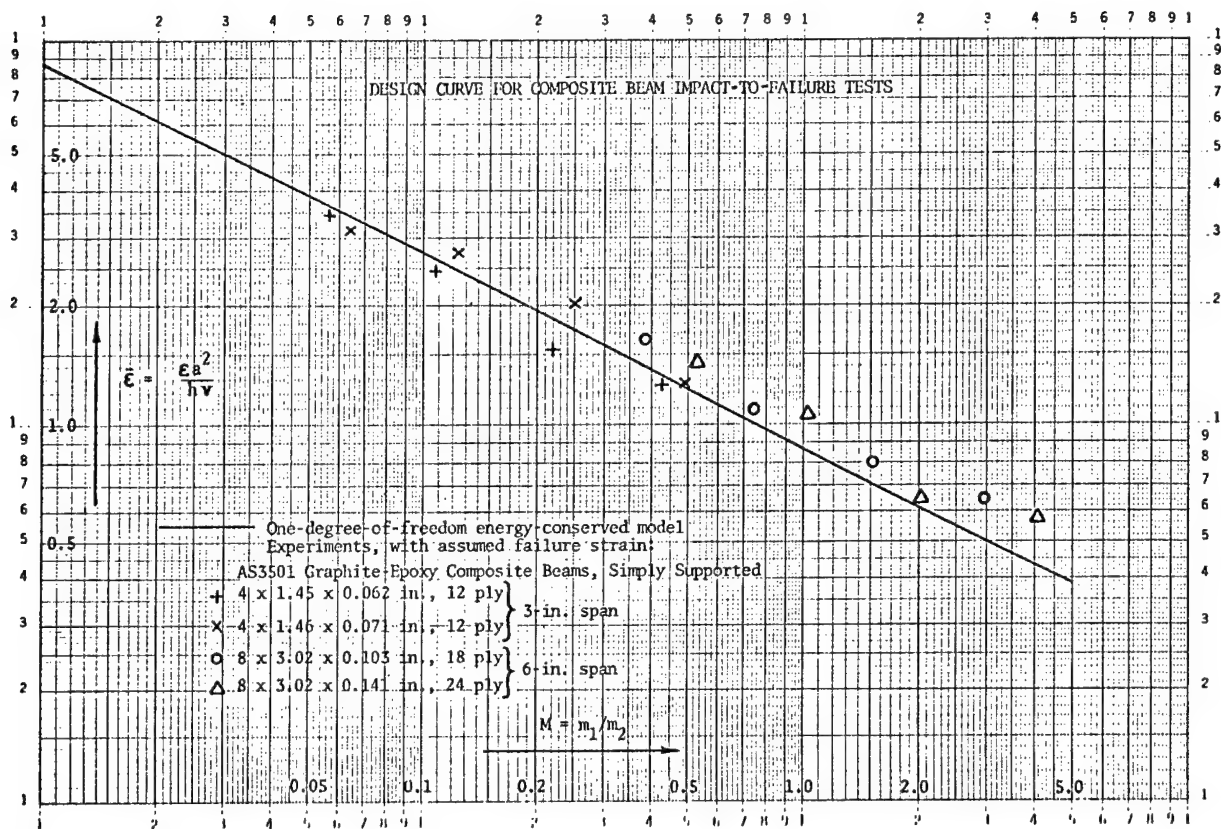
$$\bar{\epsilon} = \epsilon \frac{s^2}{hv}$$

$$\text{where } s^2 = \sqrt{D_{II}/\rho h}$$

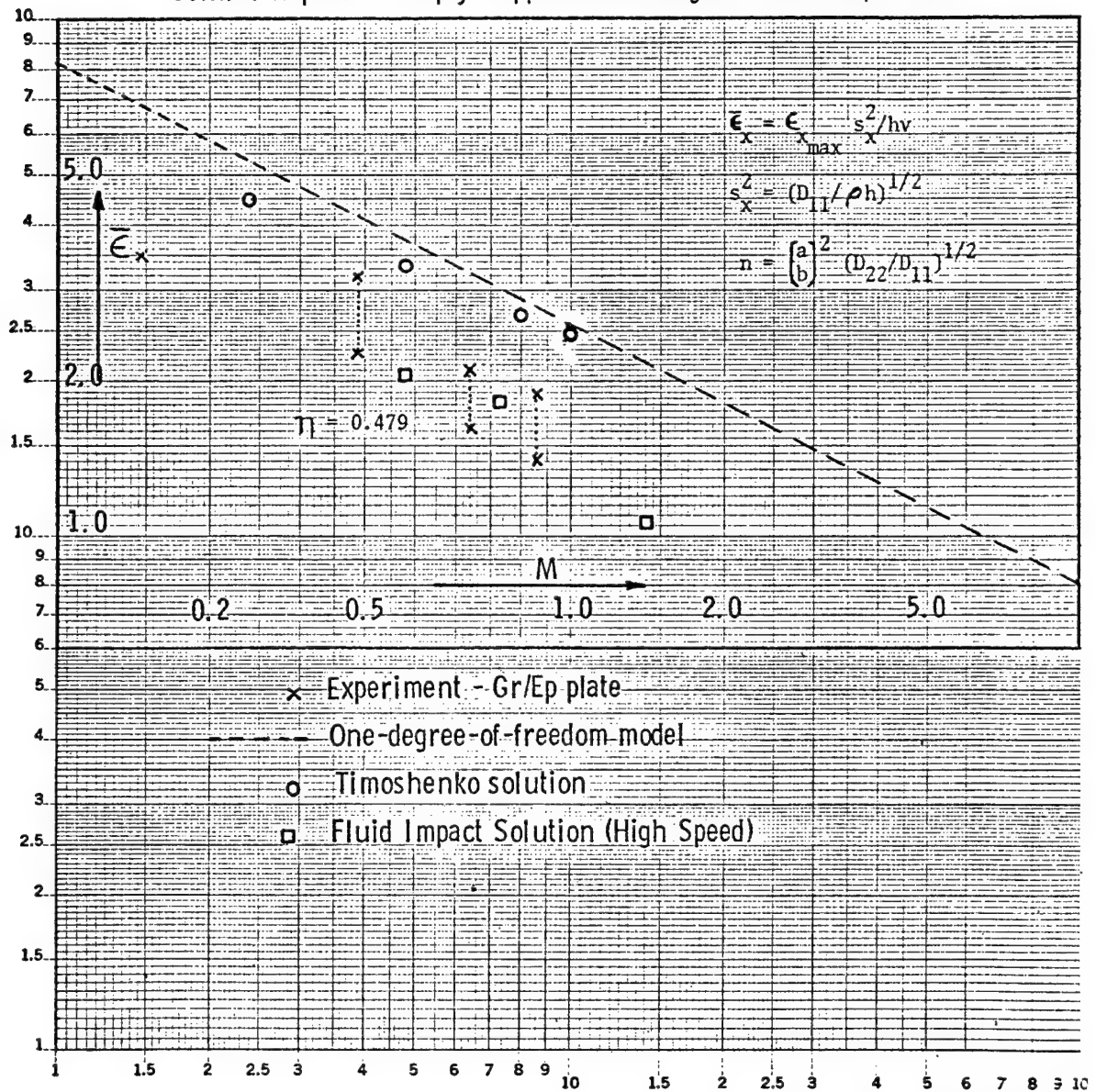
Final result:

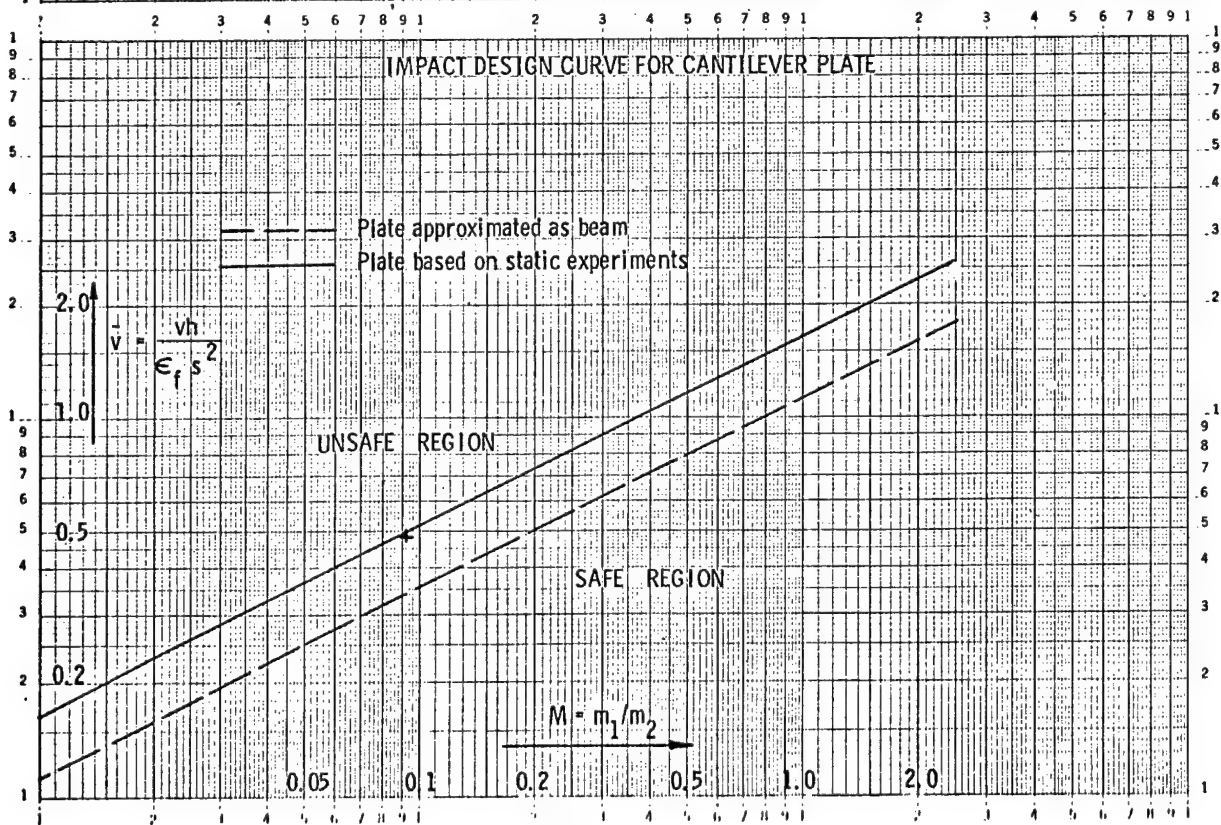
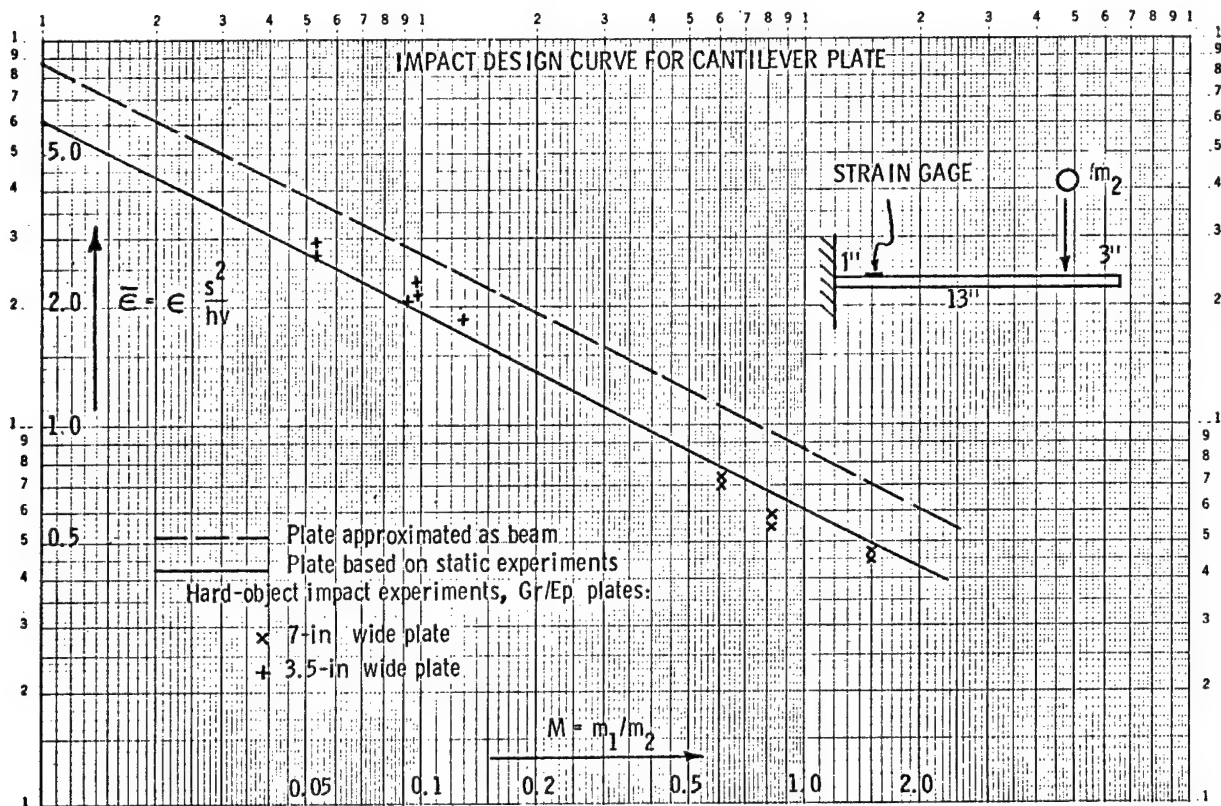
$$\epsilon = \frac{C_2}{\sqrt{M}}$$

$$\text{where } C_2 = \frac{\sqrt{D_{II} ab K_1}}{K_2 h}$$



Central Impact of Simply Supported Rectangular Orthotropic Plate





Finite-Difference Code (ANEL)
(For Local Response)

Approach : Based on HEMP

HEMP - Lagrangian, elastic-plastic-hydrodynamic, isotropic, plane strain or cylindrical symmetry.

ANEL - Lagrangian, elastic, monoclinic (plane strain or plane stress), or transversely isotropic (axisymmetric problem)

Results

1. Comparison with other calculations.
2. Comparison with experiments.

ANEL

A Finite-Difference Lagrangian Code

Governing Equations

Cauchy's Equation of Motion

$$\rho \frac{D^2 x_1}{Dt^2} = \sigma_{ij,j} + \gamma \frac{\sigma_{12}}{x_2} ; \dots$$

Conservation of Mass

$$\frac{D\rho}{Dt} + \rho \dot{x}_{i,i} + \rho \gamma \frac{\dot{x}_2}{x_2} = 0$$

Conservation of Energy

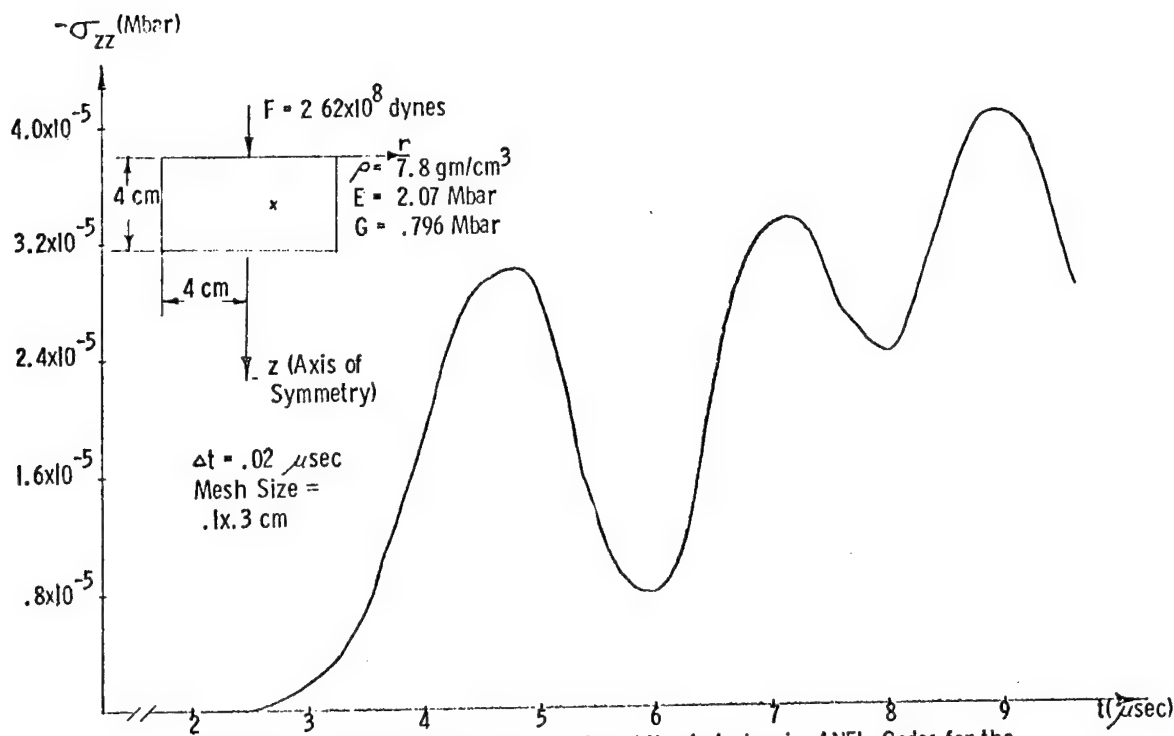
$$\rho \frac{De}{Dt} = \sigma_{ij} \dot{\epsilon}_{ij} + \gamma \sigma_{33} \dot{\epsilon}_{33}$$

Strain Displacement

$$\begin{aligned} \dot{\epsilon}_{ij} &= \frac{1}{2} (\dot{x}_{i,j} + \dot{x}_{j,i}) \\ \dot{\epsilon}_{33} &= \gamma \frac{\dot{x}_2}{x_2} \end{aligned}$$

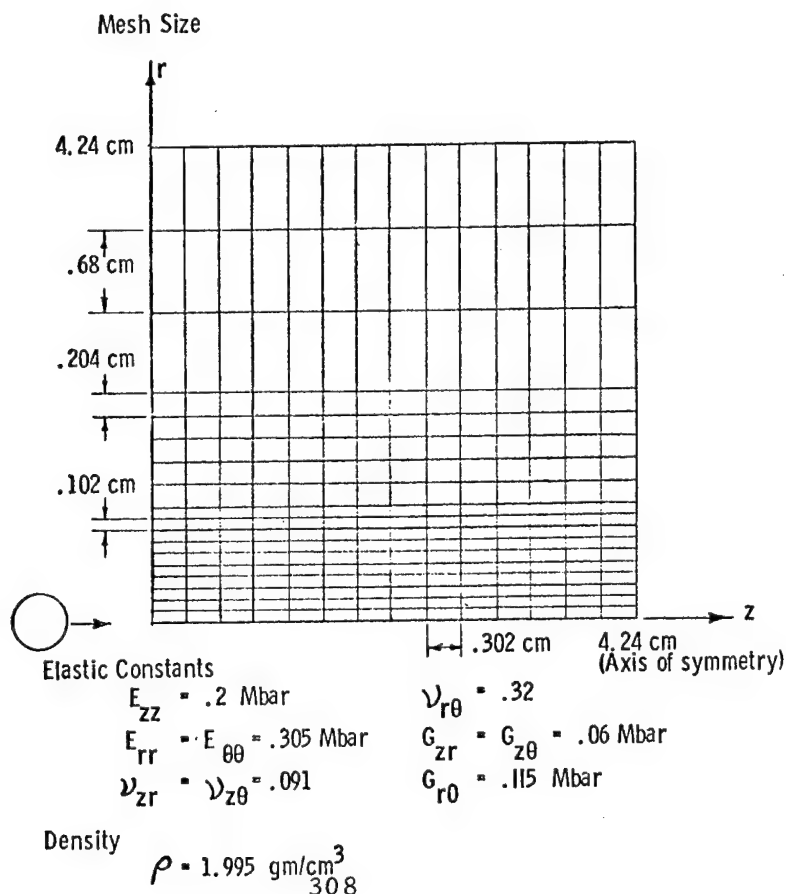
Constitutive Relations

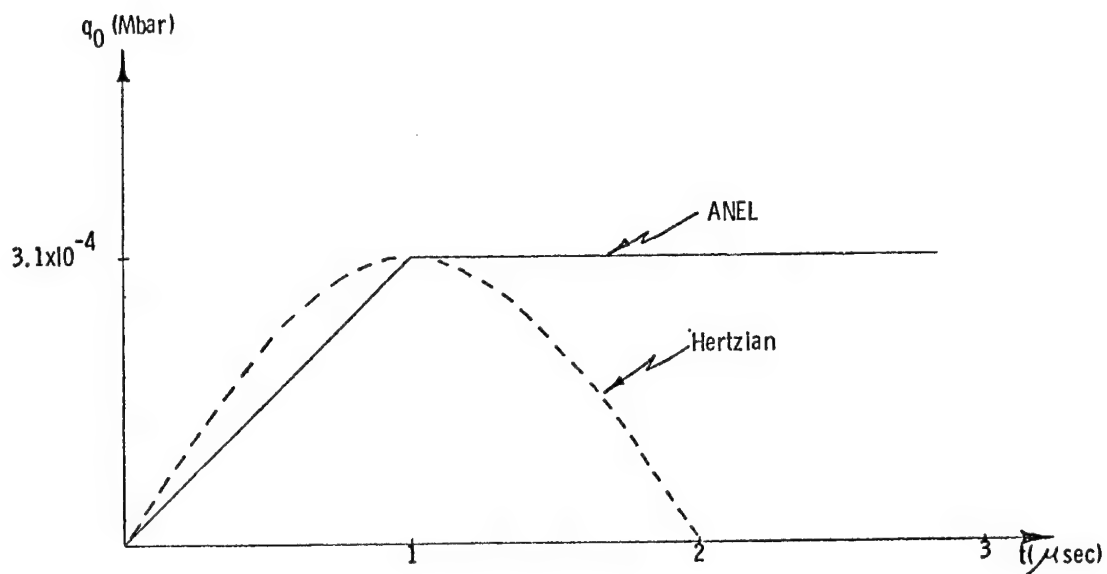
$$\begin{aligned} \dot{\sigma}_{ij} &= \frac{1}{3} \left[3 c_{ijkl} - c_{qqkl} \delta_{ij} \right] \dot{\epsilon}_{kl} \\ &\quad + \frac{1}{3} \left[3 c_{ijkk} - c_{qqkk} \delta_{ij} \right] \dot{\epsilon}_m + \dot{f}_{ij} \\ \dot{\sigma}_m &= \frac{1}{3} \left[c_{iikk} \dot{\epsilon}_{kl} + c_{iikk} \dot{\epsilon}_m \right] \end{aligned}$$



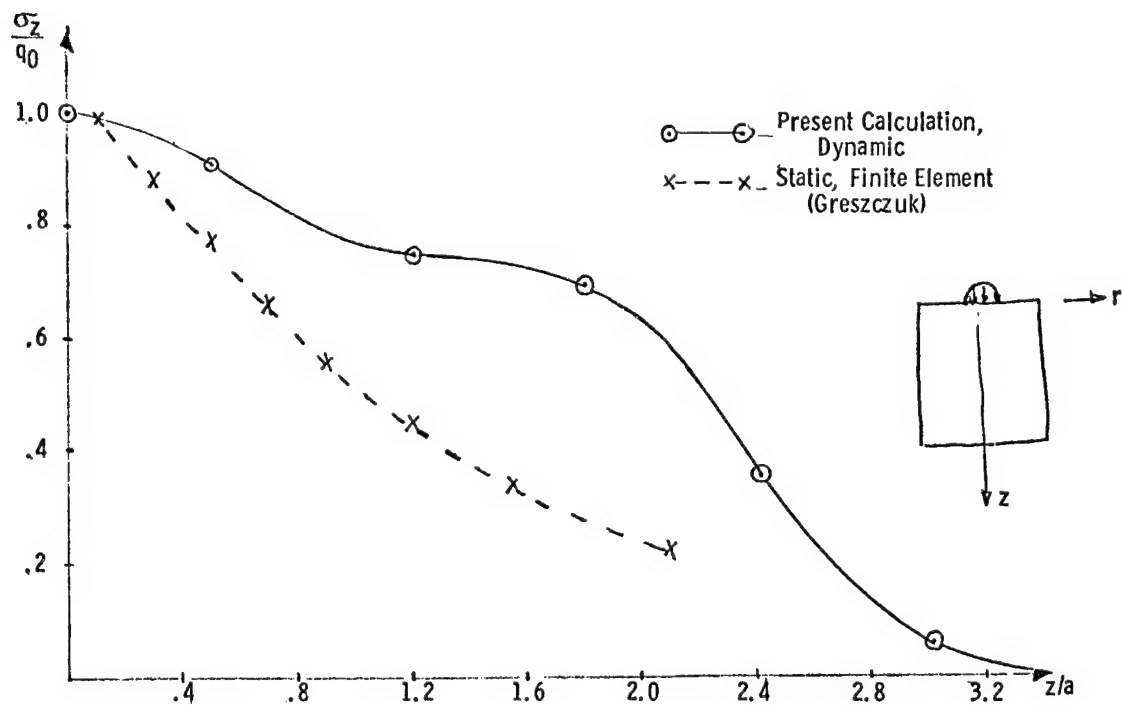
Comparison Between the Isotropic HEMP and the Anisotropic ANEL Codes for the Problem of a Concentrated Load F Suddenly Applied on an Isotropic Body. Curve shows Stress σ_{zz} at $r = 1.02$ cm, $z = 2.12$ cm for both Codes.

Glass Epoxy Under Impact of Rigid Sphere

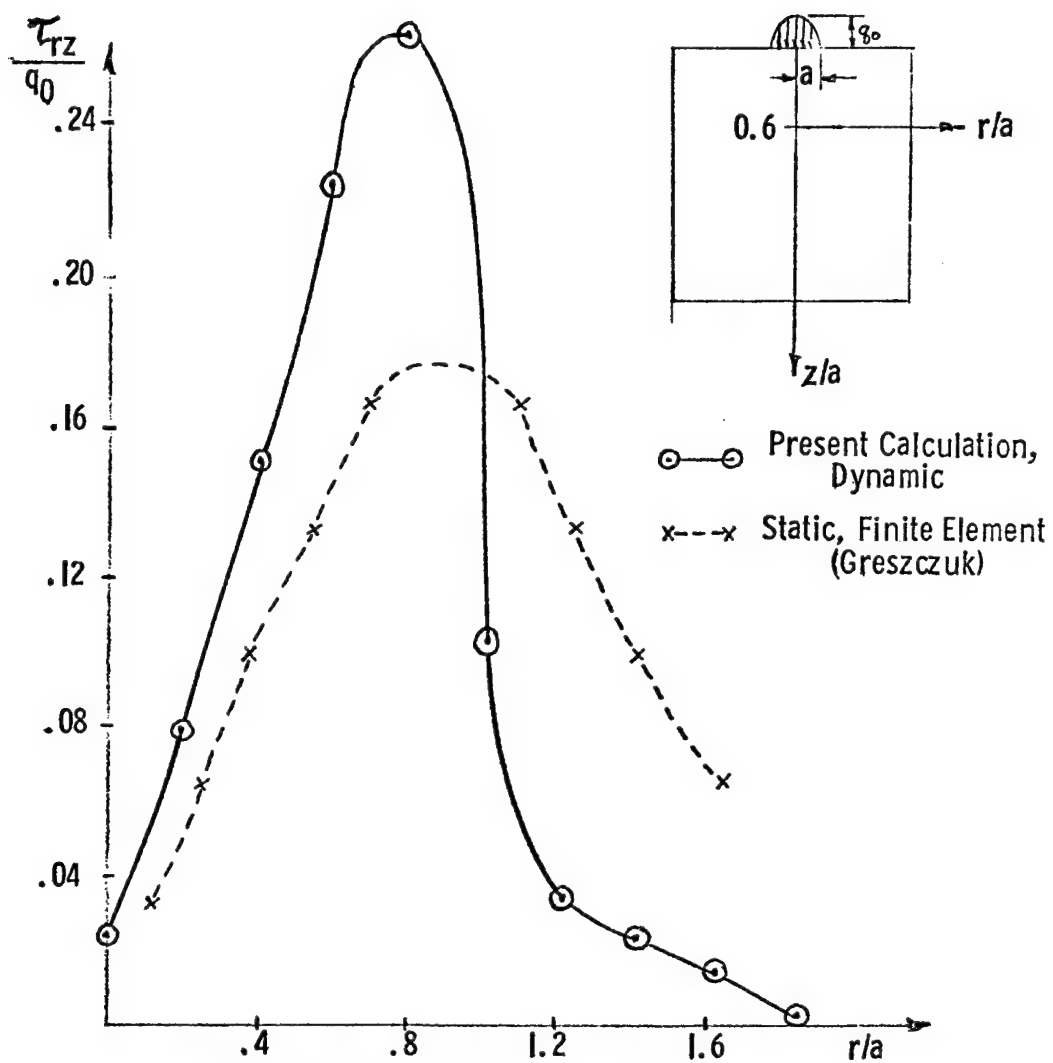




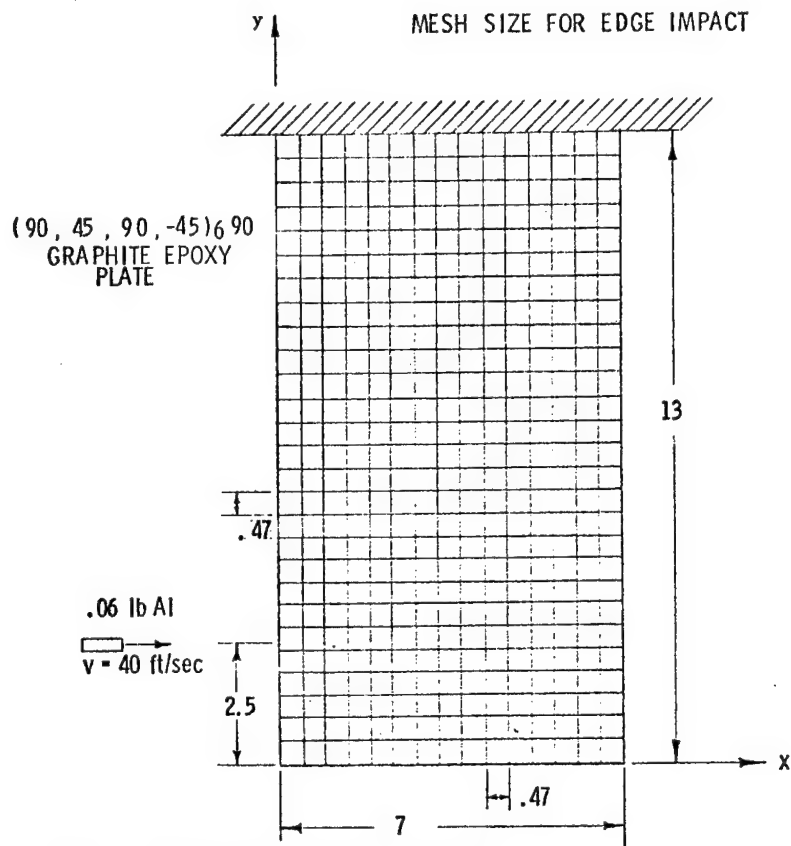
Loading Function Used in ANEL Calculation
(To be Compared with the Static Solution by Greszczuk)



Axial Distribution of Normal Stress at $4.4 \mu\text{sec}$ ($r = 0$)
Glass Epoxy Under Impact of Rigid Sphere



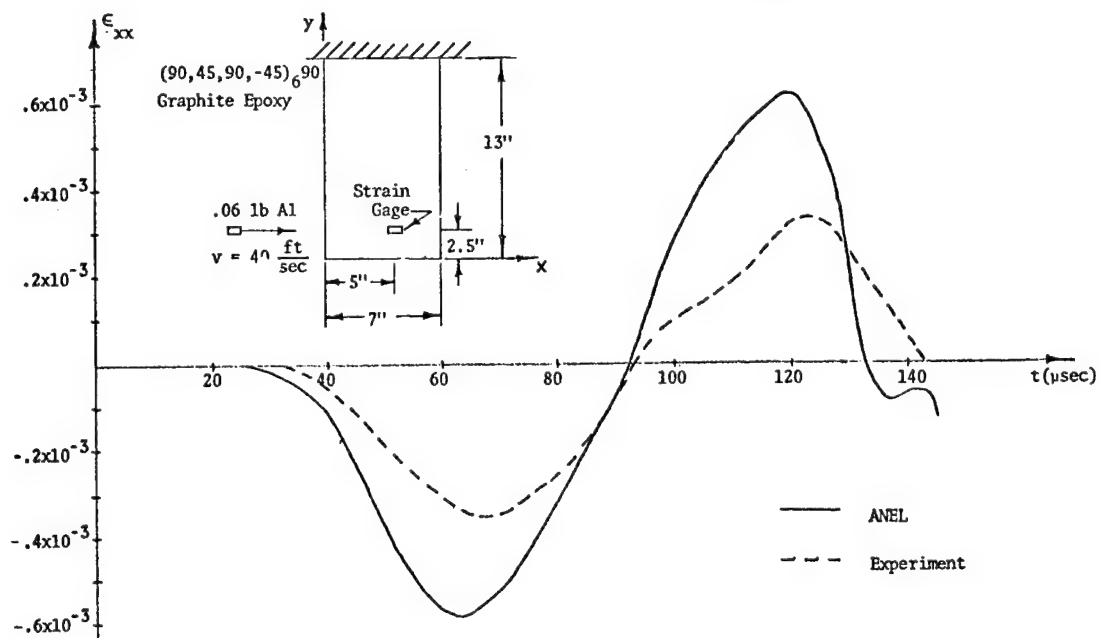
Radial Distribution of Shear Stress
 at 2.4 μ sec and $z/a = 0.6$
 Glass Epoxy Under Impact of Rigid Sphere



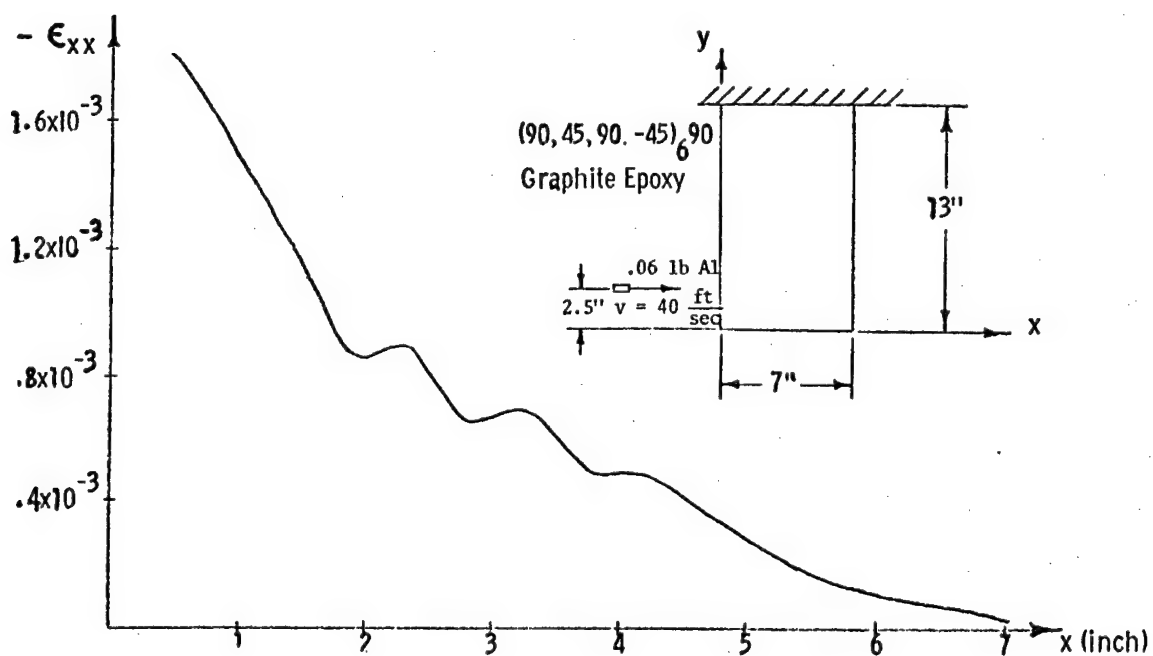
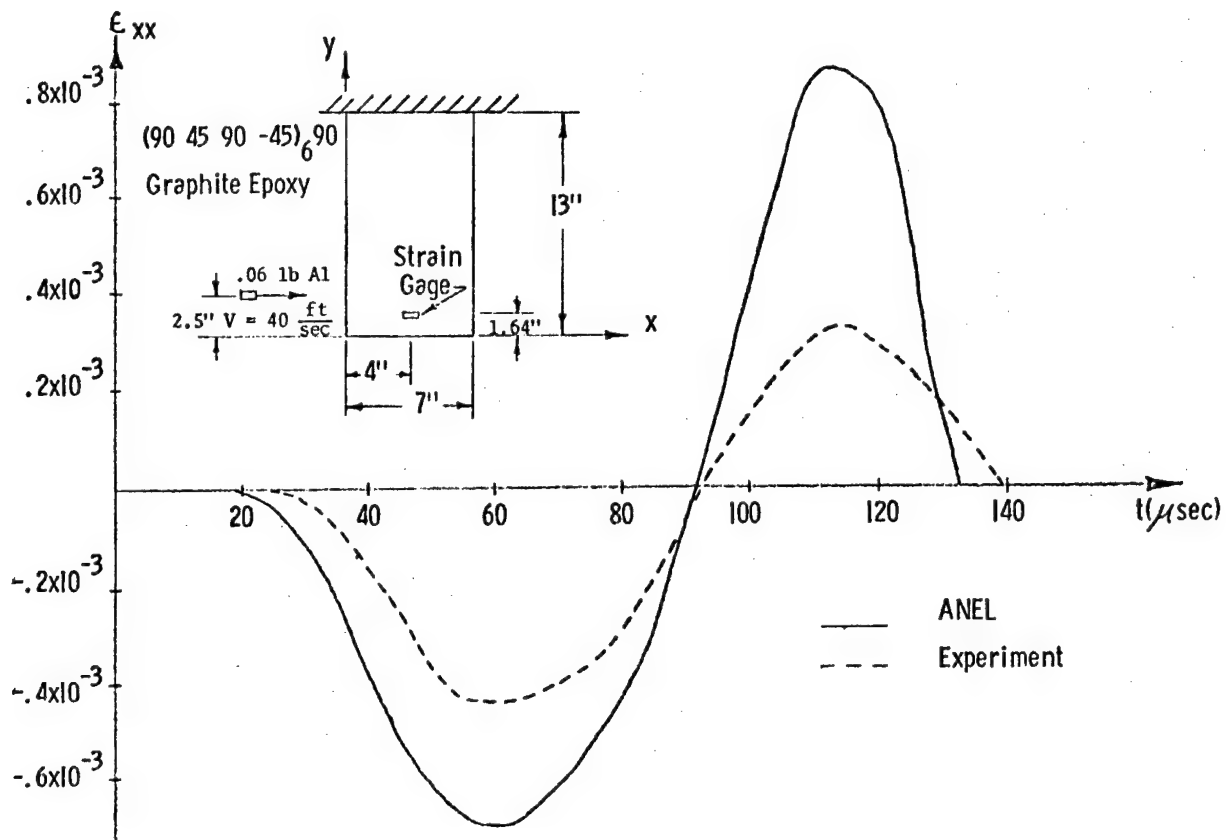
Elastic Constants for Laminated Medium

$E_{xx} = 2.9 \times 10^6$ PSI	$\nu_{xy} = .20$	$G_{xy} = 2.5 \times 10^6$ PSI
$E_{yy} = 10.3 \times 10^6$ PSI	$\nu_{yz} = .15$	$G_{yz} = .55 \times 10^6$ PSI
$E_{zz} = 1.3 \times 10^6$ PSI	$\nu_{xz} = .18$	$G_{xz} = .54 \times 10^6$ PSI

ALL DIMENSIONS IN INCH



Comparison for Edge Impact of Composite Plate



Conclusions

I. Design Curve

- A method is developed for constructing design curves for plate under impact. For a given type of structure, calculation, or testing, of a few cases is sufficient; it can be used to estimate other sizes and other impact conditions.
- Maximum strain proportional to velocity and to square root of impactor mass.

$$\sigma_{\max} \propto V \sqrt{m_2}$$

2. Anisotropic Code

- An anisotropic finite-difference computer code is developed for local impact response calculation.
- dynamic stress higher than quasi-static stress
- May be extended to include plastic and hydrodynamic constitutive equations.

MECHANICS OF COMPOSITE MATERIALS
WITH DIFFERENT MODULI IN
TENSION AND COMPRESSION

ROBERT M. JONES
SOUTHERN METHODIST UNIVERSITY
DALLAS, TEXAS

OUTLINE

- INTRODUCTION
- NONLINEAR MULTIMODULUS MATERIAL MODEL
- MATERIAL MODELING ACCOMPLISHMENTS
- MATERIAL MODELING IN PROGRESS
- SUMMARY

INTRODUCTION

BILINEAR MODEL FOR MULTIMODULUS MATERIALS

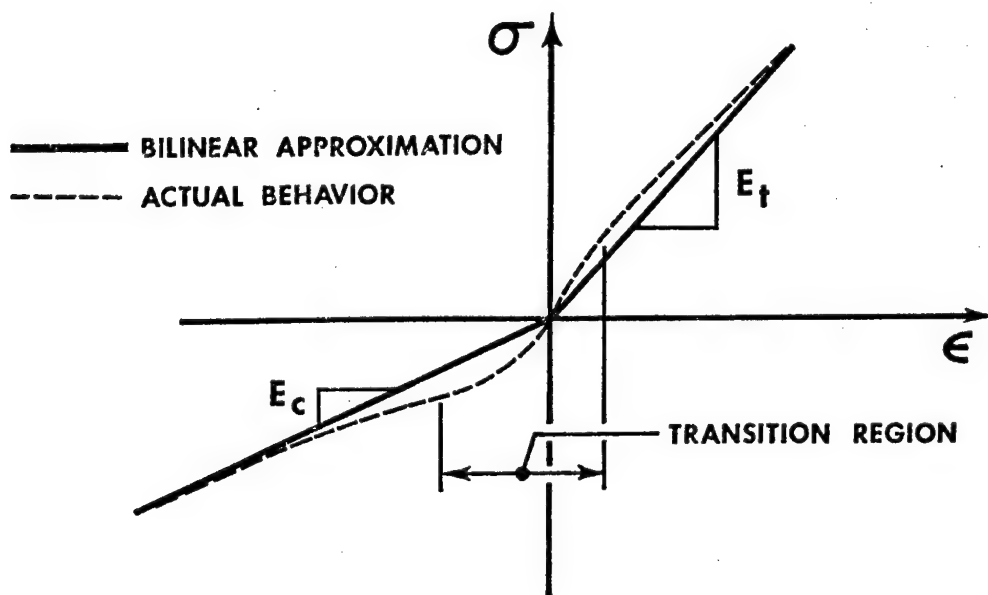
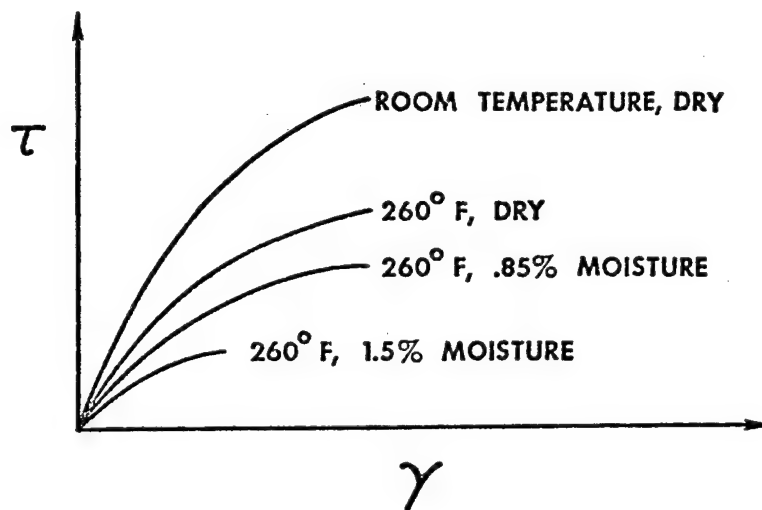


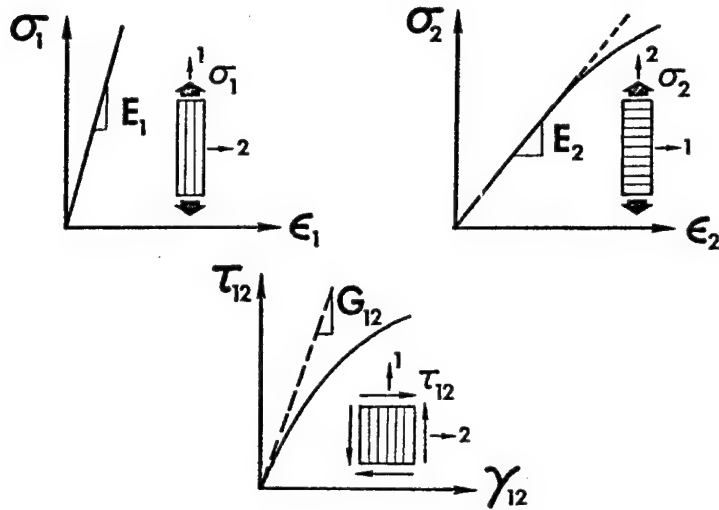
TABLE 1
TENSION AND COMPRESSION MODULI RELATIONSHIPS
FOR SEVERAL COMMON COMPOSITE MATERIALS

MATERIAL	FIBROUS OR GRANULAR	REPRESENTATIVE MODULI RELATIONSHIP
GLASS/EPOXY	FIBROUS	$E_t = 1.2E_c$
BORON/EPOXY	FIBROUS	$E_c = 1.2E_t$
GRAPHITE/EPOXY	FIBROUS	$E_t = 1.4E_c$
CARBON/CARBON	FIBROUS	$E_t = 2-5E_c$
ZTA GRAPHITE	GRANULAR	$E_c = 1.2E_t$
ATJ-S GRAPHITE	GRANULAR	$E_t = 1.2E_c$

EFFECT OF MOISTURE AND TEMPERATURE ON STRESS-STRAIN CURVE NONLINEARITY



TYPICAL STRESS-STRAIN BEHAVIOR OF FIBER-REINFORCED COMPOSITE MATERIALS



OBJECTIVES

MECHANICS OF COMPOSITE MATERIALS WITH DIFFERENT MODULI IN TENSION AND COMPRESSION

- DEVELOP MATERIAL MODEL FOR NONLINEAR MULTIMODULUS BEHAVIOR OF VARIOUS CLASSES OF COMPOSITE MATERIALS
- ANALYZE STRESS EQUILIBRIUM BEHAVIOR OF SOLID BODIES (E.G., THERMAL STRESSES \rightarrow SIMULTANEOUS TENSILE AND COMPRESSIVE STRESSES)
 - LINEAR ELASTIC MULTIMODULUS
 - NONLINEAR ELASTIC
 - NONLINEAR ELASTIC MULTIMODULUS
- ANALYZE BENDING, BUCKLING, AND VIBRATION BEHAVIOR OF LAMINATED PLATES AND SHELLS
 - LINEAR ELASTIC (LAMINATION ASYMMETRIES)
 - LINEAR ELASTIC MULTIMODULUS
 - NONLINEAR ELASTIC
 - NONLINEAR ELASTIC MULTIMODULUS

JONES - NELSON

NONLINEAR MATERIAL MODEL

ORTHOTROPIC STRESS-STRAIN RELATIONS AXISYMMETRIC BEHAVIOR

$$\begin{Bmatrix} \epsilon_r \\ \epsilon_z \\ \epsilon_\theta \\ \gamma_{rz} \end{Bmatrix} = \begin{bmatrix} \frac{1}{E_r} & -\frac{\nu_{rz}}{E_r} & -\frac{\nu_{r\theta}}{E_r} & 0 \\ -\frac{\nu_{rz}}{E_r} & \frac{1}{E_z} & -\frac{\nu_{z\theta}}{E_z} & 0 \\ -\frac{\nu_{r\theta}}{E_r} & -\frac{\nu_{z\theta}}{E_z} & \frac{1}{E_\theta} & 0 \\ 0 & 0 & 0 & \frac{1}{G_{rz}} \end{bmatrix} \begin{Bmatrix} \sigma_r \\ \sigma_z \\ \sigma_\theta \\ \tau_{rz} \end{Bmatrix}$$

MATERIAL PROPERTY - ENERGY RELATIONS

$$\text{MATERIAL PROPERTY}_i = A_i \left[1 - B_i \left(\frac{U}{U_{0i}} \right)^{C_i} \right]$$

A_i = INITIAL ELASTIC VALUE

B_i = INITIAL CURVATURE OF σ - ϵ CURVE

C_i = RATE OF CHANGE OF CURVATURE

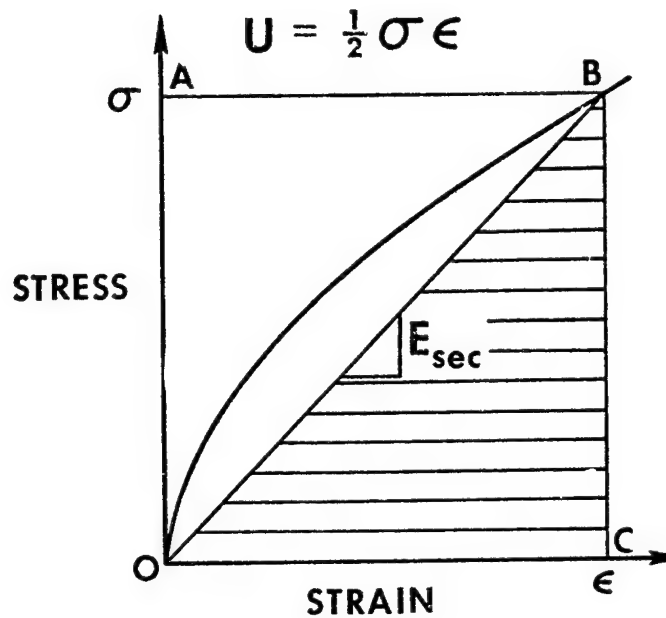
U = STRAIN ENERGY

U_{0i} = UNIT STRAIN ENERGY

STRAIN ENERGY FUNCTION

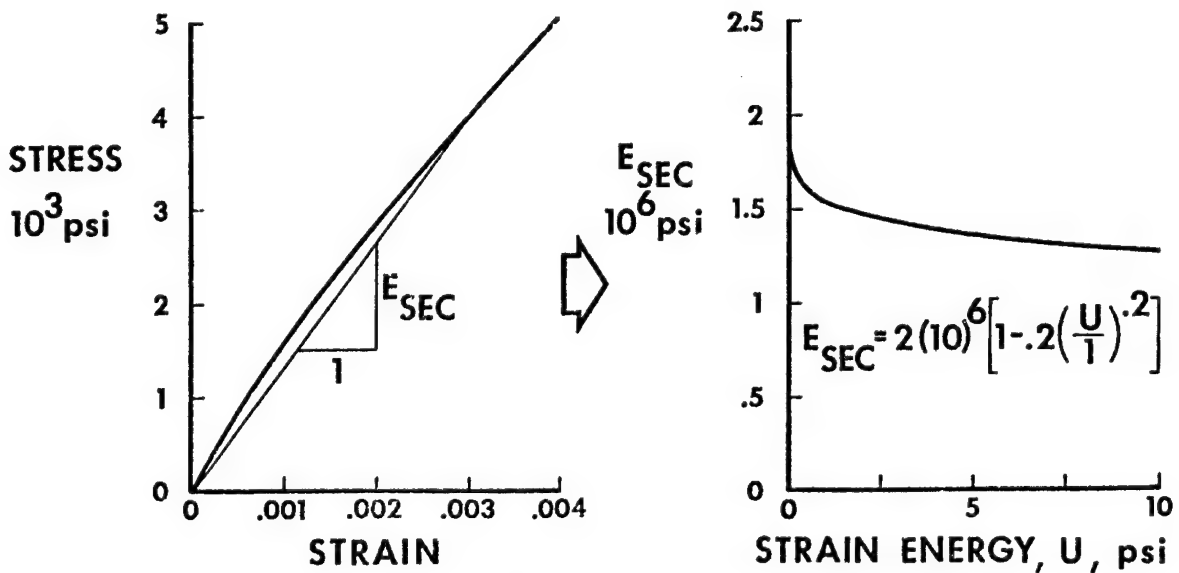
$$U = \frac{1}{2}(\sigma_r \epsilon_r + \sigma_z \epsilon_z + \sigma_\theta \epsilon_\theta + \tau_{rz} \gamma_{rz})$$

UNIAXIAL INTERPRETATION OF THE STRAIN ENERGY



REPRESENTATION OF STRESS-STRAIN BEHAVIOR

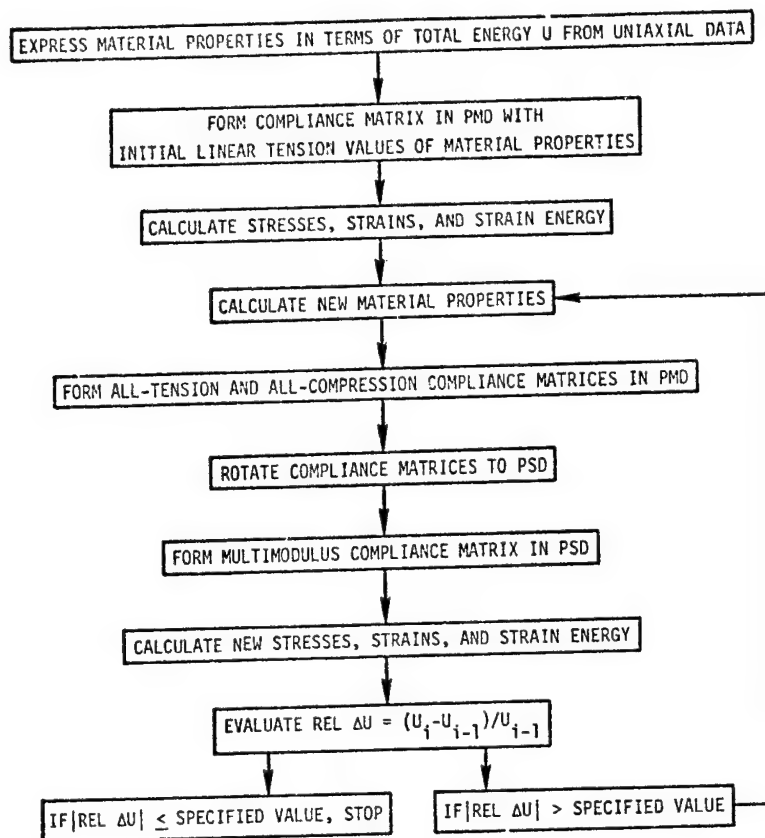
DIRECT MODULI



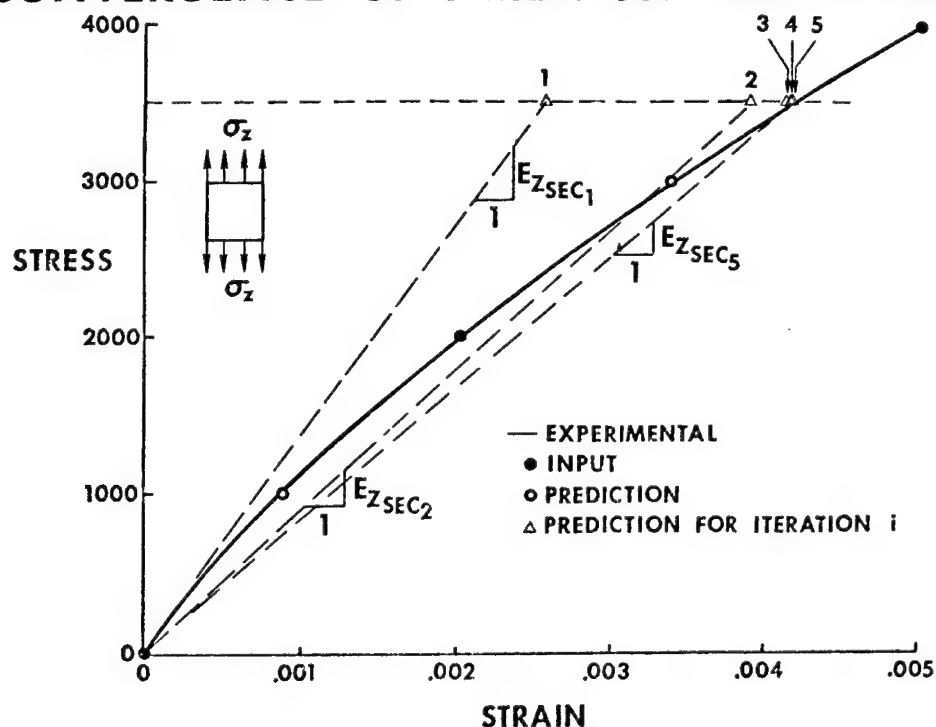
ITERATION PROCEDURE

PMD = PRINCIPAL
MATERIAL
DIRECTIONS

PSD = PRINCIPAL
STRESS
DIRECTIONS

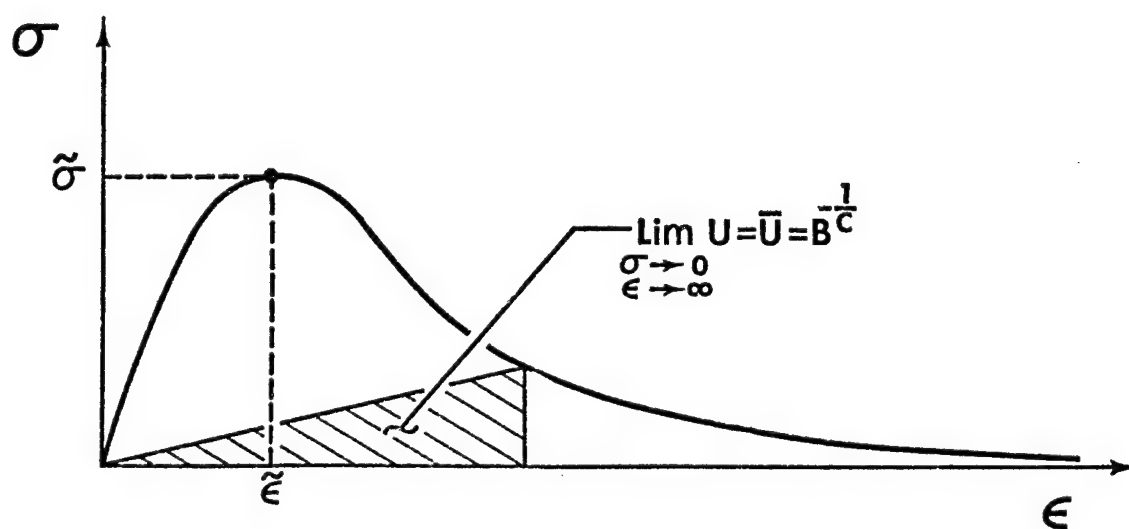


CONVERGENCE OF ITERATION PROCEDURE

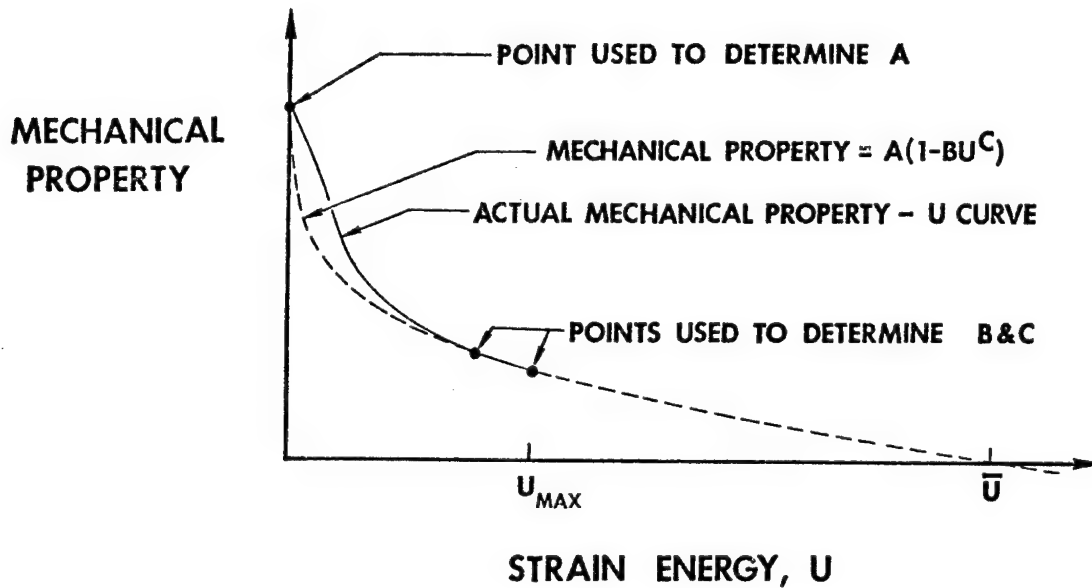


EXTENSION OF JONES - NELSON MODEL

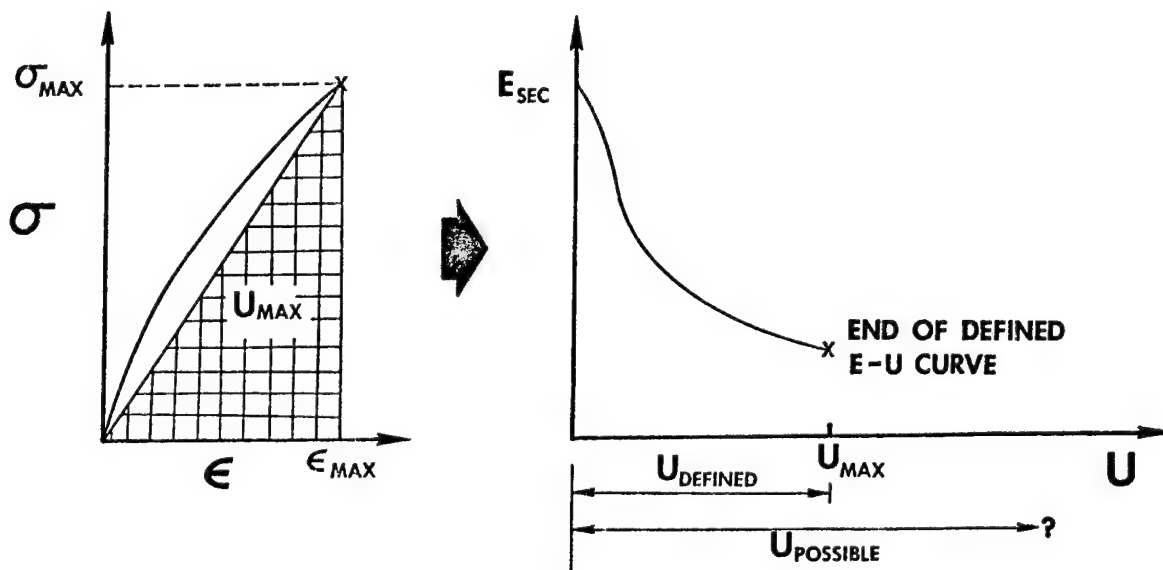
REPRESENTATIVE IMPLIED STRESS - STRAIN CURVE



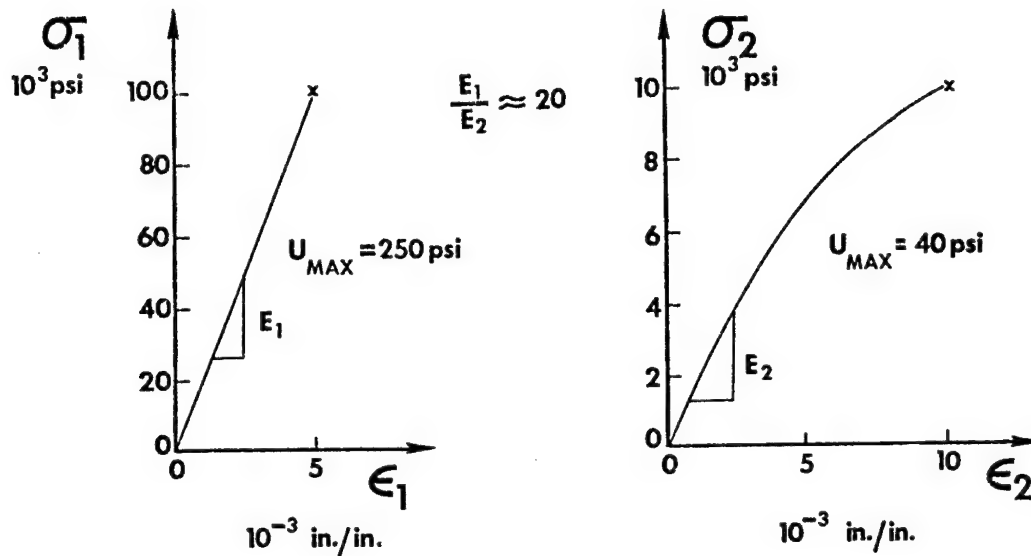
ACTUAL VS. EXTENDED APPROXIMATE MECHANICAL PROPERTY VS. U CURVE



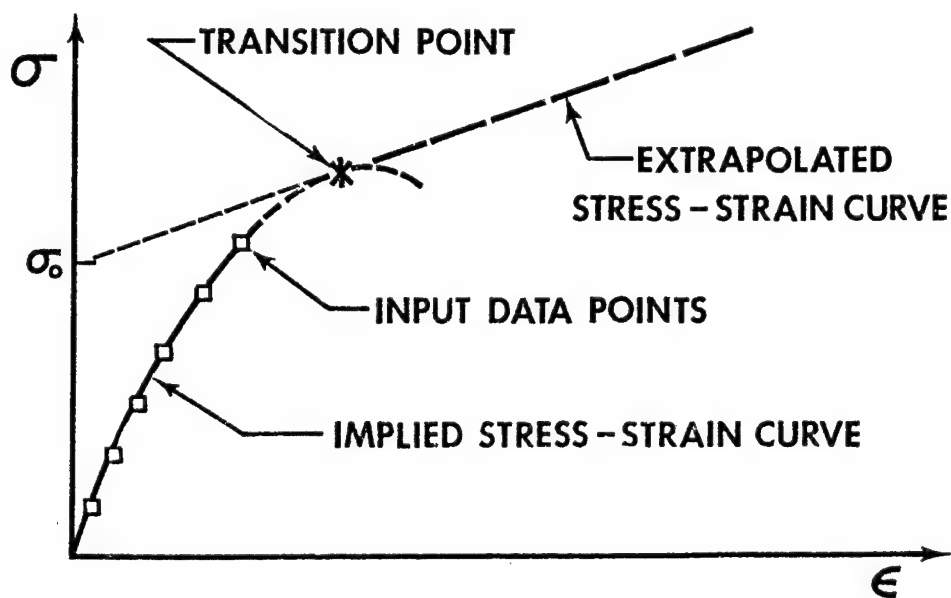
LIMIT OF MEASURED DATA FOR MECHANICAL PROPERTY VS. U CURVE



LIMITS OF STRESS-STRAIN DATA FOR DIFFERENT PRINCIPAL MATERIAL DIRECTIONS

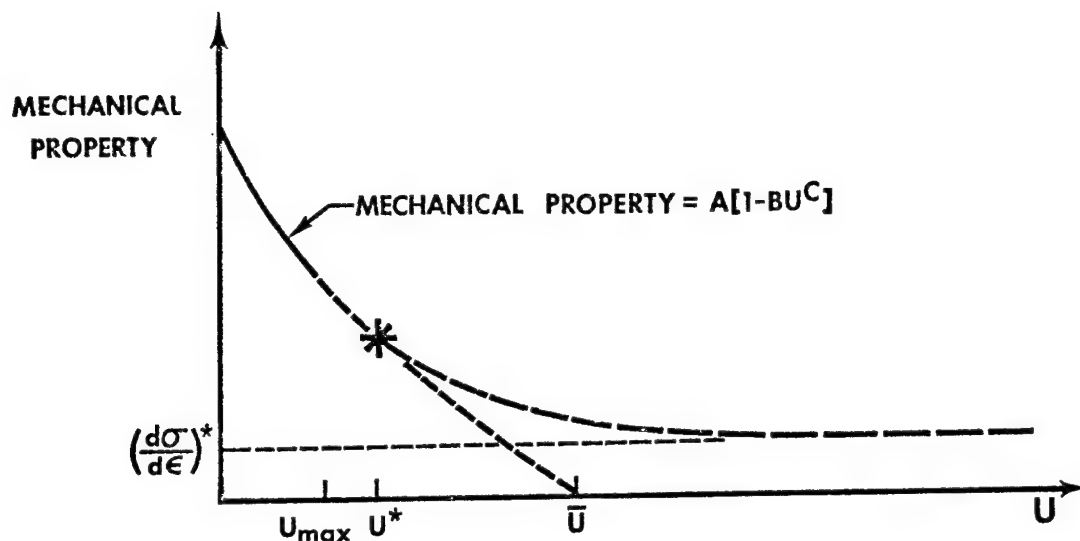


EXTENDED STRESS-STRAIN CURVE APPROACH JONES-NELSON-MORGAN A, B, AND C PLUS INPUT SLOPE



EXTRAPOLATION OF MECHANICAL PROPERTY BEHAVIOR

JONES - NELSON - MORGAN A, B, AND C PLUS INPUT SLOPE



DEFINITION OF A MATERIAL MODEL

- OFTEN -
THE STRESS-STRAIN RELATIONS FOR THE MATERIAL
- HERE -
THE SET OF MECHANICAL PROPERTY VERSUS ENERGY EQUATIONS
PLUS THE ASSOCIATED ITERATION PROCEDURE FOR THE MATERIAL

STEPS TO DEFINE AND VALIDATE MATERIAL MODELS

- (1) FIT MECHANICAL PROPERTY VERSUS ENERGY EQUATIONS
TO UNIAXIAL STRESS - STRAIN DATA IN PMD*
⇒ MATERIAL MODEL IS DEFINED
- (2) USE MATERIAL MODEL TO PREDICTED STRAINS
UNDER UNIAXIAL LOADING IN OTHER THAN PMD*
AND COMPARE PREDICTED WITH MEASURED STRAINS
- (3) USE MATERIAL MODEL TO PREDICT STRAINS
UNDER BIAXIAL LOADING IN PMD* AND OTHER THAN PMD*
AND COMPARE PREDICTED WITH MEASURED STRAINS
- (4) IF ALL COMPARISONS ARE SATISFACTORY,
THEN MATERIAL MODEL IS REGARDED AS VALIDATED

*PMD = PRINCIPAL MATERIAL DIRECTIONS

MATERIAL MODELING ACCOMPLISHMENTS

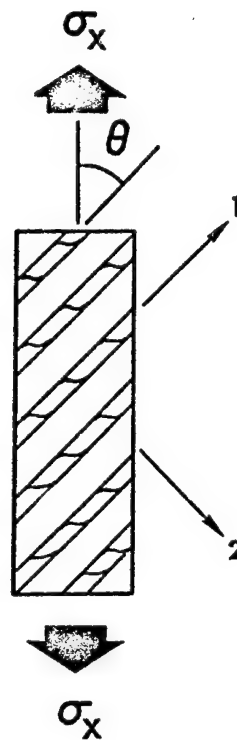
MATERIAL	TYPE OF MATERIAL	NUMBER OF NONLINEARITIES		MATERIAL MODEL		
		TENSION	COMPRESSION	MULTIMODULUS ELASTIC	NONLINEAR	NONLINEAR MULTIMODULUS
ATJ-S GRAPHITE	TRANSVERSELY ISOTROPIC	5	5			✓
BORON/EPOXY	ORTHOTROPIC LAMINA	1	1	✓	✓	
GRAPHITE/EPOXY	ORTHOTROPIC LAMINA	1	1	✓	✓	
BORON/ALUMINUM	ORTHOTROPIC LAMINA	3	3		✓	
CARBON-CARBON	ORTHOTROPIC LAMINA AND ANISOTROPIC 3-D WEAVE	4-9	4-9	✓		

MATERIAL MODELING ACCOMPLISHMENTS

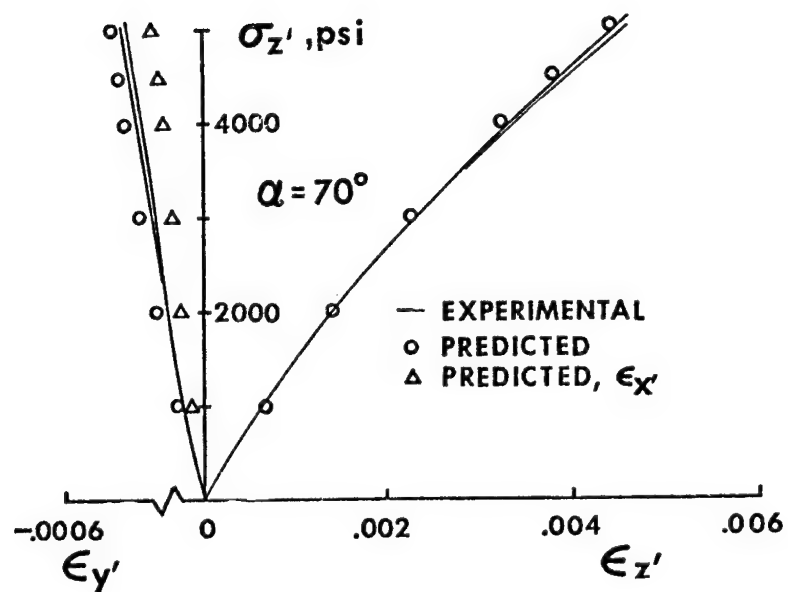
MATERIAL	COMPARISON WITH EXPERIMENT				
	UNIAXIAL		BIAXIAL		
	PMD*	OFF-AXIS	TUBE	DISK	LAMINATE
ATJ-S GRAPHITE	✓	✓	✓	✓	N/A
BORON/EPOXY	✓	✓			✓
GRAPHITE/EPOXY	✓	✓			
BORON/ALUMINUM	✓				✓
CARBON-CARBON					

*PMD = PRINCIPAL MATERIAL DIRECTIONS

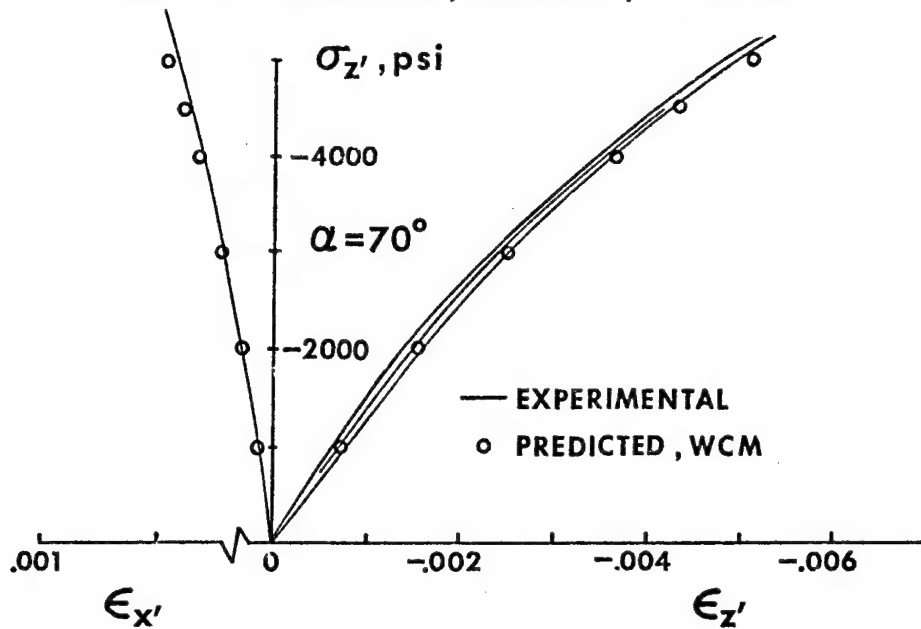
OFF - AXIS TEST



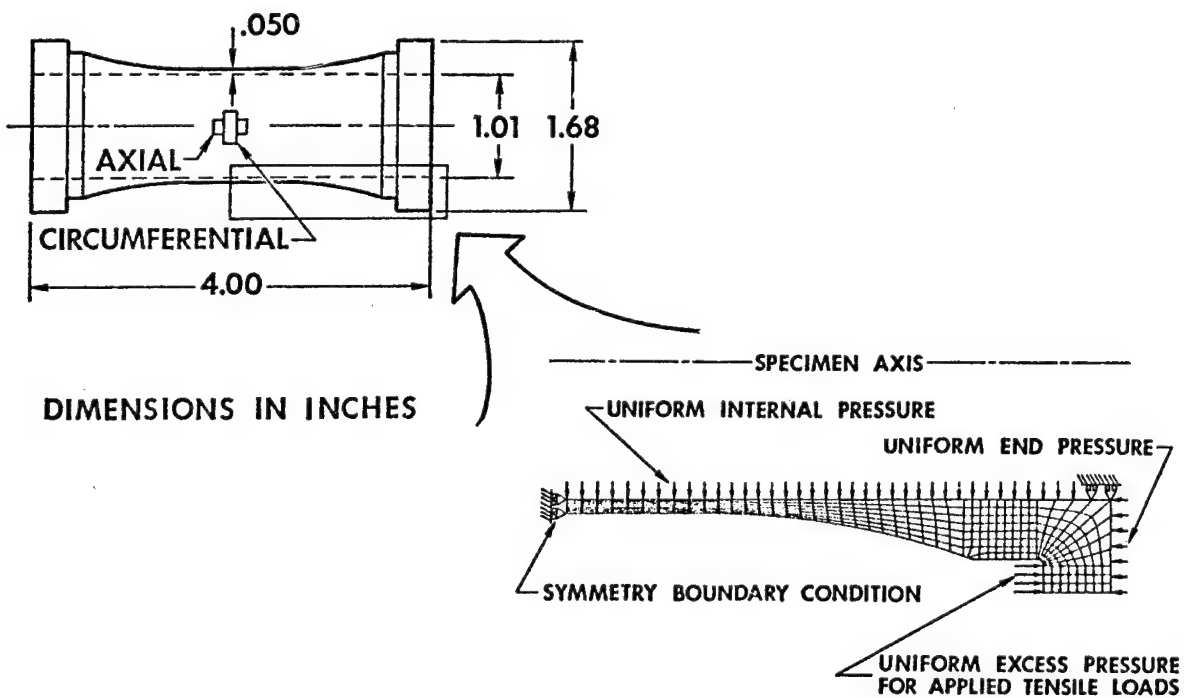
OFF-AXIS σ - ϵ BEHAVIOR TENSION, $\alpha = 70^\circ$



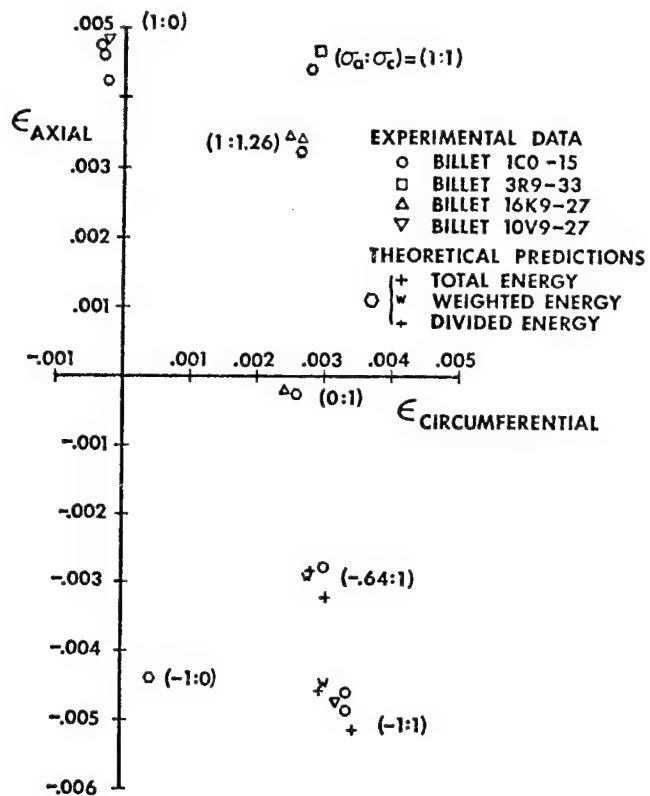
OFF-AXIS σ - ϵ BEHAVIOR COMPRESSION, $\alpha=70^\circ$, WCM



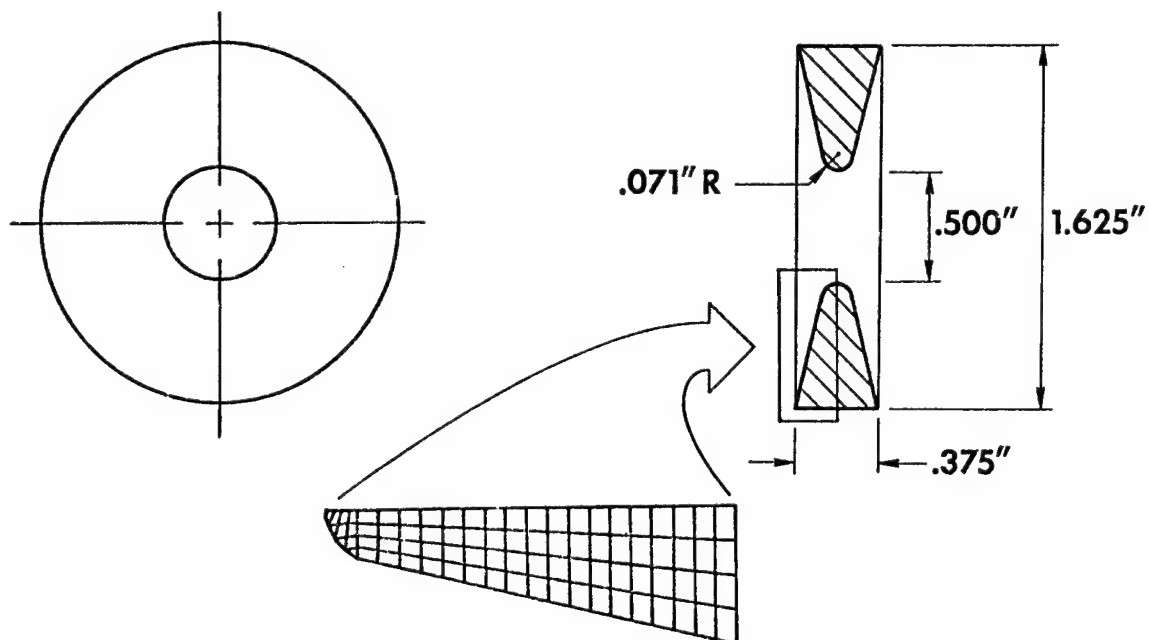
HOLLOW GRAPHITE BIAXIAL TEST SPECIMEN



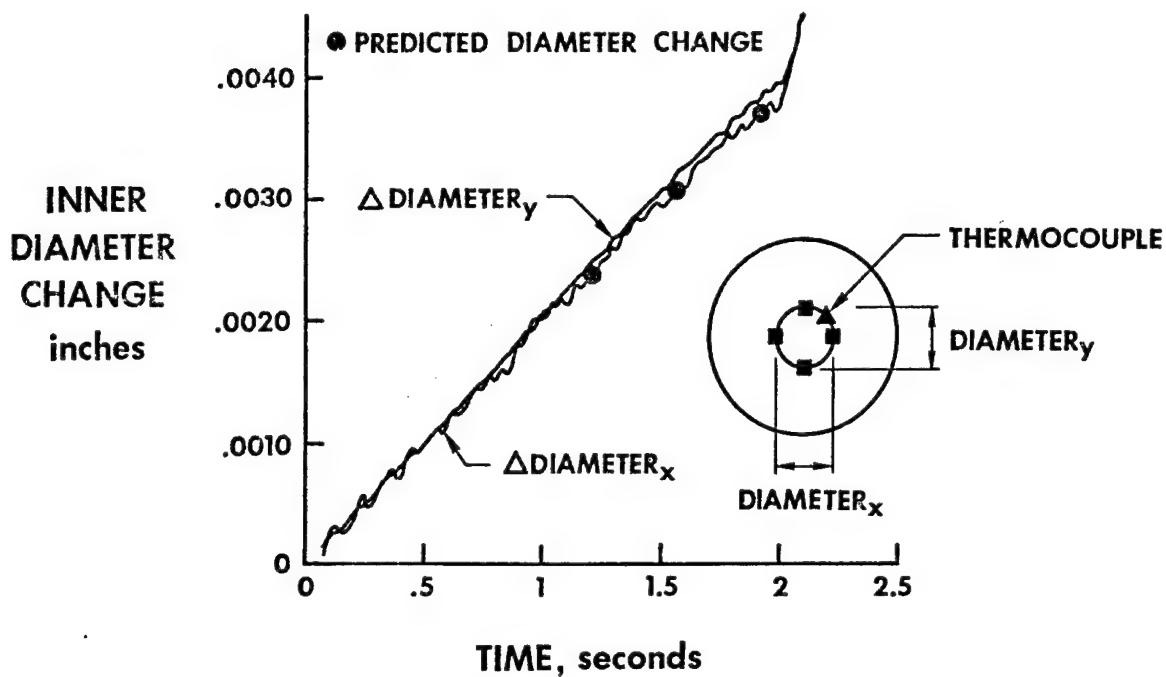
BIAXIAL STRAINS NONLINEAR WCM MODEL 16K9-27 DATA SET



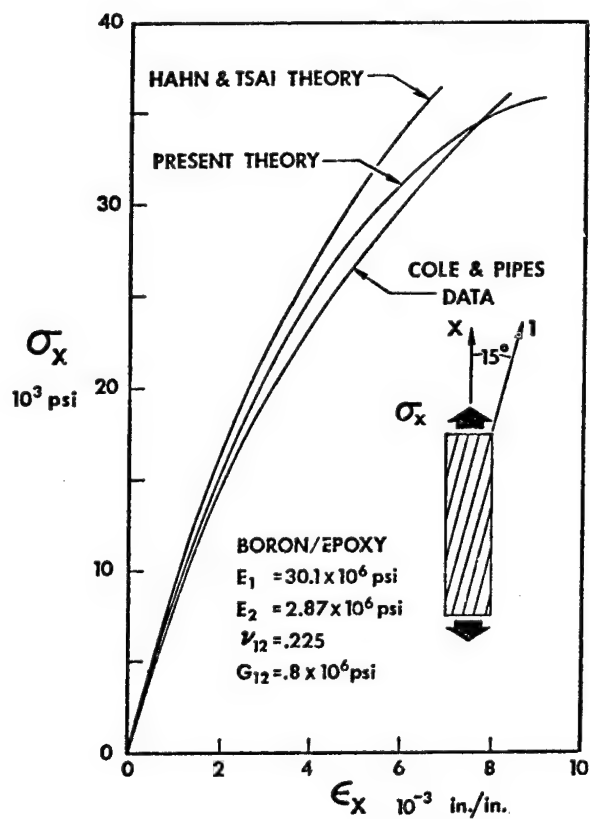
WEDGE-SHAPED DISK AND IDEALIZATION



DISK INNER DIAMETER CHANGE VS. TIME



OFF - AXIS STRESS - STRAIN BEHAVIOR

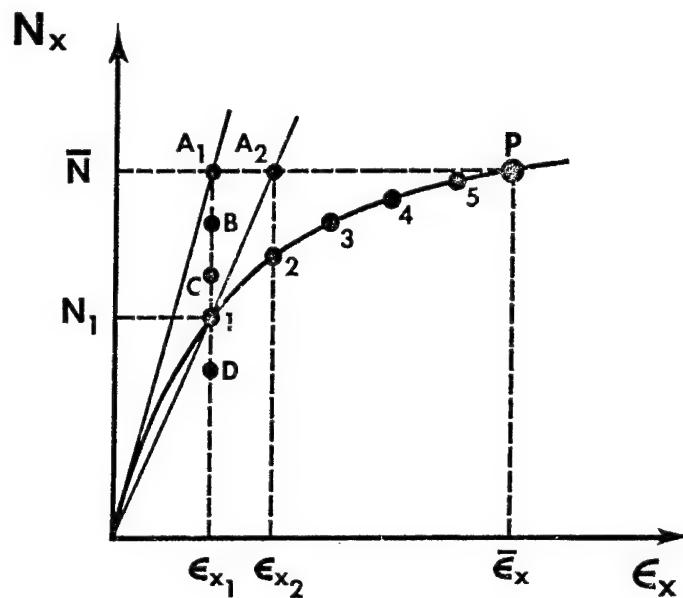


MATERIAL MODELING IN PROGRESS

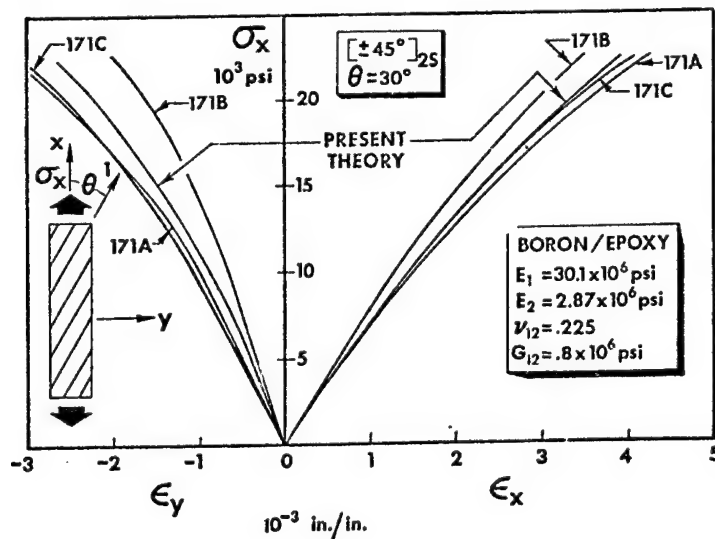
MATERIAL MODELING IN PROGRESS

- NONLINEAR LAMINATE DEFORMATION AND BUCKLING
 - BORON/EPOXY
 - GRAPHITE/EPOXY
 - BORON/ALUMINUM
- EXTENSION OF MODEL TO CARBON-CARBON
 - BEHAVIORAL CHARACTERISTICS OF CARBON-CARBON
 - BASIC CHARACTERISTICS OF MODEL
 - APPARENT FLEXURAL MODULUS AND STRENGTH
OF MULTIMODULUS MATERIALS
 - COMPARISON OF PREDICTED AND MEASURED OFF-AXIS STRAINS

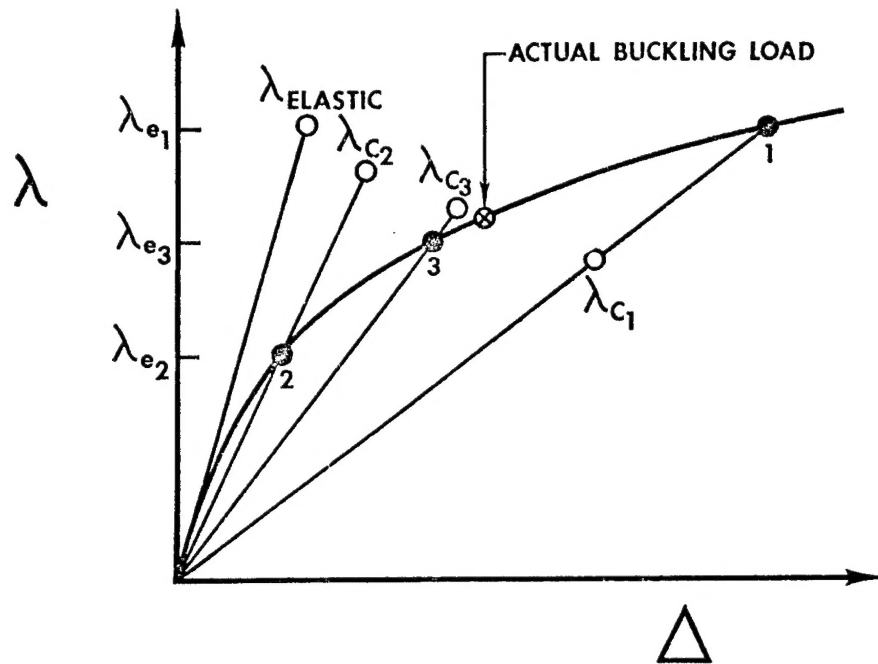
SEQUENCE OF POINTS IN AN ITERATION PROCEDURE TO FIND STRAINS CORRESPONDING TO A GIVEN LOAD



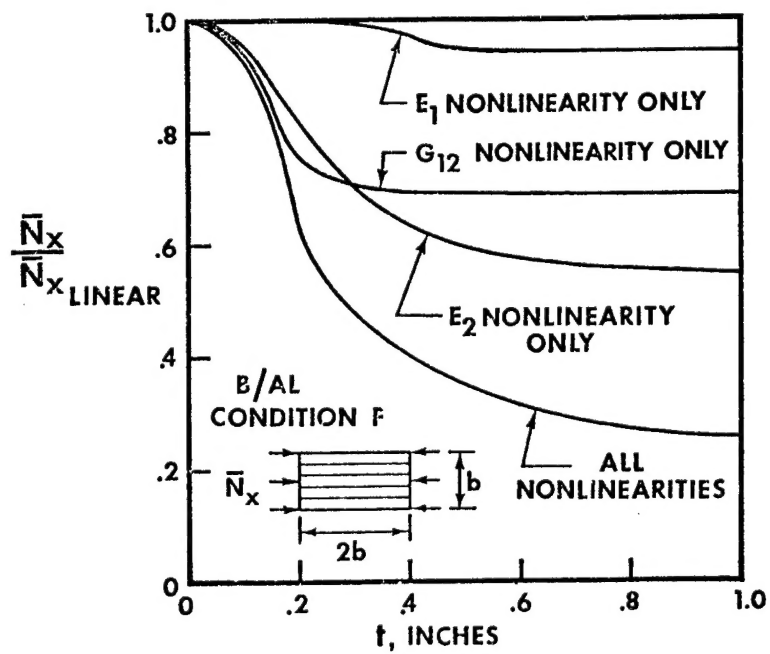
PREDICTED AND MEASURED LAMINATE LOAD-STRAIN BEHAVIOR



BUCKLING LOAD SEARCH PROCEDURE

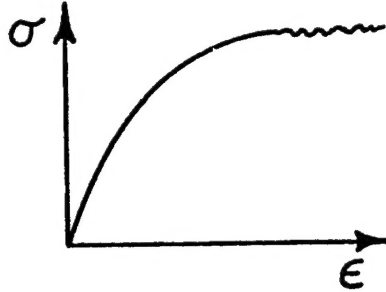


BUCKLING OF UNIDIRECTIONAL 0° LAMINATES



MODELING OF CARBON-CARBON

- NONLINEAR ORTHOTROPIC OR ANISOTROPIC MATERIAL
- MODELED AS A NONLINEAR STRESS-STRAIN CURVE WITH A LINEAR PORTION ABOVE A TRANSITION STRESS



MODELING OF CARBON-CARBON, continued

- JNM DATA COMPUTER PROGRAM (AUTOMATED MODELING AND INPUT)
 - NOW FOR TRANSVERSELY ISOTROPIC MATERIALS
 - EXTENDING TO ORTHOTROPIC MATERIALS
- APPARENT FLEXURAL MODULUS AND STRENGTH
 - NOT INDEPENDENT PROPERTIES OF MULTIMODULAR MATERIALS
 - CAN BE PREDICTED WITH AVAILABLE DATA
 - SHOULD NOT BE MEASURED
- COMPARISON OF PREDICTED AND MEASURED OFF-AXIS STRAINS
 - USE SORI DATA
 - 22 1/2° and 45° OFF-AXIS DATA

PRINCIPAL FINDINGS AND CONCLUSIONS
MECHANICS OF COMPOSITE MATERIALS WITH DIFFERENT MODULI IN TENSION AND COMPRESSION

● MATERIAL MODEL

- STRESS-STRAIN RELATIONS FOR MATERIALS WITH DIFFERENT MODULI IN TENSION AND COMPRESSION, AIAA JOURNAL, FALL 1976
- A NEW MATERIAL MODEL FOR THE NONLINEAR BIAxIAL BEHAVIOR OF ATJ-S GRAPHITE JOURNAL OF COMPOSITE MATERIALS, JANUARY 1975.
- FURTHER CHARACTERISTICS OF A NONLINEAR MATERIAL MODEL FOR ATJ-S GRAPHITE, JOURNAL OF COMPOSITE MATERIALS, JULY 1975.
- MATERIAL MODELS FOR NONLINEAR DEFORMATION OF GRAPHITE, AIAA JOURNAL, JUNE 1976.
- THEORETICAL-EXPERIMENTAL CORRELATION OF MATERIAL MODELS FOR NONLINEAR DEFORMATION OF GRAPHITE, AIAA JOURNAL, SEPTEMBER 1976.

SOLID BODIES

- ABOVE REFERENCES PLUS
- NONLINEAR DEFORMATION OF A THERMALLY STRESSED GRAPHITE ANNULAR DISK (SUBMITTED TO AIAA JOURNAL)
- APPARENT FLEXURAL MODULUS AND STRENGTH OF MULTIMODULUS MATERIALS (SUBMITTED TO JOURNAL OF COMPOSITE MATERIALS)

① LAMINATED PLATES AND SHELLS

● LAMINATION ASYMMETRIES

- BUCKLING AND VIBRATION OF UNSYMMETRICALLY LAMINATED CROSS-PLY RECTANGULAR PLATES, AIAA JOURNAL, DECEMBER 1973.
- BUCKLING AND VIBRATION OF ANTISYMMETRICALLY LAMINATED ANGLE-PLY RECTANGULAR PLATES, JOURNAL OF APPLIED MECHANICS, DECEMBER 1973.
- BUCKLING AND VIBRATION OF CROSS-PLY LAMINATED CIRCULAR CYLINDRICAL SHELLS AIAA JOURNAL, MAY 1975.
- DEFLECTION OF UNSYMMETRICALLY LAMINATED CROSS-PLY RECTANGULAR PLATES, PROCEEDINGS OF 12th ANNUAL MEETING OF THE SOCIETY OF ENGINEERING SCIENCE, OCTOBER 1975.

● LINEAR ELASTIC MULTIMODULUS

- BUCKLING OF STIFFENED LAMINATED COMPOSITE CIRCULAR CYLINDRICAL SHELLS WITH DIFFERENT MODULI IN TENSION AND COMPRESSION, AFOSR-TR-75-0547, FEBRUARY 1975.
- BUCKLING OF LAMINATED COMPOSITE CIRCULAR CYLINDRICAL SHELLS WITH DIFFERENT MODULI IN TENSION AND COMPRESSION, PROCEEDINGS OF 1975 INTERNATIONAL CONFERENCE ON COMPOSITE MATERIALS, APRIL 1975.
- BENDING AND EXTENSION OF CROSS-PLY LAMINATES WITH DIFFERENT MODULI IN TENSION AND COMPRESSION, PROCEEDINGS OF 17th AIAA/ASME SDM CONFERENCE, MAY 1976.

● NONLINEAR ELASTIC

- ANALYSIS OF NONLINEAR STRESS-STRAIN BEHAVIOR OF FIBER-REINFORCED COMPOSITE MATERIALS, PROCEEDINGS OF 17th AIAA/ASME SDM CONFERENCE, MAY 1976.

SUMMARY

- SIGNIFICANT MULTIMODULUS EFFECTS FOR GRANULAR COMPOSITE MATERIALS
- MIXED MULTIMODULUS EFFECTS FOR FIBER-REINFORCED COMPOSITE MATERIALS
 - LOW FOR BORON/EPOXY AND GRAPHITE/EPOXY AT ROOM TEMPERATURE AND LOW HUMIDITY
 - (EXPECTED) HIGHER FOR BORON/EPOXY AND GRAPHITE/EPOXY AT ELEVATED TEMPERATURE AND HUMIDITY
 - (EXPECTED) HIGH FOR CARBON-CARBON UNDER ALL CONDITIONS
- MULTIMODULUS AND NONLINEAR EFFECTS ARE SUSCEPTIBLE TO RATIONAL ANALYSIS
- FUTURE WORK WILL BE CONCENTRATED ON CARBON-CARBON